This document contains all of the abstracts presented
at IPPW-2018, held 11-15 June 2018,
at the University of Colorado Boulder

FUTURE DEVELOPMENT PLAN OF SAMPLE RETURN CAPSULE EVOLVED ON THE BASIS OF HAYABUSA SRC HERITAGE .

Kazuhiko Yamada[1], [1] Japan Aerospace Explartion Agency (3-1-1 Yoshinodai Chuo-ku Sagamihara Kanagawa Japan, yamada.kazuhiko@jaxa.jp)

Introduction: A significance and its value of sample return missions to astral bodies in the deep space is recognaized by HAYABUSA's successful sample return to asteroid ITOKAWA. The sample return mission became one of the keys in the planetry exploration. In Japan, several sample return missions have been discussed and proposed, including Mars Moon sample return mission and Jupitar Trojan sample return mission using the solar power sail.

The sample return capsle is one of the important and indispensable key technologies to support the future sample return missions. The evoluation of the sample return capsule is necessary in order to return a larger amount of samples from deeper space. JAXA and Janapnese resserchars and engineers continues the research and development of the sample return capsule evolved on the basis of HAYABUSA-SRC heritage[1].

Figure 1: Hayabusa's reentry and Hayabusa 2 sample retrun capsule.

Its reserach and development aims to not only the Jananese driven missions but international collaboration missions. In this presentation, the future development plan of the sample return capsule for the future several sample return missions. Current candidate missions to apply its sample return capsules evolved on the basis of Hayabusa's SRC heritage are three projects as follwing.

1) Martian Moons Exploration (MMX) : Sample return mission to Martian moons including phobos[2].
2) Comet Astrobiology Exploration Smaple Retrun (CAESAR) mission : One of the finalist missions in 4th NASA New Frontiers Program, that is the sample return mission to comet 67P/Churyumov–Gerasimenko[3].
3) Outsized Kitecraft for Exploration and Astro-Nautics in the Outer Solar system (OKEANOS) mission : The sample return mission to Jupiter Trojan asteroid using the solar power sail[4].

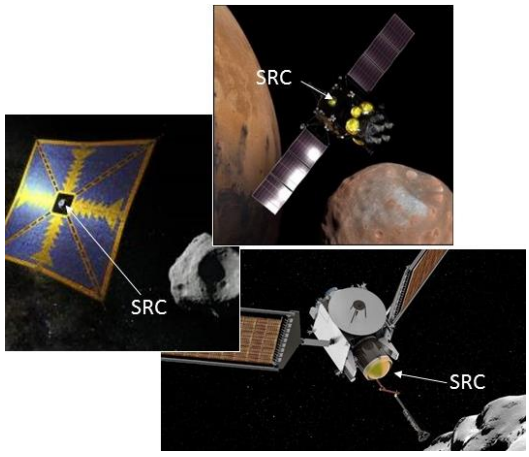

Figure 2: Artist conceptual image of MMX, CAESAR, and OKEANOS.

MMX-SRC:

The sample return capsule for MMX is being developed with the same design concept of HAYABUSA SRC. However it needs scale-up up to 60cm diameter and 50kg. To meet its mission requirement, the performace of some components including, parachute deployment mechanism, heat shield and parachute is enhanceced.

CAESAR-SRC:

The sample return capsule for CAESAR requires to install a large payload system and to keep the payload in low temperature. Therefore, its sample return capsule have to be evolved from Hayabusa SRC. The aerodynamic shape and heat shield material is same as Hayabusa SRC and the front heat shield can be jettisiond in descent phase, which is the same concept of Hayabusa SRC. However, the two stage parachute is adopted and the integration of inside devices including payload system is modified to meet the mission requirements to CAESAR SRC.

OKEANOS-SRC:

The sample return capsule for OKEANOS has to reenter to the Earth's atmosphere with a reentry speed of 14.5km/s because of the direct entry from interplanetary orbit from Jupier. The OKEANOS SRC has

to endure the serverer aerodynamic heating environment than Hayabusa SRC. However, the mass allocaton for SRC is very restricted. We are progressing the conceptual design of OKEANOS-SRC, considering with the optimization of the aerodynamic shape and the material of the heat shield.

SUMMARY :

Recentry, the sample return capsules for the future sample retrun missons, including MMX, CAESAR and OKEANOS have been developed using Hayabusa's SRC herirage. These variation of the sample return capsule will contribute to the various future planetary explration mission.

References:

[1]Yoshifumi Inatani and Nobuaki Ishii, "Design Overview of Asteroid Sample Return Capsule", The institute of Space and Astronautical Science Report SP No.17, March 2003. Page 1-15

[2] K.Kuramoto, et. al. "Martian Moons Exploraton (MMX) conceptual study update" ,49th Lunar and Planetary Science Conference 2018 (LPI Contrib. No. 2083, 2143.pdf) (2018)

[3] S. W. Squyres, et, al. "The CAESAR New Frontiers Mission : 1. Overview", 49th Lunar and Planetary Science Conference 2018 (LPI Contrib. No. 2083, 1332.pdf) (2018)

[4] T. Okada, et,al. "Science and Exploration in the Solar Power Sail OKEANOS Mission to a Jupiter Trojan Asteroid" ,49th Lunar and Planetary Science Conference 2018 (LPI Contrib. No. 2083, 1406.pdf) (2018)

A New Era and a New Tradespace: Evaluating Earth Entry Vehicles Concepts for a Potential 2026 Mars Sample Return. S. V. Perino[1], J. C. Vander Kam[2], J. M. Corliss[3], [1]Jet Propulsion Laboratory, California Institute of Technology, 4800 Oak Grove Drive, Pasadena, CA 91109, [2]NASA Ames Research Center, Moffett Field, CA, 94036, [3]NASA Langley Research Center, 1 NASA Dr., Hampton, VA 23666 [1]scott.perino@jpl.nasa.gov

Introduction: Part of any notional Mars Sample Return (MSR) Mission [1] is the need to return the collected samples from the Martian surface safely back to the Earth. This function has been studied for a large number of potential mission architectures, with most MSR architectures approaching the return as a rendezvous and capture of the Orbiting Sample (OS) in low Mars orbit, followed by some type of encapsulation and/or sterilization (containment) of the OS for planetary protection purposes, then a Mars-to-Earth transit followed by a direct atmospheric entry in an Earth Entry Vehicle (EEV) to a landing on the Earth's surface.

This presentation describes the beginnings of a collaborative multi-year effort between the Jet Propulsion Laboratory, NASA Ames Research Center, and NASA Langley Research Center to evaluate many, down select to two, and mature one baseline Earth Entry Vehicle concept for a potential 2026 launch of an MSR orbiter.

Abstract:

An early EEV concept was developed by Mitcheltree et al. [2] for the original MSR project in the late 1990s. That project was however canceled, and since then a number of architectural assumptions and design requirements have changed. Due to the significant changes, a new examination of the EEV design and trade space is warranted. The key changes influencing EEV design are 1) an increase in the size and baseline quantity of sample tubes, 2) a maturing orbiting sample container design, 3) a new on-orbit 'break-the-chain' containment approach, and 4) a higher than previously anticipated entry velocity needed for new potential return trajectories.

Challenging 'Earth return' planetary protection requirements led the original EEV concept to be simple and robust, with exceptional reliability. Now with the same design goals, this effort leverages the original MSR-EEV work by assuming EEV concepts have the following common features: minimally complex mechanisms, a passively stable aerodynamic shape for all flight regimes, a fail-safe or redundant TPS, redundant impact-tolerant containers encapsulating the OS, impact absorbing structure around the contained OS, and a required landing ellipse fully within a fenced area of the landing zone, notionally the Utah Testing and Training Range (UTTR).

For the preliminary concept development and evaluations, the EEV effort is broken into four sub-elements: TPS, Aerodynamics & Aeroshell, Containment Assurance, and Assembly and Ejection as shown in Fig. 1. Each sub-element team is evaluating a set of design options within a set of constraints. For TPS, four materials: Phenolic Impregnated Carbon Ablator (PICA), Fully Dense Carbon Phenolic (FDCP), Heat Shield for Extreme Entry Environment Technology (HEEET), and Carbon-Carbon (C/C) are being investigated. For aerodynamics & aeroshell, different cone angles (45° and 60°), blunt to sharp sphere-tip radii (45 cm – 2 cm), and several structural materials (Titanium, Aluminum, C/C, Carbon-fiber reinforced composite, and structural-HEEET) are considered. For the containment assurance element, different concepts are evaluated for stress, G-loads, and impact protection especially during off-nominal impacts. Some concepts use hard-shell designs and others using soft-shell designs. For the assembly and ejection element, each concept is evaluated to show feasible in-space robotic assembly of the EEV, snug fit, and reliable precision spin-ejection from the spacecraft.

The current status of each EEV design trade will be presented. Additionally, an overview of the most-current reference orbiter mission architecture is also a topic of this presentation.

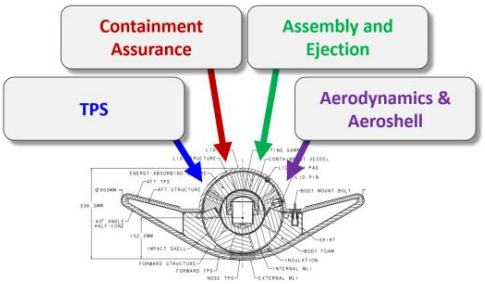

Figure 1: Four element EEV concept generation approach.

References:

[1] National Research Council (U.S.). Committee on the Planetary Science Decadal Survey. Vision and Voyages for Planetary Science in the Decade 2013-2022. Washington, D.C.: National Academies Press; 2011.

[2] Mitcheltree, R. A., et. al., "A Passive Earth-Entry Capsule for Mars Sample Return," 7th AIAA/ASME Joint Thermophysics and Heat Transfer Conference, Albuquerque, NM: AIAA, 1998

Acknowledgment:

A portion of the research described in this paper was carried out at the Jet Propulsion Laboratory, California Institute of Technology, under contract with the National Aeronautics and Space Administration. NASA has made no official decision to implement Mars sample return.

Hot-Structure Earth Entry Vehicle Concept for Robotic Mars Sample Return. M. A. Lobbia[1], S. V. Perino[1], and J. C. Parrish[1], [1]Jet Propulsion Laboratory, California Institute of Technology, 4800 Oak Grove Drive, Pasadena, CA 91109, Pasadena, CA.

Introduction: Robotic Mars Sample Return (MSR) has been of high importance to the planetary science community for over a decade. The most recent Planetary Science Decadal Survey [1] indicated a sample-caching rover should be the top priority large-class mission. The currently in-development Mars 2020 mission will fulfil this objective by incorporating sampling/handling mechanisms in its payload.

NASA's most recent MSR study architecture splits the potential architecture into several distinct elements [2]: 1) a "MSR Lander" that would land a fetch rover to collect previously-cached samples and a Mars Ascent Vehicle (MAV) to launch them into orbit, and 2) a "MSR Orbiter" which would capture the Orbiting Sample (OS) container launched into Mars orbit by the MAV, and return it to Earth's surface using an Earth Entry Vehicle (EEV).

The present work focuses on presenting details of a new hot-structure concept for the EEV utilizing a Carbon-Carbon (C-C) aeroshell. This will include discussion of the design approach, as well as trajectory and aerothermal/ablation analyses highlighting the entry system performance. Potential benefits (as well as challenges) of this concept in meeting the EEV mission requirements will be discussed.

Earth Entry Vehicle Concept: As part of the many MSR studies that have occurred over the last 20+ years, EEV concepts have been developed utilizing a variety of approaches. In general, the high-reliability requirements associated with planetary protection of Earth from Martian samples drives the EEV design approach. Based on this, these past designs implemented a passive ballistic entry vehicle design that would notionally have a relatively hard impact at the Utah Test and Training Range (UTTR). UTTR was chosen as the notional landing site for this study as the soft soil there has been shown solely sufficient for attenuating impact loads to levels that protect sample integrity. Additionally, an integrated system of impact energy absorbers and redundant impact-rated containers were incorporated in the vehicle design which would prevent inadvertent sample release, even for off-nominal impact landings.

Hot-Structure Design Approach: Past EEV designs have followed a heritage "cold-structure" aeroshell design approach, where a Thermal Protection System (TPS) material is bonded to a composite or metallic substructure – the TPS is then sized to maintain a bondline temperature requirement (typically on the order of 500 K) due to adhesive and substructure temperature limitations.

Based on the high-reliability requirements envisioned for the EEV, JPL has led development of a new "hot-structure" design approach utilizing C-C composites. C-C has a material density and strength similar to Aluminum, but with the benefit of constant/increasing strength as temperatures approach several thousand degrees. While C-C is not routinely used in NASA planetary entry missions (aside from Genesis), C-C is a mature and well-characterized material due to investments by the U.S. Department of Defense.

This hot-structure design approach is illustrated in Fig. 1, which shows the aeroshell, Containment Assurance Module (CAM), and Contained-OS (C-OS) elements. The aeroshell structure consists of a 3D C-C nosetip, an 8 mm thick frustum made of 2D C-C, and a series of C-C structural support ribs and load ring. Due to the high-temperature capability of C-C, no additional TPS is required. However, the CAM is designed with a more typical ablator TPS (in this case, Carbon-Phenolic) to provide redundant aerothermal environment protection for the C-OS.

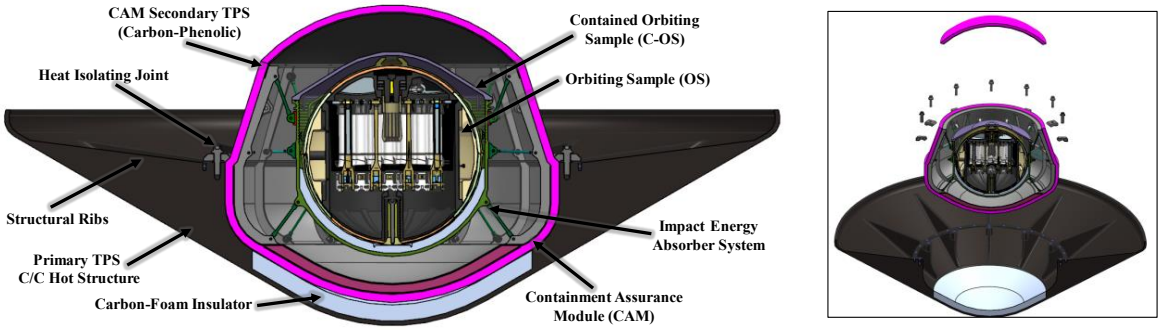

Fig. 1 *Earth Entry Vehicle concept utilizes Carbon-Carbon as a hot load bearing structure.*

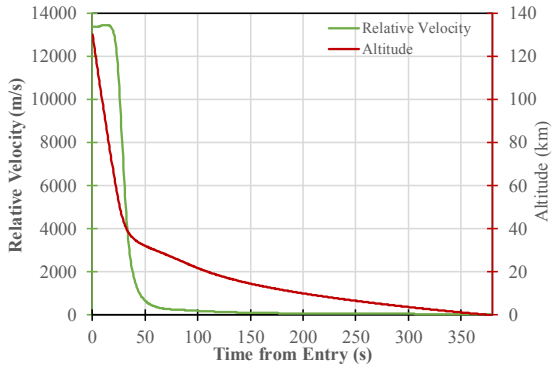

Fig. 2 *Entry and descent trajectory for Earth Entry Vehicle concept.*

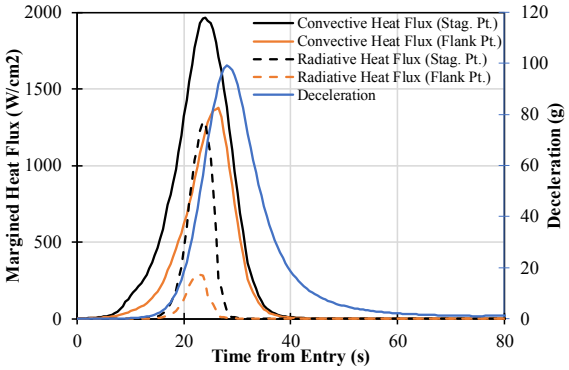

Fig. 3 *Heating and deceleration for Earth Entry Vehicle concept.*

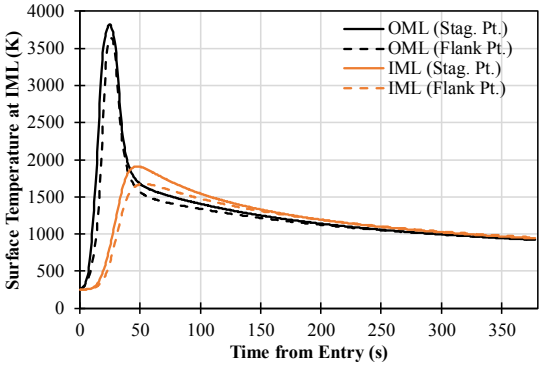

Fig. 4 *Carbon-Carbon temperature history for Earth Entry Vehicle concept..*

An important part of the overall design is the interface between the "hot" C-C aeroshell and "cold" CAM. The current design assumes the use of Zirconia spacers (for thermal isolation) and 3D C-C bolts to connect the CAM to the aeroshell, as well as a carbon-foam insulator behind the nose section of the aeroshell. Alternative CAM interface approaches are also currently being investigated to better optimize the overall design.

Reference Design Results: The concept shown in Fig. 1 was assessed for a nominal 13 km/s entry and 100 kg entry mass at Earth / notionally UTTR in 2029. The results of the entry trajectory analysis (run using JPL's DSENDS code) are shown in Fig. 2 – in this case, the entry flight path angle was designed to be -15 deg., which limits peak deceleration to approximately l00 g's during entry (see Fig. 3). NASA's CBAERO code was used to generate aerothermal environments, and indicated a peak heat flux (including 50% margin and the assumption of fully turbulent flow) of approximately 2 kW/cm^2 (convective) and 1.3 kW/cm^2 (radiative) at the stagnation point (see Fig. 3). A 1D thermal-ablation analysis using NASA's FIAT code indicated a total recession (due to C-C oxidation) of 3.2 mm at the nose and 1.2 mm at the flank (see Fig. 4). This analysis also shows peak temperatures of near 4000 K are reached during entry – due to the high thermal conductivity of C-C, it can be seen that the temperature at the inner mold line (IML) only briefly lags the outer mold line (OML), which is different than a typical ablator TPS design.

Conclusions: A new hot-structure design for a robotic MSR EEV concept demonstrates the potential for increased reliability and low mass in meeting MSR planetary protection requirements. Further design details and analysis updates will be presented at the workshop in June.

References: [1] Squyres, S., et al., "Visions and Voyages for Planetary Science in the Decade 2013-2022," National Academies Press (2011). [2] Lobbia, M., et al, "Mars Ascent Vehicle Concept - Overview and Aeroheating/Thermal Protection System Design," 14th International Planetary Probe Workshop, The Hague, Netherlands (2017).

Acknowledgment: A portion of the research described in this paper was carried out at the Jet Propulsion Laboratory, California Institute of Technology, under contract with the National Aeronautics and Space Administration.

POST FLIGHT ANALYSIS OF THE COMARS+ DATA AND BACKCOVER HEATING OF THE EXOMARS SCHIAPARELLI LANDER

A. Gülhan, T. Thiele, F. Siebe, T. Schleutker, R. Kronen
Supersonic and Hypersonic Technology Department of the Institute of Aerodynamics and Flow Technology, German Aerospace Research Center (DLR), Linder Hoehe, D-51147 Cologne, Germany

In order to measure aerothermal parameters on the back cover of the ExoMars Schiaparelli lander the instrumentation package COMARS+ was developed. Consisting of three combined aerothermal sensors, one broadband radiometer sensor and an electronic box the payload provides important data for future missions. The aerothermal sensors called COMARS combine four discrete sensors measuring static pressure, total heat flux, temperature and radiative heat flux at two specific spectral bands. The narrow band radiometers were provided by CNES. The infrared radiation in a broadband spectral range is measured by the separate broadband radiometer sensor.

Although the landing of Schiaparelli failed, a part of the flight data during the entry phase were transmitted to the TGO at low sampling rate of 0.1 Hz. All COMARS+ sensors delivered useful data with respect to total heat flux rate, radiative heat flux rate, surface temperature and surface pressure of Schiaparelli from the Martian entry point until parachute deployment with the exception of the plasma black-out phase. Since measured structure and sensor housing temperatures were below predicted pre-flight values, a further calibration using the COMARS+ spare sensors at temperatures down to 243 K was conducted. A post flight analysis has been performed by critical assessment of measured flight data of COMARS+ sensors and CFD computations. Table 1 shows the ten trajectory points with available flight data of the COMARS+ package.

Table 1: Trajectory points with COMARS+ data.

	Flight Time from EIP	Altitude Above Ground	Aerodynamic Speed	Dynamic Pressure
	[s]	[km]	[m/s]	[Pa]
S1	35,553	82,467	5829,38	86,53
BL				
S2	115,553	28,202	2595,41	5193,40
S3	125,551	25,477	2013,84	4013,02
S4	135,552	23,064	1570,58	3009,56
S5	145,551	20,862	1236,92	2265,92
S6	155,551	18,887	1001,92	1745,64
S7	165,553	16,959	823,09	1381,21
S8	175,551	15,099	685,40	1115,89
S9	185,552	13,227	584,38	938,40
S10	195,551	11,379	503,09	804,24

The first point before the the black out (S1) is at very high altitude does not cause any remarkable aerothermal heating on the base of the vehicle.At the trajectory point S2 at an altitude of 28.2 km and velocity of 2595 m/s the maxiumum heat flux rate on the back cover has been measured. The aerothermal loads at the trajectory points S3 and S4 are a bit lower but sill high enough for a credible post flight assesment. At trajectory points S5 to S10 aerothermal loads are negligible small, although the surface pressure is high enough to dominate the aerodynamic stability of the vehicle. Therefore a CFD simulation study using the DLR code TAU has been carried out only for the three trajectory points after the communication black out.

In particular the trajectory point S2 provides valuable information about the role of chemical non-equlibrium in aerothermal loads (Figure 1). Computed gas temperature profiles shows remarkable difference in the gas temperarure for chemical non-equlibrium and equilibrium assumptions. It leads to one order of difference in the CO centration and schock stand-off distance. At this trajectory point the ratio of the measured maximum back cover heat flux rate with COMARS+ and computed stagnation heat flux rate for a fully catalytic wall is approx. 0.09. At other trajectory ponts the role of the gas chemistry is weak.

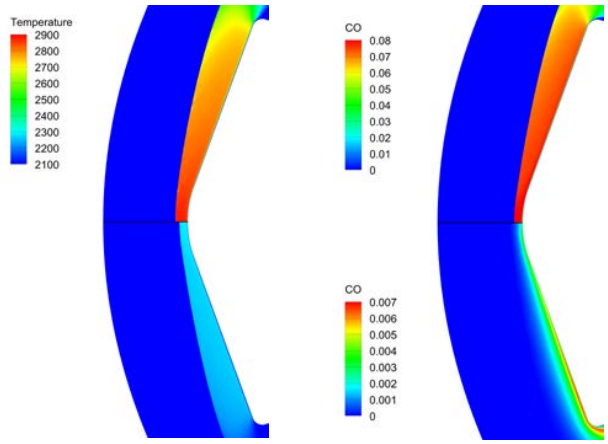

Figure 2: Computed gas temperatures and CO contentration in the schock layer at trajectory points S2 for non-eqilibrium flw (upper figures) and equilibrium flow (bottom figures).

Pterodactyl: Integrated Control Design for Precision Targeting of Deployable Entry Vehicles. S. N. D'Souza[1], B. P. Smith[1], W. A. Okolo[1], B. J. Johnson[2], and B. E. Nikaido[1], NASA Ames Research Center (P.O. Box 1, Mailstop 258-1, Moffett Field, CA 94035, sarah.n.dsouza@nasa.gov), [2]NASA Johnson Space Center (2101 E NASA Pkwy, Houston, TX 77058).

Introduction: This work seeks to do for a deployable entry vehicle (DEV) what the Wright Brothers did to propel modern day aviation: develop the guidance and control (G&C) methods that will make maneuvering and precision landing of DEV a reality. The successful development of a DEV system promises the ability to land high mass payloads on Mars due to the DEV's increased drag area and volume savings over rigid aeroshells. However, the challenge facing the aerospace community is understanding which type of advanced G&C systems will actually enable DEVs to meet precision landing performance requirements. The Pterodactyl project objective is to deliver an integrated G&C methodology for a DEV, based on a detailed analysis that utilizes a Multi-disciplinary, Design, Analysis and Optimization framework.

The current state-of-the-art for entry G&C is rooted in the precision EDL of rigid entry vehicles such as Mars Science Laboratory, Apollo and the Space Shuttle, which used Reaction Control Systems (RCS), a propulsive control system, to achieve the desired bank command profile [1]. However, landing large payloads on Mars using DEVs will require advancements of G&C methods in part because current DEV configurations are radically different from their predecessor; DEVs have no backshell. Recent research has taken a particular interest in non-propulsive control for DEVs, including direct force control [2]–[4] (angle of attack modulation via control surfaces or CG movement) and drag modulation [5], [6] (discrete change in ballistic coefficient). In these studies, the control rate and acceleration requirements are typically assumed to be similar to that of an RCS. However, it is unknown whether alternative G&C systems can actually meet these requirements and can be feasibly integrated into the DEV configuration. Building ground or flight test prototypes for each proposed G&C methodology can be cost prohibitive. Thus, system architecture simulations are needed to advance hardware prototyping efforts for technologies with the highest likelihood of success. Past architecture studies have yet to integrate a high-fidelity control system models into a Multi-Disciplinary, Design, Analysis, and Optimization (MDAO) framework, thus not providing capabilities for trade studies on optimal, integrated DEV G&C solutions. Without these types of trade studies, progress on precision landing of DEVs will stall. Pterodactyl's objectives are to deliver 1) an integrated G&C methodology for a DEV and 2) an analysis-directed prototype of a functional DEV G&C.

Technical Approach: The Pterodactyl technical approach leverages past work on DEV architectures and G&C methods through collaborations with multiple experts across NASA, University of California at Davis, and Applied Physics Laboratory. Specifically, Pterodactyl will leverage work completed to design the Lifting Nano ADEPT (LNA) configuration [7]. This was selected to provide a solid baseline for the vehicle design such that the full vehicle subsystem configuration did not have to be developed from scratch. Specifically, all known subsystems have been packaged within the available LNA volume, system components have been analyzed to meet load requirements, and the stowed LNA has been designed to meet launch vehicle (Atlas V or Falcon 9) mass and volume requirements (Figure 1).

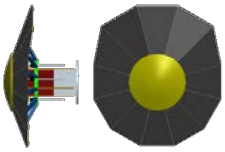

Figure 1: LNA Configuration

Additionally, initial RCS sizing was completed based on a trajectory analysis that maximized cross range capability and this RCS subsystem was included as part of the integrated LNA configuration. The LNA configuration is an asymmetrical vehicle with an L/D of 0.26, a 1+ meter diameter and known subsystem masses (including landed payload RCS mass).

In order to perform the architecture study for this integrated system Pterodactyl will develop a MDAO tool call COBRA-Pterodactyl (COBRA-Pt). This framework will leverage components of the original COBRA to develop an optimal DEV G&C design. COBRA is a modular software tool designed to complete systems-level analyses for entry vehicles (Figure 2a) and has been used extensively for previous entry system studies and

architecture development efforts at NASA [8]. The COBRA-Pt framework leverage existing COBRA tools:

- Model Center Software to integrate simulations
- CBAERO combined with Rapid Geometry Creation for aerodynamics and heating
- Multi-Objective Genetic Algorithm (JEGA via DAKOTA) to perform the full trade optimization

The novel modification to the COBRA framework requires the development and integration of three critical models:

- Guidance with Monte Carlo
- Parametric Control Models
- Vehicle Geometry

Once developed, this capability can also enable optimization of future entry vehicle G&C concepts.

JHU Applied Physics Laboratory's (APL) trajectory analysis capability will be applied to determine the optimal direct entry trajectory and initial conditions for an unguided LNA with a fixed L/D and a guided LNA targeting the beginning of the descent phase. These reference trajectories will be used to modify and implement appropriate bank and alpha modulation guidance algorithms. These guidance algorithms will be developed at NASA JSC.

The control model architectures to be developed and implemented into the COBRA model are: 1) RCS, 2) trim tabs, and 3) shape morphing. The RCS model is selected as a state-of-the-art technology baseline from which to measure performance of alternative control systems models. The trim tab control methodology was selected because the current direction for exploration class missions is to develop trim tab technologies [4]. Finally, shape morphing was selected as a means to possibly dual purpose the ADEPT deployable structure as a control system, which could reduce mass required for additional subsystems. The output from these parameterized control models are the control rates/accelerations and other limits that will be used by the guidance model to determine a feasible commanded control profile to reach the target.

The vehicle geometry is the next element for development and is the primary input to the Configuration-Based Aerodynamics (CBAERO) model. CBAERO outputs relevant aerodynamic/aeroheating databases as a function of the flight conditions, Mach number, dynamic pressure, and angle of attack. These databases are another input to the guidance algorithm and used in the determination of the commanded control profile. Each of these control methodologies will require a modification to the fixed geometry in order to generate accurate aerodynamic/aeroheating effects.

The COBRA-Pt model is illustrated in Figure 2:

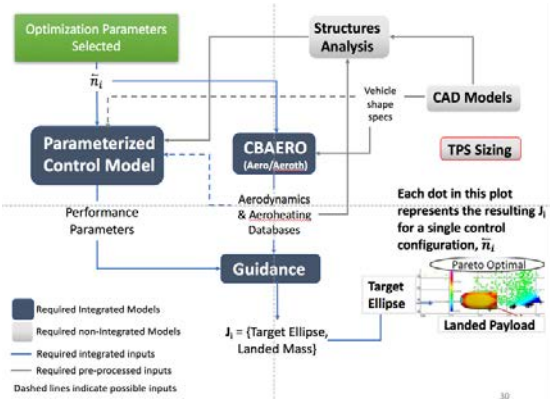

Figure 2: COBRA-Pt Framework

Upon completion of the COBRA-Pt development, a full trade study of the three architectures will be completed to determine the optimal LNA G&C system based on which system minimizes the target ellipse and maximizes landed payload.

This optimal LNA G&C design will enable the build-up of a functional prototype. The prototype will include the integration of guidance software with control actuators and will be tested by sending the vehicle simulated inputs of navigation, atmosphere, aerodynamics, etc. The completion of the test will require building a test stand that can handle the loading and movements of the prototype. The testing of this prototype should lead to the discovery and solution of software/hardware integration issues for this system and validation of the COBRA-Pt G&C models.

References: [1] D'Souza S.N. and Sarigul-Klijn N. (2014) *Progress in Aero. Sci.,* 68, 64-74. [2] Ciancolo A. M. et al. (2011) *NASA/TM-2011-*

217055. [3] Cianciolo A. D. and Polsgrove T. T. (2016) *AIAA Space 2016*. [4] Korzun A. M. et al. (2013) *31st AIAA Applied Aero. Conf.* [5] Putnam Z. R. and Braun R. D. (2014) *JSR*, 51, 128-138. [6] Saikia S.J. et al. () *Astro. Specialist Conf.* [7] Wercinski P. (2016) *FY16 Center Innovation Fund LNA Final Report*. [8] Garcia J. et al. (2010) *10th AIAA/ASME Joint Thermo. and Heat Transfer Conf.*

Aerobraking at Mars: A Machine Learning Implementation. G. Falcone[1] and Z. R. Putnam[2], [1]University of Illinois at Urbana-Champaign (Gfalcon2@illinois.edu), [2]University of Illinois at Urbana-Champaign (Zputnam@illinois.edu).

Introduction:

Aerobraking is an effective maneuver that is able to decrease the propellant mass necessary to insert a spacecraft in a target orbit through many continuous passages into the atmosphere of a planet. The reduction in the propellant mass can lead to an increase in the mass allocation for the science payload or to a reduction in the launch cost of the mission. The spacecraft, entering in the atmosphere, experiences the effect of the atmospheric drag which slows down the vehicle, decreasing its apoapsis radius. Before each atmospheric pass, an aerobraking corridor has to be adequately defined according to the characteristic of the experienced orbit and the limit condition for the passage. According to the velocity of the spacecraft, which depends on the characteristics of the orbit, the limiting factor could be respectively or the dynamic pressure, or the total or the integrated heat flux. These three factors are strictly related to the atmospheric model of the planet and can independently lead the mission to fail.

Currently, three missions have successfully performed a Mars aerobraking maneuver: Mars Global Surveyor (1996), Mars Odyssey (2001), Mars Reconnaissance Orbiter (2005). Mars Odyssey has been the mission with lowest thermal margins and, consequently, has been exposed to the most aggressive conditions. During these three missions, data were sent back to the Earth where specific teams were estimating the atmospheric profile for the next orbit. On the base of that, they were deciding if effectuate a trim maneuver for arising or lowering the periapsis altitude of the successive passage. This methodology, although, has led to three successful missions, results expensive, for its ground station cost, and conservative, since it requires more than 4 hours before the spacecraft can enter again in the atmosphere because of the uplink and downlink time. This time constraint results in an impossibility to perform an aerobraking maneuver for quasi-circular orbit. An autonomous system could overcome this limit.

Moreover, the data received from the historical missions have provided precious information about the atmosphere on Mars and its strong local variation. The data have shown possible asymmetry in the passage where the periapsis was not located in the middle point, massive increase in the density in a short amount of time or substantial deviation in the density values and shapes for two following passages, as shown in Figure 1.

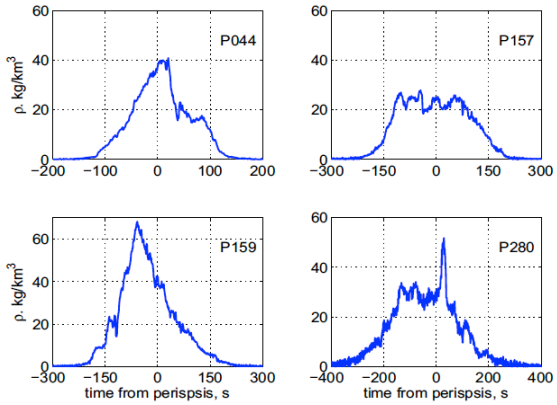

Figure 1. Four Odyssey orbits[1].

Previous works have already studied the implementation of an autonomous system with conventional techniques. The work developed in this paper wants to define an autonomous system taking advantage of the mighty methodologies of machine learning. The system has been implemented to be usable in real-time on the onboard computer and to be capable of estimating the atmospherical density and the current state of the spacecraft; of predicting the next passage trajectory, atmospheric densities and state of the spacecraft; and of autonomously deciding to perform a trim maneuvers to arise or decrease the periapsis. Preliminary results are shown.

Currently, machine learning techniques have been already employed in space to increase the accuracy of orbit prediction of debris, to study the landing problem and to design a low-thrust trajectory, to name some of them, and have shown impressive results.

References:

[1] Tolson, Robert H. and Jill LH Prince (2011) *Onboard atmospheric modeling and prediction for autonomous aerobraking missions.*

Overview of Heatshield for Extreme Entry Environment Technology (HEEET)

D. M. Driver[1], D.T. Ellerby[1], M. J. Gasch[1], M. Mahzari[1], F. S. Milos[1], O. S. Nishioka[1], K. H. Peterson[1], M. M. Stackpoole[1], E. Venkatapathy[1], Z. W. Young[1], P. J. Gage[2], T. Boghozian[3], J. F. Chavez-Garcia[3], G. L. Gonzales[3], G. E. Palmer[3], D. K. Prabhu[3], J. D. Williams[3], C.D. Kazemba[4], A. S. Murphy[5], S. L. Langston[6], C. C. Poteet[6], S. C. Splinter[6], M. E. Fowler[7], C. M. Kellermann[8], [1]NASA Ames Research Center Moffett Field, CA 94035, [2]Neerim Corp Moffett Field, CA 94035, [3]Analytical Mechanics Associates, Inc. Moffett Field, CA 94035, [4]Science and Technology Corp, Moffett Field, CA 94035, [5]Millennium Engineering and Integration Co. Moffett Field, CA 94035,[6]NASA Langley Research Center Hampton, VA 23681, [7]NASA Johnson Space Center Houston, TX 77058, [8]Jacobs Technology, Inc. Houston, TX 77058

The objective of the Heatshield for Extreme Entry Environment Technology (HEEET) projects is to mature a 3-D Woven Thermal Protection System (TPS) to Technical Readiness Level (TRL) 6 to support future NASA missions to destinations such as Venus and Saturn. Destinations that have extreme entry environments with heat fluxes upto 5000 W/cm^2 and pressures upto 5 atmospheres, entry environments that NASA has not flown since Pioneer-Venus and Galileo.

The scope of the project is broad and can be split into roughly four areas, Manufacturing/Integration, Structural Testing and Analysis, Thermal Testing and Analysis and Documentation. Manufactruing/Integration covers from raw materials, piece part fabrication to final integration on a 1 meter base diameter 45 degree sphere cone Engineering Test Unit (ETU). A key aspect of the project was to transfer as much of the manufacturing technology to industry in preparation to support future mission infusion. The forming, infusion and machining approaches were transferred to Fiber Materials Inc. and FMI then fabricated the piece parts from which the ETU was manufactured.

The base 3D-woven material consistes of a dual layer weave with a high density outer layer to manage recession in the system and a lower density, lower thermal conductivity inner layer to manage the heat load.

At the start of the project it was understood that due to weaving limitations the heat shield was going to be manufactured from a series of tiles. And it was recognized that the development of a seam solution that met the structural and thermal requirements of the system was going to be the most challenging aspect of the project. It was also recognized that the seam design would drive the final integration approach and therefore the integration of the ETU was kept in-house within NASA. A final seam concept has been successfully developed and implemented on the ETU and will be discussed.

The structural testing and analysis covers from characterization of the different layers of the infused material as functions of weave direction and temperature, to sub-component level testing such as 4pt bend testing at sub-ambient and elevated temperature. ETU test results are used to validate the structural models developed using the element and sub-component level tests. Given the seam has to perform both structurally and aerothermally during entry a novel 4pt bend test fixture was developed allowing articles to be tested while the front surface is heated with a laser. These tests are intended to establish the system's structural capability during entry.

A broad range of aerothermal tests (arcjet tests) are being performed to develop material response models for predicting the required TPS thickness to meet a missions needs and to evaluate failure modes. These tests establish the capability of the system and assure robustness of the system during entry.

The final aspect of the project is to develop a comprehensive Design and Data Book such that a future mission will have the information necessary to adopt the technology.

This presentation will provide an overview and status of the project and describe the status of the tehnology maturation level for the inner and outer planet as well as earth entry sample return missions.

HIGHLY RELIABLE 3-DIMENIONAL WOVEN THERMAL PROTECTION SYSTEM FOR MARS SAMPLE RETURN., E. Venkatapathy[1], K. Peterson[2], D. Ellerby[2], P. Gage[3], E. Christiansan, J. Vander Kam[2], T. White[2] and M. Stackpoole[2]
[1] MS 229-3, NASA ARC, Moffett Field, CA; ethiraj.venkatapathy-1@nasa.gov; [2] NASA Ames Research Center; [3] Neerim Corp.

Introduction: This paper is concerned with a Thermal Protection System technology development plan for a new generation of highly reliable Thermal Protection Systems (TPS). The current work leverages previous 3D Woven TPS (3-D WTPS) development experience, specifically HEEET and 3-D MAT, to attack the TPS reliability problem on the MSR EEV. Additionally, this effort will lay the foundation for a reliability-focused TPS design methodology that is also applicable to TPS for human missions.

The baseline design for MSR EEV, developed over the last two decades, is shown in Figure 1. The TPS consists of a Tape-Wrapped Carbon Phenolic (TWCP) on the flank, a Chop-Molded Carbon Phenolic (CMCP) nose-cap, and SLA 561-V for the back-shell.

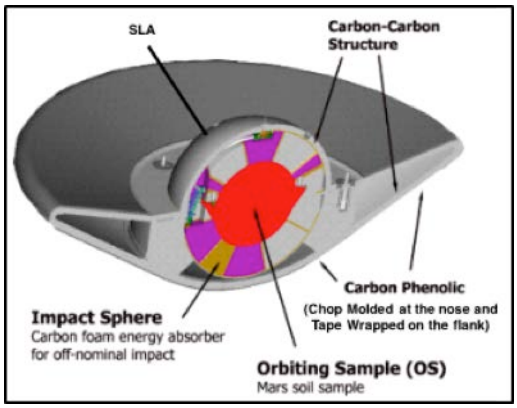

Figure 1. Baseline EEV Concept for MSR

At the time of TPS selection, these materials appeared to offer high reliability through extensive flight heritage, but TPS reliability was never verified when design decisions were made in 2002. In addition, Micro-Meteor and Orbital Debris (MMOD) impact was a concern, but only in 2010, when MMOD impact testing was performed and excessive damage was observed [1], was the baseline TPS found to have inadequate reliability.

The MSR mission has more stringent TPS reliability requirements than any mission conceived to date. Currently, there is no established practice or methodology for the design of TPS to meet reliability requirements. There is ongoing discussion regarding what level of reliability is acceptable for the MSR EEV TPS, and there are questions regarding verification feasibility, especially with realistic constraints on cost and development time. A Risk Informed Decision Making (RIDM) framework is used here to support discriminating between candidate systems based on reliability metrics.

3-D Woven Thermal Protection Systems: 3-D Woven TPS is not a single material, but a family of materials that can be tailored to meet various requirements (Ref 2). 3-D Multifunctional Ablative TPS (3-D MAT) flight hardware has been developed and delivered for the Orion EM1, vehicle, to replace carbon phenolic in regions where high compression loads are applied to the thermal protection material.

Both HEEET and 3-D MAT offer examples of innovative TPS solutions that use 3-D weaving, are robust, and meet mission performance requirements. It offers tantalizing options for the development of a series of highly reliable TPS options for the MSR EEV through an integrated approach that focuses on the reduction in severity of various failure modes through the improvement in integrated (TPS and structure) thermo-structural capability and an improved toughness against hypervelocity impacts from Micrometeoroids and Orbital Debris.

System Selection for Reliability and Verifiability: The full paper will report on initial characterization of candidate TPS architectures from a risk perspective to identify: 1) The potential failure modes of each TPS design option, 2) the likelihood of those failure modes, and 3) the consequences anticipated for each failure mode. A HEEET architecture, including seams between woven panels, will be compared with the Carbon Phenolic system that was baselined previously, with

particular attention on MMOD robustness, based on recent impact testing of HEEET material (Figure 2 is the HEEET as it is undergoing OML machining).

Figure 2. 3-D Woven dual-layer heat-shield (HEEET) undergoing outer mold line machining.

Aerothermal and thermostructural capability of HEEET, as demonstrated in extreme environment testing, will also be discussed with reference to MSR design environments.

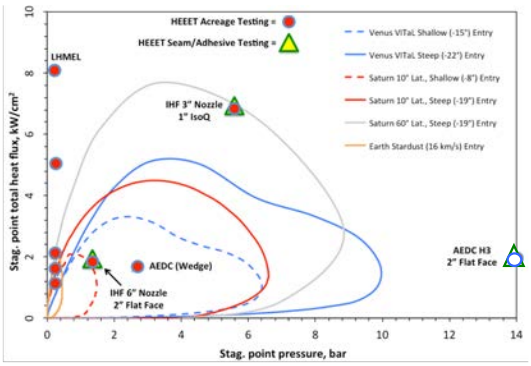

Figure 3. Comparison of Saturn, Venus and Sample Return Flight Environments (Stagnation Point Conditions) vs Test Performed

In order to improve design, it is attractive to eliminat features that might lead to failure and to add features that are robust against failure modes. Since seams between TPS panels are difficult to verify, the full paper will include initial investigation of a single piece heatshield, particularly from the perspective of manufacturing and integration-option will be evaluated.

At least two candidate implementations will be included:

1) a "hot structure" system that includes only the dense "recession layer" from HEEET, and

2) A dual layer HEEET system with tailored thickness, backed by a conventional composite structure.

Ranking of failure modes and a discussion of the relative verification challenges will be provided.

References:

[1] Christiansen, E., et al., "Micrometeoroid and Orbital Debris Threat Assessment: Mars Sample Return Earth Entry Vehicle," NASA TM 20 2013-217381

[2] Venkatapathy, E., "Modern Advances in Ablative TPS," EDL Short Course at the 10th International Planetary Probe Workshop, June 2013, San Jose, CA.

SIZING AND MARGIN METHODOLOGY FOR DUAL-LAYER THERMAL PROTECTION SYSTEMS

M. Mahzari[1] and F. Milos[2]

[1] *NASA Ames Research Center (milad.mahzari@nasa.gov),* [2] *NASA Ames Research Center (frank.s.milos@nasa.gov)*

Introduction: This presentation introduces a new sizing and margin methodology for dual-layer Thermal Protection Systems (TPS). The methodology has been tailored for application to a dual-layer 3D-woven TPS called Heatshield for Extreme Entry Environments Technology (HEEET) [1]. Sizing is performed for a reference Saturn probe mission to show how uncertainties in trajectory, aerothermal modelling and TPS response impact the sizing of each layer.

TPS Sizing: TPS sizing and margining is the process of determining the required material thickness to meet a certain design criterion for mission-defined boundary conditions, while accounting for variabilities and uncertainties in boundary conditions, material response, and manufacturing processes. Typically, the design criterion is a temperature constraint at the TPS-structure bondline defined by the performance limit of the adhesive or the structure. TPS sizing approaches for previous entry missions have ranged from methods as simple as applying engineering factors to a nominally-sized thickness to more detailed techniques that account for multiple independent sources of uncertainty. Wright et al. employed a Root Sum Square (RSS) process for the sizing of Mars Science Laboratory's single-layer heatshield [2]. The goal of this study is to expand that sizing process for application to dual-layer heatshield materials, specifically the HEEET system.

Dual-Layer TPS: Dual-layer materials allow for integration of a robust top layer with good recession performance (typically with a relatively high density and thermal conductivity) with a bottom layer with good insulation performance (lower density and lower thermal conductivity). The increased mass efficiency of a dual-layer material enables mission designers to select shallow entry trajectories that may have carried unacceptably high mass penalties for traditional single layer materials, but that are of interest due to reduced g-loads. The HEEET project is developing a dual-layer 3D woven heatshield for this exact purpose. The HEEET top layer, called Recession Layer (RL), is composed of tightly-woven carbon fibers while the bottom layer, called Insulation Layer (IL) is made with larger blended carbon and phenolic tows. The two layers are interwoven and then infused with phenolic resin to produce a rigid TPS material. Due to weaving size limitations, a flight heatshield must be made of tiles with gap fillers. The sizing and margining process must account for the uncertainties in the performance of both the acreage and gap filler materials. Dual-layer materials are likely to be designed with a requirement that the bottom layer is not exposed to the high-temperature flow, which introduces an additional constraint for thickness of the top layer.

Sizing Methodology: Figure 1 illustrates the sizing and margin methodology developed for the HEEET system. The process, as shown here, assumes a uniform TPS thickness across the entire heatshield because the current HEEET development is tailored for a uniform-

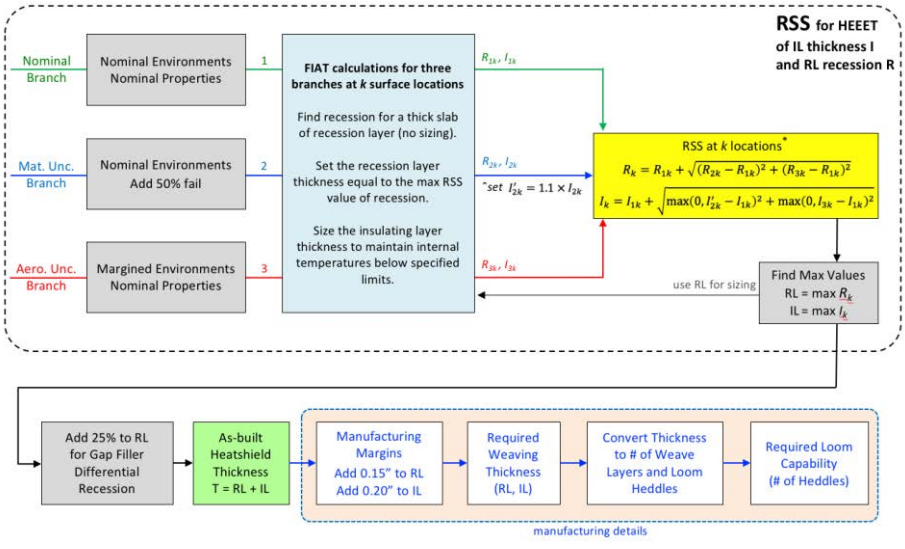

Figure 1. Sizing and Margin Process for Dual-Layer TPS

thickness heatshield ; however, the process can be easily modified for heatshields with varying thickness. This three-branch process applies margins for uncertainties associated with heating environments and material response in an RSS process to compute the required recession layer thickness. Analysis is done at multiple vehicle body points and for bounding trajectories to find the maximum RL thickness. This processes is then repeated to calculate the IL thickness for multiple body points and trajectories with the bounding RL thickness computed in the previous step. Additional considerations are included for gap filler differential recession and manufacturing tolerances.

CFD heating environments from a reference Saturn probe mission will be used to study how variabilities and uncertainties in trajectory, heating environments and material response impact the sizing of each layer.

References:

[1] Milos, F.S., *et al*., AIAA paper 2017-3353.

[2] M. Wright, et al. (2017) *J. Spacecraft and Rockets*, **51**(4), pp.1125-1138.

STUDIES IN SUPPORT OF VENUS AEROCAPTURE UTILIZING DRAG MODULATION. R.A.S. Beck[1], G.A. Allen[2], M. Aftosmis[1], P. Wercinski[1], M. Wilder[1] and E. Ventakapathy[1], NASA Ames Research Center, PO Box 1, N229, Moffett Field, CA 94035, [2]AMA, Inc. at NASA Ames Research Center, PO Box 1, N229, Moffett Field, CA 94035.

Introduction: Aerocapture has been extensively studied and these studies (Ref. 1 – 3) have shown the benefit for planetary exploration missions. While the traditional approach to aerocapture with lifting configurations and lift-guided modulations has been assessed to be technologically feasible, aerocapture using purely drag modulation was proposed and studied by Prof. Braun and his students (Ref. 4 – 7). These studies show that if one can assess the feasibility of aerocapture using drag modulation at Venus, and develop tall pole technologies needed at Venus, then this concept is much easier to execute at all other relevant destinations.

Based on the above finding, partnered proposals were submitted by Adam Nelessen at JPL and Ethiraj Venaktapathy at Ames in collaboration with Prof. Braun at the University of Colarado, Boulder (UCB). Under this partnership, Ames Research Center (ARC) is working to address some of the key entry technology challenges associated with drag modulation aerocapture at Venus. Drag modulation aerocapture is a simple, scalable, and likely cost-effective way to enhance planetary science missions. The approach envisioned is to design a small spacecraft, that would most likely be a secondary payload, with a removable drag skirt. The vehicle would enter the atmosphere at Venus with a low ballistic coefficient, decelerate rapidly, drop the skirt resulting in a smaller vehicle with a higher ballistic coefficient which would skip out of the atmosphere and enter into a desired orbit, shown in Figure 1.

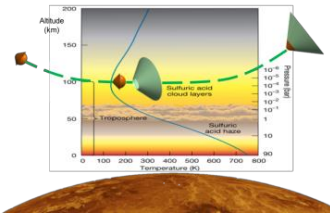

Figure 1. Illustration of Drag Modulated Aerocapture

ARC's role in this collaboration is multifold. First of which is to perform design studies on various pre- and post-jettison geometries utilizing a 3-DOF trajectory code to determine the aerodynamics and aerothermodynamics of the vehicles and evaluate viable thermal protection material system designs. Once these design studies are complete, Ames will then perform higher fidelity CFD and TPS sizing to further design the vehicles.

Second, the multi-body separation dynamics of the drag modulation event will be explored using both CFD simulations (CART3-D and US3D) as well as possible ballistic range testing. ARC's tools and expertise have been used to assess and advise on the selection of the separating configuration. In addition to the preliminary evaluation, ARC will provide tools and expertise to UCB team members to further assess aerodynamic interactions between the separating bodies and provide guidance as to the feasibility of stable transition.

Initial Studies:

Using the NASA Ames 3-DOF simulation code TRAJ, trajectory sensitivity studies were performed to understand the transition time in order to determine the environment on the two body system.

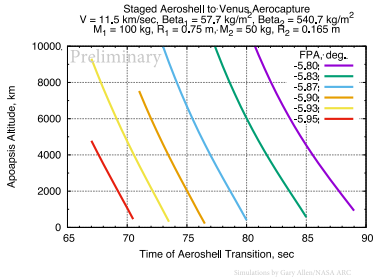

Figure 2. Sensitivity of apoapsis altitude to time of separation.

Figure 2 shows the sensitivity for a given mass and size of of the entry body, mass and size of the separate center-body, the time at which the skirt needs to separate from the center body in order to achive the desired apoapsis and also the effect of initial entry flight path angle accuracy required. Analysis of aerocapture at Venus with several entry velocities and flight path angles, have been performed and for those trajectories, the margined peak heating was less than 800 W/cm2 and stagnation pressures were approximately 0.2 atm. At these levels, lightweight PICA and/or conformal PICA can easily perform as the TPS and the higher performance materials such as HEEET and carbon phenolic will not be required.

Based on these initial studies, PICA or conformal PICA could both serve as the TPS for the center body as well as the skirt, in case the skirt is a rigid body system. If packaging a large skirt is a constraint one has to deal with, evaluation of the ADEPT concept will be part of the trade study in the future. The ADEPT concept allows the skirt to be folded and deployed prior to entry. The ADEPT concept utilizes 3-D woven carbon fabric that is amenable to and has been tested at conditions applicable for the aerocapture. The thickness of the fabric and foldability of the fabric are some of the issues that will be addressed as the study progresses in the near future.

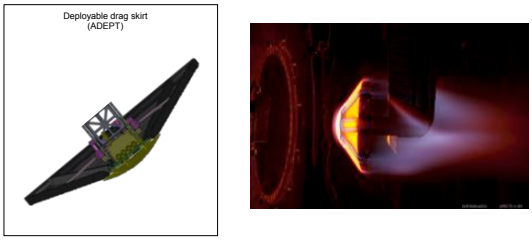

Figure 3. A deployable skirt concept made of 3-D woven carbon fabric can withstand the heating and based on ADEPT studies, the foldable construct could be an option if launch constraints require the deployable skirt to be folded during launch.

Seperation of the skirt from the center body during the atmospheric entry is a critical event. The skirt could be a single contiguous element that separates from the center body as a single piece or it could be made of multiple petals that seprate into multiple bodies. The desire is for the separation to be simple and avoid re-contact.

The CART3-D is a computational simulation tool that can deal with complex and multiple bodies. The code is designed to compute aerodynamic coefficients as part of the evolving system and use them to compute the trajectories of the multiple bodies.

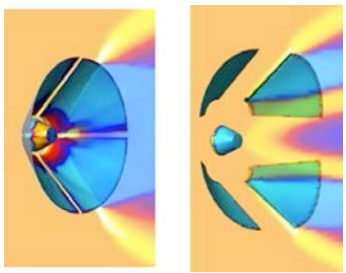

Figure 4. Dynamic simulation using CART-3D of a multiple petal skirt system.

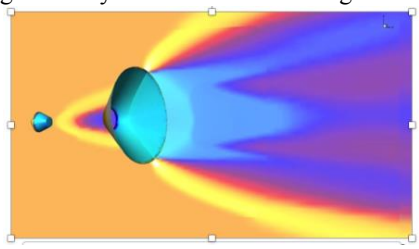

Figure 5. Dynamic simulation using CART-3D of a single piece skirt system.

The preliminary studies indicated that a single skirt system is likely to separate cleanly and could have minimal likelihood of recontact. The four petal skirt system did lead to complex separation dynamics and, without an initial kickoff force, the mulitiple petals were likely to recontact the center body. This is because the aerodynamic of each of the petals forces it to tumble into the wake and interact with the center body. This preliminary study informed the team to consider only the single piece skirt and not the multiple petal concept.

In addition to computational simulation, the Ames team will be pursuing ballistic range experiments to establish the viability of the single skirt concept.

Figure 6. Preliminary Ballistic Range Model Design.

Typically, a ballistic range model is a single piece and the Ames ballistic range can obtain aerodynamics data for both non-lifting and lifting configuration with various gas compositions and at various densities. Using the ballistic range to study the separation of multiple bodies is novel and presents challenges. The Ames team is exploring options with improved optical systems and is designing a model that will separate cleanly during free flight. We will be performing exploration studies in the coming months. Based on design and free flight computational simulations, focused model design and testing is planned for the next fiscal year.

Remarks: The novel construct of aerocapture using drag modulation proposed by Prof Braun and his students is attractive as it is simple to execute and yet provides the benefits recognized by many of the previous studies. By assessing its viability through exploring the challenges and evaluating the technology readiness at Venus, the current work performed by Ames, in partnership with JPL and UCB hopes to enable the technology, starting with future small spacecraft science missions and possibly large flagship-class Ice-giant missions.

References:

1. Walberg, G.D., "A Survey of Aeroassisted Orbit Transfer," Journal of Spacecraft and Rockets, Jan. 1985.

2. Hall, J.L., Noca, M.A., Bailey, R.W., "Cost-Benefit Analysis of the Aerocapture Mission Set," Journal of Spacecraft and Rockets, Vol. 42(2), pp. 308-320, Mar. 2005.

3. Lockwood, M.K., "Titan Aerocapture Systems Analysis," AIAA/ASME/SAE/ASEE Joint Propulsion Conference and Exhibit, July 2003.

4. Putnam, Z.R., Braun, R.D., "Drag Modulation Flight-Control System Options for Planetary Aerocapture,"Journal of Spacecraft and Rockets, Vol. 51(1), pp. 139-150, Jan. 2014.

5. Putnam, Z.R., Braun, R.D., "Precision Landing at Mars Using Discrete-Event Drag Modulation," Journal of Spacecraft and Rockets, Vol. 51(1), pp. 128-138, Jan - Feb 2014.

6. Werner, M. S., et al., "Development of an Earth Smallsat Flight Test to Demonstrate Viability of Mars Aerocapture," 55th AIAA Aerospace Sciences Meeting, Grapevine, TX, Jan. 2017.

7. Werner, M. S., Braun, R. D., "Characterization of Guidance Algorithm Performance for Drag Modula ance & Control Conference, Feb. 2017.

SCIENCE GOALS AND PAYLOADS FOR COMMON PROBE MISSIONS TO VENUS AND THE GIANT PLANETS. D.H. Atkinson[1], T.R. Spilker[2], M. Amato[3], L. S. Glaze[3], M. Hofstadter[1], K. M. Sayanagi[4], A. A. Simon[3], [1]David.H.Atkinson@jpl.nasa.gov, Jet Propulsion Laboratory, California Institute of Technology, Pasadena, CA, [2]Independent Consultant, [3]NASA Goddard Space Flight Center, [4]Hampton University, Hampton, VA

Introduction: The atmospheres of the planets in our solar system are laboratories in which the structure, chemistry, processes, climate, and climate evolution on the Earth, other atmospheres throughout the solar system, and of extrasolar planets are studied. Remote observations provide global cloud-top coverage of planetary atmospheres, but are of limited utility for studying key properties of the deeper atmosphere. For a complete characterization of an atmosphere, *in situ* sampling from one or multiple carefully targeted entry probes is necessary to supplement remote sensing measurements.

Perhaps the single most important property of an atmosphere is the composition, the abundance of noble gases including helium (giant planets) in particular. The heavy elements and noble gas abundances reflect the circumstances and processes by which the planet and atmosphere formed, and carry the signature of the origin, formation, and chemical and dynamical evolution of the atmosphere. With no microwave spectral signature, noble gases are beyond the reach of remote sensing and can therefore only be retrieved by direct *in situ* atmospheric sampling. Being chemically non-reactive, noble gases are well-mixed and measurement of noble gas abundances can be made by a single probe at any location below the homopause within the atmosphere.

Although the atmospheres of the terrestrial planets and the giant planets formed in different locations of the protoplanetary solar nebula by different mechanisms at different epochs, resulting in significantly different compositions and structures, the fundamental questions are common to all planetary atmospheres. The atmosphere of a planet is diagnostic of the formation of the planet itself, and the properties of an atmosphere therefore provide unique insight into the origin, formation, and evolution of the planet. Comparative planetology dictates that many atmospheric processes, and key aspects of atmospheric thermal and energy structure, dynamics, and chemistries are common among all atmospheres. The study of a single atmosphere therefore provides significant insight into and valuable context for the study of other atmospheres in the solar system and beyond. Terrestrial planet atmospheres present an additional complication due to the presence of a lower boundary, whether a solid surface or an ocean.

Another important quantity that requires *in situ* measurements is the deep static stability of the atmosphere. Radio occultation techniques can provide elements of the vertical structure in the upper atmosphere. However, radio occultation is only effective to one bar or slightly deeper, at which point either bending of the signal raypath by atmospheric refraction or atmospheric absorption will diminish the signal strength and make deeper measurements impossible. The deep static stability of the atmosphere is governed by various mechanisms of vertical energy transport including dry/moist convection, radiation, and atmospheric waves, and is a result as well as an indicator of the thermal energy balance and the thermal evolution of the planet.

Atmospheric entry probe missions have been made to the terrestrial planet Venus by the Pioneer multiprobes, the VeGa landers and balloons, and the Venera landers. The Galileo probe to Jupiter represents the only *in situ* exploration of a giant planet atmosphere. To date, no *in situ* measurements have been made by entry probes at the other gas giant planet Saturn, or the ice giants Uranus and Neptune. In particular, the lack of a probe to an ice giant represents the largest current gap in our understanding of solar system atmospheres.

In spite of significant differences between the composition, structure, and dynamics of the terrestrial planets in the inner solar system and the giant planets in the outer solar system, the overarching physics of atmospheres results in essential key questions that can be largely addressed by a common probe instrument payload. The composition is the most important measurement to be made of a planetary atmosphere. Remote sensing can provide some indication of the deep, well-mixed abundances of volatiles. However, measurement of noble gas and certain key isotope abundances require direct atmospheric sampling. The key instrument on a planetary entry probe is therefore a composition instrument to measure the well-mixed noble gases as well as other key atmospheric constituents including volatiles, disequilibrium species, and isotopes. With the exception of the noble gases, the abundances of other constituents may vary with altitude due to condensation into cloud layers, atmospheric convection, photochemistry, and precipitation. The overall structure of the atmosphere is defined by the thermal structure and dynamics of the atmosphere and requires instruments to measure the altitude profiles of temperature, pressure, winds, and waves. Clouds play an important role in the thermal structure and energy balance of atmospheres, and their

formation, altitude, and structure reflect the composition, the thermal profile, and the dynamics of planetary atmospheres.

Common Probe Instruments: To understand the overarching properties of an atmosphere including composition, and thermal and dynamical structure, a common atmospheric probe strawman payload comprises Tier 1 (essential) and Tier 2 (lower priority) instruments:

Tier 1

- **Mass Spectrometer**, possibly including both a neutral mass spectrometer and a tunable laser spectrometer to measure the abundances of well-mixed noble gases, volatiles, disequilibrium species, and isotopic ratios;
- **Atmospheric Structure Instrument** comprising accelerometers, pressure, and temperature sensors to measure entry and descent dynamics, and the altitude profile of temperature and pressure that defines the thermal structure and stability of the atmosphere;
- **Ultrastable Oscillator** to generate a stable radio link from which probe motions reflecting the dynamics of the atmosphere can be retrieved using Doppler techniques.

Tier 2

- **Nephelometer** to characterize the location, microphysics, number densities, and structure of hazes and clouds;
- **Net Flux Radiometer** to measure the net upward and downward thermal and visible radiative fluxes to indicate locations within the atmosphere of radiative absorption and the net energy structure of the atmosphere;
- **Speed of sound** instrument. If the atmospheric temperature is known, a measurement of the speed of sound would constrain the atmospheric composition. If the composition is known, then the measured speed of sound would provide a high spatial resolution measurement of temperature;
- **Ortho/Para Hydrogen** (giant planets only) to characterize convection that carries ortho-hydrogen upwards from the deep atmosphere;
- **Electromagnetic Instruments** including electric field sensors, magnetometers, lightning and radio sensors, and relaxation probes to detect signatures of electrical processes within the atmosphere and the electrical conductivity of the atmosphere.

A COMMON PROBE DESIGN FOR MULTIPLE PLANETARY DESTINATIONS. H. H. Hwang,[1] G. A. Allen, Jr.,[2] A. I. Alunni,[2] M. J. Amato,[3] D. H. Atkinson,[4] B. J. Bienstock,[4] J. R. Cruz,[5] R. A. Dillman,[5] A. D. Cianciolo,[5] J. O. Elliott,[4] J. D. Feldman,[6] M. D. Hofstadter,[4] K. M. Hughes,[3] M. A. Lobbia,[4] G. C. Marr,[3] F. S. Milos,[6] K. H. Peterson,[6] D. K. Prabhu,[2] and T. R. White.[6] [1]NASA Ames Research Center, M/S 230-3, Moffett Field, CA 94035, USA (helen.hwang@nasa.gov), [2*]AMA, Inc. at NASA ARC, [3]NASA Goddard Space Flight Center, [4]Jet Propulsion Laboratory, [5]NASA Langley Research Center, [6]NASA Ames Research Center.

Introduction: Atmospheric probes have been successfully flown to planets and moons in the solar system to conduct *in situ* measurements. They include the Pioneer Venus multi-probes, the Galileo Jupiter probe, and Huygens probe. Probe mission concepts to five destinations, including Venus, Jupiter, Saturn, Uranus, and Neptune, have all utilized similar-shaped aeroshells and concept of operations, namely a 45° sphere cone shape with high density heatshield material and parachute system for extracting the descent vehicle from the aeroshell. Each concept designed its probe to meet specific mission requirements and to optimize mass, volume, and cost. At the 2017 IPPW, NASA Headquarters postulated that a common aeroshell design could be used successfully for multiple destinations and missions [1]. This "common probe" design could even be assembled with multiple copies, properly stored, and made available for future NASA missions, potentially realizing savings in cost and schedule and reducing the risk of losing technologies and skills difficult to sustain over decades.

Thus the NASA Planetary Science Division funded a study to investigate whether a common probe design could meet most, if not all, mission needs to the five planetary destinations with extreme entry environments. The Common Probe study involved four NASA Centers and addressed these issues, including constraints and inefficiencies that occur in specifying a common design.

Study methodology: First, a notional payload of instruments for each destination was defined [2] based on priority measurements from the Planetary Science Decadal Survey [3]. Steep and shallow entry flight path angles (EFPA) were defined for each planet based on qualification and operational *g*-load limits for current, state-of-the-art instruments. Interplanetary trajectories were then identified for a bounding range of EFPA [4].

Next, 3-DoF simulations for entry trajectories were run using the entry state vectors from the interplanetary trajectories [5,6]. Aeroheating correlations were used to generate stagnation point convective and radiative heat flux profiles [6] for several aeroshell shapes and entry masses. High fidelity thermal response models for various TPS materials were used to size stagnation point thicknesses, with margins based on previous studies. Backshell TPS masses were assumed based on scaled heat fluxes from the heatshield and also from previous mission concepts.

Presentation: We will present an overview of the study scope, highlights of the trade studies and design driver analyses, and the final recommendations of a common probe design and assembly. We will also indicate limitations that the common probe design may have for the different destinations. Finally, recommended qualification approaches for missions will be presented.

References:

[1] Session: Outer Planets (2017) *14th IPPW*, The Hague, Netherlands, June 14. [2] Atkinson, D. H. *et al*. (2018) *15th IPPW*, Boulder, CO, June 11–15. [3] Squyres, S., et al., "Visions and Voyages for Planetary Science in the Decade 2013-2022," National Academies Press (2011). [4] Lobbia, M. A. *et al*. (2018) *15th IPPW*, Boulder, CO, June 11–15. [5] Cianciolo, A. D. *et al*. (2018) *15th IPPW*, Boulder, CO, June 11–15. [6] Allen, G. A., Jr., *et al.* (2018) *15th IPPW*, Boulder, CO, June 11–15.

[*]G. A. Allen, Jr. and D. K. Prabhu were supported by NASA Contract NNA15BB15C to AMA, Inc.

EVALUATION OF COMMON PROBE TRAJECTORIES AT MULTIPLE SOLAR SYSTEM DESTINATIONS. A. D. Cianciolo,[1] and G. A. Allen, Jr.[2] [1]NASA Langley Research Center, MS 489 Hampton, VA, 23681 USA (Alicia.m.dwyercianciolo@nasa.gov). [2]AMA, Inc. at NASA Ames Research Center, M/S 230-2, Moffett Field, CA 94035, USA (gary.a.allen@nasa.gov).

Introduction: The common probe study seeks to determine whether a single entry vehicle design is sufficient for atmospheric science exploration at multiple solar system destinations. The motivation of such a design is to reduce mission cost, risk and schedule and allow for higher cadence science investigation specifically at Venus, Jupiter, Saturn, Uranus and Neptune. The study seeks to identify a common aeroshell design, determine the size (volume and diameter) of potential scientific payloads and make recommendations for probe elements that could be manufactured and stored until a mission of use is identified [1]. Therefore, a major contributor to the aeroshell design are the results of trajectory simulations at the various destinations. This presentation outlines the study assumptions that drive probe shape and mass selection. It describes the arrival conditions and aerodynamic and aerothermodynamic model assumptions. Finally, a comparison of atmosphere models for each destination and overall trajectory performance results that determine the feasibility of designing a common probe is provided.

Initial Vehicle Assumptions: The probe is assumed to have a 45 deg sphere cone vehicle, similar to the Pioneer Venus Large probe design, with a diameter of 1.5 m and an entry mass of 400 kg. The nose radius of the vehicle is 0.375 m.

Arrival Conditions: Assuming an Evolved Expendable Launch vehicle (EELV) class, interplanetary trajectories were designed for each destination. Venus considers a direct transit arriving with an inertial velocity near 11.0 km/s entry on May 9, 2025. Jupiter considered a direct transit and arrived with an inertial velocity near 60 km/s in October, 2034. Saturn's arrival in November of 2034 had a velocity of 36 km/s. Likewise, Uranus considers an interplanetary trajectory that uses a Venus-Earth-Earth-Jupiter gravity assist arriving at the planet in May, 2043 with a velocity of 22 km/s and Neptune arrives in August, 2044 with an inertial velocity of nearly 25 km/s. A summary of the interplanetary trajectories and assumptions is provided in [2].

Model Assumptions: The aerodynamic model for the vehicle comes from a database developed for a similar shape deep space microprobe. The aerodynamic model takes into the effect the low density upper altitude regime. However, since the atmosphere constituents are different at each destination, the axial force coefficient is scaled based on respective atmospheres' specific heat.

A stagnation heating model uses the Sutton-Graves [3] constant derived for each destination. However, trades are conducted using Tauber model [4] for the destinations where it is available. A description of the aerothermal design is provided in [5].

The final major trajectory simulation model is the atmosphere. For the destinations that have a Global Reference Atmosphere Model (GRAM), it is used (Venus and Neptune). For the remaining destinations several models are considered and used in concert to generate a reference profile that most accurately represents the destinations atmosphere in the altitude range of interest to the study. The presentation will describe the various atmosphere models and how they are used to support the common probe study.

Trajectory Results: Nominal ballistic trajectories are assumed at all destinations and the concept of operations allows for two hours of flight time at each destination. Trades were performed on entry flight path angle to evaluate trajectories that encounter less than the PV-like 200 Earth g entry decelerations. Trajectories at each destination considered flight path angles that produced decelerations between 50 and 200 g's. The results inform communication system design, identify the regions of the atmosphere to be sampled and provide conditions to assess science instrument options. No dispersion analysis is considered in this study. Trajectory comparisons of flight path angle and stagnation heating and atmosphere models are presented. Finally, a summary of the impact these parameters have on the common probe design and study recommendations are presented.

References: [1] Hwang, H. H. et al. (2018) *15th IPPW*, Boulder, CO, June 11–15. [2] Lobbia, M.A. et al. (2018) *15th IPPW*, Boulder, CO, June 11–15. [3] Sutton, K. and Graves, A. G., Jr. (1971) *NASA TR-R 376*. [4] Tauber, M. E., *et al.* (1999) NASA/TM-1999-208796. [5] Allen, G. A. et al. (2018) *15th IPPW*, Boulder, CO, June 11–15.

Acknowledgements: The authors would like to thank D. K. Prabhu who served as consultant to the project and, along with G. A. Allen, Jr., was supported by NASA Contract NNA15BB15C to Analytical Mechanics Associates (AMA), Inc.

AEROTHERMODYNAMICS FOR DRAGONFLY'S TITAN ENTRY. A. M. Brandis[1], D. A. Saunders[1], G. A. Allen[1] E. C. Stern[2], M. J. Wright[2], D. S. Adams[3] and R. D. Lorenz[3], [1]AMA Inc at NASA Ames Research Center, Moffett Field, 94035, USA: aaron.m.brandis@nasa.gov. [2]NASA Ames Research Center, Moffett Field, 94035, USA. [3]Johns Hopkins Applied Physics Laboratory, Laurel, Maryland, 20723, USA

Introduction: Dragonfly is a proposed spacecraft and mission that would send a mobile robotic rotorcraft lander to Titan, the largest moon of Saturn, in order to study prebiotic chemistry and extraterrestrial habitability at various locations. Titan is unique in having an abundant, complex, and diverse carbon-rich chemistry on the surface of a water-ice-dominated world with an interior water ocean, making it a high-priority target for astrobiology and origin of life studies. The mission was initially proposed in April 2017 to NASA's New Frontiers program by the Johns Hopkins Applied Physics Laboratory. In December 2017, it was selected as one of two finalists (out of twelve proposals) to further refine the mission's concept. NASA Ames Research Center and NASA Langley Research Center are partnering as the leads for the Dragonfly's entry system to provide the completed EDL Assembly.

The aerothermal analysis for Dragonfly utilizes four simulation tools from NASA Ames Research Center. Traj for calculating the trajectory, DPLR 4.04.0 for calculating the flowfield around the vehicle (see Figure 1) and convective heating, NEQAIR V15.0 for calculating the radiative heating, and FIAT for calculating the material response and thermal protection system (TPS) sizing for the heatshield. The entry conditions are relatively benign and can readily be accommodated with a tiled PICA heatshield similar to MSL and a number of flight proven materials for the backshell. This work will demonstrate that the aerothermal entry environments can be readily solved using heritage materials and techniques.

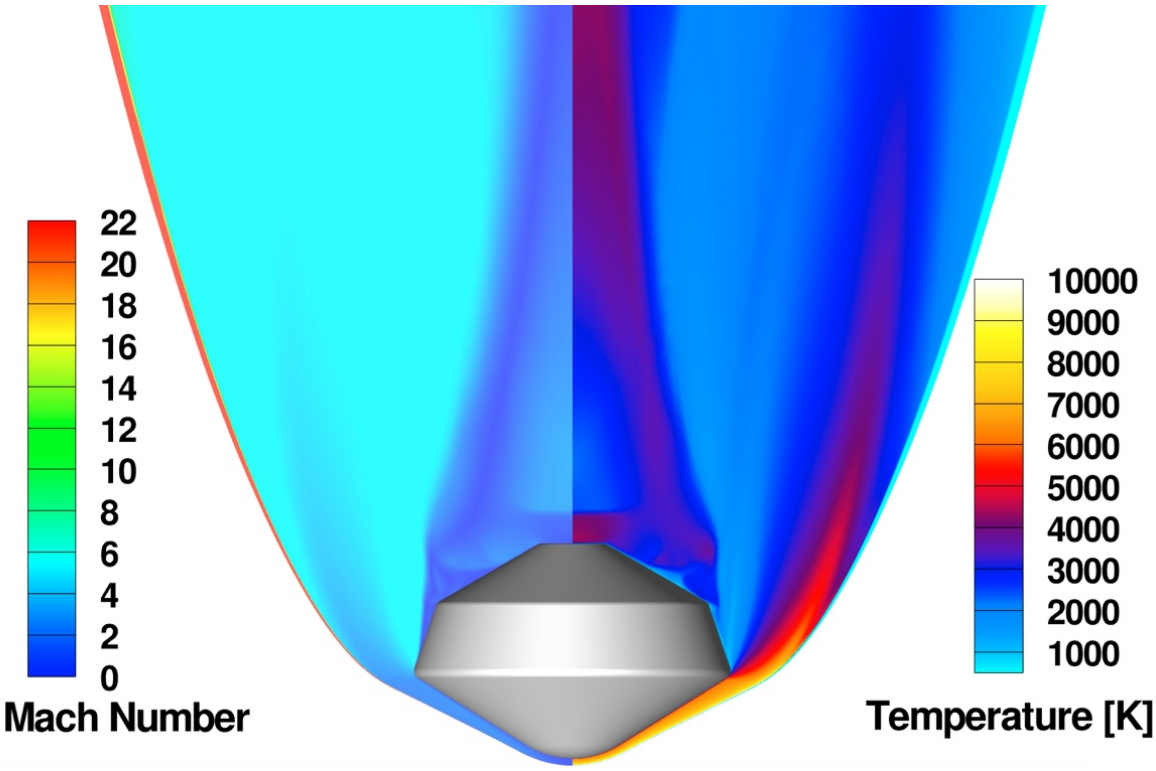

Figure 1 Dragonfly at Peak Heat Flux

STUDY ON EDL SEQUENCE OF MARTIAN PENETRATOR.

T. Kazama[1], K. Yamada[2] and J. Koyanagi[1], [1]Tokyo University of Science (125-8585 Nijuku, Katushika Ward, Tokyo, Japan, 8214028@ed.tus.ac.jp), [2] ISAS/JAXA (252-5210 Yoshinodai, Chuo-ku, Sagamihara City, Kanagawa Prefecture, Japan).

Introduction: A penetrator is one kind of the planetary probes and a stake-shape hard lander which impacts on the planetary surface in order to penetrate into the ground and make meteorological and geological observation under the ground. The penetrator can be embedded under the ground simultaneously with landing and does not require a softlanding system. This feature of penetrator is a significant advantage for the Martian probe, because an EDL system for the Martian missions is very complex and difficult. Planetary missions using the penetrator were planned or launched all over the world in the past. However, all penetrator missions have never succeeded at exploration until now. In Japan, LUNAR-A which is the penetrator to the moon was planned at ISAS[1]. While LUNAR-A project was canceled, its penetrator technology has been developed and has matured to apply it to the actual missions. Recently, some new missions using the heritage of LUNAR-A's penetrator technology is discussed and proposed. Our group are proposing a Martian penetrator mission. To realize the Martian penetrator, the EDL (Entry, De-scent, Landing) technology is necessary. And the penetrator type probe must be suitable for Martian atmosphere. In our concept, a deployable and flexible aeroshell and a cross-type parachute is adopted as EDL technique. In this study, an aerothermal environment during the EDL sequence was estimated by an atmospheric-entry trajectory simulation and EDL systems suitable to Martian penetrator was designed.

Entry and Descent system design: The deployable and flexible aeroshell developed by MAAC group which is collaboration team with many universities and JAXA, has lightweight and good packing efficiency, because it consists of the thin membrane flare and a single inflatable ring[2]. This aeroshell structure is sustained against the aerodynamic load only by single inflatable ring which uses a compressing force. It is essential to design the aeroshell system which can endure in the aerodynamic heating and the aerodynamic load condition during the atmospheric entry. The planetary probe using the deployable aeroshell avoid severe entry aerodynamic heating, because of its low ballistic coefficient due to having light weight and large area aeroshell. The aerodynamic heating environment and aerodynamic load during the atmospheric entry from the orbit around Mars was predicted, and the size of the deployable aeroshell was determined by the restriction which it is carried the LUNAR-A type penetrator to the Martian surface.

Landing system design: The Penetrator has to control its speed and attitude appropriately when it impacts on the ground in order to avoid the fail to penetrate or the breaking of the observation devices. Therefore, at the final phase of EDL sequence, our Martian penetrator system adopted a cross parachute to control the velocity and to stabilize the attitude. The cross parachute is designed based on heritage of Hayabusa's sample return capsule.

EDL sequence of Martian penetrator: We designed the EDL sequence of the Martian penetrator mission, as shown in Fig. 1. In this sequence, the penetrator with the deployable aeroshell enters Martian atmosphere, and this aeroshell is jettisoned after the probe reach the subsonic region. Simultaneously with the aeroshell jettison, the cross parachute is deployed using the aeroshell as drawing devices and the probe penetrates the Martian ground.

In this future, we will refine the EDL sequence to predict accurately aerodynamic heating by CFD simulation and measure the performance of the cross parachute at the low-density environment by the wind tunnel test.

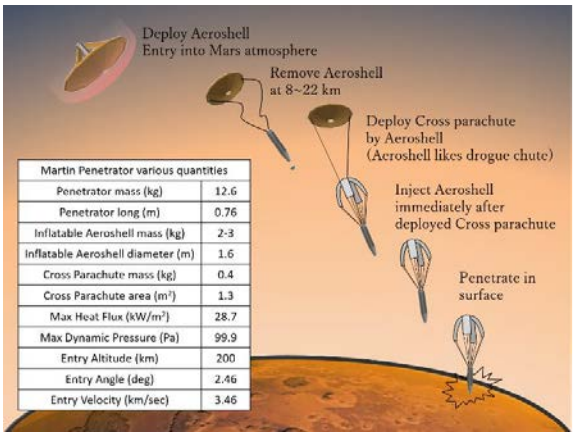

Fig. 1 EDL sequence of the Martian Penetrator mission

References: [1] T. Nakajima, M. Hinada, H. Mizutani, H. Saitoh, J. Kawaguchi and A. Fujimura (1996) LUNAR PENETRATOR PROGRAM:LUNAR-A, Acta Astronomica Vol. 39.

[2] K. Yamada, T. Abe, K. Suzuki, O. Imamura, D. Akita, Y. Nagata, Y. Takahashi and MAAC research and development group (2015) Development of Flare-type Inflatable Membrane Aeroshell for Reentry Demonstration from LEO, AIAA 2167

MISSION DESIGN OPTIMIZATION FOR CONSECUTIVE AEROCAPTURE-ENTRY SYSTEMS AT MARS. E. J. Zinner[1] and Z. R. Putnam[1], [1] University of Illinois at Urbana-Champaign

One of the limiting factors in sending large payloads to the surface of Mars is our ability to decelerate them when they arrive. This shortcoming is particularly important for a future human mission to Mars, where NASA has estimated it will need to land 40-100 metric tons on the surface. Many of the proposed methods for landing significantly more massive payloads include doing an aerocapture maneuver to dissipate energy prior to EDL. In an aerocapture, the vehicle will fly through the upper atmosphere of the planet to deplete enough energy to enter an elliptic orbit from the initial hyperbolic orbit. Following aerocapture, the vehicle must execute a propulsive maneuver to raise periapsis above the Martian atmosphere. After a deorbit maneuver, entry, descent, and landing would occur, but with a much slower entry velocity compared with a direct entry from the hyperbolic approach trajectory. This aerocapture-entry strategy provides operational flexibility and improves safety for crewed missions.

This study seeks to understand the relative benefits of how much energy is dissipated in the aerocapture compared to how much will be dissipated during the entry, descent, and landing phase to produce an optimal mission and vehicle design with respect to design parameters of interest. The goal of the optimization is to maximize payload mass by minimizing TPS mass and propellant required. Thermal protection system mass is a strong function of the heating profile, particularly total heat load and maximum heat flux. These heating properties as well as the trajectory that ensues from the aerocapture are estimated using an in-house trajectory simulation. Thermal protection system mass is estimated using NASA's Fully Implicit Ablation and Thermal Analysis Program (FIAT). The amount of energy dissipated during aerocapture is largely a function of the minimum altitude where deceleration occurs. For this analysis, the minimum altitude is only a function of initial flight path angle and velocity. For a flight system, the energy dissipation can be varied by rotating the lift vector and spending more or less time in the atmosphere. There are two propulsive maneuvers that must also be considered: raising periapsis and an entry burn. Both of these maneuvers require less delta-V for a more eccentric parking orbit.

In addition, the relative merits of performing a propulsive maneuver to raise the periapsis after the aerocapture pass or proceeding directly to entry, descent, and landing less than one orbital period after aerocapture are assessed. Following aerocapture, the outer layers of the heat shield will be very hot. Spending more time in orbit around Mars allows more time for the heat to radiate to space and provides operational flexibility. However, this approach also allows more time for the very hot outer layers of the heat shield to conduct inward toward the vehicle.

Multiple vehicle geometries are considered: a nonlifting sphere cone, a lifting sphere cone, and a medium lift-to-drag ratio aeroshell. Approach velocities ranging from 5.5 to 8.0 km/s are considered. For each hyperbolic approach velocity, initial flight-path angles are chosen to enable the vehicle to aerocapture into a specific parking orbit. For estimating the mass from the propulsive maneuvers, a liquid oxygen/methane engine is assumed along with a specific impulse of 340 s. Limited by FIAT's material database, LI 2200, reinforced carbon-carbon, and a fiction material TACOT are examined as TPS materials.

Investigation of DPG Properties as a Material in a Self-Healing Thermal Protection System. N. L. Skolnik[1] and Z. R. Putnam[1], [1]University of Illinois at Urbana-Champaign.

Thermal protection systems are mission-critical for all atmospheric entry missions. Over the course of the first 33 Space Shuttle missions (1981-1989), the number of thermal protection system tiles requiring replacement due to damage from debris ranged from 53 to 707 per flight (with a mean of 179) out of 25,000 tiles. The amount of debris in Earth orbit has only increased since 1989. Integrating a self-healing mechanism into the thermal protection system may mitigate the effect of damage from orbital debris.

Previous work has investigated the depth at which a self-healing mechanism should be placed in order to reduce system mass and complexity. This location is called the critical depth. Using hollow channels built into the Thermal Protection System at this critical depth will allow the healing fluid to be transported to the damage site when the TPS is damaged and the channels are broken in that location.

This work investigates a candidate material for the healing fluid in the channels, DPG, for a vascular self-healing thermal protection system. DPG is composed of silicone vacuum pump oil, borate glass, and silicon carbide particles. This material combination was selected based on testing performed during the Space Shuttle Return to Flight activities after the Columbia accident. The material was not down selected for further testing, but initial literature review has found this material to meet key criteria for use in a space environment.

The mass ratios of the constituents are varied and tested to see which combination has the best vacuum, thermal, and viscous properties. These will indicate the types of missions that this material is suitable for.

Vacuum properties are important because the material tested on the ground needs to withstand a space environment. If the material outgasses and changes in any way, the system will not work as designed. Outgassing will be measured using the ASTM E595 method. This method uses a vacuum oven to determine the mass loss of the material. The mass of the DPG will be measured before and after 24 hours in the vacuum oven, and the percent mass loss will be recorded.

Thermal properties are the important because the material with have to withstand the same entry environment as the TPS it is used with. Thermal properties will be measured using a Thermogravimetric Analysis machine. A small sample of the DPG is placed in a crucible and the temperature is raised to 1000°C. The mass of the crucible and material are measured and the mass loss recorded. A higher char yield, or the resulting mass after the test is run, is desirable for entry conditions.

Finally, the viscosity will be measured using a viscometer. The viscosity of the material is important as the self-healing material needs to be transported to the site of the damage so that it can heal the TPS in the appropriate location. The material needs to be fluid enough to be transported, but thick enough to not wick away into the bulk TPS material and create clogs in the transport channels.

Results from this investigation will provide insight into the suitability of the candidate material for vascular self-healing systems for thermal protection systems.

FAST DESIGN TECHNIQUE FOR CONCEPTUAL HYPERSONIC ENTRY VEHICLE. K. Bonnet[1] and R. D. Braun[2], [1]University of Colorado Boulder (kevin.bonnet@colorado.edu), [2]University of Colorado Boulder (bobby.braun@colorado.edu)

Introduction: During the conceptual design of hypersonic entry vehicle, optimal trajectories are selected and used to determine a set of vehicle parameters, such as ballistic coefficient or L/D. As these trajectories are often flown with a non-constant angle of attack, the vehicle parameters may be varying over time. Therefore, an iterative process is usually performed until the vehicle shape yields the aerodynamic performance required by the trajectory. To support trade studies, several hypersonic entry trajectories are generally considered, each requiring a long computational process to find the corresponding vehicle shape. The ability to quickly identify families of vehicle shapes that satisfy a given trajectory reveals to be essential.

This investigation focuses on the development of a technique to rapidly determine sets of vehicle geometries from a given entry trajectory. Typically, the trajectory is given in terms of altitude and velocity time histories. The planar equations of motion for atmospheric reentry can be rearranged to obtain expressions for aerodynamic parameters, that are evaluated numerically from the trajectory time history. Besides, analitycal expressions of aerodynamic coefficients can be derived from Newtonian flow theory. These expressions explicitly depend on vehicle shape parameters and can then be inverted to determine the corresponding vehicle geometry. Finally, for a given entry mass or vehicle length (diameter for the most common entry vehicles) and a desired vehicle general shape (e.g. cone, sphere-cone), constraints can be established on the vehicle design space solely based on trajectory information. This design space can be further reduced by applying common constraints such as maximum heat rate and g-loading, which can be easily applied using the information computed above.

This process can be extended to include the lateral components of the trajectory. In this case, this approach also yields useful information beyond the vehicle shape. During the process described above, lift and drag time histories can be estimated. Control laws can then be derived from these. For instance, considering a guided entry using bank-angle steering for a fixed vehicle shape flying at constant angle of attack, a corresponding bank-angle time history can be estimated.

Results: The method presented above was applied to some test cases. The trajectories were generated using the equations of motion given in [1]. For simple trajectories, with constant vehicle parameters and constant bank angle, this method yields very good results, in a short amount of time.

References: [1] Vinh N.X., Busemann A. and Culp R. D. (1980) *Hypersonic and Planetary Entry Flight Mechanics,* 2nd edition, University of Michigan Press.

DRAG-MODULATION AEROCAPTURE ON MARS: INDEPENDENT CAPABILITY INSERTION FOR SMALL SATELLITES. G. Falcone[1], J. W. Williams[2] and Z. R. Putnam[3], [1]University of Illinois at Urbana-Champaign (Gfalcon2@illinois.edu), [2]University of Illinois at Urbana-Champaign (Jamesw3@illinois.edu), [3]University of Illinois at Urbana-Champaign (Zputnam@illinois.edu).

Introduction:

Current and proposed space mission plans show an increasing interest in the exploration of Mars and its system. This increased interest, along with recent improvements in small satellite capabilities, represents a boon in the number of rideshare opportunities for small satellites to Mars. However, with current propulsion technologies, small satellites are constrained near the target orbit of their host orbiters. Nonetheless, small satellites have proved their ability to enhance scientific, reliable, low-cost missions thanks to the technological improvements in the instrumentations of the last decade. An independent insertion capability for small satellites would remove the orbital insertion constraint on rideshare missions, extending the reachable orbits through the variation of semimajor axis, eccentricity or inclination. The proposed methodology to enable independent insertion of small satellites is the drag-modulation aerocapture maneuver. This maneuver exploits a single pass through the atmosphere of the target body, by changing only the drag area during flight, to affect the same delta-V with minimal propellant requirements.

A previous study proved the feasibility of the maneuver for a fixed scenario: a flyby of Phobos with malleability in the arrival state. It also has presented results regarding the independence of the reached orbit inclination with respect to the main orbiter inclination if a small maneuver is performed in the first phase of the Earth-Mars transfer[1].

The current study focuses on four baseline missions. The analysis shows the relevant advantages in the propellant mass budget and in the simplicity of the drag-modulation aerocapture maneuver proving that the investigated maneuver would be successful in a variety of different scenarios equally scientifically interesting. The baseline missions consist in the investigation of Phobos and Deimos, the two moons of Mars, through the use of flyby/rendezvous parking orbit, polar mapping in a low parking orbit of Mars and Areosynchronous equatorial orbit of Mars. The scenarios differ from each other mainly in their semimajor axis; the conducted study proved that the aerocapture maneuver could successfully reach a range of target orbits of different altitudes, with a substantial savings in mass compared to a propulsive method.

Analyses include assessment of the sensitivity of the entry corridor size to the altitude of the four target orbits which will be extended to an analysis for a continuous variation in altitude and eccentricity of reachable orbits post-maneuver. Studies show variation in the entry corridor with respect to the ballistic coefficient ratio, which represents a design parameter defined by the area pre- and post- aerocapture maneuver. Furthermore, statistical results regarding the effectiveness of real-time aerocapture guidance and control algorithms through an extensive Monte Carlo simulations analysis for all the four scenarios are presented. The Monte Carlo simulation analysis indicates a small error in the reached apoapsis post-maneuver due to the density uncertainties. To compensate for this small inaccuracy, a planned post-aerocapture propulsive maneuver is required. This propulsive maneuver has been designed to minimize the overall propellant mass budget. Furthermore, analyses include the evaluation of acceleration peak, maximum heat load and maximum heat rate for several initial velocities. A comprehensive study has also been performed regarding acceleration, heat load and heat rate per the two boundaries paths, and the center path of the aerocapture maneuver's corridor. Finally, results regarding the savings of propellant mass in the four baseline missions are specified.

References:

[1] Falcone, G., Williams, J. and Putnam, Z.R., *Small Satellite Drag-Modulation Aerocapture Mission Design Options for Mars Small Satellites*, AAS Guidance and Control Conference, Breckenridge, CO, Feb. 2-7, 2018.

AEROTHERMAL DESIGN OF A COMMON PROBE FOR MULTIPLE PLANETARY DESTINATIONS.

G. A. Allen, Jr.,[1*] F. S. Milos,[2] T. R. White,[2] and D. K. Prabhu.[1*] [1]AMA, Inc. at NASA Ames Research Center, M/S 230-2, Moffett Field, CA 94035, USA (gary.a.allen@nasa.gov), [2]NASA NASA Ames Research Center, Moffett Field, CA, USA.

Introduction: The idea of a single design of a capsule, for atmospheric entry at Venus, Jupiter, Saturn, Uranus, and Neptune and delivery of payloads for *in situ* scientific experiments, is currently being pursued by a team of scientists and engineers drawn from four NASA centers – Ames, Langley, JPL, and Goddard [1].

For notional suites of instruments [2] (the selection depending on the destination), interplanetary trajectories have been developed by team members at JPL and Goddard [3]. Using the entry states provided by these trajectories, 3DOF atmospheric flight trajectories have been developed by Langley [4] and Ames [5]. The range of entry flight path angles for each destination is chosen such that the deceleration load lies between 50 g (shallow) and 150-200 g (steep) for a 1.5 m (diameter) rigid aeroshell based on a 45° sphere-cone geometry (Fig. 1) and an entry mass of 400 kg.

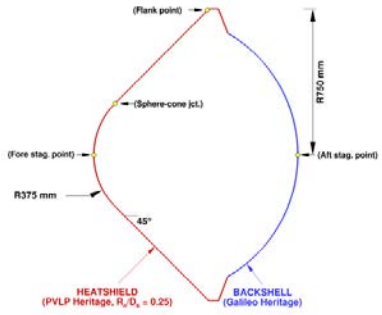

Figure 1. Reference geometry for the Common Probe. The backshell shape is notional.

Given the ambient densities and velocities along each of the flight trajectories from the 3DOF analyses, the aerothermal environments are estimated using standard correlations – Sutton-Graves [6] for convective heating, and Tauber [7] for radiative heating. The thermal protection materials are then sized using *FIAT* [8] together for several candidate materials for the heatshield and backshell: (i) fully-dense carbon phenolic (used on the Pioneer-Venus & Galileo probes); (ii) a dual-layer woven material called HEEET (new NASA technology); (iii) PICA (used on the Stardust probe); and (iv) appropriate backshell material(s).

Proposed Paper/Presentation: The presentation will focus on: (a) definition of aerothermal environments and associated uncertainties at – (i) the stagnation point, (ii) a point on the conical flank, and (iii) a point on the backshell for the various flight trajectories; (b) candidate materials and uncertainties in materials properties; and (c) margining policy. Margined TPS thicknesses that result from the analysis will be presented, along with the sensitivity of those thicknesses to: (i) the initial soak temperature, (ii) the maximum bondline temperature, and (iii) choice of structural material. Choosing the largest fully-margined thickness as the basis for the design of the TPS of the Common Probe, the design will be evaluated at all destinations to determine the degree of sub-optimality in the design.

As an example, results of zero-margin TPS mass estimates for fully-dense carbon-phenolic (FDCP) are presented in Table 1, along with mass estimates for HEEET for Venus (other destinations are still being analyzed). The sizing computations assume an aluminum structure to which the TPS is bonded.

Table 1. Results for zero-margin sizing of FDCP (all destinations), and HEEET for the case of Venus only.

Planet	V_E km.s^{-1}	γ_E deg	Dec. g	m_{TPS} kg	Mat.
Venus	10.93	-9	53	59.0	FDCP
				27.3	*HEEET*
		-16.8	135	39.0	FDCP
				18.3	*HEEET*
Jupiter	59.68	-4.1	73	165.6	FDCP
		-6.5	206	108.6	
Saturn	35.66	-11.9	51	102.4	FDCP
		-25.0	168	61.2	
Uranus	22.34	-16.5	51	101.5	FDCP
		35.0	205	54.9	
Neptune	24.73	-16.0	52	88.5	FDCP
		-23.0	177	57.0	

References:

[1] Hwang, H. H., *et al*. (2018) *15th IPPW*, Boulder, CO, June 11–15. [2] Atkinson, D. H., *et al*. (2018) *15th IPPW*, Boulder, CO, June 11–15. [3] Lobbia, M. A., *et al*. (2018) *15th IPPW*, Boulder, CO, June 11–15. [4] Dwyer-Cianciolo, A. *et al*. (2018) *15th IPPW*, Boulder, CO, June 11–15. [5] Allen, G. A., Jr., *et al.* (2005) NASA/TM-2005-212847. [6] Sutton, K. and Graves, A. G., Jr. (1971) *NASA TR-R 376*. [7] Tauber, M. E., *et al.* (1999) NASA/TM-1999-208796. [8] Milos, F. S. and Chen, Y.-K. (2013) *J. Spacecraft and Rockets,* **50**(1), pp.137-149.

* G. A. Allen, Jr. and D. K. Prabhu were supported by NASA Contract NNA15BB15C to AMA, Inc.

REDUCED LIFT-TO-DRAG VEHICLE CONCEPTS FOR NEPTUNE AEROCAPTURE. C. Heidrich[1] and S. Dutta[2], [1]University of Colorado Boulder, CCAR 431 UCB, Boulder, CO 80309, USA, [2]NASA Langley Research Center, Hampton, VA 23681, USA.

Introduction: Aerocapture has been covered extensively in literature for science objectives at Neptune. Compared to fully impulsive strategies, aerocapture drastically increases delivered payload mass to orbit. [1] The aerocapture maneuver consists of a single pass through the target planet's upper atmosphere to reduce kinetic energy through aerodynamic forces. Upon atmospheric exit, the vehicle flies a Keplerian orbit to apoapsis where a propulsive circularization burn is performed. However, aerocapture requires active guidance during the atmospheric phase of the flight and often requires large control margin that cannot be provided by typical entry vehicles with low lift-to-drag ratios. The goal of this study is to apply modern predictor-corrector guidance algorithms to enable the use of low lift-to-drag vehicle concepts for aerocapture at Neptune.

Baseline concept. The baseline of comparison in this research is a mission concept from a multi-center NASA study of Neptune aerocapture by Lockwood [2]. An inertial entry interface velocity of 29 km/s and flight-path angle of -12.818 deg are assumed. The post-aerocapture target is a high-energy science orbit with apoapsis and periapsis of 430,000 km and 3,986 km, respectively, designed to enable Triton fly-bys. The baseline vehicle concept is a flat-bottom ellipsled aeroshell with a mass of 2200 kg and ballistic coefficient of 896 kg/m^2.

The severe entry environment at Neptune is characterized by large aeroheating and g-loads due to high entry velocities. The Lockwood study indicated a moderately high L/D of 0.8 was necessary to achieve capture while satisfying aeroheating and g-load constraints. However, this study used classical guidance strategies based on pre-computed drag-altitude rate error feedback.

Modern aerocapture guidance. In recent years, numerical predictor-corrector algorithms have gained traction for real-time trajectory control. These strategies are robust to large trajectory dispersions and need not adhere to a pre-computed trajectory. Advances in on-board computational power have enabled a new generation of guidance strategies for robust and accurate in-flight trajectory control.

This study utilizes an optimal predictor-corrector algorithm called Fully Numerical Predictor-corrector Aerocapture Guidance (FNPAG) to study reduced L/D aerocapture concepts at Neptune. FNPAG takes advantage of optimal control theory results to minimize the post-aerocapture apoapsis error or circularization delta-V. [3] The algorithm utilizes a bank-to-steer prediction method. For each guidance cycle, the method applies a planning strategy where the remaining trajectory is simulated, and a corrector scheme computes the necessary bank-angle to achieve targeting conditions. Previous studies showed promising results for precision aerocapture at Mars using FNPAG. [4] Application of FNPAG to the severe entry environment at Neptune will further its potential for use in modern aerocapture guidance strategies.

Reduced-lift aerocapture concepts. Previous feasibility studies showed aerocapture at Neptune is possible with moderately high L/D. However, reducing L/D requirements greatly improves vehicle outer mold line (OML) options and increases usable delivered mass to orbit. This research applies modern guidance strategies to reduced L/D vehicles for Neptune aerocapture. First, an open-loop study is performed to determine the L/D range required to achieve capture. Then, FNPAG is applied within this range to determine the reliability of the guidance algorithm with reduced control authority. The performance of FNPAG is tested using Monte-Carlo dispersion strategies. Trajectory simulation is performed using POST2, a high-fidelity atmospheric flight simulation tool.

Acknowledgements: The authors extend their gratitude to Dr. P. Lu for his work developing FNPAG.

References: [1] Wercinski P. F. (2002) AIAA 4812. [2] Lockwood, M. K. (2004) AIAA, p. 4951. [3] Lu P. (2015) *JGCD*, 38, p. 553-565. [4] Webb K. (2017) AIAA, p. 1900.

SINGLE-STAGE DRAG MODULATION GNC FOR VENUS AEROCAPTURE DEMONSTRATION

E. Roelke[1], M. S. Werner[2], and R. D. Braun[3], University of Colorado Boulder, Department of Aerospace Engineering. 2598 Colorado Ave, Boulder, CO 80309
[1] Evan.Roelke@colorado.edu, [2] Michael.Werner@colorado.edu, [3] Bobby.Braun@colorado.edu

Introduction: Aeroassist technology is currently limited by payload mass, requires an initial orbital insertion maneuver, increases the duration of time until a nominal science orbit is attained, and typically includes minimal, if any, control authority for guidance and targeting concerns. One such improvement to modern aeroassist methods is aerocapture; this maneuver involves a single pass through the upper atmosphere of a planetary body to capture into orbit about the body, saving time and resources. Aerocapture has been shown to provide significant mass savings to all bodies within the solar system, primarily the outer solar system bodies [1].

The primary concern with aerocapture is the final orbit dependence on the entry state vector, which itself is very mission-dependent and sometimes inflexible. Introducing control authority into an aerocapture maneuver would allow the system to theoretically target a specific nominal orbit given uncertainties in the entry state vector and atmosphere, among other system uncertainties.

The chief control methods for aerocapture can be divided into discrete-event and continuous aerodynamic modulation, as modulation of both lift and/or drag forces are feasible [2]. The latter typically allows for more control authority throughout the trajectory, but demands a more complex and robust system architecture as well as GNC algorithms. Drag-modulated aerocapture systems derive their control authority from changes in the vehicle ballistic coefficient via drag area or mass changes mid-flight [2].

This investigation focuses on the GNC methodology for single, discrete event drag modulation aerocapture systems, mainly by assessing the architecture for an aerocapture demonstration at Venus. This action is performed through a single stage drag skirt jettison maneuver to raise the vehicle ballistic coefficient via mass and drag area reductions. This action can be performed manually through some parameter trigger or automatically. A numerical predictor-corrector algorithm has been developed to simulate real-time guidance and adjust the jettison time to minimize the final error for a target orbit apoapsis [2]. The predictor models the vehicle as a point mass with constant drag and the planetary body as a sphere with inverse-square gravity with J2 perturbations and nominal atmospheric table in order to account for day-of-flight uncertainties.

This guidance algorithm requires the vehicle's flight path to be bounded by a flight path angle corridor, which can be computed with the bisection method for a given entry vehicle geometry, entry state, and planetary body atmosphere.

This research seeks to quantify the trends between this flight path angle corridor and relevant aerocapture parameters such as entry velocity, target apoapsis, and ballistic coefficient ratio. In addition, this investigation is interested in quantifying the amount of control needed to target a nominal orbit apoapsis for a given entry state and orbit tolerance as a function of the ratio of ballistic coefficients before and after the jettison event for a smallsat-scale vehicle entering at Venus. Since aerocapture has never had a flight demonstration, this investigation is interested in understanding the minimum required ballistic coefficient ratio to successfully target a given orbit apoapsis, within a reasonable tolerance, to provide a lower bound on the feasibility of this specific system. The analysis will include Monte Carlo analyses to include dispersion analysis from uncertainty in the entry state vector, Venusian atmosphere, and vehicle aerodynamics. Similarly, a reasonable upper bound on the ballistic coefficient ratio can be determined to develop a range of control authorities within which such a system might operate, and the resultant system complexity/orbital targeting accuracy in each case. Dispersion analyses can then be performed on the tradespace bounded by these control requirements to identify candidate trajectory and control authority necessities.

References:

[1] Hall, J. L., Noca, M. A., & Bailey, R. W. (2005). Cost – Benefit Analysis of the Aerocapture Mission Set, *42*(2).

[2] Putnam, Z. R., & Braun, R. D. (2014). Drag-Modulation Flight-Control System Options for Planetary Aerocapture. *Journal of Spacecraft and Rockets*, *51*(1), 139–150.

Sustaining Phenolic Impregnated Carbon Ablator (PICA) TPS for Future NASA Needs

Ethiraj Venkatapathy[1], Don Ellerby[1], Matt Gasch[1], Frank Milos[1], Keith Peterson[1], Dinesh Prabhu[2], Kristina Skokova[2] Mairead Stackpoole[1] and S. Violette[3]

[1]NASA Ames Research Center, Moffett Field, CA 94035,
[2]AMA Inc, NASA Ames Research Center, Moffett Field, CA 94035,
[3]Fiber Materials Inc, Biddeford, ME 04005.

Phenolic Impregnated Carbon Ablator (PICA), invented in the mid 1990's, is a low-density ablative thermal protection material proven capable of meeting sample return mission needs from the moon, asteroids, comets and other destinations as well as for Mars (Stardust, OSIRIS REx, MSL and Mars 2020) [1, 2]. Its low density and efficient performance characteristics have proven effective for use from Discovery to Flagship class missions. It is important that NASA maintain this TPS material capability and ensure its availability for future NASA use. The rayon-based carbon precursor raw material used in PICA preform manufacturing requires immediate replacement.

Requalification has been required at least twice in the past 25 years and a third substitution is now needed as the vendors that have manufactured the rayon has discontinued the production of it. The past vendors that provided the rayon has been foreign suppliers.

The carbon precursor replacement challenge is twofold – the first involves finding a long-term replacement for the current rayon, preferably domestic source, and the second is to assess its future availability periodically to ensure it is sustainable and be alerted if additional replacement efforts need to be initiated.

Rayon is no longer a viable process in the US and Europe due to environmental concerns. In the early 80's rayon producers began investigating a new method of producing a cellulosic fiber through a more environmentally responsible process.

This cellulosic fiber, Lyocell, is a viable replacement precursor for PICA fiberform. From preliminary results Lyocell PICA is likely a "drop in" replacement for future NASA mission needs. Since Lyocell is manufactured in the US in very large quantities and the need is in the commercial sector, Lyocell based PICA could be a sustainable source for future mission needs.

This presentation reviews current SMD-PSD funded PICA sustainability activities in ensuring a rayon replacement for the long term is identified and in establishing that the capability of the new PICA derived from an alternative precursor is in family with previous versions of the so called "heritage" PICA.

References:

[1] Tran, H.K., "Phenolic Impregnated Carbon Ablators (PICA) for Discovery Class Missions", *AIAA Paper 96-1911*, June 1996.
[2] Wilcockson, W., "Stardust Sample Return Capsule design experience", 7th AIAA/ASME Joint Thermophysics and Heat Transfer Conference, *AIAA paper # 2854*, 1998.

'More honoured in the breach?' – Test as You Fly Environments for Planetary In-Situ Missions.

Ralph D. Lorenz[1] [1]Johns Hopkins Applied Physics Laboratory, Laurel, MD 20723, USA. (Ralph.Lorenz@jhuapl.edu).

Introduction: More so than the vacuum of space familiar to satellite designers and operators, the atmospheric environments experienced in planetary exploration are often difficult to completely replicate. However, as many successful missions attest, careful design of the test conditions can affordably achieve the desired test objective, to simulate the relevant phenomena with sufficient fidelity to predict performance at another world. While being a laudable guideline, strict "Test as you fly" is, as Shakespeare put it in Hamlet, 'A custom more honoured in the breach than in the observance'. This paper reviews the testing philosophy of previous missions with a view to indicating what is 'close enough'. The relatively few instances where in-flight performance has deviated from what was anticipated from test are also considered.

Philosophy: To completely reproduce conditions on another planet requires first that those conditions be known, which is not always the case. Further, while individual aspects of an environment (e.g. pressure/temperature, or gravity) can be simulated in practicable test arrangements, it would be absurdly expensive, if not physically impossible, to achieve them all simultaneously. All one can reasonably do, and indeed all that has ever been done in 50 years of planetary exploration, is to attempt to match the performance of concern. This practice is well-established in aerodynamics, where scale model tests are used with confidence as long as the key parameters (Mach and Reynolds numbers) are achieved.

Examples: The historical record suggests that complete replication is rarely if ever achieved, but tests that attempt to match the controlling parameters are good enough. For example, while the 'warm' thermal balance tests of the Viking lander – a Flagship mission - used 2.5 mbar CO_2, a 'cold' test (20 mbar) had to use Argon to avoid freezing CO_2 out on the test chamber walls [1]. No wind was simulated in these chamber tests : a higher gas pressure was used to achieve the correspondingly higher heat transfer (and a separate test was made in a conventional 1-bar wind tunnel to evaluate cooling of the RTG). Testing of Mars Pathfinder and the Mars Exploration Rovers have similarly used nitrogen atmospheres (with occasional exceptions).

A similar test environment approach was adopted for the Huygens probe [2] – a 600 mbar atmosphere in Earth gravity was considered to give the same heat transfer conditions as the expected 1500 mbar atmosphere with Titan gravity. Pure nitrogen was used, the few per cent of methane having a minimal effect on transport properties such as viscosity. (Note that generally only the bulk atmospheric constituent is used, Argon and Nitrogen being ignored in Mars tests.)

Another example is Pioneer Venus (another Flagship!) : whereas individual units were tested to the 425g qualification level for entry deceleration, the centrifuge used for probe testing could not achieve this, and so a 160g test was performed, but with the units ballasted with extra mass to give the corresponding structural loading.

One exception where the environment was relatively faithfully reproduced (cold carbon dioxide, including a fan to generate a 10 m/s wind) was the Beagle 2 lander [4]. This rigorous testing did not prevent loss of the mission, sadly.

Surprises: One example where flight results diverged appreciably from design/test expectations is the temperature evolution inside the Galileo Probe. Here, temperatures rose rather faster than predicted, such that many instruments operated outside the range in which they had been originally calibrated. The suspected cause is that internal convective heat transfer was stronger than predicted, either due to the spin of the probe, or by circulation in the vehicle induced by the dynamic pressure of descent causing inflow past (not airtight) closeout boot seals[3]. The deviation of flight from test was not a result of the (practical) choice of helium instead of Jupiter's hydrogen-helium mix, nor the failure to simulate Jovian gravity, but the purely static nature of the test. The impact of this deviation from prediction was modest - a significant post-flight recalibration effort was required for some instruments (but not all – the Helium Abundance Detector remained within limits due to better heatsinking and insulation.) Clearly, the lesson is to maintain healthy margins against phenomena that are impossible/impractical to reproduce, and against those one hasn't thought of.

Conclusions: Even Flagship-class missions in the past have deviated from strict "Test as you fly". Care is needed in formulating test conditions, but it is clear that the accepted practice is to employ conditions that are both practicable and adequately faithful.

[1] Buna, T., et al. (1973), NASA SP-336. [2] Klein, J. and Jäkel, E.K.J. (1997) ESA SP-408, 57-65. [3] Mischel, B. et al. (1997) AIAA-97-2456. [4] Shaughnessy, B. (2004) Proc. I. Mech. E. 218, C14403

EXOMARS SCHIAPARELLI FLIGHT TRAJECTORY AND ATMOSPHERIC RECONSTRUCTION.

B. Van Hove[1], Ö. Karatekin[1], F. Ferri[2], A. Aboudan[2], G. Colombatti[2], T. Schleutker[3], A. Gülhan[3]
[1]Royal Observatory of Belgium (ROB), Ringlaan 3, 1180 Brussels, Belgium, bartvh@observatory.be, [2]Università degli Studi di Padova, Centro di Ateneo di Studi e Attività Spaziali 'Giuseppe Colombo' (CISAS), Italy, [3]Supersonic and Hypersonic Technology Department of the Institute of Aerodynamics and Flow Technology, German Aerospace Research Center (DLR), Cologne, Germany.

Mission: On 19 October 2016, the ExoMars entry, descent, and landing (EDL) demonstrator module (EDM) or Schiaparelli arrived at Mars. In the ESA-Roscosmos ExoMars mission, Schiaparelli was intended to demonstrate European EDL capability on Mars [1]. The hypersonic entry of Schiaparelli into the Mars atmosphere was successful, and was followed by the deployment of a supersonic parachute. At this point a navigation error occurred, which later resulted in loss of radio contact and Schiaparelli's crash. While the mission was not successful, fortunately essential flight data were transmitted in real-time. The data record beguins before atmospheric entry and stops after parachute deployment. No data were received during radio blackout, corresponding to altitudes between about 70 and 30 km. Schiaparelli was equipped with an inertial measurement unit, which contains accelerometers and gyroscopes, as well as more novel heat shield pressure and temperature instrumentation. The pressure data are valuable to check aerodynamic models, but also for atmospheric reconstruction.

Flight instrumentation: Schiaparelli was equipped with onboard guidance, navigation and control (GNC) software that processed inertial rate data recorded by a Miniaturized Inertial Measurement Unit (MIMU), which contained 3 gyroscopes and 3 accelerometers. The GNC software also used data from two sun sensors (SDS) located on the back cover to estimate attitude before atmospheric entry, and ranging measurements from a downfacing radar Doppler altimeter (RDA) activated after front shield release. In addition to these flight sensors essential to mission success, Schiaparelli was further equipped with an instrumented heat shield. Aerothermal sensors (surface pressures and temperatures at multiple depths) were embedded within the thermal protection system (TPS) material of both the frontal heat shield and back cover. The frontal heat shield included 4 pressure sensors and 7 thermal plugs. The front heat shield pressure sensors are referred to as a Flush Air Data System (FADS), which measured the surface pressure on the heat shield along the trajectory. The received pressure data have a reduced sampling frequency of 1 Hz compared to 10 Hz for a successful landing.

Reconstruction: By combining the FADS pressure data with CFD forebody pressure models, validated in wind tunnel experiments, the atmospheric density and vehicle attitude are reconstructed [2]. FADS estimates are compared to GNC navigation that is based on the sun sensors and MIMU data. We attempt to correct the GNC navigation estimates for errors in the initial state before entry and the MIMU gyroscope measurements after parachute deployment. The consolidated ExoMars Schiaparelli trajectory is compared to the accurately known locations on Mars of the impact site, parachute, and heat shield. We compare atmospheric conditions reconstructed from flight data with atmospheric models and remote observations.

References: [1] Blancquaert T. (2017) *Space Sci. Rev.* ExoMars 2016 special issue, [2] Van Hove B. & Karatekin Ö. (2017) *J. of Spacecraft and Rockets*.

Placeholder for Orion Aerodynamics and EFT-1 Flight Experience and Lessons Learned

Abstract will be received shortly, but this should be treated as an invited talk from the Orion program.

Please direct all immediately questions to Ashley Korzun (Ashley.m.korzun@nasa.gov).

OVERVIEW OF THE FIRST TWO FLIGHTS OF THE ASPIRE SUPERSONIC PARACHUTE TEST PROGRAM.

B. S. Sonneveldt[1], C. O'Farrell[1], and I. G. Clark[1]
[1]Jet Propulsion Laboratory, California Institute of Technology, 4800 Oak Grove Drive, Mail Stop 321-220, Pasadena, CA 91109, ofarrell@jpl.nasa.gov

Abstract: The Advanced Supersonic Parachute Inflation Research Experiments (ASPIRE) test program has developed an infrastructure for the testing of parachute inflation at supersonic test conditions and dynamic pressures analogous to those encountered during Martian EDL sequence [1]. The initial series of ASPIRE flights were designed as a risk-reduction activity for NASA's upcoming Mars 2020 project and will test two candidate 21.5-m Disk-Gap-Band parachute designs for this mission [2]. This presentation will describe the first two flights of the ASPIRE sounding rocket test campaign, including footage of the inflation events, reconstruction of the sounding rocket trajectories, and recovery of the parachute and payloads.

This test program uses sounding rockets operated by NASA's Sounding Rocket Operations Contract (NSROC) to deliver the parachutes to the targeted test conditions. The sounding rocket assembly, consisting of a Terrier first stage, a Black Brant second stage, and the roughly 1200 kg payload section containing the experiment, are launched out of NASA's Wallops Flight Facility (WFF). The system is rail-launched and spin-stabilized at 4 Hz. After booster separation and de-spin, the payload attitude is controlled by a cold-gas attitude control system. The payload section reaches apogee between 50 km and 55 km before deploying the parachute at the target Mach number and dynamic pressure. After decelerating to subsonic speed, the parachute and payload descend to the ocean for recovery and inspection.

The ASPIRE instrumentation suite is designed to obtain the data necessary for reconstruction of the test conditions, determination of the parachute loading environment and aerodynamic performance, and obtaining high-resolution data of the parachute deployment and inflation events. This is achieved using state-of-the-art cameras capturing images at 1000 frames per second and at a 4K resolution, situational video cameras, parachute bridle load pins, and an inertial measurement unit.

The first ASPIRE flight test took place at Wallops Island, Virginia on October 4th 2017. The payload reached an apogee of 50 km before deploying the first candidate Mars 2020 parachute at Mach 1.77 and a dynamic pressure of 453 Pa. The parachute performed nominally in this supersonic environment and carried the payload to splashdown 35 minutes after launch. The parachute and payload were recovered 73 km off of the Virginia coast along with all instrumentation and sensor data. The next test is planned for March of 2018. It will test a second Mars2020 candidate DGB at a target deployment dynamic pressure of 667 Pa.

References:

[1] O'Farrell, C., Clark, I..G, and Adler, M. "Overview of the ASPIRE Project," presented at the 14th International Planetary Probes Workshop, The Hague, NL, June 2017.

[2] Tanner, C.L., Clark, I.G., and Chen, A. "Overview of the Mars 2020 Parachute Risk Reduction Plan" presented at IEEE Aerospace Conference Paper, Big Sky, MT, March 2018.

[3] O'Farrell, C., Karlgaard, C., Tynis, J.A. "Overview and Reconstruction of the ASPIRE Project's SR01 Supersonic Parachute Test" IEEE Aerospace Conference Paper No. 2233, Big Sky, MT, March 2018.

ASPIRE – INSTRUMENTATION RING AND EXPERIMENT SECTION SUBSYSTEMS. J. L. Hill[1] and B. S. Sonneveldt[1] and I. G. Clark[1], [1]Jet Propulsion Laboratory, California Institute of Technology, 4800 Oak Grove Drive, Mail Stop 321-220, Pasadena, CA 91109, jeremy.l.hill@jpl.nasa.gov.

Introduction: The Advanced Supersonic Parachute Inflation Research and Experiments (ASPIRE) project was established as a risk-reduction activity for the Mars 2020 project in 2016. ASPIRE is developing an infrastructure for the testing of parachutes at supersonic conditions and dynamic pressures analogous to those encountered at Mars. The project is studying the deployment, inflation, and performance of 21.5-m DGBs in supersonic, low-density conditions. The parachutes are delivered to target deployment conditions representative of flight at Mars by sounding rockets launched out of NASA's Wallops Flight Facility (WFF). The first successful launch occurred in October of 2017. Two test articles will be deployed: a full-scale version of the DGB used by the Mars Science Laboratory (MSL), and a full-scale strengthened version of the MSL parachute with the same geometry but differing in materials and construction.

In order to achieve the desired flight conditions, the ASPIRE sounding rocket platform relies on existing solid rocket motors. A new payload referred to as the Experiment Section is developed to carry the parachute and the required instrumentation. The ASPIRE instrumentation suite, housed in a structure referred to as the Instrumentation Ring, is critical to obtaining the data necessary for reconstruction of the test conditions, determination of the parachute loading environment and aerodynamic performance, and obtaining high-resolution data of the parachute deployment and inflation events.

The Instrumentation Ring interfaces with both structure of the Experiment Section and soft goods of the Parachute Decelerator System. A Parachute Decelerator System (PDS), which is comprised of a Mortar Tube, Parachute, Sabot, and Gas Generator is used to house and deploy the parachute. The Mortar Tube interfaces with the Experiment Section, while the Parachute interfaces with load pins in the Instrumentation Ring. The primary function of the Experiment Section and Instrumentation is to anchor all of the major subsystems together and provide the structural load paths necessary to support the launch, mortar fire, parachute inflation loads, and recovery. The key challenges for this hardware lie in the complex configuration, multiple load cases, and magnitude of loads.

Another key challenge for this hardware lies in the reusability requirements. Following the deployment of the parachute, the payload descends into the Atlantic oceans where the payload is recovered, disassembled, refurbished, and reused on future ASPIRE launches. In order to allow for recovery, the payload design included verifying buoyancy in the ocean water. Low density foam was integrated into Experiment Section to meet this requirement. The primary purpose of the buoyancy foam is to ensure that the Experiment Section floats following splashdown in the ocean. The Experiment Section is not sealed and can take on water after landing necessitating the presence of foam to prevent this. The foam must integrate to the structure of the Experiment Section such that it survives launch and parachute deployment related loads. The foam must also accommodate adjacent hardware and wire harnesses.

This presentation will describe the design of the Instrumentation Ring and Experiment Section subsystems as well as the key challenges and how they were met. Some of the key challenges that were faced in this design included the large scale of the hardware, the complex set of interfaces, multiple load cases with large magnitudes, and recovery and reuse after ocean landing, and extremely aggressive schedule.

The Modulated Exo-Brake Flight Testing: Modeling and Test Results

M. S. Murbach,[1] A. Guarneros,[1] A. Bowes,[3] R.W. Powell, [3] J. Wheless,[1] F. Tanner,[1] C. Priscal,[1] S. Smith,[1] A. Salas, P. Papadopoulos,[2] A. Dwyer-Ciancolo, [3]

[1]NASA Ames Research Center, Moffett Field, CA 94035 (marcus.s.murbach@nasa.gov), [2]San Jose State University, Aeronautical Engineering Department, One Washington Square, San Jose, CA, 95192, [3]NASA Langley Research Center, 8 Lindburgh Way, Hampton, VA, 23681

Abstract: The Exo-Brake is a simple, non-propulsive means of de-orbiting small payloads from orbital platforms such as the International Space Station (ISS). Two recent flight experiments on TechEdSat 5 and 6 have developed the necessary avionics/control hardware to modulate the drag area of the de-orbiting experiments. The two experiments were successfully jettisoned from the International Space Station (ISS) on March 26, and November 21, 2017. These build on the previous flight experiments with fixed surface areas and evolving two-way communications hardware/GPS for uplinking commands based on navigation information. The current TechEdSat-6 has been particularly successful,with the intent of targeting the re-entry point. Improved targeting efforts are continuing, and the subsequent flight experiment set (TechEdSat 7-9) is described. In addition, the use of the platform as an experimental Entry/ Descent/Landing platform is discussed.

COMPUTED TOMOGRAPHY SCANNING OF A 1-METER DEMONSTRATION HEATSHIELD FOR EXTREME ENTRY ENVIRONMENTS

C. D. Kazemba[1] and M. Mahzari[2]

[1] STC Inc. (cole.d.kazemba@nasa.gov), [2] NASA Ames Research Center (milad.mahzari@nasa.gov)

Introduction: The Heatshield for Extreme Environments Technology (HEEET) is maturing a new thermal protection system (TPS) for use in extreme entry environments [1]. To advance the technical maturity of the HEEET system, the HEEET project recently completed the manufacturing of 1-meter diameter Engineering Test Unit (ETU) heatshield for manufacturing demonstration and environmental testing (Figure 1). This presentation will cover the development and initial findings of the X-Ray Computed Tomography (CT) scanning conducted following manufacturing. This work extends the state of the art for scanning 1-meter class heatshields beyond the technique applied for the Stardust capsule following its return to Earth [2].

Figure 1: HEEET ETU Before OML Machining

Need for NDE: The ETU is an assembly of HEEET tiles integrated onto a composite laminate aeroshell. An epoxy film adhesive was used to bond the tiles to the outer surface of the aeroshell. The carrier structure contains a stainless steel payload adapter ring beneath the composite laminate. Between HEEET tiles, a compliant gap filler similar in composition to the HEEET material is bonded using a 0.2mm thick phenolic film adhesive (Figure 2). Verifying the integrity of this adhesive layer after manufacturing is paramount.

The post-manufacturing inspection verifies that the manufacturing processes developed for the HEEET system were successful and establishes a baseline for the ETU prior to environmental testing. Several NDE methodologies were considered and investigated at an exploratory level, however the primary NDE method implemented was CT scanning.

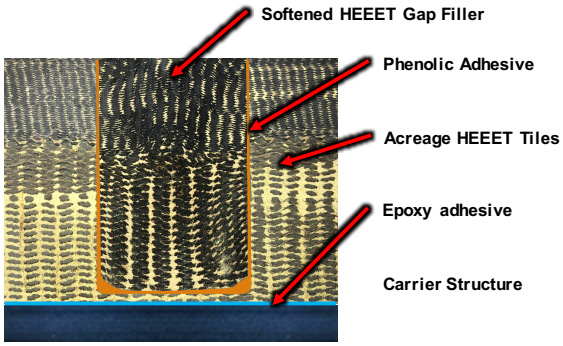

Figure 2: Key Elements in the HEEET System

Challenges: The driving inspection requirement for application of CT scanning to the ETU was the need to identify defects in the 0.2mm thick phenolic adhesive layer between gap fillers and the adjacent acreage HEEET tiles. Scanning a 1-meter article with sufficient resolution and contrast to resolve defects in this adhesive layer requires coverage across 4 orders of magnitude in scale. This difficult task was exacerbated by the similarity in material density (and therefore similar attenuation properties) of the HEEET material and the phenolic adhesive. Furthermore, challenges related to the presence of the stainless steel ring and logistical complexities were also encountered.

Results: In working with industry, the HEEET team successfully developed and demonstrated an inspection methodology using CT (Figure 3). This data set revealed a variety of features of interest; recession layer thickness for each element, missing fibers in the woven material, small adhesive voids under the base of closeout plugs, and cracks in the phenolic adhesive near the base of the gap filler were all identified and categorized (Figure 4). The structural impact of these defects was analyzed and determined to be acceptable, allowing the project to move forward into environmental testing.

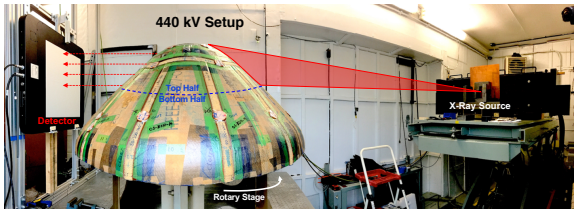

Figure 3: 440 kV Scanning Configuration

The same scanning configuration applied to the top portion was initially applied to the bottom half of the ETU. In an attempt to reduce the effects of the steel ring, an alternative scanning methodology using a high energy X-ray source (9 MeV) and a 200-micron detector was applied to the bottom portion of the ETU.

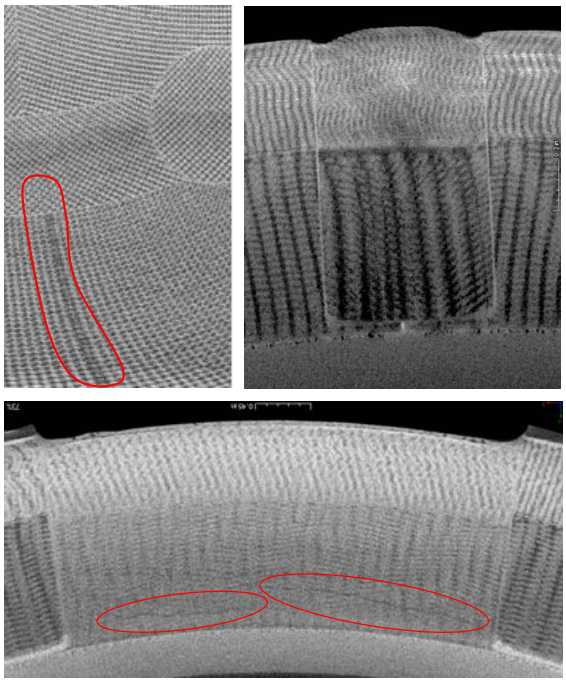

Figure 4: Representative slices from the top portion of the HEEET ETU.

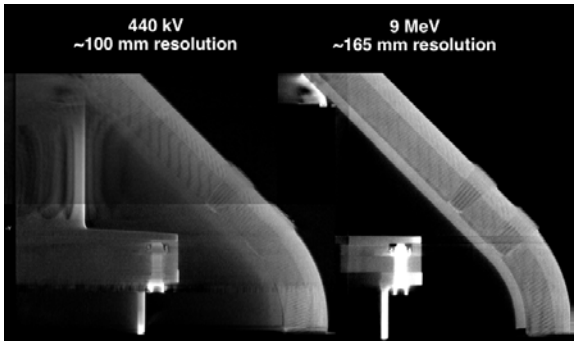

Figure 5: 440 kV and 9 MeV Scans of ETU

References:

[1] Venkatapathy, E., et al., "Progress Towards Providing Heat-shield for Extreme Entry Environment Technology (HEEET) for Venus and Other New Frontiers Missions," 15th Meeting of the Venus Exploration and Analysis Group (VEXAG), 2017.

[2] McNamara, K. M., et al., "X-Ray Computed Tomography Inspection of the Stardust Heat Shield", 7th International Planetary Probe Workshop, 2010.

FLIGHT TESTING A VISION-BASED NAVIGATION AND HAZARD DETECTION AND AVOIDANCE (VN&HDA) EXPERIMENT OVER A MARS-REPRESENTATIVE TERRAIN. C. Posse[1], J. Oliveira[2], F. Camara[3], J. Canilho[4], T. Hormigo[5]
[1-5] Spin.Works S.A., Av. Da Igreja 42-6º, 1700-293 Lisboa, Portugal. E-mail: {carlos.posse, joao.oliveira, francisco.camara, jose.canilho, tiago.hormigo}@spinworks.pt

Introduction: This article focuses on the results of the actual flight testing of a multi-copter platform that carries aloft a Vision-Based Navigation and Hazard Detection and Avoidance (VN&HDA) experiment, and autonomously flies over Mars-representative terrain, following a Mars Precision Lander (MPL)-representative trajectory in order to assess the performance of the VN&HDA system. The flight hardware that composes the payload under test is called the Avionics Test Bench (ATB). It consists of:

- a space-grade representative LEON processor and a co-processor FPGA running all HDA software modules under test,
- a VN&HDA Sensors suite, composed of COTS sensors including an IMU, visual camera, imaging LIDAR, and laser range finder,
- a COTS (CPU+FPGA) processing hardware (VBN System) running the VBN algorithms,

all the other required COTS electronic components, such as mass memory, communication & telemetry (including the Data Link and all other connections with sensors), a power source and distribution board.

The work presented in this article is the product of an on-going ESA activity with the objective of further develop and flight test visual based navigation (VBN) and hazard detection and avoidance (HDA) algorithms to serve the needs of future Mars and other planetary missions and raise them to a technology readiness level (TRL) of 5 ("critical function verification in a relevant environment"). In particular, ESA seeks as an output of this activity, validated HDA and VBN algorithms for Mars landing, as well as a fully-functional, flight-tested, Mars-landing avionics testbed.

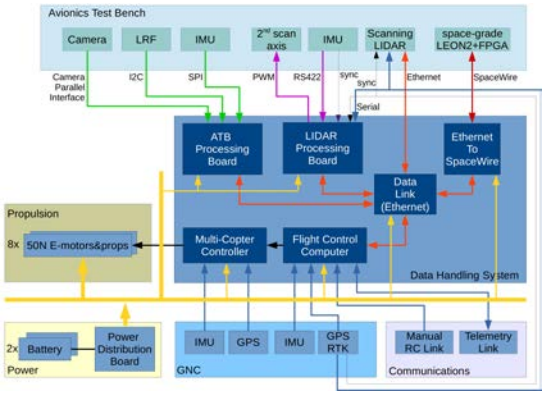

Figure 1 – Avionics functional reference architecture

The discussion presents the Flight Testing campaign and addresses the engineering issues that were taken into account when scaling the actual descent and landing (D&L) Mars trajectory into a representative Terrestrial Demonstration Mission (TDM). Namely, the TDM was designed to maintain a representative observation geometry, while respecting the LIDAR sensor range limitation to 100m and maximum descent speed allowable for multi-copters of <5m/s.

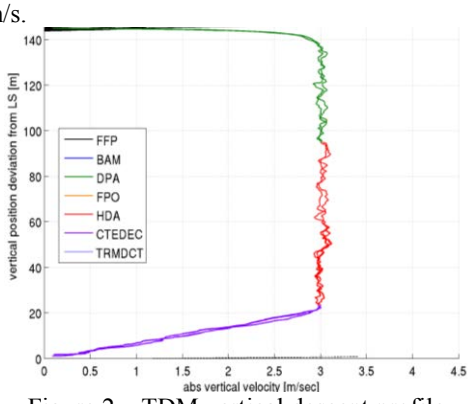

Figure 2 – TDM vertical descent profile.

The Terrestrial Demonstration Mission (TDM) is focused on the final phases of the powered descent flight, i.e., starting from the transition from the Descent Profile Acquisition Phase (DPA) to the HDA phase down to the Touchdown. During the terrestrial flight demonstrations, the HDA phase involving the operation of hazard detection sensors and on-board decision-making processes related to landing site selection is executed in real-time, such as to demon-

strate the highest achievable representativity relative to the MPL D&L mission.

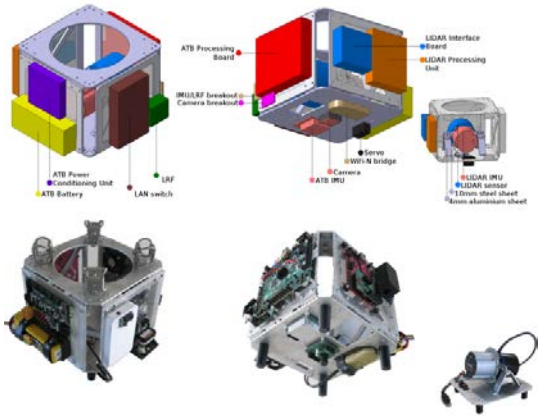

Figure 3 – ATB. Top) Design views. Bottom) As-built.

Figure 4 – Multi-copter vehicle.

The flight tests are the last step in a sequence of extensive Monte Carlo test campaigns that involved model-in-the-loop and hardware-in-the-loop testing. The simulation campaigns have shown that the HDA system raises the probability of safe landing selection from a blind landing baseline of 80% to over 99% [5]. Adding the visual-based GNC to the loop, the simulations have shown that the probability of safe landing is kept above 99%. From the time that the HDA takes a snapshot of the terrain and selects a landing site, till touchdown, the on-board VBN accumulates a horizontal positioning error that is characterized by a 3-sigma of less than 4m. The error in the attitude estimation at the time of HDA is also a contributing factor of error, denoted here as a map-tie error associated with the HDA. The total horizontal positioning error at touchdown is within 6.5m (at 99.7% percentile, a 3-sigma equivalent). Studying the synthetic terrains selected for the tests, it was found that HDA-visible patch of terrain (from which a candidate landing site must be selected) can contain between 1% to 7% of terrain that are free of hazards within a 6m radius, revealing that the testing terrains were very challenging. This article presents the results of the actual flight testing campaigns and compares the results with the simulation campaigns.

References:

[1] F. Câmara et al., "Hazard avoidance techniques for vision based landing", 6th International ESA Conference on Guidance, Navigation and Control Systems, 2005.

[2] F. Câmara et al., "A Hybrid Camera-Lidar Hazard Detection and Avoidance System for Lunar Landing", ESA GNC Conference, Karlovy Vary, Czech Republic, June 2011

[3] F. Câmara et al., "Data Fusion Strategies for Hazard Detection & Safe Site Selection for Planetary & Small Body Landings", 9th ESA Conference on Guidance and Navigation Control Systems, Portugal, 2014

[4] T. Hormigo et al., "StarTiger Dropter Project: Integrated, Closed-Loop Vision-Aided Navigation with Hazard Detection and Avoidance", 9th ESA Conference on Guidance and Navigation Control Systems, Portugal, 2014

[5] F. Câmara et al., "Data fusion strategies for hazard detection and safe site selection for planetary and small body landings", CEAS Space Journal, Vol.7, Iss.2, pp.271–290, June 2015

ADEPT SR-1 Development and Testing. B. P. Smith[1], A. M. Cassell[1], P. F. Wercinski[1], S. M. Ghassemieh[1], B. C. Yount[1], C. E. Kruger[1], O. S. Nishioka[1], C. A. Brivkalns[1], S. C. Wu[1], A. Guarneros Luna[1], and J. D. Williams[2], [1]NASA Ames Research Center (M/S 229-1, Moffett Field, CA, brandon.p.smith@nasa.gov), [2]AMA Inc. @ NASA Ames Research Center.

The Adaptable Deployable Entry and Placement Technology (ADEPT) Sounding Rocket One (SR-1) fight test will be the first sub-orbital flight of Nano-ADEPT [1]. Nano-ADEPT is a deployable heatshield for secondary payload missions desiring to re-enter the Earth's atmosphere or deliver small science payloads to Mars or Venus. Two units have been built and tested in preparation of launch: one designated the "Spare" unit and one the "Flight" unit. The general development approach has been to perform all procedures on the Spare prior to performing them on Flight. This approach has served the project well, allowing for procedures to be rapidly developed and tested on spare hardware where mistakes are less consequential. Conversely, when schedule constraints have come up, the approach has allowed the project to rapidly pivot to an approach where Flight drives the critical path rather than Spare. This approach has enabled relatively rapid development of Flight where technical risk is balanced with schedule realism. This poster will describe the various tests that have been performed on Nano-ADEPT Spare and Flight units to prepare for the suborbital flight. The purpose is to communicate the development approach we took for this low-cost, moderate-risk flight test and hopefully engage the EDL community in a wider discussion of risk-balanced approaches toward flight hardware development of secondary payload atmospheric entry systems.

The ADEPT SR-1 vehicle can be functionally divided into a Mechanical Subsystem and an Electrical Subsystem. Figure 1 below shows the components of the vehicle. The Mechanical Subsystem, consisting of the carbon fabric skirt, struts, ribs, impact attenuator, deployment mechanism, and rib release deck, is assembled and tested in parallel with the Electrical Subsystem, which consists of all other components shown in Figure 1.

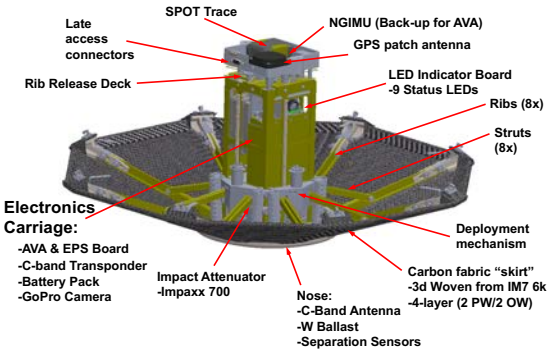

Figure 1. ADEPT SR-1 Components

The Mechanical Subsystem checkout activity is primarily focused on ensuring the carbon fabric skirt deploys reliably, is tensioned adequately, and opens to the required angle. The Electrical Subsystem checkout activity focuses on making sure all of the individual electronical components work together as designed. This "flat sat" procedure involves running through an entire mission simulation, including mission durations, to ensure battery life and data volume margins are sufficient.

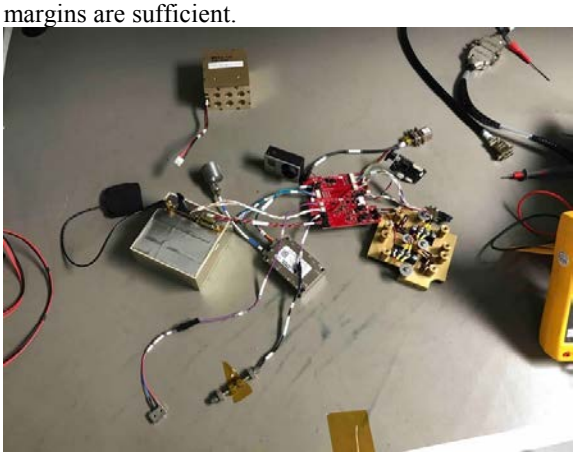

Figure 2. "Flat Sat" testing.

Once ADEPT is fully integrated, it undergoes a series of functional checks and system measurements. These include tests of deployment with the Electronic Subsystem in the loop, mass property measurements, avionics calibration at the system-level, and mission simulation operations. Photos of the testing are displayed in Figure 3-5. This poster will show a visual flow of the testing performed with more details of the objectives and outcomes of each testing activity.

Figure 3. Magnetometer calibration at Moffett Field compass rose

Figure 4. System-level accelerometer calibration on optical bench.

Figure 5. System-level rate gyro calibration on spin table.

References:

[1] Smith, B.P. et al. (2015) IEEEAC, "Nano-ADEPT: An Entry System for Secondary Payloads." [2] Smith, B. P., Wilder, M. C., Cruz, J. R., Dutta, S. (2016) IPPW14, "Free-Flight Ground Testing of ADEPT in Advance of the Sounding Rocket One Flight Experiment."

PLANNED ORBITAL FLIGHT TEST OF A 6-METER HIAD. R. A. Dillman[1,2], J. M. DiNonno[1], R. J. Bodkin[1], S. J. Hughes[1], F. M. Cheatwood[1], H. Blakeley[1], R. L. Akamine[1], and A. Bowes[1]; [1]NASA Langley Research Center, [2]Robert.A.Dillman@nasa.gov.

Abstract: NASA has funded LOFTID, the Low Earth Orbit Flight Test of an Inflatable Decelerator, for flight testing of a 6m diameter HIAD. LOFTID will launch in 2020 as a secondary payload on an Atlas V mission. After release of the primary payload, the upper stage Centaur will perform a modified de-orbit burn, then power up LOFTID for inflation from its stowed launch configuration. Once the aeroshell is inflated, the Atlas will release the HIAD for reentry. The 12G reentry trajectory will produce over twice the peak heat flux of the earlier IRVE sub-orbital flight tests, providing flight performance data relevant to LEO payload return and direct Mars entry. After splashdown in the Pacific Ocean, the reentry vehicle will be recovered for inspection and analysis. This presentation will discuss the overall mission concept, HIAD design, subsystem configurations, planned ground tests, and post-flight recovery approach.

The HIAD Orbital Flight Demonstration Instrumentation Suite. G. T. Swanson[1], B. P. Smith[2], R. L. Akamine[3], R. J. Bodkin[3] and F. M. Cheatwood[3]. [1]AMA Incorporated at NASA Ames Research Center, g.swanson@nasa.gov, [2]NASA Ames Research Center, [3]NASA Langley Research Center.

Abstract: NASA's Hypersonic Inflatable Aerodynamic Decelerator (HIAD) technology has been selected for a Technology Demonstration Mission under the Science and Technology Mission Directorate. HIAD is an enabling technology that can facilitate atmospheric entry of heavy payloads to planets such as Earth and Mars using a deployable aeroshell. The deployable nature of the HIAD technology allows it to avoid the size constraints imposed on current rigid aeroshell entry systems. This enables use of larger aeroshells resulting in increased entry system performance (e.g. higher payload mass and/or volume, higher landing altitude at Mars).

The Low Earth Orbit Flight Test of an Inflatable Decelerator (LOFTID) is currently scheduled for mid-2021. LOFTID will be launched out of Vandenberg Air Force Base as a secondary payload on an Atlas V rocket. The flight test features a 6m diameter, 70-deg sphere-cone aeroshell and will provide invaluable high-energy orbital re-entry flight data. This data will be essential in supporting the HIAD team to mature the technology to diameters of 10m and greater. Aeroshells of this scale are applicable to potential near-term commercial applications and future NASA missions.

LOFTID will incorporate an extensive instrumentation suite totaling over 150 science measurements. This will include thermocouples, heat flux sensors, and a radiometer to characterize the aeroheating environment and aeroshell thermal response. An Inertial Measurement Unit (IMU), GPS, and flush air data system will be included in order to reconstruct the flown trajectory and aerodynamic characteristics. Loadcells will be used to measure the HIAD structural loading, and cameras (both visual and infrared) will be mounted on the aft segment looking at the aeroshell to monitor structural response and temperature distribution. In addition to the primary instrumentation suite, a new fiber optic sensing system will be used to provide global temperature distributions as a technology demonstration. The LOFTID instrumentation suite leverages Agency-wide expertise, with hardware development occurring at Ames Research Center, Langley Research Center, Marshall Space Flight Center and Armstrong Flight Research Center.

This presentation will discuss the measurement objectives for the LOFTID mission, and the extensive instrumentation suite that has been selected to capture the HIAD performance during the high-energy orbital re-entry flight test.

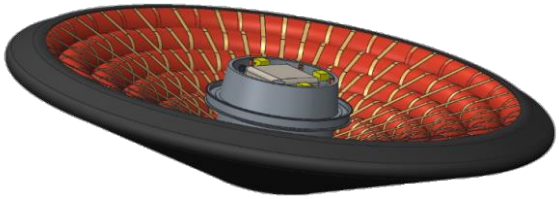

Fig 1. Drawing of the LOFTID 6m Re-entry Vehicle

Mars 2020 Entry, Descent, and Landing Verification and Validation Overview. Gregorio Villar[1], Cj Giovingo[1], Aaron Stehura[1], Allen Chen[1], [1]Jet Propulsion Laboratory, California Institute of Technology

Abstract – The Mars 2020 Entry, Descent, and Landing (EDL) team has entered the verification and validation phase, which is an extensive test and analysis campaign used to provide confidence in the performance of the EDL system. Mars 2020 EDL V&V heavily leverages the successful architecture established during the Mars Science Laboratory mission and is composed of four domains: Flight Dynamics (vehicle interactions with external environments) Subsystem (component-level hardware and software), Flight System (vehicle-internal interactions and behaviors), and Mission System (operations – team, processes, and tools) [1]. This paper presents the scope and schedule of the Mars 2020 EDL V&V campaign, and provides an overview of each domain, except Flight System V&V, which will be discussed in another presentation. All essential components of Mars 2020 EDL V&V will be completed before launch in 2020, with stress, off-nominal and robustness flight software testing and operations testing extending until landing in 2021.

References:

[1] Richard Kornfeld. et al. *Verification and Validation of the Mars Science Laboratory/Curiosity Rover Entry, Descent, and Landing System,* Journal of Spacecraft and Rockets, Vol. 51, No. 4, July–August 2014

Mars 2020 Entry, Descent, and Landing Flight System Verification and Validation Cj Giovingo[1], Allen Chen[1], Mallory Lefland[1], Aaron Stehura[1], Gregorio Villar[1], [1]Jet Propulsion Laboratory, California Institute of Technology, 4800 Oak Grove Drive, Pasadena, CA 91109.

Abstract: The Mars 2020 (M2020) project is built upon the successful design and implementation of the Mars Science Laboratory mission. The M2020 Entry, Descent, and Landing (EDL) team is leveraging this high heritage design in the planning and execution of the Verification and Validation (V&V) campaign [1]. As with MSL, the M2020 EDL V&V campaign is divided into four domains: Flight Dynamics, Flight System (FS), Mission System (MS), and Subsystems [2]. This paper details the V&V plans for the EDL FS, V&V plans for Flight Dynamics, Mission System, and Subsystems are discussed in a separate paper.

The EDL FS domain encompasses the internal functional behavior of the Flight Software (FSW) to Hardware interactions, such as guidance controllers commanding actuators, as well as the FSW to FSW interactions, such as spacecraft mode changes. To accommodate these varied interactions, the V&V campaign takes place across several test venues with varying degrees of simulation and hardware fidelity which this paper describes in detail. This paper also covers the timeline for testing nominal functional behaviors, stress and robustness performance, as well as day-in-the-life scenarios on the flight vehicle.

References:

[1] Aaron Stehura (2014) *Managing Complexity: Solutions from the Mars Science Laboratory Entry, Descent, and Landing Flight System Verification and Validation* Journal of Spacecraft and Rockets, Vol. 51, No. 4.

[2] Richard Kornfeld. et al. (2014) *Verificaiton and Validation of the Mars Science Laboratory/Curiosity Rover Entry, Descent, and Landing System,* Journal of Spacecraft and Rockets, Vol. 51, No. 4.

DLR EXPLORER-INITIATIVES: ENABLING TECHNOLOGIES FOR FUTURE ROBOTIC SPACE EXPLORATION. O. Funke, DLR German Aerospace Center, Space Administration, Navigation, Bonn, Germany (oliver.funke@dlr.de).

Introduction: The search for extraterrestrial life in the solar system is one major driving force for space flight and the design of space exploration missions. Among the other solar system bodies beside our planet Earth several candidates have been identified as promising candidates for the search for life, e.g. Mars and the ice moons Europa and Enceladus. While the early planetary history of Mars resembled in many aspects that of the young Earth life may have evolved there in a similar way. If so, it might still be present in some habitable niches, where it is protected from the harsh and life-hostile environmental conditions that the planet shows today. Such niches could be for instance the (mostly frozen) soil beneath the planetary surface, caves and lava tubes, and sheets of water ice. A very interesting site for exploration on Mars is the huge canyon system Valles Marineris: with its bottom located up to 10 km beneath the average planetary surface, atmospheric pressure there is above 6 mbar, the triple point of water. Thus, from a physical point of view, the presence of water in its liquid phase is possible. Compared to other places on Mars, where the pressure is very close to ~6 mbar and liquid water cannot occur, Valles Marineris is thus a favored exploration site.

Considering Jupiter's ice moon Europa access to the global and about 100 km deep ocean is of highest interest. Before it can be explored, however, the overlying 15 - 25 km thick ice crust that builds the moon's surface has to be penetrated by the exploration system. Saturn's tiny ice moon Enceladus shows a global water ocean beneath a thick ice crust, too, making it to a favored target for exploration as well. In difference to Europa, however, Enceladus shows a strong cryovolcanic activity in the southern hemisphere: ocean water, upwelling through cracks and crevasses within the covering ice sheet evaporates in fountains of ice particles into space.

Robotic exploration of the possibly remaining habitable niches on Mars as well as the exploration of the oceans on the ice moons of the solar system is a hard technological challenge: whether in a cave on Mars or beneath a many kilometers thick ice cover on Europa or Enceladus, an adequate robotic exploration system needs a high degree in autonomy. The requirements on autonomy increase with complexity of the chosen exploration scenario. By now, such sophisticated robotic exploration systems are not available, since enabling key technologies either still have to be developed or at least raised in TRL. This is what the DLR Explorer-Initiatives are focused on.

DLR Space Administration: Acting on behalf of the Federal Government, DLR Space Administration designs and implements Germany's Space Program, which integrates all German space activities on the national and European plane. These activities include Germany's national Space Program and Germany's contributions to the European Space Agency (ESA) as well as the European Organization for the Exploitation of Meteorological Satellites (EUMETSAT). Within the national Space Program projects are funded or commissioned. Allowed applicants are universities, research facilities and industrial companies from Germany.

DLR Explorer Initiatives: The initiatives were founded by DLR Space Administration, department of Navigation, in order to concentrate expertise from diverse running projects funded within the national Space Program. The general purpose is to coordinate running activities (as for combined field tests), discussion and development of new approaches, early identification of specific technical solutions and given synergies among these projects. The DLR Explorer Initiatives emanated from the former joint projects "EnEx - Enceladus Explorer", "VaMEx - Valles Marineris Explorer", and the single partner project "EurEx - Europa Explorer". All three projects with given future space application scenarios were funded from 2012 to 2015 by DLR Space Administration.

Enabling technologies for future space missions: In EnEx a fully maneuverable melting probe, the "EnEx-IceMole", was equipped with adequate technology for positioning, navigation, and clean sampling. The technological developments in EnEx are following a scenario, in which the EnEx-IceMole autonomously melts its way into the ice surface of Enceladus at a depth of about 200 m and towards a water filled crevasse that feeds a cryovolcano. The task of the probe is to take a liquid water sample from there for in-situ examination. The technologically more challenging attempt to melt through the complete ice surface to access the ocean beneath can thus be avoided, while in the EnEx approach the main question "is there life on Enceladus" still might be answered. In collaboration with the science team from the NSF funded MIDGE project (J. Mikucki, S. Tulaczyk) the probe was already successfully utilized in a terrestrial analog field test in Antarctica (November/December 2014) for retrieval of

a clean water sample from a subglacial lake (Blood Falls experiment).

The EurEx scenario comprises the complete penetration of Europa's ice crust by a melting probe that acts as a shuttle carrying an Autonomous Underwater Vehicle (AUV) as payload. Here, the fully autonomous exploration of Europa's ocean and its sea floor is a highly ambitious task, and it will take many efforts and much time to raise the needed technologies to the required TRL. In the EurEx project the ice shuttle "Teredo" and the AUV "Leng" were developed as first approach technology carriers and tested in laboratory and minor field tests. Although in these tests the system demonstrated the correctness of the followed approach, the complete system still has to be miniaturized significantly, and the implemented artificial intelligence has to be improved much further.

The space scenario in VaMEx intends the partially autonomous exploration of a large region within the Valles Marineris. For this purpose, a heterogeneous robotic swarm shall be utilized, consisting of rovers, hominids and flying drones. Although each category of individual swarm elements covers different and specific tasks of the exploration, the swarm shall act in a cooperative and collaborative manner as one exploration system.

The way ahead: In order to continue the started developments towards enabling technologies for possible future space missions, the EnEx-Initiative and VaMEx-Initiative were established in 2015 by DLR Space Administration, department of Navigation. Since EurEx shares with EnEx the topic of exploring the icy moons of the outer solar system, this project became part of the EnEx Initiative. Accompanying the most recently accepted funding of a new project called "nanoAUV", the creation of a third Explorer initiative should occur in 2018. In this new initiative AUV-related topics will be focused on, and EurEx will become part of it.

International collaboration welcome: The described individual initiatives are focusing on different possible future space missions for robotic exploration of Mars and the water worlds of the outer solar system. The DLR Explorer Initiatives comprise these three initiatives and can be compared to a program line of DLR Space Administration as funding agency. The main goal is the invention and development of currently missing key technologies to enable realization of the addressed scenarios as future space missions. The activities in the DLR Explorer Initiatives are open for international cooperation and collaboration, if funding for the partners from abroad can be obtained from third side.

Kentucky Re-entry Universal Payload System (KRUPS): Sub-orbital Flights. J. D. Sparks[1], G. I. Myers[1], J. T. Nichols[1], E. C. Whitmer[2], N. Khouri[1], C. J, Dietz[3], S. W. Smith[1] and A. Martin[1], [1]Department of Mechanical Engineering, University of Kentucky, Lexington, KY 40506, USA, [2]Department of Computer Engineering, University of Kentucky, Lexington, KY 40506, USA, [3]Department of Computer Science, University of Kentucky, Lexington, KY 40506, USA

KRUPS (Kentucky Re-entry Universal Payload System) is an adaptable testbed for re-entry science experiments, with an initial application to Thermal Protection Systems (TPS). Because of the uniqueness of atmospheric entry conditions that ground testing is unable to replicate, scientists principally rely on numerical models for predicting entry conditions. The KRUPS spacecraft, developed at the University of Kentucky, provides an inexpensive means of obtaining validation data to verify and improve these models.

To increase the technology readiness level (TRL) of the spacecraft, two sub-orbital missions were developed. The first mission, KUDOS, launched August 13th, 2017 on a Terrier-Improved Malamute rocket to an altitude of ~150 km. The chief purpose of this mission was to validate the spacecraft's ejection mechanism, on-board power, data collection and transmission, achieved via Iridium modem. The spacecraft diameter, due to space constraints, was limited to 7.5-inches. The spacecraft powered on as scheduled, ejected from the release mechanism, and connected with Iridium Satellites. No data packets were received with the first mission, instead two incomplete transfer emails were transmitted. On-board video footage provided feedback on the spacecraft's behavior during ejection. Results from these videos showed that the spacecraft hit the inside of the release mechanism and caused the spacecraft to spin at a high rate. This is hypothesized to be one of the main reasons for the incomplete transfers. These videos were important to the mission since it showed the improvements that needed to made for the following mission. Even though data was not obtained, KUDOS increased the overall TRL from 4 to 5, by validating these system components in a relevant environment.

The second mission, KOREVET, will launch in March 2018. This mission is expected to raise the TRL to level 6 by validating the whole system in a relevant environment. This spacecraft has a diameter of 11-inches, which is the full-scale model. Feedback and results from the 1st mission were used to improve the functionality of KOREVET. The spacecraft's Center of Gravity (CG) was physically measured out to fit in the optimum self-stabilizing range. Also, the release mechanism was re-designed so that the spacecraft would not hit anything during the release, with the hopes that this will reduce the spin rate of the spacecraft. KOREVET also developed a recovery system by adding GPS tracking and a high-visibility fluorescent orange back-shell coating. Past missions using the same 45-degree fore-shell geometry were able to self-stabilize and transmit data post-splashdown. For this mission, waterproofing were implemented to allow the spacecraft to transmit post-splashdown. Both of these missions are invaluable preparation to the project's ultimate goal of releasing multiple experimental testbeds from the International Space Station (ISS).

Figure 1: KRUPS spacecraft ejection (KUDOS mission)

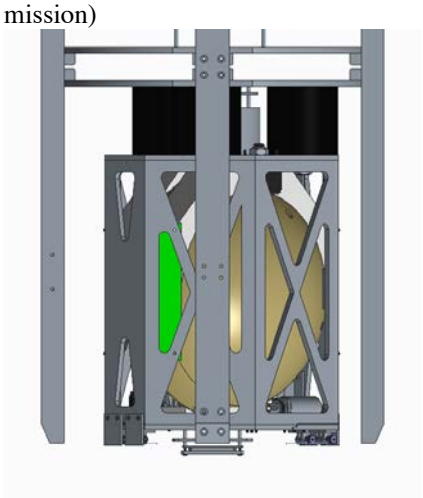

Figure 2: KOREVET CAD layout

Demonstration of a modular ascender for sample return missions. F. Ebert[1], R. Buchwald[1], O. Angerer[2], Airbus Defence and Space, email: florian.ebert@airbus.com, [2]German Aerospace Center DLR, email: oliver.angerer@dlr.de

Background: Ascent stages constitute a key element of future manned missions to moon and mars. After successful landing and completion of work on the surface, they serve as means of transportation back into orbit. After reaching the target orbit, sample containers - and astronauts in more advanced scenarios - are transferred to the awaiting return module or habitat.

Motivation: Given the high costs of such cornerstone missions and the ultimate goal to have humans in the loop or onboard for later scenarios, special emphasis has to be made to maturize the related technologies in the frame of dedicated (terrestrial) demonstration missions.

Reference missions: Currently several lunar missions including ESA's cooperations with Roscosmos on robotic lunar polar sample return (LPSR) and with JAXA and CSA on a human assisted (lunar) sample return (HERACLES) are aiming at returning samples from the lunar south pole region. In parallel NASA and ESA are progressing towards the first successful mars sample return (MSR).

The GAMMa[1] modular ascender concept: In the frame of the German national GAMMa study, a modular ascender family has been derived.

Fig.1: *left:* GAMMa LPSR ascender, *center:* GAMMa HERACLES ascender with kick-stage *right:* GAMMa MSR ascender with kick-stage

The concept is complying with all of the three reference mission scenarios. Comparative analyses show only minor mass growth with respect to a single mission design concept, making the concept a viable option for all of the three sample return missions.

Demonstration objectives: In the reference missions, the handover of the sample in orbit occurs either robotically to an earth return vehicle (LPSR, MSR) or by rendezvous and berthing of the ascender to a man-tended habitation module.

Fig.2: Free flying capture of orbiting sample (MSR, LPSR)

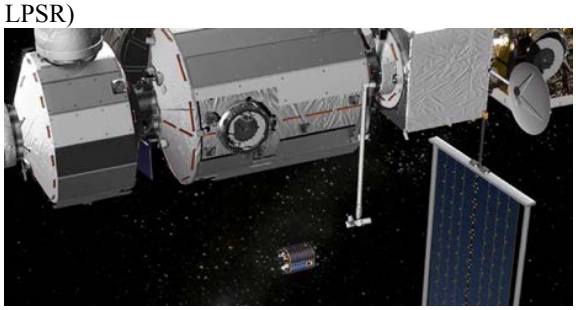

Fig.3: Rendezvous and berthing of the ascender (human assisted sample return)

Besides the technology demonstration of the ascender itself, in particular the proximity operations for sample handover are key to mission success.

GAMMa demonstration mission: A potential full-scale demonstration mission could focus on this critical mission phase. The ascender could be launched with a low cost micro launcher into low earth orbit for testing critical proximity operations and safety features using targets on a secondary payload.

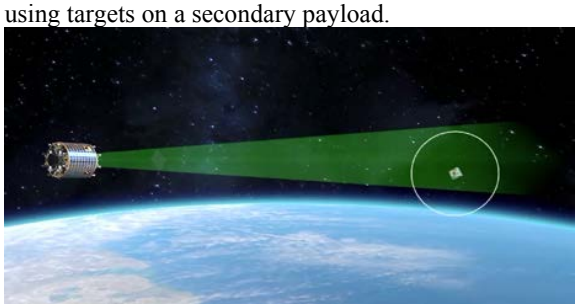

Fig.4: Proximity operations experiments in LEO

After successful primary mission, both, ascender and payload can follow secondary mission objectives in LEO.

[1] GAMMa (Gemeinsamkeiten von Aufstiegsstufen für Mond und Mars) has been supported by Federal Ministry for Economic Affairs and Energy on the basis of a decision by the German Bundestag (50JR1706)

DESIGN OF A SINGLE WHEEL TEST RIG FOR OCEAN WORLDS ROVERS. Madhura Rajapakshe[1], Ye Lu[2]*, and Sarag J. Saikia[3]*, [1]Ravenna Lab, Smithers Rapra Inc, 1150 North Freedom Street, Ravenna, OH, 44266, [2]yelu@purdue.edu, [3]sarag@purdue.edu, *School of Aeronautics and Astronautics, Purdue University, 701 W. Stadium Ave., West Lafayette, IN, 47907.

Ocean Worlds Surface Exploration: Three solar system's "Ocean Worlds"—Europa, Titan, and Enceladus—believed to harbor sub-surface oceans and the potential for habitable environments (hence life beyond Earth) are some of the most interesting targets for planetary exploration. Rugged surface characteristics (high cliffs, deep crevasses, blocky ice boulders or even tall penitentes) and extreme environments (low temperature and high radiation) are beyond the capabilities of the state-of-the-art mobility systems. A novel mobility system that is under development uses large diameter, deployable, conformal, puncture-proof, and abrasion-resistant tires. One phase of this project focuses on the design and fabrication of a single wheel test rig to support the advancement of the complete mobility system design. The proposed test rig fills the gap in rover wheel testing for ocean worlds. The design will integrate some of the features available in the existing test rigs for planetary rovers and augmented with additional test features for wheel testing in conditions envisioned to be present on the Ocean Worlds. The test rig will be versatile to allow simulating various terrain and surface conditions and low gravity.

State-of-the-Art Rover Tire Testing Facilities: Existing rover wheel testing facilities include single wheel test rigs and rover system testing facilities. A single wheel test rig assesses the wheel and terrain interaction. Such testing can help understand the dynamics of the wheel under various conditions. Rover system testing facilities are generally larger facilities that assess the dynamic performance and the durability of rover systems.

There are many single wheel testbeds across the country designed for Mars/Moon rover wheel testing. The test rigs include Robotic Mobility Group single-wheel testbed at Massachusetts Institute of Technology (MIT) [1, 2], single wheel soil imaging testbed [3] and inflatable robotic rover testbed [4] at Carnegie Mellon University (CMU), the Traction and Excavation Capabilities (TREC) testbed at NASA Glenn Research Center's Simulated Lunar Operations (SLOPE) laboratory, and single wheel testbed at Tohoku University. These test rigs can perform static testing and dynamic testing, including drawbar-pull measurement, wheel sinkage measurement, wheel slippage, etc. All previous test rigs are designed to fulfill specific testing requirements, such as Mars/Moon rover wheel testing.

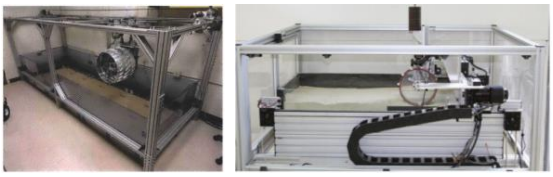

Figure 1 MIT test rig (left) and CMU test bed (right)

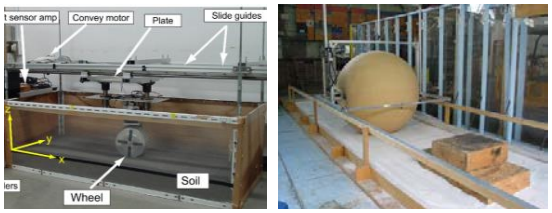

Figure 2 Testbed at Tohoku University (left) and CMU Inflatable Robotic Rover Testbed (right)

Proposed Ocean Worlds Tire Test Rig: The proposed test rig builds upon the features found on previous test rigs and accommodates the larger diameter tire (>1 m) under development. It will provide some additional capabilities as summarized below.

1. Dynamic Load Control. The test rig will be capable of dynamic load control at various test configurations while simulating low gravity conditions of the Ocean Worlds (see Table 1). The weight of a multi-axis load cell itself can exert a load in the vicinity of 22 N given in Table 1 for Enceladus. In that scenario, the weight of the tire and the other hardware on the test rig will make the tire load far exceeding the required test load. Therefore, the load control mechanism will be capable of compensating excessive load, as well as applying load dynamically.

Table 1 Example load on a single wheel on various bodies

Body	Gravity	Load for 200kg
Earth	1.00 g	1960 N
Mars	0.378 g	742 N
Europa/Titan	0.134 g	263 N
Enceladus	0.011 g	**22 N**
Ganymede	0.146 g	286 N

2. Surface Features and Simulant. Previous single wheel test rigs have restricted testing space, which limits the type of testing surfaces. As the exact surface conditions on Ocean Worlds are yet to be determined, the design of this test rig considers the possibility of varied terrain types and surface features at different scales. It will be capable of accommodating a variety

of surface types such as ice, sand-like ice and soil simulants, and surface features such as hard pointed objects and sharp edges.

3. Slip/Camber Angle Variation. Understanding of tire behavior under different slip and camber angle conditions helps improve the models for rover dynamics analysis. This test rig will have the capability to test at variable slip and camber angles, which can also be used to vary side force and overturning moment.

Relevance to Other Planetary Surfaces. As this test rig focuses on the tire testing requirements for Ocean Worlds, the design is to be versatile and partly customizable due to the lack of knowledge of the surface conditions. Hence, we expect that a variety of rover wheels can be tested at conditions that represent planetary surfaces other than the Ocean Worlds, including Mars and Moon.

Project Timeline and Status: The project is currently in the second quarter of a two-year term, and we plan to complete the design and assembly in Spring 2019 followed by validation and verification.

Acknowledgment: This project is funded through the NASA COLDTech program (80NSSC17K0518).

References: [1] Puszko, G. D. (2013) MIT Thesis. [2] Iagnemma, K. (2005) MIT Technical Report 01-05-05. [3] Moreland, S. et al, (2012) *IEEE* 10.1109/AERO.2012.6187040. [4] Apostolopoulos, D. et al. (2003) CMU-RI-TR-03-18.

Development and Testing of Precision Landing GN&C Technologies within NASA

John M. Carson III*
NASA Johnson Space Center

Michelle M. Munk†
NASA Headquarters and NASA Langley Research Center

Guidance, Navigation and Control (GN&C) technologies for precise and safe landing are essential for future robotic science and human exploration missions to solar system destinations with targeted surface locations that pose a significant risk to successful landing and subsequent mission operations. These Entry, Descent and Landing (EDL) technologies are a part of the NASA domain called PL&HA (Precision Landing and Hazard Avoidance) and are considered high priority capabilities within the space technology roadmaps from NASA and the National Research Council (NRC). The PL&HA technologies promote and enable new missions concepts to solar system destinations, including destinations prioritized in the NRC planetary science decadal survey. The NASA investments in PL&HA have been ongoing for more than a decade and have involved multiple projects, centers and supporting institutions that have developed new technologies for Terrain Relative Navigation (TRN), velocimetry, and onboard hazard detection (i.e., detection of hazards too small to identify *a priori* from orbital imagery). Numerous ground and terrestrial flight tests have been conducted for many of these new technologies in their paths toward spaceflight infusion, including tests on helicopters, fixed-wing aircraft, sounding rockets, and rocket-propelled Vertical Testbeds (VTBs) such as the NASA Morpheus vehicle and commercial suborbital rocket vehicles. The PL&HA technologies are nearing spaceflight infusion through prospective robotic lunar missions in the 2020's, and TRN will be infused onto the upcoming Mars 2020 mission, as well as a potential Europa lander mission. This presentation will provide an overview of NASA PL&HA investments, including insight into recent agency projects such as ALHAT (Autonomous precision Landing and Hazard Avoidance Technology), COBALT (CoOperative Blending of Autonomous Landing Technologies), and SPLICE (Safe & Precise Landing – Integrated Capabilities Evolution).

*Project Manager for the STMD SPLICE and COBALT Projects, IPA Detail to JSC from JPL.
†EDL System Capabilities Lead and STMD EDL Principle Technologist.

END-TO-END GN&C FOR THE POWERED DESCENT AND SAFE, PRECISE LANDING OF REUSABLE LUNAR LANDERS. J. Ferreira[1], J. Seabra[2], D. Esteves[3], T. Hormigo[4], J. Oliveira[5], F. Camara[6]
[1-6]Av. Da Igreja 42-6º, 1700-293 Lisboa, Portugal. E-mail: {joao.ferreira, joao.seabra, david.esteves, tiago.hormigo, joao.oliveira, francisco.camara}@spinworks.pt

Introduction: Within the scope of the Global Exploration Roadmap, the establishment of the Deep Space Gateway in the early 2020s is a significant milestone towards the execution of manned missions beyond LEO. One of the major challenges faced is developing the capability to quickly (within 6h), safely (P>99%) and precisely (<<100m) land after a descent from the man-tended Deep Space Gateway towards the lunar surface, nominally at the rim of Shackleton Crater in the Lunar South Pole, and strictly using technologies, sensors and processing units expected to be available today or in the very near future. The work presented here aims at applying the cumulative knowledge developed at Spin.Works towards enabling safe, precise planetary and small body landings.

First, we consider the trajectory design and navigation challenges, assumptions and guidelines, and we describe a means of obtaining a feasible descent and landing trajectory with enough margin for any retargetings which may be commanded by a smart hazard avoidance function when close to landing. Supported by detailed covariance analyses, we select a feasible set of sensors and a corresponding timeline of observations which minimizes cost and development effort while achieving sufficient landing safety and accuracy. Then, we describe both the type of image processing required to identify and/or track ground features in support of a precision landing - which takes the form of a combination of terrain matching techniques for most of the main braking phase, and of feature tracking techniques to minimize lateral drift during the late descent stages -, and we analyze the image size, the angular resolution, and the computational costs required by the image processing functions, given the target frequency at which images need to be processed.

We also define an architecture for the guidance and control modes which is able to effectively reduce the dispersions resulting from the significant NRO escape manoeuver as we leave the vicinity of the Deep Space Gateway, bringing these dispersions to within 1km early after powered descent initiation (PDI), and then, progressively, to a few tens of metres as descent approaches the landing site, such as to guarantee the feasibility of a precision landing with hazard avoidance capabilities. We further demonstrate the integration of a specific guidance mode to enable an active hazard avoidance manoeuvre as we get close to the lunar surface, and we formulate a hybrid vision, inertial and radio-based navigation filter method applicable to the complete descent.

The GN&C functions, once established, are integrated into a high-fidelity, 6 degrees-of-freedom simulation tool. A closed-loop Monte Carlo simulation campaign is then carried out to demonstrate that, for the range of mission and vehicle properties dispersions which are expected for typical commercial lunar landing missions, the integrated GN&C system is consistently able to cancel them and is furthermore able to achieve safe, precise lunar landings with a very high probability, even under the challenging lighting conditions which are expected to be present at the Lunar South Pole.

References:

[1] Klumpp A. R. (1971) Charles Stark Draper Laboratory, R-695

[2] Sostaric R. R. (2007) 30th Annual AAS Guidance And Control Conference

[3] Wilhit A. W. et al (2008) AIAA/AAS Astrodynamics Specialist Conference and Exhibit

[4] Singh G. et al (2007) Aerospace Conference, 2007 IEEE

Making an Onboard Reference Map from MRO/CTX Imagery for Mars 2020 Lander Vision System

Yang Cheng[1] Adnan Ansar[2] Andrew Johnson[3]
Richard Otero[4] Natthan Williams[5]

Jet Prolusion Laboratory, Pasadena, CA, 91007

The Mars 2020 rover will collect samples of Mars that could be returned to Earth as part of a future Mars Sample Return campaign. Therefore, Mars 2020 needs to land in or near regions of Mars that are likely to provide a diverse and compelling set of samples. Most of the best regions for sample collection happen to contain landing hazards including scarps, canyons, mesas, dune fields, rock fields and craters. Mars 2020 is using the Mars Science Laboratory (MSL) Entry, Descent and Landing (EDL) system. This system generates an inertial position by propagating an IMU from the ground navigation position fix prior to entry. The error on this position can be as large as 3.2km. The Lander Vision System (LVS) is being added to Mars 2020 to decrease this position error down to 40 meters relative to a map of the landing site. Using this position, the Guidance, Navigation, and Control (GNC) system selects a landing point that is reachable given the fuel onboard and that also avoids hazards identified a-priori in the map[1][2]. A reference map on board will be used to compare with the descent images for lander localization during the terminal stage of EDL. Therefore, it is highly desirable that the reference map has as little spatial and photometric error as possible. Photometrically, its representation should resemble as much as possible the real descent images to allow easy and reliable terrain matching. Spatially, its local distortion (errors) in both the horizontal and vertical directions should not contribute significantly to the final localization solution. In order to accomplish this, LVS has imposed the following requirements on this reference map:

1. We shall generate a seamless and gap-free LVS map composed of an LVS elevation map and co-registered LVS appearance map over a 30x30 km area at 6m/pixel centered on the targeted landing ellipse.
2. The LVS elevation and appearance maps shall be horizontally co-registered to within 6 m (99%) across the LVS map.
3. The LVS Map shall have an angular error around the normal to the map tangent plane at the center of the map that is less than 1 mrad.

[1] Principal staff member, Mobility and Robotic System Section, JPL,Pasadena, CA 91109
[2] Senior Staff member, Mobility and Robotic System Section, JPL, Pasadena, CA, 91109
[3] Principal staff member, Guidence and Control Section, JPL, Pasadena, CA 91109
[4] Systems Engineer, EDL Systems & Advanced Technologies JPL, Pasadena, CA 91109
[5] Postdoctor, Geophysics & Planetary Geosciences, JPL, Pasadena, CA 91109

4. The LVS map shall have a horizontal distortion in the map from any pixel to any other pixel in the map to less than: 9 m (99%) for distances less than 120 m between pixels and 18 m (99%) for all distances greater than or equal to 1200 m between pixels inside image foot print.
5. The LVS appearance map shall be constructed from images with sun elevation angles in the Map frame that are within +15 and –15 degrees of the sun elevation angle at nominal landing time and are within +35 and –35 degrees of the sun azimuth angle at nominal landing time.

While these requirements are trivial to meet for Earth based mapping, they present major challenges for Mars because

1. We do not have a geodetic control network for Mars with high enough accuracy and resolution. The best Mars geodetic control network from the Mars Orbiter Laser Altimeter (MOLA) is about 500 m/pixel[5]. The MOLA data is not able to provide sufficient ground control for verifying an LVS map geodetically due to the significant variation in spatial resolution associated with MOLA DEMs.
2. We do not have ideal imagery and associated ancillary data. Almost all Mars orbital imagery has been taken with push broom cameras, which are single line sensors arranged perpendicular to the flight direction of the spacecraft. Geometric distortions occur often in these images due to high-frequency spacecraft jitter, which is poorly captured by the s/c attitude sensors.
3. We do no have experience making or prototype examples of such a map. Although Mars surface mapping has a decades long history[4], none of those maps were designed with the requirements of onboard EDL. This is the first ever attempt to build a flight qualified map.

We have taken multiple major steps to ensure the required high fidelity of the map:

1. We have recalibrated the CTX camera model. Two different CTX camera models, one from USGS and another from the CTX camera team, are available[3]. After careful evaluation, we determined that both camera models have significant error intrinsically and extrinsically. In order to remove the camera model error, we chosen a CTX image (D08_030313-1751_XN_045222W) and HRSC map (H4235) over Gale crater to perform a camera calibration. We chose this area because there are corresponding MSL MARDI frame camera images. The MSL MARDI camera was carefully calibrated and has much better geometric stability than the pushbroom imagery. First, we checked the HRSC map distortion by comparing with a single MSL MARDI image (MD0_397502007EDR), and no significant error was found. Then, we matched a few rows of the CTX image to the HRSC map and those matched points were used to generate a new CTX camera model. The new camera model significantly reduces the camera model error from 100s meters to 10s meters and map orientation error from 1.5 mRad to 0.3 mRad.

2. By analyzing the ray gaps between any two CTX stereo image pairs, we found out that there is a systematic time offset between them. This offset can be as much as 30 ms and causes an apparent shift of one image relative to another of up to 100 meters along the orbit direction. A time correction is added to each CTX image resulting in ray gap error reduction to less than 10 meters.

3. After the time correction, the next largest remained error is the s/c jitter. We noticed that almost all CTX images contain some image jitter contributing up to 10s meters map distortion. We

have developed a new pushbroom bundle adjustment method to correct the s/c attitude. This new algorithm effectively reduces the ray gap error induced by s/c jitter to a few meters.

4. We took into account multiple criteria including image coverage, viewing angle, atmospheric opacity, image quality, and orbit determination solution accuracy in selecting the most suitable image sets for map building. For each site, we selected two independent data sets. In each dataset, we have two primary pairs, which can cover more than 30 by 30 km^2 area, and an additional supporting pair, which is used to enhance robustness of the bundle adjustment .

5. Two independent Jezero maps have been produced so far. We have conducted multiple validations including a cross check between the two maps and between CTX and HRSC maps. All these validation results indicate that we are able to produce a map which will meet the LVS map requirements.

Acknowledgments

This research was carried out at the Jet Propulsion Laboratory, California Institute of Technology, under a contract with the National Aeronautics and Space Administration. This work was funded by the Mars Program in the NASA Science Mission Directorate and the JPL Research and Technology Development Program.

References

[1] A. Johnson, Y. Cheng, J. Montgomery, N. Trawny, B. Tweddle, and J. Zheng, "Real-Time Terrain Relative Navigation Test Results from a Relevant Environment for Mars Landing," *Proc. AIAA Guidance, Navigation, and Control Conference*, January 2015.

[2] A. Johnson, et al. "Design and Analysis of Map Relative Localization for Access to Hazardous Landing Sites on Mar", AIAA Guidance, Navigation, and Control Conference, AIAA SciTech Forum, (AIAA 2016-0379)

[3] J.F. Bell III et al., Calibration and Performance of the Mars Reconnaissance Orbiter Context Camera (CTX), Mars, International journal of Mars science and exploration

[4] Kirk, R. L., E. Howington-Kraus, M. R. Rosiek, J. A. Anderson, B. A. Archinal, K. J. Becker, D. A. Cook, D. M. Galuszka, P. E. Geissler, T. M. Hare, I. M. Holmberg, L. P. Keszthelyi, B. L. Redding, A. W. Delamere, D. Gallagher, J. D. Chapel, E. M. Eliason, R. King, A. S. McEwen, and the HiRISE Team, Ultrahigh resolution topographic map- ping of Mars with MRO HiRISE stereo images: Meter-scale slopes of candidate Phoenix landing sites, J. Geophys. Res., 113, E00A24

[5] http://pds-geosciences.wustl.edu/missions/mgs/mola.html

AEROSCIENCES CONSIDERATIONS IN THE DESIGN OF A POWERED DESCENT PHASE FOR HUMAN-SCALE MARS LANDER VEHICLES. A. M. Korzun[1] , K. T. Edquist[1], J. A. Tynis[2], and A. M. Dwyer Cianciolo[1], [1]NASA Langley Research Center, Hampton, VA, USA, [2]Analytical Mechanics Associates, Inc., Hampton, VA USA.

Introduction: A human presence on the surface of Mars has long been a goal of space exploration. Five decades of development and seven successful landings on Mars have yielded a characteristic system for entry, descent, and landing (EDL) derived from improvements to technologies developed for the Viking landers in the 1970s. The 2018 InSight and Mars 2020 missions will fly the same basic EDL system as each of their predecessors. Human exploration on Mars will require payloads an order of magnitude larger and landing accuracy an order of magnitude smaller than a Viking-heritage EDL system [1]. To achieve the necessary deceleration for the massive, human-scale vehicles, the heritage parachute system is replaced with a powered descent phase from supersonic ignition through to a soft touchdown within tens of meters of the target.

Retropropulsion has been the primary descent and landing mechanism for spacecraft operating in near vacuum since the beginning of spaceflight. Propulsive deceleration in atmospheric flight was considered for the Viking program, prior to eventual selection of a supersonic parachute and subsonic propulsive descent and landing. It was well understood at that time that characterizing the propulsive – aerodynamic interference is the engineering challenge in moving from near vacuum to applications in an atmospheric environment.

The interference between the atmosphere and the retropropulsion exhaust plumes can significantly alter vehicle aerodynamics and impact stability and controllability. These interference effects are highly dependent on vehicle and engine configuration and operating conditions. The vehicle's local environment in flight can be very different from that in unpowered flight at the same conditions, due to exhaust plume interference. Retropropulsion exhaust is swept back over the vehicle, altering both aerodynamics and effectiveness of control systems (e.g. RCS or control surfaces) and sensors.

Subscale wind tunnel testing, coupled with analytical approximations, was the approach used to investigate exhaust plume – aerodynamics interference in the 1960s and early 1970s [2,3]. NASA conducted and sponsored a large set of such investigations. With the selection of supersonic parachutes for Viking in the 1970s and focus on exploration of low-Earth orbit with the Space Shuttle in the 1980s and 1990s, development of atmospheric powered descent did not reemerge until the mid-2000s, when NASA identified upper limits on payload delivery to the surface of Mars using supersonic parachute technology.

In the past decade, significant advances have occurred for atmospheric powered descent, from modern wind tunnel testing with inert gas [4-6] to high-fidelity computational flow solutions [7-11] to demonstration of relevant physics in flight [12]. Only in the past few years have efforts begun to emphasize conditions and configurations that are directly relevant to human-scale EDL at Mars.

Impacts of Relevant Physics on Overall Vehicle Design: Atmospheric powered descent challenges traditional processes and dependencies in system design. Changes to a design by one discipline have the potential to affect overall vehicle performance in a more exaggerated fashion than in the case of powered descent with no atmosphere as a result of the sensitivity of the propulsive-aerodynamic interference effects to small changes in configuration or operational environment. Flight mechanics, aerosciences, propulsion, and mechanical design, along with other disciplines, must iterate and integrate at the conceptual design level to produce a closed design satisfying mission requirements with reasonable confidence. As examples, aerosciences may provide limitations on engine operating conditions or engine configuration to avoid interference effects that could potentially impact vehicle controllability, and aerodynamics models can directly impact propellant usage.

This work provides an overview of the current assumptions for the human-scale powered descent phase of EDL at Mars, an overview of relevant physics, an assessment of the present baseline concepts, and discussion of the interdependencies of traditionally 'black box' disciplines in the integrated vehicle design and execution of the powered descent phase. The emphasis is on impacts of the interactions between the atmosphere and retropropulsion exhaust plumes on system performance and the work required to develop and fly such a powered descent system at Mars.

References:

[1] Dwyer Cianciolo A. M. et al. (2010) NASA TM-216720. [2] Korzun A. M. et al. (2009) *Journal of Spacecraft and Rockets, 46,* 5, 929-937. [3] Korzun A. M. (2012) *Georgia Institute of Technology*, Ph.D. Dissertation. [4] Edquist K. T. et al. (2014) *Journal of Spacecraft and Rockets, 51,* 3, 650-663. [5] Berry S. A. et al. (2014) *Journal of Spacecraft and Rockets, 51,* 3, 664-679. [6] Berry S. A. et al. (2014) *Journal of Spacecraft and Rockets, 51,* 3, 724-734. [7] Korzun A. M. et al. (2013) *Journal of Spacecraft and Rockets*, 50, 5, 950-960. [8] Korzun A. M. et al. (2013) *Journal of Spacecraft and Rockets*, 50, 5, 961-980. [9] Schauerhamer D. G. et al. (2014) *Journal of Spacecraft and Rockets, 51,* 3, 693-714. [10] Zarchi K. A. et al. (2014) *Journal of Spacecraft and Rockets, 51,* 3, 680-692. [11] Schauerhamer D. G. et al. (2014) *Journal of Spacecraft and Rockets, 51,* 3, 735-749. [12] Edquist K. T. (2017), AIAA 2017-5296.

PLANNING FOR A SUPERSONIC RETROPROPULSION TEST IN THE NASA LANGLEY UNITARY PLAN WIND TUNNEL. K. T. Edquist[1] and A. M. Korzun[2], [1]NASA Langley Research Center, Hampton, VA, USA, karl.t.edquist@nasa.gov.

Introduction: Future NASA human missions to the surface of Mars will require using retro-rockets beginning at supersonic freestream conditions (supersonic retropropulsion) in order to decelerate vehicles that are at least one order of magnitude heavier than all previous Mars landers [1]. All NASA robotic Mars missions to date, starting with the Viking missions in 1976, used a single supersonic disk-gap-band parachute prior to initiating powered descent at subsonic conditions. The renewed interest in SRP, which was first investigated prior to the Viking missions, will require testing and analysis to address the primary aerosciences risk associated with SRP: interactions between the retro-rocket exhaust plumes and the freestream flow that alter the aerodynamic behavior of the powered descent vehicle. Trajectory simulations that include a powered descent phase currently have simple aerodynamic interference models that are based on unvalidated computational fluid dynamics (CFD) flowfield predictions. Ground and flight test data are needed at relevant conditions in order to quantify uncertainties associated with the aerodynamic interference models. This paper will cover the status of planning for a sub-scale SRP wind tunnel test in the Langley Unitary Plan Wind Tunnel (UPWT) to occur in 2019, in which high-pressure air will be used to simulate the rocket engine exhaust.

Test Overview: NASA previously conducted SRP tests in 2010 (NASA Langley 4x4 UPWT) and 2011 (NASA Ames 9x7 Tunnel) as interest in SRP ramped back up after having been dormant for decades [2, 3]. The previous tests were designed to collect high-quality data against which CFD analysts could calibrate multiple codes [4, 5]. The same wind tunnel model was used in both tests, but the model was not designed to geometrically simulate any particular Mars full-scale reference vehicle. Another limitation of the previous tests is that aerodynamic (non-thrusting) forces and moments were not measured, only surface pressures.

For the upcoming test, geometric scaling and interference force and moment measurements will be added. The two available Mars reference powered descent vehicles are the low lift-to-drag (L/D) inflatable-based vehicle and the mid-L/D vehicle, shown in Figure 1. Each vehicle has eight LO_2/LCH_4 engines. Subscale versions of one or both vehicles will be tested in the UPWT.

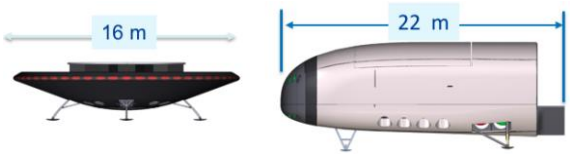

Figure 1. Low-L/D (left) and mid-L/D (right) Mars reference vehicles.

The objectives of the test are to: 1) Design and build a wind tunnel model that is geometrically-scaled from a current Mars reference powered descent vehicle. 2) Design nozzles that, when used with high-pressure air (and possibly helium), simulate the exhaust plume shapes that are predicted using CFD at Mars flight conditions. 3) Collect data across a range of Mach numbers, angles of attack, and thrust levels: discrete surface pressure, global surface pressure, high-speed schlieren video, and non-thrusting forces and moments. 4) Run multiple CFD codes at wind tunnel conditions to compare results to measured data.

Test planning still is in the early stages. Given past experience in the UPWT, it is expected that either model would be no larger than 5-in in diameter (compared to the 4-foot by 4-foot test section). The paper will discuss the latest status, including the flight CFD predictions, methods used to design the model's nozzles in order to match predicted flight exhaust plume shapes, details on planned measurements, and a preliminary test matrix (Mach numbers, angles of attack, and thrust coefficients).

References:

[1] Dwyer Cianciolo A. et al. (2010) NASA TM-216720. [2].

[2] Berry, S. et al. (2014) Journal of Spacecraft and Rockets, Vol. 51, No. 3, pp. 664-679.

[3] Berry, S. et al. (2014) Journal of Spacecraft and Rockets, Vol. 51, No. 3, pp. 724-734.

[4] Schauerhamer, D. et al. (2014) Journal of Spacecraft and Rockets, Vol. 51, No. 3, pp. 693-714.

[5] Schauerhamer, D. et al. (2014) Journal of Spacecraft and Rockets, Vol. 51, No. 3, pp. 735-749.

Detailed investigations of the Huygens spin anomaly in a subsonic wind tunnel: A. Leroy[1], J.-P. Lebreton[2], P. Devinant[1], S. Aubrun[1], S. Loyer[1], J. Simier[1], G. Thébault[1], O. Witasse[3], R. Lorenz[4], M. Perez Ayucar[5], [1] PRISME Laboratory, UPRES 4229, Université d'Orleans, Polytech Orléans, Orleans, France, annie.leroy@univ-orleans.fr, [2] LPC2E, CNRS-Université d'Orleans, Orleans, France, for first author, LPC2E, CNRS-Université d'Orleans, Orleans, France, jean-pierre.lebreton@cnrs-orleans.fr, [3]Science Support Office, ESA/ESTEC, Noordwijk, The Netherlands, [4]JHU/APL, Laurel, MD20723,USA, [5]ESAC/ESA, Villanueva de la Canada, Madrid, Spain.

Huygens is an element of the NASA/ESA/ASI Cassini-Huygens mission, launched on 15 October 1997, to explore in detail the Saturn system. After insertion of the Cassini-Huygens spacecraft in orbit around Saturn on 1st July 2004, Huygens was dropped by Cassini in late 2004. It entered in Titan's atmosphere and descended under parachute to the surface on 14th January 2005, Figure 1.

Figure 1 : Illustration of the Huygens entry and descent

The descent lasted 2 ½ hours. During its release from Cassini, Huygens was imparted a clock-wise spin of about 7.5 rpm. Huygens continued spinning at 7.5 rpm during the 21-day coast to Titan and during the entry that lasted a few minutes. After heat shield deployment, starting at Mach 1.5, a set of 3 parachutes was sequentially deployed to control the descent. The forebody of the descent module was equipped with a set of spin vanes that were designed to control the spin direction and the spin profile during the descent under parachute. For reasons still not fully explained, the spin rate slowed down under the main parachute and reversed direction within 10 min. It continued spinning in the reverse direction under the drogue parachute down to the surface [1], Figure 2.

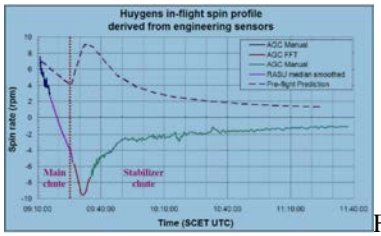

Figure 2: Huygens spin profile (design and in-flight performance)

The Huygens drop test model, which was dropped from a stratospheric balloon above Kiruna in 1995, also spun under parachute in a direction contrary to the expected one. This behavior was not explained.

A comprehensive study of the spin torque was carried out under ESA contract by a Consortium led by Vorticity [2]. This study led to conclude that the spin vanes did not have enough authority to robustly control the spin, and that the spin could have been affected by the appendages.

In order to investigate further the spin anomaly, ESA contracted out a 2-year study to CNRS Orleans that started in November 2017 (ESA Contract: 4000121841/17/ES/JD). The study is jointly carried out by CNRS at LPC2E, and the University of Orleans. The wind tunnel tests are carried out in the framework of aerospace engineering student projects (students from Polytech Orléans – the engineering school of the university of Orléans). During the 1st phase of the study, we performed a series of wind tunnel tests in the subsonic wind tunnel of the PRISME laboratory (Lucien Malavard subsonic wind tunnel). For the purpose of the tests, we constructed a 1:3 mock-up of the Huygens probe and of all its appendages. The appendages were designed to be easily removable in order to study the effects of each of them individually and of several configurations of them on the aerodynamic properties of the Huygens descent module. Aerodynamic loads and moments were measured with and without appendages for different incoming steady flow velocities.

In our presentation, the performances of Huygens will be briefly reviewed and the initial results of the 1st series of tests presented and their initial interpretation

discussed. Input for the 2nd series of tests foreseen to take place in early 2019 will be sollicited during an open discussion at the end of the talk.

References: [1] Lebreton J.-P . et al.. (2005) An overview of the descent and landing of the Huygens probe on Titan, *Nature 438, 90,785-791, doi: 10.10.1038/nature04314*. [2] Vorticity Report, Huygens in flight performance validation, ESA Contract Report : VOR-RE-1508, Iss 2. (Nov. 2015)

A Brief History of InSight Parachute Development and Acceptance for Flight D. M. Kipp[1] and D. Buecher[2], [1]Jet Propulsion Laboratory, California Institute of Technology (devin.m.kipp@jpl.nasa.gov), [2]Lockheed Martin Space Systems (david.buecher@lmco.com)

Introduction: When the Interior Exploration using Seismic Investigations, Geodesy, and Heat Transport (InSight) project was selected by NASA for development in August 2012, the InSight parachute was envisioned as a build-to-print copy of the Mars Phoenix parachute to be qualified by a drop testing campaign using heritage test procedures and equipment. Since that time there have been a continuing series of concerns, originating from ongoing testing and engineering analysis, regarding the structural capability of the parachute during supersonic inflation. This paper will discuss the series of concerns and how the InSight team responded to each in order to get the parachute accepted for flight and on to the launch pad.

Early in the development of the InSight spacecraft, it was found that the peak predicted parachute inflation load exceeded the load that the build-to-print parachute was designed and qualified to accommodate. Several changes were made to accommodate a ~20% increase in the parachute design load. In the same time period, the primary qualification method was changed from drop testing to wind tunnel testing in order to better control parachute peak loads achieved during qualification [1]. The InSight flight parachute lot was manufactured in late 2014 and successfully completed system level testing and qualification in February 2015 [2]. This effort was bookended by two Supersonic Flight Dynamic Tests (SFDT-1 and SFDT-2) that were part of NASA's Low Density Supersonic Decelerator (LDSD) technology demonstrator program. SFDT-1 [3] and SFDT-2 [4] both experienced structural failure during supersonic inflation of their test parachutes, leading to a period of great consternation and learning related to the deployment and inflation of supersonic parachutes. Lessons learned from both SFDT flights were monitored and each lesson learned was addressed by the InSight project; this led to augmentation of the InSight system-level test campaign.

After completing the test campaign, careful inspection of high-speed video revealed a previously unknown twisting behavior of the canopy during parachute extraction, leading to a substantial investigation and risk mitigation effort. [5] Ultimately, the proposed mitigation was unsuccessful, but the cause of twist was determined and the associated risks were deemed acceptable. A final determination was made in December 2015 to accept the parachute for the March 2016 launch. Shortly thereafter, the 2016 launch was suspended, causing a launch slip to May 2018.

During the hiatus, developmental testing by the Mars 2020 project discovered a previously unknown issue of degradation in broadcloth material strength after exposure to the high-temperature bake-out used to achieve the level of microbial reduction necessary to meet planetary protection spore count requirements. This issue also led to a substantial investigation and risk mitigation effort. Once again the risk mitigation effort was ultimately unsuccessful but a greater understanding of the degradation levels, and associated levels of degradation, was achieved, allowing a determination that the associated risks are acceptable for flight.

The history of the InSight parachute program is an interesting case study in the need to be responsive to new knowledge and lessons learned, from both internal and external program activities. InSight experienced a half-dozen interrupts over the course of five years that introduced new threats to the flight parachute. Each of these issues required significant project resources to respond to appropriately. In all but one of these cases, the ultimate determination was either that no mitigation was warranted, or that the attempted mitigation was unsuccessful but the resulting risk was acceptable. Focused investigations and improved understanding ultimately enabled the project to determine that no unacceptable risks have been identified related to the flight parachute.

References:

[1] A. Witkowski, D. Buecher, D. Kipp, *Overview of the Parachute Decelerator System for the InSight Mission*, IPPW-13

[2] Anon., *InSight Parachute Decelerator System Wind Tunnel Test Report*, NCYT-RP-15-0532, Lockheed Martin Space Systems, 2015

[3] E. Blood et al, *LDSD Supersonic Flight Dynamics Test 1: Post-flight reconstruction*, IEEEAC 2014

[4] C. O'Farrell, et al, *Reconstructed Parachute System Performance During the Second LDSD Su-*

personic Flight Dynamics Test, AIAA Atmospheric Flight Mechanics 2016

[5] D. Kipp, D. Buecher, A. Witkowski, *Decelerator Pack Rotation Discovery During Qualification / Acceptance Testing for the InSight Mission,* IPPW-13

RECONSTRUCTED DISK-GAP-BAND PARACHUTE PERFORMANCE DURING THE FIRST TWO ASPIRE SUPERSONIC FLIGHT TESTS.

C. O'Farrell[1], B. S. Sonneveldt[1], and I. G. Clark[1]
[1]Jet Propulsion Laboratory, California Institute of Technology, 4800 Oak Grove Drive, Mail Stop 321-220, Pasadena, CA 91109, ofarrell@jpl.nasa.gov

Introduction: The Advanced Supersonic Parachute Inflation Research Experiments (ASPIRE) project was begun in 2016 to develop a capability for testing supersonic parachutes at Mars-relevant conditions [1]. The initial series of ASPIRE flights are targeted as a risk-reduction activity for NASA's upcoming Mars 2020 project and will test candidate parachute designs for this mission [2]. Two candidate Disk-Gap-Band (DGB) parachute designs will be tested at Mach number and dynamic pressure conditions relevant to Mars 2020: a build-to-print version of the DGB used by the Mars Science Laboratory (MSL) in 2012 and a full-scale strengthened version of this parachute that has the same geometry but differs in materials and construction.

The parachutes are delivered to targeted deployment conditions representative of flight at Mars by sounding rockets launched out of NASA's Wallops Flight Facility (WFF). The sounding rockets carry the experiment to an apogee altitude of between 45 km and 55 km. The 21.5-m parachute is mortar-deployed during the descending portion of the trajectory once the payload reaches a targeted test condition. The deployment, inflation, and supersonic and subsonic aerodynamics of the parachute are analyzed by a suite of instruments including: a three-camera high-speed/high-resolution stereographic video system trained on the parachute, situational awareness video cameras, a set of load pins at the interface of the parachute triple-bridle and the payload, and a GPS and inertial measurement unit (IMU) onboard the payload.

The first ASPIRE sounding rocket flight test (SR01) took place on October 4, 2017 [3]. During this test, an MSL build-to-print DGB was deployed successfully, at a Mach number of 1.77 and a dynamic pressure of 453 Pa. The high speed camera footage captured the deployment and inflation of the parachute. The parachute was found to reach line-stretch 0.961 sec after mortar fire and to fully inflate 0.506 sec later. The peak load at full inflation was found to be 32.4 klbf. Following completion of the mission, the parachute and payload were recovered from the ocean, and data were recovered to characterize the flight environments, loads, and performance of the parachute. The second supersonic test flight, SR02, is scheduled to take place in late March of 2018. The SR02 test article will be Mars 2020's strengthened DGB design. A higher target dynamic pressure was selected for this second flight: 677 Pa, which is expected to yield a peak load at full inflation of approximately 47 klbf.

This presentation will describe the reconstructed behavior of the supersonic parachute systems during SR01 and SR02. It will discuss the performance of the mortar system, the deployment and inflation of the parachutes, and the aerodynamic performance of the test articles in subsonic and supersonic flight. The observed performance will be compared against pre-flight models [4, 5] and historical results. Lessons learned from the first two flights, avenues for further investigation using the data collected during the tests, and the impact of the results on Mars 2020's risk-reduction campaign will be discussed. Finally, plans for ASPIRE third supersonic test flight, which is scheduled for the summer of 2018, will be presented.

References:

[1] O'Farrell, C., Clark, I..G, and Adler, M. "Overview of the ASPIRE Project," presented at the 14th International Planetary Probes Workshop, The Hague, NL, June 2017.

[2] Tanner, C.L., Clark, I.G., and Chen, A. "Overview of the Mars 2020 Parachute Risk Reduction Plan" presented at IEEE Aerospace Conference Paper, Big Sky, MT, March 2018.

[3] O'Farrell, C., Karlgaard, C., Tynis, J.A. "Overview and Reconstruction of the ASPIRE Project's SR01 Supersonic Parachute Test" IEEE Aerospace Conference Paper No. 2233, Big Sky, MT, March 2018.

[4] Muppidi, S., O'Farrell, C., Tanner, C.L., Van Norman, J.W., and Clark,I. G. "Modeling and Flight Performance of Supersonic Disk-Gap-Band Parachutes In Slender Body Wakes", to be presented at the AIAA Atmospheric Flight Mechanics Conference, Atlanta, GA, June 2018.

[5] Way, D. W., "A Momentum-Based Method for Predicting the Peak Opening Load for Supersonic Parachutes", IEEE Aerospace Conference Paper No. 2817, Big Sky, MT, March 2018.

Analysis of Supersonic, Ejected Debris Far-Field Flight Envelope. D. J. Blette[1], [1]Georiga Institute of Technology – Space Systems Design Laboratory (dblette@gatech.edu).

Introduction: The succession from the current state of the art of entry, descent, and landing (EDL) technologies along NASA's goal of extending and sustaining human presence in our solar system will require landing large robotic (~10 mT) and human class payloads (~40-80 mT) on Mars with landed accuracies on the order of meters. Supersonic Retropropulsion (SRP) is one promising candidate supersonic deceleration technology currently under heavy development by both NASA and SpaceX to enable higher mass Mars missions.

To enable the use of SRP, an entry vehicle will likely need to perform a supersonic vehicle reconfiguration during descent to the Martian surface to expose SRP rocket nozzles into the oncoming atmospheric flow. The change between the hypersonic entry vehicle configuration and the SRP-ready vehicle configuration will require the supersonic ejection of the vehicle aeroshell. Once ejected, the discarded aeroshell becomes an intact, solid-mass piece of debris traveling in the same direction as the primary vehicle. This debris poses potential catastrophic recontact risks to the primary descent vehicle. Mitigating these debris recontact risks is a significant hurtle to the development of SRP as a mission-ready technology.

Supersonic descent vehicle reconfigurations have never been performed and there exists no published research in this field. However, supersonic ascent vehicle reconfigurations are routinely performed and are well documented in the literature. The most well-known example of an ascent supersonic vehicle reconfiguration comes from the Space Shuttle ejecting its spent solid rocket boosters on its ascent into orbit. While fundamental differences exist between supersonic descent and ascent vehicle reconfigurations, the two disciplines share some of the same challenges. These similarities allow for ascent analysis methodologies to be adapted and modified for use with descent analyses.

As part of my Ph.D. research I have developed a high-level, rapid analysis methodology that provides mission designers the capability to assess the initial feasibility of numerous candidate descent vehicle reconfiguration architectures during trade-study-level investigations. At IPPW14, I presented a poster giving an overview of the three primary analysis steps of this methodology. The first step develops a flight trajectory envelope for a piece of ejected debris as it undergoes an uncontrolled tumble from a specified altitude and velocity to the Martian surface. From this debris field envelope, a required offset distance between the PDV and the point at which the debris begins to tumble is calculated such that the PDV trajectory will not pass through the debris field envelope. The second step utilizes the previously-calculated offset distance as well as a three-step sequential approximation methodology (TSSAM) to determine an optimized, actively-controlled transit trajectory between the initial point of debris ejection from the PDV and the point at which the debris begins an uncontrolled tumble. This step utilized isolated aerodynamics databases. In the final step, the previously determined transit trajectory is overlaid with interference aerodynamics to increase the fidelity of the approximation of required control impulses during the transit.

This year's poster is a follow-on to last year's poster. It will present in-depth details on the first step of the rapid, supersonic descent separation analysis methodology, namely, the development of the far-field tumbling debris flight envelope and the determination of the required offset-distance for the PDV to safely navigate around said debris-field. In this work, isolated aerodynamics were developed using NASA's inviscid CFD solver, Cart3D, for a representative debris shape. The database covers Mach numbers ranging from 2 to 5 and angle of attack and sideslip angles each ranging from 0 to 360 degrees. A Monte Carlo analysis consisting of 8000 simulated tumbling debris trajectories is performed using NASA's Program to Optimize Simulated Trajectories (POST2). A random-draw approach is used to generate initial conditions for each trajectory from normal 3-sigma uncertainty distributions on aerodynamics, inertia, and initial flight state-vector components.

Slices of the 8000 simulated trajectories are taken at spaced altitude intervals such that at each altitude a constant altitude plane is generated in latitude-longitude space that has 8000 points on it corresponding to the spatial positions of the 8000 simulated trajectories at each defined altitude. For each altitude slice, a bounding ellipse is computed such that 99% of the trajectory intersection points are contained within said ellipse. The bounding ellipses are then combined in altitude, latitude, longitude space to define the composite spatial debris field envelope.

The motion of the PDV (from which the debris was originally ejected) is then simulated as it descends to the Martian surface under the influence of supersonic and subsonic retropropulsion. The PDV trajectory is

then combined with the composite spatial debris field envelope to determine the minimum initial offset distance that ensures the PDV trajectory does not pass through the debris field envelope. Three different approaches to determining the minimum offset distance are compared: debris overshoot, debris undershoot, and debris crossrange mitigation.

ADAPTIVE ATTITUDE CONTROL SYSTEM DESIGNED FOR NASA'S ADEPT ENTRY PROBES

J. Hicks[1],T. Drake[1], J. Mehta[1], S. Sherod[1], E. Zavala[1] P. Papadopoulos[2] S. Swei[2], [1]Student, [2] Advisor, San Jose State University, San Jose, California, 95192

Introduction: EDL on Mars is becoming increasingly challenging as higher payload masses are proposed for future missions. Part of the solution lies in the implementation of lift modulation and lift vector control system designed to increasing the total flight time. This enables bleeding off significant kinetic energy prior to landing. Our design demonstrates the use of active and adaptive mass property adjustments during reentry for precision landing. The technology demonstrated allows stream angle of attack adjustments in flight for reentry vehicle attitude control. This technology demonstrates how the total time of flight can be significantly increased by shifting the center of gravity to improve off nominal (non-zero) L/D vehicle performance. The GN&C strategy and hardware developed will be presented in this publication.

System Breakdown: The current iteration of the system includes a 3D printed 0.7m diameter 70° aeroshell, onboard power, sensors, flight computer, movable C.G. actuators and a structure to maintain safety and stability. The system will be test flown in a vertical wind tunnel similar to the NASA Langley's Vertical Spin Tunnel or the commercially implemented iFLY facilities while remaining untethered similar to testing done on the SR-1 [1]. The untethered nature of the testing environment is intended to allow for implementation of true fully coupled dynamics.

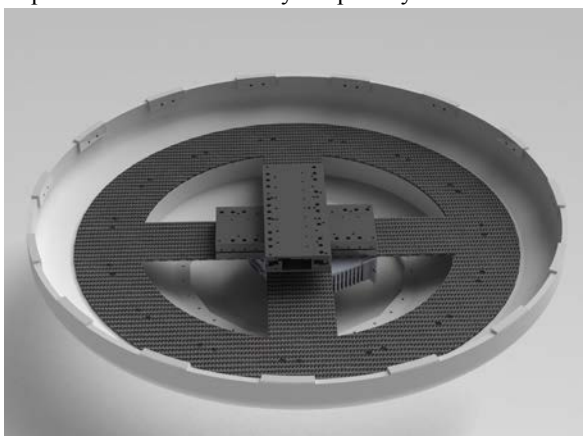

Figure 1. *System architecture of subscale prototype.*

GN&C Subsystem: The GN&C subsystem consists of actuators used for C.G. shifting, gyro and accelerometer sensors, and the onboard computational system to implement control and modeling techniques. A "pilot in the loop" system is used for simplicity and initial testing of the hardware. A modeling actuation subroutine is then implemented to fully define the dynamic model of the system.

Hardware Description: The hardware utilized includes a pair of Motion Solutions linear motor stages stacked perpendicularly, driven by a Copley Controls servo drive powered by MAX Amps Lipo battery packs. Additionally, a Raspberry Pi equipped with a Sense HAT is utilized to collect and compute data as well as enable the system to be controlled wirelessly. The aeroshell is 3D printed for this small scale prototype and the actuators are mounted on a composite bulkhead.

Design Details: The blunt body aeroshell allows for subsonic stability testing inside the iFLY facility. The aeroshell was designed using the same geometric profile of the ADEPT SR-1 [2], but was fully revolved instead of panel revolved. This was done to create a comparable drag profile to previously published data. The aeroshell structure supports and attaches all other subsystems, satisfying all strengths and stiffness requirements while allowing motion within the actuator envelope. The aeroshell structure haul's the major loads; secondary structure supports the electronics module, power box, and amplifier. Due to the weight load on the system, it is crucial to create a prototype with as little mass as possible.

Overall System Improvements: The control system developed here supports the ADEPT GN&C system requirements. This design could be used for future control system implementations on the ADEPT platform.

Impact Statement: This system provides more downrange capability for enhanced lift modulation that further extends the performance of the system. The final presentation at the event will include a detailed design of hardware developed. The study presented engages the commercialization trends of lower earth orbit and beyond with respect to EDL systems.

References: [1]Smith, B. P., Wilder, M. C., Cruz, J. R., and Dutta, S., "Free-Flight Ground Testing of ADEPT in Advance of the Sounding Rocket One Flight Experiment," *IPPW-14*, June 2017. [2] Wercinski, P., Smith B. P., Yount, B. Kruger, C. Brivkalns, C., Makino, A., Cassell, A., Dutta, S. Ghassemieh, S. Wu, S. Battazzo, S., Nishiola, E., Venkatapathy, E., Swanson, G. "ADEPT Sounding Rocket One (SR-1) Flight Experiment Overview," NASA Ames Research Center, 2017

INTEGRATED MISSION AND EARTH REENTRY CAPSULE DESIGN FOR A SAMPLE RETURN FROM THE MOONS OF MARS. T. Hormigo[1], J. Seabra[2], D. Esteves[3], J. Leite[4], R. Couto[5], C. Dias[6], V. Pimenta[7], M. Torres[8], N. Rocha[9], M. Bruxelas[10], M. Castela[11], M. L. da Silva[12], E. R. Pires[13], P. Gil[14]
[1-7] Spin.Works S.A., Av. Da Igreja 42-6º, 1700-293 Lisboa, Portugal. E-mail: {tiago.hormigo, joao.seabra, david.esteves, jose.leite, ricardo.couto, carlos.perestrelo, vasco.pimenta}@spinworks.pt
[8,9] INEGI – Institute of Science and Innovation in Mechanical and Industrial Engineering, Campus da FEUP, Rua Dr. Roberto Frias, 400, 4200-465 Porto, Portugal. E-mail: nrocha@fe.up.pt
[10-12] Instituto de Plasmas e Fusão Nuclear, Instituto Superior Técnico, Universidade de Lisboa, Av. Rovisco Pais, 1049-001 Lisboa, Portugal. E-mail: {marta.bruxelas,maria.castela,mlinodasilva}@tecnico.ulisboa.pt
[13,14] Mechanical Engineering Department, Instituto Superior Técnico, 1 Av. Rovisco Pais, 1049-001 Lisboa, Portugal. . E-mail: {eduardo.pires, paulo.gil}@tecnico.ulisboa.pt

Introduction: A significant portion of the future planetary missions currently in the planning and development phase (to Mars, to the Moon or to small bodies) involve the return of samples to Earth at very high velocities (on the order of 12-14km/s). This presents a significant challenge from the perspective of the structural and thermal preservation of Earth-bound samples during the extreme entry conditions expected (peaking at close to or over 100g). In addition, the intricate requirements applicable to these missions typically result on a minimalist approach to the Earth Return Capsule (ERC) design, yielding a fully passive capsule which needs to be able to cope with both high-g entry and moderate ground impact speeds (~30-50m/s). A multidisciplinary effort was carried out by the Portuguese research and industrial entities IPFN, IST and INEGI, in a consortium led by Spin.Works, to study the different aspects of mission planning, preliminary vehicle design (covering the disciplines of aerothermodynamics analysis, and structural and thermal design) and flight dynamics in an integrated way. A feasible configuration was obtained with a ballistic coefficient of about 50kg/m^2 (terminal velocity around 30m/s) satisfying all the requirements applicable to a mission aimed at returning samples from Phobos.

First, and in order to establish a framework for the work in each of the disciplines covered (while leaving room for iterations where required), a complete mission analysis and trajectory definition study was carried out to identify the total ΔV required. This included estimates for the outbound leg (Earth departure to the surface of Phobos, including an orbital period for detailed observation) and the return leg (where a separate Earth Return Vehicle is used, to which the ERC is attached). The mission is assumed to occur in the 2024-2028 period, and was analyzed on a segment-by-segment basis from Earth Departure to touchdown on Earth after a high speed entry. Mission design elements include the interplanetary transfer to Mars, Mars targeting, orbit insertion and transfer to Phobos, a dynamical analysis of Distant Retrograde Orbits (DROs) around Phobos, the sequence of manoeuvres required to escape from Mars Orbit, the Mars-Earth transfer, Earth Entry Targeting, and Earth atmospheric entry, descent and landing.

Within the mission analysis component, a study of the stability of DROs around Phobos was carried out to identify the robustness of those orbits to dispersed initial conditions, allowing a set of alternative manoeuvre sequences towards a potential Phobos descent and landing phase to be defined, and to identify manoeuvres that may lead to controlled, high-latitude fly-bys starting from (and returning to) a stable DRO, for the purpose of obtaining high resolution data to assist the decision making process related to landing site selection.

Upon return to Earth, the severity of the atmospheric entry environment is initially calculated by connecting an existing entry trajectory propagation tool with a tailored covariance analysis tool and widely used empirical relations to establish dispersed convective and radiative heat fluxes.

For more detailed aerothermodynamics analysis, a shape of the aeroshell similar to the Hayabusa capsule was selected, which ensures aerodynamic stability across all flight regimes. The internal design of this capsule involves an internal structure that uses a combination of metallic foams to shield samples from impact, and a selection of insulation materials aimed at preventing sample temperatures from reaching 40C within the first 4h upon landing, as required by typical sample return mission constraints.

In order to further solidify the Thermal Protection System (TPS) design assumptions beyond the use of empirical expression, aerothermodynamics analysis were carried out based on CFD simulations for both representative trajectories (inertial entry flight path angles of -15.9º and -24.2º), with a sampling of 5 points for each trajectory. These encompass peak convective and radiative heating as well as peak dynamic pressure, predicted from stagnation-point rela-

tions. The thermal nonequilibrium Navier-Stokes code SPARK has been utilized, considering a two-temperature (T,Tv) thermodynamic model, Park's chemistry [5], and a Gupta-Yos transport model [6]. The computed convective heat-fluxes agree well with the correlated results, with a slight difference in the prediction of peak heating (around 8.5km/s instead of 10km/s).

Radiative heating simulations on the stagnation point have also been carried out assuming a tangent-slab geometry. We have used the SPARK-Radiation line-by-line code, with a detailed database of atomic and molecular radiative systems, accounting for both discrete (bound-bound transitions) and continuum (bound-free transitions), with a special emphasis on VUV systems. Owing to the near-complete dissociation of the flow behind the shock, atomic ratiation has been found to be dominant. Radiative losses from absorption in the shock and boundary layer have been found to be limited, so that the flow can be considered optical-thin to a good approximation. Radiative peak heating is found to be significantly higher than the stagnation line correlations, being almost equivalent to convective heating.

A full preliminary aerothermo-structural design cycle was completed for the ERC. Two distinct thermal models were used. Initially, a 1D thermal model provided the temperature evolution in the front and back TPS during re-entry, taking as an input the heating data from each of the reference trajectories. This model enabled fast mass/shape/trajectory/heat-load iterations and first sensitivity analysis, together with the TPS material family pre-selection. Further refinement of the structural design and the 3D Finite Element (FE) thermal-structural model followed. The 3D FE model provided, in addition to a more detailed and complete geometry and mass modeling, the possibility of predicting the thermal evolution inside the ERC post-landing, which is a driving requirement. One driver for the TPS mass is clearly the TPS to base structure bond-line temperature.

Different options were compared in terms of TPS materials performance, availability and suitability for each mission specificity. Low-to-mid density carbon-phenolic ablative materials were selected as the most suitable for the targeted mission, with the reference material PICA (Phenolic Impregnated Carbon Ablator) analyzed for the design of the TPS performed through the NASA's solver PAT0 (Porous Ablation Toolbox). An alternative TPS material, based on European available raw-materials, was also considered and showed an equivalent performance when compared to PICA. However, further gains in TPS performance are typically limited by the associated extensive experimental development work that is required, due to the large number of interacting phenomena and, thus, the complex link between materials design (compositions, combinations, thickness, etc) and performance. In this project, therefore, a sensitivity analysis of the materials parameters was also performed, based on TACOT (Theoretical Ablative Composite for Open Testing), by performing a series of simulations on PAT0 with the objective to assist the development of even higher performance TPS materials. The results have shown that improved performance may be achieved if some material properties are changed. For instance, a decrease of 50% in the thermal conductivity, moving from the density of rayon-based (1.5) to pitch-based (2.2) carbon fibres, increasing 10% in the specificheat capacity, and 10% in the enthalpy of the virgin material, leads to a reduction of, respectively, 20%, 15%, 5%, 14% in the interface temperature, for the same TPS thickness. These results can be an important driver for future TPS development, requiring a careful evaluation on what is possible with currently available technologies, available materials supply and overall impact in the re-entry capsule design.

A key aspect for the vehicle design is an appropriate ERC/TPS mass distribution, something which depends on the complete structural sizing of the base structure, its reinforcements, sub-systems and equipment. Another aspect is the internal sample canister crushable shock absorption system design, and the reserve of internal volume and positions for equipment such as sample door mechanisms, hold-down and release interface points for spin-ejection devices and ballast masses. The layup for the aluminum honeycomb CFRP sandwich base structure thus took into consideration the envelope of all launch loads, aerodynamic reentry-loads, and the crash landing loads.

A fully passive ERC for sample return missions has been often suggested for simplicity and reliability reasons, and in the present work we adopted such an approach; therefore a parachute is avoided in the proposed design, and instead a crushable sample canister shock absorption system has been dimensioned based on aluminum foam alone. Landing site soil compliance (ground penetration) was considered, and the structural shell was dimensioned to maintain a minimum structural integrity so as to not limit the effectiveness of the crushable structure even for the case of impact with a hard surface. The ballistic coefficient design point (~50 kg/m2) was also selected with a low terminal velocity in mind. Two values for the maximum landing acceleration requirement were considered for the design of the crushable structure: 800g and 2000g, since this value might fluctuate depending

on the particular nature of the return samples and their analysis.

Acknowledgments: This work was partially supported by the Portuguese FCT, under Project UID/FIS/50010/2013.This work has been funded by POCI-01-0247-FEDER-003476.

[1] Tauber M. E. and Sutton K. (1991) Journal of Spacecraft and Rockets, Vol. 28, No. 1 , pp. 40-42.
[2] Martin-Mur, T. J., Kruizinga, G. L., & Wong, M. C. (2011). Mars Science Laboratory interplanetary navigaton analysis.
[3] Antimisiaris, M. E., Albers, J., & Jenniskens, P. (2011). Hayabusa re-entry: trajectory analysis and observation mission design.
[4] Desai, P., & Wawrzyniak, G. (2006). Stardust Entry: Landing and Population Hazards in Mission Planning and Operations.
[5]
Park,, C, Jaffe, R. L. and Partridge H. (2001) Chemical-kinetic parameters of hyperbolic earth entry Journal of Thermophysics and Heat Transfer, Vol. 15, No. 1, pp. 76-90.

[6] Gupta, R. N., Yos, J. M. Thompson, R. A. and Lee, K.-P. (1990). A review of reaction rates and thermodynamic and transport properties for an 11-species air model for chemical and thermal nonequilibrium calculations to 30000 K. Technical Report RP 1232, NASA, 1990.

AERODYNAMIC INSTABILITY MEASUREMENT WITH FREE-FLIGT CAPSULE MODEL IN VERTICAL FREE-JET FACILITY DLR-VMK H. Tanno[1], K. Komuro[1], H. Nagai[2] and K. Yamada[3], Sebastian Willems[4], Ali Guelhan[4]. [1]JAXA KSPC Kakuda Miyagi 981-1525 Japan tanno.hideyuki@jaxa.jp. [2]IFS Tohoku Univ. Katahira Sendai Miyagi Japan, JAXA-ISAS Sagamihara Kanagawa Japan, [4]Deutsches Zentrum für Luft- und Raumfahrt e.V, Linder Höhe, 51147 Köln, Germany.

A free-flight technique[1] was applied to measure aerodynamic instability of capsule-shaped test models in the vertical wind tunnel. In this technique, the free-stream dynamic pressure was adjusted to balance the model weight and aerodynamic force (drag force), so that the model can be floating in the vertical free-stream for a long duration (Fig.1). In this technique test model is completely non-restrained for the duration of the test, so it experiences completely free-flight conditions. It means that the technique allows the elimination of a model support sting, ending concerns about the aerodynamic interference between the sting and the base flow of the model, which interference could cause serious errors in measurement for aerodynamic instability of capsules.

The wind tunnel test was conducted with a re-entry capsule (JAXA HTV small reentry test capsule) model in the subsonic-supersonic vertical free-jet facility VMK DLR-Köln. On the test model, an onboard data recorder and six miniature accelerometers were instrumented[2] in the model to measure drag force, lift force, side force, pitching moment and yawing moment. In the wind tunnel test, the model had free-flight during 10 seconds under conditions of test free-stream Mach number 0.25 and Pitching and Yawing moments were successfully measured (Fig.2). Through the post-analysis based on a mathematical model, Pitching and Yawing damping coefficients were evaluated.

References:

[1] Preci, A., Gülhan, A., Clopeau, E., Tran, P., Ferracina, L. and Marraffa, L., "Dynamic Characteristics of MarcoPolo-R Entry Capsule in Low Subsonic Flow". 8th European Symposium on Aerothermodynamics for Space Vehicles, 02.-06. March 2015, Lisbon, Portugal.

[2] Tanno, H., Komuro, T., Sato, K., Fujita, K. and Laurence, S.J., "Free-flight measurement technique in the free-piston high-enthalpy shock tunnel", Rev.Sci.Inst, 85, 045112 (2014)

Fig 1. A capsule shaped test model free-flying in the test section of the vertical wind tunnel DLR-VMK.

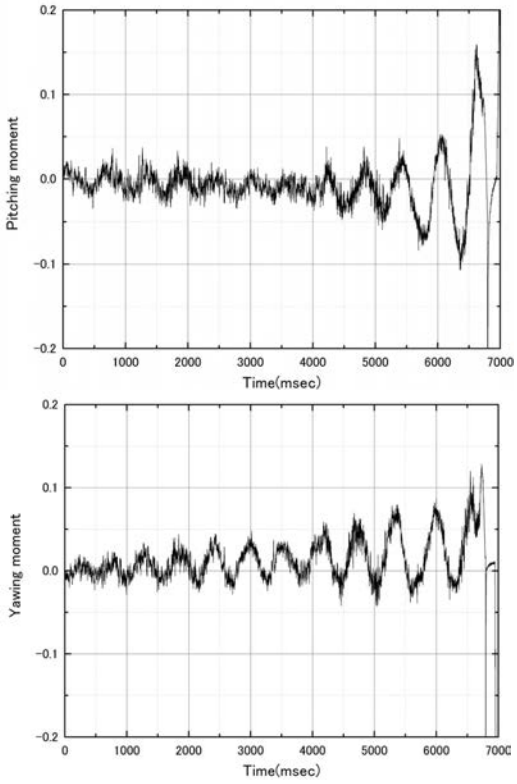

Fig.2 Pitching and Yawing moment histories measured in the VMK wind tunnel (M=0.25).

MINIMUM-FUEL POWERED DESCENT IN THE PRESENCE OF UNCERTAINTY. J. Ridderhof[1] and P. Tsiotras[2], [1]Graduate Student, Department of Aerospace Enginering, Georgia Institute of Technology, Atlanta, GA, 30332, USA. Email: jridderhof3@gatech.edu. [2]Dean's Professor, Department of Aerospace Engineering, and Institute for Robotics and Intellegent Machines.

Introduction: For a spacecraft in powered descent targeting a zero-velocity touchdown, the fuel-optimal control strategy at any given time is to command either maximum or minimum thrust. As a direct consequence, the minimum fuel cost to accomplish a powered descent maneuver *increases* as either the maximum thrust limit is decreased or the minimum thrust limit is increased. And since the same control used to steer a spacecraft in descent is used to correct for deviations from the nominal trajectory, this property leads to an interesting trade on fuel cost and robustness to disturbances. Furthermore, if there are any systematic uncertainties or external disturbances, the control effort required to track the reference is uncertain. One solution to this problem is to set conservative thrust limit margins, and then to evaluate the effectiveness of the margins through Monte Carlo simulation. However, this process is time-consuming and will most likely result in a sub-optimal design.

Method: In this work, we propose a combined approach to trajectory and feedback design using covariance control techniques. First, by restricting the uncertainty in the system to an external white-noise disturbance, we solve for a feedback gain that minimizes the expected integral of norm-squared tracking control effort while satisfying a constraint on the distribution of position and velocity deviation from the target [1], [2]. This procedure yields a closed-loop covariance in both spacecraft *state* and *control*, which we then use to set time-varying reference trajectory thrust margins such that hard throttle limits are satisfied in the presence of disturbances by a user-specified probabilistic bound.

Results: We demonstrate this method in a Monte Carlo simulation of Mars Science Laboratory (MSL)-type powered descent scenario. Results are shown in the figures on the right. In the top figure, we compare a fuel-optimal thrust profile designed with constrant thrust margins to a thrust profile designed using covariance methods. On the middle plot, we can see that the method worked as intended: when using feedback to correct to disturbances, the control magnitude remains within the bounds given by a probabilistic threshold. Trajectories for a select number of the Monte Carlo trails are shown in the bottom plot.

[1] Y. Chen, T. T. Georgiou, and M. Pavon (2016) *IEEE Trans. on Automatic Control 61,* 1158–1169. [2] Ridderhof, J., and Tsiotras, P. (2018) *AIAA SciTech Forum.*

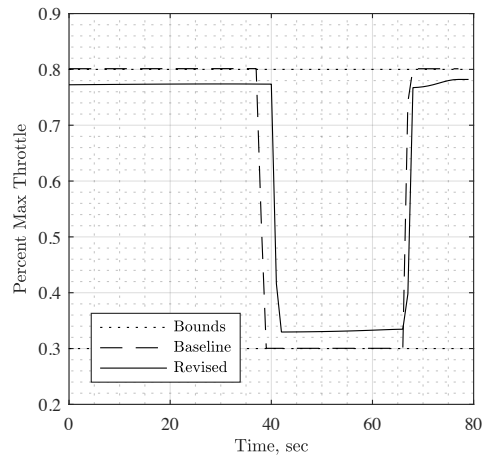

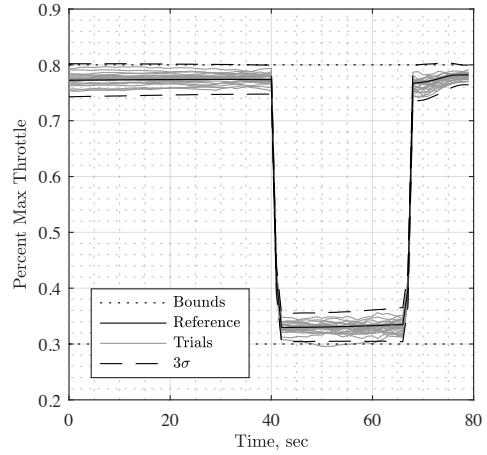

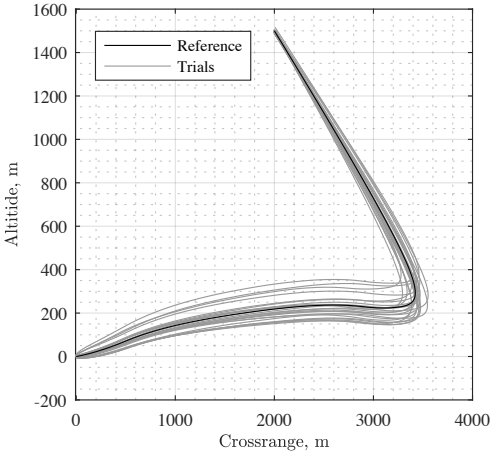

Testing of an instrumented Huygens mock-up in a subsonic wind tunnel : 1st campaign and preliminary results. G. Thébault[1], J. Simier [1], A. Leroy[1], P. Devinant[1], S. Loyer[1], J-P. Lebreton[2] , [1]PRISME Laboratory, UPRES 4229, Université d'Orleans, Polytech orléans, Orleans, France, guillaume.thebault1@etu.univ-orleans.fr , (guillaume.thebault@esa.int as of April 2018), [2]LPC2E, CNRS-Université d'Orleans, Orleans, France.

Huygens, part of the NASA/ESA/ASI Cassini-Huygens mission, is an atmospheric probe that landed under parachute on the surface of Titan, one of the several natural satellites of Saturn, on January 14th 2005. The goal of the mission was to study the physical properties and chemical composition of the atmosphere and the surface of Titan. The bottom of the probe was equipped with a set of spin vanes to control the spin during the descent. External devices accommodated on the rim of the probe also contributed to the spin torque. Although the probe was released from its carrier Cassini with the correct spin, the spin started to slow down and eventually reverse during the descent under parachute. This behavior is still not completely understood. Our work, carried out in the frame of a 2-month student project, is part of a 2-year project (that started in November 2017) whose main aim is to investigate the contribution of each of the external appendages to the spin control [1]. Our work consisted in testing a mock-up of the probe equipped with its appendages (Figure 1) in the Lucien Malavard subsonic wind-tunnel located at the University of Orleans.

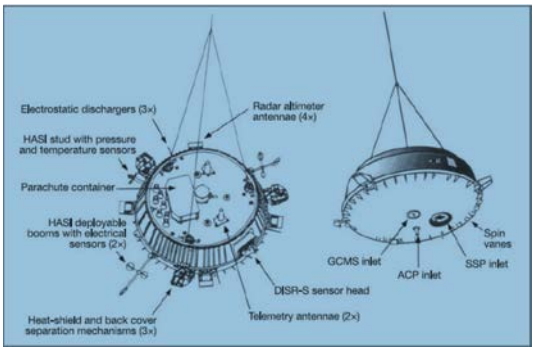

Figure 1: Two different views of the Huygens probe configuration under parachute.

A Huygens test mock-up was designed and built for the purpose of the project. The dimension of the mock-up (scale 1/3) was carefully chosen taking into consideration the descent parameters of Huygens in Titan's atmosphere and the performances of the subsonic wind tunnel (Figure 2).

A test protocol was established that included a large number of combinations of appendages in order to characterize individually the effect of each of them and their combination on the aerodynamic performances of the mock-up. About 200 tests were carried out. They provide a unique set of results that we started to analyse. The initial results of our analysis demonstrate that each individual appendage contributes differently to the aerodynamic characteristics of the mock-up. A data base of all the test data is set-up in order to archive properly the test results and to facilitate their further analyses that will be undertaken by students teams that will follow-up the project. They will also allow to prepare the work to be done by an other group of students during the 2nd year of the project.

Figure 2: Photograph of of Huygens mock-up under test: flow visualisation

References:

[1] Leroy et al, (2018). Abstract submitted to this this workshop.

REQUIREMENTS FOR PINPOINT LANDING OF SPACE RIDER. R. Haya Ramos[1],
[1] SENER Ingeniería y Sistemas, S.A. (Severo Ochoa 4, PTM, 28760 Tres Cantos, SPAIN rodrigo.haya@sener.es).

Introduction: Entry, Descent and Landing (EDL) faces several challenges in order to bring safely a vehicle from orbit flying at several km per seconds to rest onto the surface. The management of the energy drives the design and control of the EDL phases and if landing into a designated zone is required, the targeting of the landing area becomes the second EDL driver.

In case high precision at landing is required either by scientific interest or safety of the operation, more control authority is needed to reach the target within hundreds of meters. On the Earth, the use of wings allows runway landing (precise by definition) and reusability, but the penalty on dry mass cannot be afforded in missions like beyond LEO exploration due to the snow ball effect in mass. Moreover, it has been widely demonstrated, either using capsules or lifting bodies, that wings are not necessary to perform a controlled hypersonic entry flight and hence alternatives are required for the descent and landing.

If the hypersonic guidance is able to leave the vehicle within a few kilometres before initiating the descent sequence the question is how to reduce the dispersion an additional order of magnitude. In case of the Earth, one alternative to the wings is the use of a guided parafoil, that on one side as decelerator continues the philosophy of "brake by free" of the entry and on the other it provides authority for trajectory control and hence targeting capability.

Based on the Intermediate eXperimental Vehicle (IXV) success and assets, an application programme called Space Rider has been proposed to develop an affordable and sustainable reusable European space transportation system to enable routine "access to" and "return from" space, operating in-orbit, de-orbiting, re-entering, landing on ground and being re-launched after limited refurbishment. Space Rider will perform in-orbit operation, experimentation and demonstration for applications like micro-gravity experimentation, orbit applications and In-Orbit Demonstration and validation of technologies. These technologies suitable for demonstration inside Space Rider cover a wide spectrum: from Earth science to planetary Exploration. The re-entry module itself is a test bed for entry technologies as the IXV precursor was. The project is currently running Phase B2 heading towards PDR by the end of the year.

The vehicle used for re-entry is the IXV shape, which is a 5 m long lifting body weighting up to 2.5 Tons. The IXV flight demonstrated in can safely flight down to Mach 1.5 with a precision below 1 km. The first challenge for Space Rider is to pass the transonics and once we are in transonics how to achieve pinpoint landing. Based on the heritage from the X-38 program and the former Parachute Technology Demonstrator project from ESA, the landing under parafoil has been baselined in order to meet the 150 m accuracy requirement at landing on prepared terrain.

The landing under controlled parafoil has been mastered in military applications for precision cargo delivery since decades. However, significant differences arise in case of landing of a space vehicle. First, the need to compensate for the dispersion at the beginning of the descent accumulated during hypersonic and supersonic phases and second the need of a soft landing and safe ground roll.

This paper discusses the requirements and the analysis to achieve this objective, which involves the actuator (the parafoil), the Guidance, Navigation and Control system, the landing system (landing gear) and the operation. The GNC concept is presented as well as first results.

STATUS OF THE INSIGHT ENTRY, DESCENT, AND LANDING SYSTEM B. P. Harper[1], M. R. Grover[1], E. P. Bonfiglio[1], C. E. Szalai[1], D. M. Kipp[1], M. A. Johnson[2], [1]Jet Propulsion Laboratory, California Institute of Technology, Pasadena, CA, [2] Lockheed Martin Space Systems, Littleton, CO .

Introduction: The Interior Exploration using Seismic Investigations, Geodesy, and Heat Transport (InSight) is a NASA Discovery Program mission that will analyze the deep interior structure and processes of Mars. Set to land on November 26th, 2018, InSight offers the opportunity to better understand the formation and evolution of terrestrial planets.

Since being delayed in 2016 due to a persistent vacuum leak in its prime science instrument, InSight and its Entry, Descent, and Landing (EDL) system has faced new challenges in prepraration for the 2018 launch. This talk will discuss the status of the mission, and impacts on the EDL system since the launch slip. In particular, the presentation will cover the InSight project's response to the failed landing of the European Space Agency's Schiaparelli module, and application of key lessons learned.

VENUS AERIAL PLATFORMS STUDY: J. A. Cutts[1] , J. L. Hall[1], L. H. Matthies[1] and T. W. Thompson[1], [1]Jet Propulsion Laboratory, California Institute of Technology, 4800 Oak Grove Drive Pasadena, CA 91109, James.A.Cutts@jpl.nasa.gov.

Introduction: The Venus Aerial Platform Study, previously described in June 2017 at IPPW 14 , is assessing the technologies for exploring Venus with aerial vehicles in order to develop a Venus Aerial Platform Roadmap for the future exploration of the planet. Two Study Team meetings were conducted in May and December of 2017. The first Study Team meeting in late May 2017 focused on the scientific opportunities offered by aerial platforms at Venus, their operating environments, and a technical review of possible aerial platforms. The second meeting in early December 2017 examined the technologies needed for operating in the severe Venus environment. Two companion papers examine results from this study. The paper by Hall et al., describes the trade study between different types of aerial platforms and the science payload fractions achievable with different concepts. The paper by Izraelevitz et al. assesses the feasibility of deploying very small probes capable of reaching the surface of Venus from the altitude of the aerial platform. This paper focuses on other technologies needed to fully exploit the potential of aerial platforms capable of operating in the altitude range 45 km to 65 km.

Key Aerial Platform Technologies: Beyond the technologies of achieving mobility in a planetary atmosphere, other key capabilities are localization of the platform, communications of data and scientific measurement.

Localization: Determining the position of the vehicle is critical to operation of the mission and to acquisitions of certain types of scientific information such as the magnitude and time variation of zonal and meridional winds. When the platform is on the earth facing side of Venus, extremely accurate measurements of position and velocity can be made with the Deep Space Net. A constellation of CubeSats in orbit at Venus can provide comparable information for the side of Venus facing away from the Earth and can reduce the costly use of ground assets through the mission. Comparisons of the positional accuracy achievable with different approaches will be presented

Communications: Transmitting data from the platform directly to Earth is feasible but is only practical when the vehicle is on the earth facing side of the planet and even then is not an efficient approach in terms of either the amount of power consumed on the platform and the DSN antenna time that must be dedicated to data transfer. Orbital relay is the alternative and a SmallSat in a near circular orbit can provide a substantial enhancement in data return. Trade studies indicating dependence of data return on orbital parameters will be presented. Trajectory models indicate that aerial platforms inserted in the equatorial regions will remain in a near equatorial belt indefinitely. A complementary highly-inclined orbiter could guard against the possibility of drift of the platforms to high latitudes. However, solar powered aerial platforms will have limited lifetimes above 70 degrees.

Instrument Miniaturization: The limited payload mass of aerial platforms of 10 to 20 kg means that instruments that are or can be miniaturized define the science that can be performed. For investigating the physics and chemistry of the atmosphere a range of mass spectrometers, tunable diode spectrometers and nephelometers will make it possible to characterize both the active gases and the haze and cloud particles that constitute the atmosphere. For investigating the crusts and interior, a range of infrasound and electromagnetic techniques are also feasible. The capabilities of these different instrument capabilities for meeting Venus science goals will be compared and contrasted.

Next Steps: NASA is currently considering a collaboration with Russia and the Venera D mission in which NASA would furnish an aerial platform. NASA is also examining the feasibility of a program of low cost Venus missions termed Venus Bridge which would include potential balloon mission. The findings of this study will guide what kinds of platforms will be most compatible with these opportunities.

References

[1] Aerial Platform Option for Venus**,** J. L. Hall, M. de Jong, D. Sokol, K. Nock, Leyland Young, G. Landis, J. A. Cutts[1], (companion submittal to IPPW 15)

(2) Minimum Mass Limits for streamlined Venus Probes, J. Izraelevitz and J. L. Hall, (companion paper submitted to IPPW 15)

Acknowledgement: This work was carried out at the Jet Propulsion Laboratory, California Institute of Technology, under a contract with the National Aeronautics and Space Administration.

AERIAL PLATFORM OPTIONS FOR VENUS J. L. Hall[1], M. de Jong[2], D. Sokol[3], K. Nock[4], Leyland Young[5], G. Landis[6], J. A. Cutts[1], [1]NASA Jet Propulsion Laboratory, California Institute of Technology (4800 Oak Grove Drive, Pasadena, CA 91109, jeffery.l.hall@jpl.nasa.gov and james.a.cutts@jpl.nasa.gov), [2]Thin Red Line Aerospace (208-6333 Unsworth Rd., Chilliwack, BC, Canada V2R 5M3, maxim@thin-red-line.com), [3]Northrup Grumman Aerospace Systems, 1 Space Park Blvd., Redondo Beach, CA 90278, Daniel.Sokol@ngc.com), [4]Global Aerospace Corporation, 12981 Ramona Blvd Suite E, Irwindale, CA 91706, kerry.t.nock@gaerospace.com), [5]Wallops Flight Facility, Goddard Space Flight Center, 32400 Fulton St., Wallops Island, VA 23337, leyland.g.young@nasa.gov), [6]Glenn Research Center, 21000 Brookpark Rd., Cleveland, OH 44135, geoffrey.landis@nasa.gov)

Introduction: This paper summarizes the approach and results from a recent NASA-sponsored study on aerial vehicle options for flying in the Venusian atmosphere[1]. This study consisted of two multi-day workshops with intervening time for science and engineering analysis and involved a cross-disciplinary team of scientists, engineers and technologists drawn from NASA centers, industry and universities. The purpose was to identify what science could be obtained from different platforms, quantify the resource needs of mass, power and volume, assess the technological maturity of those platforms and provide guidance on required technology development investments to achieve flight readiness. The specific platforms considered were a superpressure balloon, four different types of variable altitude balloons, solar-powered airplane and a hybrid vehicle ("VAMP") where lift is generated by both aerodynamic and buoyant forces. Table 1 lists the platforms and summarizes their key features. Examples of some of these vehicles are shown in Fig. 1.

Quantitative mass comparisons between the platforms were performed in a trade study that used a cloud-level exploration scenario across a range of 50 to 60 km altitude and with a 10 kg science instrument payload. Given that Venus-relevant designs were rudimentary for most vehicle types, the analysis approach relied extensively on extrapolations from similar Earth vehicles or rules of thumb gleaned from various Venus studies and mission proposals. The study team performed cross-checks to try and ensure fair comparisons between the platforms.

Below the cloud exploration (<48 km) is also possible with the variable altitude platforms, although the large reduction in solar flux tends to preclude sustained powered flight with the airplane and hybrid vehicle options. Although no detailed trade study was performed to systematically quantify the below-the-cloud options, a number of opportunities and constraints were noted in the study to guide future mission planning and technology developments.

The paper concludes by presenting the technology development roadmap matched to future mission opportunities, along with a discussion of the status and key technical challenges for each aerial vehicle option.

Table 1: Platform Type Comparisons

Platform Type	Main Buoyancy Method	Envelope Type	Altitude Change Method
Super-pressure Balloon	He	super-pressure	None
Pumped Helium (He)	He	zero-pressure	compression and storage of He
Mechanical compression balloon	He	super-pressure	compress envelope
Air ballast balloon	He	Zero- or super-pressure	compress and store ambient air
Phase change fluid (PCF) balloon	He	zero-pressure	change of phase of PCF
Solar airplane	propulsive-driven aerodynamic lift	N/A	lift modulation
VAMP (aero-braked)	buoyancy & lift	super-pressure	lift modulation

Results: The science trade study shows a clear increase in scientific payoff as one progresses through the sequence of aerial platforms from drop probes to constant altitude superpressure balloons to variable altitude superpressure balloons to fully 3D controlled vehicles. However, the increased value for fully 3D controlled vehicles is only achieved if the vehicle can broadly target surface locations and measure them from below the clouds. If that capability is not provided then science return is maximized with simpler altitude-controlled balloons. Constant altitude balloons were found to provide significant science return but ranked significantly lower than variable altitude balloons given their inability to measure vertical changes in winds, solar and IR fluxes, trace chemical species and cloud aerosol properties.

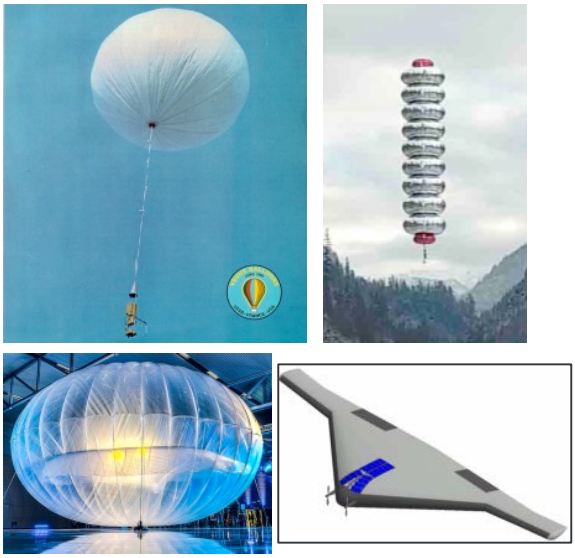

Fig. 1: VEGA superpressure balloon (top left), Thin Red Line variable altitude mechanical compression balloon (top right right), Google Loon air ballast balloon (lower left), Northrup Grumman VAMP vehicle concept (lower right).

All platform options except VAMP require aeroshell protection during the hypersonic atmospheric entry phase of the mission; VAMP enters on its own from a low orbit at < 8 km/s. We defined a metric called System Arrival Mass to be the total mass of the system arriving at Venus after separation from a carrier spacecraft including the aerial vehicle itself and all other required supporting mass such as the aeroshell, parachutes and any propulsion system required upon approach.

We found that the simplest option of a constant altitude superpressure balloon (like the Soviet VEGA balloons) requires the least system arrival mass and that the 3D controlled airplane and VAMP vehicles require the most. The set of four variable altitude balloons all have comparable system arrival mass requirements between those two extremes. Note that the solar airplane in this study is restricted to all-daylight conditions with altitudes above 66 km at the sub-solar point to have enough sunlight to run the propulsion system and maintain steady flight. All of the other options can use buoyancy to float at night and survive on stored energy.

All of the vehicle options require significant prototyping and testing to achieve sufficient technological maturation for a Venus flight mission. This includes verification of basic flight performance, packaging survivability, deployment and inflation process and, for VAMP, the hypersonic entry phase from orbit.

Acknowledgements: The research described in this paper was funded by the Jet Propulsion Laboratory, California Institute of Technology, under a contract with the National Aeronautics and Space Administration. The information in this document is predecisional, and is provided for planning and discussion only.

References: [1] Cutts et al (2018), (in press).

BALLOON-BORNE INFRASOUND AS A REMOTE SENSING TOOL FOR VENUS – PROGRESS IN 2017. S. Krishnamoorthy[1], V. Lai[2], L. Martire[3], E. Kassarian[3], A. Komjathy[1], J. A. Cutts[1], M. T. Pauken[1], R. F. Garcia[3], D. Mimoun[3], J. M. Jackson[2], D. C. Bowman[4]

[1] Jet Propulsion Laboratory, California Institute of Technology, Pasadena, CA
[2] Seismological Laboratory, California Institute of Technology, Pasadena, CA
[3] Institut Supérieur de l'Aéronautique et de l'Espace (ISAE), Toulouse, France
[4] Sandia National Laboratories, Albuquerque, NM

Introduction: Over five decades have passed since the Mariner spacecraft visited Venus in 1962. However, much of Venus' sub-surface and lower-atmospheric dynamics remains a mystery. Compared to Mars and other planets in the solar system, our knowledge of Venus has shown relatively slow progress. This is in large part due to the technological challenges in exploring Venus posed by its extremely high surface temperature and pressure conditions [1]. These adverse conditions have thus far rendered long-duration experiments on or near the surface impossible. Therefore, while Mars already has a fleet of rovers on the surface and will welcome the InSight lander in the coming months, a similar experiment on Venus is years, if not decades away. In this presentation, we will explore the possibility of performing planetary science on Venus using infrasound (pressure waves with frequencies less than 20 Hz) as a remote sensing tool and discuss the progress our group has made in the last year.

Infrasound and Atmospheric Remote Sensing: Infrasound has been recorded from a variety of events on Earth. Of particular interest to planetary science are infrasound signals from quakes, volcanic eruptions, thunderstorms, and meteors [2,3,4,5]. While infrasound generation from quakes relies on the coupling between the solid planet and the atmosphere, in the case of volcanic eruptions, thunderstorms, and meteors, energy is directly deposited into the atmosphere. Venus offers a unique opportunity for the use of infrasound as an investigative tool – due to its dense atmosphere, energy from seismic activity couples with the Venusian atmosphere up to 60 times more efficiently than Earth [6]. As a result, infrasound waves from Venus quakes are expected to be an almost exact replica of ground motion. Infrasound is also known to propagate long distances from generating events with relatively little attenuation, thereby making it an effective alternative to placing sensors on the surface of Venus. Lastly, acoustic sensors used to capture infrasound may also be used to investigate low-frequency, large-scale planetary atmospheric features such as planetary-scale gravity waves, which have recently been observed by JAXA's Akatsuki mission [7].

Balloon-based Infrasound Detections on Venus: The main advantage of performing balloon-based infrasound science on Venus is the extension of mission lifetimes by virtue of being in a more benign environment. Compared to 460 C and 90 atmospheres on the surface, the temperature and pressure are more Earth-like at 55-60 km altitude. Vega balloons floated at this altitude have already been demonstrated to survive longer than the Venera landers [8]. Further, acoustic sensors greatly benefit from being on a platform that floats with the wind. In fact, Krishnamoorthy et al. [9] recently showed that the noise level on a pressure sensor that floats with the prevailing wind can be much lower than that of a stationary platform. Lastly, the super-rotation of the Venusian atmosphere equips balloons with a much larger coverage zone than a single lander on the surface.

From a scientific perspective, there are also several challenges with performing such an experiment. Signals are often weak compared to the noisy background. Multi-channel correlation is difficult, since balloon platforms have payload restrictions and cannot feasibly support a large number of instruments. In the presence of a variety of infrasound-generating events, source discrimination and localization also represent challenges that need to be overcome.

Progress in 2017: Our team has been involved in a campaign to use the Earth's atmosphere as an analog testbed for Venus to demonstrate the feasibility of balloon-based infrasound science on Venus and address the challenges associated with it. Significant progress has been made in 2017. We conducted an extensive field experiment in Pahrump, NV in June 2017, where the ground was repeatedly struck with a seismic hammer to create small artificial earthquakes. The strikes generated infrasound signals, which were detected by ground-based and balloon-borne high precision barometers. A variety of signal processing techniques were used to discern the weak (peak-to-peak fluctuation of ~1 Pa) infrasound signal from the background, including signal filtering, stacking and wavelet transforms. Further, barometer records were correlated with ground motion gleaned from geophones deployed near the seismic hammer site. Complex simulations incorporating elastodynamics for the solid Earth coupled with Navier-

Stokes equations for the Earth's atmosphere [10] were used to generate and compare expected waveforms with the measured signals.

In another experiment in December 2017, we investigated the possibility of de-noising the pressure signal by subtracting fluctuations due to the motion of the balloon by using an inertial measurement unit.

Lastly, we have successfully conducted a campaign of recording far-field infrasound generated by rocket launches from Vandenberg Air Force Base, over 200 km away. Pressure records from these launches are being used to further develop our source inversion and localization techniques.

Results from all of the above campaign activities will be summarized in our presentation. In the future, we look forward to conducting campaigns to detect and characterize infrasonic signals in the Earth's stratosphere – the closest analog to what we would expect in Venus' atmosphere at 55-60 km altitude. Proving the feasibility of this technology in the Earth's stratosphere would make a strong case for the detection of similar signals on Venus, which would pave the way for rich opportunities in seismology and atmospheric science.

References:

[1] Wood, A. T., R. B. Wattson, and J. B. Pollack (1968), Venus: Estimates of the surface temperature and pressure from radio and radar measurements, *Science*, **162 (3849)**, doi:10.1126/science.162.3849.114.

[2] Arrowsmith, S. J., R. Burlacu, K. Pankow, B. Stump, R. Stead, R. Whitaker, and C. Hayward (2012), A seismoacoustic study of the 2011 January 3 Circleville earthquake, *Geophysical Journal International*, **189 (2)**, doi:10.1111/j.1365-246X.2012.05420.x.

[3] Matoza, R. S., A. Jolly, D. Fee, R. Johnson, B. Chouet, P. Dawson, G. Kilgour, B. Christenson, E. Garaebiti, A. Iezzi, A. Austin, B. Kennedy, R. Fitzgerald, and N. Key (2017), Seismo-acoustic waveeld of strombolian explosions at yasur volcano, Vanuatu, using a broadband seismo-acoustic network, infrasound arrays, and infrasonic sensors on tethered balloons, *The Journal of the Acoustical Society of America*, **141 (5)**, doi:10.1121/1.4987573.

[4] Farges, T. and E. Blanc (2010), Characteristics of infrasound from lightning and sprites near thunderstorm areas, *Journal of Geophysical Research: Space Physics*, **115(A6)**, doi:10.1029/2009JA014700.

[5] Donn, W. L. and N. K. Balachandran (1974), Meteors and meteorites detected by infrasound, *Science*, **185(4152)**, doi:10.1126/science.185.4152.707.

[6] Garcia, R., P. Lognonné, and X. Bonnin (2005), Detecting atmospheric perturbations produced by Venus quakes, *Geophysical Research Letters*, **32 (16)**, doi:10.1029/2005GL023558.

[7] Fukuhara, T., M. Futaguchi, and G. L. Hashimoto et al. (2017), Large scale stationary gravity wave in the atmosphere of Venus, *Nature Geosciences*, **10**, doi:10.1038/ngeo2873.

[8] Sagdeev, R. Z., V. M. Linkin, and J. E. Blamont et al. (1986), The VEGA Venus Balloon Experiment, *Science*, **231**, doi:10.1126/science.231.4744.1407

[9] Krishnamoorthy, S., A. Komjathy, and M. T. Pauken et al. (2018), Detection of artificial earthquakes from balloon-borne infrasound sensors, *submitted to Geophysical Research Letters*.

[10] Brissaud Q., R. Martin, R. F. Garcia, and D. Komatitsch (2017), Hybrid Galerkin numerical modelling of elastodynamics and compressible Navier–Stokes couplings: applications to seismo-gravito acoustic waves, *Geophysical Journal International*, **210**, doi: 10.1093/gji/ggx185.

ANALYSIS FOR LITHIUM-COMBUSTION POWER SYSTEMS FOR EXTREME ENVIRONMENT SPACECRAFT – POSTER & PRESENTATION. Christopher J. Greer[1], Michael V. Paul[2], and Alexander S. Rattner[1]. [1]Department of Mechanical and Nuclear Engineering, The Pennsylvania State University, University Park, PA 16802. Email: czg5155@psu.edu, alex.rattner@psu.edu, [2]Applied Physics Laboratory, John Hopkins University, Laurel, MD 20723. Email: michael.paul@jhuapl.edu

Introduction: Reports for both Venus [1] and Europa surface mission [2], [3] concepts and the National Research Council's Decadal Survey [4] have identified the scientific value for landing on the surface of these bodies. However, the extreme environments and low solar availability on the surfaces of these bodies impose power and cooling challenges for future missions.

The opacity of the Venus atmosphere and Europa's distance from the Sun limit the use of solar photovoltaic generators for the desired power range of hundreds of Watts [5]. Because of this low solar availability, stored energy sources are necessary to power surface landers [6]. While electrochemical batteries represent a mature power system option, they significantly limit mission scope. The longest duration mission on the Venus surface was Venera 13, at just over two hours. This time constraint was due to reliance on battery power and limited cooling capacity. A mission concept for a Europa lander suggests a battery power source for a mission duration of twenty Earth days [2]. However, with battery powered missions, the duration on either target's surface will be limited by the mass available for the mission and the ability to survive the extreme environment.

Therefore, extended mission duration concepts have focused on Radioisotope Thermal Generators (RTG) power plants. Due to the RTG's dependency on plutonium 238, a RTG powered mission effectively requires a New Frontiers ($600M – $1B) or Flagship-class ($2B+) mission budget. Low cost, power, and mass radioisotope power systems have been proposed to meet this need, but have not yet been demonstrated [7]. Recently, a metal-fueled, combustion-based power plant has been proposed as a low-cost alternative for extended duration missions [6]. On many planetary bodies, the atmosphere could be used as in-situ oxidizer for reactive metal fuels (e.g., CO2 on Venus), significantly reducing carried mass requirements. The main benefit of a metal combustion-based power plant is the more than three times greater system specific energy when compared with sodium-sulfur batteries for a Venus mission [6]. Detailed surveys of available power systems and the benefits for metal combustion-based power plants have been performed [6], [8]. However, detailed analysis of the heat transfer processes to deliver energy from such reactors to potential heat engines has not yet been performed.

Present Investigation: A detailed thermodynamic and heat transfer model has been developed to predict performance at target operating conditions. The model receives inputs of oxidizer mass flow rate and ambient conditions to predict the thermal power output of the reactor system, accounting for heat losses.

Model results show that a lithium combustion power system with an in-situ, carbon-dioxide oxidizer could power a Venus lander for up five days (24 hour, Earth day) with 185 kg of fuel, delivering 14 kW_{th} thermal energy continuously. Even greater durations are possible if lower power missions are considered. A lithium combustion power system with a sulfur-hexafluoride oxidizer could power a Europa lander at 94W with a Stirling engine for up to twenty days with 43 kg of reactants mass.

Experiments were performed to characterize the Li-CO_2 combustion technology and demonstrate the ability to deliver energy. A surface reaction with high temperature heat delivery was achieved. However, future tests are in development to increase the combustion efficiency with submerged oxidizer injectors and to demonstrate power generation with TEGs.

In ongoing work, an experimental study under the NASA Hot Operating Temperature Technology (HOTTech) program will test a concept to convert the combustion heat to electrical power with a high-temperature turbine power cycle. The system model will be refined with experimental data to aid design of a future packaged prototype system. This combination of experimentation and modeling will enable the characterization of lithium combustion power technology for spacecraft applications.

Conclusions: The goal of this study is to characterize the proposed power plant concepts for their target environments, and inform engineering design. The versatility a lithium combustion power system provides a lander opportunities, including: in-situ resource utilization, higher power instrumentation, variable power output, and longer mission durations. Experimental and modeling efforts will indicate the potential for lithium combustion power systems. These findings will also enable assessment of the potential to meet other space exploration needs.

Acknowledgements: This work is supported through NASA Innovative Advanced Concepts (NIAC) Phase II funding, and NASA's Planetary Science Division's HOTTech funding.

References: [1] M. Bullock, J. L. Hall, D. A. Senske, J. A. Cutts, and R. Grammier, "Venus Flagship

Study Report," National Aeronautics and Space Administration, Jet Propulsion Laboratory, Pasadena, California, 2009. [2] K. P. Hand, A. E. Murray, J. B. Garvin, and the Science Definition Team, "Report of the Europa Lander Science Definition Team," National Aeronautics and Space Administration, Jet Propulsion Laboratory, Pasadena, California, JPL D-97667, 2017. [3] E. S. Team, "Europa Study 2012 Report," National Aeronautics and Space Administration, Jet Propulsion Laboratory, Pasadena, California, JPL D-71990, 2012. [4] S. W. Squyers, "Vision and Voyages for Planetary Science in the Decade 2013-2022," Washington, DC, The National Academies Press, 2013. [5] G. a. Landis and E. Haag, "Analysis of solar cell efficiency for Venus atmosphere and surface missions," 11th International Energy Conversion Engineering Conference, vol. 2, no. V, Reston, Virginia: American Institute of Aeronautics and Astronautics, 2013. [6] T. F. Miller, M. V. Paul, and S. R. Oleson, "Combustion-based power source for Venus surface missions," Acta Astronautica, vol. 127, pp. 197–208, 2016. [7] J. F. Mondt, M. L. Underwood, and B. J. Nesmith, "Future Radioisotope Power Needs for Missions to the Solar System," in 32nd Intersociety Energy Conversion Engineering Conference, Honolulu, HI, USA, 1997, pp. 460–464. [8] T. Baker, T. F. Miller, M. Paul, and J. A. Peters, "The Use of Lithium Fuel with Planetary In Situ Oxidizers," in 10th Symposium on Space Resource Utilization, Grapevine, Texas, 2017, no. January, pp. 1–11.

POST FLIGHT ANALYSIS OF THE RADIO DOPPLER SHIFTS OF THE EXOMARS SCHIAPARELLI LANDER. Ö. Karatekin[1], B. van Hove[1], F. Ferri[2], S. Asmar[3] [1]Royal Observatory of Belgium, Ringlaan 3, Brussels/Uccle 1180, Belgium, (ozgur.karatekin@observatory.be), [2]Università degli Studi di Padova, Centro di Ateneo di Studi e Attività Spaziali "Giuseppe Colombo" (CISAS), Italy, [3]Jet Propulsion Laboratory, California Institute of Technology, California, USA.

Schiaparelli, the Entry Demonstrator Module (EDM) of ESA's ExoMars 2016 mission entered Mars atmosphere at 14:42 GMT on 19 October 2016. All ensuing communications during the entry and descent were transmitted by a UHF (ultra-high frequency) radio on board using an antenna on the backshell of the heatshield during entry, and then using the spiral-shaped antenna on the top deck of the lander after it separated from the parachute. UHF has been selected to be used for Proximity Relay Communications. Nevertheless, the Giant Metrewave Radio Telescope (GMRT), located at Pune, India, was able to track the Schiaparelli in real-time prior to atmospheric entry as well as during its atmopsheric descent except during the plasma blackout. The real-time signal was received with a delay of 9 minutes 47 seconds due the distance between Mars and Earth. The GMRT lost the tack of EDM shortly before the expected touchdown.

The Schiaparelli radio signal were also recorded by ESA orbiters in Mars orbit, namely, Mars Express (MEX) and Trace Gas Orbiter (TGO) and downlinked later to the ground stations. MEX Melacom communication system monitored and recorded carrier signals from the module in open-loop mode. In addition to the carrier signal, TGO Electra communication system was able to record the telemetry. The essential data as well as the Doppler information were extracted from the relayed data by ESOC following the receipt of data on ground and transfer to the mission control centre in Darmstadt. The communications during the descent were interrupted during the plasma blackout which lasted about 1 minute.

In this study we present the postflight analysis of the radio communications of ExoMars 2016 Schiaparelli during its entry and descent through the Martian atmosphere. The Doppler shifts and power levels received by radio receivers on Earth and by Mars relay orbiters will be analyzed to provide information on EDM state, trajectory and on Mars atmosphere.

MARS 2020 ENTRY, DESCENT, AND LANDING UPDATE. Erisa K. Stilley*, Allen Chen, Richard Otero, Aaron Stehura, and Gregorio Villar. Jet Propulsion Laboratory, California Institute of Technology (Pasadena, CA, 91109, *ekhines@jpl.nasa.gov)

Abstract: Building upon the success of Curiosity's landing and surface mission, the Mars 2020 project is a flagship-class science mission intended to address key questions about the potential for life on Mars and collect samples for possible return to Earth by a future mission [1]. Mars 2020 will also gather knowledge and demonstrate technologies that address key challenges for future human expeditions to Mars. Based on the highly successful entry, descent, and landing (EDL) architecture from the Mars Science Laboratory (MSL) mission [2], Mars 2020 will launch in July of 2020 and land on Mars in February of 2021.

The mission takes advantage of the favorable 2020 launch/arrival opportunity; this enables the delivery of a larger, heavier, and more capable rover to wider variety of potential landing sites. While Mars 2020 inherits most of its EDL architecture, software, and hardware from MSL, a number of changes have been made to correct deficiencies, improve performance, and increase the overall robustness of the system. Over the past year, significant deliveries in hardware and software have been made, including some that support the new Terrain Relative Navigation (TRN) system, a key capability to reaching the candidate Mars 2020 landing sites. These deliveries kick off an extensive test program for the flight system. There are continuing efforts to increase robustness of the parachute design through testing and analysis. Additionally, the Mars 2020 team continues to engage in landing site selection activities in support of selecting a final landing site in the fall of 2018.

This paper presents an update on the development and major milestones of the Mars 2020 EDL system, and a brief look at what remains ahead.

References:

[1] Mustard, J., et al. (2013) "Report of the Mars 2020 Science Definition Team," Tech. rep*., Mars Exploration Program Analysis Group (MEPAG).*

[2] Steltzner, A. (2013) *"Mars Science Laboratory Entry, Descent, and Landing System Overview", AAS 13-236.*

MARS 2020 LANDING SITE EVALUATION: DIGITAL TERRAIN MODEL DEVELOPMENT AND EVALUATION. R. L. Fergason[1], T. M. Hare[1], D. P. Mayer[1], D. M. Galuzska[1], M. P. Golombek[2], R. E. Otero[2], and B. L. Redding[1], [1]U.S. Geological Survey, Astrogeology Science Center, Flagstaff, AZ, USA, rfergason@usgs.gov, [2]Jet Propulsion Laboratory, California Institute of Technology, Pasadena, CA, USA.

Introduction: The Mars 2020 rover will explore a region of Mars where the ancient environment may have been favorable for microbial life, and will investigate martian rocks for evidence of past life. Three candidate sites are currently being considered as potential landing sites, including Columbia Hills/Gusev, Jezero crater, and NE Syrtis. Columbia Hills/Gusev was the location where the Mars Exploration Rover Spirit landed and operated from 2004 to 2010 [1-2]. This abstract focuses on the present exploration of Mars, and is relevant to the planetary probe community as it includes Digital Terrain Model (DTM) product development and the evaluation of slope and topography for the assessment of landing site safety.

The Mars 2020 mission has an ellipse ranging from 18 km by 14 km to 13 km by 7 km, depending on atmospheric conditions, and is oriented roughly east-west. Terrain Relative Navigation (TRN) is a new capability being developed at the Jet Propulsion Laboratory to enable the spacecraft to autonomously avoid small hazards (e.g., rock fields, crater rims) that exceed the relief and rock constraints. This capability allows small-scale hazards to be present in the landing ellipse, providing greater flexibility in spacecraft landing location. We are generating DTMs to fulfill two objectives: 1) to facilitate the identification and characterization of potential slope hazards on the surface within the landing ellipse, and 2) to produce a flight-quality DTM for use on-board the spacecraft in conjunction with TRN.

Digital Terrain Model (DTM) Generation Methods: To generate a DTM, the methods used for the evaluation of the InSight mission landing site [3-4] were also employed, and are summarized here. After a series of pre-processing steps using the ISIS3 software system [5], the images, trajectory, and pointing data are transferred to the commercial software system SOCET SET® from BAE Systems [6] where matching software correlates features in each image and uses the known camera orientation to determine topography. The images are then controlled and bundle adjusted using the SOCET SET® program Multi-Sensor Triangulation (MST), and then DTMs are produced by performing high-density area- and feature-based automated matching with the Next Generation Automatic Terrain Extraction (NGATE) module [7]. We then perform manual updates within a 3D editing environment to correct errors and remove artifacts (determined by visual inspection) from the automated matching process. This final editing significantly improves the quality of the DTM, and is critical for producing DTMs of high enough quality to certify a landing site.

Surface Topography Characterization: High-resolution DTMs provide critical information regarding the topography of the landing site region, and allow engineering criteria to be evaluated and certified. The Mars 2020 engineering requirements that are addressed using DTMs include: 1) Mars Orbiter Laser Altimeter (MOLA) [8-9] elevation below -0.5 km for sufficient atmosphere to slow the spacecraft during Entry, Descent, and Landing (EDL), 2) less than ~100 meters of relief at baseline lengths of 1-1,000 meters to ensure proper control authority and fuel consumption during powered descent, and 3) less than 25°-30° slopes at length scales of 2-5 meters to ensure stability and trafficability of the rover during and after landing. The needs described above are addressed by generating both Context Camera (CTX) [10] and High-Resolution Imaging Science Experiment (HiRISE) [11] DTMs at scales appropriate for identifying lander-scale hazards (1-meter baselines) and for EDL simulations (20-meter baselines). We also produce ancillary products, including maps of adirectional slope at 1-, 2-, 5-m baselines for HiRISE DTMs and 20-m baselines for CTX DTMs and orthoimages for each DTM stereo pair image.

At the time of abstract submission, we have generated six CTX DTMs and twenty HiRISE DTMs in support of Mars 2020 landing site evaluation (some DTMs generated cover regions no longer being considered). See **Table 1** for a summary of slope statistics related to each DTM that intersects landing sites currently being considered. Although Jezero and NE Syrtis contain slopes at local scales that pose a hazard to landing and traversability, the regions are small enough to be avoidable using TRN. Thus, all three candidate landing sites meet the criteria required for safe landing.

Flight Quality DTM Mosaic Development: To support landing using TRN capabilities, we will produce a CTX orthoimage mosaic and HiRISE orthoimage mosaic of the landing ellipse and surrounding region. TRN registration requirements include: 1) HRSC to CTX horizontal coregistration less than 60 meters at the 99%tile; 2) CTX to HiRISE horizontal coregistration less than 6 meters at the 99%tile; and 3) HiRISE to HiRISE horizontal coregistration less than 3 meters at the 99%tile. These are significantly stricter

horizontal and vertical registration requirements than landing site characterization and have prompted the need to develop new DTM generation procedures and capabilities. We are currently improving our DTM image pre-processing pipeline including capabilities to utilize camera model and jitter-correction improvements, using Ames Stereo Pipeline (ASP) [12] as a means to improve the starting point for DTM generation, and the ability to improve our use of MOLA, High/Super Resolution Stereo Color Imager (HRSC) [13], and CTX as ground tie points. We are also exploring existing methods, and developing new approaches, to validate the horizontal and vertical registration for DTMs in a quantitative manner (**Figure 1**). Finally, we are exploring and developing new methods to generate flight-quality DTM mosaics, including utilizing the ASP program *pc_align* in innovative ways to improve the registration between images and generating DTM mosaics using SOCET SET® and/or SOCET GXP®.

Table 1. Statistics for CTX and HiRISE DTMs in support of Mars 2020 landing site selection.

Name	Sensor	Mean Slope	Standard Deviation
ColumbiaHills_XE	CTX	1.7	2.9
ColumbiaHills_W	HiRISE	4.6	3.0
ColumbiaHills_WC	HiRISE	4.5	3.7
ColumbiaHills_EC	HiRISE	3.6	3.2
ColumbiaHills_E	HiRISE	3.2	2.5
Jezero_XW	CTX	5.5	5.1
Jezero_W	HiRISE	4.5	4.2
Jezero_C	HiRISE	6.7	4.9
Jezero_CE	HiRISE	4.0	3.6
Jezero_E	HiRISE	4.2	3.3
NE_Syrtis_XC	CTX	5.8	4.6
NE_Syrtis_N	HiRISE	6.2	4.7
NE_Syrtis_NW	HiRISE	5.1	4.0
NE_Syrtis_W	HiRISE	5.8	4.5
NE_Syrtis_WC	HiRISE	4.7	4.1
NE_Syrtis_C	HiRISE	5.0	3.9
NE_Syrtis_CE	HiRISE	5.6	4.6
NE_Syrtis_E	HiRISE	5.5	4.4

Acknowledgements: Part of this work was performed at the Jet Propulsion Laboratory, California Institute of Technology, under a contract with NASA. References to commercial products are for identification purposes and do not imply an endorsement by the U.S. Government.

References: [1] Squyres S. W. et al. (2004) *Science*, *305*(5685), 794-799. [2] Arvidson R. E. et al. (2010) *JGR*, *115*(E7), doi:10.1029/2010JE003633. [3] Fergason R. L. et al. (2016) *SSR*, doi:10.1007/s11214-016-0292-x. [4] Golombek M. et al. (2016) *SSR*, doi:10.1007/s11214-016-0321-9. [5] Sides, S. C. et al. (2017) *LPS*, *XLVIII*, 2739. [6] Miller S. B. and Walker A. S. (1993) *ACSM/ASPRS Annual Conv*., *3*, 256–263. [7] Zhang B. (2006) *GeoCue Corporation 2nd annual Technical Exchange Conference*. [8] Smith D. et al. (1999) *Science*, *284*, 1495-1503. [9] Smith D. E. et al. (2001) *JGR*, *106*, 23,689-23,722. [10] Malin M. et al. (2007) *JGR*, *112*(E05S02), doi:10.1029/2005JE002605. [11] McEwen A. S. et al. (2007) *JGR*, *112* (E05S02), doi:10.1029/2005JE002605. [12] Moratto Z. M. et al. (2010) *LPS*, *XLI*, 2364. [13] Jaumann R. et al. (2007) *Planet and Space*. *Sci*., *55*, 928-952.

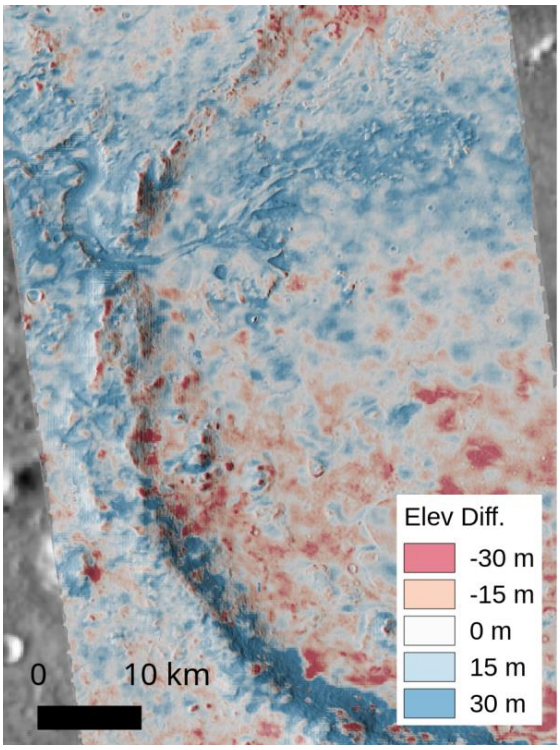

Figure 1. Elevation differences between CTX DTM of Jezero crater and HRSC reference DTM, overlain on CTX hillshade.

Recent Developments for an Orbiting Sample Container for Potential Mars Sample Return. A. J. Siddens[1,2], S. V. Perino[1], and T. A. Komarek[1], [1]Jet Propulsion Laboratory, California Institute of Technology, 4800 Oak Grove Drive, Pasadena, CA 91109, Pasadena, CA. [2]aaron.j.siddens@jpl.nasa.gov

Introduction: A significant goal of the upcoming Mars 2020 mission is to collect geological samples of the planet's rocks and regolith and store them in hermetically sealed sample tubes. The tubes could then be collected by a later mission with the goal of bringing them back to Earth for detailed study as part of a potential Mars Sample Return (MSR) effort.

The Orbiting Sample (OS) container is a key piece of hardware in most proposed sample return mission architectures. It is the primary vessel that would be sent to and brought back from Mars. The basic function of the OS would be to hold and protect the sample tubes from the time of collection on Mars through impact landing on Earth.

The proposed MSR architecture consists of four elements: three separate flight missions, (1) the Drilling and Caching mission (Mars 2020), (2) the MSR Lander, and (3) the MSR Orbiter, and (4) a ground sample handling facility. In this notional plan, the OS would be sent to Mars with the Lander in two pieces: the OS canister, and the OS shell. Once the sample tubes are placed in the canister, the two halves would be assembled and then launched into low Mars orbit on the Mars Ascent Vehicle (MAV). The Orbiter would rendezvous with the OS, capture it, package it into the Earth Entry Vehicle (EEV), then return to Earth and put the EEV with OS onboard onto an Earth impact trajectory.

It is critical that the OS design both meets structural requirements and has a fully conceived method of integration onto the MSR Lander and MAV system. The present work highlights recent efforts to mature and optimize the OS and the OS-MAV interface.

Orbiting Sample: The OS must survive Earth impact inside the EEV with peak impact loads anticipated to be 1300 G. Additionally, the OS must not amplify the loads transmitted to the sample tubes above 1300 G. From a structural standpoint, meeting these requirements is one of the most challenging aspects of the OS design and has been a key focus of previous work.

A reference OS structural design has steadily matured over several years of investigation [1]. Impact simulation of various OS concepts was performed to vet out designs and arrive at the current axially-preloaded canister design (Fig. 1). It has been shown through numerous tests and analyses that the design can meet the structural requirements for assembly and impact loading under nominal conditions [1].

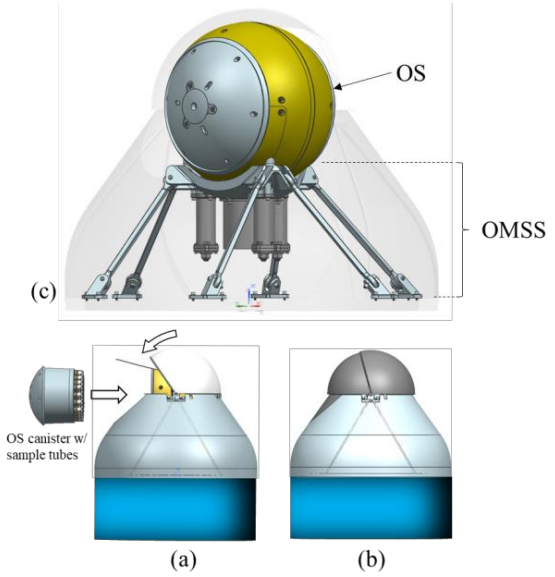

Fig. 1. Concepts for (a) OS assembly on MAV by inserting canister into shell, then closing MAV lid, (b) MAV config for Mars Ascent, and (c) OS and OMSS atop the MAV

While still evolving, the OS design and proposed MSR effort are at a point where further optimization of the reference concept and design of interface hardware to which the OS directly interfaces is pertinent.

Recent Developments: Changes to the OS directly affect the Lander and Orbiter designs. By one estimate, adding 1 kg of OS mass requires 5 kg of added MAV mass to deliver it to low Mars orbit, and adding 1 kg of MAV mass requires 20 kg of additional Lander mass [1]. Increasing the OS mass also requires a larger EEV and thus more mass on the Orbiter. Conversely, if the OS mass decreases, then the Lander and Orbiter can be lightened. Small mass reductions on the OS propagate through both systems and could have substantial mass savings across the entire multi-mission architecture.

To this end, topology optimization (top-opt) and 3D printing have recently been explored to help identify opportunities for light-weighting and alternative efficient concepts within the current OS design space (Fig. 2). While traditional top-opt uses static loads, the key driver for the OS is transient impact loading for which there is no firmly established method for optimization. Techniques and iterative workflow developed to optimize

and assess the OS for impact will be discussed, as well as the design improvements and insights gained by this top-opt effort.

An important factor in the OS design is how it interfaces with the MAV. The exact vehicle design and loading characteristics are still being determined, but a conservative random vibration environment has been developed for initial studies. The Mars ascent phase of the mission is likely the most challenging for the MAV-mounted hardware that supports the OS, dubbed the OS Mechanical Support System (OMSS).

The OMSS is responsible for restraining the OS during Mars ascent and releasing the OS once in orbit. Methods of adequately restraining and releasing the OS have been explored in detail over the past year. Most approaches require interface features on the OS itself, and thus the OMSS design directly affects the OS design. Details of the methods explored, the current OMSS design, and the corresponding effects on the OS design will be covered.

These and other recent developments and the overall projected path forward for the OS will be presented.

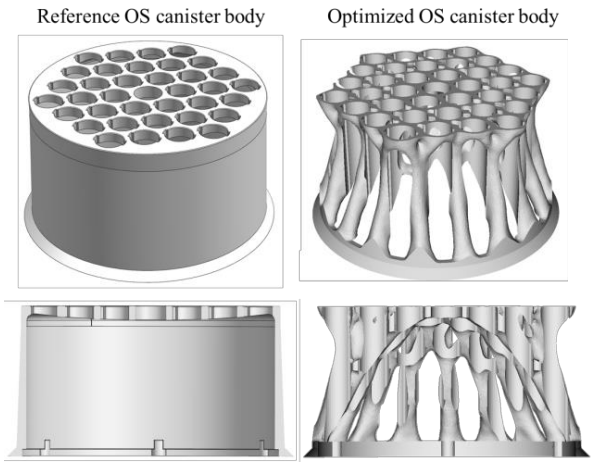

Fig. 2. Comparison of the reference OS canister body (left) and geometry resulting from initial topology optimization (right). Top row is angled view, bottom row is section cut view.

References:

[1] Perino, S., et al, "The Evolution of an Orbiting Sample Container for Potential Mars Sample Return," 2017 IEEE Aerospace Conference, Big Sky, MT, 2017, pp. 1-16. doi: 10.1109/AERO.2017.7943979

Acknowledgment: A portion of the research described in this paper was carried out at the Jet Propulsion Laboratory, California Institute of Technology, under contract with the National Aeronautics and Space Administration.

CHANGING ENTRY, DESCENT, AND LANDING PARADIGMS FOR HUMAN MARS LANDERS. A. D. Cianciolo, NASA Langley Research Center, MS 489 Hampton, VA, 23681 USA (Alicia.m.dwyercianciolo@nasa.gov).

Introduction: The design of entry, descent, and landing (EDL) systems for human Mars missions is performed in the context of a broad exploration architecture that extends from pre-Earth launch through Mars operations and crew return to Earth [1, 2]. Recent studies [3] have considered technology investments for human-scale EDL that have evolved since the release of the NASA Human Mars Design Reference Architecture (DRA 5.0) [4]. This presentation will summarize relevant updates to ground rules and assumptions that impact human-scale EDL design and describe specific entry vehicle changes made to accommodate the new guidelines. Finally, challenges associated with integrated EDL mission design that are changing the robotic mission EDL paradigms are discussed.

Background: DRA5 did not include surface asset buildup at a single location. Rather, two 10 m x 30 m mid lift-to-drag (Mid L/D) entry vehicles each delivered 40 t payloads to a single location. Subsequent missions would deliver similar vehicles to other distant locations of interest on the planet. To reduce propellant load and to expose the payload for landing, the aeroshell was jettisoned during entry, after the peak heat pulse.

Updated Ground Rules and Assumptions: The current Mars architecture assumes the use of SLS launch vehicles with a 10 m diameter fairing to launch all architecture elements including the Mars lander. The lander rendezvous and docks with a Solar Electric Propulsion (SEP) in-space transportation vehicle in low Earth orbit, which then delivers the lander to Mars vicinity. The options to use either aerocapture or the SEP stage to propulsively insert deliver the lander into a one Sol (33,900 km x 250 km) parking orbit are considered. The crew entry vehicle will loiter in orbit for up to one year waiting for the crew, while other landers may spend only a short time there prior to deorbit. The payload manifest for multiple subsequent long-stay missions (300 days), each with a crew of four, has been identified and packaged [5], which offers advantages over the black box payloads (mass only – no volume) considered for DRA5. For example, estimates of inertias and center-of-gravity locations can be calculated and used in high fidelity flight simulations. Concepts for adequately achieving the required L/D can be evaluated. Guidance and control methods are being designed to meet the desired landing within 50 m of a specified target. Now that multiple landers are sent to a single site, jettisoning elements during EDL increases the risk of impacting existing surface assets. Consequently, jettison events have been eliminated. Additionally, due to surface-plume interaction studies that indicate engine exhaust can disperse surface regolith up to 700 m from the touchdown location, the landing zone has identified "keep out" zones around each landing target of 1 km to prevent impacting other landed assets.

The cargo landers will serve as integrated flight system tests for the crew vehicle, thus all entry vehicles (cargo and crew) are required to fly in the same manner (i.e. ballistic coefficient, L/D, guidance navigation and control sensors and algorithms). Therefore, all entries are designed to maintain nominal entry decelerations of 3 Earth g's or less to satisfy deconditioned crew guidelines from the NASA Human System Integration Requirements (HSIR). Likewise, since the exact landing location has not been identified, the target landed altitude is 0 km relative to the MOLA areoid and a maximum vertical velocity of 2.5 m/s at touchdown is assumed.

Vehicle Modifications: Current EDL designs consider Mid-L/D vehicles, albeit smaller than the DRA 5.0 design, as well as Low-L/D alternatives. The EDL Systems Analysis study [6] indicated that using inflatable structures to increase the drag area of the vehicle beyond the limitations of the launch vehicle diameter offered lightweight alternatives to rigid vehicles for human-scale EDL. A 16m-diameter HIAD vehicle is considered for this study. Vehicle entry masses, on the order of 50 to 60t, are equipped with eight 100 to 120 kN descent engines. The advantage of the Low-L/D vehicle is that the forebody is made of lightweight materials and there is no backshell. However, the challenge for the Low-L/D vehicles that use heritage bank angle control is the need for L/D near 0.3, which translates to an angle of attack in flight near 20 deg. At these angles for the payload manifests considered, there is a risk of flow impingement and thus significant heating on the payload. To mitigate this risk, control alternatives were considered. Mars Science Laboratory performed analysis on trim tabs on blunt body vehicles [7]. Advancements in sizing and actuating such flaps to generate both angle of attack and sideslip control independently during entry indicate that the performance gained allows the vehicle to fly with a lower L/D (~0.15 to 0.2) and angles of attack less than 10 deg) thus reducing the risk of convective flow impingement. Radiative heating is still an issue but initial analysis shows that the radiative heating can be mitigated using thin thermal protection system or even reflective paints, depending on the payload ele-

ment. Using this direct force control (DFC) has the advantage over bank angle control of no open loop phases of flight. In addition to controlling downrange and cross range, as with bank angle control, direct force control (DFC) permits fine control of altitude which significantly reduces the powered descent propellant load.

Even seemingly straight forward decisions, such as storing the Reaction Control System (RCS) propellant for in-space transportation phases of flight (to dock, undock with SEP stage, perform aerocapture and orbital maintenance) in the lander main engine tanks requires larger tanks and higher lander deck height, which is a concern for payload offloading. Additionally, the decision to eliminate the jettison event means that the vehicles must design retractable deployables, payload bay doors, or another payload offloading mechanism. Packaging arrangements that allow for access to the surface also drive the design. Therefore, it was critically important to understand how the EDL system fits into the overall Mars exploration architecture.

Challenges: All of these aspects combined in four EDL vehicle point designs to deliver a human-scale lander that meets the outlined ground rules and assumptions with varying degrees of strengths and weakness. Yet, many challenges remain. For example, physical methods to enable DFC for Low-L/D vehicles are only now being explored. They include a range of techniques from the demonstrated flight test of center-of-gravity movement [8], shape morphing, and attaching flaps to the outer radius of the vehicle. More analysis is needed to develop guidance and control algorithms and mechanical designs to determine the most feasible approach. Likewise, all performance analyses to date assumes perfect navigation knowledge and perfect engine performance, both of which are known to be large contributors to the landing footprint dispersions.

To minimize propellant mass, the engines are initiated at supersonic speeds and remain on for durations less than 60 s. Therefore, identifying navigation sensors and defining their requirements is a challenge. Due to use of supersonic retropropulsion, the vehicle geometries, velocities, sensor accommodation, processing speed and vehicle accommodation are yet to be explored. Defining navigation requirements for new trajectory geometries is a challenge.

This presentation will summarize key human Mars architecture ground rules and assumptions, as well as the large-scale mission challenges, are changing the EDL paradigms that have developed from the robotic lander missions to Mars.

References: [1] Craig, D., et al. (2015) IEEE Aerospace Conference. [2] Craig, D. A., et al. (2015) *AIAA SPACE 2015* [3] Cianciolo, A. D. and Polsgrove, T. T., (2016) AIAA 2016-5494. [4] Drake, B. G., editor., (2009) NASASP-2009-566. [5] Toups, L., and Hoffmann, S. "Pioneering Objectives and Activities on the Surface of Mars." [6] Dwyer Cianciolo A. M. et al. (2010) NASA TM-216720. [7] Horvath, T. et al. (2002) AIAA 2002-4408. [8] Dillman, R., et al. (2013) IPPW-10.

Exploring Impact Attenuating Interfaces for a Potential Mars Sample Return Earth Entry Vehicle. C. M. Grace[1,2], S. V. Perino[1], [1]Jet Propulsion Laboratory, California Institute of Technology, 4800 Oak Grove Dr, Pasadena, CA 91109, [1]cameron.m.grace@jpl.nasa.gov [2]cmgrace3@buffalo.edu

Introduction: A proposed Mars Sample Return (MSR) mission architecture utilizes a passive and aerodynamically stable Earth Entry Vehicle (EEV) to transport Martian samples from space to the Earth's surface. The EEV would enter Earth's atmosphere and impact at terminal velocity at the notional landing site of the Utah Test and Training Range (UTTR). In the potential architecture, the EEV must be designed to absorb and redirect kinetic energy in a way that avoids damage to the Orbiting Sample (OS) and sample tubes held within [1, 2]. Fundamentally, the success of such a notional MSR effort relies on a successful design of an EEV for impact attenuation in order to safely deliver high-quality Martian rock and regolith samples.

The EEV must be designed to guarantee sample integrity and containment assurance during impact landing. This presentation discusses the various methods employed in a proposed EEV concept to dissipate kinetic energy during Earth impact. A diverse range of materials and mechanisms, such as metallic foams and a buckling ratchet concept, have been proposed and are being studied as mechanical interfaces between the OS and EEV subsystems. Geometric parameterization tools and material property tuning techniques were utilized to uncover the most competent damping interfaces for protecting the OS from transient impact loads.

Ratchet/Pawl Designs: The structures within the EEV form crucial interfaces to ensure the survival and containment of the Martian samples held within the OS. The OS attaches to the Primary Containment Vessel (PCV) while onboard a Sample Return Orbiter (SRO) by means of a ratcheting device shown in Fig. 1 (a). This ratcheting device has two primary functions: (1) In the intended landing configuration the ratchet prevents the OS from experiencing rebound translational motion perpendicular to the base of the ratchet after impact, and (2) in the case of off-nominal landing the ratcheting device minimizes load transfer through the PCV and the Secondary Containment Vessel (SCV) seals so that damage to the seals does not occur.

A custom Monte Carlo Simulation code played a pivotal role in identifying the ratchet's initial design parameters while also identifying key features that improved the overall design. Millions of combinations of pawl geometries and other design parameters were generated. Each design was then assessed for its response under both quasi-static and impact conditions, with the latter being approximated as a representative static load case. After a recommended convergent solution was identified, a transient Finite Element Analysis (FEA) model was constructed to confirm that the design could indeed survive full dynamic impact loading conditions. This FEA model was used to ensure that non-linear phenomena such as material yielding of individual pawls would not threaten the design.

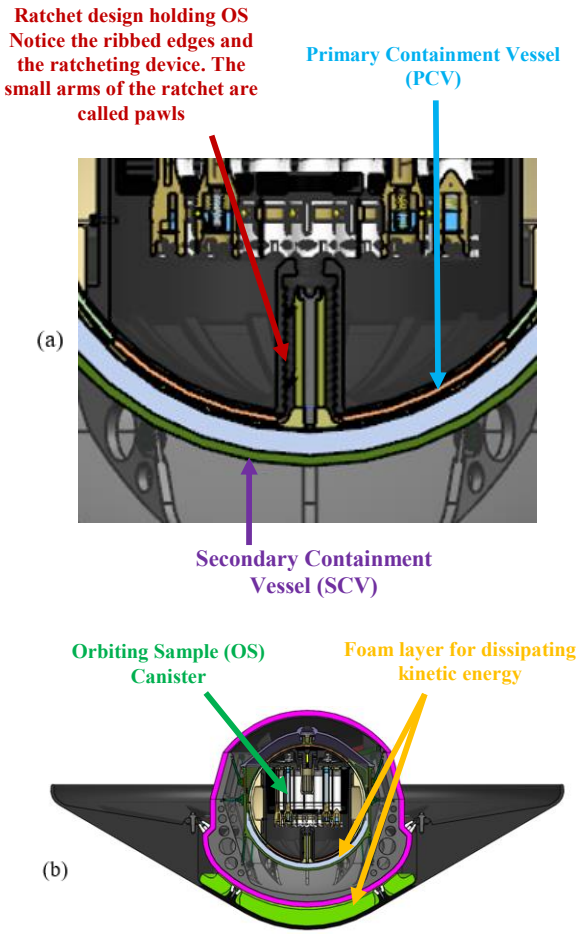

Fig. 1. (a) Earth Entry Vehicle concept cross section, **(b)** OS internal interface structures

Metallic Foams: The carefully chosen soft soil located at UTTR has been shown capable of attenuating impact loads, but additional energy dissipating interfaces may be necessary for guaranteeing the safe return of the samples contained in the OS. Thus, metallic foams have been tested both empirically and with FEA simulations to obtain the proper thicknesses and relative densities required to crush under expected impact

loads. These metallic foams possess vibration reducing properties as well as a decrease in thermal conductivity, commonly called a foam's "R-Value." Because of these properties, foam has been carefully positioned between various components of the EEV, as can be seen in Fig. 1. (b).

Two types of foams were explored in this study: (1) open cell foam, and (2) closed cell foam. Each of these types of foams has unique properties such as variable stiffnesses, damping capacities, and dynamic moduli that are all heavily contingent on their respective relative densities and strain rates. The characteristic of these foams creates an interface structure between comparatively rigid components in the EEV. These interfaces allow for a constant stress state up to 70% strain of the metal foam, and this crushing behavior alleviates both impact loads and adds additional time to otherwise ephemeral loading conditions [3].

Conclusion: The return of samples from Mars would expand our knowledge and accelerate our understanding of our solar system. However, these samples need to return intact and uncontaminated. Toward this goal, effective energy dissipation using an EEV is one critical aspect of the baseline mission design. In order to secure the payload successfully, the entire design space must be explored. This presentation will expand upon the topics discussed and the potential for future work.

References:

[1] Perino, S., et al, "The Evolution of an Orbiting Sample Container for Potential Mars Sample Return," 2017 IEEE Aerospace Conference, Big Sky, MT, 2017, pp. 1-16. doi: 10.1109/AERO.2017.7943979

[2] Mitcheltree, R. A., Kellas, S., Dorsey, J. T., Desai, P. N., and Martin, C. J., "A Passive Earth-Entry Capsule for Mars Sample Return," 7th AIAA/ASME Joint Thermophysics and Heat Transfer Conference, Albuquerque, NM: AIAA, 1998

[3] Gui, M. C., Wang, D.B.,Wu, J. J., Yuan, G. J., Li, C. G., "Deformation and damping behaviors of foamed Al-Si-SiCpcomposite," Materials Science and Engineering A, National Laboratory of Advanced Composites, Institute of Aeronautical Materials, Beijing: 2000

Acknowledgment: A portion of the research described in this paper was carried out at the Jet Propulsion Laboratory, California Institute of Technology, under contract with the National Aeronautics and Space Administration.

Altitude Control For Venus Balloons Using Phase Change And Loop Heat Pipes V.D.Patel[1] and P.E.Papadopoulos[2], [1]San Jose State University (One Washington Square San Jose, CA 95192, varun.patel01@sjsu.edu), [2]San Jose State University (One Washington Square San Jose, CA 95192, perikilis.papadopoulos@sjsu.edu)

Introduction:

Venus has an extemely harsh envriomentt, the atmosphere's chemical composition and temperature makes it challenging to land a probe on the surface without it melting or being crushed by intense pressure. In the upper atmosphere of the planet, there is a layer that is very earth like in temperature and pressure. Past missions, VEGA 1 and VEGA 2, included balloons with Teflon like coating and were superpressured but because of leaking they only about lasted 2 days each. JPL and NASA are working on balloons using a combination of Mylar and Teflon and that will be able to last almost 2 months. Superpressure balloons are designed to stay relatively stable in the upper atmosphere but even then there are 3-D winds that can disturb the balloons and cause them to bob up and down as the VEGA missions did. The problem with all of these missions is that they're all dependent on the wind to move them around while having no real control over the direction.

Loop heat pipes have been around for quite some time and have been used in satellites for thermal protection and heat distribution. For a more simpler solution they've been used in CPU coolers with a thermal interface that sits on top of the CPU and the loop heat pipes direct the heat to a heat sink that distributes the heat throughout it and a fan that acts as the cooling agent. This is an example of active cooling system because it requires the fan to cool the heat sink. For a passive system the heat would need to be dissipated without the use of more energy or an additional thermal source. Loop heat pipes have a lot of factors that determine the efficiency of the system. The thermal fluid inside, the materials used for the loop heat pipes, the diameter and shape of the heat pipes as well as the shape of the evaporator all change how efficient the system is.

This paper will consider a design for an attitude control system by implementing the use of a phase change balloon, loop heat pipes and ballasting to increase altitude stability of high altitude balloons for Venus. This system solely relies on the ambient temperature leading it to be fully autonomous. To control the altitude the primary method is to use a phase change balloon with a mixture of helium and water with the addition of a loop heat pipe. As a secondary method to use ballasting for more drastic and instantaneous control. As the balloon loses altitude the ambient temperature will increase, evaporating the water and increasing buoyancy and as a result the balloon will rise until the water condenses again from a gas to a liquid. When the balloon reaches the highest altitude possible, the temperature should drop and cause the water to freeze which will decrease the buoyancy and as a result the balloon will lose altitude again. This phase change cycle would continue indefinitely and works effectively because of the large temperature difference in the upper atmosphere of Venus. The ballast will be attached to the payload and deployed when needed.

The heat from the payload is captured and redirected using a loop heat pipe and dissipated into the balloon envelope. This would help increase the rate at which the phase change occurs by directing wasted thermal energy back into the system. While the balloon is at lower altitudes the payload and the ambient temperature would both add thermal energy into the phase change balloon and drive the liquid water to evaporate faster and driving the balloon back to higher altitudes. As the balloon reaches the upper altitudes the water vapor starts to condense and eventually into ice which would drive the balloon back towards the lower altitudes. With the addition of the loop heat pipe, the heat from the payload would be dissipated into the balloon envelope and slowing down the phase change process from liquid water to solid ice. With the combination of these methods and on board pressure sensors, the balloon should be able to maintain a stable altitude with smaller oscillations creating a good platform for long duration missions on Venus.

References:

[1] J. L. Hall, V. V. Kerzhanovich, A. H. Yavrouian, G. A. Plett, M. Said, D. Fairbrother, C. Sandy, T. Frederickson, G. Sharpe, and S. Day, Second generation prototype design and testing for a high altitude Venus balloon, Advances in Space Research, Vol. 44, 2009, pp. 93-105

[2] R.A. Preston, C.E. Hildebrand, G.H. Purcel1, J. Ellis, C.T. Stelzried, S.G. Finley, R.Z. Sagdeev, V.M. Linkin, V.V. Kerzhanovich, V.I. Altunin, L.R. Kogan, V.I. Kostenko, L.I. Matveenko, S.V. Pogrebenko I, S. Strukov E.L. AlumY, u.N. AlexandrovN, .A.Armand R.V.Bakitko, A.S.VysAh.lFo.vB, ogomYoulo. Nv,.Groshenkov, A.S.Selivanov, N.M.Ivanov, V.F.Tikhonov, J.E.Blamont,L.Boloh, G.Laurans,A.Boischot,F.Biraud,A.Ortega-Malina, C.Rosolen, G.Petit (1986). Determination of Venus

Winds by Ground Based Radio Tracking of the VEGA Ballloons, Science, 231, 1414
[3] R.Z. Sagdeev, V.M. Linkin, J.E. Blamont, R.A. Preston (1986). The VEGA Venus Balloon Experiment, Science, 231, 1407
[4] Phase changes. (n.d.). Retrieved September 29, 2017, from http : //hyperphysics.phy − astr.gsu.edu/hbase/thermo/phase.html
[5] Maydanik, Y. F. (2006). Loop Heat Pipes - Theory, Experimental Developments And Application. Keynote Papers. doi:10.1615/ihtc13.p30.190
[6] Squyres, Steven W. "Venus." Encyclopædia Britannica. Encyclopædia Britannica, inc., 24 Apr. 2017. Web. 09 June 2017
[7] A. Seiff, 'J.T. Scoffield, A.J. Kliore, F.W . Taylor, S.S. Limaye, H.E. Revercomb, L.A. Sromovsky, V.V. Kerzhanovich, V.I. Morozand M.Ya. Marov (1985). Models of the Structure of the Atmosphere of Venus from the Surface to 100 km Altitude, Adv.Space Res., 5, I 1,3-58
[8] B. Ragent, L.W. Esposito, M.G. Tomaslo, M.Ya. Marov, V.P. Shari and V.N. Lebedev (1985). Particular matter in the Venus Atmosphere, Adv. Space Res., 5 , I 1, 8516
[9] V.V. Kerzhanovich, J.A. Cutts, A. Bachelder, J. Cameron, J. Hall, J. Patzold, M. Quadrelli, A. Yavrouian, J. Cantrel1, T. Lachenmeier, M. Smith (1999). Mars Balloon Validation Pro- gram. 13'h AIM International Balloon Technology Conference, Norfolk, Virginia, Collection of papers, 8
[10] Lu, T. (2000). Thermal management of high power electronics with phase change cooling. International Journal of Heat and Mass Transfer, 43(13), 2245-2256. doi:10.1016/s0017-9310(99)00318-x
10
[11] Williams, D. R. (2016, April 12). Chronology of Venus Exploration. Retrieved September 29, 2017, http : //nssdc.gsfc.nasa.gov/planetary/chronology$_V$enus.html
[12] Landis, Geoffrey A. "Atmospheric Flight on Venus." 40th Aerospace Sciences Meeting Ex- hibit (2002): n. pag. Web. http : //citeseerx.ist.psu.edu/viewdoc/download?doi = 10.1.1.195.172rep = rep1type = pdf
[13] Mogk, David. "Gibbs' Phase Rule: Where it all Begins." Teaching Phase Equilibrium. Gibbs' Phase Rule: Where it all Begins, n.d. Web. 4 June 2017.

3D PRINTED LIQUID ROCKET ENGINE DESIGN FOR MARS SAMPLE RETURN MISSIONS

T. Saunders[1], S. Elaian[1], A. Mitchell[1], T. Soares[1], S.Sanchez[1], P. Papadopoulos[2], [1]Student, [2]Advisor, San Jose State University, San Jose, California, 95192

The current poster presentation will demonstrate a parametric study implemented to design a 3D-printed liquid rocket engine that meets the requirements of a Mars ascent vehicle for a Mars sample return mission [1]. The design, build, and manufacturing process will be presented in detail. The design and hardware presented will enable low-cost future sample return missions from Mars and will support science and technology objectives of in situ exploration on Mars.

The engine is powered by liquid methane and liquid oxygen fuel. It is designed to be manufactured out of copper c18150 utilizing direct metal laser sintering (DMLS); high conductivity copper c18150 promotes heat transfer through the walls of the engine, allowing more heat to be absorbed by the regenerative cooling system. By leveraging DMLS, a regenerative cooling system is implemented in which the cooling channels are designed directly into the walls of the nozzle and combustion chamber. After passing through a feed system, the fuel enters the engine walls though the manifold located at the base of the nozzle shown in figure 1. The injector utilizes a fuel oxidizer oxidizer fuel (FOOF) orifice pattern to prevent oxidizer from spraying on the walls. Acoustic resonator cavities are implemented to mitigate combustion instability frequencies.

Research was performed to determine the feasibility of in situ resource utilization for construction of the system on Mars. The Sabatier chemical reaction could be used to produce the engine's methane and oxygen propellant from the carbon dioxide in Mars' atmosphere along with a supply of hydrogen transported from Earth. Copper alloy and the capability to conduct DMLS on Mars would additionally need to be supplied from Earth.

The engine requirements for sample return include 42 kN of thrust and a vacuum Isp of 332 s to place a vehicle and payload of 800 kg into Martian orbit using a single stage. The system requirements sized the combustion chamber for a 40 second burn time. Sizing of the injector was based on pressure losses from the fuel and oxidizer channels and manifolds. Sizing of the cooling channels was based on the conductivity of copper c18150, the mass flow rate required by the combustion chamber, and the heat flux at the throat.

Detailed CFD and FEM analysis were used for the combustion chamber, injector, and nozzle designs. An iterative process was implemented to downselect the optimal design. Key design parameters include nozzle area ratio, O/F ratio, thrust, and mass flow rate. A 3D CFD analysis of the flow through the regenerative cooling channels has been developed using the SolidWorks flow simulation package, which takes into account a fixed wall temperature of 1,450°C. A 3D FEM structural analysis was performed to size the engine's wall thickness and accommodate the heat flux through the wall and the regenerative cooling channels.

Figure 1. *Nozzle and combustion chamber geometry*.

The work presented supports low cost Mars sample return missions by leveraging in situ resources and 3D printing, minimizing the cost and increasing the ease of manufacturing. The poster presentation will further highlight details of the design as well as the hardware developed.

References: [1] Benito, J., "Development Status of a Mars Ascent Vehicle Proposed Technology Demonstration," *IPPW-14*, 2017.

THE MARS MICROPHONE ONBOARD SUPERCAM FOR THE MARS 2020 ROVER.

David Mimoun (1), Sylvestre Maurice (2), Anthony Sournac (1), Alexandre Cadu (1), Marti Bassas (1), Murdoch Naomi (1), Baptiste Chide (1), Jérémie Lasue (2), and Roger Wiens (3)
(1) Université de Toulouse, ISAE-Supaero, DEOS/SSPA, Toulouse, France (david.mimoun@isae.fr), (2) IRAP, CNRS, Université Paul Sabatier, Toulouse, France, (3) LANL, Los Alamos, NM

The Mars Microphone has been designed as an component of the Supercam instrument onboard Mars 2020 rover, whose design is similar to the ChemCam instrument currently operating at the surface of Mars, onboard the Curiosity rover. It is the result of a collaboration between ISAE-SUPAERO, IRAP and LANL, under the supervision of CNES. [1,2,3]

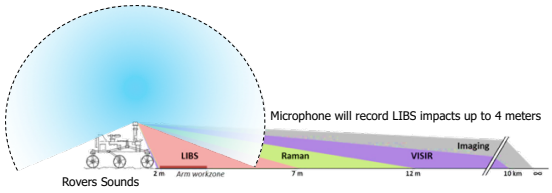

Fig 1 : The various sensor capabilities of SuperCam

The Mars microphone will be located on the mast of the Mars 2020 rover, close to the SuperCam laser head.

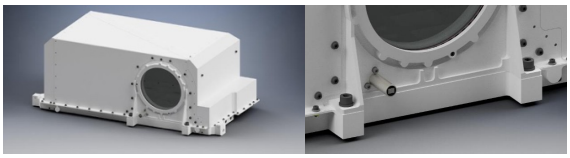

Fig 2 The Mars Microphone mechanical accommodation on the SuperCam mast unit

The Mars microphone has several scientific objectives. Its primary goal is to support the Laser LIBS investigation to enhance its capability of determining properties of Mars rocks and soils through their coupling with the laser beam. In addition, it will contribute to basic atmospheric science, by providing wind speed statistics, speed of sound as a function of the temperature, convective vortices, dust devil studies at close distance or when interacting with the rover. It will also record the unique signature of many artificial sounds: operations of the robotic arm and mast, sounds of the wheels on the ground when driving and other noise coming from the rover.

The Mars Microphone is able to record audio signals from 100 Hz to 10 kHz on the surface of Mars, with a sensitivity sufficient to monitor a LIBS impact at distances up to 4 m. To meet these requirements, a condenser microphone has been selected. The Microphone is a commercially available condenser microphone from Knowles The same model of microphone has actually flown to Mars twice before: once on theMars Polar Lander in 1998 that subsequently crashed onto the red planet, and a second time in 2007 as part of the Phoenix mission. The microphone was, however, never turned on during this mission due to compatibility issues of the hosting payload (a descent camera) with the avionic of the probe.

The amplification gains and dynamics of the instrument have been carefully chosen. The microphone has passed its qualification and performance tests, including end-to-end tests in Martian environment [4,5], and has been delivered to IRAP for integration on the SuperCam instrument.

The delivery of the Supercam instrument (and therefore of the Mars microphone) to the Jet Propulsion laboratory is expected at the end of 2018.

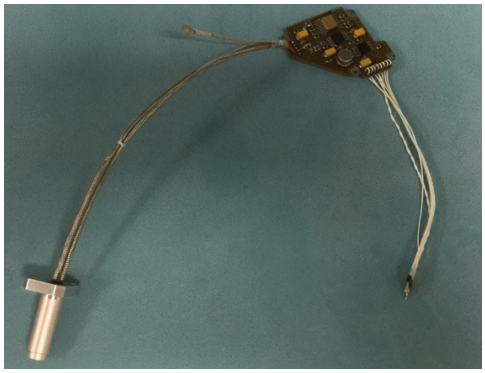

Fig 3 : the Mars Microphone flight model before delivery to IRAP

References: [1] Wiens, R. et al., (2017) Spectroscopy 32(5) [2] Maurice, S. et al. (2015) 46th LPSC, #1832. [3] Maurice, S. et al. (2016) 47th LPSC, #3044. [4] Holstein-Rathlou, C., et al. (2014), J. of Atmospheric and Oceanic Technology, 31(2) [5] Murdoch et al., (2018) submitted to PSS.

InMARS: a comprehensive program for the development of key-technologies for miniature Martian probes.

I.Arruego[1], V. Apéstigue[4], J. Martínez[4], J.J. Jiménez[1], A. Martín-Ortega[4], J.R. de Mingo[1], M. González-Guerrero[4], J. Azcue[1], N. Andrés[4], F.J. Álvarez[1], J. Rivas[1], J. Manzano[1], F. Serrano[1], I. Martín[1], A. Gonzalo[1], H. Guerrero[1], S.Espejo[2], J. Ceballos[2], A. Ragel[2], D. Vázquez[2], F. López[3], A.J. de Castro[3], F. Cortés[3].
[1]INTA, Spain (arruegori@inta.es). [2]Instituto de Microelectrónica de Sevilla (IMSE), Spain. [3]Universidad Carlos III, Spain. [4]ISDEFE as external consultant for INTA, Spain.

Introduction: the Space Sensors Engineering Area of INTA (the National Institute of Aerospace Technology, Spain) maintains a continuous activity aimed at the development of different resources and enabling capabilities, to allow the construction of compact instruments for atmospheric science on Mars and, in the long term, complete miniature atmospheric probes that could be used to deploy networks of meteorological stations on the red planet. InMARS (Instrumentation for Martian Atmospheric Research on Surface) program is part of this strategy. Under this program, we are presently developing one instrument for the JPL/NASA Mars 2020 Rover, two different sensors for the METEO package on board the ESA/Roscosmos ExoMars 2020 surface Platform (one of them led by a partner team from the Carlos III University, Madrid), and another instrument for the Dust Complex on board the same lander. We also developed a radiometer [1], [2] for the DREAMS payload [3] on board the ill-fated Schiaparelli Descent Module of ExoMars 2016. This program is complemented by another initiative we named CERES (Compact Electronic Resources for the Exploration of Space), devoted to develop horizontal capabilities for the aforementioned purpose, and also supported by our own in-orbit test-beds (INTA's Small Satellites Program). Amongst them, we include the development of Radiation-Hardened By design (RHBD) mixed-signal ASICs developed by another partner, the Institute for Microelectronics in Seville (IMSE).

The whole strategy is presented here, the main developments summarized and the next steps outlined.

Background: Taking as reference some initiatives from the big agencies, such as NASA's Mars Technology Program (MTP), including the Mars Instruments Development Project (MIDP), or ESA's Mars Robotic Exploration Preparation (MREP), we started a line of work adapted to the capabilities of a reduced group (around 20 people), with the aim of developing some horizontal capabilities with a non-specific mission approach [4]. It included activities such as the selection of high-performance electronic and optoelectronic components, development of different radiation tests (TID and particles), qualification and screening tests, and in-orbit demonstrations and validations on board several INTA platforms (Nanosat-01, 1B and OPTOS: three polar LEO satellites, the first two ones around 20kg and the last one a triple cubesat).

The selected and tested components include a number of analog parts such as operational and instrumentation amplifiers with different characteristics, voltage regulators and references, analog multiplexers and switches, etc. Also different mixed-signal parts such as Digital-to-Analog (D/A), Analog-to-Digital (A/D), Voltage-to-Frequency (V/F) converters, or Field Programmable Analog Arrays (FPAA), and finally digital/logic ones, such as FPGAs (Field Programmable Gate Arrays), CPLDs (Complex Programmable Logic Devices) and DSC (Digital Signal Controllers) (e.g. [5]-[9]).

In our small satellites we tested from conceptual developments (such as a distributed computer based on a collaborative architecture formed by ten small processing units and intra-satellite optical wireless communication [10]), to different COTS electronic parts (programmable logic, digital signal controllers, high-performance amplifiers, etc.) and several sensing technologies such as different types of magnetic sensors, optoelectronic emitters and detectors or several radiation-sensing technologies (e.g. [11], [12]).

Thanks to this effort and the high Technology Readiness Level (TRL) achieved through it, in 2008 we joined a Finnish-Russian initiative named Mars MetNet Lander, aimed at the development of small penetrators for Mars exploration, adequate for the deployment of large meteorological networks on the planet's surface [13]. We developed our first highly-compact sensors capable of withstanding the environmental conditions of a Martian mission on surface [14].

Besides, we started to set-up a national infrastructure for the development of mixed-signal ASICs intended to be used in compact instruments for Mars exploration and other Space applications. This is done in cooperation with another public research center in the south of Spain (IMSE). Work was started by creating a library of RHBD building blocks for the construction of future ASICs and verifying their resistance to TID and SEE. Then two first ASICs were developed, one implementing an optical wireless transceiver [15] and the other a front-end for the signal conditioning of a 3-axis magnetic sensor [16]. Both were also tested for operation in cold temperature (-135ºC).

InMARS at present: InMARS is now focused in Mars 2020 (JPL/NASA) and the ExoMars Program (ESA/Roscosmos), for which we deliver a number of instruments and lead their subsequent scientific exploitation. We are also developing a continuous effort to increase our horizontal capabilities, through different activities.

Development of Flight Hardware. We developed the Solar Irradiance Sensor (SIS) for the DREAMS meteorological station in ExoMars 2016 and, despite the last-minute failure of Schiaparelli's descent, we demonstrated the possibility of obtaining a real-time estimation of the optical thickness (OT) of the Martian atmosphere with a very miniaturized sensor, laying the background for the on-going and future developments of what we call "sectored" sensors. This validation was done through a test campaign carried out in the Sahara desert during the dust-storm season. Details can be found in [1].

At this moment we are developing the following units:

- Radiation and Dust Sensor for the Mars Environmental Dynamics Analyzer (Mars 2020 Rover). It is a sectored radiometer plus a "SkyCam" (zenith-pointed CCD devoted to scientific purposes), intended to estimate the OT and scattering phase function of the Martian dust [17].
- Radiation and Dust Sensors for the meteorological station of the ExoMars 2020 Lander. These are a new SIS (SIS'20) and a Dust Sensor (DS'20) evolved from a first development carried-out for MetNet in 2009. The first one is a new radiometer with improved performance, capable of determining OT, scattering-phase function and detecting the presence of clouds, with two new bands dedicated to analyze the variations in ozone concentration and a micro-spectrometer of only 5 grams that provides 10 nm resolution from 360 to 780 nm. DS'20 employs a single broad-band spectrum emitter and two pairs of detectors in two different bands within the 1-5 μm region, measuring both back and forward scattering generated by the dust particles. It allows to estimate the size of the dust grains [18]
- MicroMED: a miniature nephelometer for the Dust Complex package of the ExoMars 2020 Lander [19]. It will allow to precisely measure the volumetric density of the dust particles in the Martian air close to the lander, as well as measuring their size on-by-one. The whole electronics and software are defined and developed by INTA within InMARS. We expect to download information from more than 100.000 dust particles per Sol.

Fig. 1 shows some of the aforementioned developments.

Boosting horizontal capabilities. Besides those developments, we have also defined, developed and characterized with excellent results, a new mixed-signal ASIC capable of performing the whole signal conditioning and high-precision acquisition of up to ten photodetectors (with photocurrents in the pA range) plus thermal and other auxiliary information.

We have also carried-out, during almost three and a half years by now, an intensive thermal cycling test campaign from -135ºC to 40ºC to more than 20 different active electronic components (meaning Part Numbers; minimum 3 samples per P/N), 10 types of photodetectors, dozens of passive components and several Printed-Circuit Board mounting techniques, glues, resins, conformal coatings, paints, etc. Thanks to this effort, we have produced a comprehensive portfolio of components, materials and processes that we may use in our present and future developments with absolute confidence about their reliability in a so-stressing thermal scenario (more than 3000 thermal cycles applied to every part) [17].

Finally, we have also performed complete qualification and screening tests to some selected COTS that we use for these new developments, such as the aforementioned micro-spectrometer or the microcontroller that is the core of the MicroMED processing unit [9].

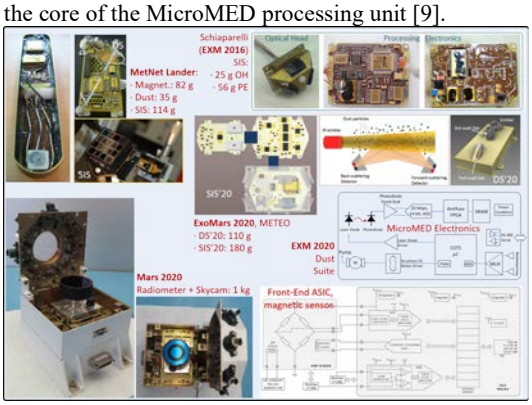

Fig. 1 Some of the described developments for different Mars exploration missions.

Synergies and Next Steps: Once the present developments for the on-going missions are finished, the InMARS activity will continue is different frameworks, both related to other Space projects and new concepts for Martian exploration.

Next steps. We intend to continue the InMARS effort in the development of complete instruments, and also to open it to non-scientific developments (platform

subsystems), aiming at the future construction of small planetary probes. In this sense, we will work with two reference concepts on mind: MetNet and MarsDrop. The first has already been mentioned. INTA was responsible of the whole Spanish contribution to this trilateral mission, back in 2008-2011. It is a penetrator-type lander around 24 kg. MarsDrop is a JPL initiative [20], a small probe in the 5 kg range, for which we intend to provide scientific instruments and, potentially, additional contributions. With those potential missions on mind, the following developments are under consideration at this moment for the 2019-2022 period:

- Scientific instruments: we are starting feasibility studies for the development of a compact LIDAR for atmospheric sounding, as well as a new CO_2 sensor together with the Carlos III University [21].
- Platform subsystems: we intend to focus our efforts in three key elements such as (a) a miniature, high-performance, Instruments Control Unit/On Board Computer, starting from the long experience we already have in the development of this kind of units for small satellites; (b) a compact radio transceiver compatible with Proximity-1 and (c) power generation and storage elements for high-efficiency and low-temperature operation.

All of that is, as stated, in a preliminary selection/feasibility analysis phase at this moment.

Synergies with other programs. Synergy between different programs is key when trying to set-up an horizontal strategy for technology development. INTA is now resuming (after some years in stand-by due to budget limitations) two activities that offer several synergistic opportunities with regard to InMARS: the Small Satellites Program and the Optical Wireless Communications initiative [22].

In the first of them, we are in the phase-A of an in-orbit demonstration of a formation-flying cluster of cubesats named ANSER. The first payload (a distributed one, with detectors in three satellites separated between 1 and 10 km from each other) will be based on the same micro-spectrometer we have integrated into SIS'20. New read-out electronics will be developed for the particular mission requirements, as well as complete optics. Also, intersatellite distance determination based on a simplified and highly compact laser ranger is considered. This could be a reduced and very simplified version of the aforementioned LIDAR, with short-distance ranging instead of atmospheric sounding application.

Regarding the optical wireless communications, we intend to take them from the intra-satellite application we developed during more than a decade, to the short-distance inter-satellite communication within a single cluster. The target data rate will be in the order of 50 to 100 Mbps, which means that the same kind of transimpedance receiver may be used for both communications, ranging and LIDAR. Thus, synergies are evident. The development of a dedicated ASIC for this purpose is also under consideration.

Conclusion: InMARS is part of a continuous effort that we started more than ten years ago, devoted to the development of different resources and enabling technologies for the construction of compact instruments, and other electronic units, devoted to Mars exploration and with strong synergy with our own Small Satellites program. We intend to continue and expand these capabilities in the next five years, always having on mind realistic mission scenarios.

Part of this work has been funded by the Spanish National Research, Development and Innovation Program, through grants ESP2014-54256-C4-3-R and ESP2016-80320-C2-1-R.

References: [1] Arruego I. et al. (2017), *Adv. Space Res., 60*, 103-120. [2] Toledo D. et al. (2017), *Planet. Space Sci 138*, 33-43. [3] Esposito F. et al., *Space Sci. Rev.*, submitted. [4] Arruego I. (2014), *in Proc. of IPM 2014,* Greenbelt, MD, USA. [5] López-Ongil C. et al. (2012), *in Proc. of 18th IEEE IOLTS*, 188-193. [6] Jiménez J.J. et al. (2006) *IEEE Rad. Effects Data Workshop*, pp. 77-84. [7] Jiménez J.J. et al. (2007) IEEE Radiation Effects Data Workshop, pp. 73-79 [8] Michelena M. et al. (2008), *J. App. Phys. Vol. 103*, *Iss. 7*, pp 07E912 - 07E912-3. [9] Martin-Ortega A. et al. (2017), *in Proc. IPPW, The Hague, Netherlands.* [10] Rivas J. et al. (2017), *CEAS Space J.* [1º] Michelena M. et al. (2010), *IEEE Trans. Aerosp. Elec. Sys., Vol. 46, N. 2*, 542-557. [11] Jiménez J.J. et al. (2012), *IEEE Trans. Nucl. Sci. 59*, *N.4*, 1092-1098. [13] Harri A-M et al. (2017), *Geosci. Instrum. Method. Data Syst. 6*, 103-124. [14] Arruego I. et al. (2010), *in Proc. EGU, Vienna, Austria*. [15] Ramos-Martos J. (2012), *in Proc. AMICSA, Noordwijk, Netherlands*. [16] Sordo-Ibáñez S. et al. (2014) *in Proc. IEEE MetroAeroSpace*, Benevento, Italy. [17] Apéstigue V. et al. (2015), *in Proc. EPSC*, Nantes, France. [18] De Castro A.J. et al. (2017), *in Proc. ExoMars Atm. Sci. Miss. Workshop, Saariselka, Finland*. [19] Esposito F. et al. (2017), *in Proc. ExoMars Atm. Sci. Miss. Workshop, Saariselka, Finland*. [20] Staehle R. et al. (2015), *in Proc. AIAA/USU Small Sat. Conf.*, Utah, USA. [21] Cortés F. et al. (2012), *SPIE Proceedings Vol. 8550, Opt. Sys. Des.* [22] Arruego I. et al. (2009), *IEEE J. Sel. Areas Commun. Vol. 27, N. 9,* 1599-1611.

TESTING CAMPAIGN OF A MARTIAN SPHERICAL WIND SENSOR AT THE AWTSII WIND TUNNEL FACILITY. L. Kowalski, S. Gorreta, M.T. Atienza, V. Jimenez, L. Castañer, M. Dominguez-Pumar, MNT-Group. UPC-Campus Nord, Ed. C4. Jordi Girona 1-3. 08034 Barcelona, SPAIN. manuel.dominguez@upc.edu

Introduction: The purpose of this paper is to present the experimental results obtained with a prototype of a 4-sector spherical anemometer, [1-2], in the Aarhus Wind Tunnel Simulator II (AWTSII) [3] reproducing Martian conditions. The main objective of the experimental campaign has been to measure wind velocity for a wide number of yaw and pitch angles, in an environment in the range of typical Mars conditions. The experimental results indicate that wind speed and angle recovery can be achieved with the proposed spherical sensor. The obtained responses are close to the empirical models found in the literature [4].

Sensor description: The sensor is composed of 4 sectors, conforming a 11 mm diameter sphere, that are placed on two superimposed PCBs, which act as supporting structure and provide signal routing (see Figure 1). A customized silicon die which includes a Pt resistor is attached to each sector in order to sense temperature and dissipate heat. Finally, two additional resistors are placed on the supporting PCBs in order to be able to control the temperature at the core of the sphere, on the PCBs.

The sensor is operated at the same constant temperature in the sectors and core. Conduction losses from the sectors to the supporting structure are minimized, since all parts are at the same temperature. The output signals are the heating powers injected on the 4 resistors within the sectors.

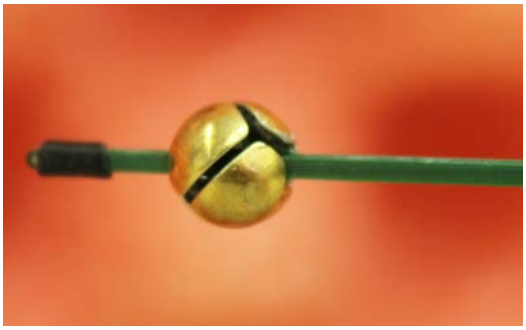

Fig. 1. Photograph of the prototype of the spherical sensor anemometer.

Main result: The paper summarizes the experimental results obtained in a measurement campaign at the AWTSII wind tunnel of the Mars Simulation Laboratory at Aarhus University. The targeted environmental conditions are: CO2 atmosphere, 7-8 mbar, temperatures from -25ºC to -15ºC. In order to test the invariability of the results to the operating temperature two constant operating temperatures have been used: T_{hot}=20ºC and T_{hot}=10ºC. The tested wind velocities span the range 0 – 16 m/s, whereas the angle span is 0-360º full yaw rotation, and pitches from -45º to +45º. The pressure and ambient temperature in the chamber were continuously monitored during the experiments.

Figure 2 shows the total heating power in the 4 sectors as a function of wind velocity in two experiments at two different target temperatures (T_{hot}=20ºC and 10ºC).

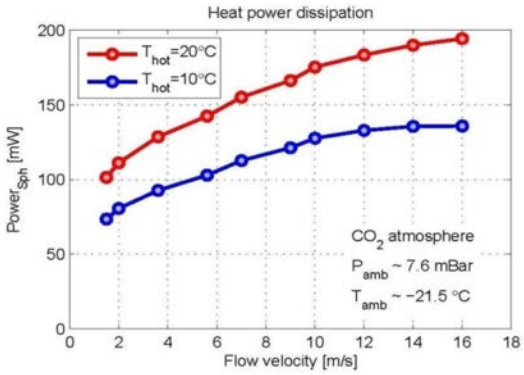

Fig. 2. Total power delivered to the 4 sectors, for different wind velocities, and two operating constant temperatures.

Figure 3 shows the calculated thermal conductance of the whole sphere, taking into account the heating power delivered to the sectors, ambient temperature and pressure variations. Superimposed is the comparison with the model in [4].

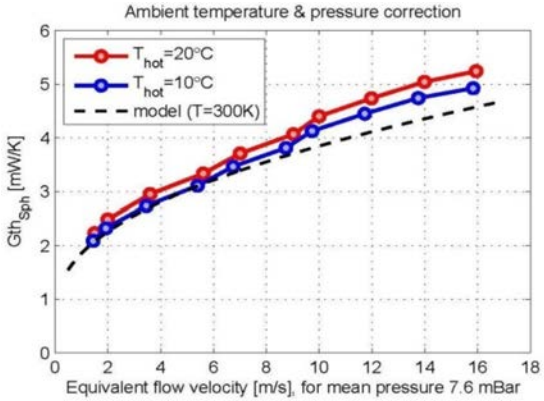

Fig. 3. Thermal conductance in the experiments obtained from the total power in the sectors, ambient temperature and pressure. Comparison with the model in [4].

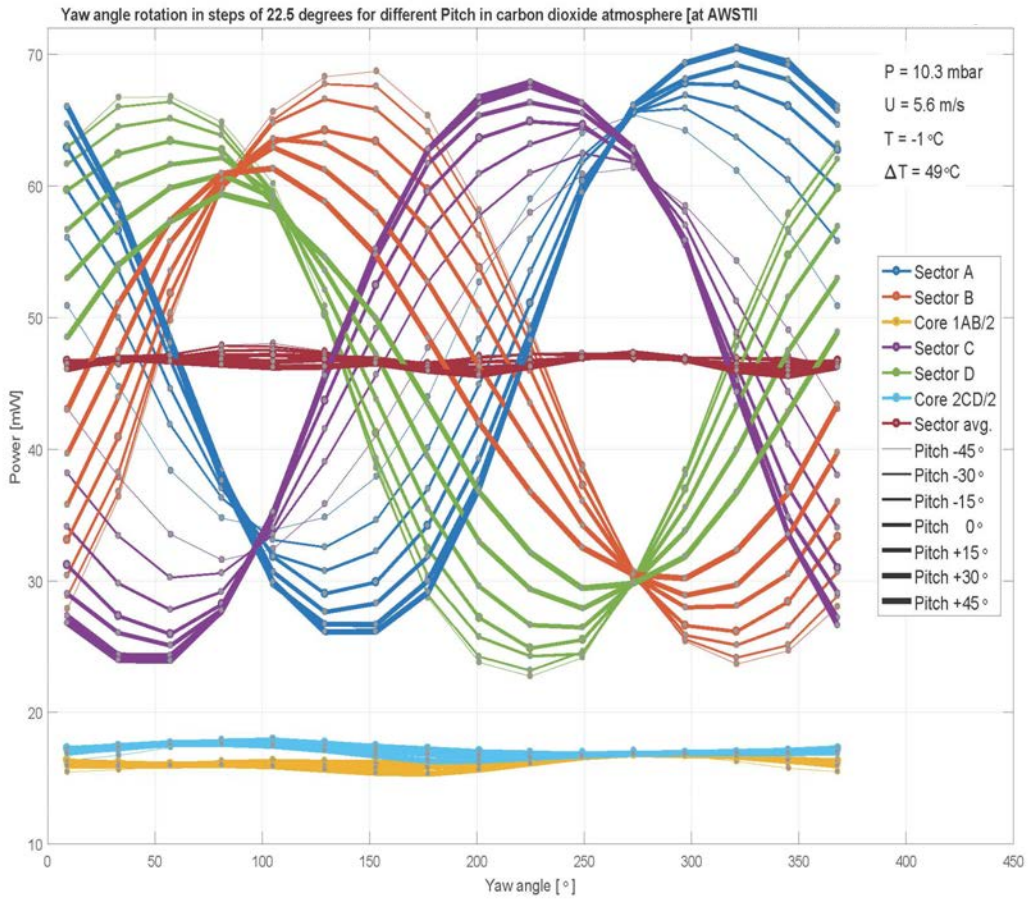

Fig. 4: Power delivered to all Pt resistors (sector A,B,C,D and 2 cores) in a experiment in which 0-360º yaw angles were swept for different pitch angles (-45º, -30º, -15º, 0, 15º, 30º and 45º), at constant wind speed (5 .6 m/s)

Finally, Figure 4 shows the powers injected in all resistors for a long-time experiment in which many different yaw and pitch angles were swept. As it can be observed in Figures 3 and 4, wind speed and angle recovery is possible: high individual sector variations for different yaw and pitch angles, whereas the sum of power of four sectors remains constant, and depends only on wind speed.

Acknowledgements:

Authors want to show their gratefulness to the Planetary Environment Facilities at Aarhus University (DK) for their hostage and professional approach. This laboratory is a member of Europlanet 2020 RI which has received funding from the European Union's Horizon 2020 research and innovation programme under grant agreement No 654208. This work was partially supported by the Spanish Ministry MINECO under Project grant no. ESP2016-79612-C3-2R.

References:

[1] L. Kowalski, et al. (2016), *IEEEE Sensors Journal*, *16*, 1887-1897. [2] M. T. Atienza, et al. (2017) *Sens. and Act. A, 267*, 342-350. [3] C. Holstein-Rathlou et al. (2014), J. Atm. Oceanic Tech., 31, 447-457. [4] Zhi-Gang Feng et al. (2000), *Int. J. Heat Mass Tr.*, 43, 219-229.

Mars Sample Return to Subglacial Polar Science on Earth.

R. Timoney[1], K. Worrall, D. Firstbrook, P. Harkness and J. Rix[2],

[1]University of Glasgow, School of Engineering, Space & Hazardous Environments Access and Research Group, G12 8QQ, Scotland, UK. r.timoney.1@research.gla.ac.uk

[2]British Antarctic Survey, Madingley Road, Cambridge, UK. CB3 0ET. jrix@bas.ac.uk

Introduction:

The global polar science community has expressed a clear desire to obtain bedrock samples from beneath glacial ice sheets as part of the ongoing, international paleoclimatology focus. While there exists drilling systems which are capable of subglacial bedrock sampling, these systems are typically bulbous and heavy by design, thus incompatible with the British Antarctic Survey (BAS) logistical effort consisting of relatively compact Twin Otter aircraft. To this end, a solution was pursued which would make use of a lightweight and low footprint ice-sampling system currently in use with BAS, the Rapid Access Isotope Drill (RAID). While the new system would retain key elements of the RAID design, the entire terrain-facing, ice auger element would be replaced by a rotary-percussive system capable of penetrating rock and consolidated terrain. This project was jointly undertaken by the University of Glasgow and BAS, harnessing Glasgow's knowledge in developing low resource sampling solutions for planetary exploration, and has resulted in the development of the Percussive Rapid Access Isotope Drill (PRAID). This paper seeks to detail the development and testing of both the proof-of-concept model of this novel system (Figure 1), highlighting the design challenges faced throughout. Results from prolonged cold chamber testing shall be discussed alongside an insight in to the development of the industrialised, full scale model which is to be tested in Antarctica during the upcoming summer season.

Figure 1: Proof of Concept P-RAID

It is thought that any lessons learned from this upcoming field test campaign of the system may also be provide an opportunity to further advance the TRL of the system for adoption by future planetary missions, advancing the European robotic sampling capability.

On behalf of the team at Glasgow, the British Antarctic Survey and members of the international polar exploration community, I look forward to presenting at the 15th International Planetary Probes Workshop.

Silicon Carbide, Vacuum Tube Nanoelectronics: Application for Exploration Missions Requiring Category III/IV Planetary Protection

International Planetary Probe Workshop (IPPW) 15
University of Colorado, Boulder Colorado
June 9-17, 2018

J. O. Arnold[1] and M. Meyyappan[2]
[1]NASA Ames Research Center N229-3, Moffett Field CA 94035, James.O.Arnold@NASA.gov
[2]NASA Ames Research Center N229-3, Moffett Field CA 94035, M.Meyyappan@NASA.gov

Spacecraft and instruments used to explore moons and planets where alien life might exist are required to meet COSPAR Category III/IV Planetary Protection (PP) requirements [1]. Quoting [1], "Specific destinations are Mars, Europa, Enceladus and others TBD". Processes that can be used to meet PP requirements for these destinations and impediments involving their application are discussed in [2]. The purpose of this paper is to acknowledge attributes of an emerging technology that can address impediments arising in the Dry Heat Microbial Reduction (DHMR) and Thermoradiation PP sterilization processes.

The 1976 Mars Viking - 1 Lander was sterilized by the DHMR process by baking the entire spacecraft at 117 ^{O}C for 30.2 hours at a humidity of 1.3 mg/mL [3]. The spacecraft was encapsulated in a biological barrier until it was in space, on its way to Mars, to help ensure that terrestrial biota would not confound the search for a second genesis on the red planet. While the Viking style DHMR is considered the "gold standard" process for PP, there are incompatibilities in its application including the requirement for onboard electronics to be rated for temperatures of 95 to 100 ^{O}C [2].

NASA's Space Mission Directorate is supporting a research program to develop electronic systems that will employ nanoscale vacuum tubes made of silicon carbide [4], as depicted in Figure 1. One motivation for this research is to provide future spacecraft electronics that can withstand the severe radiation fields in the vicinity of Europa. The SiC devices can be fabricated with modern integrated circuit manufacturing processes. The electrodes shown in Fig. 1 are 10 nm in size and the evacuated region between them is several tens of nm in length. Since the spacing between the electrodes is small, high vacuum is not required for operation. The SiC vacuum tube nanoelectronics project has a deliverable to produce demonstration devices within 2 years.

Importantly, the SiC nanoscale vacuum tube devices will be able to withstand temperatures of 500 ^{O}C. Their use on future spacecraft headed for Category III/IV destinations would address the requirement for a temperature rating of ~ 100 ^{O}C for onboard electronics for the DHRM PP method [2].

The Thermoradiation PP method involves the application of both heat and gamma radiation; sterilization benefits are realized when both of the penetrating processes are applied simultaneously [5]. As pointed out by the authors of [2] the Thermoradiation method may be promising for parts, subsystems or integrated systems that can tolerate test parameters for temperature and radiation. Scalability of gamma radiation has been addressed by the DoD, postal service and food processing suppliers [2]. An impediment stated for the application of the thermoradiation process is that onboard electronics need to be rated for 100 - 150 Krad and temperatures from 95 to 100 ^{O}C [2]. Since the SiC nanoscale vacuum tube devices will be able to withstand radiation to 1 Mrad and temperatures of 500 ^{O}C, it seems safe to say that their use on future spacecraft for Category III/IV missions would address the radiation and temperature impediment for application of the Thermoradiation PP process.

The authors understand that the impediments considered herein are examples of those that may be involved in future applications of the DHMR and Thermoradiation sterilization processes. Clearly, the attributes of emerging SiC nanoscale electronics technology discussed in Ref. [4] can address impediments discussed in [2], and that benefits for future missions requiring Category III/IV planetary protection will be achieved by their maturation. The focus here has been to discuss attributes of SiC vacuum tube electronics that address impediments to PP processes, but it is noted that many applications for the emerging technology exist where sensitivity to radiation can be an issue.

The authors acknowledge Jin-Woo Han for his contributions to nano vacuum tube fabrication.

References

[1] "Space Research Today, COSPAR's Information Bulletin", No. 200, pp 11-25, December 2017.
[2] Pugel, D. E., Rummel, J. D., and C. Conley, "Brushing Your Spacecraft's Teeth: A Review of Biological Reduction Processes for Planetary Protection Missions", IEEE Aerospace Conference March 2017.
[3] https://planetaryprotection.nasa.gov/requirements

[4] Han, J.W., Moon, D.I., and Meyyappan, M. " Nanoscale Vacuum Channel Transistor, Nano Letters, 17, 2146-2151 (2017).

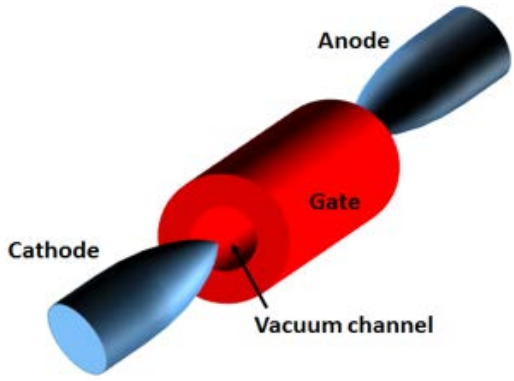

Fig1. Elements of a Nanoscale SiC Vacuum Tube [4].

[5] NASA SP-5105, Advances in Sterilization and Decontamination, A Survey" 1978.

SILICON CARBIDE PRESSURE SENSORS FOR VENUS ENVIRONMENT. R. S. Okojie[1], D. Lukco[2], R. D. Meredith[1], L. M. Nakley[1], and K. Phillips[3], [1]NASA Glenn Research Center, Cleveland, OH 44135; robert.s.okojie@nasa.gov, [2]Vantage Partners, LLC, NASA Glenn Research Center, Cleveland OH, [3]Sierra Lobo Corporation, NASA Glenn Research Center, Cleveland OH.

Introduction: We report on the evaluation of 4H-SiC piezoresistive pressure sensors in the simulated Venus environment of the NASA Glenn Extreme Environments Rig (GEER) [1]. The purpose of the evaluation was to determine the survivability of the pressure and temperature sensors and ancillary packaging components when subjected to the high pressure and aggressive chemical media that are characteristic of the Venus environment. Interest in Venus has been stimulated by the ongoing debate about Earth's planetary evolution, particularly in regards to its climate, and NASA has proposed a flagship mission to Venus to be launched in the near future [2]. Quantifying how the Venus evolution ran its course will greatly aid researchers trying to model Earth's climate dynamics.

Though probes have landed on the surface of Venus, none have conducted significantly long geodynamic characterization of the planet. It is in the context of the flagship mission's objectives that the Long-Life In-Situ Solar System Explorer (LLISSE) project aims to develop robust electronics and sensor technologies that would survive long duration on the Venus surface and perform reliably while making critical measurements, data processing, and transmission of information [3]. Among the suite of sensors proposed is pressure sensors. The criteria demanded by the Venus environment are as follows: The average atmospheric pressure is 92 bar (~9.2 MPa) and surface temperature is 462 ºC. In terms of chemistry, the near surface atmosphere is predominantly carbon dioxide, low level nitrogen, sulfur dioxide (SO_2) and traces of sulfides and corrosive halides [2].

In this current work, legacy SiC piezoresistive pressure sensors that had been demonstrated to operate reliably for long duration at 600 ºC in air and engine test rigs [4] were packaged in a configuration that would allow for insertion into the GEER chamber. The chamber was gradually pressurized to 1346 psi (9.28 MPa) and held for 22 hours at room temperature to determine the existence of leaks in the chamber. With no leaks detected, the pressure was gradually ramped back down to atmospheric pressure. During the pressure ramp-up, the response of the sensor to pressure was observed to be linear, with a pressure sensitivity of approximately 0.21 μV/psi obtained. The low sensitivity was expected, since the sensor diaphragm thickness was designed to sustain a burst pressure of 2X operational pressure. Sensors for the future campaigns would have a 1.5X operational burst pressure and would result in higher sensitivity.

The chamber was subsequently purged again with nitrogen to 1346 psi (9.28 MPa) and the temperature raised to 451 ºC. These conditions were held for approximately 50 hours after which the pressure and temperature were decreased to near vacuum and 150 ºC, respectively. All relevant gases were then delivered into the chamber at these conditions, after which the temperature was ramped up to Venus-like temperature of 462 ºC, with pressure reaching 1346 psi. These were the conditions of the chamber for the next 60 days, except for the ocassional boosting of the SO_2 that was consumed as a result of reactions inside the chamber. Data from the pressure sensors was acquired every 2 minutes during the 60-day campaign.

While the pressure sensor survived the 60 days of exposure in the simulated Venus environment, it operated reliably and accurately for 12 days. The primary failure mechanisms for the sensor were associated with chemical reactions of the sensor feedthrough connections in the chamber, the details which would be presented at the workshop.

This work was performed in support of the NASA Innovative Measurement theme of the Transformative Tools and Technologies and LLISSE projects.

References:

[1] https://geer.grc.nasa.gov/

[2] Hall, J. L., Senske, D. A., Grammier, R., Bullock, M., Cutts, J. A., "Venus Flagship Mission Study: Report of the Venus Science and Technology Definition Team," NASA TO-NMO710851, 2009.

[3] Kremic T., Hunter G. W., Neudeck P. G., Spry D. J., Ponchak G. E., Beheim G. M., Okojie R. S., Scardelletti M. C., Wrbanek J. D., Vento D. M., Nakley L. M., and Balcersk J., "Long-Life In-Situ Solar System Explorer (LLISSE) Probe Concept and Enabling High Temperature Electronics," 48th Lunar Planetary Science Conference, March 20-24, 2017, The Woodlands, TX.

[4] Okojie R. S., Nguyen V., Savrun E., and Lukco D., "Improved Reliability of SiC Pressure Sensors for Long Term High Temperature Applications," 16th International Solid-State Sensors Actuators and Microsystems Conference, pp. 2875-2878, 2011.

Development of a Pneumatic Sample Transport System for Ocean Worlds. Joseph Sparta[1], Tighe Costa[1], Fredrik Rehnmark[1], Jameil Bailey[1], Kris Zacny[1], and Ralph Lorenz[2], [1]Honeybee Robotics, Pasadena CA, USA (jsparta@honeybeerobotics.com), [2]Johns Hopkins Applied Physics Laboratory, Laurel, MD 20723, USA (Ralph.Lorenz@jhuapl.edu).

Introduction: A pneumatic sample transport system is being developed under the NASA COLDTech program for the transfer of cryogenic material from a planet's surface to a vehicle's on-board science instruments. This project focuses on the design of a pneumatic transport system for the exploration of Titan; it is feasible, however, that such a system could be used to explore other destinations.

Titan is geologically diverse (with methane lakes and rivers, sand dunes, craters, and cryovolcanoes) [1], and its surface conditions are likely to be similarly diverse. Initial testing accounts for this diveristy by including a wide variety of Titan mechanical analogs with ranging physical properties. An overview of the current status of the project follows.

Background: Sensitive scientific instruments deployed to ocean worlds to search for traces of past or extant biological activity will almost certainly be housed in a thermally controlled environment within the vehicle. A sample acquisition and delivery system presenting surface material to these instruments must be capable of operating at cryogenic temperatures (Titan's surface temperature is 94K) and in reduced gravity (Titan's surface gravity is 0.14g).

A vacuum cleaner uses airflow to pickup, transport, and collect loose material. The same applies to the pneumatic conveying of drill cuttings and surface material from the ground to an instrument for analysis. The process is simple and fast, and transport takes only a fraction of a second. Conveying material with a fast-moving air stream has a dual benefit of reducing the risk of adhesion along the transport path and minimizing temperature rise of the sample.

Pneumatic transport was successfully performed on Venus during the Venera 13, 14 and Vega 2 missions [2]. Pneumatic sample transport is also possible on airless worlds using a supply tank of gas and a manifold to seal around the target sample: injecting gas into the manifold pushes the sample through the pneumatics, as demonstrated by Honeybee's proposed PlanetVac sampling system [3].

Modeling: The pneumatic conveyors used in terrestrial process industries are typically designed to transport a specific dry material, such as grain or cement, under controlled conditions. Pneumatic transport involves complex, two-phase dynamic interactions between gas and solid particles and even three-phase flow (if the material being conveyed is wet). Consequently, the physics of pneumatic transport are not completely understood and existing models are largely empirical [4]. While these models can provide a useful starting point for design, testing is required to properly size and characterize the performance of any pneumatic transport system.

Experiments: The goal of current testing efforts is to characterize the transport of Titan simulants in a system with an architecture analogous to the flight design. These tests will determine the baseline fluid velocity for high sample collection efficiencies ([mass deposited in the sample cup] / [total mass of sample ingested]) of the target simulants in STP air. Operating at high collection efficiencies reduces buildup of material in the lines, helps prevent clogging, and minimizes crosstalk between samples. Tests are performed at standard room conditions using a sample transport testbed powered by a commercial vacuum cleaner (**Figure 1**). Future testing will be performed in environments more representative of Titan's atmosphere.

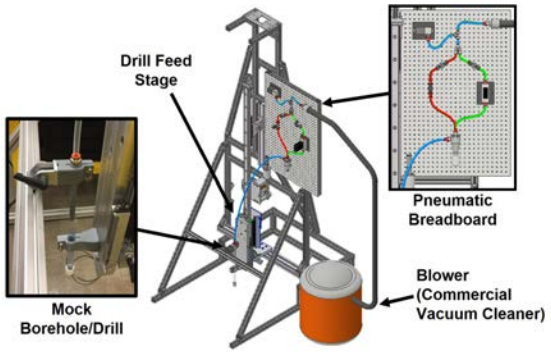

Figure 1. Pneumatic sample transport testbed.

Design: The first prototype will be designed for terrestrial operation and used for higher-fidelity simulant transport testing. The system will then be scaled for operation in Titan atmosphere.

The accepted models for pickup, choking, and saltation velocities account for the fluid properties of the carrying medium. [5] Comparison of the predictions for transport velocities on Titan to those on Earth show that the fluid velocity required to pneumatically convey a certain sample on Titan is approximately 4-5x lower than that required on Earth. This prediction will be tested with the Titan-scaled design at relevant conditions (cyrogenic GN2 at 1.5atm).

The Titan blower will be designed for the baseline fluid velocity determined in Earth atmosphere tests (adjusted for the different atmosphere and with an added margin). The scaling of the blower will be guided by the fan affinity laws, which describe the relationships of fan speed, fan size, and air density to pressure drop, flow rate, and power consumption.

The Titan cyclone separator will be scaled from the Earth atmosphere prototype according to Lapple's model of cut diameter, which accounts for fluid properties and flow rate. [6] The geometry may be fine-tuned for improved separation of sticky materials: Titan simulant transport results have so far shown that standard cyclone geometries (designed to work with dry materials) are not optimized for separation of wet and cohesive materials.

Conclusions and Future Work: This work represents a critical first step toward the design and qualification of a pneumatic sample transport system for ocean worlds. A custom blower will be designed and tested at room temperature based on the initial test results. Eventually, the design will be scaled for a Titan environment and tested at Titan temperature, pressure and atmospheric composition.

Acknowledgements: This work was funded by NASA's Concepts for Ocean worlds Life Detection Technology (COLDTech) program. The authors would like to thank the program director Ryan Stephan.

References: [1] Lorenz, R. et al, (2017) APL Tech Digest. [2] Badescu, V. and Zacny, K., (2015) *Inner Solar System: Prospective Energy and Resources*, 193-194. [3] Zacny et al, (2014) *IEEE Aerospace*. [4] Klinzing, G. (2018) *KONA Powder and Particle 35*, 150-159. [5] Klinzing, G. et al, (2010) *Pneumatic Conveying of Solids*. [6] Dirgo, J. and Leith, D., (1985) *Aerosol Science and Technology, 4, 401-415*.

ION SELECTIVE ELECTRODES FOR SOLUBLE SALT MEASUREMENTS ON ICY WORLDS. A. C. Noell[1], E. A. Oberlin[1], A. M. Fisher[1], R. C. Quinn[2], A. J. Ricco[2], R. E. Gold[3] and S. P. Kounaves[4,5], [1]Jet Propulsion Laboratory, California Institute of Technology, Pasadena, CA (anoell@jpl.nasa.gov), [2]NASA Ames Research Center, Moffett Field, CA, [3]Johns Hopkins University, Applied Physics Laboratory, Laurel, MD, [4]Department of Chemistry, Tufts University, Medford, MA, [5]Department of Earth Science & Engineering, Imperial College London, UK.

Introduction: The Wet Chemistry Lab (WCL) experiment was part of the Microscopy, Electrochemistry, and Conductivity Analyzer (MECA) instrument suite on the 2007 Mars Phoenix Lander that searched for and discovered ground ice in the Martian northern lattitudes [1, 2]. WCL was made of four indentical single-use 25 mL beakers with electrochemical sensors embedded in the walls for measuring soluble species leached from Martian regolith. Ion selective electrodes (ISEs) were one of the major classes of electrochemical sensors in WCL [3]. ISE measurements were used to speciate the major cations sodium, magnesium, calcium, and potassium, as well as to look for thruster contamination of the landing site during entry/descent/landing (EDL) by determining elevated levels of ammonium. The ISEs were the first to measure the high levels of perchlorate in the Martian soil that have since been confirmed by Curiosity and have stymied efforts to measure organics on Mars since Viking [4-6].

As NASA begins its in-situ exploration of Icy Worlds such as Enceladu, Europa, and Ceres, measurements of soluble salts will be critical to understand the dominant physio-chemical conditions in the oceans and ices on these bodies. With their proven flight heritage, ISEs and the WCL electrochemical sensors are attractive instrument technologies for implementing these important soluble salt measurements.

Nonetheless, a number of challenges need to be overcome to demonstrate that the WCL ISE sensors and related technology are suitable for missions in parts of the solar system further away than Mars. The general robustness of these sensors for long-duration storage and higher radiation levels need to be proven. Additionally, demonstrating robustness to alternative fluidic implementation and packaging, including in microfluidic arrays, is highly desirable to enable measurements on much smaller quantities of sample. A good example of a high-value small sample is from the Enceladus Life Signatures and Habitability (ELSAH) mission concept [7], recently selected for technology development, that would analyze collected plume particles from Enceladus.

Experimental: In order to address the robustness of the ISE sensors, a number of different tests have been performed or are in progress. To test long duration storage of the sensors, WCL flight spare beakers and engineering models were pulled out of storage after ~10 years since their previous testing. Typically, accelerated aging tests are required for determining the shelf life of such tecnology, but we were able to take advantage of the unique opportunity to work with flight spares and engineering models built over ten years ago.

New versions of the WCL-style ISE sensors were also built following the exact protocols of the original sensors and testing of their radiation resistance and their preservation under dry storage preservation is underway.

Sample size reduction was also pursued through the development of a microfluidic array of 14 WCL-style ISEs with a total sample volume of 100 µL. The development of novel solid-contact ISEs, that make use of the WCL ion selective membranes but change the signal-transduction portion of the sensor, are also under development to allow further miniaturization and ruggedization. These sensors are undergoing simultaneous testing for radiation, dry storage, and overall performance to assess them alongside the WCL-style sensors. These solid-contact ISEs hold the promise of further reducing the sensor size and potentially further reducing the amount of sample required by an order of magnitude.

Results: Two flight spares and two engineering models of WCL beakers were tested using the identical calibration and test procedure prior to their ~10-year storage. In all four beakers, the ISEs calibrated and measured within their stated specifications from ~ $3 \times 10^{-5} - 1 \times 10^{-1}$ M ion concentrations. One of the engineering model beakers was off nominal because of the failure of one of the two reference electrodes, and a general shift in the offset voltage, but still performed well because of the purposeful instrument design to carry two reference electrodes.

A 100 µL total volume ISE array was also designed and tested, demonstrating the compatibility of the WCL-style ISEs and microfluidic sample handling [8]. Good calibration slopes and measurement performance were demonstrated in this configuration.

Ongoing side-by -ide radiation, performance and storage testing of both WCL and novel solid-contact ISEs is underway and preliminary results will be presented.

References:

[1] Smith, P.H., et al. (2008) *Journal of Geophysical Research: Planets*, *113*, n/a-n/a.

[2] Smith, P.H., et al. (2009) *Science*, *325*, 58-61.

[3] Kounaves, S.P., et al. (2009) *J. Geophys. Res. [Planets]*, *114*.

[4] Glavin, D.P., et al. (2013) *J. Geophys. Res. [Planets]*, *118*, 1955-1973.

[5] Hecht, M.H., et al. (2009) *Science*, *325*, 64-67.

[6] Kounaves, S.P., et al. (2010) *Geophys. Res. Lett.*, *37*.

[7] *Enceladus life signatures and habitability*. 2018; Available from: https://en.wikipedia.org/wiki/Enceladus_Life_Signatures_and_Habitability.

[8] Oberlin, E.A., et al. (2017) *Astrobiology Science Conference*, Abs# 3251

DEVELOPMENT OF A DOUBLE HEMISPHERICAL PROBE (DHP) FOR IMPROVED SPACE PLASMA MEASUREMENTS. X. Wang[1,2], J. I. Samaniego[1,2], H. –W. Hsu[1,2], M. Horányi[1,2], J.-E. Wahlund[3], R. E. Ergun[1], and E. A. Bering[4]. [1]Laboratory for Atmospheric and Space Phsics, University of Colorado, Boulder, CO 80303, USA. [2]NASA/SSERVI's Institute for Modeling Plasma, Atmospheres, and Cosmic Dust, Boulder, CO 80303, USA. [3]Swedish Institute of Space Physics, Box 537, SE 751 21 Uppsala, Sweden. [4]Physics Department, University of Houston, Houston, TX 77204, USA. (First author's address: 3665 Discovery Drive, Boulder, CO 80303; Email: xu.wang@colorado.edu)

Introduction: Langmuir probes have been extensively used on sounding rockets, satellites, and interplanetary spacecraft (SC) for in-situ measurements of space plasmas, such as planetary magnetospheres and ionospheres. However, space environment is complicated, causing challenges in the probe measurements and their interpretation. Due to the interaction of the ambient plasma with the SC and onboard probe itself, the local plasma conditions around the probe could be very different from the true ambient plasma of interest. These local plasma conditions are often anisotropic and/or inhomogeneous. Current Langmuir probes are mostly made of a single electrode. These local plasma effects make their measurements and data interpretation difficult, introducing errors in the derived plasma characteristics.

Directional probes are able to characterize anisotropic and inhomogeneous plasmas. The first in-situ directional probe, the split Langmuir probe, was developed in 1970's and used for measuring the plasma flow in Earth's ionosphere [1]. The probe consisted of two planar plates or two hemicylinders that were insulated from each other, and were simultaneously swept with the same bias potentials. The current difference measured between the two electrodes was used to derive the plasma ion flow. Later, the Segmented Langmuir Probe (SLP), onboard French DEMETER [2] was also designed with 6 disc-shaped segments for characterizing the velocity vector of the ion flow.

Here we advance the directional probe technology by introducing a Double Hemispherical Probe (DHP) [3] to improve the space plasma measurements in a broad range of scenarios: i) low-density plasmas (the probe immersed in the SC sheath); ii) high surface-emission environments (photo and/or secondary electron emission from the probe and SC); iii) flowing plasmas (supersonic ions with respect to the SC); and iv) dust-rich plasma environments (local plasma generated by dust impact on the probe).

Instrument Design: The DHP working principle is similar to the split Langmuir probe described above. The probe consists of two hemispheres swept with same voltages simultaneously. The addition of the currents of two hemispheres is identical to the current of a single spherical probe (SSP) of the same radius. The difference currents between the two hemispheres are used to characterize the anisotropic/inhomogeneous plasma conditions created around the probe, which will be then removed or minimized on the interpretation of their current-voltage (I-V) curves.

A prototype DHP system is shown in Fig. 1. The DHP sensor is a few centimeters in diameter. The sensor consists of two metal hemispheres and an insulating ring-shaped spacer (Fig. 1b). The middle of the spacer is 0.25 mm thick to separate the two hemispheres. The threads are machined on the inner and outer surfaces of the hemispheres, and both sides of the spacer, respectively. The two hemispheres are fastened on both sides of the spacer. The spacer is hidden 2 mm below the outer surface of the sensor (Fig. 1c) to avoid charge buildup due to exposure to ambient plasma or UV radiation.

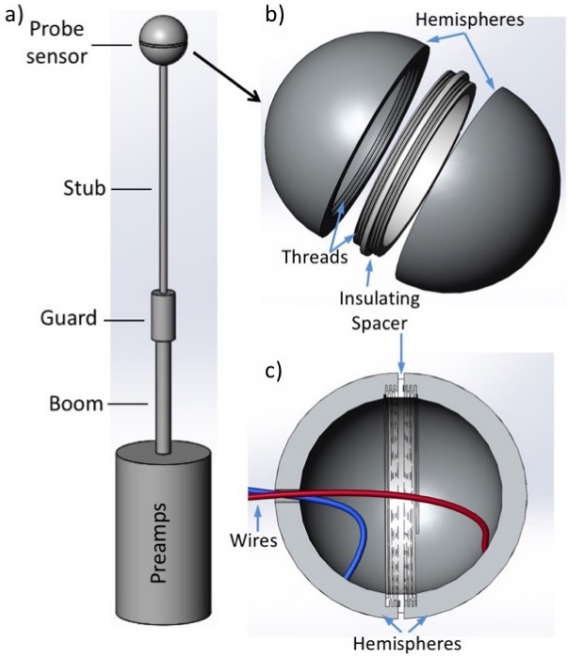

Fig. 1 a) Overview of a prototype DHP system; b) Exploded view of two hemispheres and an insulating spacer; c) Cross-section of the assembled DHP sensor with two wires connecting to each hemisphere.

The sensor is attached to a boom system, including a stub, a 'guard', a boom and two preamps (for the two hemispheres) enclosed inside a cylindrical housing. The stub can be optionally configured on both hemispheres to improve the symmetry of the probe geometry. The electronics use the technologies that

are readily available from the current Langmuir probes.

Preliminary Tests: A laboratory model made using two halves of stainless-steel ball bearings was used to demonstrate the capabilities of the DHP measurements in the scenarios described above. Significant differences in the I-V curves were shown in recognition of the anisotropic effects creaeted around the probe. Below are two examples (Figs. 2 and 3).

Figure 2 shows that the I-V curves of two hemispheres are identical in the bulk plasma (10 cm) and start to diverge in the sheath where a small potential drop emerges toward a plate (6 cm). The deviation becomes large as the probe moves into a 'deeper' sheath in which the potential drops more rapidly (4 cm). In the bulk plasma, the potentials around two hemispheres are uniform, resulting in the same current at a given probe voltage. In the sheath, the electron density decreases toward the plate. Therefore, the electron current of the plasma facing hemisphere (HS1) is greater than the plate facing hemisphere (HS2) as the probe voltage is larger than the local potential (i.e., in the electron saturation region).

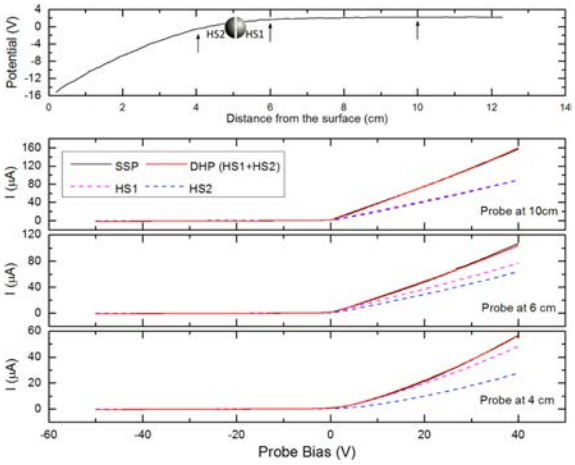

Fig. 2 Top panel: Potential profile above a plate surface measured using an emissive probe. The arrows indicate the three locations of the DHP and SSP measurements; Bottom panels: I-V curves of the probes at the three locations.

Figure 3 shows the I-V curve difference between the electron beam facing and shadowed hemispheres. Secondary electrons are emitted from the beam facing hemisphere while the shadowed hemisphere only collects the ambient plasma electrons and ions.

Discusstion and Summary: We described the concept of using a new DHP to characterize local plasma effects created around the probe due to the interaction of ambient space environments with the SC and the probe itself. Initial results tested with the simulated space plasma environments in laboratory demonstrated the capabilities of using the DHP in several scenarios described in the paper. The methods for characterizing and then removing or minimizing these local plasma effects on the probe measurements are currently being developed and examined.

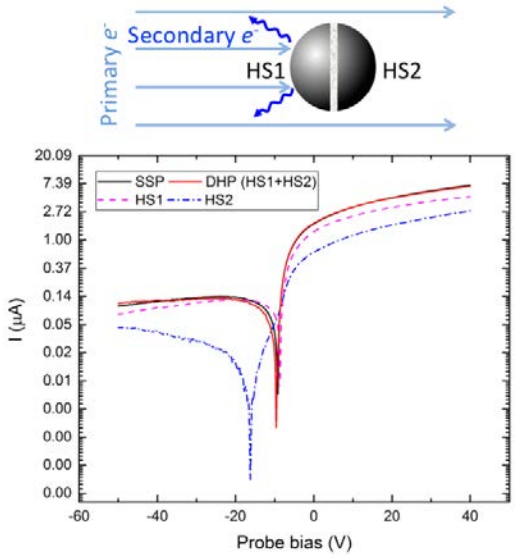

Fig. 3 Top: Diagram showing the DHP immersed in an electron beam; Bottom: Semi-logarithmic I-V curves of both the DHP and SSP.

References: [1] Bering, E. A., M. C. Kelley, F. S. Mozer and U. V. Fahleson (1973a), Planet. Space Sci., 21, 1983-2001. [2] Lebreton, J.P., et al (2006), Planet. Space Sci., 54, 472–486. [3] Wang, X., J. I. Samaniego, H.–W. Hsu, M. Horányi, J.-E. Wahlund, R. E. Ergun, and E. A. Bering (2018), submitted to JGR.

SHOCK LAYER RADIATION MEASUREMENTS FOR PLANETARY PROBES

S. M. White[1], M. E. Macdonald[2] and R. A. Miller[3],
[1]NASA Ames Research Center, Moffett Field, CA 94035, susan.white@NASA.gov,
[2]Jacobs Technology, NASA Ames Research Center Moffett Field, CA 94035, megan.e.macdonald@nasa.gov,
[3]Analytical Mechanics Associates, NASA Ames Research Center, Moffett Field, Ca 94035, ruth.miller@nasa.gov.

Introduction: Shock layer radiation to a planetary probe's heat shield has been investigated since the 1960s, using ground tests, flight tests, and theoretical modelling. As a probe enters any planetary or lunar atmosphere, entry heating to the TPS can include both convection and radiation. At high masses and speeds, the energized, shocked gas emits significant levels of radiation, characteristic of the gascap's state. High fidelity radiation simulations are used to model shock layer radiation for past and future missions. Radiation was a key component of entry heating to Jupiter's Galileo probe, and for Cassini's Huygens probe lander to Saturn's moon Titan.

Radiometers and a spectrometer were embedded in the TPS of NASA's Project FIRE II, Apollo 4 and 6, as well as PAET. PAET (Planetary Atmosphere Entry Experiment Test) is particularly relevant to planetary probes since it successfully demonstrated detecting the atmospheric composition using shock-layer radiometry. For high-speed entries such as planned Orion lunar return missions, modelling predicts shock layer radiation will have a major impact on TPS heating, which has been experimentally validated with high resolution spectrometers in EAST tests (Figure 1). The NASA Orion program and Mars 2020 include and propose for future use embedded small scale, low-mass radiometers and mini-spectrometers.

Both historic and current experiments and flight test experience have identified challenges and guided improvements in embedded sensors (Figure 2). The performance of radiation sensors embedded in heated ablative TPS offer unique challenges. Ground tests with high levels of incident radiation combined with relevant total heat flux levels enable refinement and improvements.

Recent work used a specific COTS fiber-optic mini-spectrometer, selected for wide wavelength range for testing flexibility. Tests with non-embedded mini-spectrometers, focused on the boundary layer from outside, successfully demonstrated the sensitivity to measure boundary layer emission both in NASA Arcjet tests as well as in separate laser tests. Figure 3 shows a proof of concept: these broad range mini-spectrometers (with subsequent lower resolution) detected the strongest Na and K spectral lines in both Arcjet test and Laser tests superimposed above thermal radiation. Higher resolution is attainable.

Characterization of the radiometer and spectrometer devices' components includes the radiative transport properties of the optical components and surfaces in Figure 4. Environmental and launch load testing and potential future improvements in sensor design and scale are discussed.

Figure 5 shows other instruments, with intriguing future possibilities including quantum dots. For future tests, the Laser Enhanced Arcjet Facility (LEAF) offers the unique combination of flight-relevant levels of radiant heating with convective heating over an appropriate area to allow ground testing in this challenging combined heating environment over a greatly enhanced test space.

References: [1] Brandis A. et al., JTHT 31, 1, 2017. [2] TPS Instrumentation Tutorial, Empey D. and Martinez E., IPPW9, 2012.

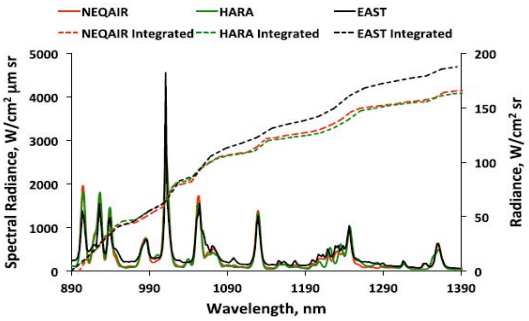

Figure 1 Shock layer radiation experiments agree well with modelling [1]

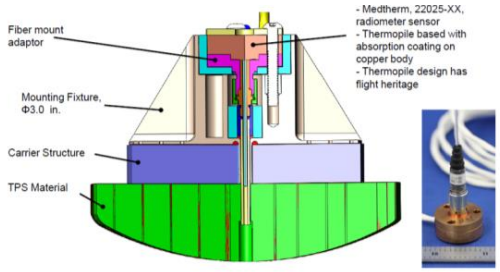

Figure 2 Arcjet model with embedded radiometer [2]

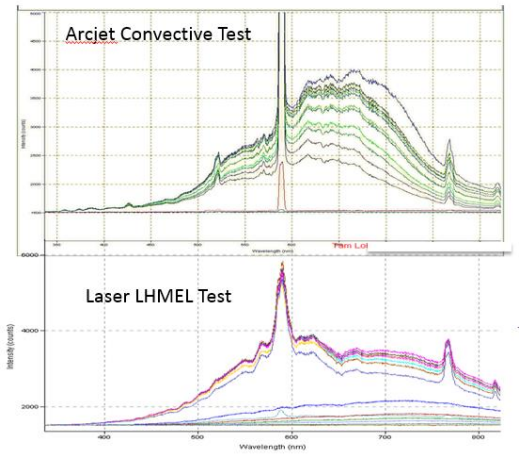

Figure 3 Mini-spectrometers detect key lines and thermal in testing

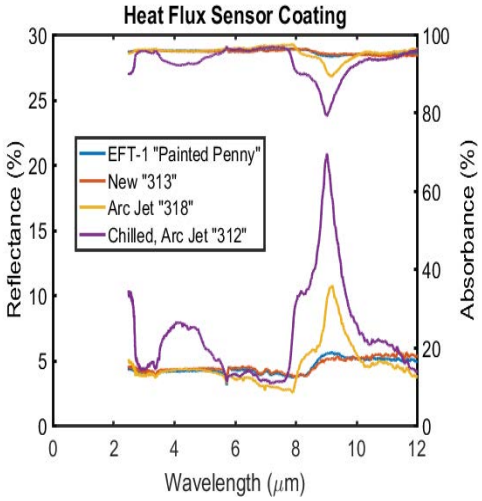

Figure 4 Reflectance and absorbance changes due to thermal cycling

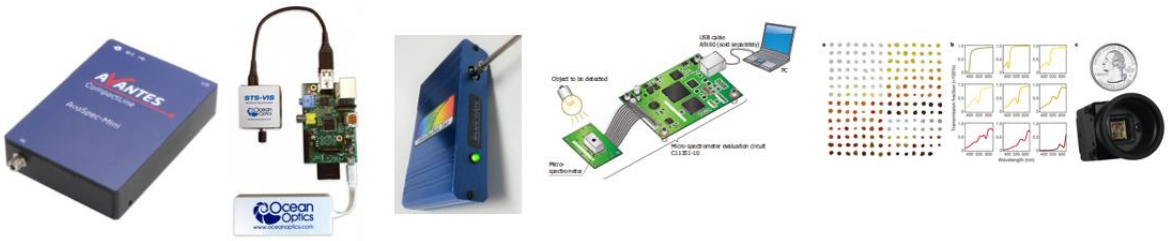

Figure 5 Decreasingly massive COTS mini-spectrometers, down to quantum dots size.

HIGH-TEMPERATURE, ANTI-FOULING COATINGS FOR VENUS EXPLORATION. R. Chen[1], C. A. Chapin[2], D. L. Chiu[3], H. So[4], L. Brockway[5], D. C. Walther[6], and D. G. Senesky[7], [1]Aeronautics and Astronautics, Stanford University, rchensix@stanford.edu, [2]Mechanical Engineering, Stanford University, cchapin3@stanford.edu, [3]Mechanical Engineering, Stanford University, dchiu08@stanford.edu, [4]Mechanical Engineering, Hanyang University, hyso@hanyang.ac.kr, [5]Nelumbo Inc., lance@nelumbo.io, [6]Nelumbo Inc., dave@nelumbo.io, [7]Aeronautics and Astronautics, Stanford University, dsenesky@stanford.edu

Introduction: Venus is the closest planet to Earth in our solar system, and yet scientists still have questions about the evolution of the atmosphere, the geophysics of the planet, and the interaction between the surface and atmphoshere. This lack of scientific knowledge is partially due to the difficulty in sending landers to Venus. *Venera 13* was the most successful Venus lander, surviving for 127 minutes on the surface, taking the first color photograph of the surface, and the first soil composition measurements [1]. Due to the harsh conditions on Venus (~460°C, 93 bar, sulfuric acid clouds, and supercritical CO_2 atmosphere) [2], landers have to be designed and fitted with extremely robust electronics. Research into high-pressure, high-temperature electronics based on gallium nitride [3][4] and silicon carbide [5] have yielded promising results, but these electronics must also come with robust external packaging to protect them from the corrosive atmosphere [6]. While the packaging material itself provides significant protection, additional coatings and surface treatments may be used to enhance the overall corrosion resistance of the electronics package and, ultimately, mission duration.

Methods: We present the development and characterization of a unique high-temperature coating intended to protect electronics and structural surfaces from the harsh Venusian atmosphere.

Fabrication: Various packaging substrate materials (stainless steel, titanium, alumina, and gold-plated alumina) were coated with an inorganic film (via Nelumbo Inc.'s propriety process). The coating material is known for its superhydrophobic properties and utilizes geometric structures to repel ice, water, and contamination on large-scale surfaces. In addition, the inorganic nature of the film enables high-temperature operation, and can be applied to thin, flexible substrates. Finally, the coating is able to withstand and repel concentrated sulfuric acid droplets, as shown in Figure 1.

Room Temperature Characterization: Water contact angle measurements were taken on the as-deposited films using a contact angle goniometer (Rame-Hart 290) and are shown in Figure 2 As expected, the inorganic coatings exhibit superhydrophobicity, with water contact angles exceeding 155° for all four substrates. Also, the films showed good adhesion to the various underlying substrate materials.

High Temperature Characterization: In order to assess the coating's ability to survive in high temperature evnvironments, the coated samples were heated up to a specified temperature between 200°C and 400°C using a box furnace (ThermoFisher) with a 2 SFCH flow of argon for 1 hour. After 1 hour, the samples were left in the furnace to cool to room temperature in the argon atmosphere, then removed. Water contact angle measurements were taken after the thermal exposure at room temperature. This process was repeated on the same samples at temperatures in the range of 200°C to 400°C in 50°C increments. The evolution of the water contact angles during the thermal exposure testing is shown in Figure 3. At temperatures of 300°C and below, there is no significant change in the water contact angle. However, at 350°C, a steep decrease in the measured water contact angle is observed, as shown in Figure 4. At this temperature, the coating is also heterogeneous, with some locations on the sample still exhibiting superhydrophobic properties while other locations did not. Finally, at 400°C, the water contact angles exhibited hydrophilic behavior comparable to the pre-coated values, suggesting that the coating had degraded due to the elevated temperatures.

Future Work: To examine the surface energies of the coated samples at room temperature, high-speed video analysis will be used. In addition, the wetting behavior of concentrated sulfuric acid will also be explored. Additionally, the samples will be exposed to varying pressures of supercritical CO_2 gas, with water contact angle measurements taken after each exposure. This data will be used to refine the coating deposition process parameters and fundamentally understand the limitations of the inorganic films.

References: [1] Moroz, V. I. (1983) *Venus*, 45-68. [2] Basilevsky, A. T. and Head, J. W. (2003) *Rep. Prog. Phys., 66,* 1699-1734. [3] Chapin, C. A. *et al.* (2017) *Sensors and Actuators A, 263,* 216-223. [4] Suria, A. J. *et al.* (2016) *Semicond. Sci. Technol., 31,* 115017. [5] Neudeck, P. G. *et al.* (2016) *AIP Advances, 6,* 125119. [6] Hunter, G. W. *et al.* (2006) *Electr. Eng, 8*.

Figure 1: Optical image of the wetting behavior of sulfuric acid (98% concentration) on inorganic nanocoatings provided by Nelumbo Inc.

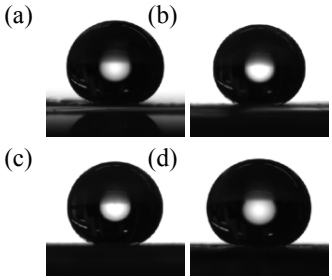

Figure 2: Optical images of water droplet measurements at room temperature of as-deposited inorganic coatings on (a) stainless steel, (b) titanium, (c) alumina, and (d) gold-plated alumina.

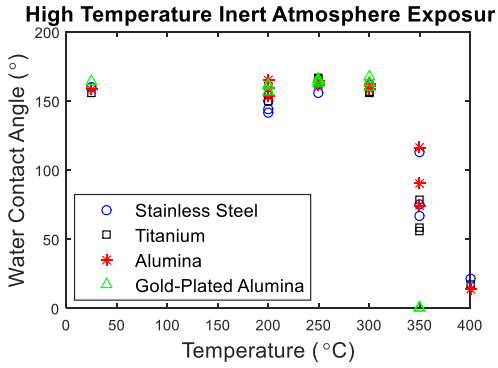

Figure 3: Evolution of water contact angle as samples were exposed to elevated temperatures.

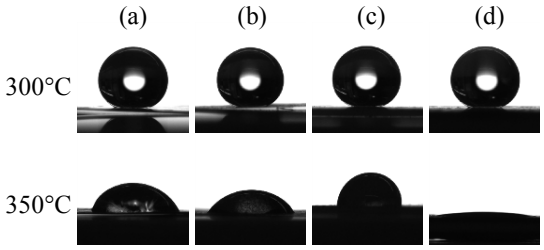

Figure 4: Optical images of water droplet measurements show the coatings transition from superhydrophobic to hydrophilic between 300°C and 350°C. Substrates are (a) stainless steel, (b) titanium, (c) alumina, and (d) gold-plated alumina.

Gas Barrier Thermal Testing for Convective Heating Improvement for Emergency Fire Shelters (CHIEFS).

J. S. Cheatwood[1], Z. M. A. Grady[2], and J. M. Fody[3], [1]Virginia Tech, [2] University of Connecticut, [3]NASA Langley.

Introduction:

On June 30, 2013, nineteen members of the Granite Mountain Hotshots were lost in the Yarnell Hill Fire in Arizona. The existing fire shelter, known as the M2002, is not designed to withstand direct contact with flames. Dynamic weather conditions had produced unexpected changes in fire behavior, and there was insufficient time to properly clear a site of combustible materials for fire shelter deployment. Shelters were fully immersed in flames and all were lost. After Yarnell Hill, the US Forest Service initiated a search for a more flame resistant technology. The initiative to address these concerns resulted in a partnership between NASA's Langley Research Center and the United States Department of Agriculture's Forest Service, called CHIEFS (Convective Heating Improvement for Emergency Fire Shelters). NASA Langley engineers sought to leverage expertise gained in the development of flexible heatshield insulations for the Hypersonic Inflatable Aerodynamic Decelerator (HIAD), an inflatable aeroshell intended for use in planetary entry, in order to make a more flame resistant fire shelter while meeting strict mass and packing volume requirements.

Fire shelters are subject to numerous constraints including mass, volume, durability, cost, and material toxicity. These requirements preclude heavy or bulky insulations, expensive materials, and a host of high temperature, but potentially toxic, material choices. As a result, these constraints must also be prioritized during thermal testing and down-select.

Given these constraints, CHIEFS engineers embarked on a four year development effort screening various hand sample scale insulations at NASA and full scale shelter prototypes in both laboratory and controlled wildfire tests in Canada. This HIAD spinoff addresses both mass and volume constraints, while providing a solution that extends survival times by as much as a factor of two compared with the M2002 when exposed directly to flames. By extending the shelter's ability to provide a survivable environment when immersed in flames, the CHIEFS effort intends to improve the odds for firefighters in the event of a future situation similar to Yarnell Hill.

During the Summer of 2017, the CHIEFS team developed a thermal test apparatus to quickly screen candidate gas barrier material for the fire shelters. A gas barrier is a layer of material designed to prevent hot gasses from penetrating the highly permeable wall insulations and advecting heat to the shelter interior. In these gas barrier screening tests, 13 unique candidate materials were exposed to propane flames in air calibrated to 86.7 ± 5.6 kW/m^2 for 150 seconds. Images of the materials, as well as thermcocouple data, was collected during testing. Materials which readily produced heavy smoke or extremely irritable or flammable decomposition biproducts were eliminated immediately. Down selected candidates were tested for additional iterations in order to increase confidence in the results. The testing allowed the team to identify best performing materials to be carried forward to the next round of full scale fire shelter tests.

INVESTIGATION OF COATINGS FOR LANGMUIR PROBES IN AN OXYGEN-RICH SPACE ENVIRONMENT. J. I. Samaniego[1,2,4], X. Wang[1,4], L. Andersson[4], D. Malaspina[4], R. E. Ergun[3,4], and M. Horanyi[1,2,4]. [1]NASA/SSERVI's Institute for Modeling Plasma, Atmosphere, and Cosmic Dust (IMPACT) at University of Colorado Boulder (3400 Marine St. Boulder, CO 80303 USA, josa3077@colorado.edu). [2]Department Physics, University of Colorado, Boulder CO 80303 USA. [3]Department for Astrophysical and Planetary Science, University of Colorado, Boulder CO 80303 USA. [4]Laboratory for Atmospheric and Space Physics (LASP), Boulder CO 80303 USA.

Introduction: Over the past 50 years Langmuir probes have been the most frequently used instruments for in-situ characterization of space plasmas. By sweeping a voltage across the probe, a current-voltage (I-V) curve is obtained and interpreted for deriving plasmas density, temperature, and spacecraft (SC) potential. However, in atmospheres and ionospheres of planets, oxygen in many forms (e.g., O, O_2, O^+ and O_2^+) is present in relatively high densities. When the probes are exposed to such environments, the surfaces of the probes have the high risk of being oxidized to have reduced conductivity, causing a mischaracterization of the ambient plasma. Currently, the most common coatings for Langmuir probes are DAG (a resin based graphite dispersion, Gold, and TiN (Titanium Nitride). They all have issues in an oxygen-rich environment.

DAG coatings react with oxygen and can cause erosion over time and therefore has the risk of exposing the naked probe surface [1]. Gold is soft and the coating layer can be damaged by ground handling or eroded in dust-rich environments. It was also shown that Gold may become oxidized when the oxygen energy is high [4]. TiN coatings, developed for its highly uniform surface conductivity and hardness, showed anomalies in their I-V curves after MAVEN dipped into the Martian ionosphere, which were suggested to be caused by the oxidation effect [2].

In contrast to DAG, Gold, and TiN, Iridium and Rhenium show promise as new Langmuir probe candidates for missions with high densities of O and O_2 because: 1) They are difficult to oxidize; 2) Their oxidized forms maintain high conductivity [3]; and 3) They have high corrosion resistance and high hardness.

We investigate and validate Iridium and Rhenium as new coating materials for applications in oxygen-rich plasma environments by comparing them to current probe coating materials (DAG, TiN, Gold) and metals known to oxidize readily (Copper and Nickel) as controls.

Method: To test the oxidation effect on the Langmuir probe made of each metal, the probes were first swept in an argon plasma chamber as a control for comparison.

The probes were then moved to a second vacuum chamber in which an oxygen plasma was created with both O_2^+ and O^+ present. A UV lamp was used to dissociate O_2 to O. The probes were held at a potential of -1.5 and -10 volts with respect to the plasma in order to bombard their surfaces with oxygen ions corresponding to 1.5 and 10 eV, respectively. These energies cover the SC speeds between 4 and 10 km/s. The probes were exposed for 20 minutes at a total flux of 10^{18} [Ions/m^2/sec] which is equivalent to approximately 3 hours to 5 months in the ionosphere of Earth, depending on O^+ densities and orbiting altitudes.

The probes were then returned to the argon plasma chamber where they were swept again to characterize the I-V curves after oxidation that were compared to the ones before oxidation. Additionally the probes were recleaned via in-situ heating by attracting the electrons to see if the oxidized layer could be removed.

Results: Expectedly the Copper and Nickel probes showed the most drastic change to the I-V curves after oxidation and characterized the following general features:

1. Reduced current at a given probe potential.
2. The derived plasma potential becomes more positive.
3. The derived electron density decreases.
4. The derived electron temperature becomes hotter.

The TiN probe measurements showed the significant changes in both the I-V curves and derived parameters. Interestingly, unlike all other testing probes, the TiN probe's I-V curve did not return to the control after the probe was reclined, indicating irreversible changes in the surface properties from the oxidation.

Additionally, the Gold showed moderate oxidation effects on the probe measurements despite the fact that at room temperature Gold is highly resistant to oxidation. This result is in agreement with other studies that have shown Gold can be oxidized when exposed to oxygen at higher energies [4].

DAG showed a noticeable but overall small oxidation effect on the probe measurements. However, as described above, erosion is likely a bigger issue affecting its performance [1].

Of the new coating candidates, Rhenium showed a similar oxidation effect on the probe measurements to

DAG. Iridium outperformed all other testing materials with the least oxidation effect shown on the probe measurements, which likely benefits from the high conductivity of its oxide form [3]. Figure 1 shows the I-V curves of TiN, Gold, DAG and Iridium before and after oxidation as well as after recleaning.

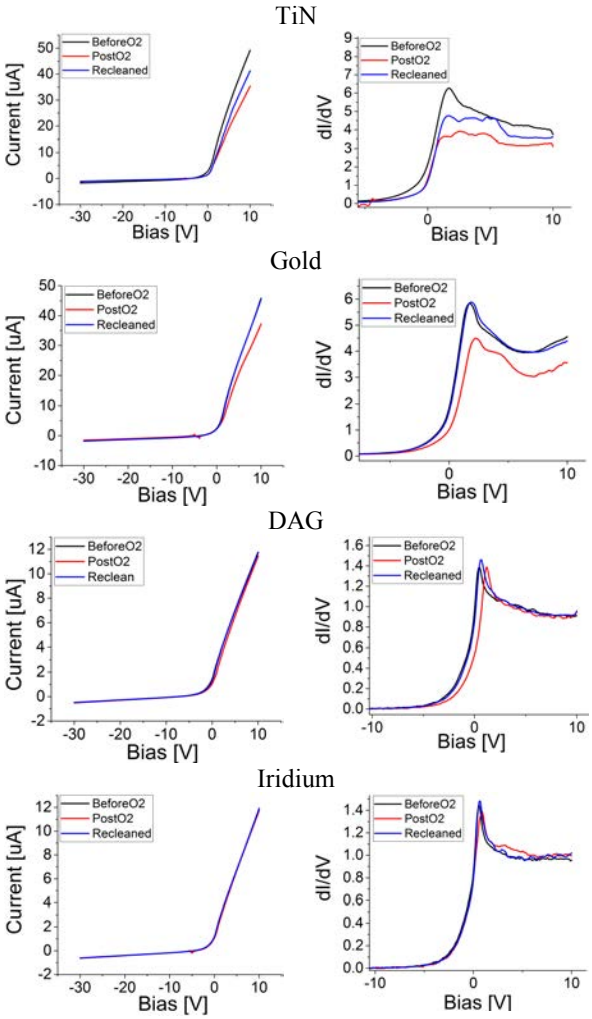

Figure 1: The I-V curves (Left) and first derivatives of I-V curves (Right) of TiN, Gold, DAG, and Iridium.

Conclusions: We have tested a variety of samples in a laboratory oxygen plasma to validate a new coating material for in situ Langmuir probes to accurately measure the plasma parameters in an oxygen-rich environment, such as planetary atmospheres and ionospheres. It was found that, in the three most commonly used coatings (TiN, DAG and Gold), both TiN and Gold showed a significant to moderate oxidation effect on the probe measurements. DAG showed less oxidation effects; however, it has a problem of being eroded over time [1]. Iridium showed the least effect due to oxygen exposure on the probe measurements, which likely benefits from the high conductivity of its oxide form [3]. Additionally, Iridium has extremely high hardness and conductive oxide form [3], making it more suitable and robust than current coatings for Langmuir probes. This new coating can be also applied for other plasma instruments in which the electrode surfaces pose a risk of being exposed to oxygen, such as Retarding Potential Analyzers (RPAs), Ion Drift Meters (IDMs), and electrostatic analyzers. The photoemission properties of Iridium and other coatings will be investigated in future work to explore the potential application of these coatings to electric field probes.

References:

[1] Visentine, J. (1983).NASA Technical Memorandum 100459. NASA LBJ Space Center. [2] Ergun, R. et al. (2015). Geophysical Research Letters, 42(21), 8846–8853. [3] Chalamala, B. et al. (1999). Applied Physics Letters, 74(10), 1394–1396. [4] Gottfried, J. M. et al. (2003). Surface Science, 523(1–2), 89–102

A DOUBLE HEMISPHRECIAL PROBE (DHP) FOR INTERPRETING PROBE MEASUREMENTS IN THE SPACECRAFT SHEATH. J. I. Samaniego[1,2,3] , X. Wang[1,2], M. Horanyi[1,3]. [1]NASA/SSERVI's Institute for Modeling Plasma, Atmosphere, and Cosmic Dust (IMPACT) at University of Colorado Boulder (3400 Marine St., Boulder CO 80303 USA, josa3077@colorado.edu). [2]Laboratory for Atmospheric and Space Physics (LASP), Boulder CO USA. [3]Department Physics, University of Colorado Boulder, CO 80303 USA.

Introduction: Langmuir probes have been the most frequently used in-situ instruments for measuring the plasma density, temperature, and spacecraft (SC) potential. However, even after decades of use, there are still challenges in the analysis and interpretation of Langmuir probe measurements. Due to the interaction of the ambient plasma with the SC and the onboard probe itself, the local plasma conditions may be created around the probe to affect its measurements. These local plasma conditions are often anisotropic and/or inhomogeneous, making the measurement and data interpretation of current single Langmuir probes difficult, and consequently introducing errors in the derived plasma characteristics.

Directional probes, including both the split Langmuir probes [1, 2] and the Segmented Langmuir Probe (SLP) [3, 4], have been developed mainly for characterizing the plasma flow in Earth's ionosphere. Based on these prior designs, we develop a Double Hemispherical Probe (DHP) to improve space plasma measurements in the much broader scenarios: i) low-density plasmas; ii) high surface-emission environments; iii) flowing plasmas; and iv) dust-rich plasma environments.

In this paper, we specifically address the problem of the probe measurements in the low density plasmas, such as planetary magnetospheres. When the plasma density is low, a large Debye sheath up to a few meters can be created around the SC. Due to the limited length of the probe boom, the SC sheath may engulf the Langmuir probe and create a localized plasma environment that is different from the true ambient plasma, causing its mischaracterization. This issue has been recognized for Langmuir probes on the Cassini and Rosetta missions [5, 6].

Here we introduce the basic concept of the DHP and the method developed to derive the true ambient plasma parameters from the the probe measurements in the SC sheath.

Experiment: Similar to the split Langmuir probes, the DHP consists of two hemispheres electrically insulated from each other. These two hemispheres are swept with the same voltages simultaneously, yielding two current-voltage (I-V) curves. The addition of the each hemisphere's I-V curve yields the I-V curve that is same to the one of a single spherical probe (SSP) of same radius. A laboratory DHP model was made of two halves of ball bearings (2 mm in radius), as shown in Fig. 1a.

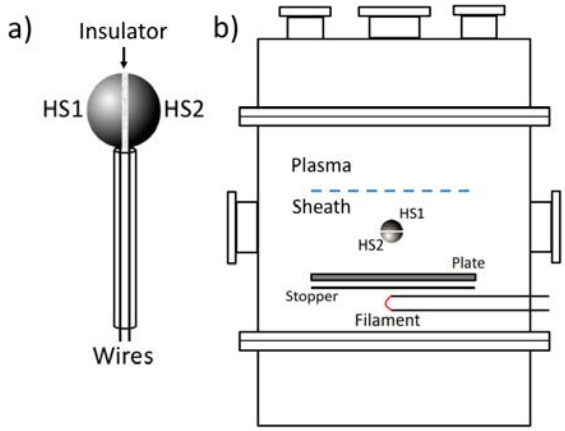

Figure1: a) Schematic of the DHP lab model; b) Schematic of the experimental setup for testing the DHP in the sheath of a metal plate.

Figure 1b shows the schematic for testing the DHP in the sheath of a SC. A conducting plate that is allowed to charge to a floating potential in a plasma, simulating a SC in a space plasma. A Debye sheath is created above the plate. An emissive probe is used to map the sheath potential profile. The DHP is swept in the bulk plasma along with a SSP to ensure matching I-V curves. The DHP and SSP are then moved incrementally into the sheath to measure how the I-V curves of each hemisphere of the DHP differ at different locations in the sheath.

Results: Figure 2 shows an example of the sheath profile measured by the emissive probe and the I-V curves of the DHP and SSP as they are moved deeper into the sheath. It shows that 1) the currents of the two hemispheres are identical when the probe is in the bulk plasma; and 2) the currents begin to diverge as the probe moves deeper into the sheath, more diverged the deeper sheath. In the bulk plasma, the potentials around two hemispheres are uniform, resulting in the same currents at a given probe voltage. In the sheath, due to the potential gradient, the electron density in the sheath decreases exponentially toward the plate. Therefore, the electron current of the plasma facing hemisphere (HS1) is greater than the plate

facing hemisphere (HS2) as the probe voltage is larger than the local potential.

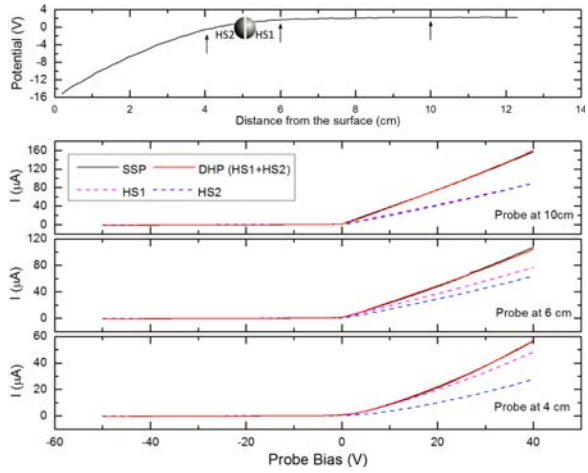

Figure 2: Top: potential profile of the Debye sheath measured by an emissive Probe as a function of distance from the plate. Bottom: I-V curves taken by the DHP and SSP at three different depths (indicated by three arrows in the top panel) in the Debye sheath of the charged plate (SC).

It was shown that the difference in the electron saturation current between the two hemispheres increased as the probe was moved 'deeper' into the sheath. This relationship could be used to determine how `deep' the probe is in the sheath. Figure 3 shows the current ratio as a function of the probes location in the sheath for various plasma conditions. The probes location in the sheath is measured not by distance from the plate, but by the difference between local potential at the position of probe (φ_{Local}) and the potential in the bulk (φ_{Bulk}), and normalized by the Debye length (λ_{De}). This approximately linear relationship can be used to determine how `deep' the DHP is within the sheath of a SC.

Retrieving True Ambient Plasma Parameters. In addition to the above relationship, using lab experiments, we will establish another relationship between the plasma parameters (i.e., density, temperature and SC potential) derived from the probe measurements in the sheath and the measuremnts in the bulk. Based on these two relationships, we are able to retrieve the true ambient plasma characteristics from the probe measurements in the SC sheath. Note that the degree of the I-V curve distortion increases as the probe is in a deeper sheath. The limit at which the true plasma parameters are unable to be retrieved will be also defined through experimental investigations.

Discussion and Conclusions: The Langmuir probe immered in the SC sheath is a challenging problem for many missions measuring plasmas with low densities, such as planetary magnetospheres. Here we showed a new concept of using a new type of directional probe, the DHP, to regonize the scenario of the probe immersed in the SC sheath. and to retrieve the true ambient plasma characterisitcs. Initial testing results of the DHP showed that it is able to determine how 'deep' the probe is in the Debye sheath around the SC from the difference in the electron saturation current between the two hemispheres. The method for retrieving the ambient plasma characteritics are described and to be tested.

References: [1] Bering, E. et al. (1973) JGR, 78, 2201-2213. [2] Bering, E. et al. (1973) Planet. Space Sci., 21, 1983-2001. [3] Lebreton, J. et al. (2006) Planet. Space Sci., 54, 472–486. [4] Imtiaz, N. et al. (2013) Phys. Plasmas, 20, 052903. [5] Wang, X. et al (2015), JGR Space Physics, 120, 2428–2437. [6] Odelstad, E. et al (2015) Geophys. Res. Lett., 42, 10,126–10,134.

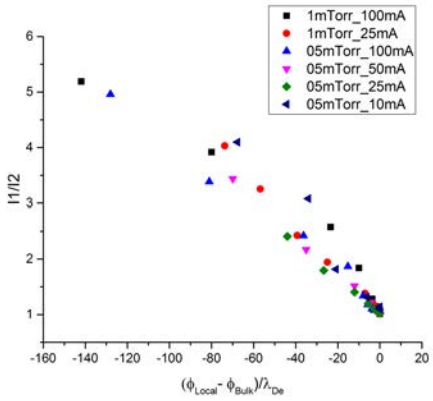

Figure 3. Ratio of the electron saturation current of HS1 (I1) to HS2 (I2) of the DHP as a function of the sheath potential depth normalized to the Debye length (λ_{De}). The sheath potential depth is defined as the difference between local potential (φ_{Local}) at the position of probe and the potential in the bulk plasma (φ_{Bulk}). Each data set taken at different pressures (1 and 0.5 mTorr) and filament emission current (10-100mA) to yield different sheath thicknesses ranging from about 2cm to 8cm.

The Comet Astrobiology Exploration Sample Return (CAESAR) New Frontiers Mission

M.J. Amato[1]. S. W. Squyres[2], K. Nakamura-Messenger[3], D.P. Glavin[1], D. F. Mitchell[1], V. E. Moran[1], M. B. Houghton[1], A. G. Hayes[2], D. S. Lauretta[4], S. Messenger[3], K. Yamada[5], T. Nakamura[6], J. P. Dworkin[1], A. N. Nguyen (Jacobs)[3], S. Clemett[3], T. J. Zega[4], Y. Furukawa[6], Y. Kimura[7], A. Takigawa[8], G. Blake[9], M. Mumma[1], S. N. Milam[1], P. A. Gerakines[1], L. F. Pace[3], C. D. K. Herd[10], S. Gorevan[11], K. Zacny[11], P. Chu[11], C. Güttler[12], H. Sierks[12], J.-B. Vincent[13], H. Campins[14], Y. Fernandez[14], J. Makowski[15], D. Oberg[15], J. M. Soderblom[16], D. Bodewits[17], M. Kelley[17], B. Davidsson[18], and the CAESAR Project Team. [1]NASA Goddard Space Flight Center, Greenbelt, MD, USA, [2]Cornell University, Ithaca NY, USA, [3]NASA Johnson Space Center, Houston TX, USA, [4]University of Arizona, Tucson AZ, USA. [5]JAXA/ISAS, Yoshinodai, Chuo, Sagamihara, Kanagawa, Japan. [6]Tohoku University, Sendai, Miyagi Prefecture, Japan. [7]Hokkaido University, Sapporo, Hokkaido, Japan. [8]Kyoto University, Kyoto, Kyoto Prefecture, Japan. [9]California Institute of Technology, Pasadena, CA, USA. [10]University of Alberta, Edmonton, AB, Canada. [11]Honeybee Robotics, Pasadena, CA, USA. [12]Max Planck Institute, Göttingen, Germany. [13]DLR Institute of Planetary Research, Berlin, Germany. [14]University of Central Florida, Orlando, FL, USA. [15]Orbital ATK, Inc, Dulles, VA, USA. [16]Massachusetts Institute of Technology, Cambridge, MA, USA. [17]University of Maryland, College Park, MD, USA. [18]Jet Propulsion Laboratory, Pasadena, CA, USA.

CAESAR Introduction: The Comet Astrobiology Exploration Sample Return (CAESAR) mission was recently selected by the NASA New Frontiers Program for Phase A study. CAESAR and Dragonfly were the two selections for Phase A. CAESAR will return surface material from the nucleus of comet 67P/Churyumov-Gerasimenko (67P). The Principal Investigator is Steve Squyres from Cornell University. NASA Goddard provides project management, systems engineering, safety and mission assurance, contamination control, gas containment system, arm, mission operations, and many other important functions. Orbital ATK develops the spacecraft based on Dawn mission heritage.

CAESAR Mission: CAESAR will acquire and return to Earth for laboratory analysis a minimum of 80 g of surface material from the nucleus 67P. CAESAR will characterize the surface region sampled, preserve the collected sample in a pristine state, and return evolved volatiles by capturing them in a separate gas reservoir. Like the Dawn mission, CAESAR uses solar electric propulsion. CAESAR will use the NEXT C ion thruster system. CAESAR launches in 2024 arriving at 67P in 2029 to perform pre sample imaging, mapping and target refinement. The sample acquisition con ops benefits from previous mission work and will utilize sample acquisition rehearsals to further reduce risk.

Detailed laboratory analyses of the sample from 67P will trace the history of volatile reservoirs, delineate the chemical pathways that led from simple interstellar species to complex molecules, constrain the evolution of the comet, and evaluate the role of comets in delivering water and prebiotic organics to the early Earth. CAESAR will achieve these goals by carrying out coordinated sample analyses that will link macroscopic properties of the comet with microscale mineralogy, chemistry, and isotopic studies of volatiles and solids. Most of the sample (≥75%) will be set aside for analysis by generations of scientists using continually advancing tools and methods, yielding an enduring scientific treasure that only sample return can provide.

Collection of a sample from the surface of comet 67P is facilitated by a set of cameras that together provide images to support sample site selection, perform optical navigation, and document the sample before, during, and after collection. The sample acquisition operations in the rehearsals closely match the operations used in final sampling. The sample is collected at the end of an arm during a touch and go maneuver with the Sample Acquisition System (SAS) led by Honeybee Robotics for the surface properties of comet 67P observed by the Rosetta/Philae mission. After sample collection, and while the sample is still cold, the arm inserts the sample container into the Sample Containment System (SCS) mounted inside the Sample Return Capsule (SRC). The SCS is sealed, preventing the sample from escaping into space. The sample is slowly warmed inside the SCS to enable sublimation of volatiles, which are collected in the Gas Containment System (GCS), a passively cooled gas reservoir. Separating the volatiles from the solid sample protects the solid sample from alteration. Once H2O has sublimated from the solid sample, the GCS is sealed to capture the volatiles it contains, and the SCS is vented to space to maintain the solid sample under vacuum. The SCS vent is closed before Earth entry to prevent atmospheric contamination.

The CAESAR SRC is being developed by the Japanese Aerospace Exploration Agency (JAXA). Its design is based on the SRC flown on the Hayabusa and Hayabusa2 missions. The CAESAR SRC design benefits from extensive JAXA investment and testing. The SRC lands at the Utah Test and Training Range (UTTR) and is immediately placed in cold storage for transportation to the NASA Johnson Space Center, where the solid and gas samples are removed and delivered to a dedicated CAESAR curation facility.

KEY CHALLENGES IN CAPTURING A BOULDER FOR THE ASTEROID REDIRECT ROBOTIC MISSION B. Cichy[1] and S. Mukherjee[2], [1]Goddard Space Flight Center, 8800 Greenbelt Road, Greenbelt, MD 20771, [2]SGT, 7701 Greenbelt Rd Ste 400, Greenbelt, MD, 20770

Introduction: NASA's proposed Asteroid Redirect Robotic Mission (ARRM) planned to demonstrate the capability to collect a large boulder from the surface of a Near Earth Asteroid, use the mass of the boulder to demonstrate enhanced asteroid deflection, and return the boulder for future exploration as part of the Asteroid Redirect Crewed Mission [1]. In June of 2017 NASA decided not to continue the Asteroid Redirect Mission. Prior to this decision, the team had made tremendous progress on detailed designs for precision landing, active touchdown, boulder collection, and formation-flying planetary defense.

This talk will give an overview of one of the key risks the team was tackling prior to project cancelation - boulder extraction. The talk will examine the uncertainties in the asteroid environment and how the project mitigated the risk in an architecture trade study completed just prior to the end of the project.

Design Refernce Asteroid and Boulder Requirements: For an asteroid to be a potential target for the ARRM, it had to be in an accessible orbit, of interest to the scientific and In-Situ Resource Utilization (ISRU) community, and have been previously characterized by ground observations. From early in development, the project used 2008 EV_5 as the design reference asteroid. (Figure 1)

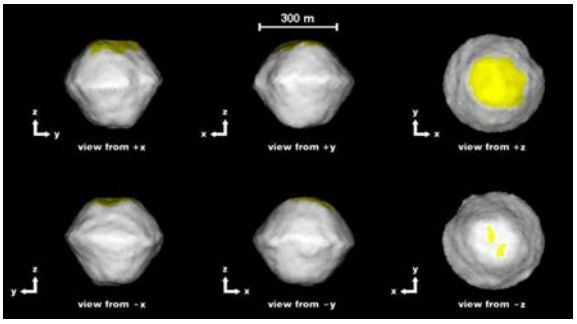

Figure 1. 2008 EV5 shape model from radar observations. Yellow shading indicates areas that were not viewed by radar[3].

However even with the best characterization through ground observations, no objects smaller than 10 m in diameter were able to be resolved on the surface. Our knowledge of how these boulders are held to the surface had even less empirical data, with the best estimates determined for the project by a group of experts convened by the project as part of the Formulation Assessment and Support Team (FAST) [2]. Their estimates on surface cohesion had over an order of magnitude uncertainty causing large uncertainties in the extraction force required by the robotic vehicle to liberate a boulder.

Robotic System Overview: To capture the boulder, the mission used an advanced robotic arm system derived from NASA Goddard's Satellite Servicing Division, robotic legs developed at NASA's Langley Research Center, and a novel robotic gripper developed at NASA's Jet Propulsion Laboratory. (Figure 2)

Figure 2. 7-DOF robotic arm and Microspine Gripper

The robotic system had to autonomously land over top of the target boulder, place and actuate the robotic grippers on the boulder's surface, extract the boulder, and depart the asteroid.

Key Challenges: The key challenges the robotic system needed to address were:

1. Uncertainty in boulder size and shape
2. Uncertainty in boulder cohesion to the surface
3. Uncertainty in boulder strength
4. Uncertainty in boulder surface features and roughness
5. Uncertainty in surface bearing strength

The team used a combination of testing, Monte Carlo simulations, dynamics analyses, and parameteric design studies to determine the most robust system given the above challenges.

References: [1]D.D. Mazanek, R.G. Merrill, S.P. Belbin, D.M. Reeves, K.D. Earle, B.J. Naasz, and P.A. Abell, "Asteroid Redirect Robotic Mission: Robotic Boulder Capture Option Overview." AIAA SPACE 2014, August 2014. [2] Asteroid Redirect Mission (ARM) Formulation Assessment and Support Team (FAST) Final Report with Public Comments. http://www.nasa.gov/feature/arm-fast. Accessed January 7, 2015

PROBING PSYCHE: MISSION OVERVIEW AND OPERATIONS CONCEPT. C. A. Polanskey[1], L. T. Elkins-Tanton[2], N. Amiri[1], S. H. Bairstow[1], T. D. Drain[1], D. J. Lawrence[3], W. Hart[1], S. Marchi[4], D. Y. Oh[1], R. Oran[5], T. H. Prettyman[6], C. T. Russell[7], D. A. Seal[1], D. Wenkert[1], D. Williams[2], and the Psyche Team, [1]Jet Propulsion Laboratory, California Institute of Technology, (4800 Oak Grove Drive, Pasadena, CA 91109, Carol.A.Polanskey@jpl.nasa.gov, Nikta.Amiri@jpl.nasa.gov, Sarah.H.Bairstow@jpl.nasa.gov, Tracy.D.Drain@jpl.nasa.gov, David.Y.Oh@jpl.nasa.gov, seal@jpl.nasa.gov, Daniel.Wenkert@jpl.nasa.gov), [2]Arizona State University (Tempe, AZ 85281, ltelkins@asu.edu, David.Williams@asu.edu), [3]Johns Hopkins Applied Physics Laboratory (11100 Johns Hopkins Road, Laurel, Maryland 20723, David.J.Lawrence@jhapl.edu), [4]Massachusetts Institute of Technology (77 Massachusetts Ave., Cambridge, MA 02139, roran@mit.edu), [5]Southwest Research Institute (1050 Walnut St. #300, Boulder, CO 80302, marchi@boulder.swri.edu),[6]Planetary Science Institute (1700 E. Fort Lowell Rd. #106, Tucson, AZ 85719, prettyman@psi.edu), [7]University of California, Los Angeles (Los Angeles, CA 90095, ctrussel@igpp.ucla.edu).

Introduction: The January 2017 selection of the Psyche Mission by the Discovery Program provides NASA with its first opportunity to directly probe a planetary core. The main belt asteroid, (16) Psyche, is composed primarily of metal and is thought to be the remnant of an early planetesimal that was stripped of its mantle by multiple hit-and-run collisions during early solar system formation [1]. With a mean diameter of 226 km [2], Psyche ranks tenth in size for the asteroids in the main belt. While the Psyche spacecraft will remain in orbit above Psyche, its suite of science investigations will enable exploration of the asteroid's remanent magnetic signature, composition, exterior morphology, and interior structure. The mission is led by principal investigator Linda Elkins-Tanton of Arizona State University (ASU) and managed by the Jet Propulsion Laboratory (JPL) with spacecraft chassis built by SSL. Launching in August 2022, the spacecraft arrives at Psyche in early 2026 where it will begin gathering data of ever greater resolution as the spacecraft altitude decreases over the course of the 21-month mission.

Science Objectives and Instrumentation: The Psyche Mission is driven by its five science objectives to:

A. Determine whether Psyche is a core, or if it is primordial unmelted material;
B. Determine the relative ages of regions of Psyche's surface;
C. Determine whether small metal bodies incorporate the same light elements into the metal phase as are expected in the Earth's high-pressure core;
D. Determine whether Psyche was formed under conditions more oxidizing or more reducing than Earth's core;
E. Characterize Psyche's topography.

Of these objectives, the first is the most far reaching, involving each of the four science investigations. The most unequivocal indicator of Psyche's origin is whether it retains a remanent magnetic field from an earlier planetary dynamo. If so, then Psyche must be a core; however, the core diagnosis is not ruled out if a field is not detected as there are other signatures that can discriminate between origin hypotheses. To address this magnetic field detection, the spacecraft will carry a fluxgate magnetometer with two sensors mounted on a two-meter boom in a gradiometer configuration. This enables the instrument to be sensitive to magnetic fields from 2 nT to 100,000 nT. The large dynamic range is needed because it is unknown how disrupted the core became during the impact stripping process. The magnetometer is provided by a team at the University of California, Los Angeles led by Chris Russell and the magnetometry investigation is led by Ben Weiss at the Massachusetts Institute of Technology (MIT).

Another discriminator is the nickel content of the metallic material on Psyche's surface. While Psyche is expected to be mostly made of iron, nickel content may range from 4 to 12 wt% [3]. Low nickel content (<4 wt%) indicates highly reducing conditions and material that never melted. Core formation typically results in 4-12 wt% nickel, whereas <6 wt% indicates the core solidified from the outside in and higher concentrations indicate that the core solidified from the inside out. The highest nickel concentrations (> 12%) indicate highly oxidizing conditions. To determine elemental composition, we carry a gamma-ray and neutron spectrometer (GRNS) developed by David Lawrence at the Johns Hopkins Applied Physics Laboratory (APL). In addition to iron and nickel, the GRNS will measure the abundance of light elements to determine the metal-to-silicate ratio.

The presence of silicates on Psyche's surface, which can be detected with the GRNS and a multispectral imager, and their relationship to the metallic materials provides another means of determining whether Psyche is a core or unmelted primordial material. If the silicates are intimately mixed with the metal at a scale we cannot detect with our images, as with primitive

chondrites, then Psyche most likely never melted. However, if large silicate provinces are detected, then Psyche is most likely a remnant core. Silicates may also be deposited on Psyche's surface from impacts. The images also contribute to other objectives by providing cratering statistics to support surface age determination and to characterize Psyche's shape and morphology. The multispectral imager investigation is led by Jim Bell at ASU partnering with Malin Space Science Systems. The spacecraft carries two identical imagers to provide redundancy for the mission critical optical navigation function.

Psyche's interior structure will be revealed through the gravity science investigation, which is led by Maria Zuber at MIT, using the X-band telecommunications antenna on the spacecraft. Internal density variations provide clues to the degree of disruption Psyche experienced in its history. Gravity science serves dual purpose, along with the imaging investigation, of providing key scientific results as well as critical data needed for operations.

Spacecraft: The Psyche spacecraft is a joint development between the commercial telecommunications-satellite manufacturer, SSL located in Palo Alto, CA, and the Jet Propulsion Laboratory (JPL) in Pasadena, CA. SSL is the largest provider of solar electric propulsion (SEP) spacecraft, a capability required for the Psyche mission. SSL will provide the SEP chassis, including the structure, propulsion, solar arrays, high gain antenna, thermal control, and attitude control hardware, while JPL provides the avionics, flight software, communications, and fault protection in a unique partnership leveraging the strengths of each institution [4]. In addition to the three science instruments, it is planned that the spacecraft would also host the Deep Space Optical Communication (DSOC) technology demonstration. DSOC is a high-speed laser communications package intended to increase spacecraft communication performance and data return by 10 or 100 times over conventional radio frequency communications on future missions.

Operations: Psyche is a massive body that has not yet been visited by previous spacecraft. To navigate the spacecraft safely in the presence of an unknown gravity field, the first orbit must be at a high altitude, insensitive to gravitational perturbations. Psyche is characterized from this altitude, obtaining a preliminary shape model from the images, an initial gravity field model from the X-band tracking, and a potential magnetic field detection. With this knowledge, the spacecraft uses the SEP system to transition to the next lower orbit where the primary imaging campaign produces a multispectral map of the body as well as an updated shape model from the stereo imaging acquired at a range of off-nadir attitudes. The improved gravity field determination enables transition to the next lower orbit where the highest fidelity global gravity map is obtained. The fourth and final orbit at the lowest altitude is customized for elemental mapping with the GRNS. The magnetometer and imager will continue to acquire data throughout the orbital operations phase. This type of operational plan has already been twice demonstrated with the Dawn mission at Vesta [5] and Ceres [6].

Prospects: The Psyche mission is now well over a year into the preliminary design phase and so far, there has been negligible deviation from the goals, objectives and implementation outlined in the proposal that was selected. While the mission is still four years from launch, the team has sustained its focus on designing the highest-heritage approach that meets the science requirements and works within the SSL product line. The allure of this mission has always been the destination, Psyche, and finding the simplest means to get there and explore.

References:

[1] Asphaug E. and Reufer A. (2014) *Nature Geosciences, 7,* 564–568. [2] Shepard M. K. et al. (2017) *Icarus, 281,* 388–403. [3] Wasson J. T. and Choe W. H. (2009) *Geochimica et Cosmochimica Acta., 73,* 4878-4890. [4] Oh D. Y. (2017) *35th International Electric Propulsion Conference,* IEPC-2017-153. [5] Polanskey C. A. et al. (2012) *SpaceOps 2012*. [6] Polanskey C. A. et al. (2016) *SpaceOps 2016* AIAA 2016-2442.

A modular ascender concept for sample return missions. R. Buchwald[1], F. Ebert[1], O. Angerer[2], Airbus Defence and Space, email: robert.buchwald@airbus.com, [2]German Aerospace Center DLR, email: oliver.angerer@dlr.de

Introduction: Ascent stages constitute a key element of future manned missions to moon and mars. After successful landing and completion of work on the surface, they serve as means of transportation back into orbit. After reaching the target orbit, sample containers, and astronauts in more advanced scenarios, are transferred to the awaiting return module or habitat. While rendezvouz and docking manoeuvres in orbit could be performed almost identically for moon and mars, the differences between both celestial bodies have to be thoroughly considered regarding the technical concept design of the ascent stages and the transferability of the related technology to other scenarios. Therefore, the question arises as to whether actual similarities between both scenarios exist and, if yes, how they can be utilized for cost and risk reduction.

Reference mission scenarios: Historically, lunar landing missions have been focussing on the lunar near side at landing regions with low to medium lunar latitudes. After the confirmation of great amounts of water at the poles, most recent scenarios are focusing on polar regions. In particular the Aitken basin, a large impact crater at the lunar far side in the vicinity of the south pole allows addressing both - high priority science goals as well as in-situ resource utilization (ISRU) demonstration needs. In this context, several missions including ESA's cooperation with Roscosmos on robotic lunar polar sample return (LPSR) and with JAXA and CSA on a human assisted (lunar) sample return (HERACLES) are aiming at returning samples either robotically to an earth return vehicle in low lunar orbit or to a man-tended habitation module in the near rectilinear halo orbit.

In parallel, significant steps towards the first successful robotic mars sample return (MSR) have been undertaken. While some elements of the MSR architecture (e.g. the transfer module, the entry capsule or the sky crane) do have flight heritage, some other elements (e.g. the MSR lander, the sample fetch rover, the ascent vehicle, and the earth return vehicle) require substantial development. A common development approach for moon and mars would avoid unnecessary and expensive competition between both programs and could ultimately reduce cost and risk if a viable technical solution exists.

Synergies and differences: While the high level objective – to lift a payload from the surface into orbit – is identical for all scenarios, significant differences exist regarding the environmental conditions. It is obvious that in particular the different gravitational environment and the absence of atmospheric pressure on the moon lead usually to different designs.

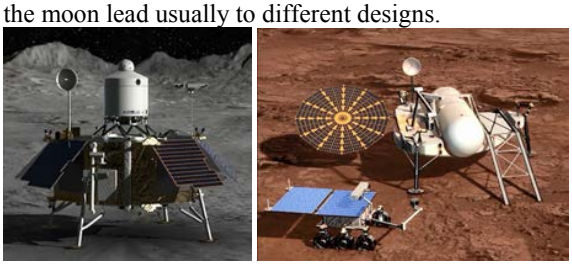

Fig.1: *left:* GAMMa LPSR lander, *right:* GAMMa MSR lander with sample fetch rover

However, while atmospheric drag does play effectively no role on the moon, an aerodynamic shape optimized for martian atmosphere does not necessarily lead to drawbacks on a lunar ascender. Further, gravitational differences can be compensated by strap on boosters or kick-stages, utilizing the mass saving effects from staging for a martian ascent vehicle whilst allow using a single stage to orbit lunar ascent vehicle as upper stage.

GAMMa modular ascender family: In the frame of the German national GAMMa study[1], a modular ascender family has been derived.

Fig.2: *left:* GAMMa LPSR ascender, *center:* GAMMa HERACLES ascender with kick-stage *right:* GAMMa MSR ascender with kick-stage

The concept is complying with all considered reference mission scenarios. Comparative analyses show only minor mass growth with respect to a single mission design concept, making the concept a viable option for several sample return missions.

[1] GAMMa (Gemeinsamkeiten von Aufstiegsstufen für Mond und Mars) has been supported by Federal Ministry for Economic Affairs and Energy on the basis of a decision by the German Bundestag (50JR1706)

PROSPECT – THERMAL DESIGN CHALLENGES FOR LUNAR VOLATILE EXTRACTION. P. B. Hager[1], V. Laneve[1], H. Rana[1], R. Trautner[1], R. Fisackerly[1], [1]European Space Agency, ESTEC, Keplerlaan 1, 2200AG Noordwijk, The Netherlands.

Introduction: To access and asses potential resources on the Moon is the main objective of the 'Package for Resource Observation and in-Situ Prospecting for Exploration, Commercial exploitation and Transportation' (PROSPECT). The primary objective is to find and characterize cold-trapped volatiles in lunar sub-surface samples at the south polar region of the Moon. A secondary objective is the demonstration of in-situ resource utilization (ISRU) capabilities. PROSPECT is designed as an ESA instrument embarked on the Russian Luna-27 mission to the Moon. Launch is expected to be in the 2022 to 2023 timeframe and it is planned to land at a location between 73° and 85° south.

The design of PROSPECT is driven by the preservation of volatile elements on one side and their extraction and analysis on the other side. A major design driver are the environmental heat fluxes.

In order to quantify lunar landing site dependent heat fluxes on the PROSPECT units, topography maps with varying levels of detail were used in a thermal analysis parametric study.

System Architecture: PROSPECT is composed of several mechanisms (ProSEED) to drill, retrieve and deliver 25 lunar sub-surface samples. Five different depths at five different lateral locations are foreseen. The drill is capable of retrieving samples from a maximum depth of 1.2 m. The samples are delivered to a Russian robotic arm and also to ProSPA, the sample analysis part of PROSPECT. ProSPA consists of several components to seal, heat, and eventually analyze & characterize the samples.

As PROPSECT is sensitive to environmental heat fluxes, thermal requirements and boundary conditions govern the design of its units.

Thermal Requirements: The lunar regolith temperature at the landing site and at sampling depth is predicted to be as low as 120 K on average, which some models consider to be consistent with the conditions necessary for sub-surface ice stability [1]. To preserve the volatiles, the entire sample handling chain is required to ensure that the bulk sample temperature is maintained within ~120-150 K, until the sample is placed and sealed in the ovens. In contrast, it is required to heat up the ovens to about 1300 K to allow for the *in-situ* demonstration of ISRU concepts. The extreme wide temperature range is challenging for materials and processes used in the ProSPA subassemblies.

From a thermal point of view, the lunar surface environment is extremely challenging for the entire PROSPECT package. Radiative heat exchange governed by environmental heat fluxes and conductive heat fluxes at the interface to the lander drive the thermal design. The interfaces to the lander can range between 93 K and 323 K for ProSEED and 222K to 323 K for ProSPA. Radiative fluxes from the environment are driven by the material and optical properties of the lunar regolith and the landing site, in terms of terrain slope and shadowing effects. The envisaged landing site between 73° and 85° South leads to lunar surface temperatures between approx. 90 K and 270 K for undisturbed flat surfaces [2-5]. Slopes or surface features such as boulders or craters can lead to even higher local temperatures [6].

Thermal Modeling Approach: In the present study several different approaches for modelling the lunar surface temperatures were compared and the resulting heat fluxes on a black cube was evaluated. An empirical approach was used to calculate local surface temperatures depending on lunar latitude and time of lunar day. In a second model a 30 m diameter disc was used and placed in 38 locations around one lunar day. The temperatures for this second model was calculated in steady state in each time step. This simplification was deemed acceptable as it allows to avoid a detailed model of the lunar surface and gives shorter computation times. In the last model, two topographic surface patches were used, of 1 km x 1 km and 30 km x 30 km diameter, respectively [7]. LRO LOLA data [8] was used to create the topography. The topography based thermal models were evaluated for selected orbit positions and results were compared to the 30 m disc results. Similar to the 30 m disc model, thermal inertia of the lunar soil was neglected in the detailed topography models. The high number of surface elements for the topography maps, led to long computational times. All models except the empirical model were set-up and run in ESATAN-TMS.

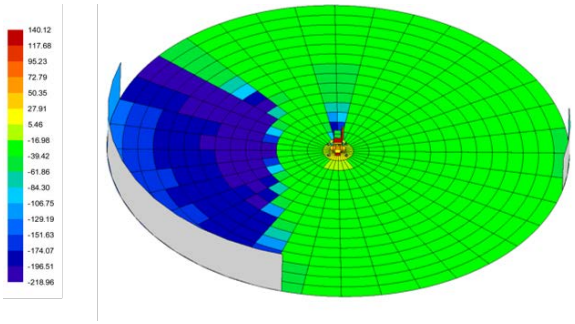

Figure 1: 30 m diameter disc with obstructions mimicking local shadows. Centered at lunar coordinates 82.7°S, 33.5°E. Colors indicate temperature in [K] for maximum solar elevation.

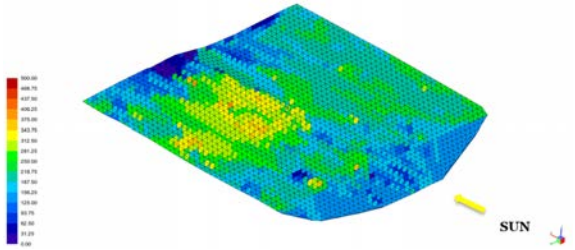

Figure 2: 1 km x 1 km topographic map. Centered at lunar coordinates 82.7°S, 33.5°E. Colors indicate heat flux [W/m²] for maximum solar elevation.

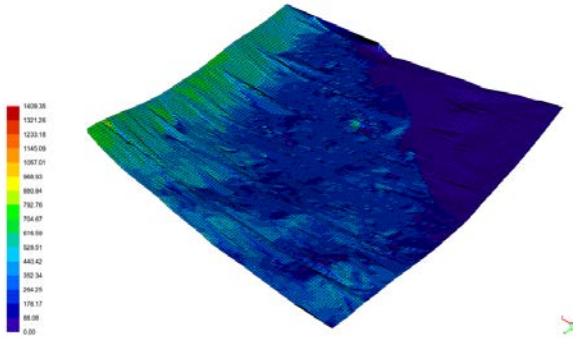

Figure 3: 30 km x 30 km topographic map. Centered at lunar coordinates 82.7°S, 33.5°E. Colors indicate heat flux [W/m²] for maximum solar elevation.

Results: The maximum deviation in calculated solar heat flux between empirical equation and 30 m disc model results was less than 0.37%. Lunar surface temperature from empirical equations was 245.6 K and between 244.65 K and 245.65 K in the 30 m disc thermal model for undisturbed, i.e. flat and not shadowed surface elements. The detailed topographic map of 1 km x 1 km diameter led to 18.36% higher infrared heat fluxes compared to the 30 m disc model. Yet, infrared heat fluxes of the 30 km x 30 km topographic map yielded in comparable results with the 30 m disc model. It was concluded that the received heat flux from mountains 20 km to 30 km away from the landing site is negligible.

Conclusions: It can be concluded that the 30 m disc model, featuring simplified obstructions to include shadowing effects, and a stepwise steady-state solution is a suitable representation for the selected landing site. It yields a good compromise between computational effort and result accuracy for thermal analysis of PROSPECT. High resolution local lunar topographic models would lead to higher and potentially more accurate results but the computational effort would be in no relation to the gained insight. Hence it was decided to use the 30 m disc model and to include an additional environmental heat flux of 20 W/m² for the worst hot cases.

References: [1] Siegler M., et al. (2014), *Icarus, 255,* 78-87. [2] Vasavada et al. (2012) *JGR,* 117. [3] Paige D.A. et al. (2010) *Science, 330,* 479-482. [4] Hayne P.O. et al. (2017) *JGR, 122*, 2371–2400. [5] Racca G.D. (1995), *Planet. Space Sci.,43, 6,* 835-842. [6] Bandfield J.L. et al. (2011) JGR, 116. [7] Laneve V. and Rana H. (2017) *ESA-HRE-PROSPECT-MEM-0001*. [8] http://ode.rsl.wustl.edu/moon/index.aspx (2012)

SIRONA-1: A SELENOCENTRIC PLATFORM HOSTING INTERNATIONAL PAYLOADS G. Bailet[1], R. Bossis[2], F. Clouvel[2], R. Derollez[2], B. Eich[2], T. Errabih[2], J.-M. Klein[2], E. Kostaropoulou[2], T. Hancock[2], M. M. Hott[2], F. Hübner[2], E. Jehanno[2], E. Lindsay[2], E. Pachoud[2], E. Rouanet-Labé and C. O. Laux[1], [1]Laboratoire EM2C, CNRS, CentraleSupélec, Université Paris-Saclay, 3, rue Joliot Curie, 91192 Gif-sur-Yvette cedex, France (gilles.bailet@centralesupelec.fr), [2]CentraleSupélec, Université Paris-Saclay, 3, rue Joliot Curie, 91192 Gif-sur-Yvette cedex, France.

Introduction: Over the millennia of recorded human history, the Moon has been the focus of great fascination and a goal to reach. Lunar exploration started with the Luna-1 flyby (1959), culminated during the Apollo era (1961-1972) and provided numerous scientific accomplishments and a tremendous source of inspiration for students, engineers and the general public.

The Lunar and Planetary Institute established a list [1] of major questions still not answered after the numerous probes/missions started in 1959. On that impulse, space agencies and universities are projecting new missions to the Moon. Although these missions are of great potential scientific return, their development costs do not fall within the budgets allocated by the funding agencies and only few projects are allowed to go forward. For the sake of illustration, since 2004, there have been fours projects in the USA (LRO 2009; Artemis P1/P2 2011; Grail A/B 2012; LADEE 2014) and only one in the EU (SMART-1 2004-2006).

We present in this paper a new platform based on the CubeSat standard [2], named SIRONA (20 kg), dedicated to bringing in lunar orbit a suite of payloads developed by universities around the world. Led by the student Space Center of CentraleSupélec, the collaborative effort to conduct this mission will provide innovative and exploratory science return with a low budget, and will foster new impetus for Lunar exploration.

On the way to the Moon: two options are available for the cislunar trajectory depending on payloads constraints and funding. The first option (OP1) is to use a commercial Polar Orbit (PO) and an off-the-shelf Electric Engine (EE) to progressively bring the spacecraft to selenocentric orbit. The second option (OP2) involves a direct cislunar trajectory insertion with a dedicated launch.

OP2 has the advantages of a short exposure to radiation during transit through the Van Allen belt, affording a better mission lifetime/radiation shielding ratio. Moreover, for the same platform mass, the OP2 scenario increases the mass available for the payload.

OP1 scenario has the advantage of a much simpler and flexible mission planning (several PO launches per year with CubeSat piggyback slots available). PO launches make the OP1 scenario the cheapest of the two options. An autonomous guidance, attitude control and propulsion system to the Moon ensures a flexible design for the payloads and future SIRONA-type missions.

Payloads: a scientific board will be formed with a panel of Lunar exploration experts and representatives of space agencies. The universities and research laboratories worldwide will be invited to respond to a call for proposal to embark payloads onto the SIRONA platform. The call will emphasize a priority on the scientific and technology demonstration objectives such as study of the Moon's water ice, development of a deployable high gain antenna, characterization of the far side of the Moon…

The scientific board will review the proposals taking in account the scientific merit of the expected return, the expected mass/volume/energy consumption of the experiment, as well as the educational impact. The board will select payload packages and backups to ensure a wide diversity of science objectives.

Funding: The total cost of the mission is expecting to be in the range 2-5 M€, depending on the scenario and launch arrangements. The SIRONA platform will be proposed for a Horizon 2020 grant to cover the hardware, manpower and the consortium/scientific board collocation meetings. A contribution to the launch cost will be requested from the payload teams as a function of their payload mass over the total mass (between 50-100k€/100g).

Conclusion: SIRONA is a unique low cost opportunity to fly multiple university-developed payloads to the Moon. The mission will investigate several critical Lunar exploration questions, allowing the scientific community to test different approaches for more in-depth studies in future flagship missions.

References:

[1] D. A. Kring, et al. (2012), *A Global Lunar Landing Site Study to Provide the Scientific Context for Exploration of the Moon*, LPI Contribution No. 1694, Lunar and Planetary Institute, Houston, TX.

[2] A. Mehrparvar (2014), *CubeSat Design Specification*. The CubeSat Program, CalPoly SLO.

INITIAL RESULTS OF SHELL LANDER IMPACT TESTS FOR THE EXPLORATION OF MEDIUM-SIZED AIRLESS BODIES.

C. D. Grimm*[1] and S. Schröder[1] and L. Witte[1],
[1]German Aerospace Center (DLR), Insitute of Space Systems, Robert-Hooke-Str. 6, 28359 Bremen, Germany, Christian.Grimm@dlr.de, Silvio.Schroeder@dlr.de, Lars.Witte@dlr.de,

Introduction: In recent years, the exploration of small solar system bodies has increased significantly. Due to both, the scientific interest for the role of small bodies during the development of the solar system and life within, as well as the potential threat for such objects to collide with Earth, they present a corner stone in the international space exploration endeavour. Apart from surveys of ground- and space based remote sensing instruments, multiple fly-by and rendezvous missions have been conducted already. However, especially spacecraft landing missions, designed to physically interact with the surface and near-surface environment enable the study of these objects from very close distance and to bring even samples back to Earth. As a result, they take up a key role in order to understand, identify and establish the most effective prevention measures, gather insights to the objects and possible mankind's origin as well as act as a demonstration to resource handling and precursor for future manned missions.

Small carry-on landers, like the European Rosetta Lander Philae which successfully landed on the comet 67P/Churyumov–Gerasimenko in November 2014 [1], or the German/French Lander MASCOT on-board the Japanese Hayabusa2 mission currently on its way to its target asteroid 162173 Ryugu and scheduled for landing in Ocober 2018 [2] , have proven to be a valuable asset by avoiding additional complexity of the main satellite and keeping project development times and costs in manageable bounds. Landing on small bodies is particular difficult due to the weak gravitational field and means to secure the lander to the surface have to be taken into account. However, with increasing size and density of the target the gravitational attraction on a lander increases also. Currently, non-propelled landers have been designed to land on very small bodies only, but medium-size class objects between diameters of 10 - 50~km are of great interest as well. For example, the Martian moons Phobos (D = 22 km) and Deimos (D = 12.5 km) as well as many Jupiter trojan asteroids have mean diameters of more then 10 km. Rendezvous missions to those targets [3] considering a detachable lander will have to focus on a dedicated landing support system. Depending on the capabilities of the mother spacecraft and resulting landing strategy, mainly the separation altitude and following free fall acceleration defines the final landing velocity at touch-down. Higher landing velocities introduce high shock loads and can cause damage to lander subsystems and instruments. Reducing the need of an optional retro-propulsion system, other means of absorbing the impact energy have to be taken into careful consideration. Non-propelled landing strategies can be devided into three categories. (i) Landing without a dedicated landing sub-system (MASCOT), (ii) Landing with energy absorbtion to reduce the imapt velocity to stay below the target's escape velocity (Philae), and (iii) heavy duty landing with a dedicated protection system to lower internal shock loads.

In order to enable the exploration and landing on medium-sized airless bodies, this talk will outline the concept of advancing small body landers with a crushable-shell protection system to sustain higher landing velocities in the range of 1 - 4~m/s. Apart form design aspects, results of initial crushable-shell impact tests will be given including test principles and test setup design.

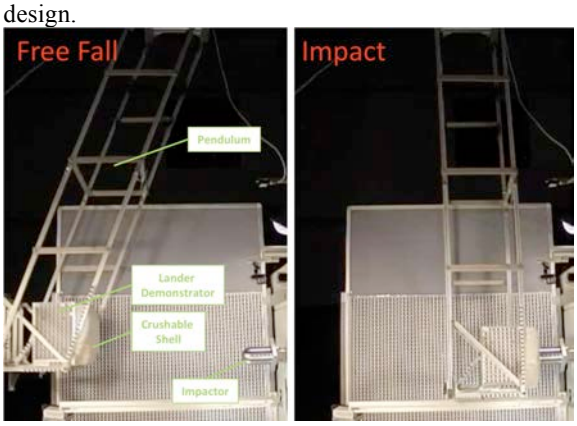

Figure 1: Pendulum Test Setup - Release, free fall and impact of a lander demonstrator with a crushable shell absorber.

References:

[1] Biele, J. et al. (2015) *The landing(s) of philae and inferences about comet surface mechanical properties, Science vol. 349 no. 6247.*

[2] Ho, T.-M. et al. (2017) *Mascot - the mobile asteroid surface scout onboard the hayabusa2 mission, Space Science Reviews vol. 208 no. 1 pp. 339–374.*

[3] Fujimoto, M. et al. (2017) *JAXA's Martian Moons eXploration, MMX, European Planetary Science Congress, Riga.*

CUBESAT ELECTROSTATIC DUST ANALYZER (CEDA) FOR MEASURING ELECTROSTATIC DUST TRANSPORT ON AIRLESS BODIES. X. Wang[1,2], Z. Sternovsky[1,2], M. Horányi[1,2], and Dust BUSTER Team[3]; [1]Laboratory for Atmospheric and Space Phsics, University of Colorado, Boulder, CO 80303, USA. [2]NASA/SSERVI's Institute for Modeling Plasma, Atmospheres, and Cosmic Dust, Boulder, CO 80303, USA. [3]Ann and H.J. Smead Aerospace Engineering Sciences, University of Colorado, Boulder, CO 80309, USA. (First author's address: 3665 Discovery Drive, Boulder, CO 80303; Email: xu.wang@colorado.edu)

Introduction: Electrostatic dust charging and transport on airless planetary bodies, due to the exposure of their regolith to the solar wind plasma and solar radiation, has been a long standing problem. This process has been hypothesized to explain a number of unusual space observations [1] from the Moon (e.g., the lunar horizon glow) to asteroids (e.g., dust ponds on Eros) to comets (e.g, Rosetta's dust collection from comet 67P) and to planetary rings (e.g, the radial spokes in Saturn's rings). It has remained an open question to understand its role in shaping the surface properties of airless bodies.

However, one fundamental problem about the exact charging and transport mechanisms remained unsolved for decades. Recent laboratory studies have greatly advanced our understanding [1,2]. In the laboratory experiments with simulated space conditions, micron-sized dust particles were lofted to several centimeter high by exposure to ultraviolet (UV) radiation and/or plasmas (Fig. 1).

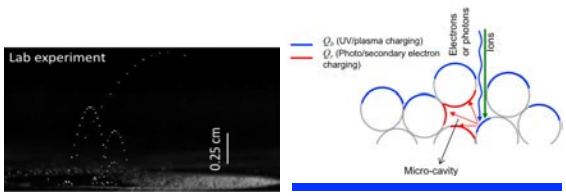

Fig. 1 Left: Trajectories of lofted dust particles under UV radiation; Right: Patched charge model.

A new "patched charge model" (Fig. 1) has been developed and validated with the experiments. It explains that the emission and re-absorption of photo- or secondary electrons inside microcavities between dust particles results in large negative charges on them, and the resulting inter-particle repulsive force causes them to be lifted off the surface. These experiments also showed that electrostatic dust transport can be an efficient process in shaping the surfaces of airless bodies, such as the surface morphology and porosity, surface materials redistribution, and alteration of space weathering effects, providing a new paradigm for the surface formation and evolution.

In-situ measurements with a dedicated dust instrument are required to find out how electrostatic dust transport contributes to reshape regolith surfaces on airless bodies. These measurements will provide an insight into their effects on the regolith physical properties and near-surface dust environments. In addition, these measurements will estimate and evaluate the potential dust hazards and enable the development of mitigation strategies for future robotic and/or human exploration.

Instrument and Mission: A new dust instrument, called the Cubesat Electrostatic Dust Analyzer (CEDA), is under development by the Dust BUSTER student team at the University of Colorado. CEDA is a 6U cubesat with an integration of a 2U dust sensor to be deployed on the surface of an airless body. This instrument measures the charge, velocity, mass of lofted dust particles, and provides their lofting rate in order to estimate their role in surface processes.

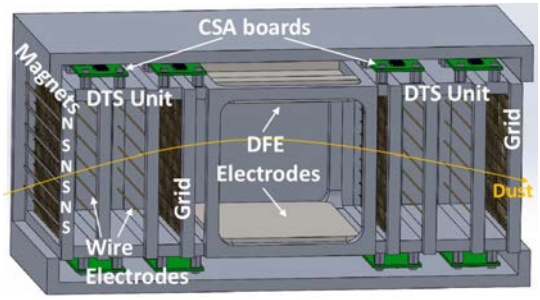

Fig. 2 Cut-view of the 2U dust sensor.

The design of the dust sensor is based on a prototype of the Electrostatic Lunar Dust Analyzer (ELDA) [3]. The sensor consists of two identical Dust Trajectory Sensors (DTS) on both ends of the sensor and a Deflection Field Electrodes (DFE) unit between the two DTS's, as shown in Fig. 2. A charged dust particle can enter the sensor from either end. The charge and velocity are measured with two arrays of the wire electrodes in the DTS on which the image charge of the dust particle is induced. The charged particle will be then deflected by the DFE and exit through the second DTS on the other end. The mass is derived from the deflected trajectory. The charge signals are measured using the Charge Sensitive Amplifiers (CSA).

The 2U dust sensor is accomadated in the 6U cubesat (Fig. 3). CEDA has a symmetric design so that the dust sensor measurement is independent of the random landing positions. The cubesat will be tilted for larger field-of-view (FOV) using miniature linear motion actuators (mLMA). Solar wind plasma and

UV radiation are blocked by door covers. The tilted side and open door are away from the Sun which position is determined by the sun sensors.

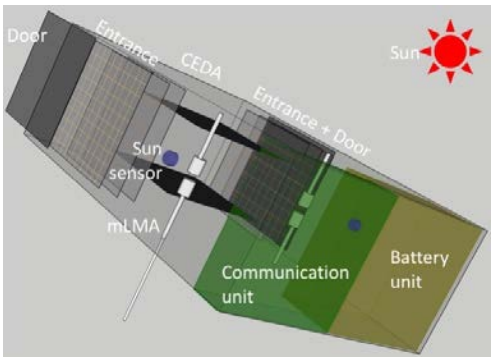

Fig. 3 Schematic drawing of CEDA. It includes the 6U cubesat system with an integration of the 2U dust sensor.

Summary: Electrostatic dust charging and transport has been suggested to explain a number of phenomena on airless bodies, and has been shown in recent laboratory observations with simulated space conditions. In-situ measurements provided by CEDA would verify and better characterize this phenomenon in order to estimate its effect on the surface processes and near-surface dust environment as well as potential dust hazards to future robotic and human exploration.

References: [1] X. Wang, J. Schwan, H.-W. Hsu, E. Grün, and M. Horányi (2016), GRL, 43, 6103–6110. [2] J. Schwan, X. Wang, H.-W. Hsu, E. Grün, and M. Horányi (2017), GRL, 44, 3059–3065. [3] N. Duncan, Z. Sternovsky, E. Grün, S. Auer, M. Horányi, K. Drake, J. Xie, G. Lawrence, D. Hansen, H. Le (2011), PSS, 59, 1446-1454.

EFFECTS OF PROBE SHAPE AND SURFACE TOPOGRAPHY IN DEPLOYMENT TO SMALL BODIES.
S. Van wal[1] and D.J. Scheeres[1], [1]University of Colorado Boulder (stefaan.vanwal@colorado.edu, 431 UCB, Boulder, CO 80309)

Introduction: The exploration of the small bodies of our Solar System is the goal of an increasing number of Discovery- and New Frontiers-class missions, and attempts to address three goals. First, small bodies are considered to be remnants of the early Solar System and may provide insight into its formation and evolution. Second, such missions provide a proving ground for planetary defense strategies to mitigate destructive impacts of near-Earth asteroids. Finally, small-body exploration enables the development of in-situ resource utilization techniques, which have the potential of reducing the cost of spaceflight.

Although some of these goals can be addressed with an orbiting mothership, the Philae lander onboard Rosetta demonstrated the increased scientific return that is possible with the inclusion of surface exploration operations. Similarly, the Hayabusa-2 mission plans to (ballistically) deploy the MINERVA-II and MASCOT rovers to the surface of asteroid Ryugu, where they will hop around using momentum exchange mechanisms and obtain scientific measurements from multiple surface sites [1, 2].

The ballistic deployment of scientific probes to small-body surfaces is challenging, due to the weak gravitational environment and resulting bouncing dynamics. This was first witnessed by the MINERVA-I hopper onboard Hayabusa-1, which failed to reach the surface [3], and later by the Philae lander. The latter bounced several times on the surface of comet 67P/C-G, before settling in a poorly-lit region [4].

These examples illustrate the need for high-fidelity simulation of probe dynamics in the small-body environment. This enables the development of a deployment strategy, subject to regional exclusion, line-of-sight, and insolation requirements. Similar analyses can be performed for hopping operations to explore the surface. In this work, we present a parallelized framework for the simulation of small-body exploration probes, that leverages the GPU to perform a large number of simulations. We apply this framework to quantify the effects of a probe's shape and of the small-body surface topography on the probe dynamics.

Modeling: The small-body shape is modeled with an implicit signed distance field (SDF), which can be pre-computed offline and interpolated online to allow for collision detection at a computational cost far lower than that of the classically-used polyhedron shape model. Although we continue to use the latter for gravity field evaluations, this field is also pre-computed and stored for online interpolations, allowing for cheap gravity field evaluations. More specifically, we store the polyhedral perturbation from a central gravity field, in order to minimize storage requirements.

Surface interactions between a probe and the small-body surface are evaluated using an impulsive contact model that takes into account restitution and Coulomb friction. The magnitude of these forces and their corresponding torques are governed by the respective coefficients of restitution and friction, which can be tuned. The model is able to handle probes with an arbitrary shape, that often experience non-trivial velocity changes during surface impacts [5].

Given the limited resolution of global shape models, they cannot account for small surface features such as rocks and boulders that may affect the motion of a surface exploration probe. We therefore procedurally generate such features using fractional Brownian motion (fBm), which imposes statistical noise onto the otherwise smooth surface at various amplitudes and frequencies [6]. These can be tuned to mimic the features observed on small-body surfaces, see Fig. 1.

Finally, the presence of regolith on top of a hard surface layer, as observed by Philae on 67P/C-G [4], is accounted for through a modulation of the coefficient

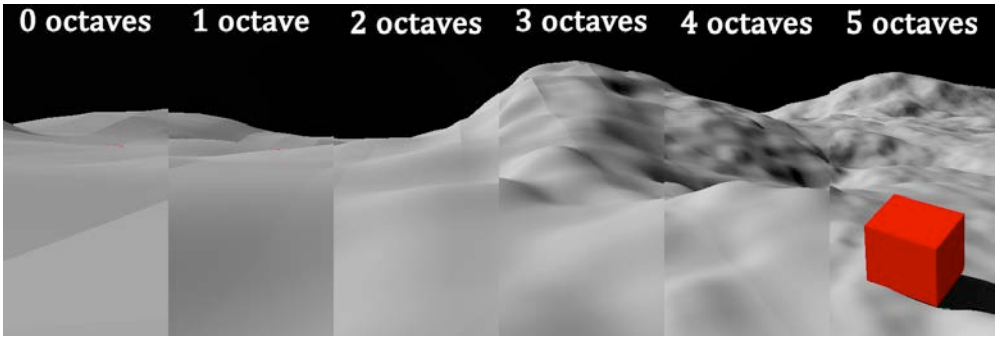

Figure 1: Generation of surface features with increasing number of fBm octaves.

of restitution based on the effective impact angle. This is done in agreement with experiments that observed greater damping in normal vs. tangential impacts in granular media [7, 8].

Probe shape: We apply the resulting simulation framework to investigate how the shape of a small-body exploration probe affects its dynamics. For this, we repeat a nominal deployment scenario (see Fig. 2) for the five platonic solids, which provide a fairly continuous sampling of realistic mass distributions. We also simulate the three rovers included on Hayabusa-2, resulting in a total of eight different probe shapes. All eight are given the same mass and volume, such that they carry the same 'malleable' payload. We find that the tetrahedron settles the fastest and with the smallest surface dispersion, followed by the octahedron, cube, icosahedron, and dodecahedron (see Fig. 3).

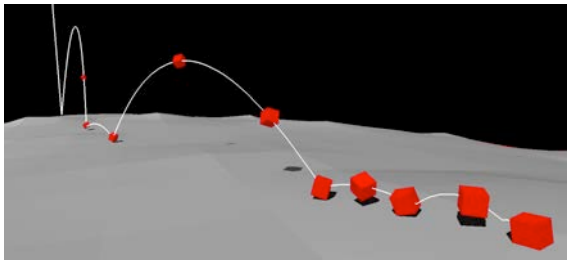

Figure 2: Sample deployment of a cube.

The MASCOT lander shows similar behavior to the cube, while MINERVA-II-2 settles slightly slower. The MINERVA-II-1 rover has the longest settling time and greatest surface dispersion. These results can be explained based on the feasible geometries at which the various shapes can impact a flat surface. This in turn determines the rate at which their energy is dissipated, and thus how far they can bounce. The duration of continued contact motion is found to be negligible for most of the tested shapes. These results have implications for the suggested design of an exploration probe, if it is to settle on the surface in minimum time.

Probe mass distribution: Varying the internal mass distribution of the mentioned probe shapes, we find that more outwards mass distributions are associated with longer settling times. This trend can be explained through the mechanics of Coulomb friction.

Shapes that are more spherical (the dodecahedron) are not as affected as less spherical shapes (the tetrahedron). The effect is of smaller magnitude than that of probe shape, but should still be considered when designing a surface exploration probe. The placement of high-density components at the center of the probe will minimize the settling time and surface dispersion.

Surface topography: Using fBm, we generate surface features on the otherwise smooth small-body surface. The inclusion of surface features larger than the simulated probe impose a randomization on the surface normal during impacts. This randomization increases the energy dissipation rate of a shape and results in shorter settling times.

The inclusion of features smaller than the probe size affect the collision geometry in a wslightly ay that increases the settling time for the tetrahedron and octahedron, while notably decreasing it for the icosahedron and dodecahedron. The inclusion of such features also strongly reduced the settling time of the MINERVA-II-1 rover, which was particularly high when deployed to smooth small-body surfaces. These results underscore the importance of accounting for small surface features such as rocks and boulders, and quantifies the effects of different-sized features on probe motion.

References: [1] Tra-Mi, H. et al. "*MASCOT – The mobile asteroid surface scout onboard the Hayabsusa-2 mission*." Space Science Reviews, 2017. [2] Yoshimitsu et al. "*Hopping rover Minerva for asteroid exploration.*" Artificial Intelligence, Robotics, and Automation in Space, 1999. [3] Yoshimitsu et al. "*Minerva rover which became a small artificial solar satellite.*' Small satellite conference, 2006. [4] Biele et al. "*The landing(s) of Philae and inferences about comet surface mechanical poperties*." Science, 2015. [5] Stronge "*Impact Mechanics*." Cambridge University Press, 2004. [6] Ebert et al. "*Texturing & modeling: A procedural approach*." Morgan Kaufmann, 2003. [7] Murdoch et al. "*An experimental study of low-velocity impact into granular media in reduced gravity*." Monthly notices of the royal astronomical society, 2017. [8] Nishida et al. "*Effects of density ratio and diameter ratio on critical incident angles of projectiles impacting granular media.*" Granular Matter, 2010.

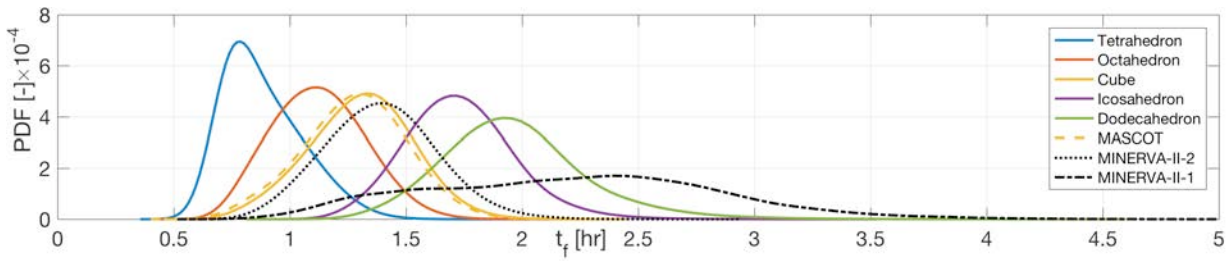

Figure 3: Settling time PDFs of tested probe shapes.

A DESIGN FOR REPEATABLE NEO FLYBY MISSIONS. O. Fuentes-Munoz[1] and D.J. Scheeres[1*], [1]Department of Aerospace Engineering Sciences, The University of Colorado, Boulder, CO 80309-0429, USA. *Corresponding author: E-mail address: scheeres@colorado.edu (D.J.Scheeres)

Introduction: The study of Near Earth Objects (NEOs) is of great relevance to the understanding of the origins of the solar system. NEOs hide the secrets of the origin of life, but they also are the greatest threat to life on Earth. Due to this, the science community around the world is making huge efforts to detect and catalogue the population of NEOs. The main systems currently used are ground based telescopes like Pan-STARRS [1] or Catalina. In addition, space telescopes like NEOWISE [2] are operational and few others are either proposed or will fly in the next years like James Webb Space Telescope or NEOCam. These sources provide hundreds of new NEOs every year.

NEOs are commonly discovered months, days, before their flyby to Earth. In 2017 alone, 857 new NEOs were discovered, 54 of which passed within a lunar distance to Earth. For example, we know of 5 objects that will flyby within 5 LD of Earth in the remainining part of 2018. However, 52 new objects were identified and had their closest approach in this range until March.[3]

This paper proposes the design of a space observatory to be ready in orbit to perform a flyby when an interesting NEO target is found. The mission would consist in the injection of the observer into a highly elliptical orbit to flyby the object without rendezvous. The original parking orbit can be restored or modified to reuse the system for future flybys (See figure 1).

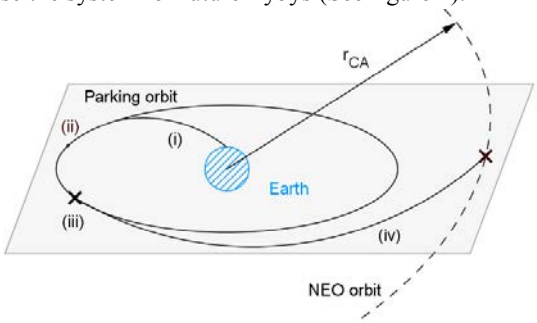

Figure 1. Flyby Mission: (i) deployment of the observer to a parking orbit. (ii). NEO surveillance. (iii). Staging of the flyby (iv)

Proposed Design: The design consists of finding the best parking orbit from which to stage the flyby. A statistical analysis of the population was performed to evaluate this. The dataset consists of all recorded objects that have flown by Earth with aim to characterize the orbit characteristic distribution of the population.

The analysis of the population starts by fixing the orientation of the parking orbit. Every object can be targeted for a flyby at the intersection of its orbit with the parking orbit plane. This allows the transfer orbit to not involve plane change, making it more Δv efficient. By changing the orientation of the parking orbit, the distribution of the intersections changes. The goal is to find the orientation that results in the minimum mean distance of flyby (See figure 2).We find that the mean distance is minimized in polar planes with respect to the ecliptic.

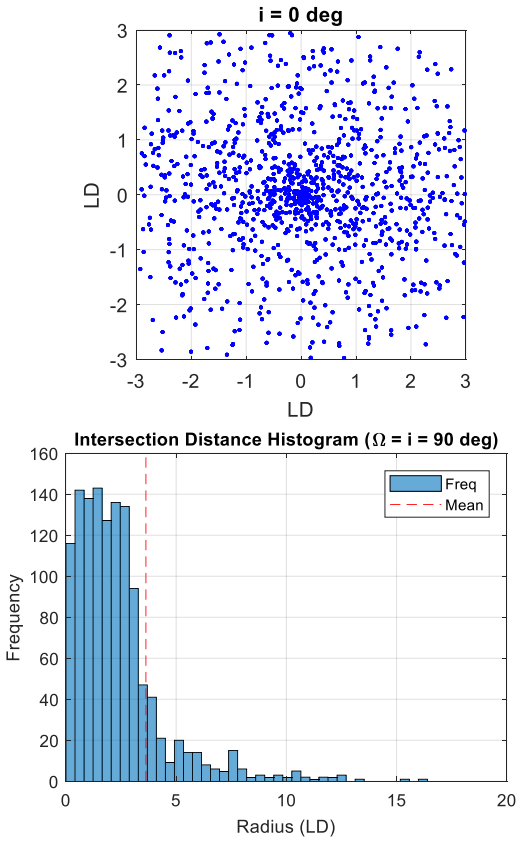

Figure 2. Distribution of the intersections of the NEO population (top) and radial component of the distribution (bottom).

An added benefit is that perturbations caused by planetary oblateness and solar tides form a natural equilibrium solution called Laplace Planes in this same orientation. The application of Laplace Planes is used in the mission design process to determine the stability of the high earth orbits considered as parking orbit [4].

Maneuver costs of the mission depend heavily on the available time. Assuming there is plenty of time, a first approach is studied by considering Hohmann transfers to that flyby. We show that we can always find a proper phasing to enable flyby observations. In a more generic approach, different Lambert problem solutions are considered.

Due to the high earth orbit nature of the orbits, the dynamic stability is assessed numerically. A numerical solution of the 3-body problem is implemented for the Earth-Sun system and the 4-body problem solution for Earth-Moon-Sun system. These are used to verify how realistic are the designed maneuvers and the resulting orbits.

Finally, the flyby geometry is considered, to evaluate conditions and constraints on the imaging system to be successful.

References: [1] The Pan-STARRS1 Database and Data Products,(2016) Flewelling, H.A., et al. [2] NEOWISE project. Mainzer et al. (2011) ApJ 731, 53. [3] Small-Body DataBase Close-Approach Data API. (2016). JPL SSD/CNEOS API Service. [4] Tremaine, et al. (2009) The Astronomical Journal, 137(3):3706-3717.

ESTIMATION EVALUATION OF THE RADIO SCIENCE PHASE OF THE OSIRIS-REX MISSION. D. N. Brack[1], A. S. French[1], J. W. McMahon[1], and D. J. Scheeres[1], [1]University of Colorado Boulder (ECNT 320, 431 UCB, University of Colorado Boulder, CO 80309).

Introduction: The Origins Spectral Interpretation Resource Identification Security Regolith Explorer (OSIRIS-REx) mission was launched in September 2016. The spacecraft is in route to its target near-Earth asteroid 101955 Bennu. The NASA mission is planned to survey the carbonaceous asteroid and orbit it during 2018 and 2019 after which the spacecraft will obtain a regolith sample from the asteroid surface to be returned to Earth in 2023. In addition to the sample return, OSIRIS-REx's scientific objectives include mapping and documenting Bennu's global properties, chemistry, and mineralogy, measuring the orbital perturbations that affect the asteroid, and characterizing global properties of carbonaceous asteroids for comparison with other observed asteroids.

OSIRIS-REx Radio Science Campaign: In the mission's Orbital B phase the spacecraft will orbit Bennu in a close-to-circular terminator orbit with a semi-major-axis of ~1.0 km. During this phase time will be dedicated for the Radio Science Campaign (RSC) in which the spacecraft's non-gravitational perturbations will be minimized. During this 9-day period the spacecraft orbit will be perturbed by the asteroid's non-uniform gravity field, enabling the low degree and order gravity coefficients to be estimated. Several measurement types will be used in the estimation process and include: range and Doppler measurements from Earth, optical imagery of the asteroid surface, and altimeter measurements of the surface topography.

Gravity Field Spherical Harmonics Expansion: In addition to improving the dynamical model for simulating and planning operations around the asteroid Bennu, estimating the spherical harmonics coefficients provides an insight into the density distribution of the asteroid. When constrained with the asteroid volume, obtained from building a shape model for the asteroid, a variety of density distributions can be compared to the spherical harmonics expansion deducing possible internal structures for the asteorid. The conclusions of this comparison will only provide an observation into Bennu's current structure and shape but could also be inferred to other asteroids of similar characteristics and assist in planning future small body missions.

Orbit Determination and Parameter Estimation: The Radio Science team at the University of Colorado Boulder has selected NASA Goddard Space Flight Center's GEODYN-II software as the orbit determination and geodetic parameter estimation tool for solving for the spherical harmonics coefficients. GEODYN-II uses the partitioned Bayesian least squares method to estimate the a-priori dynamical variables and orbital parameters of a spacecraft orbiting a celestial body. As part of the estimation process the software propagates the spacecraft orbit for the selected estimation periods.

Estimation Evaluation: Using GEODYN-II, an Orbital B phase is simulated, and corresponding measurement inputs are generated. In addition to different orbital parameters examined, the scenarios which are simulated include a variety of dates, durations and numbers of orbit arcs of the RSC as well as different spacecraft pointing schemes which dictate the measurement types available at any portion of the RSC. These simulated measurements are input back into GEODYN-II with added noise. This setup assists in evaluating the estimation process for different Orbital B scenarios and variations in orbital parameters and operational measurement schemes. The key parameters for the analysis being the spherical harmonics coefficients' estimation errors and covariances. In particular, a combination of radio, optical, and altimeter measurements is compared to a radio-optical only scheme. The analysis is then compared to results from additional tools used by the Radio Science team and will assist in determining recommended operational schemes and orbital parameters for the Radio Science portion of the Orbital B phase. The analysis will also be taken into consideration when planning the orbit determination parameters such as a-priori covariances and state noise compensation.

References: [1] McMahon J. W. et al. (2018) *Space Sci Rev, 214:43.* [2] Mink R. (2014) *"OSIRIS-REx Project Design Reference Mission and Mission Plan, Revision C" Internal Document.*

Analysis of Structural Effects on Seismic Instruments On-board Space Exploration Landers. Vikram Krishnaswamy[1], Dr. Alexandre Cadu[1], Dr. Naomi Murdoch[1], [1]ISAE-SUPAERO.

Introduction. Due to several causes including solar heating and impacts, asteroids undergo seismic activity [1]. However, this has never been measured directly. Measuring these effects can improve understanding of the asteroid's composition and structure. One mission aimed at this is the Asteroid Impact and Deflection Assessment mission [2]. The ESA component of this mission would observe an asteroid as it was impacted.

As part of the ESA mission, a 3U CubeSat, the SeisCube [3] is designed to house instruments to record the seismic vibrations of the asteroid. These instruments include 3 geophones and 3 accelerometers. The satellite would measure vibrations up to 200 Hz. Electronic boards would handle data processing, and solar panels would power the system together with a battery.

Landing on an asteroid with a specific orientation is difficult due to the low-gravity environment. In addition, during the operation of such a lander, it is possible that the low gravity and seismic activity causes the lander to leave the surface and land in another orientation, as in the Rosetta/Philae mission [4]. Asteroids have similar gravitational field strength, so landing can pose similar challenges. To solve this problem, the SeisCube will be omni-directional, and land uncontrolled.

Such a lander would require solar panels on all faces, and thus would experience increased heat flux. This can be problematic for internal sensors and batteries. To avoid this issue, the SeisCube has a two-layered structure, with layers separated by thermally-resistive spacers. The protective structure imposes transfer functions (which vary based on lander and force orientation) between the asteroid and the sensors. The purpose of this project is to identify and improve these transfer functions within the 200 Hz frequency range.

Transfer Function Identification and Improvement. It is theoretically possible to use FEA to calculate the transfer functions between the asteroid and the sensors. This can be done by applying a fluctuating force to one side of the structure, varying its frequency, and then repeating this process on all 6 faces and 3 force orientations. This, in turn, would need to be repeated every design iteration. With the available computing resources, this would take a prohibitively long time.

This problem is avoided by modelling the system as a group of connected plates and beams. With simplifying assumptions (such as thin plates, long beams, and small deflections), the reactions of these components to an input force can be approximated analytically. This would reduce computational time drastically, at the cost of some loss in accuracy (depending on the validity of the assumptions made). Using this model, the system can be optimized to remove vibration modes in the operating frequency range, and to minimize heat incursion into the protected components of the system.

Force Specification. Input forces to the system can vary with time and location on each of the outer faces of the SeisCube. They can be applied to parts of a face, or the entire face. Fourier series can be used to represent the forces as functions of time and location on each face [5]. One example of this is shown in Fig. 1, which uses Fourier series to approximate square-wave forces in two plate dimensions.

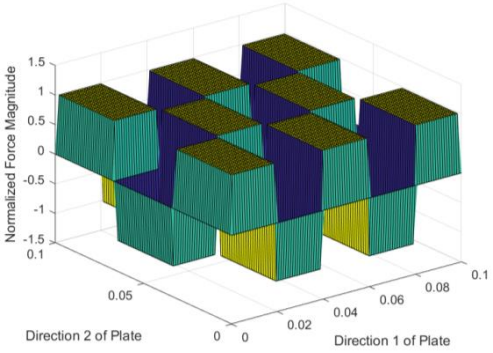

Figure 1: Arbitrary Force Distribution on Plate

Beam Deformation. Some elements of the SeisCube, such as the thermal spacers connecting the inner and outer layers, are sufficiently slender as to be representable as beams. These beams would encounter both longitudinal and transverse forces, as well as moments. Using the assumption of linear elasticity [6], the combined deformations from these forces can be calculated analytically using Hooke's Law and buckling theory, and Euler-Bernoulli beam theory respectively.

Plate Deformation. Similarly, the plates in the structure would likely experience combined loading. Axial loads produce deformations according to Hooke's law. Transverse loads on plates cause plate bending. Describing the deformation and reaction forces due to this loading can be done for specific expressions of the load. One such expression is a Fourier series, and this is the main reason for choosing this method to specify forces in Fig. 1. Given this expression of forces, the displacement can be determined as a similar series of sines. This results in a deformation & stress field across the plate, the first of which is shown in Fig. 2.

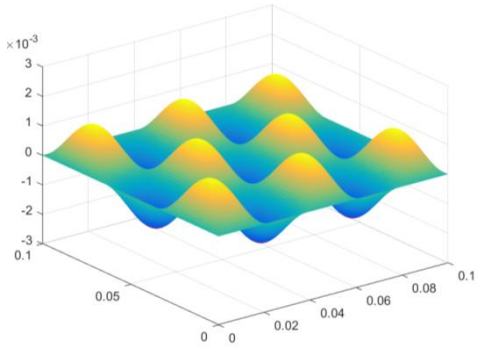

Figure 2: Deformation due to Plate Forces

The solution of this formula is dependent on the boundary conditions applied to the edges of the plate. This is the case for simply-supported edges, where the plate edges do not move. The deformation and reaction forces change with different boundary conditions, such as elastic supports and point supports. For the majority of components on this satellite, the supports are more rigid than the plate, so simple supports are a good assumption.

This model for plate deformation with no edge movement can be combined with a model for the movement and rotation of the entire plate, producing the total movement of all points along the plate.

Electrical Analogues for Mechanical Systems. For each of the beam and plate elements, the reactions to a force can be found analytically. The same is not true of the system as a whole, as the components' inertias and reactions affect all components they are connected to. Thus, the components must be connected in a network that allows them to affect one another, and the resulting system solved numerically.

One way of doing this is through the force-current analogue [7]. This converts mass to capacitance, compliance to inductance, lubricity to resistance, and force to current. Here, each node between elements represents an absolute position. This analogy preserves the topology of the system, allowing for easier conversion between the two systems.

With this system, it is possible to solve for the response at the geophones to an input force somewhere on the surface. Because the number of elements is much smaller than a typical finite-element system, the computational time required to do so is much shorter.

Design Optimization. With an easily-solvable system, it is possible to optimize the structure, given the constraints and a definition of the objectives. In this project, there are two objectives for the structure:

1. Minimize heat transfer to internal components.
2. Maximize flatness of transfer function, inside the operating frequency range of 200 Hz.

The structure is iterated upon to improve these characteristics. This optimization improves the accuracy of the sensors and enables the cancellation of the transfer function of the structure. This in turn improves the usefulness of the generated data.

Conclusion. A CubeSat lander is proposed to land on asteroids and measure their seismic activity. Due to the difficulty of landing on these bodies, the satellite will descend uncontrolled to the surface. This has architectural implications for the satellite. These mean that the structure between the sensors and the asteroid surface has a complex transfer function.

To understand the data from the sensors, it's necessary to understand this transfer function. However, the many different possible loading configurations and operating frequencies prohibit the use of traditional FEA. Each iteration of the structural design would require this simulation, which is not viable with the computing power available. Instead, we develop a simplified satellite model based on analytical deformation models of plates and beams. This model would greatly increase the speed of the simulation, at the cost of some accuracy. As such, it would allow the improvement of the satellite structure for its application.

References.

[1] N. Murdoch, et. al., "Asteroid Surface Geophysics", Asteroids IV, 2015.

[2] Cheng, A.F., Atchison, J., et. al., "Asteroid Impact and Deflection Mission", Acta Astronautica, Vol. 115, 2015.

[3] Cadu, A., N. Murdoch, et. al., "SeisCube Instrument and Environment Considerations for the Didymos System Geophysical Exploration", Geophysical Research Abstracts, Vol. 18, 2016.

[4] Biele, J., Ulamec, S. et. Al., "The Landing(s) of Philae and Inferences about Comet Surface Mechanical Properties", Science, Vol. 349, Issue 6247, 2015.

[5] S. Timoshenko, S. Woinowsky-Krieger, *Theory of Plates and Shells*, USA: McGraw-Hill Book Company, 1959.

[6] J. M. Gere, B. J. Goodno, *Mechanics of Materials*, Toronto: Cengage Learning, 2009.

[7] E. Cheever, "Analogous Electrical and Mechanical Systems", Swarthmore College Department of Engineering, 2005.

Current and future researches at ISAE-SUPAERO in autonomous operations orbiting an unknown asteroid through imagery

Paolo Panicucci[1]*, Emmanuel Zenou[2], Michel Delpech[3], Jérémy Lebreton[4], Keyvan Kanani[5]

[1] DISC, ISAE-SUPAERO, 10 Avenue Edouard Belin, 31400, Toulouse, France
paolo.panicucci@isae-supaero.fr
[2] DISC, ISAE-SUPAERO, 10 Avenue Edouard Belin, 31400, Toulouse, France
emmanuel.zenou@isae-supaero.fr
[3] IF Department, CNES, 18 Avenue Edouard Belin, 31400, Toulouse, France
michel.delpech@cnes.fr
[4] Airbus Defence and Space, 31 Rue des Cosmonautes, 31400, Toulouse, France
jeremy.lebreton@airbus.com
[5] Airbus Defence and Space, 31 Rue des Cosmonautes, 31400, Toulouse, France
keyvan.kanani@airbus.com

Abstract

Space science and Solar System exploration are continuously stimulating the design of new missions and efforts in developing innovative solutions for probes operations and navigation. The increasing interest for small bodies in the Solar System paves the way, on the one hand, to a deeper comprehension of the Solar System formation and, on the other hand, to the engineering challenges associated with the limited knowledge of the body characteristics. In particular, the stringent requirements associated with the small body missions impose high-precision navigation that cannot be fulfilled with conventional inertial sensors as, in operational cases, the small body gravity field is poorly known from radar and optical measurements. This leads to the choice of non-conventional techniques such as vision-based system despite its computational complexity.

This research aims at presenting the recent and future advancements at ISAE-SUPAERO, in collaboration with the Centre National des Études Spatiales (CNES) and Airbus Defence and Space, of the application of vision-based navigation to the problem of orbiting around an unknown asteroid. The main goal of this research is to increase the probe autonomy around the small body in order to allow longer arcs without communication with ground stations and improve the observability of gravity fiels higher order coefficients. This results in the limitation of the man-in-the-loop component in an operational framework and reduces the number of communications with ground stations. It is a crucial change with respect to current and past missions as, on the one hand, the man-in-the-loop component is extremely expensive and resource demanding and, on the other hand, this approach allows the probe to orbit closer to the asteroid without the need of delayed communications with Earth.

The research is developed on three different but complementary axes:

- The estimation of the satellite relative position with respect to the small body by computer vision techniques
- The characterization of the asteroid shape and rotational state through imagery
- The recursive estimation of the asteroid gravitational field in order to allow guidance, navigation and control (GNC) autonomous operations

Current researches are focusing on the estimation layer, i.e. the gravity estimation algorithm and its architecture. The vision-based

* Corresponding author

navigation layer - named visual layer - of the navigation architecture is temporarily emulated by the actual probe position, i.e. the ground truth, at any given time in the inertial reference frame. Moreover different gravity field models are tested to understand which is the most suitable from an estimation point of view.

Future points of interest are focused on:

- Integration of the estimation layer with the visual layer, i.e. the part of the vision-based navigation in charge of landmark extraction and matching or relative navigation, in order to simulate the visual navigation with synthetic and real images. As far as synthetic images are concerned, they will be generated with the SurRender software that allows the generation of space scene with an high level of physical details. Furthermore, the terrain models will be complemented by gravity field simulations using dedicated tools developed at ISAE-SUPAERO

- The use of infrared images to limit the influence of the light reflection and to avoid shadowing from the Sun

- The integration of the vision-based navigation system with other types of measurements, such as laser telemetry, to obtain more precise estimations. This allows a better understanding of the small body characteristics as the optical camera provides exploitable data in the perpendicular plane to the asteroid-probe direction and the LIDAR resolves the scale factor ambiguity due to the projection of the 3D space on the image plane

FREE RETURN TRAJECTORIES TO MOON

E. Unal[1]
[1]Roketsan Missile Industries Inc., PO Box 30, Elmadağ 06780 Ankara, TURKEY. emre.unal@roketsan.com.tr

Figure-8 trajectory is a path followed by the Apollo Mission in order to send the human to the Moon. Spacecrafts are sent to the Moon on the half of the 8-shaped trajectory and when it is reached to the perilunar point, the velocity is decreased in order to orbit the Moon. When the Moon part of the mission is completed, the velocity of the spacecraft is increased to complete the other half of the 8-shaped trajectory. It is also known as free return trajectory, since, once the spacecraft is placed on such a path, the mission will not require any fuel expenditure to return to Earth, except for the trajectory correction maneuvers. In Apollo project, this path has been deliberately chosen in case there might be a problem in the mission before entering to the Moon orbit. On April 11th, 1970, Apollo-13 mission carrying three astronauts has been launched. Two days later, during coast to the Moon, an accident occurred and the mission has been canceled [1]. The only way to bring the people back to Earth safely was to complete the Figure-8 path. In other words, it was inevitable for the astronauts to be stranded in the Earth&Moon system had the figure-8 trajectory was not chosen in the first place.

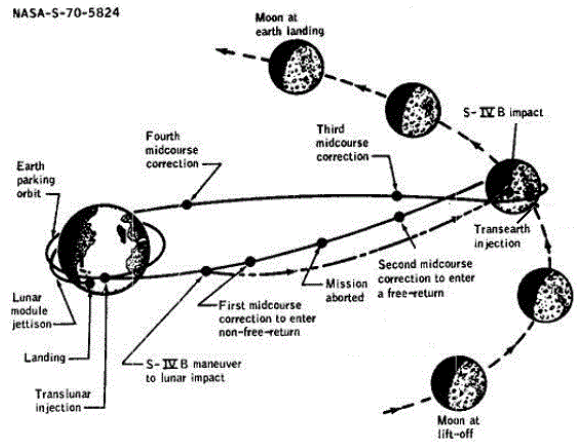

Figure 1: Apollo 13 mission profile
* The figure taken from Apollo 13 mission report [1].

In this study, the route followed in this dramatic event is investigated. In order to achieve a Figure-8 free return trajectory to the Moon, three solution methods are used: Lunar patched conic approach, numerical integration of the motion of equations, and restricted three body problem approach. Starting from the actual Apollo-13 flight parameters at the lunar injection point, the solution methods have been used to achieve the resulting goals of the mission and the results have been compared. The advantages and the disadvantages have been discussed. The effects of the Sun's and Jupiter's gravitational attraction on the trajectory have also been studied.

In "Lunar patched conic approach", the Earth and the Moon are considered to affect the spacecraft by their gravitational attraction. Outside the sphere of influence, SOI, of the Moon the spacecraft is considered under the gravitational effect of the Earth only. Inside the SOI of the Moon, the effect of the Earth is neglected. Two solutions have been matched at the edge of the SOI by setting the arrival angle. This method may be used only to get the initial estimates of the initial conditions, since the effects of the other celestial bodies could not be considered in the calculations. In addition to that, it is seen that since the Earth and the Moon are too close to each other, designing such a trajectory with the patched conic approach is only to understand the order of initial guesses.

The equations of motion for n-body system have been solved numerically for Earth, Moon and spacecraft system. The effects of the Sun and the Jupiter have also been included in further calculations. It is seen that the Sun`s effects should be considered while planning such mission trajectory. Although it is the largest planet, the effects of the planet Jupiter do not affect the results remarkably. In all of these three cases, all the orbits of the celestial bodies and the trajectory of the spacecraft are considered to be in the same plane.

The problem could also be considered as a "Restricted three body problem". In this part of the study, the equations of motion of the spacecraft have been solved numerically in the Earth&Moon system. The evaluated results and the n-body numerical solution have been compared and it is seen that both methods provide almost the same resultant altitudes when the spacecraft arrive to the Earth's vicinity after completing the Figure-8 trajectory. Although, the effect of another celestial body, such as the Sun, could not be considered here, this approach may give a quite accurate quantitative understanding of the problem and a limit for the initial conditions.

As a result, in the process of designing a trajectory from the Earth to the Moon, it is seen that the lunar

patched conic approach may be used in order to get the initial estimates for the initial conditions. Then, restricted three body approach can enhance the accuracy. Finally, though this approach requires heavy computational load, the n-body equations should be solved numerically in order to get the final parameters that will provide the desired goals of the mission under the gravitational effect of the Sun which may change the trajectory considerably especially in the second part of the Figure-8 path.

References

[1] National Aeronautics and Space Administration, Manned Spacecraft Center (1970) *Apollo 13 Mission Report*, p. 3-1

ORBIT DETERMINATION USING MARKOV CHAIN MONTE CARLO. A.S. French[1] and J.W. McMahon[2], [1]Ann and H.J. Smead Aerospace Engineering Sciences, 429 UCB, Boulder, CO 80309-0429

Abstract: This paper proposes the use of Markov-chain Monte Carlo techniques to better quantify uncertainty in the orbit determination problem. In both the Extended and Unscented Kalman filters the posterior state distribution is approximated as a Gaussian probability density function. In highly non-linear systems this is often a poor approximation that can lead to inaccurate results [1]. Particle filters attempt to address this issue by propagating a cloud of points through the nonlinear system so that, in theory, the complete posterior distribution can be recovered. Unfortunately, there are many challenges associated with particle filtering, particularly the issues of degeneracy and sample impoverishment [2]. Markov-chain Monte Carlo provides a robust alternative, with recent examples of its applicability showing up in the fields of planetary science [3], astronomy [4] and astrophysics [5]. This paper investigates the effectiveness of using an adaptive Metropolis-Hastings Markov-chain Monte Carlo ensemble sampler for the orbit determination problem as compared to conventional Kalman filtering methods.

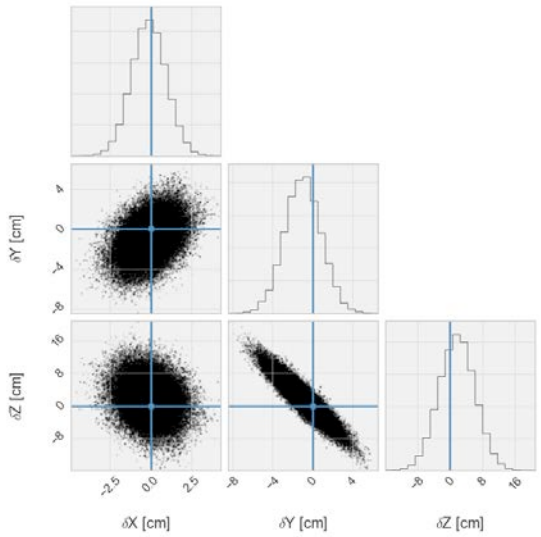

Figure 1. Example estimated posterior distribution as computed by the MCMC algorithm for a LEO satellite. Two dimensional histograms for position are shown in the bottom left corner with histograms along the diagonal. The blue lines indicate the true state.

Extended Abstract: Orbit determination is the process of collecting observations of a spacecraft, typically via up and down-link telemetry, and solving for the set of trajectory and model parameters that best explain the data. No system can be modeled perfectly and observations made of a system invariably contain noise, both of which limit the level of precision that is achievable. Conventionally, algorithms such as the Kalman filter are used to generate the minimum variance and maximum likelihood estimates of the spacecraft trajectory and relevant model parameters given a set of observations. Kalman filters, in particular, rely on the linearization of the dynamical and measurement models. This restriction prevents the estimation of moments higher than the second moment of the probability density function. In practice, this limitation generally does not have a huge impact during operational orbit determination and mission design however assuming that the final estimated covariance is truly Gaussian can be misleading. In the context of scientific analysis, this has the potential to lead to the drawing of inaccurate conclusions.

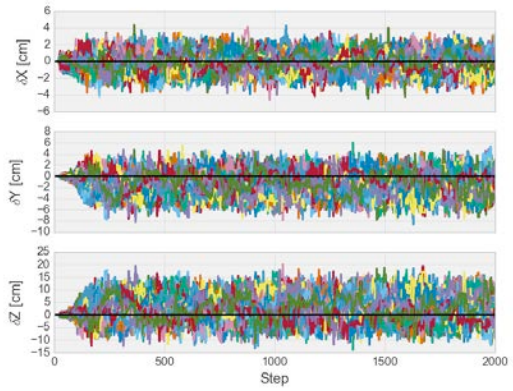

Figure 2. Example MCMC run. The above plot depicts the paths in position space of 64 random walks on the chain, relative to the true trajectory indicated in black. Note the initial burn in period of approximately 200 steps.

The aim of Markov-chain Monte Carlo is to come up with a Markov-chain that has a stationary distribution that is equal to the true posterior probability density function. Once this chain has been found, samples can be drawn directly from the posterior distribution by simulating random walks on the chain [6]. In most MCMC methods, each chain is determined via the well-known Metropolis-Hastings (MH) algorithm. In short, the standard MH algorithm is initialized at some state, which becomes the first state in the chain. Then, a new state is proposed at random using some proposal distribution. The likelihood function for the current state and the new state is computed. If the new state is found to be more likely, then it is accepted and added to the chain. Otherwise, the new state is accepted with

a probability corresponding to their relative likelihoods. The challenge with applying this technique to real systems, in which, for instance, the posterior distribution may be multi-mode or severely skewed, is the selection of an appropriate proposal distribution. It can be shown that, as the number of iterations approaches infinity, the MH process will converge to the stationary distribution regardless of the proposal distribution, so long as it satisfies detailed-balance. However, a poor selection can cause the algorithm to reject the majority of the proposed states, which dramatically effects performance [7].

The past decade or so has seen many advances in MCMC algorithm design, pioneered in large part by the astrophysics community, that address the proposal distribution issue. For systems whose likelihood functions are differentiable, the Hamiltonian Markov chain Monte Carlo provides an extremely efficient way of generating proposals, which allows for quick convergence [8]. Unfortunately, there are many systems whose likelihood functions are not differentiable, as is the case in the orbit determination problem where the likelihood is based on a trajectory that is numerically integrated to each measurement time. Other methods have been proposed that do not rely on differentiation of the likelihood function. Instead, these methods propagate an ensemble of chains and use the relative positioning of each chain to generate a proposal distribution. These methods include differential evolution Markov chains (DEMC) [9], the affine invariant ensemble sampler for Markov chain Monte Carlo (EMCEE) [10], among others. DEMC in particular was designed to efficiently explore densities that are characterized by line-of-sight measurements.

The work presented in this paper will explore the applicability of the above MCMC algorithms for orbit determination. In particular, their use in characterizing the highly non-linear environments around small-bodies will be investigated. Performance will be compared to standard batch least squares and Kalman filtering algorithms to highlight any gains made from using MCMC.

References:

[1] Tapley, B.D., Schutz, B.E., Born, G.H. (2004) Statistical Orbit Determination. *Elsevier Academic Press*. [2] Pardal P. Kuga H. de Moraes R. (2015) *Mathematical Problems in Engineering*, 168045 [3] Linares, Richard & Crassidis, John. (2017). Space-Object Shape Inversion via Adaptive Hamiltonian Markov Chain Monte Carlo. *Journal of Guidance, Control, and Dynamics*, 41, 1-12. [4] Siltala L. Granvik M. (2017) Asteroid Mass Estimation using Markov-chain Monte Carlo. *Icarus*, 297, 149-159 [5] Acquaviva V. Gawiser W. Guaita L. (2011) *The Astrophysical Journal*, 737 [6] Mackay D.J.C. (2003) Introduction to Monte Carlo Methods. [7] Foreman-Mackey, Daniel & Hogg, David & Lang, Dustin & Goodman, Jonathan. (2013). *Publications of the Astronomical Society of the Pacific.* 125. 306-312. [8] Betancourt, Michael. (2017). A Conceptual Introduction to Hamiltonian Monte Carlo. [9] Nelson B. and Ford E. and Payne M. (2014) *The Astrophysical Journal*, 210. [10] Goodman J. and Weare J. (2010) *Communications in Applied Mathematics and Computational Science*, 5, 65-80.

Simulations of a Gas Concentrator for Mass Spectrometry of Tenuous Atmospheres. Savio J. Poovathingal,[1] Chenbiao Xu,[1] Vanessa J. Murray,[1] Thomas E. Schwartzentruber,[2] and Timothy K. Minton.[1] [1]Department of Chemistry and Biochemistry, Montana State University, Bozeman, MT, USA 59717, savio.poovathingal@montana.edu. [2]Department of Aerospace Engineering and Mechanics, University of Minnesota, Minneapolis, MN, USA 55455.

Introduction: Identifying the composition of the gases emitted by a planetary body can provide insight into the geological and chemical composition of the near-surface layer below and contribute to better knowledge of potentially habitable surface conditions [1]. Mass spectrometry (MS) is typically used in such applications with open-source and closed-source inlets [2], which have several drawbacks [3]. A prototype gas concentrator has been proposed to mitigate the drawbacks of the current MS designs, including improved species detection through increased signal-to-noise ratios [3]. Initial efforts using molecular beam experiments with incident O atoms and test particle simulations demonstrated that a concentrator made of highly oriented pyrolytic graphite (HOPG) results in maximum concentration [3]. New molecular-beam experiments are being conducted with a prototype concentrator to measure the concentration ratios of several gases, such as Ar, N_2, CO_2, H_2O, and various organic molecules. Direct simulation Monte Carlo (DSMC) provides a method to understand the intricate processes that result in gas concentration. The eventual goal of these simulations is to provide a toolkit for designing a concentrator for use on a flight instrument and for generating a reference database of corrections that need to be applied for MS-based composition measurements facilitated by a concentrator.

Geometry Setup: While the HOPG surface preferentially scatters the molecules in the forward direction, the rough surface of the detection setup can result in molecules exiting the system through backward scattering before detection. Hence, the entire setup is modeled in DSMC. The final geometry used as the input is shown in Figure 1.

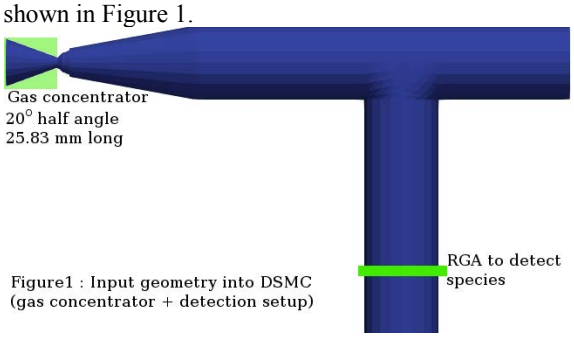

Figure1 : Input geometry into DSMC (gas concentrator + detection setup)

Method: DSMC simulations are performed using the Molecular Gas Dynamics Simulator (MGDS) code developed at the University of Minnesota [4]. Gas-surface interactions on the concentrator are modeled with the Cercignani-Lampis-Lord (CLL) model that captures the super-specular scattering of molecules from HOPG surfaces [3], while the scattering from the detection setup is assumed to be diffuse. The simulations explore the concentration of Ar and N_2 in detail, as these are the focus species of concurrent experiments with the prototype concentrator. The validated simulations will subsequently be extended to analyze other molecules of interest.

Results: The density of Ar (Fig. 2) suggests significant gas build-up at the throat of the gas concentrator which demonstrates the concentration effect of the gas concentrator. The concentration ratio (C) is computed from the ratio of the density at the RGA location (Fig. 1) with and without the concentrator (shown in Fig. 3). The inflow flux and bulk velocity are set to match the experimental conditions. The bulk flow velocity has minimal impact on C. Although the angle of attack lowers C (Figure 3), it is still greater than 1 suggesting that the gas concentrator can be used under a wide variety of flow conditions. Initial results suggest that DSMC simulations can provide valuable information and further refinement of the calculations is being performed to provide a reliable toolkit for the characterization of the gas concentrator.

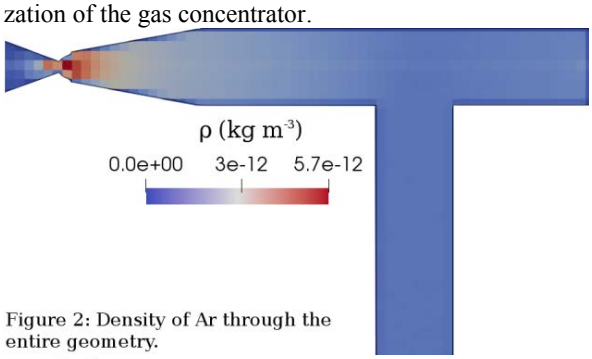

Figure 2: Density of Ar through the entire geometry.

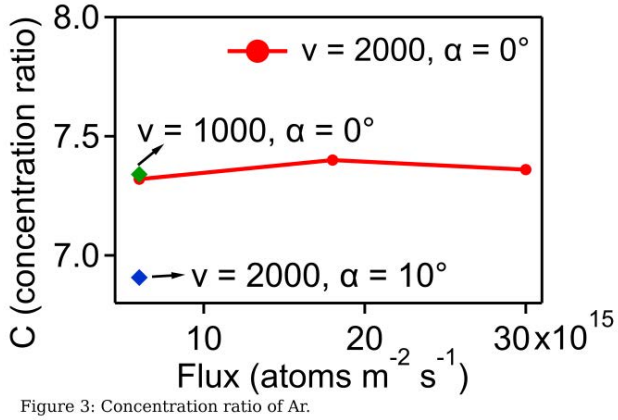

Figure 3: Concentration ratio of Ar.

Acknowledgments: The work was supported by the Jet Propulsion Laboratory (JPL), California Institute of Technology, under contract with NASA. Discussions with Drs. M.D. Pilinski and M. Coleman are greatly appreciated.

References: [1] Mahaffy P. R. et al. (2015), Space Sci. Rev. 195, 49-73. [2] Waite J. H. et al. (2004), Space Sci. Rev. 2004, 114, 113-231. [3] Murray V.J. et al. (2017), *J* Phys Chem C*.,* 121, 7903-7922. [4] Nompelis I. and Schwartzentruber T.E. (2013), AIAA 2013-1204.

In situ Characterization of Ablation Processes by High-speed X-ray Imaging

Isil Sakraker[1] and Hannah Böhrk[1], Daniel Haenschke[2], Angelica Cecilia[2]
[1]Research Scientist in German Aerospace Center (DLR), Stuttgart, Germany.
Isil.Sakraker@dlr.de and Hannah.Boehrk@dlr.de
[2]Research Scientist in Karlsruhe Institute of Technology (KIT), Karlsruhe, Germany

Introduction: One of the major issues of the hypersonic entry of spacecraft is the interaction of the vehicle surface with the planet's atmosphere. The thermal protection systems (TPS) must be sized sufficiently however without excessive safety margins that could lead to inefficient designs. Low density ablative TPS materials provide significantly efficient insulation during high speed flights such as Moon return or Mars entry. DLR has the competence and experience in manufacturing a variety of TPS materials. This study includes a cork based ablative material, DLR Cork.

It is our aim to extend the limits of the current abilities of ground test facilities e.g. arcjets, inductively couples plasma tunnels, etc. with in-situ X-ray tomography of ablation testing. Tomographic techniques can provide time resolved information about char front/pyrolysis layer propagation, pore evolution, fiber shape change, tortuosity, etc. However, it is expensive and difficult, if not impossible, to combine a large scale high enthalpy facility with X-ray tomography. Therefore, two portable high enthalpy facilities have been designed in DLR Stuttgart; a Radiation-only and an Arcjet furnace. Such in-situ experimental data will significantly improve the thermo-physical model accuracies where commonly, the pre- and post-test virgin and charred states are interpolated.

Fig. 1: Radiation facility [1].

Previous Work: A preliminary study has been conducted with the radiation furnace (Fig. 1) by exposing a DLR Cork sample to radiative heat flux, while being monitored by an industrial computed tomograph [1] and at a synchrotron radiation facility [2]. The sample was heated by three halogen lamps focusing on the center of the circular surface.

The latest synchrotron experiments consisted of 2D and 3D imaging, where the results are briefly shown in Fig. 2 and Fig. 3. The swelling of cork together with the char front propagation and cracking are monitored. Additionally, Fig. 3 also shows two cork granules inside the sample, of which the size, shape and position are tracked over time. The surface topology change in time is also observed.

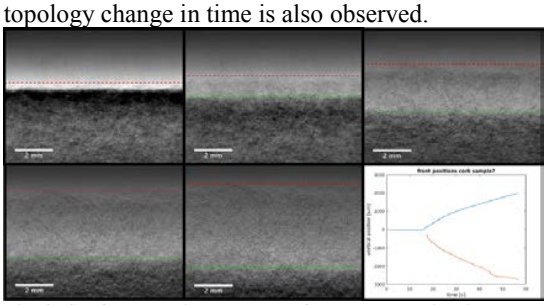

Fig. 2: Surface swelling and char front propagation in a cork sample quantitatively characterized by white beam in situ radiography with 70fps.

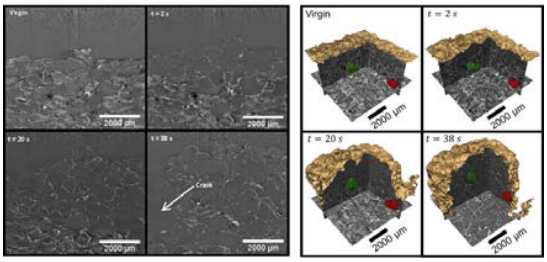

Fig. 3: 3D microstructure evolution of a cork sample imaged by fast in situ tomography, enabling e.g. the tracking of individual cork grains during the complete process.

New Synchrotron Experiments: The lessons learned from the first synchrotron campaign lead to a new furnace design with improved x-ray windows made of 80 µm thick Kapton and an integrated precise high-speed rotary stage. This will allow us to perform X-ray tomography measurements with both several full 3D scans per second and few micrometer spatial resolution. The new radiation and arcjet furnaces for x-ray imaging are shown in Fig. 4 and Fig. 5. The experimental campaign takes place in April 2018 and the results will be presented at the workshop in June 2018.

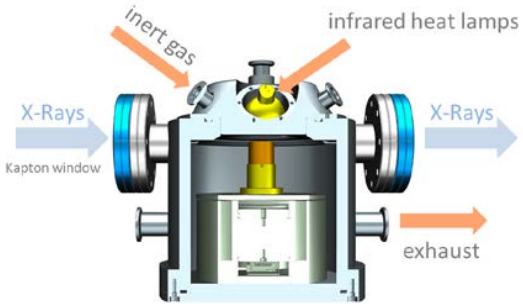

Fig. 4: New Radiation furnace.

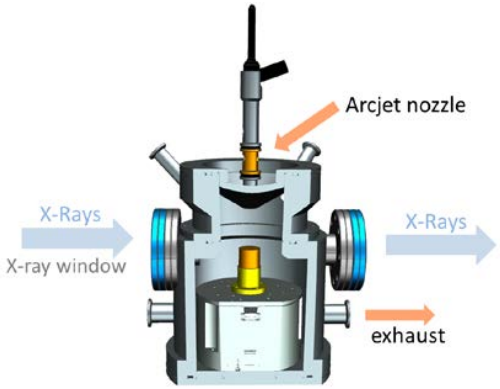

Fig. 5: Arcjet furnace with Kapton windows and integrated high speed rotary stage.

References:

[1] Hannah Böhrk and Rauf Jemmali, "Time resolved quantitative imaging of charring in materials at temperatures above 1000 K," *Review of Scientific Instruments,* vol. 87, no. 7, p. 073701, 2016.

[2] I. Sakraker, A. Joshi, H. Boehrk, A. Cecilia, D. Haenschke and T. Santos Rolo, "In-Situ X-Ray Tomography of Ablation in a Portable Arcjet and a Radiation Facility," in *14th International Planetary Probe Workshop*, The Hague, 2017.

[3] H. Böhrk, "Kinetic Parameters and Thermal Properties of a Cork-Based Material," in *20th AIAA International Space Planes and Hypersonic Systems and Technologies Conference*, 2015.

[4] H. Böhrk, "Thermal Response of an Ablator: Model and Time Resolved Imaging," in *21st AIAA International Space Planes and Hypersonic Systems and Technologies Conference*, China, 2017.

EDL MODELING CHALLENGES FOR PAST AND PRESENT PLANETARY MISSIONS. M. J. Wright,[1] M. D. Barnhardt[1] and M. F. Hughes,[3] [1]NASA Ames Research Center, [2]NASA Langley Research Center.

Introduction: Entry, Descent and Landing Modeling & Simulation encompasses a multitude of disciplines, ranging from flight mechanics to define overall system performance and determine landing footprint, to computational fluid dynamics to determine the aerodynamics and aerothermodynamics, to material response analysis used to select and size the thermal protection system. M&S is on the critical path for all EDL missions because in general it is impossible to fully test and validate the performance of an EDL system in a flight like environment. For many aspects of the EDL sequence, no ground test can simultaneously reproduce all aspects of the flight environment. For example, arc jets are the primary facility used to verify TPS performance. However, while an arc jet can generally match peak heat flux and pressure encountered during an entry (although usually not simultaneously), many other critical parameters, including enthalpy, boundary layer thickness, shear stress, and freestream composition, can only be approximated. Therefore, a good understanding of the underlying physics is required to trace ground test results to flight; extrapolation without a good understanding of the relevant physics can have catastrophic results.

This talk will discuss the importance of high-fidelity physics based modeling and simulation for EDL missions with a focus in two areas of particular interest: aerosciences and material response. Examples drawn from Science Mission Directorate missions past, present and future will be used to highlight areas where accurate simulation capabilities were important for mission success, or conversely where a lack of capability led to costly design changes and/or mission operations with unrealized (and unmitigated) risk.

One clear example of this phenomenon is aeroheating due to shock layer radiation during Mars entry. Conventional wisdom had long held that at low entry velocities (below about 7 km/s), the radiative heating on a Mars entry heatshield would be minimal. For example, pre-flight estimates of the radiative heating for MSL predicted less than 0.1 W/cm2 – a completely negligible amount as compared to the predicted 100 W/cm2 of convective heating. However, those estimates failed to include radiation from the CO2 molecule. At higher velocities where radiation is typically considered to be important, CO2 is largely dissociated and therefore not a significant radiation source. However, at lower speeds the shock is energetic enough to excite, but not dissociate, the molecules. This so-called vibrational transition radiation was not modeled in NASA radiation codes until recently. We now believe that shock layer radiation, predominantly from CO2, contributed more than 25% of the total heat load on the heatshield during the MSL entry, a prediction validated with ground test data and at least partially verified by the MEDLI flight experiment. Although the MSL heatshield carried sufficient margin to protect against this additional heating, the mere fact that 25% of the total heating could be due to a phenomenon that until recently was not even considered in the aerothermal analyses was a worrisome conclusion.

Finally, the talk will briefly outline some current investments in the NASA Entry Systems Modeling Project that are targeting key remaining uncertainties in these disciplines.

EXOMARS 2016: A PRELIMINARY POST-FLIGHT STUDY OF THE ENTRY MODULE HEAT SHIELD INTERACTIONS WITH THE MARTIAN ATMOSPHERE.

G. Pinaud[1], J. Bertrand[1], Y. Mignot[1], J. Soler[2], P. Tran[2], H. Ritter[3], O. Bayle[3], S. Portigliotti[4]

[1]Ariane Group SAS, *gregory.pinaud@ariane.group*, Issac, France, 33165
[2]Ariane Group SAS, Les Mureaux, France, 78120
[3]European Space Agency, ESA, Technical Center ESTEC, Noordwijk, The Netherlands, 2200
[4]Thales Alenia Space Italia, Torino, Italy, 10146

Introduction: The EXOMARS 2016 mission was the first (of two) join European-Russian mission aiming at searching the evidence of past extra-terrestrial life on Mars. After a successful launch of the Russian Proton rocket on the 14th of March, 2016, from Baikonur, and several liberation maneuvers while orbiting the Earth, the Breeze M upper stage carrying the Trace Gas Orbiter (TGO) and the Schiaparelli Entry Descent and Landing module started a long journey to Mars. Seven months later, on the 16th of October 2016, the space probe was released on a direct entry path to the red Planet. After a nominal entry and an expected aerodynamic braking, saturation of the GNC algorithm during the highly dynamic deployment phase of the parachute, leaded to a final free fall of the module and a destructive impact on ground.

However, telemetry of the entry phase was recorded and enabled a post-flight analysis of the heat shield behavior. This paper provides an initial assessment of the thermal instrumentation data that is comprised of in-depth temperatures in the TPS made of Norcoat Liege (a phenolic impregnated cork based ablator). In addition to an ablation scheme sensitivity analysis and material thermal diffusivity correction, a preliminary inverse analysis is performed where the time-dependent surface heating is estimated from flight-measured subsurface temperature data.

Instrumentation and Aerothermodynamic database rebuilding:

The capsule aeroshell was a 2.4 m diameter spherically-blunted 70-degree half-angle cone with a truncated conic after body (Fig. 1). Schiaparelli's front and back heatshield was made of an ablative material called Norcoat Liege®. This material is made of cork granules impregnated with phenolic.

The thermal instrumentation consists in several thermoplugs located in 3 different meridians separated by 120 deg .

Thermal plugs are strategically placed from the stagnation region up to the shoulder to cover as much as possible all the possible effects of the angle of attack, laminar to turbulent transition and wind relative velocity azimuth on the in-depth thermal response.

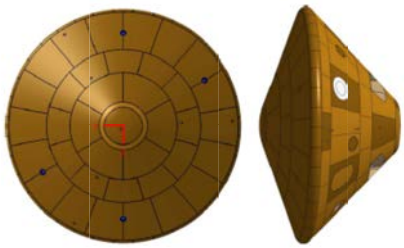

***Figure 1**: Front and side view of the 70 angle Schiaparelli entry probe.*

Figure 2 presents an overview of the raw in depth thermocouples measurements as received from in board telemetry acquisition system.

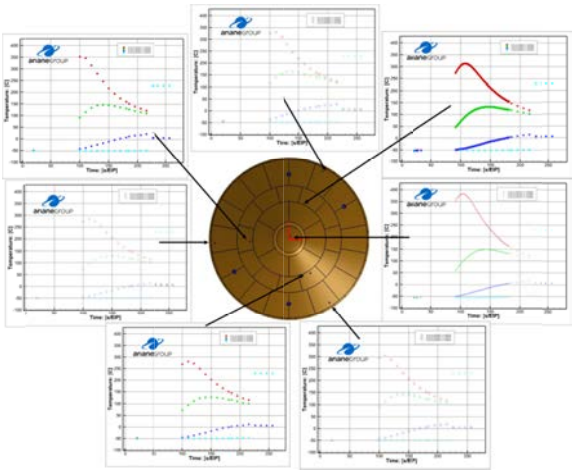

***Figure 2**: In depth raw thermocouples readings on Schiaparelli front heat shield*

After tuning the thermal and pyrolysis material model with direct thermocouple driving approach, an inverse algorithm involving a 1D finite element model of the plugs is run to retrieve the apparent net surface aero-

thermodynamic heat flux both on the front and back shield.
The preflight predictions of the aerothermodynamic loads based on engineering tools and the best estimate are then come up against the inverse total heat flux to increase model accuracy and refine the margin policy.
In the future, this data could also be compared with the imbedded DLR's radiometer instrumentation (COMARS+) in order to separate convective from radiative contribution.

References:

[1] EXOMARS 2016 Schiaparelli EDLS design, development and post-launch status, O. Bayle, T. Blancquaert, L. Lorenzoni, T. Walloschek, IPPW13, Laurel, Marylan, USA, 13 -17 June 2016

[2] EXOMARS 2016 Mission -Schiaparelli's Heatshield, Y. Mignot, A. Pisseloup, R. Velasco, Y. Camacho. Laurel, Marylan, USA, 13 -17 June 2016

[3] EXOMARS 2016 - Schiaparelli Anomaly Inquiry, T. Tolker-Nielsen, ESA IG, DG-I/2017/546/TTN, Issue 1, Rev 0, 18/05/2017

[4] EXOMARS 2016: Post flight mission analysis of Schiaparelli coasting, entry, descent and landign, D Bonettidavide, G. De Zaiacomo, G. Arnaoshow, O. Bayle, IPPW14, La Haye, NL, June 2017

[5] Ongoing European Developments on Entry Heatshields and TPS Material, H. Ritter , O. Bayle, Y. Mignot , P. Portela, J-M. Bouilly, R. Sharda, IPPW-8, Portsmouth, USA, 6-10 June 2011

DSENDS SIMULATION OF MARS 2020 ENTRY, DESCENT, AND LANDING. P. D. Burkhart[1], S. Aaron[1] and C. O'Farrell [1], [1]NASA Jet Propulsion Laboratory, California Institute of Technology (4800 Oak Grove Drive, Pasadena CA 91109).

Abstract: The Mars 2020 project will land a large rover on Mars in February of 2021 similar to Curiosity, which landed in August 2012. Mars 2020 has an entry, descent, and landing (EDL) architecture that is mostly inherited from Curiosity [1].

As was the case for Curiosity and is the case for all Mars landers, analysis of the EDL design must be done via simulation, as an end-to-end test of EDL cannot be performed on Earth. With the reliance on simulation analysis to show the EDL system works, two independent simulation tools will be deployed for Mars 2020. One of these tools is Dynamics Simulator for Entry, Descent and Surface landing (DSENDS), which is a high-fidelity simulation tool from JPLs Dynamics and Real-Time Simulation Laboratory for the development, test, and operations of aero-flight vehicles. DSENDS inherent capability is augmented for Mars 2020 with project-specific models of atmosphere, aerodynamics, sensors and thrusters, along with GN&C flight software, to enable high-fidelity trajectory simulation. In addition, a modified setup is used to choose the entry conditions that will ensure a safe landing at the desired target. In this setup, DSENDS is configured to integrate the EDL trajectory without the FSW and device models in the loop, along with modified aerodynamics and parachute modeling, to compute an EDL reference trajectory. These configurations support the two primary tasks for the DSENDS flight dynamics team, namely to support planetary approach targeting and to perform independent EDL system verification and validation (V&V).

While much of this capability is inherited from Mars Science Laboratory [2], significant updates in DSENDS capability have been made and new functionality is needed for Mars 2020. This presentation will describe the the simulation and simulation tasks, provide simulation component checkout details, show an end-to-end checkout summary, and provide details of future work.

CL#18-1296.

References:

[1] Allen Chen et al. (2015) *2015 Update: Mars 2020 Entry,Descent, and Landing System Overview,* IPPW12 Presentation #2104

[2] P. Daniel Burkhart et al. (2013) *Mars Science Laboratort Entry Descent and Landing Simulation Using DSENDS,* AAS 13-421

Blackout Analysis of Martian Reentry Missions. S. Ramjatan[1], A. Lani[1], S. Boccelli[1], B. Hoeve[1,2], O. Karatekin[2], T. E. Magin[1], and J. Thoemel[3]
[1]von Kármán Institute for Fluid Dynamics, 1640 Rhode-Saint-Genese, Belgium
[2]Royal Observatory of Belgium, Ringlaan 3, Brussels/Uccle 1180, Belgium
[3]GomSpace Sarl – 9 Avenue des Hauts-Fourneaux, 4362 Esch-sur-Alzette, Luxembourg

Introduction: With future space missions aimed towards Mars including NASA's Mars 2020 and ESA's ExoMars 2020, there is a motivation to improve the understanding of the physics regarding the communication blackout phenomena. When the electron number density traversing the signal path gets sufficiently high exceeding the critical value for a particular frequency, communication blackout can occur as shown in Fig. 1 [1]. Transmission becomes possible as the electron number density is reduced as the spacecraft decelerates itself to lower velocities. Furthermore, as the compressed gas in the shock layer flows toward the rear of the vehicle, the plasma flow is rapidly cooled and rarefied by expansion which can allow for the propagation of electromagnetic waves [2]. As a result, missions such as MSL, Mars Pathfinder, and ExoMars Schiaparelli has an antenna located at the aft of the vehicle. This work investigates the radio blackout period for a Martian reentry with a focus on the ExoMars Schiaparelli mission.

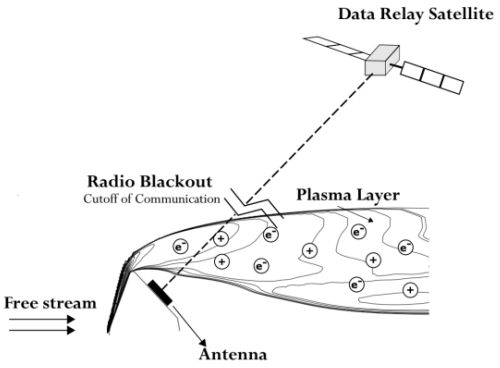

Figure 1: Radio-frequency blackout for axis-symmetric flow over reentry capsule.

Novelty of Research: Regarding blackout for Martian reentries, a limited amount of work has been conducted where the critical electron density along the Line-of-Sight (LOS) to the receiving spacecraft has been used in determining blackout conditions [1]. However, it might be possible that radio waves still reach the receiving spacecraft through refraction and reflection. As a result, this work applies a raytracing method for predicting the blackout of ESA's ExoMars 2016 mission, which experienced 60 seconds of blackout. In addition, examining radio blackout using CFD can be computationally expensive due to advanced thermo-chemical modeling that require the simulation of numerous ionized species and internal temperatures. Another novelty of this work is to apply a computationally inexpensive Lagrangian approach to extract the electron density field from a baseline CFD solution that was solved with 6 neutral species. A more elaborate thermo-chemical model consisting of 14 species is applied to recompute the electron density along streamlines. Thus, a computationally inexpensive way to retrieve the electron density field for blackout analysis is developed.

Approach: The methodology and approach used in examining the blackout period of the ExoMars Schiaparelli spacecraft include performing 2D axis-symmetric simulations using the VKI's aerothermodynamic code COOLFLuiD. Subsequently, the electron density field is extracted using a Lagrangian approach and then given to a raytracing algorithm to examine the propagation of electromagnetic waves where a conclusion on radio communication is made.

Results & Conclusions: This work applies an improved physics modeling approach in examining the blackout period by applying a raytracing method to examine how the radio frequency waves are bent by electron density gradients in the flow. Results show that the LOS method will be accurate around the maximum blackout point in the trajectory for the spacecraft but could be inaccurate in calculating the onset and end of the blackout period. Significantly, a computationally inexpensive Lagrangrian approach is able to accurately recompute ionization levels similar to the flight data from using neutral CFD simulations. Results are in good agreement with the ExoMars flight data suggesting that the blackout modeling approach presented in this work could potentially be used to reduce the computational effort of the blackout analysis process. Most importantly, the results acquired in this work provides insight into designing the EDL phase for upcoming Martian missions and results in a greater understanding of Martian thermo-chemical modelling.

References:

[1] D. Morabito, "The Spacecraft Communications Blackout Problem Encountered During Passage or Entry of Planetary Atmospheres," Jet Propulsion Laboratory, IPN Progress Report 42-150, Pasadena, 2002.

[2] Y. Takahashi, R. Nakasato and N. Oshima, "Analysis of Radio Frequency Blackout for a Blunt-Body Capsule in Atmospheric Reentry Missions," Aerospace , 2016.

DESIGN AND CHARACTERISTICS OF THE SUBORBITAL EXPANSION TUBE HEK-X FOR AFTERBODY HEATING OF SAMPLE RETURN CAPSULE. K. Shimamura[1] , K. Yamada[2], and H. Tanno[2], [1]University of Tsukuba (1-1-1 Tennnodai, Tsukuba, Japan 305-8573 and shimamura@kz.tsukuba.ac.jp), [2]JAXA.

Understanding of the aerothermal condition on the planetary entry vehicles is important for the future missions. Especially, the quantitative investigation of the afterbody heating affects the gross weight of thermal protection system. CFD simulations and real flight data suggested that the afterbody heat transfer is 1-2 % of the stagnation heat transfer. To study the re-entry condition of the post-HAYABUSA capsule, a new free-pisotn driven expansion tube HEK-X has been operated since 2015 The total length of HEK-X is 35 m which is reconstructed from the free-piston shock tunnel HEK. The specifications of HEK-X are shown in Fig. 1. In terms of the binary scaling law, the HEK-X is possible to cover the Mars re-entry mission (over 50 MJ/kg stagnation enthalpy). However, only a few study shows the test time evaluation of expansion tube at suborbital speed condition because the test time and the noise signal are respectively decreased and increased with the flow velocity.

In the present paper, the highspeed Schileren visualization was conducted to investigate the test time of HEK-X on the suborbital condition. Because the flow temperature is discontinuously changed at the contact surface, the 15 degree wedge probe was used to observe the oblique shock wave. The non-contact temperature measurement using the high speed camera is avalibale because the shock wave angle was increased with the temperature. The end of test time is found from the 8 static pressure probe history on the low pressure tube (expansion tube). According to the theoretical maximum test time condition, the pressure ratio of expansion tube/shock tube was 0.02. The initial pressure of the compression tube, shock tube, and expansion tube were 94.2 kPa, 10 kPa, and 200 Pa, respectively. The velocity of shock wave was 7.2 km/s. The 1 W 532 nm DPSS laser was used as a light sourcce. The Schlieren visullization is obtained by a high speed ICCD camera (ULTRA CAM, NAC Inc.) with 1.5 MHz maximum FPS and 120 frames. Each picture have a 320 by 400 picel color image. As shown in Figure 2, the shock wave and the contact surface were observed at No.2-3 and No.27-33, respectively. As compared with the pitot pressure, the contact surface is observed at 50-60 us in the Mach number curve. The static pressure history suggested that the end of test time was 98 us. Consequentrly, the sequence of Scheren images, the pitot pressure and the static pressure showed that the test time was 40 us at 7.2 km/s shockwave velocity.

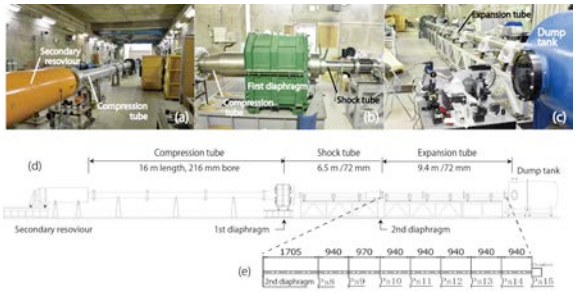

Fig.1 Schematics of the suborbital expansion tube HEK-X

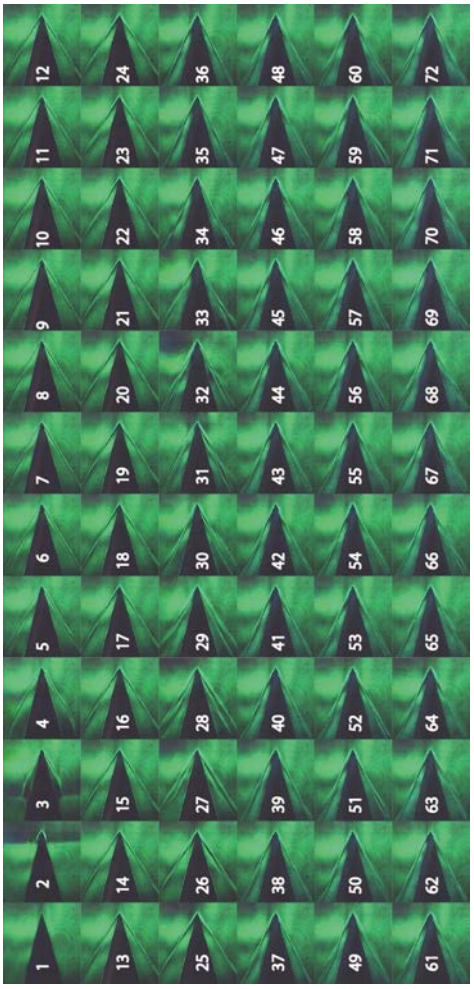

Fig.2 Sequence of Schlieren images for the 15 degree wedge probe in the range from 0 us to 140 us using a 0.5 MHz FPS camera with 300 ns exposure time. Shock wave is observed at No.2 and 3. Contact surface is observed in the range from No.27 to 33.

OVERVIEW OF GLOBAL REFERENCE ATMOSPHERIC MODEL (GRAM) UPGRADES. H. L. Justh[1], A. M. Dwyer Cianciolo[2], K. L. Burns[3], J. Hoffman[4], R. W. Powell[5], and P. W. White[6]. [1]NASA, Marshall Space Flight Center, Mail Code EV44, Marshall Space Flight Center, AL, 35812, hilary.l.justh@nasa.gov, [2]NASA, Langley Research Center, Mail Stop 489, Hampton, VA 23681, alicia.m.dwyercianciolo@nasa.gov, [3]Jacobs Space Exploration Group, 1500 Perimeter Pkwy., Suite 400, Huntsville, AL 35806, kerry.l.burns@nasa.gov, [4]Analytical Mechanics Associates, 21 Enterprise Pkwy., Suite 300, Hampton, VA 23666, james.hoffman-1@nasa.gov, [5]Analytical Mechanics Associates, 21 Enterprise Pkwy., Suite 300, Hampton, VA 23666, richard.w.powell@nasa.gov and [6]NASA, Marshall Space Flight Center, Mail Code EV44, Marshall Space Flight Center, AL, 35812, patrick.w.white@nasa.gov.

Introduction: The inability to test planetary spacecraft in the flight environment prior to a mission requires engineers to rely on ground-based testing and models of the vehicle and expected environments. One of the most widely used engineering models of the atmosphere is the Global Reference Atmospheric Model (GRAM) developed and maintained by the NASA Marshall Space Flight Center (MSFC). Over the past decade GRAM upgrades and maintenance have depended on inconsistent and waning project-specific support. The NASA Science Mission Directorate (SMD) has agreed to provide funding support in Fiscal Year 2018 and 2019 to upgrade the GRAMs. This presentation will provide an overview of the current status of the GRAMs as well as the objectives, tasks, and milestones related to the GRAM upgrades funded by the NASA SMD.

Global Reference Atmospheric Model (GRAM): The GRAMs are engineering-level atmospheric models applicable for engineering design analyses, mission planning, and operational decision making. They provide mean values and variability for any point in the atmosphere as well as seasonal, geographic, and altitude variations. GRAM outputs include winds, thermodynamics, chemical composition, and radiative fluxes. They have been widely used by the engineering community because of their ability to create realistic dispersions; GRAMs can be integrated into high fidelity flight dynamic simulations of launch, entry, descent and landing (EDL), aerobraking and aerocapture. MSFC has been developing and updating GRAMs since 1974 with GRAMs currently available for Earth, Mars, Venus, Neptune, and Titan.

GRAM Upgrade Objectives, Tasks, and Milestones:

Objectives. The GRAM upgrade effort will focus on three primary objectives: upgrade atmosphere models within the GRAMs, modernize the GRAM code, and socialize plans and status to improve communication between GRAM users, modelers and GRAM developers.

Model Upgrade Task. The priority of this effort is to update the atmosphere models in the existing GRAMs and to establish a foundation for developing GRAMs for additional destinations. This will include determining which models have upgrades currently available and implementing the model data into the GRAMs. Planetary mission atmospheric data, when available and appropriate, will also be used as the basis for verification and validation of the GRAMs. Adding the highest resolution topography available/reasonable to each of the GRAMs will also be addressed by this effort.

Code Upgrade Task. Another key element of this effort is modernizing the GRAM code. This task involves development of a new framework that transitions the original Fortran code to C++. This effort will use the best practices of the Agile software development approach take advantage of the object-oriented capabilities of C++.

Model Socialization Task. In addition to the model and code upgrades, socializing the status of the upgrades and advocating and promoting its continued use in proposals and projects will be conducted by the GRAM upgrade team members. This includes attending advisory group meetings, workshops and conferences.

Milestones. Project milestones for fiscal year 2018/2019 and beyond have been developed and include: surveying users to prioritize investments, meeting with key modeling groups, identifying, obtaining and implementing atmosphere model upgrades for GRAMs as well as observational and mission data sets for GRAM comparisons, upgrading the GRAM code framework, and releasing updated and new GRAMs that will include programming and user guides.

Conclusions: The GRAMs are a critical tool set that influence mission selection and decisions. The funding provided by the NASA SMD is vital to address current limitations and accomplish GRAM developmental goals.

Acknowledgments: The authors gratefully acknowledge support from the NASA SMD.

MARS 2020 ATMOSPHERIC MODELING FOR FLIGHT MECHANICS SIMULATION. S. Dutta[1], D. Way[1], C. Zumwalt[1], and G. Villar[2]. [1]NASA Langley Research Center, Hampton, VA 23681 (soumyo.dutta@nasa.gov), [2]Jet Propulsion Laboratory, Pasadena, CA 91109.

Abstract: Mars 2020 is the next planned U.S. rover mission to land on Mars based on the design of the successful 2012 Mars Science Laboratory (MSL) mission [1]. The Mars 2020 spacecraft will launch in July 2020 and will land on Mars in February 2021. Mars 2020 retains most of the entry, descent, and landing (EDL) sequences of MSL, including the closed-loop entry guidance scheme based on the Apollo guidance algorithm and the Skycrane landing system [2], while replacing a velocity trigger with a range trigger for the parachute deployment sequence and also incorporating Terrain Relative Navigation system on-board the spacecraft that will allow the vehicle to land at a more hazardous landing site than was possible for MSL. These and other changes are tested at a systems level through many modeling and simulation environments, including flight mechanics simulations [3-4].

A key component for the flight mechanics simulation is the choice of the atmospheric model that is used to model aerodynamic effects on the spacecraft. During the early conceptual phase of projects, global reference atmospheric models (GRAM), such as those provided by NASA Marshall Space Flight Center, are useful [5]. However, when flight simulations are run for specific landing sites, a higher fidelity atmospheric model may be required. In some cases engineering wind models, created by assuming fixed horizontal and vertical wind speeds, are suitable to gauge EDL flight performance [6]. In other cases, historic data from Mars orbiters have been used to generate profiles of atmospheric properties in flight mechanics simulations. However, since MSL was targeting a smaller landing ellipse than any previous mission with closed-loop entry guidance, a physics-based model using computational simulations of Mars weather for the landing time was used to assess the flight system in simulations. These physics-based models were mesoscale atmospheric models developed and run by Oregon State University and Southwest Research Institute. Mars 2020 retains the use of these mesoscale atmospheric profiles. This paper will discuss the methodology of how these raw mesoscale model data can be used for statistical Monte Carlo analysis. Although the current incorporation method was used for MSL and is going to be used for Mars 2020, there are certain idiosyncrasies associated with the method. The paper will discuss these issues and provide some solutions that can be used in flight mechanics simulations for future flights.

References:

[1] Mustard, J., et al. (2013) "Report of the Mars 2020 Science Definition Team," Tech. rep*., Mars Exploration Program Analysis Group (MEPAG)*. [2] Steltzner, A. (2013) *"Mars Science Laboratory Entry, Descent, and Landing System Overview", AAS 13-236*. [3] Way, D. W., Davis, J. L, and Shidner, J. D. (2013) *"Assessment of the Mars Science Laboratory Entry, Descent, and Landing Simulation", AAS 13-420*. [4] Dutta, S., and Way, D.W. (2017) "Comparison of the Effects of Velocity and Range Triggers on Trajectory Dispersions for the Mars 2020 Mission", *AIAA 2017-0245*. [5] Justh, H., Justus, C.G., and Ramey, H.S. (2011) "The Next Generation of Mars-GRAM and its Role in the Autonomous Aerobraking Development Plan", *AAS 11-478*. [6] Tamparri, L. et. al (2008) "Expected atmospheric environment for the Phoenix landing season and location," *J. Geophysical Research, 113, pp 1-18*.

PROGRESS ON FREE-FLIGHT CFD SIMULATION FOR BLUNT BODIES IN THE SUPERSONIC REGIME.

Joseph M. Brock[1] and Eric C. Stern[2], [1]Analytical Mechanics Associates, Inc., [2]NASA Ames Research Center, Moffett Field, CA, USA (joseph.m.brock@nasa.gov)

Abstract: Simulations of the free-flight behavior of entry bodies using high-fidelity CFD has been actively developed under the Entry Systems Modeling (ESM) project [1]. Comparisons against ballistic range data for the Supersonic Inflatable Aerodynamic Decelerator (SIAD) were first shown at IPPW13 [2]. Progress on the continued development and application of the Free-Flight CFD (FFCFD) solver for the supersonic regime was presented by Stern et. al. at IPPW14[3]. This presentation will show recent developments in maturing the FFCFD ability down into the lower supersonic regime.

First, simulations of the Adaptable Deployable and Entry Placement Technology (ADEPT) ballistic range campaign [4] have been performed. The methodologies and best practices developed for the earlier simulations of the SIAD geometry were applied to the ADEPT experiments. A visualization of the highly unsteady and separated flow can be seen in Figure 1. This set of experiments provides data for an open-backed aeroshell at Mach numbers; 2.36, 1.38, 1.23, and 1.21. The comparison between CFD predicted pitch and yaw angles with the experimental reconstuction is shown in Figure 2. The difference between free-flight CFD simulated total angle-of-attack is within 5% for 2.36 case, and within 15% for the lower Mach number cases (1.38, 1.23, and 1.21).

Additionally, preliminary results from FFCFD simulations of selected cases from an Orion MPCV ballistic range experiment[5] will be presented. These simulations will allow us to assess the performance of the FFCFD capability in the challenging transonic regime, for more traditional aeroshell shapes. Finally, the outlook for future development and maturation of the technology will be discussed.

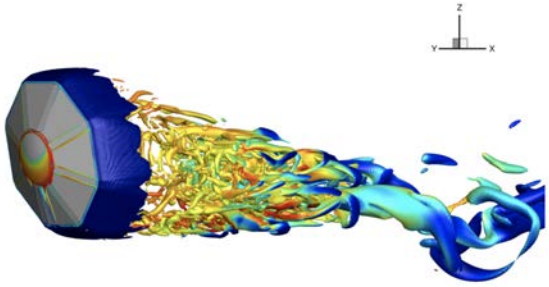

Figure 1: Iso-surfaces of the Q-criterion showing the complex wake flow from a Free-Flight CFD simulation behind the ADEPT ballistic range model.

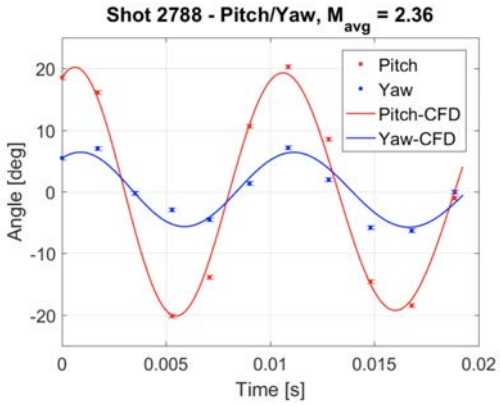

Figure 2: Pitch and yaw predictions from Free-Flight CFD for the ADEPT geometry compared to ballistic range data.

References: **[1]** Eric C. Stern, Vladimyr M. Gidzak, and Graham V Candler. "Estimation of Dynamic Stability Coefficients for Aerodynamic Decelerators Using CFD". In: *30th AIAA Applied Aerodynamics Conference*. New Orleans, June 2012, pp. 1–14. **[2]** Joseph M Brock and Eric C. Stern. "Dynamic CFD Simulations of the Supersonic Inflatable Aerodynamic Decelerator (SIAD-R) Ballistic Range Tests". In: *International Planetary Probe Workshop*. Laurel, Maryland, June 2016. **[3]** Eric C. Stern et al. "Progress on Free-Flight CFD Simulation for Entry Capsules in the Supersonic Regime ". In: *International Planetary Probe Workshop*. The Hague, June 2017. **[4]** Jakob Hergert et al. "Free-Flight Trajectory Simulation of the ADEPT Sounding Rocket Test Using US3D". In: *35th AIAA Applied Aerodynamics Conference*. Denver, Colorado: American Institute of Aeronautics and Astronautics, June 2017, pp. 207–21. **[5]** Jeffrey D Brown et al. "Transonic Aerodynamics of a Lifting Orion Crew Capsule from Ballistic Range Data". In: *Journal of Spacecraft and Rockets* 47.1 (Jan. 2010), pp. 36–47.

DYNAMIC PROPAGATION OF DISCRETE-EVENT DRAG MODULATION FOR VENUS AEROCAPTURE. M. S. Werner[1], E. Roelke[1] and R. D. Braun[1].
[1]University of Colorado Boulder, Department of Aerospace Engineering, 429 UCB, Boulder, CO 80309

Introduction: Aerocapture is an aeroassist technology in which a spacecraft uses drag from a single atmospheric pass to capture into a target orbit. For certain missions, aerocapture can greatly increase the payload mass delivered to orbit compared to traditional propulsive orbit insertion methods [1].

An elegant way to reduce the complexity of aeroassist missions is to employ a drag modulation control scheme. Discrete-event drag modulation methods utilize discrete changes in the ballistic coefficient of a vehicle to alter the vehicle's trajectory. Drag modulation control can reduce the need for center-of-gravity offsets and a propulsive reaction control scheme when compared to traditional bank-to-steer lift control schemes. Drag modulation is broadly applicable to planetary entry [2], and has been coupled with aerocapture in prior studies [3] [4].

One of the simplest means of accomplishing drag modulation is through the jettison of an attached drag device, such as a trailing ballute or a rigid drag skirt. This type of single-event-jettison system has been shown to provide ample control authority for aerocapture missions [5]. Although the simplicity of such a system is promising, one key area of risk is the dynamic evolution of the separation event. While dynamic analyses of events like fairing separation [6] and asteroid break-up [7] are readily available in the literature, there have been comparatively few studies on hypersonic separation events. Proper understanding of the dynamics of single-event-jettison systems will help characterize the risk associated with the technique and may make drag modulation an even more attractive control option.

This investigation is focused on modeling the dynamics and aerodynamic interactions associated with single-event-jettison drag modulation for aerocapture. To ensure the relevance of the results obtained by this study, a Venus aerocapture mission concept is analyzed. This mission concept utilizes the discrete jettison of an attached rigid drag skirt to provide the necessary control authority for aerocapture at Venus, and is currently under development by a multi-organizational team from the Jet Propulsion Laboratory, Ames Research Center, and the University of Colorado Boulder.

In this study, the Cart3D computational fluid dynamics (CFD) software, developed by NASA Ames Research Center, is used to prepare aerodynamic force and moment time histories immediately surrounding the nominal drag modulation jettison event. This information is used to dynamically propagate the spacecraft and the drag skirt, in order to assess the dynamic stability of the spacecraft and the risk of drag skirt re-contact (both near- and far-field). These analyses are then repeated for a range of different separation points along multiple trajectories within the mission's entry corridor, to probabilistically constrain re-contact risk.

This study represents an important step towards understanding the dynamics associated with hypersonic separation events. The probabilistic re-contact risk assessment will be a key factor in future development of the single-event-jettison aerocapture mission concept to Venus, and can later be validated through ballistic range testing of scale models of the spacecraft and drag skirt. These results may also be scalable to similar hypersonic drag modulation systems at other planets.

References:

[1] Hall, J. L., Noca, M. A., and Bailey, R. W., "Cost-Benefit Analysis of the Aerocapture Mission Set," *Journal of Spacecraft and Rockets*, Vol. 42, No. 2, 2005, pp. 309-320.

[2] Putnam, Z. R., and Braun, R. D., "Analytical Assessment of Drag Modulation Trajectory Control for Planetary Entry," *Advances in the Astronautical Sciences*, Vol. 156, 2016, pp. 4309-4324.

[3] Putnam, Z. R., and Braun, R. D., "Drag Modulation Flight Control System Options for Planetary Aerocapture," *Journal of Spacecraft and Rockets*, Vol. 51, No. 1, 2014, pp. 139-150.

[4] Werner, M. S., et al., "Development of an Earth Smallsat Flight Test to Demonstrate Viability of Mars Aerocapture," *55th AIAA Aerospace Sciences Meeting*, Grapevine, TX, January 2017.

[5] Werner, M. S., and Braun, R. D., "Characterization of Guidance Algorithm Performance for Drag Modulation-Based Aerocapture," AAS 17-032, *2017 AAS Guidance, Navigation and Control Conference*, Breckenridge, CO, February 2017.

[6] Cheng, S-C, "Payload Fairing Separation Dynamics." J*ournal of Spacecraft and Rockets*, Vol 36, No. 4, 1999, pp. 511-515.

[7] Aftosmis, Michael J., et al, "Numerical Simulation of Bolide Entry with Ground Footprint Prediction." *54th AIAA Aerospace Sciences Meeting,* 2016.

COUPLED AERO-STRUCTURAL MODELLING AND OPTIMISATION OF DEPLOYABLE MARS AERO-DECELERATORS. L. Peacocke[1], P.J.K. Bruce[1], and M. Santer[1], Department of Aeronautics, Imperial College London, London, SW7 2AZ, United Kingdom, l.peacocke16@imperial.ac.uk.

Abstract: Forthcoming missions to Mars will be required to land large payloads of up to 20 tonnes on the surface. Such landed masses are not feasible with current Mars entry vehicles, due to the size limitations of existing launch vehicle fairings. Deployable aero-decelerators are a solution that addresses this issue, by increasing the diameter of entry vehicles post-launch, which in turn improves deceleration in planetary atmospheres. Larger diameters can enable the delivery of high mass payloads to the surface of atmospheric bodies, decrease the ballistic coefficient and peak heat fluxes experience, increase the timeline available for precision guidance, or enable landing at higher elevation landing sites.

The deployable nature of this type of aero-decelerator implies some flexibility in the deployed elements, so an assessment of acceptable deflection is a key design activity. To aid the preliminary design of such configurations, a 6 DOF entry trajectory and aero-structural simulator has been developed within Matlab. This tool can simulate the atmospheric entry of different heatshield configurations and shapes, taking into account the deflection of the external shape due to pressure. Aerodynamic pressures and forces are continuously updated at each timestep of the trajectory, based on the Modified Newtonian local surface inclination method. The equations of motion are numerically integrated using a Runge-Kutta method. The simulator is a reduced-order engineering tool that allows for fast analysis and assessment of different early phase concepts. Correlation against an industry tool has been performed and has shown excellent alignment for rigid heatshields, giving confidence that the tool can be used for performance assessment of potential deployable configurations.

A coupled aero-structural module has been added to the simulator, to model the deformation experienced by the deployable elements throughout entry, as in Fig. 1. Deployed ribs are modelled as Euler-Bernoulli beams, valid for slender elements, and deflections are integrated along the length of the beam based on the aerodynamic forces experienced. Material properties, rib dimensions, cross-section shapes, and the locations of support struts (if included) can be varied and optimized as required. Abaqus FEA cases have been used to validate the deflections predicted by this method, and determine the minimum required mesh resolution that ensures acceptable accuracy. As well as the deflection, the bending moment and maximum principal stress throughout the deployed element can be output to ensure the material yield strength is not exceeded.

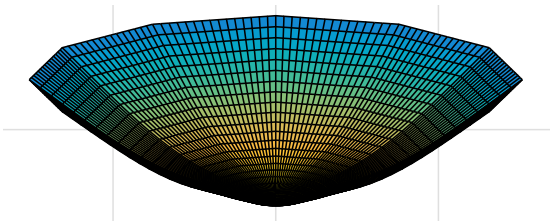

Fig. 1: Deflection modelling of a 16 m diameter deployable aero-decelerator.

An optimization activity has taken place, trading off between deployable element flexibility, mass and volume. Although flexible elements can be significantly lower mass and volume, the resulting deformation reduces the drag coefficient, leading to a faster entry and increased peak heat flux and peak dynamic pressure. However, a reduction in peak g-load is also seen. A tapered beam presents significant advantages, allowing mass savings while retaining sufficient strength at the location of maximum principal stress – near the support strut. The mass savings from flexible and tapered ribs can be used to increase the diameter of the entry vehicle if desired, which leads to deceleration at higher altitudes, as shown in Fig. 2.

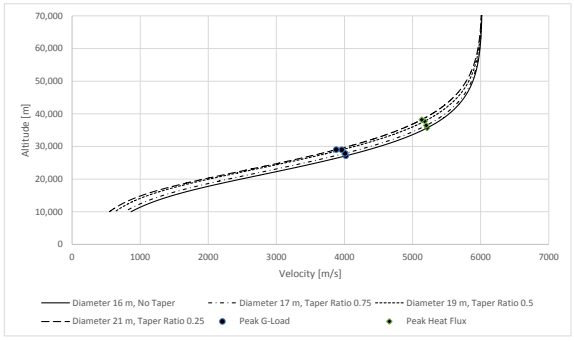

Fig. 2: Entry trajectory optimization with tool.

This presentation will outline the coupled aero-structural trajectory simulator, and present the results of the optimization of deployable aero-decelerator configurations, to demonstrate the advantages and disadvantages of flexible deployable aero-decelerators. It will also outline the upcoming experimental test campaign planned for 2019 that will utilize Imperial's high speed wind tunnel facilities.

The Case for High-fidelity Material Response Modeling. M. D. Barnhardt[1], M. J. Wright[1], N. N. Mansour[1], F. Panerai[2], and T. R. White[1], [1]NASA Ames Research Center, Moffett Field, CA 94035, [2]Analytical Mechanics Associates, Inc., Moffett Field, CA 94035.

Introduction: Material response modeling of heatshields for planetary entry vehicles has remained largely unchanged since Aerotherm Corp. introduced the CMA program in 1967. Modern models, like FIAT, have tread the same path, introducing efficiencies and better material property data along the way, but otherwise following the same underlying model paradigm. The CMA approach has worked well for heatshield design up to this point. However, there are three motivations for the material response community to pursue higher fidelity beyond simplified, CMA-derived models. The first motivation is that missions are becoming increasingly demanding and complex and, as they do, confidence in simplified models naturally decreases. Second, reliability of materials is now as much or more of a driving concern for mission designers than thermal response. Third, NASA and other agencies are increasingly interested in flight instrumentation for engineering science. This latter motivation places far stricter requirements on model accuracy in order to meet requirements for flight environment reconstruction.

Increasing Mission Complexity: Human exploration and planetary science missions will always grow more ambitious over time. Two costs of that ambition are that performance requirements become more stringent and engineering complexity rises. For the former, this typically means that modeling tolerances must become tighter in order to meet system constraints. Increased engineering complexity, meanwhile, can lead to fundamental breakdowns in the assumptions underpinning analysis. One example of this is the growing multidimensionality of thermal protection systems, where features like windows and attachment points fundamentally break down the one-dimensional assumption found in many state-of-the-art models.

Reliability of Thermal Protection Materials: It is often the case that thermal margins are a lesser worry than specific concerns about TPS reliability. A prime example is the concern regarding performance of damaged TPS, such as from a micrometeoroid impact, but extends also to built-in features like tile gap fillers. Today's tools are not at all equipped to provide insight into onset and growth of TPS failure modes and, as a result, they cannot help engineers to quantify risk of failure. This is pointedly illustrated by the 1:1,000,000 allowable failure rate imposed by planetary protection requirements for a Mars sample return mission. This requirement is so great that there is no cost-effective way to verify it through testing alone. High-fidelity models, anchored with experimental validation, must become good enough to confidently provide engineers with failure estimates.

Engineering Science Investigations: Finally, in recent years there has been a strong turn toward engineering science investigations, including MEDLI/MSL, MEDLI2/Mars 2020, DFI/Orion, and COMARS/Schiaparelli. In order to achieve desired return on these multi-million dollar investments, agencies need models capable of reconstructing the TPS performance and flight environments with maximum accuracy. Studies **[1,2]** of flight data have pointed to a number of common issues that drive reconstruction uncertainty and are not addressed by engineering models: The effect of in-depth water vaporization; uncertainties in material properties and variability; lack of finite-rate chemistry for gas-surface interactions and pyrolysis decomposition; modeling of interfaces (like gap fillers or adhesives) and surface coatings; and melt flow, to name a few.

References:

[1] Mahzari, M. et al. (2013) *JSR, 50,* 1171-1182.
[2] Bose, D. et al. (2014) *JSR, 51,* 1174-1184.

Mars 2020 Second Chance Flight Software

Aaron Stehura[1], Allen Chen[1], CJ Giovingo[1], Mallory Lefland[1]
[1]Jet Propulsion Laboratory, California Institute of Technology, 4800 Oak Grove Drive, Pasadena, CA 91109

Abstract:

Mars 2020 is a largely heritage mission, especially from an entry, descent, and landing (EDL) perspective, drawing heavily from the successful Mars Science Laboratory (MSL) flight system architecture [1]. The primary flight computer is present on the rover stage and controls the entire spacecraft throughout all phases of the mission, with other avionics hardware distributed across the descent stage, cruise stage, and heatshield. A second string was added for core avionics components (flight computers, power and analog switching modules, etc.) during MSL's development to improve surface phase reliability of the mission. Despite the addition of a second string, the single string approach was maintained for EDL to avoid complicating the EDL design itself and simplify time-of-response requirements for the multi-string fault detection, isolation, and recovery architecture. Late during MSL, an exception was made to EDL's preferred single string approach and ways to use the backup flight computer were explored.

This paper details how Mars 2020 uses its backup flight computer during EDL and how this approach is analogous to MSL's. A streamlined version of flight software (FSW) was designed specifically to run on the backup flight computer and take over if the primary flight computer relinquished control [2] [3]. This software is called "Second Chance" (SECC). It shares many common components with the mainline FSW while a handful of unique components were created to facilitate SECC's ability to follow the activities of the primary computer. Key design parameters include the capability to rapidly assume control (within 2 seconds) and land the vehicle within the same performance envelope as the mainline FSW. Also of paramount importance is that SECC should do no harm to the mainline FSW, either during operation or development. On MSL, development was conducted by a separate team to avoid drawing too much attention away from the main-line FSW while Mars 2020 has employed a more integrated development approach. Realtime concerns are alleviated by designing SECC to operate in a listen-only mode and using the same operational approach as MSL while also rectifying selected coverage gaps. Current development status and early test results are presented.

References:

[1] Allen Chen et al. (2017) *Mars 2020 Entry, Descent, and Landing System Overview*, IPPW14 Presentation.

[2] Chris Roumeliotis et al. (2013) *The Unparalleled Systems Engineering of MSL's Backup Entry, Descent, and Landing System: Second Chance,* 8th Annual System of Systems Engineering Conference, 2013, 13-1045.

[3] Mallory Lefland et al. (2017) *Mars 2020 Flight Computer Redundancy for EDL*, IPPW14 Poster.

CFD ANALYSIS OF THE CORK-PHENOLIC HEAT SHIELD OF A REENTRY QUBESAT IN ARC-JET CONDITIONS INCLUDING ABLATION AND PYROLYSIS. A. O. Baskaya[1*], A. Turchi[1†], G. Bellas-Chatzigeorgis[1‡], P. F. Barbante[2§], T. E. Magin[1¶].
[1] *von Karman Institute for Fluid Dynamics, Chaussée de Waterloo, 72, B-1640 Rhode-St-Genèse, Belgium*
[2] *Politecnico di Milano, MOX, Department of Mathematics, Piazza Leonardo da Vinci 32, 20133 Milano, Italy*

Introduction: Atmospheric entry has been a field of ceaseless curiosity since the beginning of the space age due to the high temperatures and heat fluxes the vehicle is exposed to during its hypersonic flight. Survival of the crucial components of the spacecraft within this environment is ensured by the installation of Thermal Protection Systems (TPS). Developing an understanding for the behavior of TPS materials is pivotal for space exploration missions as lightweight materials that inhibit the transfer of heat more effectively to the interior of the structure could enable critical design choices.

In this regard, the von Karman Institute for Fluid Dynamics (VKI) has developed the QubeSat for Aerothermodynamic Research and Measurements on AblatioN (QARMAN). QARMAN's main objective is to demonstrate the viability of a CubeSat as a re-entry platform. One of the main challenges QARMAN faces is the thermal protection of its components. To overcome this difficulty a cork-phenolic TPS is used around the nose of the structure and titanium is used at the side walls.

A model of QARMAN will be tested at the SCIROCCO arc-jet plasma wind tunnel in CIRA as part of the critical system review before the actual flight. This work aims to present the CFD simulations of a full-scale QARMAN model under SCIROCCO-like conditions by employing the COSMIC in-house finite volume code [1]. The code is coupled with the Mutation++ thermodynamic and transport properties library [2], utilizing its gas surface interactions (GSI) module [3] to perform simulations including the effect of mass injection due to ablation and pyrolysis. Scope of the analysis is enhanced by investigating the effect of shape change due to ablation on the evolution of the heat flux distribution along the vehicle nose.

Gas-surface interactions: The thin lamina approach [4] is used to formulate mass and energy balances in a reference frame fixed to the ablating surface. All energy fluxes arriving at the surface are considered to dissipate by heat conduction and pyrolysis gas generation through the solid material. For receding surfaces, and under few simplifying hypotheses, the temperature profile inside the material becomes time-independent. The heat conduction through the material is governed by this steady-state approximation.

For the surface species mass balance, a finite-rate ablation model is implemented to calculate the source term and the total mass loss of the ablated material. Accordingly, the effect of blowing is considered by computing the mass blowing rates directly, which eliminates the need for any further corrections for the resulting heat fluxes. Furthermore, the aforementioned steady-state approach allows the quantification of the pyrolysis gas mass flux when sufficient material information is known.

Pyrolysis: In addition to exhibiting ablation, charring ablator materials undergo in depth decomposition caused by the presence of heat moving deeper into the material to trigger pyrolysis reactions which release an outburst of gaseous species to the ambient boundary layer while leaving some amount of carbon as residue. The endothermic nature of the pyrolysis reaction together with the bulk motion of the gases generate a cooling effect that considerably influences the heat fluxes at the surface and therefore demand careful attention.

When cork-phenolic is exposed to heat, in addition to the resin, the cork itself pyrolyzes, unlike the carbon fibers of more common ablators. The additional gaseous species arising from these reactions significantly complicates the estimation of the overall pyrolysis gas chemical composition. To account for these species in this analysis the elemental compositions of cork, phenol, and the resultant pyrolysis gas have been determined by making use of scientific data published in the last three decades about cork [5, 6, 7, 8] and the experimental results for the material layer thicknesses of cork samples heat treated in the VKI Plasmatron plasma wind tunnel [9].

Surface Evolution: Mass loss due to ablation and pyrolysis is inherently accompanied by shape change in the form of surface recession. However, development of an adaptive methodology capable of reforming the

[*]baskaya@vki.ac.be
[†]turchi@vki.ac.be
[‡]georgios.bellas.chatzigeorgis@vki.ac.be
[§]paolo.barbante@polimi.it
[¶]magin@vki.ac.be

geometry during a simulation is often neglected owing to its rigorous implementation. The necessity for this advancement is assessed in this analysis through evolving the surface of the model by an uncoupled approach to attain steady-state solutions at specific intervals.

Evolution of the surface in time is determined by extracting mass blowing rates retrieved from an initial solution to obtain recession speeds at each point along the surface. Surface shape is then recessed for a specified period according to these speeds by utilizing the code developed to obtain the evolved geometry. Successive solution of these geometries provides an uncoupled way of evaluating the significance of the shape change due to recession by emphasizing the drastic reduction of heat flux along the surface of the model subsequent to evolution. As it can be seen in Fig. 1, recessing the geometry solely based on the initial recession speeds gives an overestimation. Whereas, the surface recessed with updated recession speeds at 5-second intervals provides a more realistic result. Different time intervals will be considered in this analysis to efficiently capture the relation between the shape change and the reduction in heat flux.

Conclusions: This work serves as a comprehensive analysis regarding cork-based TPS materials and ablative CFD simulations as it gives insight into the characteristic thermochemical features of cork and proposes an efficient methodology for assessing the need for adaptive implementations to capture shape deformations. Results will provide a comparison between the cases with and without pyrolysis as well as the cases of primitive and evolved geometries. Thus, by elucidating the aforementioned phenomena this work will convey a practical understanding to improve the TPS design of probes and related entry vehicles.

References: [1] Barbante, P. F. (2001). Von Karman Institute for Fluid Dynamics. [2] Scoggins, J. B., & Magin, T. E. (2014). *AIAA Paper*, *2966*, 16-20. [3] Bellas-Chatzigeorgis, G., Turchi, A., Viladegut, A., Chazot, O., Barbante, P. F., & Magin, T. (2017). In *23rd AIAA Computational Fluid Dynamics Conference* (p. 4499). [4] Keenan, J. A., Ph.D. thesis, North Carolina State University, Raleigh, North Carolina, 1994. [5] King, H. H., Avni, E., Coughlin, R. W., & Solomon, P. R. (1983). *Prepr. Pap., Am. Chem. Soc., Div. Fuel Chem.;(United States)*, *28*(CONF-830814-). [6] Smith, E., Laub, B., Beck, R., & Fretter, E. (1992). In *27th Thermophysics Conference* (p. 2905). [7] Silva, S. P., Sabino, M. A., Fernandes, E. M., Correlo, V. M., Boesel, L. F., & Reis, R. L. (2005). *International Materials Reviews*, *50*(6), 345-365. [8] Miranda, I., Gominho, J., & Pereira, H. (2013). *Journal of wood science*, *59*(1), 1-9. [9] Sakraker, I. (2016). (Doctoral dissertation, Université de Liège, Liège, Belgique).

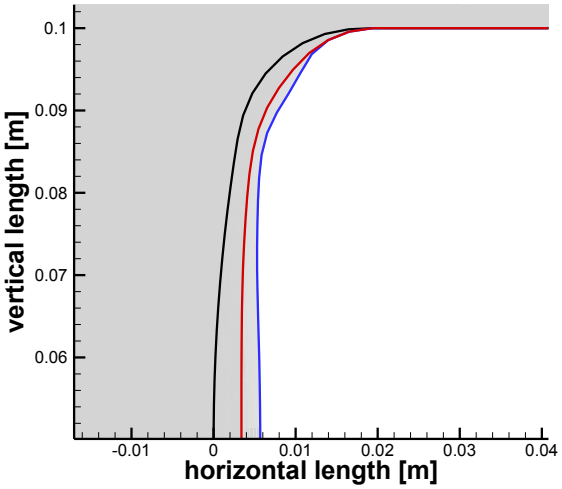

Figure 1: Surface profiles of the geometry prior to heat exposure (black), the geometry recessed for 10 seconds with the initial recession speeds (blue), and the geometry recessed for 5 seconds with initial recession speeds and another 5 seconds with the updated recession speeds (red).

HOW GRAVITY AND ICE TEMPERATURE AFFECT THE PERFORMANCE OF THERMAL MELTING PROBES, J. Kowalski[1] and K. Schüller, [1]Aachen Institute for Advanced Study in Computational Engineering Science, RWTH Aachen University, Schinkelstr. 2, 52062 Aachen, Germany, kowalski@aices.rwth-aachen.de.

Introduction: The Ocean Worlds of our Solar System are covered with ice. Hence the water is not directly accessible, yet of high interest, as it is attributed some potential to host extraterrestrial life. Using advanced melting probe technology [1,2] is one of the promising technological approaches to reach those scientifically interesting water reservoirs. Melting probes basically consist of a heated melting head on top of an elongated body that contains the scientific payload.

The traditional engineering approach to design such probes starts from a global energy balance around the melting head and determines the power necessary to sustain a specific melting velocity while preventing the probe from refreezing and stall in the channel. Though this approach turned out to be sufficient to design melting probes for terrestrial use, it is too simplistic to study the probe's performance in environmental conditions found on some of the Ocean's Worlds, e.g. a low value of the gravitational acceleration on Enceladus. This is crucial, however, when designing exploration technologies for extraterrestrial purposes.

A design model for thermal melting probes In this contribution, we will describe an improved simulation-based design model for thermal melting probes based on contact melting theory [3], see figure 1. This means that we explicitely model the physical processes in the thin melt film between the probe and the ice as they affect the macro-scale dynamics of the melting robot.

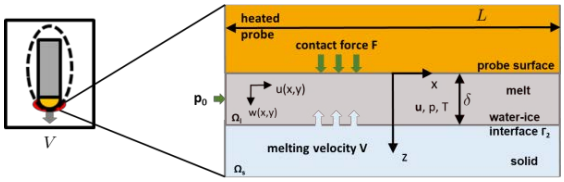

Figure 1: Micro-scale processes in the vicinity of the melting probe.

Our model is capable of

- assessing the performance of thermal melting probes on bodies of different (lower) gravitational acceleration,
- assessing the performance of complex melting head designs, e.g. built-in sensors.

We will briefly describe the basic model concept and introduce our computational implementation before discussing three results in greater detail:

The role of gravity Based on our model, we compare the melting performance of an axisymmetric melting probe (25kg) on Europa, Enceladus and Mars conditions [4], see figure 2. Note that for this study, we restrict ourselves to the probe's ice transit that is believed to take place in a 'closed' melt channel, which sustains a pressure above the triple point.

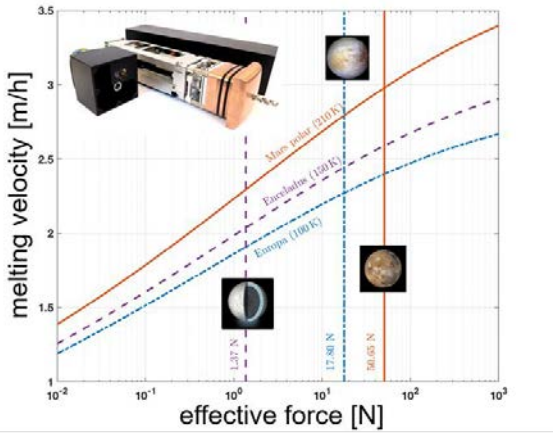

Figure 2: Computed melting velocity over effective force for a 25kg melting probe under Mars, Enceladus and Europa conditions [4].

Critical Refreezing length We will continue with a model-based quantification of heat losses due to convective transport around the probe. We will discuss to which extent these heat losses can be utilized to avoid (or reduce) a side wall heating system to prevent stall due to refreezing. In that context, we introduce the notion of the 'Critical Refreezing Length' and again compare Mars, Europa and Enceladus conditions.

Optimal sensor distribution Finally, we will describe how our computational contact melting model can be used to infer on the optimal sensor distribution on a melting head. We will briefly introduce our computational strategy and present first results for the optimized distributed placement of piezometric sensors.

Acknowledgements: The project is supported by the Federal Ministry of Economics and Technology, Germany, on the basis of a decision by the German Bundestag (FKZ: 50NA 1502).

References: [1] Dachwald B. et al. (2014) *Ann. Glaciol.,* 55, 14–22. [2] Kowalski J. et al (2016), Cold Reg Sci Technol. 123, 53-70. [3] Schüller K., Kowalski J. (2016), Int J Heat Mass Trans 92, 884–892. [4] Schüller K., Kowalski J. (2018) submitted (preprint: http://arxiv.org/pdf/1803.04883.pdf).

DESIGN EXPLORATION, OPTIMIZATION AND MODEL-BASED ENGINEERING FOR NANO-SATELLITE MISSION DESIGN. J. Ancheta[1], P. Papadopoulos[1], [1]San José State University.

Introduction: Nano-satellite missions are an inexpensive tool used to perform scientific research functions and test new space technologies. From 2000 to 2016 there were 371 nanosatellite launches with 15.4% shown to complete their mission and another 22.6% which completed some aspect of their mission [1]. The high failure rate of nano-satellites can be attributed to multiple factors such as system integration, non-space rated hardware, launch failure, and untested technology. By integrating design exploration, optimization and model-based system engineering techniques, some portion of nano-satellite risk may be mitigated.

This work presents a multi-disciplinary system exploration, design, and simulation approach for low-budget nano-satellite builders to get a better estimate of system performance before beginning the actual build. The use of design exploration minimizes the number of variables in optimization by finding which design variables have little options or impact on system performance and allows the design team to parameterize them. The system optimization process will give initial goals for the hardware mass, power and performance metrics which can then be simulated in a high-fidelity simulation to analyze mission and systems level requirements. This approach was implemented using a combination of open source tools and commercial programs. Open source packages such such as pyOpt and OpenMDAO were used to perform design space exploration and multi-objective optimization. MatLabs Simulink was used as the model based engineering program as it provides a format which would is readily available and familiar to students and engineering teams with little to no formal systems engineering background.

Design space exploration was performed by tools provided in the OpenMDAO package. Optimization was implemented by aggregating the constraints and objectives using the Kreisselmeier-Steinhauser method and using an unconstrained solver to minimize the envelope [2]. The implementation of this was algorithm was provided by the pyOpt package.

The current level for the models for each system is currently in an early development stage which should be used with caution for actual system engineering. However this proposed approach can be easily expanded with higher-fidelity models, design equations, and parameterization based off of historical data which will result in an initial starting point for nano-satellite build teams who can then make design decisions based off of currently available technology, time and monetary constraints.

References:

[1] M. Swartwout, “CubeSats and Mission Success: 2017 Update (with a closer look at the effect of process management on outcome)” in 2017 Electronics Technology Workshop, Goddard Space Flight Center,2017.

[2] G. Wrenn “An Indirect method for Numerical Optimization using the Kreisselmeier-Steinhauser Function”, NASA Contractor Report 4220, March 1989.

USING BEZIER TRIANGLES FOR MODELING SMALL BODY SHAPES AND THEIR INERTIA PROPERTIES IN THE PRESENCE OF UNCERTAINTY . Benjamin Bercovici[1] and Jay W. McMahon[2], [12] Ann and H.J. Smead Aerospace Engineering Sciences Department, University of Colorado Boulder

Introduction The knowledge of a small body shape is paramount to the determination of its inertia properties such as volume, center of mass, inertia… as well as the computation of the gravity field exerted by the body onto neighboring objects, should they be natural or artificial. In this work, we explore Bezier triangles as an alternative to traditional planar triangles as elemental surface elements to represent a small body shape [1]. A Bezier triangle is a parametric surface element formed by the interpolation of control points by means of the so-called Bernstein polynomials, effectively producing an open surface of arbitrary degree controlled by the number and position of the control points. A quadratic Bezier shape is illustrated on Figure 1. Contrary to planar triangles, an individual Bezier triangle can feature non-zero curvature, and is thus able to capture larger surface areas without requiring a commensurate increase in its order. Similarly, collections of Bezier patches can cover greater areas than planar facets without significant underfitting using a lower number of surface elements than if planar triangles were used. For the sake of illustration, a shape model of Itokawa that was fit using simulated point cloud data and only 1998 Bezier patches with global RMS fitting residuals of 0.35 meters is shown on Figure 2. Using higher-order surface patches, one can also enforce tangent continuity, a desirable property for surface mobility analyses [2].

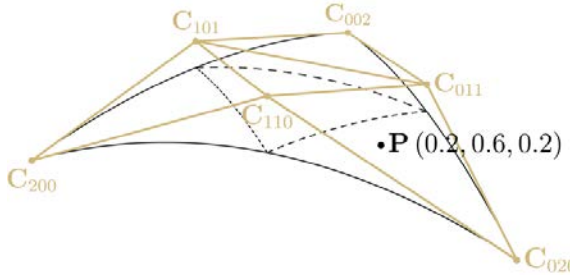

Figure 1 - A quadratic Bezier patch sampled at the barycentric coordinates (0.2,0.6,0.2)

Contributions We derive the analytical expressions of the volume, center-of-mass and inertia tensors of arbitrary collections of Bezier triangles. These expressions are explicit functions of the control mesh coordinates generating the shape. Their implementation is embarrassingly parallel, and can be further optimized due to the presence of constant factors that need not to be recomputed upon variation of the control mesh. These expressions arise from the application of the divergence theorem to a 'Bezier tetrahedron` akin to the one shown on Figure 3. They come as the complement to existing formulas for polyhedral shapes [3], with greater generality since they are applicable to Bezier triangles of arbitrary degree, while also being valid for polyhedra. Indeed, Bezier triangles of degree are no else but planar triangles. For instance, the signed volume of a single Bezier tetrahedron reads

$$V = \sum_{|\mathbf{i}|=n} \sum_{|\mathbf{j}|=n} \sum_{|\mathbf{k}|=n} \alpha_{\mathbf{ijk}} \mathbf{C}_\mathbf{i}^T \left[\mathbf{C}_\mathbf{j} \times \mathbf{C}_\mathbf{k}\right]$$

where the $\alpha_{\mathbf{ijk}}$ are weighed integrals of a product of Bernstein polynomials where the triplets of indices **i**, **j** and **k** each obey $|\mathbf{i}| = \mathbf{i}(0) + \mathbf{i}(1) + \mathbf{i}(2) = |\mathbf{j}| = \mathbf{j}(0) + \mathbf{j}(1) + \mathbf{j}(2) = |\mathbf{k}| = \mathbf{k}(0) + \mathbf{k}(1) + \mathbf{k}(2) = n$, the order of the Bezier triangle. As pointed out before, the $\alpha_{\mathbf{ijk}}$ are constant with respect to the control mesh coordinates and are only a function of n, and should thus be computed in advance.

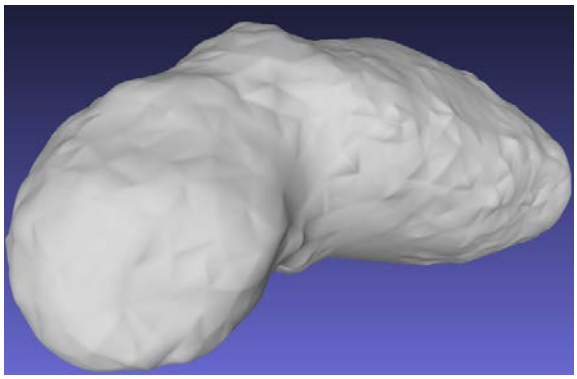

Figure 2 - A Bezier fit of Itokawa comprised of 1998 quadratic patches

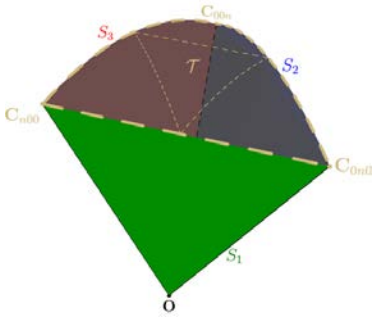

Figure 3 - Bezier tetrahedron subtended by a Bezier triangle τ and an arbitrary origin O

Current work focuses on analyzing the effect of shape uncertainty on the small body's inertia properties. To this end, we treat the control mesh coordinates of each Bezier triangle as a Gaussian random vector of known mean and covariance and derive a mapping relating the uncertainty in the control mesh to the statistics in the volume, center of mass and inertia tensor. We are making the assumption that each control point has a fully populated covariance but is uncorrelated with the other control points forming the shape, so as to facilitate the subsequent derivations. The mean and covariance of the inertia quantities of interest will then be expressed as a function of the input parameters: the mean and covariance in each control point Once available, this mapping will be useful to scientists and navigators willing to gain more insight into the variability of inertia properties of small bodies given a measure of the uncertainty in their shape parametrization. A natural extension to this work is to relate the shape uncertainty measure to that in the gravity potential and accelerations, starting with the well-established Polyhedron Gravity Model [4] providing the exact gravity field generated by a constant density polyhedron (i.e a collection of first-order Bezier triangles) .This result would be of interest to the community as the dynamics of an object orbiting the small body must must be properly modeled or have at least a sufficiently well constrained uncertainty so that subsequent navigation about the small body can safely take place.

References

[1] Farin, G. (1986). Triangular Bernstein-Bezier patches. *Computer Aided Geometric Design, 3, 83–127.*

[2] Yu, Y., & Baoyin, H.-X. (2014). Routing the asteroid surface vehicle with detailed mechanics. *Acta Mechanica Sinica, 30*, 301–309.

[3] Dobrovolskis, A. R. (1996). Inertia of Any Polyhedron. *Icarus, 124*, 698–704.

[4] Werner, R. A., & Scheeres, D. J. (1997). Exterior gravitation of a polyhedron derived and compared with harmonic and mascon gravitation representations of asteroid 4769 Castalia. *Celestial Mechanics and Dynamical Astronomy, 65(3)*, 313–344.

FULL-SCALE MSL HEATSHIELD MATERIAL RESPONSE USING DSMC AND CFD TO COMPUTE THE AEROTHERMAL ENVIRONMENTS.

A. Borner[1], J. B.E. Meurisse[1], F. Panerai[2] and N. N. Mansour[2], [1]Science and Technology Corporation at NASA Ames (arnaud.p.borner@nasa.gov), [2]AMA Inc. at NASA Ames, [3]NASA Ames Research Center.

During Mars atmospheric entry, the Mars Science Laboratory (MSL) was protected by a 4.5 meters diameter ablative heatshield assembled in 113 tiles [1]. The heatshield was made of NASA's flagship ablative material, the Phenolic Impregnated Carbon Ablator (PICA) [2].

Prior work [3] compared the traditional one-dimensional and three-dimensional material response models at different locations in the heatshield. It was observed that the flow was basically one-dimensional in the nose and flank regions, but three-dimensional flow effects were observed in the outer flank. Additionally, the effects of tiled versus monolithic heatshield models were also investigated. It was observed that the 3D tiled and 3D monolithic configurations yielded relative differences for in-depth material temperature up to 18% and 28%, respectively, when compared to the a 1D model.

The Porous material Analysis Toolbox based on OpenFOAM (PATO) [4, 5] is used for this study. The governing equations are volume-averaged forms of solid mass, gas mass, gas momentum and total energy conservation, including pyrolysis gas production. The thermodynamics and chemistry properties are computed using the Mutation++ library [6]. The boundary conditions at the heatshield front surface are interpolated in time and space from the aerothermal environment at discrete points of the MSL trajectory.

The objective of this work is to study the effects of the aerothermal environments on the material response. We propose to extend prior work [3] by computing aerothermal environments using the direct simulation Monte Carlo (DSMC) code SPARTA [8] and the CFD code Data Parallel Line Relaxation (DPLR) [9]. SPARTA will be used to compute environments in the rarefied regime prior to 50s of entry where the Knudsen number is such that the Navier-Stokes equations can be inaccurate. As an extension to previous work, the DPLR software will be used to compute the hypersonic environments for a fully turbulent boundary layer assumption from 50s up to 100s of entry along the MSL 08-TPS-02/01a trajectory.

References:

[1] K. T. Edquist, et al. (2009) *AIAA Paper* 2009-4075.

[2] M.J. Wright et al. (2009) *AIAA Paper* 2009-4231.

[3] J. B.E. Meurisse et al. (2018), *Aerosp Sci Technol*, 76, 497-511.

[4] J. Lachaud and N. N. Mansour (2014), *J Thermophys Heat Tran,* 28, 191–202.

[5] J. Lachaud et al. (2017), *Int J Heat Mass Tran,* 108, 1406–1417.

[6] J. B. Scoggins and T. E. Magin (2014), *AIAA Paper* 2014-2966.

[7] T. R. White et al. (2013), *AIAA Paper* 2013-2779.

[8] M. A. Gallis et al. (2014), *AIP Conf Proc* 1628, 27.

[9] M. J. Wright et al. (2009), *DPLR Code User Manual: Acadia-Version 4.01. 1*.

CFD CODE VALIDATION FOR MARS ENTRY SIMULATIONS. L. Cutrone[1], A. Schettino[1], M. Ventriglia[1], and E. Zaccagnino[1], [1]Italian Aerospace Research Center (CIRA), Capua (CE), Italy

Introduction:

Mechanical and thermal loads encountered by a capsule entering the Mars atmosphere are key issues in determining the type and size of its Thermal Protection System. Advanced CFD numerical tools can be used in order to estimate these loads, provided that they are able to simulate real-gas thermo-chemical non-equilibrium processes, along with the gas surface interaction, that are fundamental in the determination of aerodynamic heating. To this aim, a CFD numerical code developed at the Italian Aerospace Research Center, and largely used in the last decades in the field of aerothermodynamics of earth re-entry vehicles, has been recently extended to be able to simulate Mars atmosphere, that consists primarily of carbon dioxide at relatively low pressure, with 3% of Nitrogen.

The goal of the present work is to validate the code with respect to experimental data in representative conditions available in literature. Furthermore, a code-code comparison has been carried on with the well known commercial code FLUENT, widely used in industrial activities.

Numerical solver:

The CFD code NExT is the last version of a family of numerical solvers for aerothermodynamics developed at CIRA since the beginning of 90's. It is a structured multiblock finite volume solver that allows the treatment of a wide range of compressible fluid dynamics problems for aerothermodynamics and propulsion applications. The Chemkin® input interface allows treating different mixtures of reacting gases, specifying mixture composition and chemical kinetic scheme. A thermal and chemical database contains the transport coefficients and the thermodynamics data for each species.

The fluid can be treated as a mixture of gases in thermochemical non-equilibrium. For aerothermodynamics applications, the energy exchange between vibrational and translational modes (TV) is modelled with the classical Landau-Teller non-equilibrium equation, with average relaxation times taken from the Millikan-White theory modified by Park. For what concerns transport coefficient, the species viscosity, and thermal conductivity, are calculated by means of the Eucken law, whereas the mixture viscosity and thermal conductivity are calculated by using the semi-empirical Wilke formulas.

The diffusion coefficients are computed through a sum rule of the binary diffusivities for each couple of species.

Concerning the numerical formulation, conservation equations are written in integral form, and discretized with a finite volume, cell centred technique. Convective fluxes are computed with a Flux Difference Splitting (FDS) upwind method. Second order formulation is obtained by means of an Essentially Non-Oscillatory (ENO) reconstruction of interface value.

Viscous fluxes are computed with a classical centred scheme. Time integration is performed by employing a point-implicit algorithm coupled with an automatic evaluation of the CFL number.

Different physical models have been used; on one side, computations with and without the presence of the nitrogen have been performed, in order to verify the importance to use a more complex mixture modelling also this additional species; moreover, two different thermal models have been used for the CO_2, characterized respectively by 1 and 3 vibrational temperatures.

Test cases and preliminary results:

Two test cases were used for code validation.

The first reference is a test campaign performed at DLR in L2K wind tunnel facility [2]; pitot pressure was measured in two different positions in the test chamber, at 90 mm and 380 mm from the nozzle exit respectively (Fig. 1); in Fig. 2 a comparison between numerical and experimental data is shown.

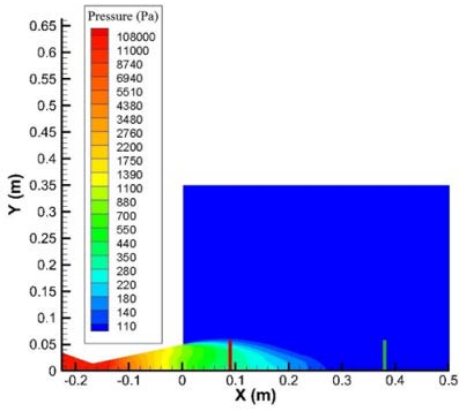

Figure 1: Simulation of L2K nozzle and test chamber. Pressure contour

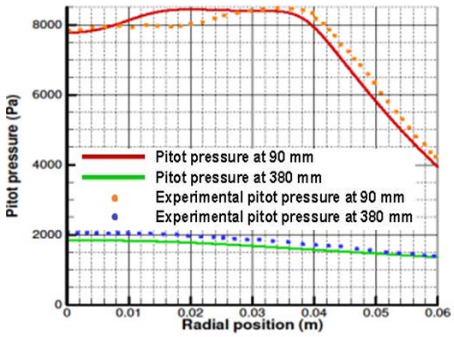

Figure 2: Pitot pressure in L2K test chamber. Comparison between CFD and experimental data.

In figure 3 the contour of the same case, including also the probe in the test chamber, is shown. The heat flux measured by means of a Heat Flux Microsensor is compared with the numerical results (Fig. 4); in this case, the numerical value overestimates by approximately 15% the experimental value. Further analyses are been performed in order to assess this difference, also considering the estimated experimental error bar. A sensitivity analysis will be performed to verify the effects of the different numerical and physical models on the heat flux prediction.

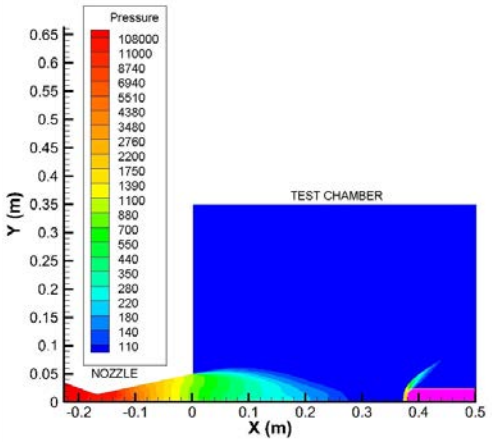

Figure 3: Simulation of L2K nozzle and test chamber, including the probe. Pressure contour

The second test case that was taken into account was the Phoenix capsule, a preliminary computation is shown in figure 5. Numerical results will be compared with data available in [3] and [4]; the attention will be also focused on the separation in the backshield region, comparing the results with the on es obtained by other authors [3].

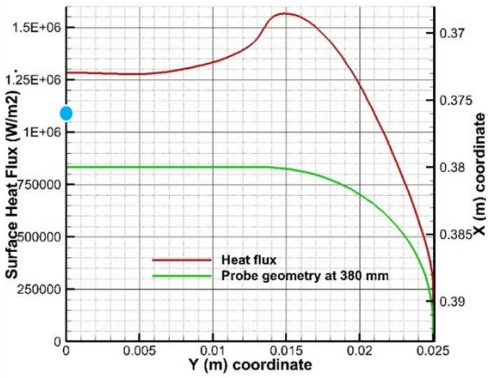

Figure 4: Heat flux over the probe in L2K. Comparison between CFD and experiments (blue point)

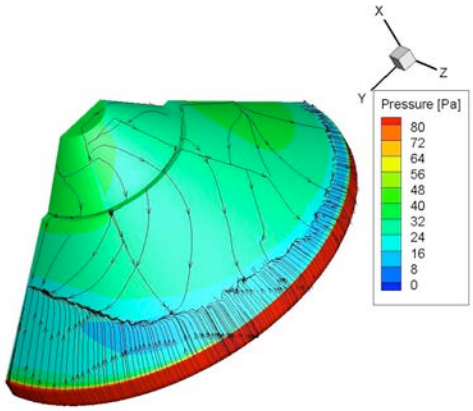

Figure 5: Phoenix capsule. Pressure contour and streamlines on the backshield.

References:

[1] Chul Park, John T. Howe, Richard L. Jaffe and Graham V. Candler. "Review of Chemical-Kinetic Problems of Future NASA Missions, II: Mars Entries", *Journal of Thermophysics and Heat Transfer*, 1994, 91-0464.

[2] M. De Stefano Fumo, P. Catalano, B. Esser and A. Gulhan. "Numerical Modelling of the CO2-N2 Hypersonic Flow for Simulations of Mars Entry conditions", *63rd International Astronautical Congress, Naples*, Paper IAC-12,A3,3A;19.p1.

[3] A.A. Dyakonov, C.E. Glass, P.N. Desai, J.W. Van Norman "Analysis of Effectiveness of Phoenix Entry Reaction Control System", *Journal of Spacecraft and Rockets*, Vol. 48, No. 5, September–October 2011.

[4] K.T. Edquist, P.N. Desai, M. Schoenenberger, "Aerodynamics for Mars Phoenix Entry Capsule",

NASA Langley Research Center, Hampton, Virginia, 2011.

Development of a Thermo-elastic Solver for Modeling Woven Thermal Protection Systems. D. Z. Dang[1], E. C. Stern[2], and I. D. Boyd[1], [1]University of Michigan, [2]NASA Ames Research Center.

Introduction: A coupled thermo-elastic solver is being developed for modeling woven thermal protection systems (TPS). For woven TPS, the architecture and material composition can be precisely tailored to meet the requirements of specific missions. The Adaptable Deployable Entry and Placement Technology (ADEPT), Heatshield for Extreme Entry Environment Technology (HEEET), and 3-D Multifunctional Ablative TPS are the three main projects at NASA leveraging the use of woven TPS.

Experimentalists from these projects have identified coupled thermo-structural phenomena that may affect the behavior of these materials under various atmospheric entry conditions. The presence of dust found on Mars could significantly augment the recession of TPS in the form of mechanical erosion, a structural phenomenon that could impact thermal performance. Under certain arc jet conditions, experimentalists have also observed increased recession possibly due to coupled thermo-structural phenomena, where prior modeling with purely thermal response codes have underestimated the recession.

The modeling in this work uses a macroscopic approach, using volume-averaged material response (solid material decomposition, pyrolysis gas continuity, and gas and solid energy conservation) and structural (linear elastic) equations for modeling coupled thermo-structural physics. A mixed central differencing and trapezoidal integration method is used to solve the governing equations (linear elasticity with damping), and regularized least squares with quadratic basis functions is used for computing gradients in the finite volume formulation. The computational science library, PETSc, is used for sparse data storage and GMRES is used for solving the linear system of equations.

Thermal stress, pressure (poroelasticity), and mesh movement coupling will be implemented to increase the fidelity of the solver by coupling multiple thermal parameters to structural variables. Stress-dependent material property relationships (e.g., porosity, conductivity, permeability) will be implemented through parametric relationships or from experimental data, if present.

The solver has been verified for one dimensional compression in both transient and time-independent scenarios. Excellent agreement was achieved between the simulation and analytical results as shown in Figs. 1-2. A multi-dimensional and coupled physics verification process will follow, along with an extensive validation campaign.

The current project targets the thermo-structural modeling of the three woven TPS projects. Due to the availability of experimental results, the current work aims to perform coupled thermo-structural modeling of a recent HEEET experiment of a woven test sample undergoing bending and heating simultaneously. Results from past, current, and future arc jet testing of woven TPS will be used to assess the validity of the modeling.

The methodology, implementation, and preliminary results for test cases will be presented in this workshop for both structural and coupled thermo-structural response. Preliminary verification of the solver and preliminary results will also be presented.

This project is particularly relevant to the planetary probe community as this work is expected to yield essential tools to guide the design of woven TPS for future space exploration missions to planets such as Mars and Venus. Coupled thermo-structural TPS modeling is essential to the safe design of entry systems, and the focus of this project is to provide innovative tools, with key physicochemical phenomena properly characterized, modeled and simulated, to better guide woven TPS design for future space exploration missions.

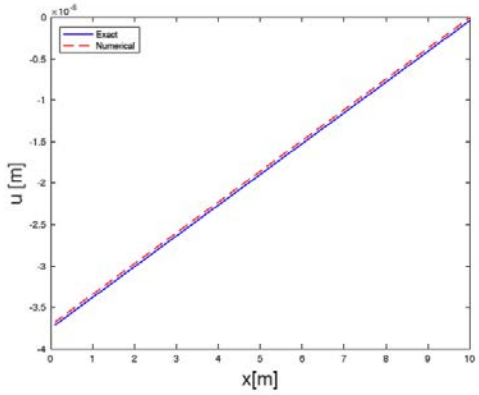

Figure 1. Verification of Steady Compression

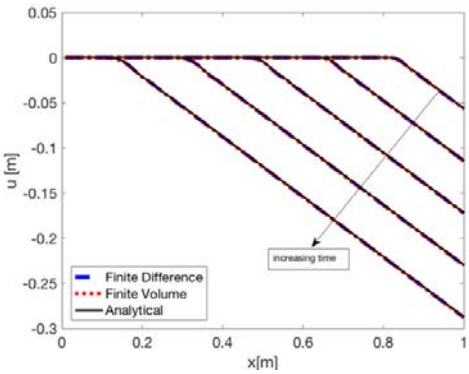

Figure 2. Verification of Transient Compression

Common-Probe: Interplanetary Trajectory Design. K. M. Hughes[1], C. L. Yen[2], J. R. Johannesen[2], and G. C. Marr[1]; M. A. Lobbia[2]; [1]NASA Goddard Space Flight Center, 8800 Greenbelt Road, Greenbelt, MD 20771; [2]Jet Propulsion Laboratory, 4800 Oak Grove Drive, Pasadena, CA 91109, Pasadena, CA.

Introduction: Planetary entry probe missions are an important part of obtaining ground-truth data to inform solar system formation models, characterize the age of the planetary bodies, and obtain in situ vertical sampling measurements of density, temperature, and winds in a given atmosphere that can be compared and contrasted with the structure and dynamics of Earth's atmosphere. These entry probe missions typically include instruments for performing mass spectroscopy (e.g., to measure noble gas abundances and isotopic ratios), as well as atmosphere structure sensors (e.g., temperature probes, pressure sensors, inertial measurement units) to measure the atmosphere structure/dynamics.

The Galileo Probe and Pioneer-Venus Multi Probe missions are examples of NASA atmosphere sampling probes that met these objectives at Jupiter and Venus, respectively. The most recent Planetary Science Decadal Survey [1] also indicated an atmosphere sampling probe to Saturn should be considered as part of the next New Frontiers call – this occurred in 2017, and (while not selected) the Saturn PRobe Interior aTmosphere Explorer (SPRITE) concept was proposed for this [2].

The present work focuses on the interplanetary modeling aspects of a recent NASA Common Probe study. Trajectories to several destinations will be presented, including highlighting key details such as timelines and delta-V requirements. Discussion of other drivers in the analysis will also be provided – for example, the data transmit geometry was a key part of the trajectory design process.

Common Probe: The Galileo Probe, Pioneer-Venus probes, and SPRITE concept all share a number of common characteristics. They all follow a similar entry and descent sequence, using an aeroshell to protect against entry environments, and parachutes to aid in extrusion and descent speed control of the descent vehicle containing the science instruments. The descent vehicles all contained similar instruments (e.g. mass spectrometers and atmosphere structure sensors), and data was either relayed back to a carrier spacecraft (Galileo Probe, SPRITE) or transmitted direct to Earth (Pioneer-Venus).

Based on these similar characteristics, NASA initiated a study to investigate a "common probe" that might be designed to perform similar science in a variety of planetary environments. This concept would leverage a common aeroshell design, and descent vehicle designs that could be made as similar as possible (the primary exception being that Venus will require a pressure vessel due to the extreme pressures and temperatures seen in the lower portion of the descent).

Interplanetary Trajectory Design: To support the Common Probe study, JPL and GSFC performed a series of interplanetary trajectory analyses to help develop the mission designs for Venus, Jupiter, Saturn, Uranus, and Neptune. Primary considerations in the trajectory modeling included: a maximum of 12-year time of flight to the destination, generation of both steep and shallow entry trajectories to each destination (where steep and shallow resulted in approximately 150 g and 50 g peak deceleration during entry at each location), and consideration of the data relay (for the outer planet destinations). Gravity assists and trajectories with low delta-V requirements (typically much less than 500 m/s) were also incorporated into the design process to enable launch on existing vehicles such as the Atlas V.

Figure 1 shows an example of the Saturn (steep) trajectory. Figure 2 shows the corresponding data relay characteristics for this, where the trajectory was designed to have a max probe-carrier range of approximately 100,000 km and elevation angle of >60 degrees for the assumed 2-hour descent timeline. As the probe will likely use a low-gain antenna, optimizing the geometery to enable higher data rates is an important part of the mission design.

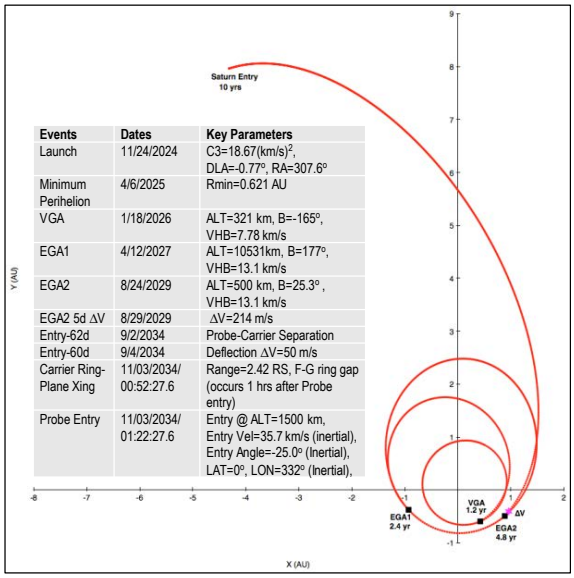

Fig. 1 *Interplanetary trajectory for Saturn (steep) trajectory.*

Summary: This interplanetary trajectory analysis was a key part of developing the Common Probe concept. Further details on the trajectories to all destinations will be provided in the final presented material.

References: [1] Squyres, S., et al., "Visions and Voyages for Planetary Science in the Decade 2013-2022," National Academies Press (2011). [2] Lobbia, M., et al, "Saturn PRobe Interior and aTmosphere Explorer (SPRITE): Mission Implementation Overview," 14th International Planetary Probe Workshop, The Hague, Netherlands (2017).

Acknowledgment: A portion of the research described in this paper was carried out at the Jet Propulsion Laboratory, California Institute of Technology, under contract with the National Aeronautics and Space Administration.

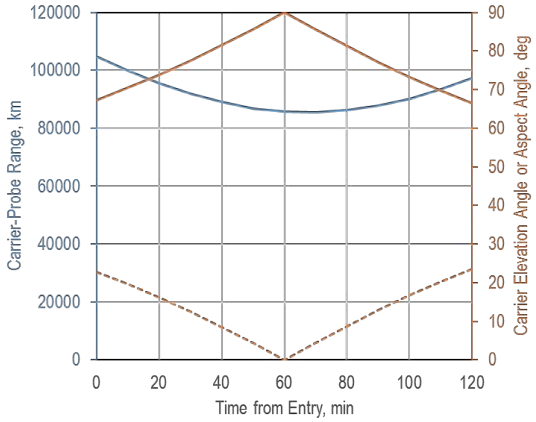

Fig. 2 *Data relay geometry for Saturn (steep) trajectory – assumes the probe is fixed at entry interface and rotates with the atmosphere during the carrier flyby.*

INVERSE DETERMINATION OF AEROHEATING AND CHARRING ABLATOR RESPONSE

J. B.E. Meurisse[1] and N. N. Mansour[2], [1]Science and Technology Corporation at NASA Ames Research Center (jeremie.b.meurisse@nasa.gov), [2]NASA Ames Research Center (nagi.n.mansour@nasa.gov).

The Mars Science Laboratory (MSL) was protected during its Mars atmospheric entry by an instrumented heatshield that used NASA's Phenolic Impregnated Carbon Ablator (PICA) [1]. PICA is a lightweight carbon fiber/polymeric resin material that offers excellent performances for protecting probes during planetary entry. The Mars Entry Descent and Landing Instrument (MEDLI) suite on MSL offers unique in-flight validation data for models of atmospheric entry and material response.

MEDLI recorded, among others, time-resolved in-depth temperature data of PICA using thermocouple sensors assembled in the MEDLI Integrated Sensor Plugs (MISP). These measurements have been widely used in the literature as a validation benchmark for state-of-the-art ablation codes [2,3]. The objective of this work is to perform an inverse estimate of the MSL heatshield aerothermal environment during Mars entry from the flight data. The Porous material Analysis Toolbox based on OpenFOAM (PATO) software [4,5,6] is used to perform the inverse analysis. PATO models PICA ablation by solving the conservation equations of solid mass, gas mass, gas momentum and total energy, using a volume-averaged formulation that includes production of gases from the decomposition of the polymeric matrix. Thermodynamic and chemistry properties are computed using the Mutation++ library [7].

Parameters estimation and the inverse problem are handled by the DAKOTA optimization library [8], coupled to PATO. A multi-objective genetic algorithm and a trust-region method for nonlinear least squares are used to estimate key uncertain material parameters that influence the material response model.

We follow the strategy of Mahzari et al [2] by using first the thermocouple driver approach to estimate uncertain parameters of the material model. In this case the temperature is imposed at the location of the shallowest MISP thermocouple. Then, the aerothermal environments (i.e surface temperature and heat flux) at the probes are estimated by fitting the in-depth measured thermocouple response flight measurements.

This work represents an important milestone toward the development of validated predictive capabilities for designing thermal protection systems for planetary probes.

References:

[1] M.J. Wright et al. (2009), *AIAA Paper,* 2009-423.

[2] M. Mahzari et al. (2015), *Journal of Spacecraft and Rockets*, 52.4, 1203-1216.

[3] T.R. White et al. (2013), *AIAA Paper*, 2013-2779.

[4] J. Lachaud and N. N. Mansour (2014), *J Thermophys Heat Tran,* 28, 191–202.

[5] J. Lachaud et al. (2017), *Int J Heat Mass Tran,* 108, 1406–1417.

[6] J. B.E. Meurisse et al. (2018), *Aerosp Sci Technol*, 76, 497-511.

[7] J. B. Scoggins and T. E. Magin (2014), *AIAA Paper,* 2014-2966.

[8] SANDIA (2014), retrieved from https://dakota.sandia.gov/documentation.html on 03/14/18.

PLANETARY PROBE ENTRY MODELS FOR CONCURRENT AND INTEGRATED INTERPLANETARY MISSION DESIGN A. J. Mudek[1]*, K. M. Hughes[2], S. J. Saikia[1], J. A. Englander[2], E. Shibata[1], and J. M. Longuski[1], [1]School of Aeronautics and Astronautics, Purdue University, 701 W. Stadium Ave., West Lafayette, IN, 47907, [2]Navigation and Mission Design Branch, Goddard Space Flight Center, 8800 Greenbelt Rd, Greenbelt, MD, 20771, *amudek@purdue.edu

Introduction: There are many prospective mission opportunities involving atmospheric entry probes. The Planetary Science Deep Space SmallSat Studies (PSDS3) recently selected probe missions to Venus, Mars, and the outer planets as part of the 10 selected studies. Two of the six themes in the most recent New Frontiers call were a Saturn probe and a Venus in situ explorer. The 2013-2022 Planetary Science Decadal Survey includes probe missions at Venus, Mars, Saturn, Titan, Uranus, and Neptune.[1] Across mission destinations and mission classes there is growing interest in planetary probes.

In the early stages, atmospheric probe missions require both an interplanetary trajectory specialist and a probe specialist, often working in separate camps and with limited experience in the other's area of expertise. Interplanetary trajectory specialists select candidate trajectories for the probe and pass the entry conditions on to the probe specialist. The probe specialist then determines if a probe design is feasible for the given trajectory. Sometimes small tweaks to the interplanetary trajectory can make the entry probe feasible, other times the trajectory designer needs to restart the process and pick entirely new interplanetary trajectories. In either case, closing the design is not a simple process and requires many iterations. This iterative design approach is a decoupled solution to a coupled problem, which would be better served by a concurrent design process.

While interplanetary trajectory specialists may like to use a broad sweep of low-fidelity solutions to find a wide array of trajectory options, probe specialists typically start off with mid- to high-fidelity point designs for the entry probe since the equations of motion for atmospheric probes require numerical integration and are so directly linked with some of the probe's subsystem design. Currently, there are no alternatives to this design approach as there are no tools capable of automatically and concurrently designing interplanetary and atmospheric trajectories. Unfortunately, this makes us reliant on point designs in the early stages of the mission design process. The reliance on point designs for atmospheric probes hinders the flexibility of the design, making the design process cumbersome and restricting decision-making down the road. The research presented here addresses this problem by providing low-fidelity models for the automated, rapid design of atmospheric trajectories and probes—models which may be solved concurrently with the interplanetary trajectory.

Methods: The goal of this work is to enable rapid trajectory and probe designs. In order to fit into current trajectory design tools, a two-point shooting architecture is used to model the approach trajectory to the body of interest. This two point shooting technique is used by many tools such as Goddard's Evolutionary Mission Trajectory Generator (EMTG) software and is depicted in Figure 1.

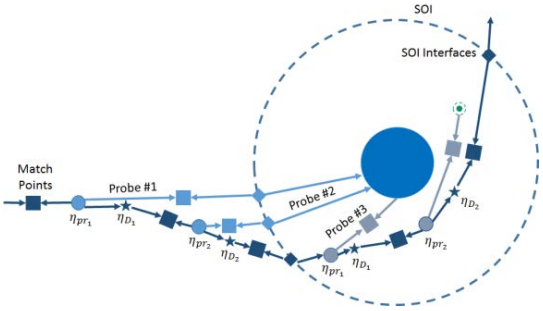

Figure 1 Approach geometry in a two-point shooting architecture. The stars represent maneuvers and the circles represent probe release points.

The models are formulated as a nonlinear programming (NLP) problem so that they may be solved using sequential quadratic programming (SQP)—in this case, SNOPT. Accordingly, the models are analytical, continuous, and differentiable. In order to fit into SQP solvers, we first must have an analytical atmospheric trajectory model.

In 1958, Allen and Eggers created the first analytical equations of motion for ballistic missiles.[2] These equations, however, were derived to describe missile trajectories at Earth and assume a constant flight path angle. This assumption works well for steep flight path angles, but loses accuracy at shallower flight path angles.

Following Allen and Eggers, further analytical work in atmospheric entry was developed in the 1960's by Loh[3,4,5] and Yaroshevskii[6,7]. Loh devised a generalized solution for ballistic entry as well as for lifting bodies (with constant lift-to-drag) based on simplified entry equations of motion. Yaroshevskii developed semi-analytical solutions based on a circular trajectory assumption, creating equations that work well for shallow flight path angles but lose accuracy at steeper flight path angles. The result of this work was a dichot-

omy of theories divided by shallow versus steep flight path angles.

To address this split in analytical theories, Vinh published a new unified analytical theory capable of addressing shallow and steep flight path angles to greater accuracy—work which was expanded upon by Longuski in the same year.[8,9] Following the work done by Vinh and Longuski, a more robust analytical theory for atmospheric trajectories has been developed by Saikia and Longuski, whose equations provide analytical, continuous, and differentiable functions describing the atmospheric trajectory of a ballistic probe.[10]

Having the analytical trajectory design provides the path of the probe, but this work also performs high-level system design for an atmospheric probe in order to estimate probe mass. The probe mass is approximated as the summation of the scientific payload mass, the thermal protection system (TPS) mass, and the structural mass. A generic probe design is defined assuming a sphere-cone geometry (depicted in Figure 2) based off of flown missions such as the Galileo probe.

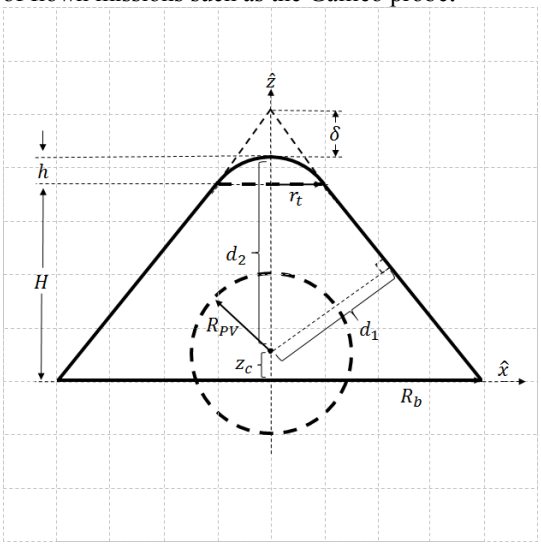

Figure 2 Probe geometry definition in the x-z coordinate plane.

Some aspects of the design, such as the cone angle, are determined by the target body and are known *a priori* while other parameters such as nose radius may be variables within the optimization problem. Much of the TPS and structural mass estimation is based off empirical fits to flown missions as well as high-fidelity simulations from proven software tools. The empirical heating equations combined with the probe geometry formulation and TPS thickness relationships provide an analytical model capable of estimating the total mass of a planetary probe.

Expected Results: The atmospheric trajectory of a planetary probe will be analytically obtained and the atmospheric probe models outlined in this work will provide TPS mass estimates for the probe as well as structural mass estimates for the aeroshell and pressure vessel. When combined with a specified science payload, the result is an estimate of the total probe mass. All of this is computed within a framework capable of being optimized with respect to a number of design variables and capable of being inserted into a number of trajectory design software packages. Probe results at Venus and Neptune will be presented corresponding to missions of interest out of the Planetary Science Decadal Survey.

References: [1] National Research Council (U.S.) Committee on the Planetary Science Decadal Survey (2011) *National Academies Press,* "Visions and Voyages for Planetary Science in the Decade 2013-2022," [2] H. J. Allen and A. J. Eggers (1958) *NACA-TR-1381*, "A Study of the Motion and Aerodynamic Heating of Ballistic Missiles Entering the Earth's Atmosphere at High Supersonic Speeds," [3] W. H. T. Loh (1963) *Prentice Hall*, *Dynamics and Thermodynamics of Planetary Entry*, [4] W. H. T. Loh (1968) *Springer-Verlag*, *Re-Entry and Planetary Entry Physics and Technology I—Dynamics, Physics, Radiation, Heat Transfer, and Ablation*, [5] W. H. T. Loh (1962) *Journal of Aerospace Sciences*, "A Second-Order Theory of Entry Mechanics into a Planetary Atmosphere," [6] V. A. Yaroshevskii (1964) *Kosmicheski Issledovaniya*, "The Approximate Calculation of Trajectories of Entry into the Atmosphere I," [7] V. A. Yaroshevskii (1964) *Kosmicheski Issledovaniya*, "The Approximate Calculation of Trajectories of Entry into the Atmosphere II," [8] N. X. Vinh, A. Busemann, and R. D. Culp (1980) *The University of Michigan Press*, *Hypersonic and Planetary Entry Flight Mechanics*, [9] J. M. Longuski and N. X. Vinh (1980) *PhD Dissertation University of Michigan*, "Analytical Theory of Orbit Contraction and Ballistic Entry into Planetary Atmospheres," [10] S. J. Saikia and J. M. Longuski (2015) *PhD Dissertation Purdue University*, "Analytical Theories for Spacecraft Entry into Planetary Atmospheres and Design of Planetary Probes"

6-DoF CFD Simulations of Cobra Mid-L/D Rigid Vehicle Ballistic Range Test. B. E. Nikaido[1] and J. A. Garcia[2], [1]MS 258-1, NASA Ames Research Centern Moffett Field, CA 940235

Introduction: Six Degree-of-Freedom (6-DoF) Computational Fluid Dynamics (CFD) simulations were conducted in support of a 0.5% scale ballistic range test of NASA's Cobra Mid-L/D Rigid Vehicle (MRV) Mars entry concept[1] which was performed to improve the current control system design of the CobraMRV concept[2]. These simulations supported ballistic range tests conducted at the US Army's Aberdeen Proving Grounds. The ballistic range tests were conducted at an initial Mach of 3 and investigated the vehicle's dynamic stability in the supersonic regime. The 6-DoF simulations were obtained from the Kestrel CFD software[3] and were utilized to assist in pretest configuration evalutations, including predicted pitch dynamics. In addition, Kestrel simulations were performed on post-test results in order to help understand an unexpected large pitch oscillation observed during the ballistic range test.

References: [1] Cerimele C. J., Robertson A. R., Sostaric R. R, Campbell C.H., Robinson P., Matz D. A., Johnson B. J., Stachowiak S. J., Garcia J. A., Bowles J. V., Kinney D. J. and Theisinger J. D. (2017) *AIAA SciTech Forum,* AIAA 2017-1898. [2] Johnson B.J., Cerimele C.J., Stachowiak S.J., Sostaric R. R., Matz D.A., and Lu, P., (2017) *AIAA SciTech Forum,* AIAA 2018-0615. [3] Morton S.A, (2012) kestrel

POST-FLIGHT RECONCILIATION MODELING FOR THE ADVANCED SUPERSONIC PARACHUTE INFLATION RESEARCH AND EXPERIMENT (ASPIRE) PROGRAM. M.E. Pizzo[1], S. Dutta[2], A.L. Bowes[2], and E.M. Queen[2], [1]Old Dominion University, Norfolk, VA, USA; mpizzo@odu.edu., [2]NASA Langley Research Center, Hampton, VA 23681.

Introduction: The Advanced Supersonic Parachute Inflation Research and Experiment (ASPIRE) Program began in 2016 following its predecessor, the Low-Density Supersonic Decelerator (LDSD) Program. LDSD started in 2012 with the objective to design and demonstrate performance of improved supersonic aerodynamic decelerator technologies, such supersonic inflatables, which may be required to successfully land future robotic and manned spacecraft on Mars [1-3]. ASPIRE follows the work of LDSD but focuses on the performance of the supersonic parachute, especially during the inflation phase. For both LDSD and ASPIRE, pre-flight prediction of vehicle performance and targeting flight constants to reach experimental phase were conducted via high fidelity flight dynamics simulations. One of these flight dynamics simulations was the Program to Optimize Simulated Trajectories II (POST2) [4]. POST2 is a generalized point mass, rigid body, discrete parameter targeting and optimization trajectory simulation program that can model multiple, six degree-of-freedom vehicles within and above an atmosphere.

LDSD Program. Two LDSD supersonic flight dynamics flight (SFDT) tests were performed in 2014 and 2015 off the coast of Hawaii. For the first flight, the nominal conditions predicted the vehicle to accelerate to Mach 4, despin and deploy a supersonic inflatable aerodynamic decelerators (SIAD), and at approximately Mach 2.5 deploy a supersonic disksail parachute that would decelerate the vehicle until the vehicle splashdowned in the ocean [2]. The second LDSD flight followed a similar concept of operations, but instead of a disksail parachute, the vehicle deployed a ringsail parachute [3]. In both LDSD flights, the disksail and ringsail parachutes were designed to handle loads during inflation at speeds greater than Mach 2. However, in both flights, the parachutes developed large tears in the fabric and failed to deploy successfully [2, 3]. These failures, along with other off-nominal flight behaviors, led to questions regarding the understanding of parachute inflation and vehicle flight dynamics at Mars-like conditions.

ASPIRE Program. The ASPIRE Program developed as a way to answer questions surrounding the parachute failures and off-nominal flight conditions of the two LDSD flights. The program objective was to understand the inflation and peak load performance of supersonic parachute designs. The program involves a series of sounding rocket flight tests deploying various supersonic parachute designs both at flight conditions near and exceeding previous Mars missions.

Motivation: Following the two LDSD flights, trajectory and flight performance were reconstructed using flight data. Moreover, to characterize the off-nominal conditions seen in the two LDSD flights, the POST2 pre-flight trajectory predictions were then compared against the reconstruction models to reconcile the off-nominal conditions observed during flight. The idea behind reconciliation is to understand what conditions in the pre-flight models of vehicle characteristics lead to performance that would match the post-flight reconstruction. The reconciliation efforts provided better understanding of the simulation models and behavior of the vehicle during flight and suggested changes to models that were made for future flights [2, 3].

Proposal: This work aims to follow the reconciliation efforts from LDSD for the ASPIRE SR01 and SR02 flights. SR01 flew in October 2017 and SR02 is scheduled for March 2018. For both SR01 and SR02, pre-flight vehicle performance and targeting of mortar fire trigger needed to reach the desired parachute performance were modeled with several flight dynamics tools, including POST2. This work will compare the reconstructed post-flight conditions to the pre-flight trajectory predictions from POST2 and reconcile any potential off-nominal flight conditions. The ASPIRE reconstruction efforts can significantly improve the understanding and accuracy of trajectory simulations and parachute performance as well as provide design recommendations for future ASPIRE flights currently scheduled later in 2018. Results will be presented for the ASPIRE flights in a poster format.

References: [1] I. Clark and E. M. Blood, *"Low-Density Supersonic Decelerator (LDSD) Supersonic Flight Dynamics Test-1 (SFDT-1) Post-Test Report*," JPL Document D-81940, NASA Jet Propulsion Laboratory, California Institute of Technology, Pasadena, CA, 2015. [2] S. Dutta, A. L. Bowes, S. A. Striepe, J. L. Davis, E. M. Queen, E. M. Blood, and M. C. Ivanov, "*Supersonic Flight Dynamics Test 1 – Post-Flight Assessment of Simulation Performance*," 25th AAS 15-219, AAS/AIAA Space Flight Mechanics Meeting, Williamsburg, VA, 2015. [3] S. Dutta, A. L. Bowes, J. P. White, S. A. Striepe, E. M. Queen, C. O'Farrell, and M. C. Ivanov, "*Post-Flight Assessment of Low Density Supersonic Decelerator Flight Dynamics Test 2 Simulation*," AAS 16-222, 26th AAS/AIAA Space Flight Mechanics Meeting, Napa, CA, 2016. [4] S. A. Striepe et al., "Program To Optimize Simulated Trajectories II (POST2): Utilization Manual." Vol. II, Version 4.1., 2018.

Dynamics of FiberForm Oxidation. Savio J. Poovathingal, Min Qian, Vanessa J. Murray, and Timothy K. Minton. Department of Chemistry and Biochemistry, Montana State University, Bozeman, MT, USA 59717. savio.poovathingal@montana.edu.

Introduction: Understanding the oxidation mechanisms of ablative heat shields is key to reliable design with low uncertainties. Phenolic Impregnated Carbon Ablator (PICA) used in Stardust and Mars Science Laboratory (MSL) missions consists of a network of carbon fibers, called FiberForm, impregnated with phenolic resin. Pyrolysis of the resin exposes FiberForm to atomic oxygen in the hypersonic boundary layer, which can result in surface and in-depth oxidation [1]. The oxidation dynamics of FiberForm with ground-state atomic oxygen has been investigated in the temperature range of 1023-1823 K. This effort follows a similar study that investigated the oxidation of vitreous carbon [2] and highly oriented pyrolytic graphite (HOPG) [3] in our laboratory and is part of a broad effort to understand the oxidation of carbon surfaces relevant to atmospheric entry missions and hypersonic flight. The experimental results are being used to develop finite-rate models for CFD [4].

Experimental Method: The experiments were performed with a laser-detonation molecular beam source that produced ground-state O and O_2 with a mole ratio of 92:8 and a nominal velocity of 8 km s^{-1}. The FiberForm sample was resistively heated using a custom-designed sample mount [2]. The products that non-reactively scatter or reactively desorb from the surface were recorded with a rotatable mass spectrometer detector operating in a pulse counting mode. The primary data are number density distributions as a function of arrival time at the detector, which are referred to as the time-of-flight (TOF) distributions. These distributions allow the simultaneous characterization of the products and the timescale of the reactions.

Results: The TOF distributions of the four species that were detected as a function of FiberForm temperature are shown in Figure 1. The dominant reactive product is CO, while CO_2 is a minor product of the reaction. CO exhibits an apparent non-Arrhenius behavior where the product intensity reaches a plateau at the higher temperatures. Analysis of the O_2 signals suggests that they arise from non-reactive scattering of the 8% O_2 that is present in the beam. The non-reactive signals from O exhibit impulsive scattering (IS) and thermal desorption (TD) components, and the TD component increases with surface temperature. Theoretical work [5] suggests that the formation of CO occurs through the participation of adsorbed O atoms on the carbon surface. Comparing the signals of CO and O indicates a competition between the formation of CO and the desorption of O. The increasing desorption rate of O with surface temperature reduces the O-atom reagents available to produce CO, thus limiting the formation of CO at higher temperatures. The apparent non-Arrhenius behavior of CO arises from these competing processes. The signals of O and CO exhibit hysteresis with respect to temperature, and they have opposing trends (Figure 2). The TOF distributions of CO demonstrate that CO exits the sample promptly or after relatively long residence times. Two populations of CO with long residence times were distinguished (Figure 3). Qualitatively, similar results have been observed in analogous molecular beam studies of vitreous carbon and HOPG, indicating that the oxidation mechanisms on sp^2 carbon surfaces are chemically similar and that the main differences arise from the morphology of the composites.

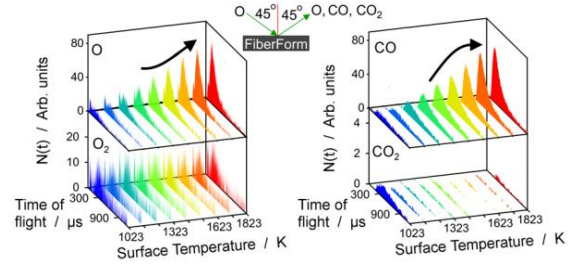

Figure 1: TOF distributions of O, O_2, CO, and CO_2.

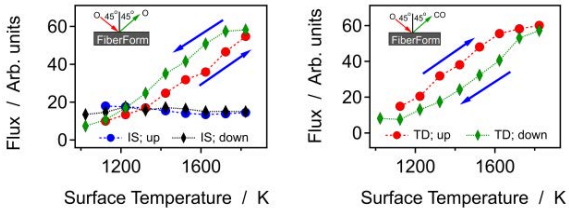

Figure 2: Flux of O and CO for increasing temperature (up) and decreasing temperature (down).

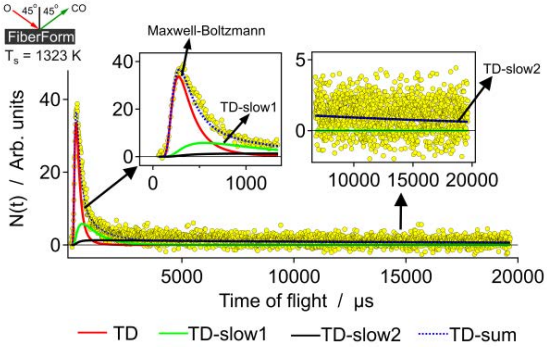

Figure 3: Timescales of three populations of CO formation.

Acknowledgments: Financial support was provided by NASA under Grant No. NNX15AD77G.

References: [1] Lachaud et al., J. of Spacecrafts and Rockets (2010), 47, 910-921. [2] Murray et al., J. Phys. Chem. C (2015), 119, 14780-14796. [3] Murray et al., J. Phys. Chem. C (2018), doi: 10.1021/acs.jpcc.7b11772. [4] Poovathingal et al., AIAA J. (2017), 55, 1644-1658. [5] Sun et al., J. Phys. Chem. C (2018), 115, 4730-4737.

AEROGRAVITY ASSIST MANEUVER VARIABILITY ANALYSIS USING GLOBAL REFERENCE ATMOSPHERE MODELS. S. R. Pujari[1] E. G. Lightsey[2] and M. J. Holzinger[3], [1]Graduate Student, Georgia Institute of Technology, spujari21@gatech.edu, [2]Professor, Georgia Institute of Technology, glenn.lightsey@gatech.edu, [3]Associate Professor, Georgia Institute of Technology, holzinger@ae.gatech.edu, 270 Ferst Drive, Atlanta, GA, 30332, USA

Deep space maneuvers such as planetary gravity assist (GA) flybys have been extensively used in historical interplanetary missions to reduce travel time and conserve spacecraft resources. The transfer of momentum from a planet to a spacecraft changes both the direction and magnitude of the spacecraft's heliocentric velocity vector and effectively bends the hyperbolic trajectory. Infrequent planetary flyby configurations meet requirements that are necessary to reach the outer planets as they are limited by launch energies, flyby periapsis, and geometric opportunities.

Analogous to a gravity-assist flyby, an aerogravity assist (AGA) maneuver, first proposed by Randolph and McRonald [1][2], performs a gravity assist flyby at a periapsis altitude low enough to enter the atmosphere of the planetary body. By allowing a spacecraft to flyby at a lower periapsis radius and by augmenting the aerodynamic forces generated on the spacecraft with the planet's centripetal acceleration, an AGA allows for an increase in the bending angle. Despite their promise, AGAs are challenging due to the extreme entry environment faced. The waverider vehicle, first introduced by Nonweiler [3], provides a high lift-to-drag ratio (L/D) and could survive the high aerodynamic and heating loads – thus enabling AGA maneuvers to become feasible. Although an AGA has never been demonstrated on a flight mission, many previous studies on its feasibility, optimization of trajectories, and simulations of vehicle body shapes can be found in the literature [6][7].

This paper contributes to the subject of AGA maneuvers by studying the effects of atmospheric variability on the trajectory through the use of higher fidelity atmospheric density models. Past studies have mainly used exponential scale models of the atmospheric density, which introduces greater risk. This risk can be reduced by utilizing NASA Marshall Space Flight Center's Global Reference Atmospheric Models (GRAM). GRAM is synthesized from collected climatology data and/or precomputed science models which simulate the perturbations and time variations of the atmosphere [8]. A Monte Carlo simulation framework is constructed to simulate the stochastic nature of the atmosphere by incorporating results from GRAM. The trajectory is then propagated through the variable atmosphere to get distributions for exit conditions. AGA maneuvers for this analysis are considered for three inner solar system bodies: Earth, Mars, and Venus.

Significant work regarding AGA trajectory feasibility and optimization has also occurred, each with differing levels of dynamics and controls modeling. For this analysis, atmospheric entry dynamics for a non-thrusting, lifting vehicle are modeled using 3-DOF spherical equations of motion assuming a point mass vehicle flying over a rotating planet with the atmosphere fixed to the planet surface [4][5]. Since this analysis focuses on the effects of the atmospheric variability, a fixed, constant, and downward-pointing bank angle is assumed to characterize the variations.

Validation of the trajectory model is done by selecting initial states that previous AGA trajectory analyses have used. For example, Hess and Mooij used the Mars flyby entry condition states for the Rosetta mission [6] and those same states are used in the analysis. During the AGA maneuver, after atmospheric entry, a constant altitude was reached by the vehicle and the flight path angle remained at zero. However, a lower altitude AGA maneuver is obtained in Hess and Mooij's results which could be due to the use of optimal control of the bank angle; in contrast, this simulation assumes a constant bank angle throughout the maneuver. The general shape and order of magnitude are similar for both maneuvers, confirming the validity of the propagator.

When extending this simulation to all three planets, the gravity, atmosphere, aerodynamic, G-loading, and heating values are computed over the course of the trajectory to assess the feasibility of the trajectory design. To compare the various trajectories, the bending angle of the velocity vector was deemed as a good figure of merit and computed by the methodology detailed by Casoliva et al [7]. Initial results for Mars using the exponential atmospheric model, the velocity vector bending angle was 450% greater for an AGA than for a GA at the same periapsis altitude. The GRAM Monte Carlo simulation produces mean and standard deviation of the bending angles, relevant model parameters, and atmospheric entry/exit altitudes that are tabulated.

Sensitivity studies on the exit hyperbolic velocity and bending angle are performed on varying entry velocity magnitude, vehicle L/D ratio, ballistic coefficient, and three different planetary atmospheres.

The results presented in this paper will enable future mission planners to understand the trends of these mission input parameters with more robust consideration given towards atmospheric variability during an aerogravity assist maneuver around bodies with an atmosphere.

[1] J.R. and D. M., A., (1992) Journal of Spacecraft and Rockets, 29, 05 [2] D. M. and J.R., (1992) Journal of Spacecraft and Rockets 29, 05 [3] T. N, (1959) The Journal of the Royal Aeronautical Society, 63, 585, 521-528. [4] N. V., et al., (1980) University of Michigan Press [5] J. C. and R. B., (2007) Georgia Institute of Technology, Masters. [6] J. H. and E. M., (2017) AIAA SciTech Forum. [7] J.C., et al., (2008) AIAA GNC [8] A. D, et al., (2005) AIAA Aerospace Sciences Meetings

A COMPARISON OF DIFFERENT FILTERING TECHNIQUES APPLIED TO AUTONOMOUS NAVIGATION USING X-RAY PULSARS. Vishal Ray[1], Sachin Patwardhan[2], Arnab Maity[3], Hari B. Hablani[4]
[1]University of Colorado Boulder (Vishal.Ray@colorado.edu),[2]Indian Institute of Technology (IIT) Bombay (sachinp@iitb.ac.in), [3]Indian Institute of Technology (IIT) Bombay (arnab@aero.iitb.ac.in), [4]Indian Institute of Technology (IIT) Indore (hbhablani@iiti.ac.in)

Introduction: Navigation is one of the most crucial subsystems of a spacecraft as most of its operational sequence is dependent on its position and velocity. Over the last three decades, GPS has been predominantly used for providing autonomous navigation of satellites in the Low Earth Orbit (LEO) regime. New developments in GPS receivers are allowing the possibility of using GPS up to geosynchronous altitudes [1]. But beyond a certain altitude in deep space, GPS receivers are rendered ineffective for navigational solution. Ground based methods, the primary navigation method for interplanetary missions are subject to degrading accuracy as the spacecraft moves farther away from Earth. There is also the issue of time delay associated with relaying the processed solution to the spacecraft which can be of concern with increasing distance. Therefore, there is a need for alternate navitation schemes which can complement existing methods in providing an autonomous navigation solution.

In the recent years, there has been a growing interest in developing a navigation method based on signals received from X-ray pulsars. The extreme rotational stability of a certain class of pulsars called millisecond pulsars allows a very accurate prediction of the pulse arrival times at an inertial location, making this method a promising alternative. Experimental demonstrations in the past few years have proven the feasibility of using pulsars for navigation [2,3]. The main advantage of this method for deep space missions is the autonomy it provides to the spacecraft in terms of its navigational capability.

In this research, we study recursive estimation of spacecraft states using signals from X-ray pulsars. The available literature on pulsar based navigation makes use of the extended Kalman filter (EKF) [4,5] and unscented Kalman filter (UKF) [6]. Over the last few decades however, there have been many developments in the area of nonlinear Bayesian state estimation. In particular, smoothing techniques [7], which use current measurements to improve state estimates in the past, can approach the accuracy of the complete data arc processed in a batch. A salient feature of pulsar based navigation is time varying standard deviation of the measurement noise. The precision of the measurements improves as the time progresses. As we show in this work, smoothing done over even a single time step [8], serves to be an important tool in such a scenario and provides a vast improvement in accuracy of the estimated state trajectory over EKF [9].

The smoothing based pulsar navigation is implemented on the Lunar Transfer Trajectory (LTT) phase of Chandrayaan-2, Indian Space Research Organization's (ISRO's) planned mission to Moon. Gravitational forces due to Earth, Moon and Sun, and solar radiation pressure (SRP) are included in the filter model. A cannonball model is used to model SRP. However, a cannonball model, though extensively used, does not capture the forces perpendicular to the sun and hence leads to unmodelled accelerations in the filter [10]. Coming up with an accurate model of SRP is difficult since it depends on the interaction of the spacecraft surface with photons from the Sun which can vary over time with solar activity and as the spacecraft spends more time in space. In such a case, simply estimating parameters such as the radiation drag coefficient does not suffice since the parameters are time varying and they may not all be observable. We model these accelerations as a first order Gauss-Markov process with the process noise and time constant as tuning parameters [10]. Such a dynamic model compensation (DMC) prevents the filter from saturating and gives improved state estimates.

Finally, we tackle the problem of numerical issues in the filter as the state vector grows in length. In the pulsar navigation method, along with estimating the states and parameters related to the state dynamics, various measurement model parameters such as the position of the pulsars also need to be estimated. The covariance for these parameters may vary by orders of magnitude rendering the overall covariance matrix ill-conditioned. Working with the square root of the information matrix in such a case makes the filter numerically robust by getting rid of the covariance matrix inverse and reducing the condition number by half. The square root information filter (SRIF) is therefore used to avoid numerical instabilities which can develop in the Kalman filter with time [11,12].

References:

[1] Winternitz, Luke et al. (2016) *Annual AAS Guidance, Navigation and Control Conference, 39.*

[2] Zhang, Xinyuan (2017), *International Journal of Aerospace Engineering, 2017.*

[3] L.M.B Winternitz et al. (2016), *IEEE Aerospce Conference,* 1-11.

[4] Sheikh, S.I. and Pines D.J (2006) *Navigation, 53,* 149-166.

[5] Du, Jian et al. (2012), *Procedia Engineering, 29,* 4369-4373.

[6] Wang, Yidi et al. (2013), *Advances in Space Research, 51,* 2394-2404.

[7] Jazwinski, A.H. (1970), *Stochastic Process and Filtering Theory.*

[8] Wishner, R.P. et al. (1969), *Automatica, 5,* 487-496.

[9] Ray, Vishal (2017), *Master's thesis, IIT Bombay.*

[10] Tapley et al. (2004), *Statistical Orbit Determination*, 230-233.

[7] McMahon, Jay and Scheeres, Daniel (2015), *JGCD*, *38,* 1366-1381.

[11] Dyer, P. and McReynolds, S. (1969), *J. Optim. Theory Appl., 3,* 444-458.

[12] Kaminski, P.G. et al. (1971), *Trans. Auto. Cont., AC-16,* 727-735.

Multi-Fidelity Modeling for Efficient Aerothermal Prediction of Hypersonic Inflatable Aerodynamic Decelerators M. Santos[1], A. Hinkle[2], S. Hosder[3], and T. K. West[4], [1]Missouri University of Science and Technology, Department of Mechanical and Aerospace Engineering, ms474@mst.edu , [2] Missouri University of Science and Technology, Department of Mechanical and Aerospace Engineering, ah896@mst.edu, [3] Missouri University of Science and Technology, Department of Mechanical and Aerospace Engineering, hosders@mst.edu, [4] NASA Langley Research Center, Vehicle Analysis Branch, thomas.k.west@nasa.gov.

Introduction and Motivation: Over the past few years, cutting edge deployable re-entry technologies have been developed that allow for an increase in mission possibilities and flexibility over that of rigid aeroshells by allowing for an increase in possible landing sites and increasing the maximum deliverable payload mass to the surface of multiple planets in our solar system such as Mars, Venus, and Titan. These technologies include NASA's Hypersonic Inflatable Aerodynamic Decelerator (HIAD) and the Adaptable Deployable Entry and Placement Technology (ADEPT) shown in Fig 1. The entry, descent, and landing (EDL) phase is one of the most dangerous phases of any space mission because of the significant aeroheating experienced by the vehicle due to the high entry velocities. Accurate prediction of the surface heat flux experienced by the vehicle is needed to ensure that a thermal protection system (TPS) is in place that is designed to withstand this heating. The system also needs to be robust and reliable, which can be achieved through extensive laboratory testing or through uncertainty quantification (UQ) integrated to the analysis and design.

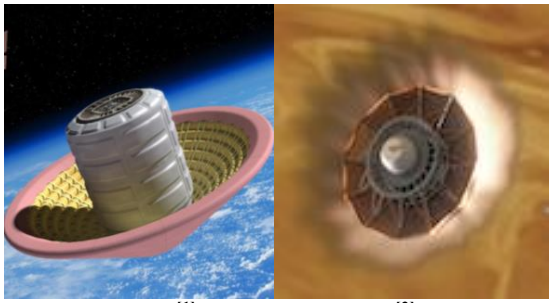

Figure 1. HIAD[1] (left) and ADEPT[2] (right) conceptual designs.

The flow conditions seen by hypersonic vehicles many times cannot be re-created in the laboratory and thus one must turn to computer modeling. Unfortunately, high-fidelity computational fluid dynamics (CFD) and thermal response simulations can be computationally very expensive due to the complex physics seen at these flow regimes (turbulence modeling, non-equilibrium thermo-chemistry, radiation heat transfer, etc.) and may not be practical for direct use in the analysis, design, and reliability assessment under uncertainty with traditional UQ approaches such as Monte-Carlo, which generally requires a large number of simulations. Multi-fidelity modeling approach is uniquely suited to solve this problem, however has not been explicitly investigated for use in the study of re-entry vehicles. Surrogate modeling of high-fidelity CFD simulations has been previously used to reduce computational cost [3] however multi-fidelity modeling offers an alternative method that achieves the accuracy of high-fidelity simulations but at a much reduced computational cost. The main idea behind multi-fidelity surrogate modeling is to combine a large number of data points from low and mid-fidelity models with a small number of data points from the high-fidelity models in a way that obtains a corrected model which maintains the accuracy of the high-fidelity model while reducing the computational cost as illustrated in Fig. 2. **The objective of this poster** is to give an overview of implementation and demonstration of surrogate-based methods for multi-fidelity modeling of convective heating, surface pressure, and skin-friction prediction for HIAD technologies.

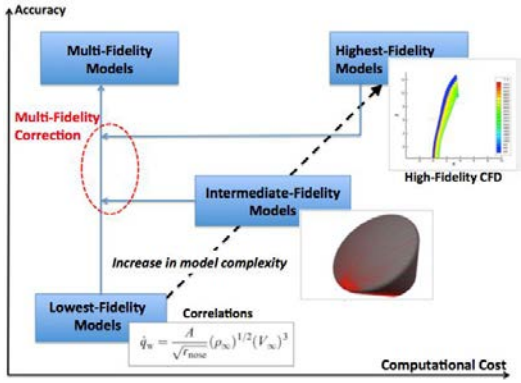

Figure 2. Accuracy vs. computational cost.

Approach: To predict the aerothermal response of HIAD geometries, currently the co-Kriging multi-fidelity method is investigated. This method includes determining the samples from the design space, evaluating the low-fidelity model, evaluating the high-fidelity model, and finally building the co-Kriging multi-fidelity model.

Trajectory and Sample Space. To model the aerothermodynamic response of a 18.8 m diameter HIAD geometry in Mars entry, the different possible trajectories seen by the geometries must first be determined. To determine these trajectory ranges a six degree-of-freedom (DOF) model was used to calculate the velocity altitude profiles, including the maximum deceleration and heating locations, for a range of vehicle masses and entry velocities at ballistic entry. Using NASA's exploration feed-forward [4] (EFF) study as a guide, a velocity range of 3.35 to 7.3 km/s and a mass range of 7.2 to 40 MT was used in the six DOF trajectory model. The resulting trajectories are shown in Fig. 3. The velocity-density space used in the study is illustrated by the red dashed lines in Fig. 3. This region was chosen as the design space because it captures the locations of the maximum heating while maintaining reasonable velocity-density combinations. Finally, vehicle nose is used as a third design variable. The nose radii used in this

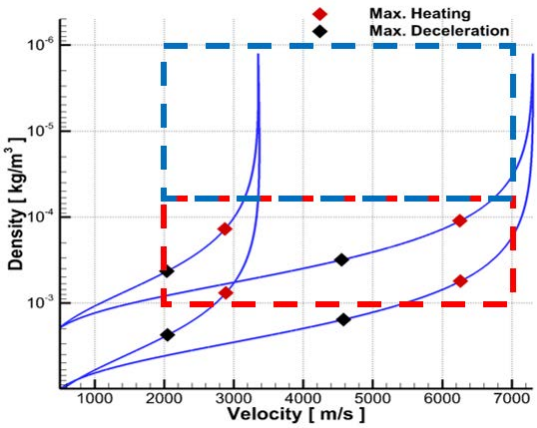

Figure 3. HIAD trajectory range for ballistic Mars entry.

study, again determined using NASA's EFF study as a guide, ranges from 4 to 20 meters.

Low-Fidelity Model. The primary function of the low-fidelity code is to provide a fast, correlation based prediction of the heat flux on an arbitrary blunt body at given flight conditions. This heat flux prediction is based first upon the stagnation point heating, which is assumed to be at the centerline of the body for this study. The stagnation heating is found using a Fay-Riddell correlation with a laminar boundary layer in thermo-chemical equilibrium and a fully catalytic wall. The heat transfer at the stagnation point is found using,

$$q_w = 0.76Pr^{-0.6}(\rho_e\mu_e)^{0.4}(\rho_w\mu_w)^{0.1}\sqrt{\left(\frac{du_e}{dx}\right)_e}(h_{0e}-h_w)\times\left[1+(Le^{0.52}-1)\left(\frac{h_d}{h_{0e}}\right)\right] \quad (1)$$

Where,

$$\frac{du_e}{dx} = \frac{1}{R_n}\sqrt{\frac{2(P_e-P_\infty)}{\rho_e}} \quad (2)$$

The equation assumes a laminar boundary layer in thermo-chemical equilibrium with a fully catalytic wall. The flow field parameters (density, velocity, pressure, and temperature) directly behind the shockwave are assumed to be the conditions at the boundary layer edge. For heating downstream of the stagnation point, correlations for the ratio of heating at an arbitrary point to the stagnation point are used [5].

High-Fidelity Model. For the high-fidelity data, the LAURA CFD software of NASA was used to determine the convective stagnation point heating. The LAURA software utilizes an upwind relaxation algorithm and includes grid adaptation to effectively capture and model the shockwave. For all data points, the geometries used a fixed base radii, shoulder radii, half-cone angles, and shoulder angles of 9.4 meters, 0.47 meters, 70 degrees, and 70 degrees, respectively. These values were chosen as they correspond to typical geometry values for the HIAD vehicle.

The grids used had cell dimensions of 96x64, with 96 cells in the direction perpendicular to the surface and 64 cells in the direction parallel to the surface. The solutions utilized a 10 species model with a super-catalytic, cold wall condition using a two temperature model. A typical grid and flow solution for the temperature is shown in Fig. 4. Both the L2 norm and convective stagnation heating history were used to determine if a converged solution was obtained. A solution was considered converged if the L2 norm was below 10-12 and if there was minimal change in the convective stagnation heating over the previous 100,000 iterations.

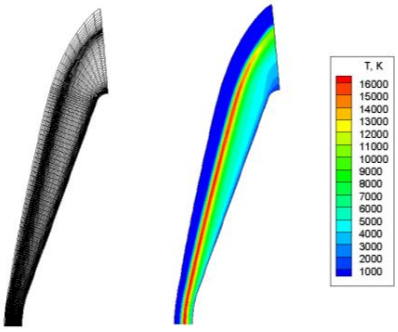

Figure 4. Typical 96x64 grid and flow solution using LAURA CFD program.

Multi-Fidelity Model. In co-Kriging modeling the Kriging method is applied twice to a set of low and high fidelity data. First the Kriging method is applied to the low-fidelity data to create a surrogate model of the low-

fidelity data, then it is applied again to the difference model between the high-fidelity model and low-fidelity surrogate [6].

Kriging models are surrogate models used to interpolate an unknown function, *f*, given n number of data points. Specifically, in Kriging models the interpolated data points are modeled by a Gaussian process in the form of $\mathbf{y}=\mu+\mathbf{b}\boldsymbol{\Psi}$, where $\mathbf{y}$ is a column vector of model responses, μ is the maximum likelihood estimate (MLE), $\mathbf{b}$ is a column vector of coefficients, and $\boldsymbol{\Psi}$ is a correlation matrix between the sampled data points, $\mathbf{x}^{(i)}$, predicted data points, $\mathbf{x}^{n+1}$, with k dimensions. In the Kriging approach, each element of $\boldsymbol{\Psi}$ is radial basis functions of a specific form given in Eq. (3).

$$\psi^{(i)} = \exp\left(-\sum_{j=1}^{k} \theta_j \left| x_j^{n+1} - x_j^{(i)} \right|^{p_j}\right) \quad (3)$$

Thus the covariance matrix for the low-fidelity data is given by,

$$\mathrm{Cov}(\mathbf{y},\mathbf{y}) = \sigma^2 \Psi \quad (4)$$

And the covariance matrix for the difference model is given by,

$$\boldsymbol{C} = \begin{pmatrix} \sigma_c^2 \boldsymbol{\Psi}_c(\boldsymbol{X}_c\boldsymbol{X}_c) & \rho\sigma_c^2 \boldsymbol{\Psi}_c(\boldsymbol{X}_c\boldsymbol{X}_e) \\ \rho\sigma_c^2 \boldsymbol{\Psi}_c(\boldsymbol{X}_e\boldsymbol{X}_c) & \rho^2\sigma_c^2 \boldsymbol{\Psi}_c(\boldsymbol{X}_e\boldsymbol{X}_e) + \sigma_d^2 \boldsymbol{\Psi}_d(\boldsymbol{X}_e\boldsymbol{X}_e) \end{pmatrix} \quad (5)$$

The multi-fidelity model is then constructed by optimizing theta, P, and rho to maximize the likelihood estimate for both the low-fidelity and difference model surrogate. The co-Kriging model can then be queried at any point in the sample domain to obtain a prediction of the high-fidelity model.

Preliminary Results: To build the co-Kriging models, 1,000 low-fidelity training points linearly spaced across the sample space were used. For the high-fidelity training points, 30 locations were used determined by an adaptive sampling scheme. Twelve random test points were selected at which to compare the performance of the multi-fidelity model against the low and high-fidelity models.

For the convective heating, both the low and high fidelity heating profiles were scaled by the stagnation point heating then parameterized using Hicks-Henne bump functions, with 22 control points and a bump width factor of 100. The width and location of each bump was kept constant and a co-Kriging model was built for each bump amplitude resulting in 22 co-Kriging models for each bump amplitude and 1 co-Kriging model for the stagnation point heating. The results for the convective heating profile at a randomly selected test point of a velocity of 6.08 km/s, density of $1.24\text{x}10^{-4}$ kg/m^3, and nose radius of 17.91 m is shown in Fig. 5.

The same method used for the convective heating was used for the surface pressure coefficient. The resulting pressure distribution at the same randomly selected test point can be seen in Fig. 6. From Figs. 5 and 6 it can be seen that the co-Kriging model provides an accurate prediction of the LAURA CFD results. The results for this test point are representative of the results for all the test points. Using dual core Intel Xeon 2.2 GHz processors, a single run of the high-fidelity model takes approximately 36 hours, a single run of the low fidelity model takes less than 1 second, and building the co-Kriging model takes 4 hours. Thus the computational cost to build the surrogate model is approximately 1084 cpu hours. However, once built the co-Kriging model requires only 1 to 2 seconds to evaluate.

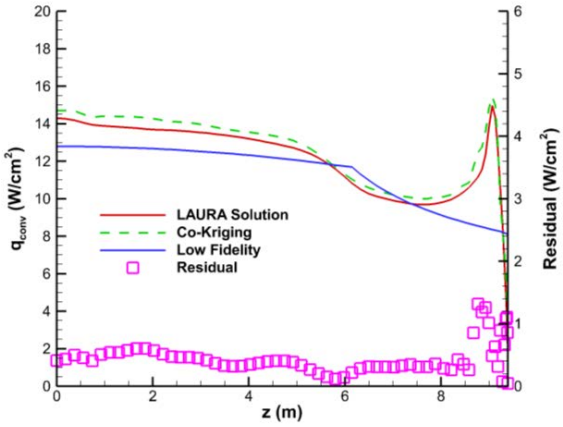

Figure 5. Convective heating prediction at randomly selected test point.

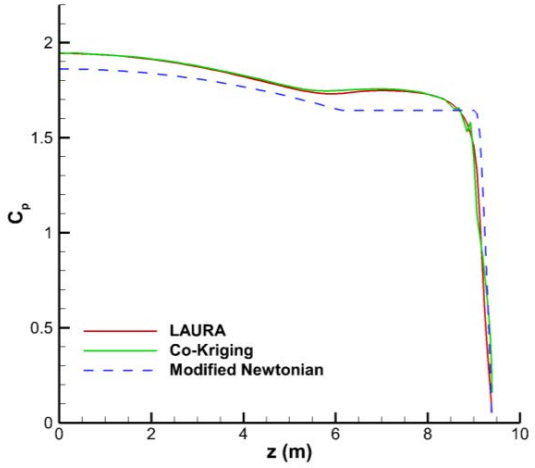

Figure 6. Surface pressure coefficient prediction at randomly selected test point.

References:

[1]http://www.nasa.gov/directorates/spacetech/game_changing_development/HIAD, Accessed: 2017-06-12. [2]https://flightopportunities.nasa.gov/technologies/139, Accessed: 2017-06-12. [3] Brune A. et al. (2015), *JSR, 52, 3*, 776-788. [4] Dwyer-Ciancolo A. et al. (2011) *Tech. Rep. TM-217055,* NASA. [5] Krasnov N.

(1970) *Aerody. of Bodies of Rev*. [6] Forrester A. et al. (2008) *Eng. design via surr. modelling: a practical guide*.

Shock Shape Transition on Spherically Blunted Cones in Hypersonic Flows

J. Martinez Schramm[1], K. Hannemann[2]
German Aerospace Center, DLR, Institute for Aerdynamics and Flow Technology
Spacecraft Department, Bunsenstraße 10, 37073 Göttingen, Germany
[1]Groupleader Aerthermodynamics, Jan.Martinez@dlr.de
[2]Head of Spacecraft Department, Klaus.Hannemann@dlr.de

H.G. Hornung[3]
CALCIT, Caltech, 1200 E. California Blvd, Pasadena, CA91125, USA
[3]hghornung@gmail.com

Introduction: A common shape for re-entry and entry capusules is that of a spherically blunted cone.In flight a transition of the main flow may occur. Depending on the cone angle, the shock shape is either dominated by the spherical nose or the conical part. The transition between these two states can result in undesirable effects on the aerodynamic stability. To understand the shock shape transition behaviour in more detail, a systematic numerical and experimental study is ongoing. In the present article, the influence of vibrational non-equilibrium compared to frozen flow is discussed for sphere-cone configurations at zero degree angle of attack. Wen & Hornung [12] showed that the shock stand-off distance in front of a sphere for a calorically perfect gas is proportional to the density ratio across the shock wave. If we consider the same flow over a sharp cone of a given half-angle, the stand-off distance increases linearly with the desity ration across the shockwave from a critical onset point. Details of this flow are described by Taylor & Maccoll [11]. As the half cone angle is increased beyond the detachment angle, the Taylor-Maccoll solution does not exist and the shock wave is detached. Here we aim to test the theoretical/empirical considerations by performing experiments in the High Enthalpy Shock Tunnel Göttingen, HEG of the German Aerospace Center and by conducting a computational study utilizing the DLR TAU code [10],[7]. The investigations were conducted using a fixed free stream condition and capsule models of varying half-cone angles at zero degree angle of attack. The condition was chosen such that the influence of vibrational excitation on the shock shape transition can be analysed.

Experiment: The HEG of the German Aerospace Center, DLR is a free piston driven shock tunnel which was commissioned for use in 1991 (see e.g. [2], [3], [4], [7]). The HEG operating condition used for the experiments described here is condition XIII. The mean free stream conditions of HEG condition XIII are summerized in Table 1. Detailed calibration of HEG condition XIII revealed that the free stream is in chemical and thermal equilibrium[3], [7].

Ma	ρ	u	T	p
[-]	[g/m^3]	[m/s]	[K]	[Pa]
7.36	26.7	2416	267	2054

Table 1 HEG condition XIII.

The models are made out of aluminium and have a typical mass of 0.5 kg. The present shock shape transition studies were combined with force measurements utilizing the free flight force measurement technique [1], [4].

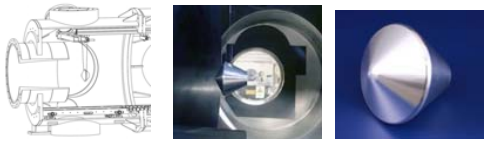

Fig. 1 Schematic (left) and photograph (middle) of the model setup in HEG; photograph of the model (right).

Two small holes of 0.6 mm diameter are drilled into the top at the axial position of the centre of mass and glued plastic threads hold the models at an angle of attack of 0°. The threads are wrapped around a holder installed at the test section ceiling. Fig. 1 (left, middle) shows a schematic and a photograph of the model set-up in the test section. Fig. 1 (right) shows a photograph of the model itself. While the shoulder radius of the capsules is 40 mm, the expansion radius on the shoulder is 4 mm, the nose radius with 16 mm and the base angle with 27° are kept constant the half cone angle is varied between 50° and 75°. Special care was taken to align the models without any yaw with respect to the nozzle exit plane. Upon flow arrival the threads break and the model flies freely during the test. A sequence of Schlieren images showing the detachment process and the free flying phase is given in Fig 2. The free-flight technique in conjunction with optical tracking requires recording high-contrast images of the model during the free flight. From these images the model location and orientation can be evaluated. The tracking algorithm used is based on the algorithm con-

cepts as given e.g. in [9]. The algorithm used for the experiments presented here is described in [1].

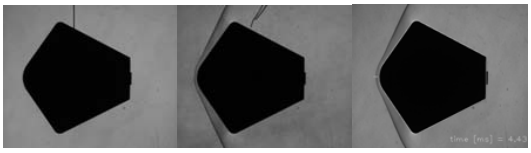

Fig. 2 Visualization of a capsule model prior to the run, at detachment from the threads and during the free flight phase during the test time (from left to right). The white line on the outer contour shows the detected geometry and the white line on the stagnation region the interrogation zone for the shock stand-off distance detection.

Summary: A comparison of the measured and computed shock stand-off distance clearly shows the influence of the different physico-chemical models. The measured values are best fitted by the assumption of a chemical and thermal non-equilibrium flow. However, the com-parison between the chemical equilibrium and non-equilibrium assumption reveals that the chemistry can be considered to be in equilibrium. It is assumed that this effect will be further increased at higher total specific enthalpy conditions where stronger dissociation of the oxygen and nitrogen molecules will occur and the flow is in chemical and thermal non-equilibrium.The paper will present the measurements obtained for shock stand-off distance, shock shape and drag and compare it to the numerical results obtained for chemical/thermal equilibrium and non-equilibrium and discuss the comparison.

References:

[1] Friedl, D., Martinez Schramm, J., Hannemann, K., Measurements by Means of Optical Tracking in the High Enthalpy Shock Tunnel Göttingen, HEG. 8th European Symposium on Aerothermodynamics for Space Vehicles, 02. - 06. March 2015, Lissabon, Portugal, 2015

[2] Hannemann, K., Martinez Schramm, J., Karl, S., Recent extensions to the High Enthalpy Shock Tunnel Göttingen (HEG), Proceedings of the 2nd International ARA Days "Ten Years after ARD", Arcachon, France, 21-23 October, 2008

[3] Hannemann, K., Karl, S., Martinez Schramm, J., Steelant, J., Methodology of a Combined Ground Based Testing and Numerical Modelling Analysis of Supersonic Combustion Flow Paths, Shock Waves, Springer, Volume 20, Number 5, pp. 353-366, 2010

[4] Hannemann, K, Martinez Schramm, J., Karl, S., Laurence, S.J., Enhancement of Free Flight Force Measurement Technique for Scramjet Engine Shock Tunnel Testing, AIAA 2017-2235, 21st AIAA International Space Planes and Hypersonics Technologies Conference Xiamen, China, 2017

[5] Hayes, W.D., Probstein, R.F., Hypersonic flow theory, Academic Press, 1959

[6] Hornung, H.G., Martinez Schramm, J. and Hannemann, K., Sonic line and stand–off distance on re–entry capsule shapes, Proceedings of the 28th International Symposium on Shock Waves held in Manchester UK, 17 to 22 July 2011, Vol 1, Konstantinos Kontis (Ed.), Springer, 2012

[7] Karl, S, Numerical Investigation of a Generic Scramjet Configuration, PhD thesis, Technical University Dresden, 2011

[8] Klomfaß, A., Hyperschallströmungen im thermischen Nichtgleichgewicht, PhD thesis, RWTH Aachen, Berichte aus der Luft- und Raumfahrt, Shaker, 1995

[9] Laurence, S.J., On tracking the motion of rigid bodies through edge detection and least-squares fitting, Exp Fluids, 52(2):387—401, 2012

[10] Schwamborn, D., Gerhold, T., and Heinrich, R., The DLR Tau-Code: Recent Applications in Research and Industry, Proceedings of the European Conference on Computational Fluid Dynamics ECCOMAS, edited by Wesseling, P., Onate, E., and Periaux, J.,TU Delft, The Netherlands, 2006

[11] Taylor, G.I., Maccoll, J.W., The air pressure on a cone moving at high speed, Proc. Roy. Soc., A 139, 278-311, 1933

[12] Wen, C.-Y., Hornung, H.G., Non-equilibrium dissociating flow over spheres, Journal of Fluid Mechanics, 299, 1995

Validation of the KATS Material Response Code with Arc Jet Data O. M. Schroeder[1], J. Cooper[1], H. Weng[1] and A. Martin[1] , [1]University of Kentucky, Lexington KY 40507.

Introduction: Spacecraft planetary entry is a complex, multi-physical and multi-scaled process. In order to provide reliable design margins for sizing thermal protection systems, these must be extensively modeled and tested. Because flight testing is, for the most part, prohibitively expensive, ground testing facilities such as arc jets are used for recreating high enthalpy flow environments encountered during entry. However, due to the cost and difficulty of recreating these environments, it is not statistically feasible to design TPS based solely on experimental data. Furthermore, not every flight condition can be extrapolated to from ground testing. For these reasons, numerical modeling tools are developed for both research (high-fidelity codes) and design.

The Kentucky Aerothermodynamics and Thermal-response System (KATS) [1] is a modified conservation equation solver used for phenomenalogical research in hypersonic gas flow and material response of TPS. Although KATS has been proven to qualitatively predict expected trends for extreme cases such as Stardust, it has not yet been validated against ground testing evironments. The objective of this work is validate the KATS material response solver with experimental data obtained from the NASA Ames AHF and IHF facilities, with Phenolic Impregnated Carbon Ablator (PICA) [2]. Particular attention will be given to unique treatment of the pyrolysis gas transport through momentum equations in contrast to the explicit solution of Darcy's Law for gas velocity employed in most codes. The formulation of the grid advection terms will be explored within the KATS framework, as well as their relative impact on the solutions, see Fig. 1. Finally, the effect multi-dimensionality has on gas transport within orthotropic materials is of interest, particularly regarding the cumulative effect of surface recession and shape change.

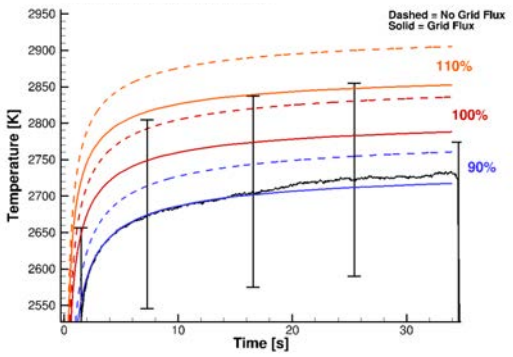

Figure 1: Effect of grid advection fluxes on the surface temperature of a PICA sample exposed to arc jet environment.

However, in order to be able to simulate the multi-dimensional material response of arc jet samples, a flow solver, capable of recreating the boundary layer properties is needed. Thus, the KATS-FD [3] solver is used for recreating surface heating and pressure profiles for the samples, as well as the boundary layer edge properties i.e. enthalpy and chemical composition. This solver is first verified against solutions available in the literature, where a legacy code, Data Parallel Line Relaxation (DPLR), was used for simulating the arc jet flow in the IHF (using the same nozzle)[4].

Although experimental data from ground testing is extremely useful for validation of numerical models, these can also assist in the characterization of some heating facilities. In this work, upon the validation of the KATS code with well characterized heating facilities, the latter is also used for assessing the flow heating environment of the NASA Langly HYMETS facility and thermal response of TPS material samples.

First, flow velocity data obtained using Planar Induced Fluorescence [5] is leveraged to assess the code's prediction of the Mach 5 nozzle flow discharge. Secondly, a parametric study on the effects of the nozzle wall boundary conditions, the nozzle exit geometry and the bulk enthalpy is conducted [6], see Fig. 2.

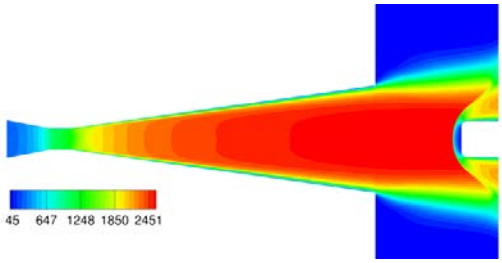

Figure 2: Axial Velocity contours (m/s) from KATS simulation of Mach 5 HYMETS Nozzle.

Finally, the flow and material solvers are used to conduct end-to-end simulations of new data obtained from the HYMETS facility using various types of TPS materials as well as model geometries.

References:

[1] Weng, H. and Martin, A. (2014) *JTHT, 28, No. 4*, 583–597. [2] Milos, F. and Chen, Y. K. (2010) *JSR, 47, No. 5*. [3] Zhang, H. (2015*) Ph.D. thesis*, U. of Kentcuky. [4] Gökçen, T., Balboni, J., Alunni, A. *AIAA 2015-3103*. [5] Düzel, Ü., Schroeder, O. M., and Martin, A. *AIAA 2018-1719*. [6] Inman, J., et al. (2013) *AIAA Journal, 51, No. 10*

DEVELOPMENT OF THE ICARUS MATERIAL RESPONSE SOLVER

Joseph C. Schulz[1], Eric C. Stern[2], Grant E. Palmer[1], Justin B. Haskins[1], Joshua D. Monk[1], Olivia M. Schroeder[1], and David Dang[1], [1]Analytical Mechanics Associates, Inc.,Moffett Field, CA (joseph.c.schulz@nasa.gov), [2]NASA Ames Research Center, Moffett Field, CA, [3]University of Kentucky, Lexington, KY, [4]University of Michigan, Ann Arbor, MI

Abstract: The Entry Systems Modeling (ESM) project, under NASA's Space Technology Mission Directorate (STMD), has been supporting development of a new multi-dimensional material response tool for predicting the performance of spacecraft thermal protection systems (TPS) [1]. Icarus is a parallel, three-dimensional, finite volume material response solver, capable of simulating complex geometries by utilizing unstructured meshes [2]. Figure 1 shows an example of the type of systems that we endeavor to simulate with the new solver. Shown is an arc jet experiment performed in support of the ADEPT entry system. It is evident from this image that material response is highly three-dimensional, with complex features and interfaces. Heritage one-dimensional TPS modeling tools could be used to simulate the material response near the stagnation point, or on the acreage, but would be inadequate for predicting the performance of the full system, in particular near the seams and interfaces. Figure 2 shows a demonstration where Icarus has been used to compute the surface temperature distribution on the ADEPT arc jet configuration, utilizing a multi-block hybrid unstructured mesh to account for the complex seams and interfaces.

This poster will present a brief overview of the solver architecture, numerics, and physical models. Verification and validation studies show that Icarus maintains expected numerical accuracy, and computes the same material response as heritage solvers when run with notionally equivalent physics. Icarus is intended to be utilized in engineering design of TPS systems, and thus computational efficiency is paramount. Studies showing computational efficiency, and scalability for mission-relevant, large-scale, material response problems will be presented.

Icarus is already being used in NASA technology development efforts, and mission design. Examples from recent applications of Icarus to TPS development and design will be presented. Specifically, we present simulations performed in support of the development of the the HEEET woven TPS material which has been extensively presented at prior IPPW's. In addition, simulations of the TPS for the Dragonfly Titan lander will be presented. Finally, we discuss on-going developments of the solver, and future work.

Figure 1: High-definition video capture of the ADEPT arc jet article in the Interaction Heating Facility (IHF) at NASA Ames Research Center.

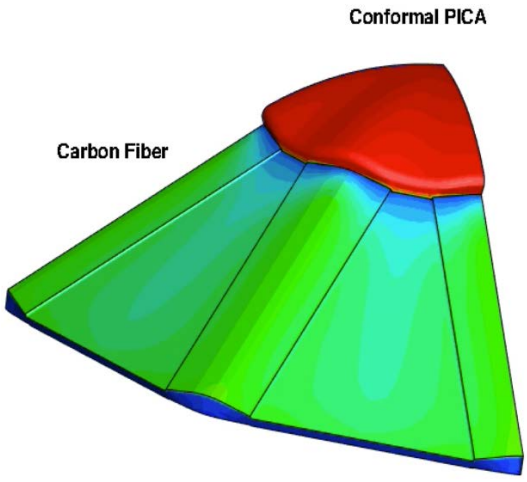

Figure 2: Visualization of the surface temperature distribution predicted by Icarus for the ADEPT arc jet experiment.

References: **[1]** Eric C. Stern et al. "Overview of the Icarus Material Response Solver". In: *7th Ablation Workshop*. Bozeman, Montana, Sept. 2017. **[2]** Joseph C Schulz et al. "Development of a three-dimensional, unstructured material response design tool". In: *55th AIAA Aerospace Sciences Meeting*. Grapevine, Texas: American Institute of Aeronautics and Astronautics, Jan. 2017.

Satellite and Payload Simulator of EntrySat 3U CubeSat. A. Van Camp[1] and Supervisor R. Garçia[2], [1]Institut Supérieur de l'Aéronautique et de l'Espace (ISAE-SUPAERO), Université de Toulouse, 31055 Toulouse, FRANCE, adriaen.van-camp@student.isae-supaero.fr, [2]Institut Supérieur de l'Aéronautique et de l'Espace (ISAE-SUPAERO), Université de Toulouse, 31055 Toulouse, FRANCE

Abstract: In-Orbit collisions and satellite orbital decay have demonstrated that orbital debris represents a potential threat to access to space as well as a threat to ground safety. One promising solution under investigation at CNES – and based on a large Orbital Test Vehicle – aims to clear low Earth orbit of debris by injecting debris into re-entry orbits which ensure a direct controlled atmospheric re-entry destruction. However, equipping a passive target with a suitable spacecraft bus for de-orbitation through an orbital rendezvous is a complex operation. Such missions often suffer critical failures, and several missions which had planned for controlled de-orbit saw failures of the de-orbit subsystems that resulted in low-slope, uncontrolled atmospheric re-entry. Meanwhile, existing knowledge on the survivability of a satellite or launch vehicle element during atmospheric re-entry remains incomplete. Further, tracking and predictive capability for the trajectory of small objects, either debris or otherwise, is lacking. Although valuable information has been obtained during complex atmospheric re-entries such as during the ATV program, no dedicated orbital debris inflight experiment has been performed to date.

Therefore, the EntrySat experiment consists of inserting a nano-satellite in the form of a 3U CubeSat into low-Earth orbit (which is similar in principle to secondary debris typically issued from launch vehicles or satellites). A science module operating during the re-entry phase will be able to perform in-situ measurements of the CubeSat environment (temperature, acceleration, pressure …) as well as integrity (position, rotation speed …) up to its destruction. Acquired data will be sent in real time through the Iridium constellation back to the ground segment. This CubeSat is to be injected into a trajectory representative of an uncontrolled atmospheric re-entry with both very low slope and high orbital velocity. Furthermore, no propulsion subsystem or re-entry protection subsystems will be used during the destructive phase of flight – thus the satellite will respond to the atmosphere in a similar manner as some orbital debris. In verifying the aerothermodynamic models of re-entry, EntrySat will help to increase the accuracy of trajectory predictions for known space debris and other small orbital objects. EntrySat CubeSat will be controlled by ISAE-SUPAERO's ground station, through the local ground station. Raw science data shall be sent to the ground station via UHF/VHF (during nominal decay phase) or the Iridium network as necessary through SBD transmission (Short Burst Data). EntrySat is a mission proposed by ISAE-SUPAERO and supported by CNES in the frame of the JANUS student projects.

The objective of the satellite and payload simulator (created in Matlab Simulink) is to predict all measurements that EntrySat will make during the mission. The inputs of this simulator are a starting position, velocity and time and the content of the satellite data base. As output it predicts all measurements produced by the satellite to simulate which measurements will be received once the satellite is in orbit. To simulate these measurements, the simulator models the orbit and rotation of the satellite together with the environment around the satellite.

The ultimate goal of the model will be to predict the satellite's response to a parameter change performed by a command we send to it, and to calibrate the various sensors of the satellite in flight. The model was also used to confirm the capability of EntrySat to perform air density retrieval experiments through the analysis of torques applying on the satellite.

AERODYNAMIC STABILITY ANALYSIS OF A CUBESAT IN RAREFIED FLOW. J. W. Williams[1] and Z. R. Putnam[2], [1]Graduate Student, University of Illinois at Urbana-Champaign (Jamesw3@illinois.edu), [2]Assistant Professor, University of Illinois at Urbana-Champaign (Zputnam@illinois.edu).

Smallsats and CubeSats operating in low Earth orbit, specifically below 200 km altitude, interact with flows which provide small but measurable aerodynamic effects over even short time horizons. These small satellites often have modest control authority, meaning that the resultant aerodynamic torques incident on the vehicles may overpower their actuators. For missions with strict pointing requirements, aerodynamic effects may lead to premature mission termination due to aerodynamic instabilities causing the vehicle to be incapable of maintaining pointing. As the onboard control system becomes less effective, vehicles must rely on passive aerodynamic stability to maintain pointing. It is necessary to understand the aerodynamics of satellites in the CubeSat form factor to ensure missions designed for this regime of flight can operate for the entire desired mission duration.

To analyze the aerodynamics of a CubeSat, a free-molecular aerodynamic solver was created. This solver calculates the normal and shear pressures incident on the faces of the CubeSat and integrates these to find the forces and moments on the vehicle. The CubeSat is modeled as a collection of three orthogonal flat plates, for which there are analytical solutions for the normal and shear pressures. Only three plates are required due to shadowing effects creating an effective vacuum behind the vehicle.

The most important effect of the flow on the stability of the craft the is the aerodynamic torque. All torques act around the center of gravity. In general, a craft with its center of gravity fore of its neutral point has a negative pitching moment coefficient with respect to angle of attack, which is desirable for stability. The aerodynamic torques can be split up into those resultant from forces fore of the center of gravity, and those aft of the center of gravity.

To analyze the transient stability response of the CubeSat, a rigid-body dynamics solver was created. The craft is modeled as orbiting around the Earth in inverse-square gravity, with the angle of attack of the flow resulting from the instantaneous velocity vector and the craft's attitude in inertial space. Currently, circular orbits between 80 and 200 km are modeled for craft with centers of gravity positioned between 10% and 45% of the total craft length.

Figure 1 shows the angle of attack vs. time trace for a 150 km altitude circular orbit starting at an angle of attack of 45° and an angle of attack rate of 0°/sec. It is apparent from this figure that there is little to no damping inherent in the free molecular flow, so the best case for stability of a craft in this regime of flight is oscillatory stability. With the addition of onboard control, it is possible to damp the attitude to asymptotic stability.

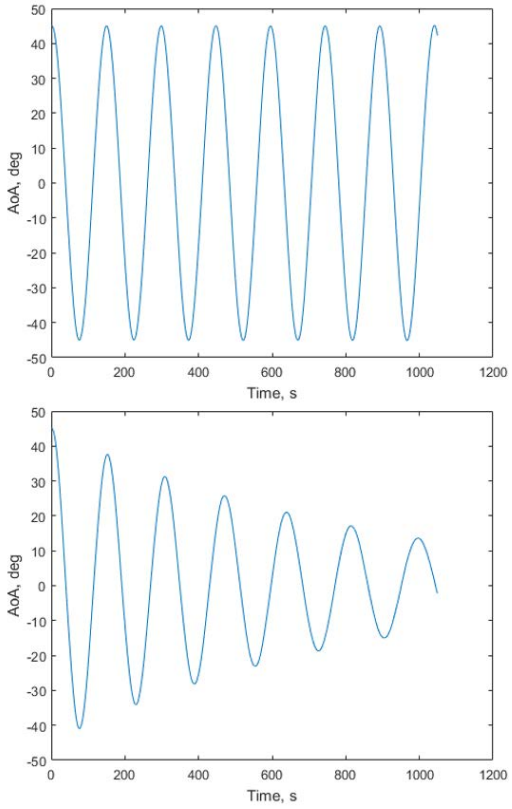

Figure 1: Angle of Attack vs. Time for a 150-km altitude orbit with center of gravity position = 45% craft length. (Top) Without artificial damping (Bottom) With rate damping using onboard control

Further examples are offered to better characterize the stability of vehicles with differing properties and initial states and inform the development of more comprehensive control models to incorporate the limitations of common CubeSat control systems. Prototype real-time control algorithms are presented that can provide damping across a range of vehicle and environmental properties.

WE NEED YOUR HELP - The Planetary Probe "Blue Book" Refresh

Gary Allen[1], Dean Kontinos[2], Sharon McKee[1], Ethiraj Venkatapathy[2], Todd White[1]

[1] AMA Inc., Entry Systems and Technology Division, NASA Ames Research Center
[2] NASA, Entry Systems and Technology Division, NASA Ames Research Center

In the 1990's, engineers at NASA Ames Research Center gathered a comprehensive summary of several planetary entry probes into a small handbook that was shared with students, mission planners, and EDL technologists. The focus of the handbook was on entry vehicle geometry, trajectory, aerothermal design environments, and thermal protection system materials. This Planetary Probe handbook became known as the "Blue Book" because of its bright blue cover, and was subsequently updated in 2002, and 2006 as a NASA technical memorandum. [1]

With the recent entry missions and EDL technology demonstration missions at NASA, ESA, and beyond, NASA Ames has undertaken to update the Blue Book, and solicit input from the IPPW community to correct and expand the scope of an updated Blue Book. The update of the Blue Book is planned for IPPW 2019.

This poster session will solicit input on future content and mission information sought, and the process for an online and print version of the Blue Book.

[1] NASA/SP-2006-3401, Planetary Probe Data Book at https://ntrs.nasa.gov/search.jsp?R=20070022789

Europa Lander Mission Overview and Update. S. W. Sell[1], [1]Jet Propulsion Laboratory, California Institute of Technology, 4800 Oak Grove Drive, Pasadena, CA 91109

The Europa Lander project held its Mission Concept Review last year. In response to this review, the development of the Europa Lander Mission concept has seen several significant changes aimed at reducing cost and complexity. Rather than using the carrier vehicle as a cummunications relay, the mission will instead use its updated telecommunications system to communicate directly to Earth. This change reduced both cost and mass, but also brought unique challenges such as communications during the critical event of Deorbit, Descent, and Landing. Additionally, a new landing trajectory to allow for a planetary protection compliant disposal of the carrier vehcle had to be implemented. The Flight system has also undergone several updates to the spacecraft configuration aimed at increasing robustness as well as reducing mission cost. This paper outlines and updates the Europa Lander Mission concept as well as the new approaches to the many challenges of landing on Europa.

Landing on Europa: Key Challenges and Architecture Concept. A. K. Zimmer[1], E.D. Skulsky[1], A.M. San Martin[1], S. W. Sell[1], T. P. Kulkarni[1], D. M. Kipp[1], [1]Jet Propulsion Laboratory, California Institue of Technology, 4800 Oak Grove Dr., Pasadena, CA 91109, USA

Abstract: NASA has extended the scope of the potential exploration of Europa beyond the planned Europa Clipper mission and initiated a Pre-Phase A mission concept study of a potential Europa Lander. With a massive liquid water ocean beneath its icy crust, Europa is one of the Solar System's prime candidates for hosting life. Consequently, there is a strong desire in the scientific community to perform in-situ Europa science through a landed mission. Jupiter's hostile radiation environment and the lack of information about the moon's terrain at the scale of a lander spacecraft would require significant technology development to overcome the inherent landing challenges. This paper provides a brief overview of the Europa Lander mission concept and describes the significant challenges associated with landing on Europa, the technologies required to overcome those challenges, and a strategy for Deorbit, Descent, and Landing (DDL). In the current baseline, DDL would begin with the separation of the lander, descent stage, and deorbit vehicle from the carrier stage. Due to Europa's tenuous atmosphere, a propulsive deorbit maneuver would be required to slow the spacecraft down from orbital velocity. After burnout and jettison of the deorbit stage, the descent stage and lander would use a camera and lidar altimeter to compute its position and velocity relative to an onboard map provided by Europa Clipper reconnaissance. Based on this updated map-relative state, the spacecraft would calculate and follow a powered approach profile to a few hundred meters above the targeted landing region. Now in vertical descent, the spacecraft would scan the surface terrain with the lidar and in real time construct a digital elevation model, generate a safety map, and select a safe landing location. In the last stage of landing, the lander would be lowered on tethers from the descent stage in a sky crane configuration before final touchdown, after which the descent stage would fly away and crash-land at a safe distance from the lander. Due to the long light-time between Europa and Earth and the fast sequence of events during DDL, landing would be completely autonomous. The information to be presented about the Europa Lander is pre-decisional and is provided for planning and discussion purposes only.

Concepts on Maximizing Data Return for a Potential Europa Lander Using Direct to Earth Communications. G.H. Tan-Wang[1], P. Estabrook[1], M. Smith[1]. [1]Jet Propulsion Laboratory, California Institute of Technology, 4800 Oak Grove Drive, Pasadena, CA 91109

For cost and complexity reasons, the Europa Lander concept has evolved to a mission using Direct To Earth (DTE) communications only. The new architecture is a result based the recommendations from the Mission Concept Review held in June 2017 and a subsequent Formulation Adviory Group study led by Standing Review Board member Dr. Bobby Braun. The removal of relay via the Carrier vehicle challenges the short lived, primary powered lander to send the entirety of the surface science mission data from the surface of Europa to Earth as well as the data from the Deorbit, Descent and Landing (DDL). In fact, this architecture was not fully explored previously due to perceptions that a surface mission at 5 AU from Earth would be near impossible given the experiences so far with recent Mars surface missions. However, while a DTE mission architecture has a significant reduction in the capability of the total data return, the concept developed by the lander design team made modifications on both the flight system (telecommunications hardware, battery, etc) and the ground system (arraying of antennas) as well as reworked project level requirements to ease the design needs while still meeting the science needs as defined by the Science Definition Team (SDT). This presentation will address the myriad of changes across the project that allowed for a concept to close around a Europa Lander mission as defined by the SDT.

Surface and Subsurface Sampling Drills for Life Detection on Ocean Worlds. Fredrik Rehnmark[1], Tighe Costa[1], Joey Sparta[1], Jameil Bailey[1], Kris Zacny[1] and Ralph Lorenz[2], [1]Honeybee Robotics, Pasadena CA 91103, USA (FLRehnmark@honeybeerobotics.com), [2]Johns Hopkins Applied Physics Laboratory, Laurel, MD 20723, USA (Ralph.Lorenz@jhuapl.edu).

Introduction: The authors propose two very different drilling machines to search for life on ocean worlds. SLUSH Drill (Search for Life Using Submersible Heated Drill) is a drilling probe that could penetrate several kms through Europa ice to reach the warm ocean below. CryoSADS (Cryogenic Sample Acquisition and Delivery System) is a transportable surface drill that could penetrate a few cm deep into the Titan regolith at various landing sites.

Background: Because liquid water plays such a central role in biological processes on Earth, the search for life elsewhere begins with a search for oceans, either present or past. There is evidence that Europa and Titan both have plentiful liquid water buried deep underground and, therefore, insulated from the cold temperatures (~100K) at the surface. On Europa, these subsurface oceans could be accessed by drilling through kilometers of ice. Titan, on the other hand, also has surface oceans consisting of liquid methane, which has a much lower freezing point than water but participates in the Titan climate in ways analogous to water on Earth. If they exist, heretofore undiscovered lifeforms that depend on methane, rather than water, could be detectable at or near the Titan surface. Therefore, a sampling drill for Titan would only need to penetrate a few cm deep. For maximum flexibility, both drills will use a proven rotary percussive drilling approach [1] that traces heritage back to the Apollo Lunar Surface Drill (ALSD).

SLUSH Drill for Europa: Drilling tests were performed in cryogenic ice to compare power consumption with room temperature drilling trials conducted in similar strength (~100 MPa) rock (**Figure 1**). Although different drill bits were used and it is, therefore, dangerous to draw too many comparisons, the specific energy (Whr/cc) measured while drilling in ice (unheated bit) was at least two orders of magnitude lower than in rock. In warm (~240K) ice, however, internal heating was necessary to prevent the drill bit from getting stuck, even at a very modest depth of 20 cm [2]. This increased the specific energy of drilling in ice to roughly one order of magnitude lower than drilling in rock. Internal heating would also provide a related benefit of facilitating the transport of cuttings from the drill, past the probe body and up to the open hole behind the probe, allowing it to make forward progress.

Figure 1. Drilling in cryogenic ice (unheated bit).

CryoSADS Drill for Titan: One of the requirements of sampling on Titan is to preserve the composition and physical properties of surface material by limiting temperature rise to no more than 10K above ambient. This motivates the use of pneumatic sample transport using Titan air. The drill will be powered by electromagnetic motors that can operate at Titan ambient conditions to minimize heating of the drill bit. Extreme environment electromechanical actuators have been built and tested in both cold [3] and hot [4] environments.

Surface observations of Titan provided by the Huygens probe are consistent with damp sand [5], raising concerns that the surface material at the landing site could be difficult to transport. To reduce the risk of fouling the sample acquisition system, the CryoSADS drill will first probe the ground and relay imagery and sensor data to Earth for landing site evaluation before initiating the sampling sequence. Testing in a range of wet and dry simulants with a range of particle sizes is planned and will be correlated with soil property measurements in an effort to define high-confidence screening criteria.

Conclusions and Future Work: Penetrating the surface of ocean worlds such as Europa and Titan is feasible by enhancing existing planetary drilling technology. SLUSH and CryoSADS offer unique capabilities necessary to expand the search for life to these destinations.

Acknowledgements: This work was funded by NASA's Concepts for Ocean worlds Life Detection Technology (COLDTech) program and by NASA's Small Business Innovative Research (SBIR) program. We owe our sincere thanks and appreciation to the COLDTech program director Ryan Stephan and the SBIR COTR Juergen Mueller.

References: [1] Zacny, K. et al. (2013) *Astrobiology 13(12)*, 1166-1198. [2] Zacny, K. et al. (2018) *IEEE Aerospace*. [3] Tyler, T. et al. (2011) *Proc. Of*

14th ESMATS. [4] Rehnmark, F. et al. (2017) *Proc. Of 17th ESMATS.* [5] Lorenz, R.D. et al. (2006) *Meteoritics and Planetary Science 41(11)*, 1705-1714.

Key Technology Needs for Accessing the Ocean of an Icy Moon

Tom Cwik, Wayne Zimmerman, Andrew Gray, Bill Nesmith
Jet Propulsion Laboratory, California Institute of Technology, Pasadena, California, United States
cwik@jpl.nasa.gov
Anita Sengupta
Hyperloop One, Los Angeles CA, United States

The icy moon oceans beckon with ingredients that potentially may harbor extant life. Beginning with the Galileo and Cassini missions, measurements have revealed the presence of global oceans under the icy crust of several moons of Jupiter and Saturn. Among those moons, Europa and Enceladus have their ocean in contact with the rocky core, providing an environment similar to the conditions existing on the terrestrial sea-floor where life has developed at hydrothermal vents. Accessing these oceans presents considerable difficulty due to a number of issues including the depth and composition of the icy crust, the time needed to travel through the crust, the power needed to propel a probe, communication of scientific and engineering data though the ice and back to earth, entry and mobility in the ocean and autonomous operations for the life of the mission.

A detailed trade space study was conducted to develop a technology architecture defining a system that would access an icy moon's ocean. To specifically bound the architecture, Jupiter's moon Europa was chosen as the target body. The current understanding of the scientific properties of the ice crust and ocean was used to guide the development. A strawman scientific payload was devised to further develop a baseline set of requirements. Beginning with a launch and trajectory that can bring a system to Europa's orbit, a complete trade space was developed outlining the engineering systems needed to access the ocean. The launch system and trajectory provided a bound for the amount of mass that would be available to Europa's surface. The architecture was divided into specific phases for i) deorbit, descent and landing, ii) surface operations, iii) ice descent and iv) ocean access. The needed functions for each phase were then identified with potential options for each sub-system evaluated. The technical maturity of each of these sub-systems was assessed for systems that could be developed to a maturity ready for a preliminary design in 5-10 years. Integrated system parameters on power, communication capacity, and mass were developed to further define the overall system. To constrain the design, a total time in the ice, from the ice crust surface to accessing the ocean was limited to two years, and 10Km of ice was baselined with a temperature profile through the ice estimated from the scientific literature.

The results of this architecture will be presented in the paper. A complete system has been defined for a system that can access the ocean after two years of travel through the baseline 10km of ice. Models with a range of fidelity are being developed to bring additional prediction to the effort. A description of testbeds that can validate the models as well as provide experimental validation of subsystems will be described. The trade space and key technology needs will be reported.

EXPLORING ICY WORLDS: ACCESSING THE SUBSURFACE VOIDS OF TITAN THROUGH AUTONOMOUS COLLABORATIVE HYBRID ROBOTS

Ali-akbar Agha-mohammadi[1], Jason Hofgartner[1], Pradyumna Vyshnav[1], Jose Mendez[1] , Daniel Tikhomirov[1], Fernando Chavez[1], Jonathan Lunine[2], Issa Nesnas[1]
{aliagha, jason.d.hofgartner, pradyumna.vyshnav, jose.a.mendez, daniel.tikhomirov, fernando.chavez, issa.nesnas}@jpl.nasa.gov, jlunine@astro.cornell.edu,

[1]NASA Jet Propulsion Laboratory, California Institute of Technology, 4800 Oak Grove Drive, Pasadena, California 91109, USA.
[2]Cornell Center for Astrophysics and Planetary Science, Cornell University, 616A Space Science Building, Ithaca, New York 14853, USA

Introduction: Saturn's giant moon Titan is one of the most fascinating bodies in the Solar System. It is the only moon with a dense atmosphere, vast dune fields, rain, rivers, and seas that are part of a methane hydrologic cycle analogous to Earth's water cycle [1] [2]. Titan also has the most complex atmospheric chemistry in the solar system that may include prebiotic chemistry similar to that on early Earth before life began [3]. The Sotra Patera region has Titan's deepest known pit adjacent to its highest known mountain, a morphology suggesting cryovolcanism [4]. Additionally, Sotra Patera is regarded as the best candidate, by far, for volcanic topography anywhere documented on an icy extraterrestrial surface, making it immensely important from a geological perspective. Long-range mobility and capability to negotiate rugged terrains is a critical capability to extract valuable information from Sotra Patera region while also expanding surface access on Titan.

Related Work: Recent progress on several fronts has suggested that due to Titan's dense atmosphere, utilization of rotorcrafts and aerial vehicles may be an effective and affordable method to achieve these mobility capabilities. Additionally, NASA has recently selected the "Dragonfly" concept as one of the finalists for its New Frontiers program to study Titan's surface using a rotorcraft lander [5] [6]. In this work, we extend previous state-of-the-art mission ideas to explore Titan's subsurface voids [7]. This calls for a system with high degree of mobility and resiliency to cope with narrow passages and extreme terrains in subsurface voids, a capability beyond traditional concepts such as landers, tethered rovers, balloons, airplanes, and [8] [9] [10] [11] [12] [13].

Exploring Titan's subsurface presents two main challenges: 1) many of the scientifically enticing locations are difficult to access due to challenging surface conditions such as steep slopes, narrow passages, seafloors etc., and 2) a desire to explore all of Titan's diverse terrains, but inability to traverse the long distances between them.

Mission Objectives: A team of collaborative, resilient, autonomous, and long-endurance assets will be deployed by a lander to explore the Sotra Patera region to confirm its cryovolcanic origin and determine the extent to which lavas have interacted with organic surface materials. The mission starts with landing near Sotra Patera. In order to fulfill the science objectives, the assets will be designed so as to complete the various tasks, including:

- *Low/high resolution local mapping*
- *Stratigraphy*
- *Deep excursion*
- *Cave exploration*

Technical Approach: To address severe energy and mobility limitations in exploring subsurface voids, we use recent developments in energy-efficient, resilient hybrid (ground/aerial) mobility (discussed below). We rely on a team of such hybrid robots to complete our mission objectives. Rotorcrafts operating in teams have considerable advantages over single robot systems in the context of exploration. First, a team of robots can cover a given target area more quickly than a single robot, by searching it in parallel. Second, using a robot team provides robustness by adding redundancy and eliminating single points of failure that may be present in single robot or centralized systems.

Mobility: Rollocopter is a six degrees-of-freedom autonomous hybrid aerial-ground robot (Figure 1). This mobility system is a mechanically-simple, agile, energy

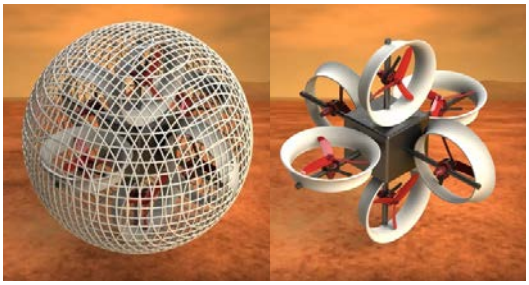

Figure 1. (Left) Rollocopter is a novel mobility autonomous robot design for exploring extreme environments. It is capable of multiple locomotion modes from: flying, rolling, hovering, and bouncing. (Right) Shows a 6-motor Rollocopter configuration.

efficient, and collision-resilient vehicle recently developed at NASA's Jet Propulsion Laboratory (JPL) for both aerial and terrestrial modes [14]. Compared to aerial-only rotorcraft, it provides a vastly increased range and operation time. Unlike ground robots, it can negotiate obstacles by simply flying over them.

Energy Considerations: Due to extremely cold temperatures on Titan, development of energy-efficient power sources and managing them to operate robotic assets on the surface is a challenge. Further, as our mission concept involves robotic assets performing stratigraphy and exploring deep excursions/caves, long-range mobility with persistent situational awareness is pivotal. In order to fulfil these diverse objectives, our autonomy framework allocates the tasks to the robots based on mission specifications, and the vehicle energy level [15] [16]. Due to the energy-aware mode-switching ability, rollocopters can traverse and map the area for long distances without the need for recharging. They roll to save energy and fly only when necessary. The mission planner schedules optimal visits to the recharging base station located on the lander, while another rollocopter repeats this process. This procedure is executed simultaneously with different groups of rollocopters until the region of interest is fully explored.

Multi-agent Autonomy: In the proposed exploration scenario, rollocopters will be used as a robotic network capable of collaborating with each other for navigating autonomously across various domains. To this end, robust motion planning methods will be incorporated into our autonomy framework (e.g., [17]). Once the assets are deployed by the lander, a group of scouting rollocopters will be dispatched to create an initial low-resolution map of the nearby environment (Figure 2).

After the scouting phase, a high-resolution science (HRS) mapping behavior starts, where the autonomous mission planner deploys a set of rollocopters equipped with an advanced sensory suite and science instruments to selected parts of the terrain. To enable HRS-mapping over long distances, we adopt a range-sweeping technique: At each episode, a rollocopter traverses the mapped area with high-speed (using trajectory following), reaches the frontier of the mapped area, and then explores the unmapped area via low-speed, higher-energy mapping behavior.

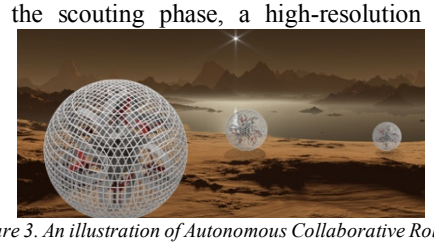

Figure 3. An illustration of Autonomous Collaborative Rollocopter network performing vision-based mapping on Titan's surface.

While a preliminary set of target measurement regions may be part of the initial mission plan, autonomy enables opportunistic science and updates the mission plan based on observations made onboard. This behavior can be accomplished collectively by communicating any significant discoveries made by one rollocopter to other team members.

Communication Protocol: Effective distributed autonomy in self-governing exploration requires a reliable method for ensuring information delivery and state synchronizing, capable of handling severe subsurface communication challenges from limited line-of-sight, signal degradation, and effects of varying geology. We will rely on Disruption-tolerant Networking (DTN) protocol techniques that allow autonomous management of communication links and data transmission [18]. DTN is a highly reliable and resilient scheme to enable a communication network between a group of mobile nodes [18] [19] [20] [21] with assured data delivery using automatic store-and-forward mechanisms; Each data packet is forwarded immediately or stored for the next transmission possibility. DTN ensures successful communication between all assets in the system even if an end-to-end communication path does not always exist (Figure 3). The acquired data will be relayed back to the lander, which will then be sent to Earth for further processing and analysis.

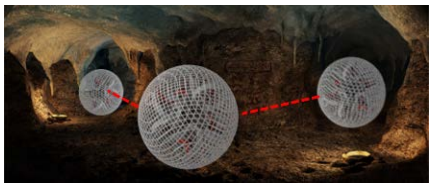

Figure 2. An illustration of Rollocopter network exploring a cave on Titan using DTN protocol.

Conclusion: Technology for small autonomous rotorcrafts has matured dramatically in the last decade and Mars helicopter is receiving intensive study for a potential technology demonstration on Mars [22]. This suggests that rotorcrafts may have great potential for exploring Titan, which has a denser atmosphere and weaker gravity than Earth and Mars, making it very favorable for aerial mobility from an aerodynamics perspective. Furthermore, using a team of robots would allow high-redundancy in the system where not only specific targets on Titan could be closely observed, sampled and cached, but also high-risk, high payoff measurements could be taken (since the loss of one rollocopter would not spell the end of the mission). Incorporation of autonomous capability-aware mission planner and DTN in our autonomy framework and communication protocols respectively further strengthens our approach to achieve the mission objectives in an efficient manner.

References: [1] O. A.Haronson, A. Hayes, P. Hayne, R. Lopes, A. Lucas and J. Perron, "Titan's surface geology in Titan", Cambridge, *Cambridge University Press*, 2013, p. 63.
[2] A. Hayes, "The Lakes and Seas of Titan", vol. 44, *Annual Review of Earth and Planetary Sciences*, 2016, p. 57–83.
[3] S. Horst, "Titan's atmosphere and climate", vol. 122, Pasadena, CA: *Journal of Geophysical Research: Planets, 2017, p. 432–482*.
[4] Lopes et al., "Cryovolcanism on Titan: New results from Cassini RADAR and VIMS", *Journal of geophysical research: planets, vol. 118, 416–435*.
[5] R.D. Lorenx et al., "Dragonfly: A rotorcraft lander concept for scientific exploration of Titan", *APL Tech Digest.*
[6] E. Turtle, J. Barnes, M. Trainer, R. Lorenz, S. MacKenzie, K. Hibbard, D. Adams, P. Bedini, J. Langelaan and K. Zacny, "Dragonfly: Exploring Titan's Prebiotic Organic Chemistry and Habitability", *Lunar and Planetary Science Conference,* 2017.
[7] L.Jones et al., "Titan Explorer NASA Flagship Mission Study", *JHU/APL*, Laurel, MD, 2007.
[8] J.Lebreton et al., "An overview of the descent and landing of the Huygens probe on Titan", *Nature*, vol. 438, no. 7069, pp.758-764, 2005.
[9] J. Barnes, C. McKay, L. Lemke, R. Beyer, J. Radebaugh and D. Atkinson, "AVIATR: Aerial vehicle for in-situ and airborne Titan reconnaissance", *Lunar and Planetary Science Conference,* vol. 41, p. 2551, March 2010.
[10] M. Lockwood et al., "Titan Explorer", *in proc. AIAA/AAS Astrodynamics Specialist Conference*, Honolulu, paper AIAA-2008-7071, 2008.
[11] R.D.Lorenz, "Flight Power Scaling of Airships, Airplanes and Helicopters: Application to Planetary Exploration, *J.Aircraft* 38 (2), 208-214, 2001.
[12] L.Matthies et al., "Titan Aerial Daughtercraft (TAD) for surface studies from a lander or balloon", *11th International Planetary Probe Workshop*, Pasadena, CA, 2014. .
[13] I. A.D. Nesnas et al., "Axel and DuAxel Rovers for Sustainable Exploration of Extreme Terrains", *Journal of Field Robotics (JFR)*, 2012.
[14] A.-a. Agha-mohammadi, "Rollocopter: Novel Hybrid Aerial-Ground Vehicle for Failure-Resilient, Energy-Efficient, and Agile Mobility", *Submitted to The United States Patent and Trademark Office*
[15] P. Nilsson, S. Haesaert, . Thakker, K. Otsu, C. Vasile, A.-a. Agha-mohammadi, R. Murray and A. Ames, "Specification-guided Active Exploration: Application to Risk-averse Rover/Copter Mars Missions", *Robotics: Science and Systems(RSS)*, 2018.
[16] S. Haesaert, P. Nilsson, C. Vasile, R. Thakker, A.-a. Agha-mohammadi, A. D. Ames and R. M. Murray, "Temporal Logic Control of POMDPs via Label-based Stochastic Simulation Relations", *IFAC Conference on Analysis and Design of Hybrid Systems,* 2018.
[17] A.-a. Agha-mohammadi, S. Chakravorty, N.M. Amato, "FIRM: Sampling-based feedback motion-planning under motion uncertainty and imperfect measurements", *International Journal of Robotics Research (IJRR)*, 2014.
[18] E.J Wyatt et al., "Exploring Mars Via Autonoumously Networked Spacecraft", *Concept and Approaches for Mars Exploration,* 2012.
[19] National Aeronautics and Space Administration, "Disruption Tolerant Networking Reliable Solar System Internet Connection", *National Aeronautics and Space Administration*, [Online].
[20] S. Burleigh, A. Hooke, L. Torgerson, K. Fall, V. Cerf, B. Durst, K. Scott and H. Weiss, "Delay-tolerant networking: an approach to interplanetary Internet", *IEEE Communications Magazine ,* vol. 41, no. 6, pp. 128 - 136, 2003.
[21] K. Fall, K. Scott, S. Burleigh, L. Torgerson, A. Hooke, H. Weiss, R.Durst, and V.Cerf, "Delay-tolerant networking architecture", *National Aeronautics and Space Administration*, [Online], 2007.
[22] B.Balram, T.Canham, C.Duncan, H.F.Grip, W.Johnson, J.Maki, A.Quon, and D.Zhu, "Mars Helicopter Technology Demonstrator", 2018 *AIAA Atmospheric Flight Mechanics Conference*, AIAA SciTech Forum, (AIAA 2018-0023).

Sample Acquisition and Transfer for a Titan Lander.

Ralph Lorenz[1], Kris Zacny[2], Tighe Costa[2], Fredrik Rehnmark[2], Joseph Sparta[2], Niklaus Traeden[2], Zachary Mank[2], Jameil Bailey[2]. [1]Johns Hopkins Applied Physics Laboratory, Laurel, MD 20723, USA. (Ralph.Lorenz@jhuapl.edu). [2]Honeybee Robotics, Pasadena CA, USA. (KAZacny@honeybeerobotics.com)

Introduction: We report on an effort sponsored in part by the NASA COLDTech program to demonstrate acquisition and transfer of low-temperature surface materials. This investigation has application to the Dragonfly mission [1] currently undergoing a Phase A study for possible flight to Titan in NASA's New Frontiers program (NF-4).

Background: The challenge of ingesting material that may be a bulk solid on a planetary surface into an instrument on a lander is readily decomposed into two steps : generating particulate material from the bulk, and conveying those particulates into an instrument a meter or two away. The first step is readily accomplished by a variety of systems (drills, rasps, etc. – or scoops if natural particulates are already present) and traditionally the second step has employed a robotic arm with several actuators to raise the scoop and pour samples into an orifice, the transfer being effected by gravity. This has not always been successful, as the experience on the Phoenix lander attests. An alternative approach, particularly applicable for low-gravity world with a dense atmosphere, is to employ a current of gas : pneumatic transfer is widely used in the mining, food and pharmaceutical industries (indeed, coal lumps are lifted hundreds of meters in mines by this method). The extraction of particulates from the gas stream can be performed by a cyclone separator, perhaps most familiar in Dyson™ vacuum cleaners. On airless worlds or Mars, pneumatic transfer can be performed by positive pressure (gas from a tank), and this has been demonstrated by Honeybee's 'Planetvac' experiments sponsored by the Planetary Society [2]. On Titan no gas tank is needed – ambient air is simply drawn through the transfer hose with a blower, just as in a domestic vacuum cleaner (although Titan's dense atmosphere makes particle transport easier).

Effect of Gravity: The gravity on large icy satellites is ~1/6-1/7 that of Earth, which in principle reduces the flow speed needed to transport material aerodynamically up into a sampling hose is less since the weight of a given particle is less. Thus pickup experiments in Earth gravity are conservative. On the other hand, the reduced gravity makes particles drizzle down the cyclone walls a little slower.

In fact, pneumatic transfer has been demonstrated to be effective in 1/6 gravity conditions simulated in NASA parabolic flight experiments (related to in-situ resource utilization for lunar applications [3]). Experiments showed a ~20% drop in reduced-gravity conveyance efficiency at the (50%) threshold particle size (d50), but at nominal larger sizes the difference was not measureable and efficiency was ~100% in both Earth and reduced gravity.

Experiments: Our initial efforts aim to achieve a robust understanding of the transfer process and its performance with a wide range of materials, including fine- and coarse-grained particulates with a variety of characteristics (hard/soft/moist etc). The mouth of a transfer tube is advanced at a constant rate into a sample : slow advance ensures that the solid:air ratio is very low (dilute flow). Our test setup allows us to monitor pressures, fan speed and gas flowrate : our room temperature tests use clear plastic hoses so that the transfer behaviour can be monitored visually (if selected for oral presentation we will show video). Transfer efficiency is evaluated by weighing the solids delivered through the mouth of the cyclone separator : we find some cyclone designs offer superior performance even for more challenging materials, and some preliminary results will be presented.

Operations Concept: Dragonfly is equipped with two independent sample drills, one on each landing skid. This provides redundancy against failure, and possible sample diversity at each landing site (although of course the vehicle can be relocated at will). Sensors in the skids, as well as a workspace imager and a microscopic imager, allow characterization of the surface. The ground can be probed with a shallow bite from the drill, and the texture of cuttings and hole assessed to evaluate cohesion and other properties. With this information, the science team can determine whether the drill sites can be safely sampled.

Conclusions and Future Work: Pneumatic transfer is an effective and versatile approach and has been proposed for several target bodies. We are extending the application to Ocean Worlds : after thoroughly demonstrating room-temperature operation of the transfer system alone, our program will integrate the transfer system with a drill to demonstrate end-to-end sample acquisition, and we will extend the work to cryogenic materials.

References: [1] Lorenz et al, APL Tech Digest. [2] Zacny, IEEE [3] Sullivan et al., AIAA_92-01667 [4] Crosby et al., Wisconsin Space Grant, 2008

NEW TECHNOLOGIES FOR POWERING A SURFACE MISSION ON TITAN: CAPTURING ENERGY FROM TITAN'S WINDS FOR SCIENCE EXPLORATION (CETIWISE). M. E. Evans[1] and W. J. O'Hara[2], [1] Johnson Space Center, Houston, TX, [2]Sierra Nevada Corporation, Louisville, CO.

Summary: Titan is the largest moon of Saturn with a gravity approximately 1/7 of Earth and an average surface temperature of ~94°K (-180°C) near the triple point of methane [1]. Titan's atmosphere is four times as dense as Earth's atmosphere, is composed of ~95% nitrogen and ~5% methane, and has a surface atmospheric pressure one and a half times that of Earth [2]. Extensive dunes on the surface suggest winds (at least seasonally) with aeolian transport of sediments [3]. Fluvial systems and lakes/seas of liquid hydrocarbons with lower viscosity than liquid water exist [4]. Exploration of this environment requires technologies capable of surviving cryogenic temperatures and hydrocarbon liquids. Solar power is not feasible for Titan surface operations due to the persistent haze that blocks the faint sun. Nuclear powered systems generate waste heat that could envelop an instrument in a methane gas cloud, or sink a hulled vessel from reduction in buoyant force as the hydrocarbon liquid boils.

The goal of this proposal is to develop long lived planetary exploration platforms that operate at extremely cold temperatures using in situ resources for power, thus eliminating the need for a surface nuclear power source. We propose exploration of the Titan surface by harvesting wind energy. This technology proposal has been submitted to the NASA Innovative Advanced Concepts (NIAC) Phase I Step B process in Nov. 2017 with the slogan "going green on an orange moon".

The concept is to develop a Mobile Science Platform (MSP) that captures wind energy and converts it to electricity that is stored in a cryogenic superconducting capacitor, then to use the electrical energy to power a suite of instruments, communications equipment, and a propulsion system for the MSP (see Figure 1). Alternate propulsion systems are proposed for 1) solid surfaces with a Ground Rover Base (GRB), 2) liquid surfaces with a Lake Vessel Base (LVB), or a combination of both with an Amphibious Base (AB). This proposal includes many novel and exciting technologies for exploring Titan, including:

- Energy capture from the atmospheric winds
- Cryogenic electrical energy storage using superconductive materials
- Biology instruments to detect possible microbial life in liquid hydrocarbons, lakebed sediments or lakeshore regolith
- Scientific instruments to measure liquid hydrocarbon lake profiles, meteorology and subsurface, geological structures

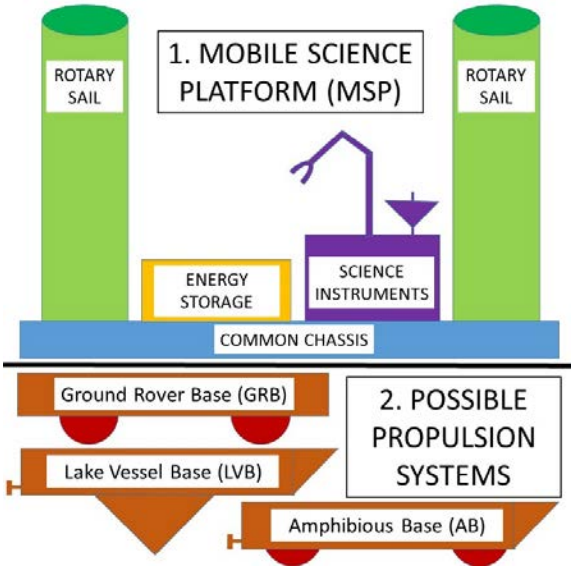

Figure 1: CETiWiSE Concept

Surface Wind Energy Capture: Titan experiences long seasons, diurnal heating, and infrequent storms with methane rainfall [1]. A Titan General Circulation Model (GCM) of the near surface environment suggests wind speed thresholds of 0.4-0.7 m/s at an altitude of 10m [5]. This proposal includes additional modeling of localized surface atmospheric winds and lake wave properties as input to the engineering designs.

Traditionally, wind energy can be harvested using flexible, rigid, or rotating sails; however, a rotary sail is desired since it captures wind energy from any direction and drives a generator to create electricity. The rotating sail also creates a "Magnus Effect" propulsive force perpendicular to the wind direction [6, 7]. Successful terrestrial marine applications of rotary sails include the Flettner Rotor Concept [8-10]. Compared to Earth, the use of a rotary sails on Titan is appealing due to higher atmospheric density (more force) and lower gravity (less structural weight).

Cryogenic Electical Energy Storage:

Electrical energy can be stored in a chemical form in a battery, in a magnetic field in an electrical coil, or in an electrical field in a capacitor. A typical, chemical, terrestrial battery requires temperatures from -20°C to +100°C with optimum performance around 20°C [11]. On cryogenic Titan, batteries are less desirable since they require energy consuming heaters to operate. Below a critical temperature, T_c, certain materials will exhibit zero electrical resistance [12]. Recent

advances in materials have identified "high temperature" superconducting ceramic oxides with a T_c at 127°K. On the Titan surface at 94°K, superconducting wires in a coil configuration could support a persistent current thus storing energy in the resultant magnetic field. Superconducting wire can also be used to create a direct drive electrical generator eliminating mechanical rotational components and mass. These techniques have been demonstrated at colder temperatures [13, 14] and will be investigated with new "high temperature" superconducting wire types for the Titan surface.

Biology Surface Instruments: A common organic molecule in Titan atmosphere could be a source of biologic energy for microbial life in surface hydrocarbon lakes [15]. The MSP includes a spectrometer atop the rotary sails to search for color changes in the nearby surface as an indicator of possible microbial blooms [16]. The propulsion system delivers the MSP to the possible bloom location. Once there, the robotic arm (designed to function in cryogenic temperatures) captures liquid or solid samples and places them in a new instrument. This instrument, based on the ISS mini-DNA sequencer [17], can identify polarity in repetitive patterns indicating the presence of a charged particle "backbone". This "backbone" have been suggested as a potential marker for identification of life on Titan [15, 18, 19].

Other Surface Science Instruments: The MSP also includes camera equipment and meteorology instsurments for measuring atmospheric temperature, pressure, humidity, winds and precipitation. The LVB and AB option includes oceanography instruments to measure bathymetry, liquid surface waves and currents, liquid chemical and physical profiles at depth, and a sediment grabber to capture samples from the lake floor for biological analysis. The GRB and AB option includes deployable geological instruments to measure surface and subsurface structures with seismometers and a magnetometer.

Mission Architecture: A solar powered Titan Orbiter (TO), modeled from the NASA JUNO mission, includes relay equipment for communications between the Titan surface and Earth, and scientific instruments for surface radar mapping and atmospheric studies. The planned Space Launch System (SLS) lifts assets from Earth and delivers the TO and one lander to Titan orbit. The lander is composed of the MSP on a propulsion platform, which could be a GRB (for solid surfces), the LVB (for liquid surfaces), or an AB (for both solid and liquid surfaces). The lander descends through the atmosphere with a parachute and captures wind energy to charge batteries for MSP deployment, which then captures surface wind energy to power the scientific instruments and propulsion platform. The minimum mission design life is 5 Titan days (80 total Earth days).

References: [1] Oleson, S.R., R.D. Lorenz, and M.V. Paul, (2015), *NASA/TM 2015-218831*, [2] Grotzinger, J., et al., (2013), *Comparative Climatology of Terrestrial Planets*, [3] Malaska, M.J.L., et al., (2016), *Icarus, 270,* 183-196, [4] Stofan, E.R., et al., (2007), *Nature, 445(7123),* 61, [5] Hayes, A., et al., (2013), *Icarus, 225(1)*, 403-412, [6] Kornei, K., (2017), http://www.sciencemag.org/news/2017/09/spinning-metal-sails-could-slash-fuel-consumption-emissions-cargo-ships, [7] Scientia, (2017), https://www.freedawn.co.uk/scientia/2015/07/23/what-is-the-magnus-effect-and-how-does-it-work/, [8] De Marco, A., et al., (2016), *International Journal of Rotating Machinery*, *2016*, [9] Pearson, D., (2014), *Proceedings of the Influence of EEDI on Ship Design Conference*), [10] Kuuskoski, J., (2017), *Norsepower rotor sail solution*, [11] CADEX Battery University, (2017), http://batteryuniversity.com/learn/, [12] Onnes, H.K., (1911), *Comm. Phys. Lab. Univ. Leiden, 122,* 124, [13] Chen, H., et al., (2009), *Progress in Natural Science, 19(3),* 291-312, [14] Cao, (2011), in *Wind Turbines. InTech*, [15] McKay, C., (2016), *Life, 6(1),* 8, [16] Thurman, H.V., et al., (2011), *Essentials of oceanography*, [17] Wallace, S., (2017), *NTRS JSC-CN-39208*, [18] McLendon, C., et al., (2015), *Astrobiology, 15(3),* 200-206, [19] Benner, S.A., (2017), *Astrobiology, 17(9),* 840-851

Dragonfly: Rotorcraft Landing on Titan

K. E. Hibbard[1], D. S. Adams[1], R. D. Lorenz[1], E. P. Turtle[1], P. Bedini[1],
[1]Johns Hopkins Applied Physics Lab., Laurel, MD (Kenneth.Hibbard@jhuapl.edu)

J. W. Langelaan[2]
[2]Pennsylvania State University, University Park, PA

Introduction: Titan's abundant complex carbon-rich chemistry, interior ocean, and past presence of liquid water on the surface make it an extremely compelling science target to explore potential habitability [1-6]. The diversity of Titan's surface materials and environments [7] drives the scientific need to be able to sample a variety of locations, making mobility key for *in situ* measurements. This largest moon of Saturn is also ideally suited for atmospheric flight. Compared to Earth, Titan's gravity is lower by a factor of seven, and its atmospheric density is higher by a factor of four. This combination of factors means that the power required to hover in Titan's atmosphere is 2.5% of that required in Earth's atmosphere for the same mass. Dragonfly leverages this unique environment with a relocatable lander system that provides long-range mobility for exploration of Titan [8, 9].

Rotorcraft: The rotorcraft lander with a mobility subsystem consisting of sensors (lidar, radar, cameras, IMU), actuators (motors and rotors), structure (booms and skids), electronics (navigation processor and rotor drive electronics), and surface Guidance, Navigation, and Control (GNC) processing, combines traditional subsystems to enable atmospheric flight. Dragonfly's octocopter (dual quadcopter) design is well suited for flight in Titan's environment and provides full redundancy. A quadrotor configuration maximizes the net disk area for a given aeroshell radius, and thus minimizes the power required for flight [9].

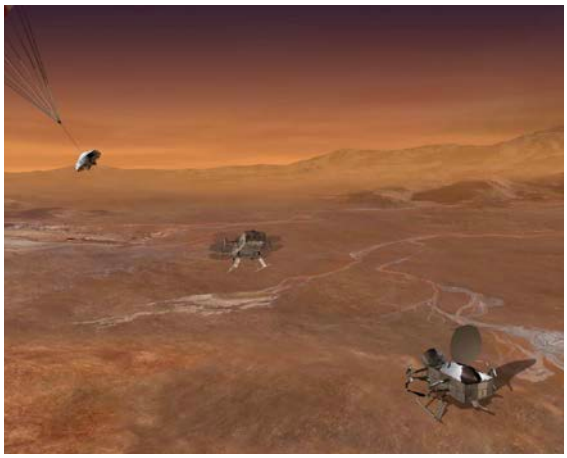

A unique landing approach: Titan's dense atmosphere allows entry and descent to proceed at a relaxed pace in comparison to Mars or Earth entries. The capabilities of Dragonfly's rotorcraft mobility system provide the means to employ powered flight upon separation from the backshell, perform reconnaissance of the local environment, and then safely descend and land on known interdune flat fields that have been characterized by the *Cassini* orbiter and the *Huygens* probe, which descended through Titan's atmosphere and landed on the surface at a similar latitude and time of year as planned for Dragonfly [*e.g.*, 10, 11]. The entire landing sequence from atmospheric entry to landing takes just under two hours and will demonstrate a new paradigm for mobility on planetary bodies with atmospheres beyond Earth.

References: [1] Raulin F. *et al.* (2010) Titan's Astrobiology, in *Titan from Cassini-Huygens* Brown *et al.* Eds. [2] Thompson W.R. & Sagan C. (1992), C. Organic chemistry on Titan: Surface interactions, *Sympos. on Titan, ESA SP-338*, 167-176. [3] Neish C.D. *et al.* (2010) *Astrobiology 10*, 337-347. [4] Neish C.D. *et al.* (2018) *Astrobiology* in press. [5] https://astrobiology.nasa.gov/research/life detection/ladder/ [6] Hand K. *et al.* (2018) *LPSC 49.* [7] Barnes J.W. *et al.* (2018) *LPSC 49.* [8] Lorenz, R. D. (2001), Journal of Aircraft, Vol. 38, No. 2, 208 and 214. [9] Langelaan, J. W., Schmitz, S., Palacios, J., and Lorenz, R. D. (2017), IEEE Aerospace Conference, [10] Lorenz, R. D., et al. (2006), Science, Vol. 312, No. 5774, 724 727, [11] Barnes, J. W., et al. (2008), Icarus, Vol. 195, No. 1, 400-414.

ENCELADUS PROBE MISSION DESIGN USING TITAN AEROGRAVITY-ASSIST. Ye Lu[1] and Sarag Saikia[2], [1]yelu@purdue.edu, [2]ssaikia@purdue.edu, School of Aeronautics and Astronautics, Purdue University, 701 W. Stadium Ave., West Lafayette, IN, 47907.

Motivation: The possibility of finding life on Ocean Worlds (i.e., Enceladus, Titan, and Europa) is of increasing interests to the science community, the public, and the politicians [1]. Cassini measurements have established the habitability of oceans on Enceladus; a search-for-life mission is logically the next step, for example, an orbiter or a lander mission. This work evaluates the benefit of Titan aerogravity-assist (AGA) in capturing around Saturn in an elliptical transfer orbit to Enceladus.

What is Aerogravity-Assist? Aerogravity assist is a maneuver where the spacecraft enters the body's atmosphere upon hyperbolic approach and exits the atmosphere to an escaping orbit. Traditional AGA maneuver achieves a higher turn angle using aerodynamic forces to gain a higher velocity boost compared to gravity assist (GA). However, traditional AGA maneuver may require that vehicles have *L/D* of 3.0 or higher [2]. Such vehicle design minimizes the aerodynamic drag forces [3]. AGA at Titan for missions in Saturnian system differs from the traditional AGA. Figure 1 shows the concept of aerogravity-assist.

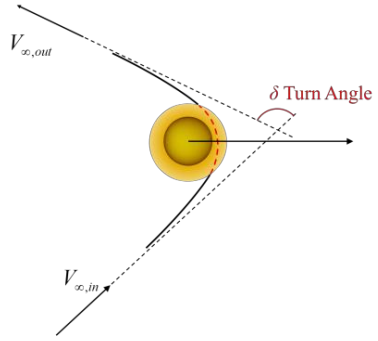

Figure 1 Illustration of aerogravity-assist

Upon hyperbolic approach at Titan, the spacecraft slows down significantly and gets into orbit around Saturn, and this is very different from both the GA [4] and the traditional AGA. Titan has a small gravity well and a very thick atmosphere; it is an appealing target to perform aerocapture/aerogravity-assist for missions to the Saturnian system. Entry environment at Titan is very benign, and AGA maneuver can potentially enable a higher arrival velocity at Saturn. Ramsey and Lyne [5, 6] conducted a preliminary analysis of missions to Saturn and Enceladus using aerogravity-assist. They have evaluated the corridor width and the target orbit and showed that it is feasible using vehicles with *L/D* of 1.0 and 0.48 (depending on the entry speed). Low-*L/D* vehicles (i.e., 0–0.4) can be used for Aerocapture at Titan [7]. One of the goals of the present study is to assess if the current entry technology is sufficient for Titan AGA.

Enceladus Mission Concept: There exist many transfer orbits from Titan to Enceladus after Titan AGA maneuver. With the same arrival trajectory ($V_{\infty,IN}$), the spacecraft can enter a transfer orbit crossing Enceladus orbit with many values of exit velocities, $V_{\infty,OUT}$, and turn angles, δ. Figure 2 shows two illustrations that result in different saturnocentric velocity (i.e., labeled as 3.18 km/s and 3.7 km/s).

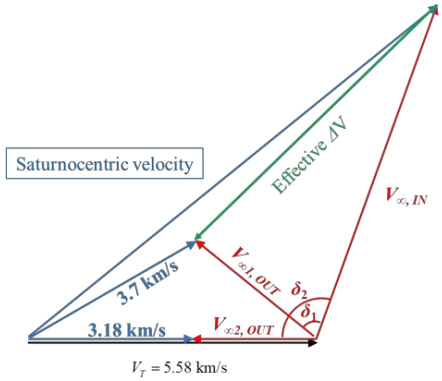

Figure 2 Saturnocentric velocity before and after an AGA maneuver

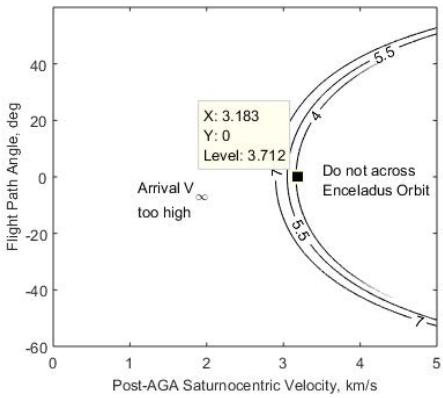

Figure 3 Contours lines of arrival V_∞ at Enceladus at a range of saturnocentric velocity and post-AGA flight path angle.

Figure 3 shows the minimum arrival V_∞ at Enceladus is 3.7 km/s and the corresponding post-AGA saturnocentric velocity is 3.18 km/s. The region to the right of the line denoted "4" indicates the higher energy

orbit where the spacecraft does not cross Enceladus orbit. The region to the left of line denoted "7" shows where Enceladus orbit insertion or landing is unlikely to realize due to the limit of the propulsion system. As an example, Figure 4 shows a mission concept with the minimum energy transfer orbit (i.e., Hohmann transfer orbit), and the post-AGA saturnocentric velocity is 3.18 km/s.

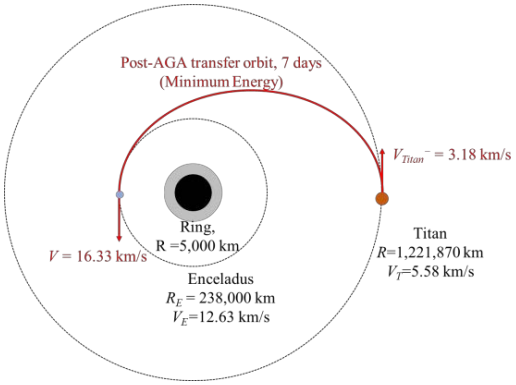

Figure 4 Schematics of Minimum energy transfer orbit after Titan AGA maneuver.

AGA Vehicle Design—Preliminary Results: To successfully perform Titan AGA, the spacecraft must have control authority to overcome the uncertainties in spacecraft guidance and navigation, atmosphere models, and vehicle aerodynamics. Theoretical corridor width (TCW) measures the vehicle's control authority.

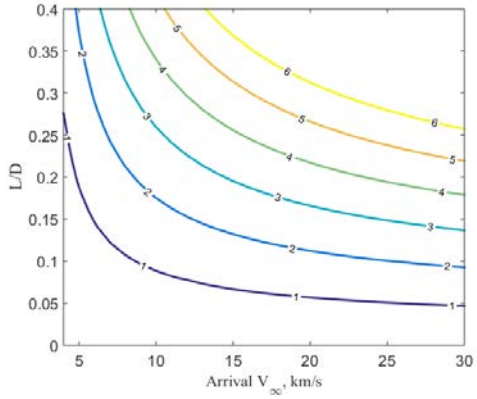

Figure 5 Contour lines of constant theoretical corridor width at a range of arrival V_∞ and vehicle *L/D*.

Figure 5 shows the TCW using a vehicle with a ballistic coefficient of 500 kg/m^2. The results shown assume a target atmospheric exit velocity of 3.28 km/s, equivalent to an outbound V_∞ of 2.4 km/s. The lower TCW occurs at the bottom-left in Figure 5, which is at a low arrival velocity and low vehicle *L/D* and TCW increases as the arrival velocity and vehicle *L/D* increases. Ref. [8] has observed the same trend for aerocapture. Vehicle designs for aerogravity-assist share common grounds with atmospheric re-entry. Peak heat rate, total heat load, and peak decelerations are the key design parameters for entry vehicle design and will be evaluated in this study.

Trajectory Feasibility: The exit velocity (or outbound V_∞) must be consistent with the turn angles. Since the vehicle has control over the atmospheric trajectory, there is a range of turn angles that an AGA maneuver can achieve. The minimum turn angles occur when the vehicle points its lift vector fully upwards, which may result in a negative turn angle; whereas the maximum turn angles are achieved by pointing the vehicle's lift vehicle fully upwards. For vehicle with *L/D*=0.4, the maximum turn angles at V_∞ of 4 km/s and 25 km/s are 38 and 68 deg respectively.

Expected Results: We will present on the feasibility of Titan aerogravity assist for Enceladus missions by considering the entry vehicle design, in terms of structure, packaging, and heating constraints. Also, we will evaluate Titan aerogravity-assist using a comprehensive approach that combines the interplanetary arrival geometry, time of arrival (i.e., moon phasing), and atmospheric flight performance.

References: [1] Hendrix, A. et al. (2018) *OPAG ROW*. [2] Edelman, P. and Longuski, J. M. (2017) JGCD, 40, 2699–2703. [3] Bonfiglio, E. et al. (2000) *JSR*, 37, 768–775. [4] Strange, N. J., and Longuski, J. M. (2002) *JSR*, 39, 9–16. [5] Ramsey, P. and Lyne, J. E. (2006) *JSR*, 43, 231–233. [6] Ramsey, P. and Lyne, J. E. (2008) *JSR*, 45, 635–638. [7] Lu, Y. and Saikia, S. (2018) *JSR*. [8] Lockwood, M. et al. (2006) NASA/TM-2006-214273.

SCIENTIFIC RATIONALE FOR URANUS AND NEPTUNE IN SITU EXPLORATIONS. O. Mousis[1], (olivier.mousis@lam.fr), D.H. Atkinson[2], T. Cavalié[3], L.N. Fletcher[4], M.J. Amato[5], S. Aslam[5], F. Ferri[6], J.-B. Renard[7], T. Spilker[8], E. Venkatapathy[9], P. Wurz[10], and the Ice Giants team, [1]Aix Marseille Université, CNRS, Laboratoire d'Astrophysique de Marseille, UMR 7326, 13388 Marseille, France, [2]Jet Propulsion Laboratory, California Institute of Technology, 4800 Oak Grove Dr., Pasadena, CA 91109, USA, [3]LESIA, Observatoire de Paris, Meudon, France, [4]Department of Physics & Astronomy, University of Leicester, University Road, Leicester, LE1 7RH, UK, [5]NASA Goddard Spaceflight Center, Greenbelt, MD, 20771, USA, [6]Università degli Studi di Padova, Centro di Ateneo di Studi e Attività Spaziali "Giuseppe Colombo" (CISAS), via Venezia 15, 35131, Padova, Italy, [7]CNRS-Université d'Orléans, 3a Avenue de la Recherche Scientifique, 45071, Orléans Cedex 2, France, [8]Solar System Science & Exploration, Monrovia, USA, [9]NASA Ames Research Center, Moffett field, CA, USA, [10]Physics Institute, University of Bern, Sidlerstrasse 5, 3012, Bern, Switzerland

Introduction: The ice giant planets Uranus and Neptune represent a largely unexplored class of planetary objects, which fills the gap in size between the larger gas giants and the smaller terrestrial worlds. Uranus and Neptune's great distances have made exploration challenging, being limited to flybys by the Voyager 2 mission in 1986 and 1989, respectively. Therefore, much of our knowledge of atmospheric processes on these distant worlds arises from remote sensing from Earth-based observatories and space telescopes. Such remote observations cannot provide "ground-truth" of direct, unambiguous measurements of the vertical atmospheric structure (temperatures and winds), composition and cloud properties. With the exception of methane, these observations have never been able to detect the key volatile species (NH_3, H_2S, H_2O) thought to comprise deep ice giant clouds, and a host of minor species remain undetected. Because of the physical limitations of these remote observations, and the deficiency of *in situ* or close-up measurements, Uranus and Neptune's physical and atmospheric properties are poorly constrained and their roles in the evolution of the Solar System are not well understood.

Uranus and Neptune are fundamentally different from the better-known gas giants Jupiter and Saturn. Interior models generally predict a small rocky core, a deep interior of ~70% of heavy elements surrounded by a more diluted outer envelope. Uranus and Neptune also have similar 16 to 17-hour rotation periods that shape their global dynamics. For all their similarities, the two worlds are also very different. Uranus is closer to the Sun at 19 AU versus Neptune's 30 AU and the two planets receive solar fluxes of only 3.4 W/m^2 and 1.5 W/m^2, respectively. However, while Neptune has an inner heat source comparable to the heating received by the Sun, Uranus lacks any detectable internal heat, possibly due to a more sluggish internal circulation and ice layers. Additionally, the two planets experience very different seasonal variations, as Uranus's 98° obliquity results in extreme seasons, compared with Neptune's more moderate 28° obliquity. These extremes of solar insolation have implications for the atmospheric temperatures, cloud formation, photochemistry and general circulation patterns.

Because of the lack of dedicated exploration missions, our knowledge of the composition and atmospheric processes of these distant worlds is primarily derived from remote sensing from Earth-based observatories and space telescopes. As a result, Uranus's and Neptune's physical and atmospheric properties remain poorly constrained and their roles in the evolution of the Solar System not well understood. Exploration of an ice giant system is therefore a high-priority science objective as these systems (including the magnetosphere, satellites, rings, atmosphere, and interior) challenge our understanding of planetary formation and evolution. Here we describe the main scientific goals to be addressed by a future *in situ* exploration of an ice giant. An atmospheric entry probe targeting the 10-bar level, about 5 scale heights beneath the tropopause, would yield insight into two broad themes: i) the formation history of the ice giants and, in a broader extent, that of the Solar System, and ii) the processes at play in planetary atmospheres. The probe would descend under parachute to measure composition, structure, and dynamics, with data returned to Earth using a Carrier Relay Spacecraft as a relay station. In addition, possible mission concepts and partnerships are presented, and a strawman ice-giant probe payload is described. An ice-giant atmospheric probe could represent a significant ESA contribution to a future NASA ice-giant flagship mission.

References: [1] Mousis, et al., Scientific rationale for Uranus and Neptune in situ explorations Planetary and Space Science, 2018. In Press https://doi.org/10.1016/j.pss.2017.10.005

A Concept for a Joint NASA/ESA Mission for In Situ Exploration of an Ice Giant Planet. D.H. Atkinson[1] (David.H.Atkinson@jpl.nasa.gov), O. Mousis[2], T.R. Spilker[3], A. Coustenis[4], M. Hofstadter[1], J.-P. Lebreton[5], K. Reh[1], A.A. Simon[6]

[1]Jet Propulsion Laboratory, California Institute of Technology, 4800 Oak Grove Dr., Pasadena, CA 91109, USA, [2]Aix Marseille Université, CNRS, Laboratoire d'Astrophysique de Marseille, UMR 7326, 13388 Marseille, France, [3]Independent Consultant, [4]LESIA, Observ. Paris-Meudon, CNRS, Paris Univ., France, [5]CNRS-Universitè d'Orlèans, 3a Avenue de la Recherche Scientifique, 45071, Orlèans Cedex 2, France, [6]NASA Goddard Space Flight Center, Greenbelt, MD, USA

Introduction: The top-listed goal in the NASA 2018 Strategic Plan is to "Expand Human Knowledge through New Scientific Discoveries", with a key Strategic Objective to *Understand the Sun, Earth, Solar System, and Universe*. The outer solar system comprises many unexplored bodies within which exists evidence of solar system origin, formation, and processes central to the evolution of the solar system. Uranus and Neptune represent the entire population of a largely unexplored class of planets that has received only the briefest of glimpses by the Voyager 2 spacecraft. The value of further studying the ice giants as essential to understanding the solar system is reflected in the Planetary Sciences Decadal Survey Vision and Voyages 2013-2022 recommendation of an ice giants mission as the highest priority new start flagship mission [1].

The ice giant planets fill the gap in size between the larger gas giants and the smaller terrestrial planets including Earth. Aside from the initial reconnaissance by Voyager 2, to date much of our knowledge of ice giant cloud-top composition and atmospheric processes arises from distant observations from space-based telescopes and observatories on Earth. However, whether from Earth or from a local spacecraft, remote observations cannot directly provide unambiguous measurements of the abundances of noble gases and key isotopes, as well as the altitude profiles of atmospheric thermal and energy structure, stability and dynamics, composition, and cloud properties. [2]

Due to the physical limitations of remote sensing and the lack of *in situ* measurements, many of the most important physical and atmospheric properties of the ice giants are poorly constrained and the ultimate role of the ice giants in the evolution of the Solar System is currently impossible to ascertain. Only *in situ* exploration by a single or multiple descent probes can reveal the secrets of the deep, well-mixed atmosphere that contains pristine materials from the epoch and location of ice giant formation. Of particular importance are the chemically inert noble gases. With no detectable radio signature and therefore requiring direct sampling, the noble gases reflect the processes of ice giant origin, formation, and evolution, including the delivery of heavy elements, and evidence of possible giant planet migration.

A mission concept for a flagship mission to one of the ice giants includes a NASA-provided spacecraft that would carry and deliver a European probe to the ice giant atmospheric entry interface point, and would subsequently act as a relay receiving station for the atmospheric probe science telemetry. The primary goal of the European ice giant atmospheric probe would be to measure the well-mixed abundances of the noble gases He, Ne, Ar, Kr, Xe and their isotopes, the altitude profile of the heavier elements C, N, S, and P, key isotope ratios $^{15}N/^{14}N$, $^{13}C/^{12}C$, $^{17}O/^{16}O$ and $^{18}O/^{16}O$, and D/H, and disequilibrium species CO and PH_3 which act as tracers of internal processes. The atmospheric probe would sample well into the cloud-forming regions of the troposphere where many cosmogenically important and abundant species are expected to be well-mixed, far below regions directly accessible to cloud top remote sensing.

Throughout the atmospheric descent, the probe would measure pressure and temperature to provide valuable context for the composition measurements, the vertical thermal and energy structure and static stability, the location, density, and composition of the upper cloud layers, as well as direct tracking of the planet's atmospheric dynamics including zonal winds, waves, convection and turbulence.

The ice giant planets represent the last unexplored class of planets in the solar system and the most frequently observed type of exoplanets. Extended studies of one or both ice giants, including *in situ* with an entry probe, are necessary to further constrain models of solar system formation and chemical, thermal, and dynamical evolution, the formation and evolution of atmospheres, atmospheric processes, and to provide additional ground-truth for improved understanding of exoplanetary systems. Additionally, the gas and ice giants offer laboratories for studying the dynamics, chemistry, and processes in other planetary atmospheres including that of Earth. By extending the legacy of the Galileo Jupiter probe mission and possibly a future Saturn entry probe mission, an ice giant probe or probes would further discriminate between and help refine theories addressing the formation, and chemical, dynamical, and thermal evolution of all the giant planets, the solar

system including Earth and the other terrestrial planets, and lend significant insight into the formation and structure of exoplanetary systems.

References:

[1] Squyres, S., et al., "Visions and Voyages for Planetary Science in the Decade 2013-2022," National Academies Press (2011).

[2] Mousis, et al., Scientific rationale for Uranus and Neptune in situ explorations Pl. Sp. Sci., 2017. In Press https://doi.org/10.1016/j.pss.2017.10.005

HYBRID AEROCAPTURE USING LOW L/D AEROSHELLS FOR ICE GIANT MISSIONS. A. Pradeepkumar[1†], A. Arora[2†], J. A. Cutts[‡], and S. J. Saikia[3†], [1]apradee@purdue.edu, [2]arora31@purdue.edu, [3]ssaikia@purdue.edu, [†]School of Aeronautics and Astronautics, Purdue University, 701 W. Stadium Ave., West Lafayette, IN, 47907, [‡]NASA-Caltech Jet Propulsion Laboratory, 4800 Oak Grove Drive, Pasadena, CA, 91109, james.a.cutts@jpl.nasa.gov.

The "Ice Giant" Planets: Uranus and Neptune, known as the ice giants are mainly composed of elements such as oxygen, carbon and nitrogen. The ice giants are fundamentally different from the gas giants and the terrestrial planets and most exoplanets discovered so far appear to be ice giant size bodies. The Planetary Science Decadal Survey 2013-2022 has identified an ice giant mission as a priority for a Flagship-class mission after Mars Sample Return and a Europa mission [1].

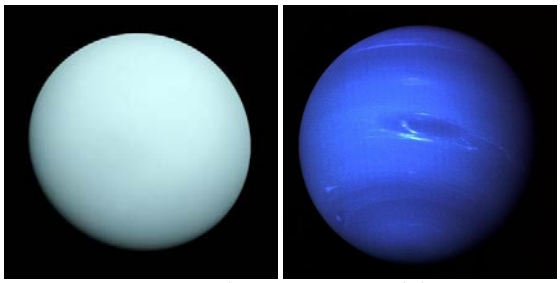

Figure 1: *Uranus and Neptune, imaged by Voyager 2 during its flyby in 1986 and 1989 respectively [2].*

NASA Ice Giants Pre-Decadal Study: JPL has completed the NASA Ice Giants Pre-Decadal Study which investigated in detail six mission architectures to Uranus and Neptune. The architectures include an orbiter and probe, orbiter alone, flyby with probe, SEP and chemical trajectories, and a variety of launch vehicles. Nominal flight times to Uranus and Neptune are 11 and 13 years respectively using SEP [3].

Assuming a nominal radioisotope power system (RPS) life of 15 years, this allows for 2–3 years for the science mission. While this is likely to be sufficient to accomplish the primary science objectives, it is unlikely to allow the spacecraft to follow up and further investigate new discoveries.

Reducing time of flight to the Ice Giants: One solution to decrease the time of flight is to use aerocapture, which performs a single atmospheric pass upon arrival and is captured into orbit. Aerocapture was studied as a part of the NASA Ice Giants Pre-Decadal Mission Study and has been classified as an "enhancing" option if the technology is available.

In contrast to propulsive orbit insertion, aerocapture allows for a larger range of arrival velocities. This allows for a broader range of interplanetary trajectories for a mission designer to choose from and can thus potentially reduce the time of flight, increase delivered mass, or both, and may allow the use of cheaper launch vehicle.

Ice Giants Aerocapture Assessment: An assessment of aerocapture for ice giant missions was performed at Purdue University in support of the NASA Ice Giants Pre-Decadal Survey. The study concluded that aerocapture can potentially increase delivered mass and reduce time of flight by three or more years while maintaining useful delivered mass provided an aeroshell with a mid L/D of 0.6 to 0.8 is available [4].

Aerocapture theoretical corridor width and the need for a mid L/D aeroshell at Ice Giants: Figure 2 shows the contours of theoretical corridor width (TCW) for Neptune as a function of arrival V_∞ and vehicle L/D for a specific ballistic coefficient and target capture orbit apoapsis altitude.

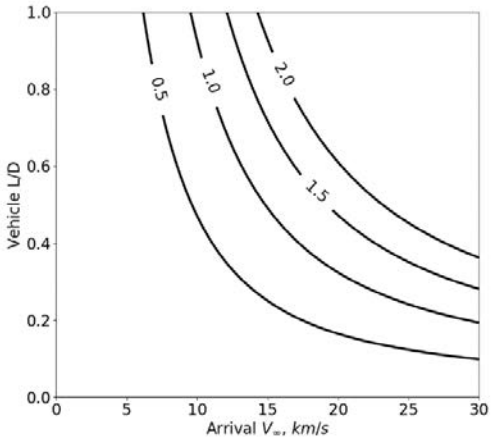

Figure 2: *Theoretical corridor width (TCW) contours, in degrees for aerocapture at Neptune for a range of vehicle L/D and interplanetary arrival velocities. Vehicle with β=200 kg/m^2, target apoapsis radius=1.578E6 km, corresponding a 20-day capture orbit which is also a desired science orbit [4].*

To account for spacecraft delivery errors, atmospheric, aerodynamic and other uncertainties, a minimum required corridor width can be computed. If the TCW exceeds the required corridor width, vehicle control authority is deemed to be adequate for aerocapture.

Preliminary analysis indicates that the required corridor width is at least 1.5 degrees for aerocapture at Ice Giants [4]. From Fig. 2, to obtain 1.5 degrees of TCW, an arrival V_∞ of approximately 15 km/s or higher is required along with a vehicle with mid L/D of 0.6 to 0.8. Higher arrival V_∞ than 25 km/s or higher enable use low L/D (0.2 to 0.4) vehicles but exceeds the capability of currently available TPS materials.

Aeroshells with flight heritage: Aeroshells with flight heritage such as Apollo and MSL, or those under development such as Orion Crew Module has a maximum L/D of 0.3 – 0.4 [5-7]. Currently there are no programs to develop a mid L/D vehicle in the US, and it is unlikely that NASA will pursue the development of such a vehicle in the near term due to budgetary constraints. Given this scenario, it would be advantageous to investigate techniques that may enable aerocapture at ice giants to be performed using heritage aeroshells with a maximum L/D of 0.4.

Potential options to perform ice giants aerocapture using low L/D aeroshells [4]**:**

1. Reduce the required corridor width by reducing uncertainties: Improvements in knowledge of ephemeris and atmospheric profiles, as well as improved navigation techniques can reduce uncertainties and hence reduce the required corridor width. For example, if the required corridor width can be reduced to 0.5 degrees or lower, then aeroshells with L/D of 0.4 become feasible for arrival V_∞ of at least 10 km/s as seen in Fig. 2.

2. Use a hybrid chemical-aerocapture approach to widen the theoretical corridor width: One example of this technique could be using aerocapture to achieve an initial target apoapsis lower than what is desired for the science orbit, and then use propulsion to boost the apoapsis. Cost-benefit analysis of this technique has been suggested as a potential follow on study by a recent NASA aerocapture assessment report [6].

3. Use a pathfinder entry probe: Sending a pathfinder probe to enter the atmosphere several days in advance of the orbiter aerocapture maneuver can measure the atmospheric structure and thus reduce atmospheric uncertainties.

Hybrid aerocapture analysis: This work will investigate the feasibility and perform a cost-benefit analysis of two hybrid chemical-aerocapture orbit insertion strategies at Uranus and Neptune.

1. Target a capture orbit with lower apoapsis. A lower apoapsis altitude than what is desired for the final science orbit is targeted during aerocapture. Preliminary results indicate this can increase the theoretical corridor width (TCW) as shown in Fig. 3. If the required corridor can be decreased to 1 degree using improved navigation, aerocapture with L/D of 0.4 becomes feasible for arrival V_∞ of at least 15 km/s.

Taregting a smaller capture orbit requires a propulsive burn at the apoapsis to raise the periapsis (ΔV_1), and a second burn at the periapsis to raise the apoapsis (ΔV_2) to that of the desired science orbit. The required propulsive ΔV for the two burns to transfer from a 1 day capture orbit to higher period science orbits (with a periapsis of 1.1 Neptune radius) is shown in Table 1.

Feasibility charts will be presented to understand the trade-offs between increased TCW and propulsive burn ΔV for a range of vehicle L/D, arrival velocities, ballistic coefficient initial target apoapsis for aerocapture, and final science orbits.

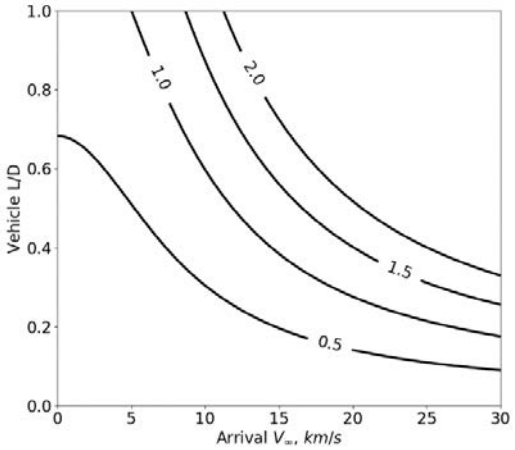

Figure 3: *Theoretical corridor width (TCW) contours for aerocapture at Neptune for a smaller 1-day capture orbit in contrast to a 20-day capture orbit shown in Fig. 2. Vehicle β=200 kg/m^2, target apoapsis radius=1.907E5 km, corresponding to a 1-day capture orbit which can be boosted to a 20-day science orbit using chemical propulsion.*

Table 1: *ΔV_1 and ΔV_2 for periapsis and apoapsis raise maenuvers respectively from a 1-day capture orbit to various desired science orbits at Neptune. Vehicle β=200 kg/m^2, L/D=0.4, V_∞=15 km/s, Entry altitude=1000 km.*

Final science orbit (days)	Apoapsis Radius (km)	ΔV_1 (m/s)	ΔV_2 (m/s)
10	9.841E5	137	1139
20	1.578E6	137	1252
120	5.273E6	137	1385
180	6.918E6	137	1399

2. Use atmospheric pass to reduce energy, but not enough to get captured. This study will perform a cost-benefit analysis of a vehicle which makes one pass through the atmosphere and removes a significant portion of the velocity, but not enough to get captured. A propulsive burn is used to complete the capture maneuver and accomplish the initial capture orbit, and subsequently the science orbit. The implications of such an aeroassist maneuver on TCW has not been studied in literature and is worth investigation.

References: [1] SSB (2011), *Planetary Science Decadal Survey 2013-2022*. [2] JPL Photojournal, PIA18182, PIA01492. [3] Elliot J. *et al*. (2017), JPL-D 100520 [4] Saikia S. J. *et al.* (2016), PU-AAC-2016-MC-0002. [5] Hillje E. R. (1969), NASA TN D-5399. [6] Spilker T. R. *et al*. (2016), JPL D-97058. [7] Moss J. N. *et al.* (2006), AIAA-2006-8081.

EXPLORATION OF PLUTO WITH A NEW-FRONTIERS-CLASS LANDER OR ORBITER MISSION.

B.D. Goldman[1], K. T. Nock[1], D. K. Lo[1], C. R. Sandy[2], [1]Global Aerospace Corporation, 12981 Ramona Blvd, Ste E, Irwindale, CA 91706, Benjamin.d.goldman@gaerospace.com, [2]ILC Dover LP.

Introduction: With water-ice mountains, expansive glaciers, possible cryovolcanism, and an extended Nitrogen atmosphere, Pluto is a dynamic world shrouded in mystery. Surface features aligned with Pluto's tidal axis suggest that it has a hidden subsurface ocean of liquid water. Pluto could be the most distant "Ocean World" in our solar system. The best way to unravel the mysteries of Pluto is stop and stay a while with a new mission concept to explore the interior, surface and atmosphere.

A low-cost, *New-Frontiers*-class Pluto lander or orbiter mission with a launch in 2029, Jupiter gravity assist in 2030, and arrival at Pluto in 2040 is possible. The next opportunity for a similar mission will not be possible until a 2042 launch when Jupiter is again positioned for a gravity assist.

So how can we land on or orbit Pluto without several hundreds of millions of dollars in nuclear power sources, a next generation launch vehicle, or a massive propulsion system? One way is to launch a probe on a trajectory similar to the Jupiter flyby trajectory of *New Horizons*, target it for entry at Pluto at 14 km/s, and deploy a large, ultra-lightweight inflatable drag device prior to entry at an altitude of 1600 km. The low density Pluto atmosphere has a scale height of ~60 km, nearly 8 times larger than at Earth, enabling atmospheric drag to slowly dissipate the 50 gigajoules of kinetic energy of entry.

Contrary to prior thought, recent studies show that the Pluto atmosphere does not collapse and may have increasing atmospheric pressure with time in the current epoch[1], making the 2029 window a real possibility for this mission.

Only one Multi-Mission Radioisotope Thermoelectric Generator (MMRTG), currently in production by DOE, is needed to power onboard spacecraft systems. Depending on the trajectory and flight path angle, the probe can either descend to the surface and deliver a 200-kg lander-hopper or insert an orbiter via aerocapture. We deem this architecture *Entrycraft*.

This mission concept is enabled by the use of ultra-lightweight, Enveloping Aerodynamic Decelerator (EAD) technology*. The Entrycraft combines the decelerator system with the lander or orbiter payload that also performs all the needed function during the cruise to Pluto without a separate stage.

In one ConOps (Figure 1), the lander separates from the deceleration system a few hundred meters above the surface and performs a small burn for landing. Once at the surface, initial science experimentation can begin. Science operations could include imaging, surface sampling and soil mass spectrometry, geophysical sounding, heat flow and seismometry, as well as atmospheric sampling. Once the initial landing site science objectives are completed, a hop to another landing site is planned based on a combination of *New Horizons* data and the optical navigation camera images taken on entry. A small propulsive burn is executed to put the lander on a parabolic trajectory toward a second landing site. During the hop, imaging and spectroscopy data of the surface can be obtained. A final propulsive burn is preformed just prior to touchdown for landing.

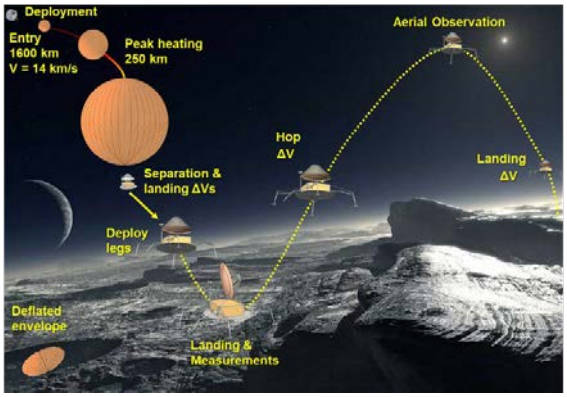

Figure 1. Concept of Operations

The preliminary results of a NASA Innovative Advanced Concepts (NIAC) study will be presented including the results of the interplanetary and approach mission design; structural, aeroelastic, aerothermodynamic, and thermal modeling; aerodecelerator and lander/hopper system design; and possible orbiter mission design efforts.

References:

[1] C. Olkin, "Evidence that Pluto's atmosphere does not collapse from occultations including the 2013 May 04 event," Icarus, vol. 246, pp. 220-225, 2015.

* US Patent 9,884,693 issued February 6, 2018.

Nuclear Thermal Propulsion: Enabling Robust Missions to the Outer Solar System

Les Johnson, Mike Houts, and Mitchell Rodriguez

NASA is developing nuclear thermal propulsion (NTP) stages for future human and robotic scientific exploration of the solar system. First generation systems under development, when coupled with the lift capability of NASA's Space Launch System, will enable spacecraft with dry masses between two and five metric tons to be captured into orbit at Uranus and Neptune with reasonable trip times. No state-of-the-art or near-term new propulsion system can come close to matching this performance. This capability may enable robotic landers the size and mass of *Curiosity* (900 kg), used for exploring Mars, to be landed on the moons of the Ice Giants. Spacecraft comparable to the Cassini (2500 kg) may also be sent to explore the Ice Giants and their moons.

First generation NTP system will provide high thrust at a specific impulse above 900 s, roughly double that of state of the art chemical engines. And, using Low Enriched Uranium (LEU), comparable to that use in university-class research reactors worldwide, will allow these systems to be developed at a much lower cost than previously-considered NTP systems.

An overview of the propulsion systems being developed, estimated performance for first generation NTP systems (for exploration of the outer solar system and beyond), as well as a status of the NASA program will be discussed.

A SURFACE MOBILITY SYSTEM WITH LARGE DEPLOYABLE AND CONFORMAL TIRES FOR OCEAN WORLDS EXPLORATION. R. Agrawal[1I], B. Aiken[2ǂ], M. de Jong[3ǂ], A. Pradeepkumar[4I], J. Longuski[5I], S. J. Saikia[6I], [1]agrawa77@purdue.edu, [2]brian.aiken@thin-red-line.com, [3]maxim@thin-red-line.com, [4]apradee@purdue.edu, [5]longuski@purdue.edu, [6]ssaikia@purdue.edu, [I]School of Aeronautics and Astronautics, Purdue University, 701 W. Stadium Ave., West Lafayette, IN 47907, USA. [ǂ]Thin Red Line Aerospace, Chilliwack, British Columbia, V2R 5M3, Canada.

Why Ocean Worlds? Europa and Enceladus are widely believed to harbor sub-surface oceans—and therefore offer the potential for habitable environments—making them prime candidates in the search for life beyond Earth [1–3]. The presence of salty liquid water oceans (in contact with a rocky surface), hydrothermal vents, and active geology make Europa and Enceladus (Figure 1) compelling candidates in the search for life beyond Earth. Therefore, mobility technologies that enable robotic in situ exploration of the surfaces of these Ocean Worlds are of high interest to NASA for future missions. However, no current state-of-the-art (SOA) mobility system can operate in the rugged terrains of the Ocean Worlds.

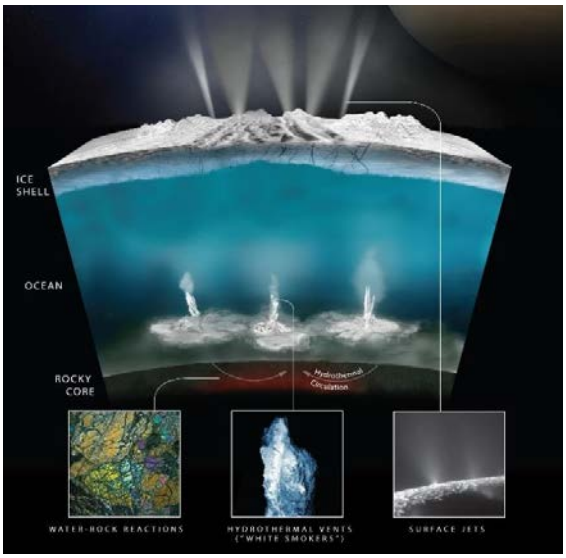

Figure 1: Ocean Worlds such as Europa and Enceladus are prime candidates in the search for life beyond Earth [4].

Exploration Cadence: Europa and Enceladus have so far only been studied from orbit. While the planned Europa lander mission envisions a stationary lander that can target a focused set of scientific questions, a mobility system will be an essential step in the mission cadence (Figure 2). In addition, the proposed Europa lander, with a 3-σ landing accuracy of about 40m, cannot necessarily land near an area of greatest scientific interest [5]. Ocean Worlds exploration will evolve from a stationary lander, to a mobility system, and ultimately to a sub-surface explorer to explore the liquid water oceans (Figure 2).

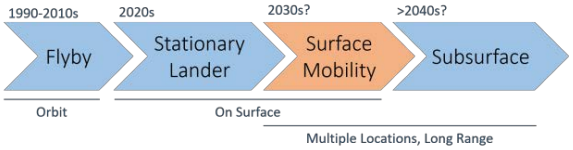

Figure 2: Ocean Worlds exploration cadence

Challenges for an Ocean Worlds Mobility System: Ocean Worlds will likely offer terrain varying from the smoothness of sea ice to as rugged as high cliffs, deep crevasses, blocky ice boulders, soft powdery snow, or even tall penitentes. Europa's highest resolution images (6–12 m/pixel resolution) [3,5] of the surface from the Galileo mission, identify scientifically attractive exploration targets. These images indicate a heavily textured surface down to the pixel level, terrain presenting fractures, steep inclines, and scarps. Enceladus's young and active "tiger stripe" region (Cassini, 4 m/pixel) near the south pole is strewn with ice blocks and boulders ranging in size from 10 to 100 meters, along with intervening smooth patches [6] (Figure 3).

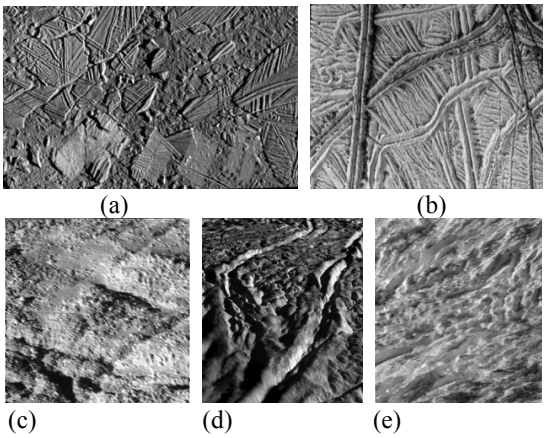

Figure 3: Ocean Worlds Surfaces (a) Europa's Chaos Terrain (b) Double ridges on Europa (c) Ice-block covered surface of Enceladus's Tiger stripes (4 m/pixel) (d) Perspective view of Baghdad Sulcus, tiger stripes (12-30 m/pixel) (e) Close-up of tiger stripe (15m/pixel) [6–8].

Europa's dark lineae are also important science targets as they might have resulted from recent (and active) upwelling, signifying thinner regions in the ice shell. However, the rugged terrains (caused by eruptions of warmer ice—similar to Earth's mid oceanic ridges) around these regions will likely pose severe mobility challenges, as would subduction or compression zones.

State-of-the-Art (SOA) Mobility Systems: The SOA NASA Mars rover mobility system (six-wheel rocker bogie) is not designed for the extreme and rugged environment of the ocean worlds: The six-wheel rocker bogie system uses a large number of actuators. Also, the wheels are not scalable or conformal, and vastly larger, flexible tires are required to traverse such rugged terrain. Hoppers potentially offer an alternative, but these are propellant-intensive and inherently risky during landing [9–10]. The most common terrestrial mobility systems for polar regions such as snowmobiles and other tracked vehicles would also be unsuitable for the. Operating the mobility systems at the temperatures of 50-100 K is infeasible.

Proposed Expandable Tire for Ocean Worlds: Our team proposes to develop and test an innovative and game-changing mobility concept for the exploration of surfaces of the Ocean Worlds. The proposed effort includes analysis, simulation, prototyping of a tire, and evaluation and testing in an analog test environment. The proposed rover for Ocean Worlds overcomes the shortcomings of the current SOA mobility systems by employing large expandable tires with wide, conforming surface tread that provides excellent traction on rugged terrain and jagged surface features while offering outstanding wear resistance.

Large Diameter Deployable Tire: The expandable and scalable, puncture-proof tire is based on a cutting edge fabric structure called Ultra High Performance Vessel (UPHV) (Figure 4). The UHPV architecture was developed by Thin Red Line Aerospace (TRLA) to address NASA's problems with performance unpredictability in inflatable structures [11–12]. Figure 4 shows the various elements of the deployable tire along with their descriptions.

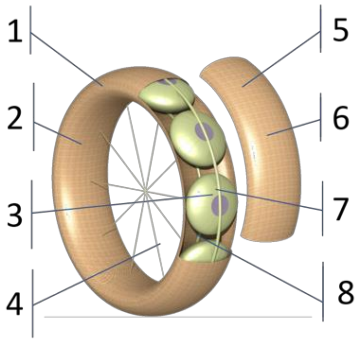

Figure 4: Cross-sectional view and various elements of the deployable tire: 1. UHPV fabric 2. Large diameter, expandable tires. 3. Oblate spheroid, unpressureized UHPV, tensioned using internal leaf springs 4. Spokes tensioned during deployment. 5) Wide conforming surface, tread for traction. 6. Wear resistant exterior 7. and 8. Outer and inner annuli for deployment and structural rigidity [13].

Tire Packaging and Deployment: The wheels are capable of compact stowage and simple lightweight construction to facilitate efficient packaging. In stowed position, annular rings and spheroids are deflated and folded. To deploy the tire, the annular rings are first inflated after which the tire unfolds and the spokes are tensioned. After the tire fully unfolds, the leaf springs in the spheroids deploy and the spheroids expand (Figure 5). The outer annulus is only important during initial inflation, and once inflated, is no longer essential.

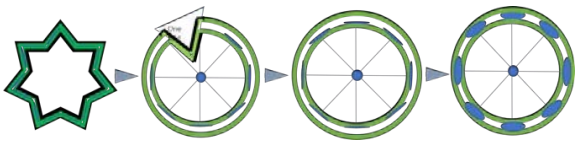

Figure 5: Tire deployment concept of operations [13].

Proposed Work: Current efforts involve characterizing the surface features of Europa and Enceladus, specifically for the scientific regions of interest. Surface detail is simply not adequately understood at the rover scale. Improved insights of terrain types and surface materials will be applied to tire design. Our team will present results from the following studies and analysis:

- *Material selection for all tire components*
- *Tire sizing and mass estimation*
- *Stowage, packaging and deployment*
- *Conceptual tire design for Mars rocker-boogie rover application*

Relevance to NASA: With potentially habitable environments, Ocean Worlds are of prime interest to NASA. While the current Europa lander mission concept envisions a stationary lander, a rover with mobility capabilities like the one proposed can greatly expand the data collection of a potential Europa/Encleadus landed mission by accessing multiple sites. A mobility platform could potentially approach the vicinity of an active geyser for collection of subsurface materials. Therefore, the proposed mobility system is potentially game-changing and is an "enabling" technology for an Ocean World mission, not otherwise possible with current state-of-the-art systems.

References: [1] SSB (2003), *New Frontiers in the Solar System.* [2] NASA (2014), *Science Plan*. [3] SSB (2011), *Planetary Science Decadal Survey 2013–2022*. [4] JPL Photojournal, PIA21442. [5] Miguel San Martin A. (2015), *IPPW-12*. [6] Greenberg R. *et al.* (1998), *Icarus 135.1: 64-78.* [7] Europa Study Team (2012), JPL D-71990. [8] Porco, C.C. *et al*. (2006), *Science, 311,* 1393-1401. [9] Cohanim B. (2013), Ph.D. Dissertation, MIT. [10] Montminy S. (2008), *Acta Astronautica 62.6:* 438-452. [11] de Jong M. (2010), NASA Phase II SBIR Report, NASA-ARC. [12] de Jong M. *et al*. (2016), *IPPW-13*. [13] Pradeepkumar A. *et. al.* (2018), *NASA Outer Planets Assessment Group Meeting.*

DRAGONFLY: NAVIGATING TITAN'S SURFACE. D. S. Adams[1], B. F. Villac[1], K. E. Hibbard[1], R. D. Lorenz[1], E. P. Turtle[1], B. D. Cichy[2], and F. Amzajerdian[3], [1]Johns Hopkins Applied Physics Laboratory, Laurel, Maryland 20723, [2]NASA Goddard Space Flight Center, Greenbelt, Maryland 20771, [3]NASA Langley Research Center, Hampton, Virginia 23681.

Introduction: The Dragonfly relocatable lander requires *in situ* navigation capability in order to traverse the surface of Titan. Doing so requires the ability to identify previously-scouted and known-safe landing sites, and to navigate from those sites to both scout and subsequently to land at new sites. The rotorcraft lander is equipped with a carefully selected suite of sensors to follow a ground-determined flight plan in order to safely negotiate the surface of Titan in pursuit of the mission science objectives..

GNC Instrumentation: The Dragonfly landing-system design combines multiple existing guidance, navigation, and control (GNC) technologies for multi-rotor vehicle control, terrain-relative navigation, and safe-landing-site characterization, into a robust and realizable space flight system. Dragonfly's core element is a rotorcraft lander with a mobility subsystem consisting of the sensors (lidar, radar, cameras, IMU, and atmospheric pressure), actuators (motors and rotors), structure (booms and skids), electronics (navigation processor and electronic speed controllers), and GNC processing, that all combine with traditional subsystems to enable relocation to multiple sites via atmospheric flight.

The Flight Mode Manager (FMM) is the heart of the flight control system. The FMM receives data from the navigation filter and sensors, processes them along with uploaded flight profiles and constraints, and autonomously switches between flight guidance modes (waypoint/trajectory following, climb, cruise, descent, landing, etc.) and flight control modes (rotor speed, differential rotation). The low-level multi-rotor flight control laws are based on well-known approaches commonly used for terrestrial systems.

While the general landing site target is specified by ground command, the lander-scale touchdown position is determined on-board in real time using data from a flash lidar. This instrument is ideal for interrogating the local slope and terrain features in order to assess landing site safety and to implement hazard detection and avoidance (HDA). One of the key features of the Dragonfly architecture in the Titan environment is the flight endurance and the ability to loiter over a target landing site allowing the lander to be discerning in the landing position selection. The onboard ability to identify safe landing sites permits subsequent exploration of more complex (and thus more scientifically appealing) terrain, and can also be used for unplanned landings should the need arise.

Optical Navigation: While IMU-only navigation can be used for short hops, for high precision on longer traverses Dragonfly employs optical terrain-relative navigation (TRN). This is acomplished using two well-established and simple operational modes, optical velocimetry (OV) and optical landing site recognition (OLSR), and does not require real-time map generation. The system uses wide field-of-view (FOV) cameras that are optimized for Titan lighting conditions. A navigation system based on these overlapping capabilities provides multiple functional redundancies to maximize navigation precision and allow extended flights.

Sensor Redundancy: In order to maximize resiliencey, the sensor system design can leverage multiple sensors (some of which can make redundant measurements) to provide these capabilities. Radar velocimeters have flown on missions to the Moon and Mars, and provide both altitude and velocity data relative to the surface, independent of lighting conditions. Flash lidar systems provide the ability to directly measure the surface topography of terrain beneath the lander and also provide altitude. OLSR and OV provide lateral position and redundant and velocity measurements respectively, and can use either radar or lidar altitudes for processing.

Sticking the Landing: Rotorcraft within a few rotor diameters of the ground may create recirculating air that can result in brown-out conditions. This would only occur in the last seconds of Dragonfly's descent, which are therefore executed using only the IMU and the navigated position and velocity. Extensive simulations and testing verify that Dragonfly will achieve soft, stable landings with minimal surface disturbance.

Using Radiation Sails to Transport Interplanetary and Interstellar Probes. Ronald L Bennett[1], Jovian Inc. 2550 E Desert Inn, Las Vegas, NV 89121.

Introduction: Imagine if you will, a spacecraft that can travel to Mars within a couple days, to Jupiter within a week or sooner without carrying a huge amount of propellant. A truly alien type spacecraft with the power of a small power plant that may look like what we commonly refer to as an Unidentified Flying Object, UFO. Now imagine a spacecraft that can sail to our nearest star within 10 years, that is if humans can withstand time dilation past twenty percent the speed of light. That all sounds like something out of a science fiction novel or movie doesn't it. It is not as complicated as it seems. Most of you are going to be amazed about what I'm about to tell you if this stands up to critical examination that is sure to follow making such bold extraordinary claims. If it does, then we may be on a truly fast paced exploration of our solar system.

Nuclear fission is where a neutron decays into a proton and gives off an immense amount of energy, some of the particles escaping nuclear material such as gamma rays travel the speed of light. That energy if used like a rocket exhaust speed can technically propel an object close to the speed of light.

The current use of nuclear fission in nuclear power plants is that they use the radioactive decay of a fission material by turning the kinetic energy into thermal energy then into electrical power, the nuclear material radiates energy over a known set amount of time. The fission process from an atomic nuclear bomb releases all the energy at once from most of the energy within the nuclear material.

For this abstract that is Patent Pending the nuclear material I'm going to use to explain it in detail is Strontium 90, Sr^{90} with a half-life of 28.7 years which decays into Yttrium 90, Y^{90} with a half-life of 64 hours, then into stable Zirconium. As a result, it's a combined Sr^{90}/Y^{90} decay. Sr^{90} /Y^{90} gives off high speed Beta, β decay only, it also gives off a very miniscule amount of Gamma rays that is so small it's not harmful to humans. Different nuclear material can be used with varying results. Strontium 90 is very abundant in nuclear waste sites, it's dangerous to humans if inhaled or if it gets in the food supply chain yet the Russians use it extensively in space for a long-term power supply to generate continuous electricity in a Radioisotope Thermoelectric Generator, RTG.

This invention is about using most of the initial energy from radioactive decay to create thrust of a spacecraft on one side while using the resulting waisted thermal energy to produce electrical energy on the other side. The claims and diagram below briefly tell you what I'm talking about

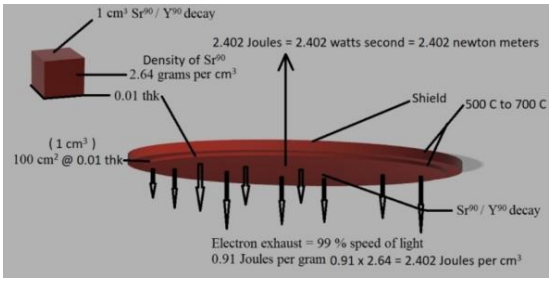

Fig 1

In Fig 1 shows how this will work. The secret hear is to take radioactive material and adhere it or splatter it onto a surface as a surface coating about 0.01 min deep. In this case we use Sr^{90}/Y^{90} that emit β particles.

During radioactive decay of Sr^{90}/Y^{90} most of the high-speed β particles will escape a depth of 0.01 of the Sr^{90} on the unshielded side that is used to lift the device up. In that way most of the radiation that needs to escape will do so on one side, lower side, while most of the radiation on the other shielded side, upper side, conserves the energy therefore moving the object in an upper direction. If both sides were unshielded then the object upwards force would equal 0. The shielded side conserves the kinetic energy turning it into thermal energy, the unshielded side lets the radiation escape as a result it is used as thrust. For example, if you take 1 cubic cm of radioactive Sr^{90}/Y^{90} and slice it up into 0.10 thick pieces spreading it our over 100 cm^2 surface area it will give an object lift, if that same mass was in a cube most all the kinetic energy will be turned into thermal energy and not thrust.

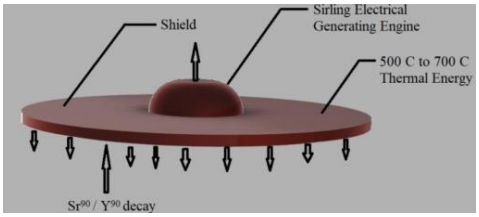

Fig 2

In Fig 2 the shielded sides is waisted thermal energy that can be convert into electrical power several differ-

ent ways either by using a Sirling engine, by using a co-generator steam power, or a Radioisotope Thermoelectric Generator, RTG.

We now know if placed in space using chemical rockets, over time it theoretically can travel up to 99 percent the speed of light with hundreds of times more thrust per newton than any ion drive or solar sail proposed today. We know that it would be sustainable 30 years or however long the radiations decay lasted and can be used to generate its own electricity.

Now let's do some math to see how much energy we have in a gram of Sr^{90}/Y^{90}. We're going to use two different methods.

Knowns

1 Joule (J) = 6.242^{18} ev
1 calorie = 4.184 J
1 newton (n) = 786.831 calories (c)
1 n = 3292.1 J or 1 J = 0.0003 n

The first method we will find out how much energy is in the speeding β particle that's ejected from the decaying atom in electron volts, ev, due to its momentum and convert that into Joules. There's 6.242^{18} ev in a Joule.

What's the amount of decay in 1 gram of pure Sr^{90} in Becquerel, One Bq = 1 radioactive decaying atom due to fission. Sr^{90} has an average of 5.21 trillion Bq, 5.21TB/q activity per second per gram with an average energy of 546,000 ev, 0.546 Mev, per particle.
5.21×10^{12} Bq x 0.546Mev = 2.845×10^{18} ev Sr^{90} decay energy per gram/second, 2.845×10^{18} ev / 6.242×10^{18} ev (1 Joule) = 0.455 Joules per gram or 0.000138 n

The amount of decay in 1 gram of pure Y^{90} is 1.99×10^{16} Bq-g, that's 19,900 trillion of decays every second per gram with an average decay energy of 2.841 Mev., 1.99×10^{16} Bq-g x 2.841 Mev = 5.654×10^{22} ev / 6.242×10^{18} ev = 9,057.34 J-g or 2.717 n per gram.

How does the Sr^{90} decay happens? 5.21 TBq per second per gram Sr^{90} decay into Y^{90}, even though that's a very large number it is nowhere near the number of atoms in a gram of Y^{90}, in order to calculate that up the right way for the decay of Sr^{90} into Y^{90} we would need to use, mols and avocados number and still your talking about a number that changes over time. At best what I found is that the total average energy of the Sr^{90}/Y^{90} decay to be 0.91 Joules. How they came up with that number is by multiplying the Sr^{90} 0.455 Joules number by 2 you get from above, meaning that is what they surmise out of both Sr^{90}/Y^{90} decay. They used the assumption, for every β particle decay energy of Sr^{90} there was an equal amout of β decay energy from Y^{90}. So, to find the actual amount of energy released per second in a gram of Sr^{90}/Y^{90} decay, we may want to try the second method.

The second method we will find out how much thermal energy is released in the fission of a Sr^{90}/Y^{90} decay using Calories per Celsius, for instant it takes 1 Calorie to raise a gram of water one-degree C. Pure Sr^{90} radiates between 500 C to 700 C of thermal energy. Using the lower end of the thermal energy shown above, 500 C, and specific heat of the metal we can convert it to joules, 1 Calorie = 4.186 Joules. The specific heat of Strontium and Yttrium is the same 0.300 kj/kgK, the energy needed to raise one gram of Strontium from 20 C to 500 C (480) as a result 0.300 kj/kgK x 1 g x 480 = 144 Joules per gram or 0.0432 n

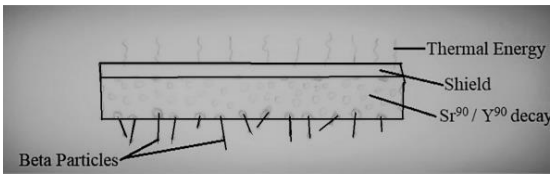

Fig 3

In Fig 3 there is 5.21 trillion of Sr^{90} decays every second per gram of nano-size explosion's, which launched the β particle from the surface to close the speed of light with much greater energy than the combined energy of the β particles. In a solid most, β particles don't escape the mass, it conserve's the energy thus turning the kinetic energy into thermal energy, only the β particles close to the surface radiate β particles outwards that escape the mass.

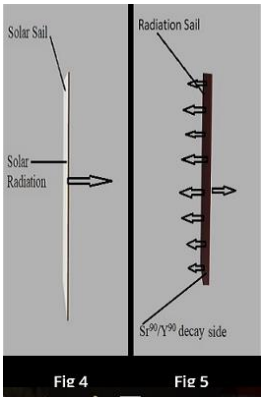

Fig 4 Comparison of a 32-square meter Solar Sail 2, 320,000 square centimeters, developed by The Planetary Society and this invention with the same size proposed, Fig 5, Radiation Sail that has a 0.010 min coat-

ing with Sr^{90}/Y^{90} radiation with a thicker solar sail material that acts as a shield.

The total force acting on the said Solar Sail by the force of the solar radiation is 2.91 x 10^{-4} N = 0.000291 N with a maximum speed of 240, 000 kph, 150,000 mph. The radiation shield which uses 3,200 cm^3 of Sr^{90} /Y^{90} radiation that covers the entire 320,000 square centimeters sail at a depth of 0.010 minimum. Using 0.91 Joules per cm^3 x 2.64 grams per cm^3, Sr^{90} /Y^{90} = 2.402 Joules per cm^3 = 2.402 Nm per cm^3. 2.402 x 3,200 cm^2 we get 7,686 J from the Radiation Sail pushing the sail with an exhaust speed at up to 99 percent the speed of light which is over 4,500 times faster than the Solar Sail. Using just 10 percent efficiency of the Radiation Sail 768.6 J or 0.230 n as a result the Radiation Sail has at least 792 times more force to accelerate an object using the same surface area as a Solar Sail while accelerating it close to the speed of light.

By using a commercial application that will splatter on pure Y^{90}, at 9,057.34 J per gram on the 5.66 m^2 (18.4 ft^2) sail the resultant force on the same size sail as the Planetary Society Solar Sail would be 76,516,386 J or 22,955 n.

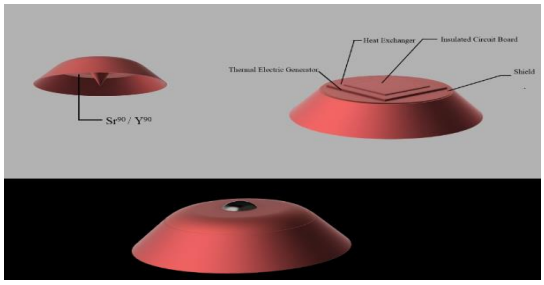

Fig 6

Fig 6 Future Light Weight Test launched in orbit into Interstellar Space

There are several other ways this invention, patent pending, can be used including ion drives, plasma induced magnetic field. etc. To get more lift ionizing feed stock may be used by colliding the fisionary electrons at speeds up to 99 percent the speed of light with protons, atoms, water vapor, or gas resulting in 1,000 times more ev's energy used that ionizes the feedstock into plasma than is currently used in ion drives.

Another research is in inducing more fission in nuclear material by injecting neutrons into the material as a result it induces neutron decay chain reaction that extract out more energy, a large solid mass in U235 or PL239 can have a meltdown when neutrons get out of control, but a thin coating of radioactive material that's been bombarded with added neutrons will not. Therefore, more energy can be extracted with neutron enriched radioactive decay supplying more needed acceleration at the time we need it. Like new groundbreaking inventions this is the start of something much bigger.

The first use of this invention may be after it is launched into space as a Radiation Sail Shuttle in between planets, moons, and even the stars. It can be used to mimic artificial gravity by its constant acceleration and deceleration. The first use may be landing and launching from low gravity worlds, once refined in the future maybe even launched from earth.

This invention is only the beginning of our quest to visit our neighbor stars unshackling humans from the pale blue dot we live on.

"The vast distances that separate the stars are providential. Beings and worlds are quarantined from one another. The quarantine is lifted only for those with sufficient self-knowledge and judgment to have safely traveled from star to star." - Carl Sagan, Pale Blue Dot

References: [1] Author Ronald L Bennett. (2018)

SIMULATING CAVITATION ON THE TITAN SEAS. D. Chen[1], S.R. Carberry Mogan[1], and A. Tafuni[1], [1]Dept. of Mechanical and Aerospace Engineering, Tandon School of Engineering, New York University, Brooklyn, NY, 11201, USA, damonchen@nyu.edu.

Introduction: Because of their accessibility, the hydrocarbon seas on Titan are exciting targets for future in-situ exploration missions. However, the seas are very effervescent and solubility models predict that the introduction of small heat fluxes, temperature, or pressure gradients are likely to cause exsolution of the nitrogen gas dissolved within the solution [1]. For an analogous comparison, the composition of the seas on Titan are similar to that of soda or sparkling water in that they are very bubbly due to the presence of dissolved gas. Moreover, the issue is further exacerbated by the fact that hydrocarbons, due to their higher vapor pressure, are more prone to vaporization when compared with water. As such, a particularly unique challenge for probes is posed since there is a potential for the nitrogen gas bubbles to (1) manifest from waste heat from the radioisotope generators present on a lander which may interfere with the performance of scientific instruments and (2) elicit from the pressure gradient of a propulsion system like a marine propeller which may cause significant cavitation damage. These issues are present on many proposed Titan landers such as the Titan Mare Explorer, JPL Team X Titan lake probe, and Titan Submarine [2]. Previous small-scale experimental work have been done to investigate this issue by determining the bubble incipience point at various compositions [3].

The present work aims to use computational fluid dynamics (CFD) code, ANSYS Fluent, to characterize the effervescence issue on Titan that arises from planetary probes as it is crucial for evaluating their feasibility and performance. Rather than investigating the issue as it occurs in its full complexity, two comparatively simpler cases are studied.

Heat Based: First, a two dimensional case is modeled in which a heat flux is introduced to the bottom of an insulated tank of a fully saturated LCH_4 + DN_2 mixture at 90 K and 0.15 MPa to visualize bubble formation and determine the required heat flux for significant bubble incipience. The model used in this case assumes that the mass transfer rate between DN_2 and GN_2 is linearly proportional to the supersaturation ratio of the mixture and is implemented via UDF. Model parameters are tuned and benchmarked against experimental data. Various cases in which a specified heat flux on the bottom of the tank is simulated. Visualization of the GN_2 volume fraction with a heat flux of 10 kW/m^2 is shown in Fig 1. The model assumes infinite nucleation points for bubble formation which is appropriate for this case. The nucleation of the bubbles are investigated in a further study. Bubbles begin to onset after the required Gibbs free energy needed to liberate a bubble from its initial surface tension is supplied.

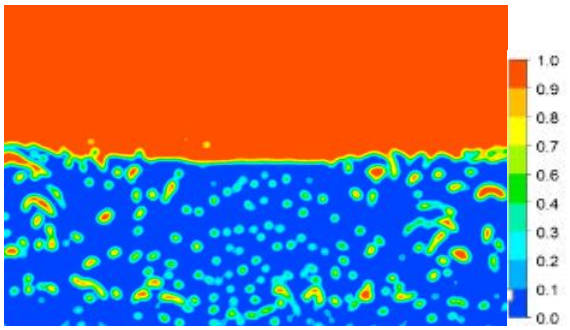

Fig 2. GN_2 volume fraction (q = 10 kW/m^2)

Pressure Based: Second, a two dimensional case of a Laval converging-diverging nozzle using a model that is similar to the well-known Sauer cavitation model is implemented [4]. A modified Sauer model is adopted in this work to account for the dissolved nitrogen in solution. This model is ideal for this case because although it makes quite a bit of assumptions, the only required parameters are the vapor pressure and the bubble density. Additionally, results are obtained for a saturated mixture at various Re and Re = 75000 is shown in Fig 3. Here, nitrogen exsolution is modeled without the inclusion of CH_4 vapor phase.

In addition, dimensional test case of a marine propeller is simulated for methane vaporization and nitrogen exsolution to evaluate propeller cavitation. Future work includes performing experiments to further benchmark and tune the simulation parameters.


Fig 3. LCH_4 + DN_2 Saturated mixture at 90 K (Re = 75000)

References:

[1] Hartwig, J. et al. (2018) *Icarus,* 299, 175-186 [2] Oleson, S.R. et al. (2015) *NASA TM* 2015-218831. [3] Richardson, I. et al. (2018) *FPE,* 462, 38-43 [4] Dunn. P.F. et al. (2010) *Physics of Fluids,* 22, 117102-1-22.

MODELING EXOSPHERIC ESCAPE AND TRANSFER PROCESSES IN THE PLUTO-CHARON SYSTEM USING A HYBRID SPH-BALLISTIC METHOD. S. R. Carberry Mogan[1§], D. Chen[1], A. Tafuni[1]; [1]New York University Tandon School of Engineering ([§]ShaneRCM@nyu.edu; 6 MetroTech Center, RH517D, Brooklyn, NY 11201).

Background: Until the New Horizons (NH) flyby of Pluto in 2015, atmospheric models were inspired by telescopic observations that suggested Pluto's atmosphere was complex. Its global structure and evolution, however, were not well understood [1]. Thus, the data from NH was highly anticipated as it would provide a detailed snapshot of the current state of its atmosphere. Figure 1 illustrates the difference between telescopic and NH's in-situ observations.

Pluto's atmosphere was once widely believed to undergo escape in a process that was slow and hydrodynamic (e.g., see review in [2]). Previous studies discussed the various escape drivers, cooling processes and the role of conduction and viscosity in determining the structure of and escape from Pluto's atmosphere [3-7]. In all of these cases, however, they used hydrodynamic (i.e., continuum) models. The failure in the continuum model is indicated by the increasing Knudsen number, Kn, which is the ratio of the mean free path over a characteristic length scale and indicates whether a continuum or molecular approach should be applied [8]. Thus, continuum models break down well before simulations approach the nominal exobase, which is typically taken to be at the Kn = 1 interface, necessitating the use of a kinetic model for upper atmospheres. Indeed, the accuracy of a continuum model has been shown to be adequate for atmospheric escape if coupled to a molecular approach above Kn ~ 0.01 [9-10].

Thus, for one of the focuses of my Ph.D. research, I have chosen to apply a novel, hybrid computational method, coupling a continuum to a molecular solver, to model the complex gas dynamics of the Pluto-Charon system described by the NH encounter. This research will serve as a means to improve our ability to simulate the evolution of planetary systems.

Figure 1. Telescopic (*left*) and in-situ (*right*) images of Pluto.

Methodology: A multi-dimensional and species code will be devised and adapted to model flow combining the computational efficiency and grid-free adaptation of the smoothed particle hydrodynamics (SPH) method in the continuum regime with the broad applications of a molecular kinetics (MK) method in the very low density regime. The SPH method was originally introduced and used for stellar [11]. It is a purely Lagrangian, meshless approach for solving the Navier-Stokes (N-S) equations. MK methods are used to track molecular dynamics in a variety of flow fields [12]. If molecules move in a highly rarefied region, such as in a planet's exosphere, their ballistic trajectories can be traced using free molecular flow models [13].

The benefits of such a hybrid method are immense for describing atmospheric dynamics in complex planetary systems. However, the SPH method cannot be applied in the rarefied gas dynamics regime due to the breakdown of the N-S equations and an MK method, such as a free molecular flow model, can be computationally intensive when trying to span very large density differences. Thus, a hybrid method would allow for SPH to efficiently describe regions in which the geometry is such that grid based methods are problematic before coupling to a MK method when in the low density, non-equilibrium regimes.

This hybridization would be a significant advancement of the coupling described in [14] for a 1-D spherically symmetric atmosphere. Pluto's exosphere and Charon's atmosphere, if one exists, however, are not spheres and escape is not spherically symmetric. This is due non-uniform illumination of the system; non-uniform distribution of volatile ices across Charon's surface resulting in varying sublimation; Charon's gravitational influence on Pluto's ex-tended atmosphere; and centrifugal forces acting on the molecules in Pluto's atmosphere due to its rotation [2, 13]. The magnitude of these effects change according to varying solar insolation stemming from Pluto's elliptical orbit about the sun. Thus, this system possesses a geometry that is problematic for standard mesh-based methods that could be efficiently solved by coupling to a particle-based method. SPH would solve for the continuum fluid dynamics up to a certain Kn before transitioning to the latter method to describe the nearly collisionless gas dynamics in the upper thermosphere exosphere. This would allow for a transition from a deterministic to a probabilistic approach, in which global properties of mass, kinetic energy, and linear and angular momen-

tum must be conserved. To implement such a transition, each simulated particle would be treated as a system carrying a set of equations governing its dynamic behavior. Thus, transitioning flow scales does not erquire particles to be destroyed or new ones to be inserted into the regime; instead, their description would change according from one to the other via their equations of motion within a "buffer." An ideal location for a buffer region would be at the Kn where the continuum model begins to breaks down. Figure 2 highlights this buffer with a NH occultation of Pluto's atmosphere and an illustration of this hybrid methodology applied within its extended regions. Thus, the methods would transition from SPH to ballistic when the N-S equations begin to fail as particles ascend to the rarefied regime in order to simulate the effect of a non-uniform exobase on the escape rates and density profiles.

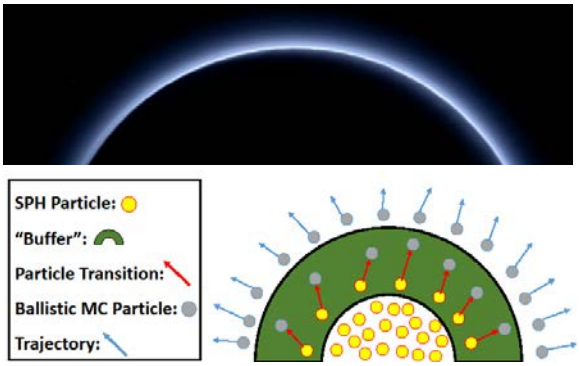

Figure 2. An image of a NH occultation of Pluto's atmosphere (*above*) and a simplified portrayal of the buffer where transition from a SPH to ballistic solver occurs within the exosphere (*below*).

Future Work: Upon validation of the SPH-Ballistic model, the latter method would be replaced by a spherical direct simulation Monte Carlo (DSMC) grid [12]. This would allow for the two methods to be coupled deeper into the atmosphere, i.e., below the exobase, where the frequency of molecular collisions increase and ballistic trajectories no longer apply.

Other applications of this novel method to this system could include implementing improved and more complex boundary conditions for Charon as frost properties, fractional maps, and surface temperature distributions are expected to be in forthcoming NH results. By applying a global map of surface temperature to Charon, a boundary condition could be implemented such that only some of the impacting particles stick to the surface. Moreover, if frost properties are known, a residence time for the sticking particles could also be introduced before particles are released back into the flow. Further analysis could be done simulating the transport of these "hopping" particles along the surface to determine escape rates from Charon or travel to and deposition in colder regions [2].

There is now a wealth of spacecraft and telescopic data available on the upper atmospheres of a number of topical solar system bodies. For example, MAVEN is making regular passes through the upper atmosphere of Mars and Cassini made hundreds of passes through Titan's upper atmosphere. Despite this wealth of data, there remains a clear lack of understanding of the evolution of these atmospheres. Thus, my proposed hybrid simulation scheme is also applicable towards modelling other solar system bodies that have collisional atmospheres, such as Titan and/or Mars, where there is a plethora of existing models coupled with in-situ observations. Moreover, this hybrid method would be uniquely suited to model the cryovolcanic processes of Enceladus where pluming gas is released into space from various surface vents which represent complex geometries. Such phenomena was first detected in-situ by the Cassini satellite and any future simulations would be validated against existing observational data.

Conclusion: The research described herein has been shown to address needs of the IPPW community by validating in-situ observational data and previous models of various planetary atmospheres via a novel, hybrid method which can simulate complex solar system phenomena. Although Pluto is the main focus, the long term goal is to develop a set of simulations for efficiently describing a 3-D atmosphere in a system that does not have a simple geometry.

References: [1] Gladstone G.R. et al. (2016) *Science*, 351(6279). [2] Hoey W.A. et al. (2017) *Icarus*, 287, 87-102. [3] McNutt R.L. (1989) *Geophys. Research letters*, 16(11), 1225-1228. [4] Yelle R.V. and Elliot J.L. (1997) *Pluto and Charon*, 347-390. [5] Krasnopolsky V.A. (1999) *JGR: Planets*, 104(E3), 5955-5962. [6] Tian F. and Toon O.B. (2005) *Geophysical Research Letters*, 32(18). [7] Strobel D.F. (2008) *Icarus*, 193(2), 612-629. [8] Teschner et al. (2016) *Microfluidics and Nanofluidics*, 20(4). [9] Tucker et al. (2013) *Icarus*, 222(1), 149-158. [10] Tucker et al. (2016) *Icarus*, 272, 290-300. [11] Gingold R.A. and Monaghan J.J. (1997) *Monthly notices of the Royal Astronomical Society*, 181(3), 375-389. [12] Bird G.A. (1994) *Clarendon, Oxford*, 508. [13] Tucker et al. (2015) *Icarus*, 246, 291-297. [14] Tucker et al. (2012) *Icarus*, 217(1), 408-415.

THE PROPOSED HERA SATURN ENTRY PROBE MISSION CONCEPT. D.H. Atkinson[1] (David.H.Atkinson@jpl.nasa.gov), O. Mousis[2], T.R. Spilker[3], E. Venkatapathy[4], A. Coustenis[5], M Hofstadter[1], J.-P. Lebreton[6], K. Reh[1], A. Simon[7], and the Hera team, [1]Jet Propulsion Laboratory, California Institute of Technology, 4800 Oak Grove Dr., Pasadena, CA 91109, USA, [2]Aix Marseille Université, CNRS, Laboratoire d'Astrophysique de Marseille, UMR 7326, 13388 Marseille, France, [3]Independent Consultant, [4]NASA Ames Research Center, Moffett Field, California, USA, [5]LESIA, Observatoire de Paris, Meudon, France, [6]CNRS-Universite d'Orleans, 3a Avenue de la Recherche Scientifique, 45071, Orleans Cedex 2, France, [7]NASA Goddard Space Flight Center, Greenbelt, MD, USA

Introduction: The formation and evolution of the giant planets and their atmospheres is fundamental to understanding the origin of the solar system including the initial stages, conditions, and processes by which the solar system formed, the initiation of the formation process, the nature of the interstellar seed material from which the solar system was born, and the subsequent dynamical and chemical evolution of the solar system. Additionally, the atmospheres of the giant planets serve as laboratories for studying the chemistries, dynamics, processes, and climates of all solar system atmospheres including that of the Earth, and provide a context and ground truth for exoplanets and exoplanetary systems including potentially habitable planetary systems.

Remote sensing is of limited use to measure the bulk atmospheric composition of the giant planets. Entry probes represent the only method by which the chemically inert noble gases can be measured and provide ground truth for directly correlating remote sensing measurements with the physical properties of the atmosphere. Additionally, *in situ* measurements provide access to atmospheric regions that are beyond the reach of remote sensing, enabling the dynamical, chemical and aerosol-forming processes at work to the troposphere below the cloud decks to be studied.

Hera is a Saturn entry probe currently under consideration as an ESA M-class flight mission proposal. The proposed Hera mission comprises an atmospheric entry probe built by the European Space Agency with contributions from NASA, to be released into the atmosphere of Saturn by a companion solar-powered Saturn Carrier-Relay spacecraft (CRSC) possibly provided by NASA. The CRSC would deliver the probe to the Saturn entry interface point and subsequently act as a relay station to receive the probe science telemetry for recording and later transmission to Earth. Hera would descend under a sequence of parachutes to depths of at least 10 bars in approximately 75 minutes. By probing deep into the cloud-forming region of the troposphere to locations where certain cosmogenically abundant species are expected to be well mixed and far below regions accessible to remote sensing, Hera would measure the atmospheric composition, most notably noble gases and key isotopes not accessible by remote sensing, as well as the thermal and dynamical structure of Saturn's atmosphere at the probe descent location.

The battery-powered Hera probe would be designed from ESA elements with contributions from NASA, with the Carrier Relay Spacecraft possibly supplied by NASA. The only major subsystem to be provided either by direct procurement by ESA or by contribution from NASA is the probe entry aeroshell and thermal protection system.

Following the example set by the highly successful example of the Cassini-Huygens mission, the Hera probe science team would comprise an international science team and would carry European and American instruments, with scientists and engineers from both agencies and many affiliates participating in all aspects of mission development and implementation. The basic Hera probe science payload would include a Mass Spectrometer to measure the bulk composition of Saturn's atmosphere, an Atmospheric Structure Instrument to measure the thermal structure and stability of Saturn's atmosphere, and a Doppler Wind Experiment to measure the dynamics of Saturn's atmosphere.

Other possible instruments in the Hera scientific payload include a Net Flux Radiometer to measure the energy balance of the Saturn atmosphere and a Nephelometer to measure cloud location and structure.

The Hera Saturn probe would provide critical measurements of composition, structure, and processes not accessible by remote sensing and place Saturn into the context of giant planet science provided by the Galileo, Juno, and Cassini missions to Jupiter and Saturn. The results of Hera would help test competing theories of solar system and giant planet origin, chemical, and dynamical evolution.

The information presented about the Hera mission concept is pre-decisional and is provided for planning and discussion purposes only.

DRAG MODULATION AEROCAPTURE FOR SMALLSAT SCIENCE MISSIONS TO VENUS.

A. Nelessen[1], E. Venkatapathy[2], R. Braun[3], A. Austin[1], B. Strauss[1], J. Ravich[1], A. Didion[1], R. Beck[2], G. Allen[2], M. Aftosmis[2], P. Wercinski[2], M. Wilder[2], M. Werner[3], E. Roelke[3].

1. Jet Propulsion Laboratory, California Institute of Technology, 4800 Oak Grove Dr., Pasadena, CA, 91109.
2. NASA Ames Research Center, PO Box 1, N229, Moffett Field, CA 94035
3. University of Colorado Boulder, Boulder, CO 80309

Introduction: Aerocapture has long been considered a compelling technology that could significantly enhance orbital missions to Mars, Venus, Titan, Uranus, and Neptune.[1,2,3,4] Aerocapture uses the drag from a single hyperbolic atmospheric pass to provide the delta-V needed for orbit insertion. Studies suggest that, compared to propulsive orbit insertion, aerocapture could increase delivered payload by 15% at Mars, 70% at Venus, more than 200% at Titan and Uranus, and an estimated greater than 800% at Neptune.[2]

Many aerocapture studies to date have focused on bank-angle lift modulation, which requires complex control algorithms and an integral propulsive reaction control system (RCS). The aerocapture technology described in this presentation is drag modulation aerocapture, which shows promise of being simpler and more cost-effective than bank-angle lift methods.[5] Drag modulation aerocapture uses in-flight transformations of an entry vehicle's drag area to control the amount of deceleration produced during an atmospheric pass.

Single-Stage Discrete-Event Drag Modulation Aerocapture: The simplest form of drag modulation aerocapture is the single-stage discrete-event architecture, which is depicted in Figure 1. One possible way to execute the single-stage discrete-event maneuver is to enter the atmosphere in a low ballistic coefficient configuration, with a large drag skirt deployed, and then to transition to high ballistic coefficient by jettisoning or folding the drag skirt. Such a single-stage discrete-event architecture was previously studied within the context of an Earth SmallSat Flight Test of Aerocapture.[6]

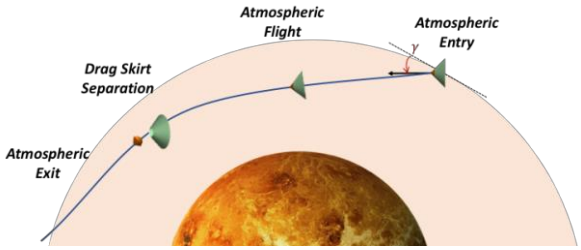

Figure 1: Single event drag modulation aerocapture is a potentially cost-effective and mass-efficient approach to achieve orbit insertion with a small satellite

Study Objective: This work is maturing a single-stage discrete-event drag modulation aerocapture system that could deliver a SmallSat into orbit at Venus for a fraction of the mass of propulsive systems.

Study Description: The key challenges associated with drag modulation aerocapture for Small Satellites at Venus, which are the focus of this presentation, include:

1. Vehicle stability throughout atmospheric flight, and the effects of tipoff and/or potential recontact between the two bodies after separation
2. Guidance and control (G&C) architecture for targeting a precise science orbit despite navigational and atmospheric uncertainties
3. Aerothermal stresses on the vehicle due to high heat rates at Venus

In order to address these key challenges and determine the feasibility of this aerocapture system for use in planetary missions, a multi-organizational team was formed from collaborators at the Jet Propulsion Laboratory (JPL), Ames Research Center (ARC), and the University of Colorado at Boulder (CU Boulder). Spanning various areas of expertise, this team brings a wealth of experience to address the key challenges of drag modulation aerocapture. The collaborating organizations in this effort and their focus areas are shown in Table 1 below.

Table 1: Organizations and focus areas

Organization	Focus Areas
JPL	Flight System Engineering Mechanical Design G&C and Trajectory Simulation Navigation
ARC	Aerothermal Analysis Thermal Protection System Sizing Computational Fluid Dynamics Ballistic Range Test Development
CU Boulder	Computational Fluid Dynamics G&C and Trajectory Simulation

In the first half of Fiscal Year 2018 (FY18), the team has focused on developing an understanding of the constraints and initial conditions of an aerocapture mission to Venus. Navigation and entry corridor

targeting capabilities have been assessed, and initial sizing of the aerodynamic surfaces and flight system hardware has been completed. Along the way, modeling tools and simulation capabilities have been developed for continued use in maturing the design. Future work in FY18 will involve several more design iterations, sensitivity studies, and preparation for an experimental test in a ballistic range. Work for FY19 will execute a series of ballistic range tests, which will constrain the dynamics of drag skirt separation.

Key Findings to Date: Study findings to date indicate that while challenging, drag modulation aerocapture at Venus using a small satellite is indeed feasible. A design which enters the Venusian atmosphere at an entry velocity near 11 km/s at a flight path angle of $5.6 \pm 0.2°$ could potentially achieve a final orbit of 2000 km x 175 km. Smaller orbits are possible, but may reduce the flight path angle corridor further. While the flight path angle corridor of 0.4° is very narrow, it is not beyond the navigational capabilities of modern interplanetary spacecraft.

While the design continues to evolve, the current iteration leverages the Pioneer-Venus aerodynamic shape, and has a pre-jettison diameter of 1.5 m and a post-jettison diameter of 0.4 m. The entire system constitutes about 80kg in total mass, places roughly 40 kg in orbit, and delivers nearly 12 U of useful flight system volume. As a point of comparison, a vehicle performing propulsive orbit insertion would require almost 160 kg of fuel to deliver the same 40 kg of useful payload mass to the same orbit. This shows that the 80 kg aerocapture vehicle is significantly more mass efficient-than the 200 kg propulsive vehicle.

The current aerocapture system design utilizes a PICA thermal protection system, a predictor-corrector G&C algorithm based on linear accelerometer data for triggering drag-skirt separation, and a guide rail system for reducing the risk of re-contact after Drag Skirt Separation.

References:

[1] Walberg, G. D. (1985) *Journal of Spacecraft and Rockets*. [2] Hall J. et al. (2005) *Journal of Spacecraft and Rockets*. [3] Rohrschneider, R. R. and Braun. R. (2007) *Journal of Spacecraft and Rockets,* Vol. 44(1). [4] Lockwood M. K. (2003) *AIAA/ASME/SAE/ASEE Joint Propulsion Conference and Exhibit*. [5] Putnam, Z.R. and Braun, R.D. (2014) *Journal of Spacecraft and Rockets*, Vol. 51(1). [6] Werner, M. S. et al (2017) *55th AIAA Aerospace Sciences Meeting.* [7] Webster R. (2013) *AIAA/ASME/SAE/ASEE Joint Propulsion Conference and Exhibit.*

MINIMUM-MASS LIMITS FOR STREAMLINED VENUS ATMOSPHERIC PROBES. J. S. Izraelevitz[1] and J. L. Hall[1], [1]NASA Jet Propulsion Laboratory, California Institute of Technology (4800 Oak Grove Drive, Pasadena, CA 91109, jacob.izraelevitz@jpl.nasa.gov, jeffery.l.hall@jpl.nasa.gov)

Introduction: Small, expendable drop probes are an attractive method for making measurements in the lower atmosphere of Venus. These miniaturized probes are motivated by potential future mission opportunities for adding one or more probes as secondary payloads onto a spacecraft or aerial platform, and clearly smaller probes are more readily accommodated than larger ones.

However, drop probe miniaturization is impeded by the need to provide thermal and pressure protection. All past Venus in-situ missions have used insulated pressure vessels to protect the payload, providing it with a benign environment for the short time needed to reach the surface and make scientific measurements along the way [1, 2]. This approach has been very successful, but has resulted in relatively large vehicles ranging from 99 kg for the Pioneer Venus [1] small probe to 716 kg for the VEGA-2 lander [2]. Alternatively, if much of the protection is excluded by instead ruggedizing the payload to some extent, Lorenz [3] concluded that extremely small probes on the order of 1 kg are possible.

Objective*:* The purpose our study is to determine, when full temperature and pressure protection of the payload is provided, what are the lower mass limits for a short-duration probe using a simple thermo-mechanical analysis. In addition to traditional bluff-body probe designs, we also determine relationships for how streamlining the probe can further adjust the insulation mass required.

Methodology: First we describe a simple conservative drop probe model that captures the relevant physics while enabling extensive trade studies. Our model assumes that entry into the atmosphere has been completed and heat shield ejected, leaving the probe to be dropped from its carrier craft or an aerial vehicle. This probe, illustrated in Fig. 1, consists of a layered construction in analog of the design of the Pioneer Venus Probes [1] and the Venera/Vega landers [2], with the addition of an optional external cowling designed to reduce or augment the drag during descent.

Next, we perform a parametric study on a variety of probe designs and derive the scaling laws for the thermal and pressure vessel subsystems. We then invert these scaling laws to address the design problem, determining the minimum mass cut-off. For our model, we also derive analytic expressions for optimizing the mass of insulation and heat sink for any given design point.

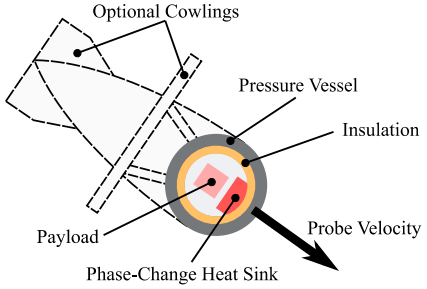

Fig. 1: *Miniature probe model, with external cowlings*

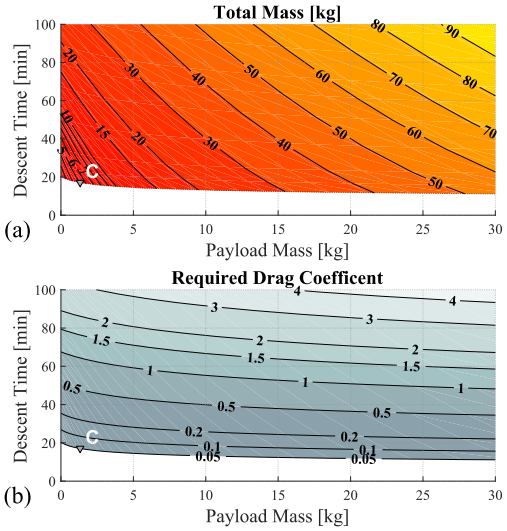

Fig. 2: *Mass Costs for a target Venus Payload and Descent Time (derived for payload density = 0.7g/cm³)*

Results: We have found that probes of substantially lower mass than Pioneer Venus appear plausible, provided that streamlining is used to shorten the descent time through the atmosphere (Fig. 2). Falling faster mitigates the timeline that heat conduction can occur, thereby reducing the heat load and associated thermal system mass. For example, one of our proposed 5.7kg probe designs carries 1.4kg of payload at an accelerated 17 minute descent (Probe C in Fig. 2).

However, an ideal Venus probe would have both a large payload *and* a long descent time for science collection and transmission. We therefore additionally

derive the marginal mass costs, material selection criteria, and a variety of specific design points for navigating the tradeoff space.

Acknowledgements: The research described in this paper was funded by the Jet Propulsion Laboratory, California Institute of Technology, under a contract with the National Aeronautics and Space Administration.

References: [1] Bienstock B. J. (2004), "Pioneer Venus and Galileo entry probe heritage," International Workshop on Planetary Probe Atmospheric Entry and Descent Trajectory Analysis and Science, 544, 37–45. [2] Huntress, W. T. et al. (2011) "Soviet Robots in the Solar System". Springer Science & Business Media. [3] Lorenz R. D. (1998), "Design considerations for Venus microprobes," J Spacecraft Rockets, 35, 2, 228–230.

MISSION DESIGN OF SMALL DEPLOYABLE CAMERAS FOR THE CLOSE INVESTIGATION OF PHOBOS. Onur Celik[1], Nicola Baresi[2], Ronald-Louis Ballouz[2], Yasuhiro Kawakatsu[2], Kazunori Ogawa[3], Koji Wada[4], [1]The Graduate University for Advanced Studies (SOKENDAI) (onur.celik@ac.jaxa.jp), [2]Japan Aerospace Exploration Agency, [3]Kobe University, [4]Chiba Institute of Technology.

Introduction: The scientific and engineering communities have a profound interest in returning to the Martian moons for a spacecraft mission. An exploration mission could finally settle the debate on the origin of the moons, as well as provide a better understanding on the Martian systems to support the future manned exploration of Mars.

To address this interest, JAXA is currently planning the launch of the "Martian Moons eXploration" (MMX) mission in 2024 [1]. If successful, MMX will be the first spacecraft in history to retrieve samples from the surface of Phobos.

A number of Deployable CAMera 5 (DCAM5) probes have been identified as promising candidates to enhance the science return. Each of these probes consists of a 0.75 kg cylindrical canister of size 105 mm (side) x 95 mm (diameter), and it carries two visible-infrared range multiband cameras, four close-up cameras, and three-axis accelerometer to investing ate the environment in the vicinity of Phobos. The probe will accomplish several tasks to understand the regolith-covered surface of Phobos and the local gravitational environment: They will image the moon's surface, and measure the total acceleration throughout the trajectory until the final location. These investigations are expected to provide invaluable information about Phobos' internal structure and the geophysical properties of the potential landing sites of MMX, and in the regions that are too risky for MMX to approach, due to complex topography.

This paper presents the mission design studies of DCAM5 system. The fact that DCAM5 is purely passive system makes its deployment challenging, as the probe has the potential to escape from the system after the first impact. This issue is addressed in this research using realistic gravitational environments and considering the inelastic collisions in the surface via the state-of-the-art N-body contact dynamics code "pkdgrav." The results provide a framework for scientific and engineering requirements for the mission and new insights into the geophysical environment of Phobos.

Deployments of DCAMs: There are many challenges associated with the deployments DCAMs. First of all, DCAM5 release mechanism can provide injection speeds only within 0.2 m/s and 1 m/s, which essentially rules out the deployments from the nominal low-altitude science orbits of MMX, i.e. quasi-satellite orbits around Phobos. Second, strict attitude constraints are imposed on DCAM trajectories because of the imaging requirements during the descent. Finally, DCAMs have to survive the impact, relay the data back to its mothercraft before its battery depletes, and not escape from Phobos after touchdown.

To investigate the possible outcomes and derive the requirements for the mission success, a high-fidelity simulation toolbox is developed during this research. The initial attitude and orbit state of DCAM trajectories are propagated in the polyhedron gravity field of Phobos until the point of impact. The states shortly before the impact are next input to pkdgrav, which accurately simulates the interaction between the cylindrical probe and the regolith of Phobos. The output of pkdgrav is input back to the trajectory simulations and a new trajectory is computed. In the case of a re-impact with the surface, the same cycle is repeated until the probe comes to rest on the surface. It is worth noting that the parameters of the toolbox can be varied in order to identify potential deviations from the nominal trajectory due to the many uncertainties of the problem. Furthermore, interesting geophysical information, such as the surface coefficient of restitution can be monitored and collected during the probe's contact with the surface.

Mission analysis results: The analysis was performed for various landing sites of interest. The general results can be summarized in two categories:

Descent. The current DCAM5 deployment scenario considers deployments during the landing or the landing rehearsal of MMX at an altitude of 3 km above Phobos surface. With these initial conditions, the probe touches down the surface in ~1 h and experiences landing speeds ≥10 m/s, i.e., two orders of magnitude higher than the touchdown speeds of the analogous probes (e.g. MASCOT). Regardless of these challenging constraints, candidate trajectories were found to the scientifically interesting blue/red regions of Phobos, which exhibits high surface slopes, therefore not suitable for MMX landing. Furthermore, the attitude requirements have also been met.

Contact. The results suggest that Phobos surface is quite dissipative, with an effective coefficient of restitution values between 0.1-0.2 for successful DCAM landings. Bounces are expected; however, the distance travelled after bounce varies based on the design parameters.

Conclusions: This paper presented the deployment of DCAM, as part of JAXA's Martian Moons eXploration (MMX) mission. These simple probes can provide unprecedented data about the interesting regions of Phobos surface. The same information can be used to support the surface operation of MMX during sampling activities.

References: [1] Kuramoto, K. et al. (2017) *LPS XLVIII* Abstract #2086.

SMALL PLATFORMS for PLANETARY EXPLORATION : ESA's SPP study outcomes. S. Bayon and T. Voirin[1] [1]European Space Agency (Thomas.voirin@esa.int and silvia.bayon@esa.int).

Introduction:

Following a Call for "New Science Ideas", the Science Future Missions Department of the European Space Agency (ESA) is taking some steps to investigate the use of small satellites for deep space planetary mission applications to open new affordable opportunities for ESA-led planetary missions. The first of those steps has been to, after iteration with representatives from the European and Japanese planetary scientific communities, select three reference mission scenarios to run a short internal study at ESA'S Concurrent Design Facility (CDF).

Two of the selected scenarios revolve around the idea of performing multi-point, simultaneous observations around a small body, either an active one in the Main Asteroid Belt (volatiles investigation mission) or a non-active NEO (radar tomography mission). In these two cases, the multi-point measurements are achieved thanks to a flotilla of 4 nanosatellites (20 kg class) operated 6 months around the body – the nanosatellites being brought to destination by a mother spacecraft (500kg class) which is also in charge of interplanetary transfer and data relay.

The third concept studied the application of small satellites for a multi-target mission to the Main Belt. In that case, there is no nanosat involved and the scientific payload consists of remote sensing instruments (optical and IR). The mission allows up to 10 consecutive asteroids flybys in one mission arc of typically 3 years for a spacecraft mass in the 300kg class.

In view of cost constraints, in any of the studied scenario, SPP would share as a passenger an Ariane 62 launch of an ESA Science mission to the Sun-Earth Lagrange point L2. The targeted launch date would be in the 2025-2030 time frame.

These reference architectures do not correspond to real or candidate missions but were chosen for defining typical/envelope needs and to better understand the areas where technology developments are needed before the small satellites can be considered for implementation within the ESA Science Programme, e.g. in one of the next cosmic vision call for mission proposals. This presentation will outline the studied concepts and summarise the major trade-offs, outcomes and findings of the ESA CDF study on Small Planetary Platforms (SPP).

MULTIPROBE MISSION DESIGN WITH APPLICATIONS TO THE OUTER PLANETS. A. Arora[1†], S. J. Saikia[2†], and J. M. Longuski[3†], [1]arora31@purdue.edu, [2]sarag@purdue.edu, [3]longuski@purdue.edu, [†]School of Aeronautics and Astronautics, Purdue University, 701 W. Stadium Ave., West Lafayette, IN, 47907-2045.

Introduction: The 2014 NASA Science Plan and 2013 Planetary Science Decadal Survey detail high-priority science goals for planetary exploration [1–2]. Based on these science priorities, several missions have been proposed for the Discovery, New Frontiers (NF), and Flagship (FS) mission classes, as well as for other missions of opportunity. NF- and FS-class missions are flown about every five and ten years and cost $1B and $2B+ (in today's $), respectively, making them rare and quite expensive. The planetary exploration community and NASA believe that one way to improve the science return from these missions is to add an additional spacecraft, as indicated in its 2016 NASA Solicitation for Planetary Science Deep Space SmallSat Studies (PSDS3): "*NASA's Planetary Science Program is considering including small secondary payloads on every future planetary science launch*" [3]. The recent emergence of such small spacecraft and their associated technologies has opened up interesting possibilities for multi-spacecraft missions.

What are Multiprobe Missions? For this study, we constrain ourselves to missions that include one primary spacecraft and two atmospheric probes. However, results could easily be extrapolated for any *n* number of atmospheric probes. There are three types of multiprobe missions possible with these spacecraft:

- Both probes deployed at the destination body
- Both probes deployed during a single flyby
- One probe deployed at each an intermediate gravity-assist body and the destination

In this study, we focus on the first two mission types, as the third mission type could be designed as two independent single-probe missions.

Motivation: In 1995, NASA delivered an orbiter and atmospheric probe to Jupiter during the Galileo mission. However, the atmospheric probe entered a section of Jupiter's atmosphere that was not well-mixed and not representative of the whole atmosphere [4]. The only way to obtain accurate data is to send another atmospheric probe to Jupiter; however, these missions to the outer planets are very rare (the next Jupiter mission was Juno in 2016). The cheapest remaining option is a dedicated New Frontiers mission to Jupiter, costing at least ~$1 billion ($FY17, not including launch) and only providing the atmospheric data. Instead, if the Galileo mission had included another atmospheric probe, costing ~$100-400 million ($FY17, launch cost not required), it is very likely that we would have data for a well-mixed section of Jupiter's atmosphere.

The lack of representative atmospheric data from the Galileo mission accentuates the advantages of a multiprobe architecture for any upcoming Flagship missions to the outer planets. JPL recently completed its Ice Giants Pre-Decadal Survey Mission Study Report [5], examining potential Flagship missions to the Ice Giants. However all of the analyses were limited to single atmospheric probe missions, despite the potential value of an additional probe, because no tool or methodology currently exists to analyze the design of such a multiprobe mission.

Multiprobe Mission Design: Though we have flown multiprobe missions such as Pioneer-Venus and Deep Space 2 in the past, there is no generalized methodology to design such missions. As a result, no tool exists that can determine if a multiprobe mission is possible for a given set of interplanetary trajectories. Therefore the feasibility, impact on mission design, potential benefits, and risks of multiprobe architectures are not well-understood. A study was recently conducted for NASA PSDS3 regarding these multiprobe missions [6]. From this study, we know that there are several interconnected considerations while designing a multiprobe trajectory, including but not limited to:

Multiprobe Architecture: Regardless of the number

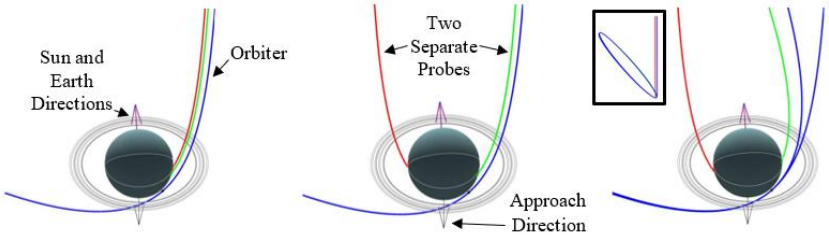

Figure 1. *Multiprobe Mission Architecture Schematics (to scale). The blue line represents the orbiter and the red and green lines represent two separate probes. (Left): Both probes are deployed to one side of the planet. (Middle): The two probes are deployed to opposite sides of the planet. (Right): One probe is deployed during the planetary approach, and the other probe is deployed to the other side of the planet after capture.*

of probes deployed in a mission, we first need to determine when they are released and where we want them to go (see Figure 1). A couple of the architecture options include:

- Releasing both probes either during hyperbolic approach, after capture, or using a combination of the two
- Delivering the probes on the same or the opposite side of the planet as each other

Probe-Orbiter Communication: In order for a probe to be worth the extra cost, it must be able to transfer sufficient science data to the orbiter during descent. The amount of data that can be transferred is dependent on the distance between the orbiter and the probe, the amount of time that they are in contact, and the relative geometry of the two spacecraft during contact period. Changing either the mission architecture or the maneuvers used during the mission will greatly affect the amount of data that the probe can transfer back to the orbiter.

In order to accurately determine the relationships between these different mission parameters, we perform simulations with high enough fidelity in three dimensions. Once the probe enters the atmosphere, we assume a planet with a co-rotating atmosphere and a density profile derived from historical measurements. As a result, we can take into account factors such as the out-of-plane rotation of the probe due to the atmosphere, and determine how that change in relative geometry affects the communication between the probe and the orbiter.

Maneuvers Required: Any probe mission will require additional deflection maneuveres in order to target the probe's entry location, adjust the probe-orbiter geometry (see Figure 2), etc. Some of the important maneuvers include:

- A timing deflection to slow down the orbiter after probe release, so that the orbiter passes over the descending probe
- A plane change to ensure the orbiter passes directly over the descending probe, which rotates with the atmosphere—out-of-plane relative to the orbiter

Probe G-Load Tolerance: Depending on the mission architecture and selection of the probes' entry flight path angles, the probes will need to withstand different aerothermodynamic stresses. This in turn affects the communications possible between the probe and the orbiter, as changing the entry flight path angle will result in differing probe-orbiter relative geometries during descent.

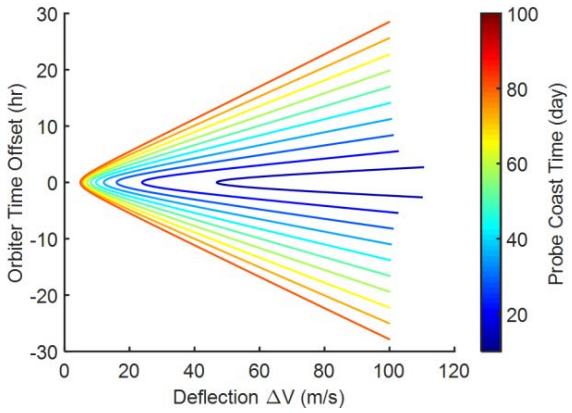

Figure 2. *Timing Deflection ΔV. After the probe is released, the orbiter performs a maneuver to adjust its speed so it passes over the probe as it descends. The amount of ΔV required to make the orbiter go faster or slower relative to the probe is plotted for various probe coast times.*

Orbital Insertion: The selection of the orbiter's insertion periapsis radius will result in lower propellant costs to capture, but will cause unfavorable probe-orbiter relative geometries for communication. As the orbiter is closer to the planet, it will have much less time to communicate with a probe due to the higher probe-orbiter relative angular velocity. Additionally, orbital insertion can be a time-consuming maneuver, so it important that there is a sufficient gap between this maneuver and the communication window with any probes.

Expected Results: We plan to analyze each of the potential multiprobe mission architectures, and examine the impact of each of the mission parameters. By considering all of the important factors, we can get a sense of what characteristics most greatly affect the mission design. Understanding these general trends will allow for the more rapid design of these multiprobe missions, and help in developing a more generalized methodology for designing these missions in the future. The methodology can be used along with existing state-of-the-art trajectory design tools and EDL simulations tools used by JPL and NASA centers for rapid concurrent mission design studies.

References: [1] "2014 NASA Science Plan." (2014). [2] "Vision and Voyages for Planetary Science in the Decade 2013-2022." (2011). [3] "C.23 Planetary Science Deep Space SmallSat Studies." (2016). [4] G. Orton et al. (1996) *Science, 272, 839-840*. [5] M. Hofstadter et al. "Ice Giants Pre-Decadal Survey Mission Study Report" (2017). [6] K. Sayanagi. "Small Next-generation Atmospheric Probe (SNAP)." (2017).

Simulation and Assessment of Magnetohydrodynamics (MHD) impact on a CubeSat sized re-entry capsule MIRKA 2 for heat flux mitigation during re-entry.

R.A. Müller[1], P.P. Upadhyay[2], A.S. Pagan[3], G. Herdrich[4] , S. Fasoulas[5]
[1,2,3,4,5](Institute of Space Systems (IRS), University of Stuttgart, Pfaffenwaldring 29, 70569 Stuttgart, Germany)
[1]*rmueller@irs.uni-stuttgart.de,* [2]*upadhyay@irs.uni-stuttgart.de,* [3]*pagan@irs.uni-stuttgart.de,*
[4]*herdrich@irs.uni-stuttgart.de,*[5]*fasoulas@irs.uni-stuttgart.de*

Abstract:

The present research focuses on the influence of an applied magnetic field on plasma flows during re-entry. The motivation was to assess the effects of Magnetohydrodynamics (MHD) on the conical re-entry capsule geometry MIRKA2 developed at Institute of Space Systems (IRS) in Stuttgart to assess its potential as a secondary thermal protection system (TPS).

The influence of Lorentz-force is used to manipulate the plasma flow. The applied magnetic field induces a circular ring current which interacts with the magnetic field to create a resultant Lorentz-force acting on the charged particles. **Figure 1** visualizes this principle, especially the axial part of the Lorentz force is very useful to decrease convective heat flux, as charged particles are pushed away from the stagnation point.

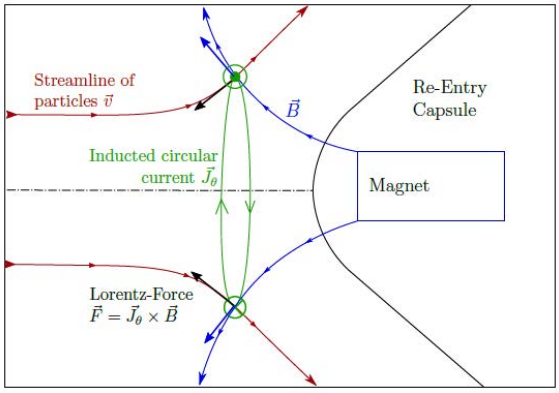

Figure 1: MHD-effects on re-entry capsule with magnet

The investigation was conducted with numerical methods, using the IRS in-house code SAMSA, which employs a finite-volume scheme on unstructured grid in an axisymmetric calculation domain. SAMSA was initially developed for the testing of MPD-thrusters and has been adapted to simulate re-entry problems [1].

The influence on temperature distribution, convective heat flux and bow shock geometry in front of the capsule's stagnation point was evaluated. Furthermore, thermal conductivities of both electrons and heavy particles and the total pressure in the plasma flow were examined.

A freestream and a ground facility case in the plasma wind tunnel PWK1 at the Institute of Space Systems were examined, based on earlier experimental works conducted by A. Knapp [2]. The Magnetoplasmadynamic Generator (MPG) RD5 was used to generate an argon plasma flow. SAMSA's capability to simulate PWK1 conditions was validated by simulating the experiments conducted in PWK1 [3,4].

The re-entry capsule which was modelled is the MIRKA2, which was developed by the small satellites students association KSat at the Institute of Space Systems in Stuttgart. MIRKA2 is part of the CAPE project, which includes the deployment and return of the capsule from lower orbit via a CubeSat module [5]. The project is intended to introduce students to the tasks and challenges of an aerospace engineer and to test new heat protection materials and plasma thrusters (PTT) [6].

Two different design variations were implemented to incorporate permanent neodymium magnets which were then implemented into SAMSA. **Figure 3** shows a picture of the retrieved MIRKA2 capsule, which was dropped from an altitude research rocket.

Figure 2: MIRKA2

For this investigation, five standardized magnetic field strengths at the tip of the capsule were modelled

for the two design variations: 0.1 T, 0.2 T, 0.3 T, 0.6 T and 1.0 T. One design case includes a cylindrical magnet, which replaces part of the tungsten weight at the bottom of the capsule. The other design case replaces the tungsten weight with a conical neodymium magnet.

With the current state of technology, it is possible to attain a magnetic field strength of 0.2 Tesla to 0.3 Tesla at the tip of the capsule by employing a neodymium magnet with a magnetic field strength (remanence) of 1.25 Tesla. **Figure 3** shows the design adaption for the MIRKA2-capsule to incorporate a cylindrical magnet.

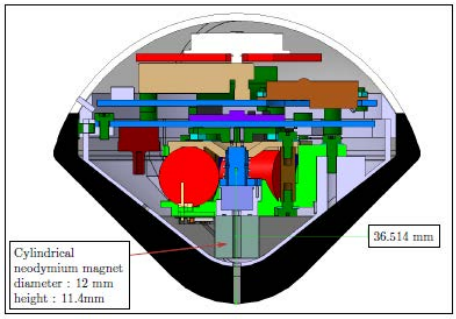

Figure 3: Design adaption for cylindrical magnet

Especially for the larger magnetic field strengths, which are very complex to achieve with the current state of technology, a conclusive influence of applied magnetic fields was proven. It is possible to decrease the temperature gradient and to increase the distance to the Mach 1 isoline in front of the tip significantly.

Figure 4 shows a heavy particle temperature distribution over the computational domain. The shift of the boundary layer and stagnation point is clearly visible.

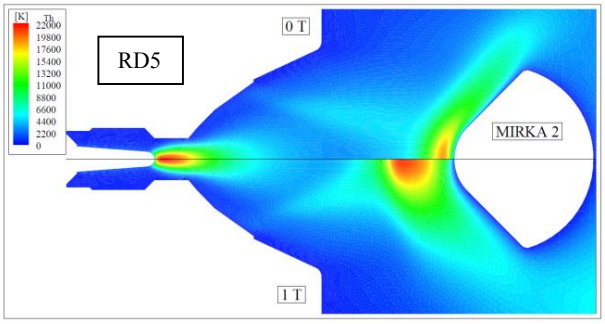

Figure 4: Heavy particle temperature plot

The heat flux at the capsule's tip was calculated and there is a significant decrease the convective heat flux at the capsule's tip by up to 57 % in the 0.3 T case.

Surprisingly, this result was not achieved for the highest magnetic field strength, as applied magnetic fields also raise the thermal conductivity in both electrons and heavy particles in addition to changing its distribution. Ultimately, the convective heat flux for high magnetic strengths like like 0.6 T and 1.0 T is roughly the same or even higher than for all other magnetic field strengths, including the case with no magnets.

References:

[1] Haag D. et. al. (2009) *JSASS Space Tech. Japan, Vol.7, No. ISTS26, 19-28*

[2] Knapp A. et al. (2012) *Open Plasma Phys. J., 5,* 11-22.

[3] P.P. Upadhyay et. al. (2017)*, 31st ISTS & 26th ISSFD & 8th NSAT*.

[4] P.P.Upadhyay et. al. : Numerical and experimental investigation of boundary layer manipulation with magnetic fields for heat flux mitigation during atmospheric entry, *IPPW-2017, Den Haag*

[5] KSat MIRKA2 project, URL: http://www.ksat-stuttgart.de/en/our-missions/mirka2-rx/

[6] J.P. Baumann et. al. (2015): Aerothermodynamic re-entry analysis of the CubeSat-sized entry vehicle MIRKA2

Abbreviations:

IRS	Institute of Space Systems
SAMSA	Self- and Applied Field MPD Thruster Algorithm
PWK1	Plasmawindkanal 1
CAPE	CubeSat Atmospheric Probe for Education
KSat	Kleinsatellitengruppe KSat e.V.

VENUS AIRGLOW MEASUREMENTS AND ORBITER FOR SEISMICITY (VAMOS): A MISSION CONCEPT STUDY, A. Komjathy[1], S. Krishnamoorthy[1], A. M. Didion[1], B. Sutin[1], B. Nakazono[1], A. Karp[1], M. Wallace[1], G. Lantoine[1], , M. Rud[1], J. Cutts, J. Makela[2], M. Grawe[2], P. Lognonné[3], B. Kenda[3], M. Drilleau[3] and Jorn Helbert[4]

[1]Jet Propulsion Laboratory, California Institute of Technology, USA
[2]University of Illinois at Urbana-Champaign, USA
[3]Institut de Physique du Globe-Paris Sorbonne, France
[4]Deutsches Zentrum für Luft- und Raumfahrt e.V. (DLR), Germany

Introduction: The planetary evolution and structure of Venus remain uncertain more than half a century after the first visit by a robotic spacecraft. To understand how Venus evolved it is necessary to detect the signs of seismic activity. Due to the adverse surface conditions on Venus, with extremely high temperature and pressure, it is infeasible, even using flagship missions, to place seismometers on the surface for an extended period of time. Due to dynamic coupling between the solid planet and the atmosphere, the waves generated by quakes propagate and can be detected in the atmosphere itself.

Science Investigation: The Venus Airglow Measurements and Orbiter for Seismicity (VAMOS) would be a mission architecture concept to enable a small spacecraft in Venus orbit to detect and characterize the perturbations of the neutral atmosphere and ionosphere induced by seismic waves. Venus is surrounded by the brightest naturally occurring airglow layer known in the Solar System. Airglow is a result of various atoms, molecules, and ions that get photoionized by ultraviolet radiation from the Sun and then release energy as visible and infrared light when they recombine and return to their normal state. Perturbations in the neutral atmosphere caused by seismicity on Venus leave an imprint in this airglow layer, which spans altitudes from 90-110 km. We use remote optical observations of this layer to study these perturbations, allowing us to infer the currently unknown seismicity and crustal structure of the solid planet below. In *Figure 1* (play Venus Airglow movie: http://goo.gl/j3I1bG) we display the resulting airglow fluctuations for a M_w=5.8 quake calculated on the nightside of Venus using stacked processing. The detection threshold would then be about M_w=5.3.

Additional perturbations from atmospheric sources (i.e., gravity waves) are also present in this airglow layer and provide insight into Venus' atmospheric dynamics, particularly the variability in the zonal wind on dayside and nightside. The unexplained day-to-day variability in the airglow and hence the oxygen atom abundance would be an additional target of investigation.

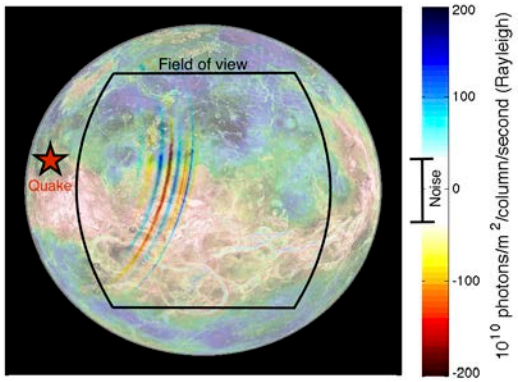

Figure 1. Modeled airglow fluctuations due to 20-sec seismic waves generated by a M_w=5.8 quake. (See Airglow Movie [1] in References). The star is quake location and the colors indicate airglow fluctuations above the conservative ±30 Rayleigh detection noise estimate using 0.3° planetary resolution.

Science Implementation: Two specific airglow emissions are investigated in the mission concept study, one occurring at 1.27 µm (visible on the night-side) and the other at 4.3 µm (visible on the dayside). The significant advantage of observing nightglow on Venus is that it is much brighter on Venus than on Earth [*2*] and that airglow lifetime (~4000 sec) is significantly longer than the period of seismic waves (10-30 sec) required to be detected to answer the aforementioned questions [*3*]. This makes it very attractive for directly detecting surface waves on Venus. This is in sharp contrast with Earth where the lifetime of airglow is about one order of magnitude smaller (~110 sec) than, e.g., the tsunami waves we routinely observe on Earth with 630 nm airglow instruments [*4*]. We also investigate the use of a 4.3 µm infrared (IR) channel to detect slow moving processes including gravity waves and signals of non-adiabatic heating of the atmosphere generated by the Venus quakes. The 4.3 µm channel complements the 1.27 µm one in possibly sensing epicentral waves generated by quakes at higher altitude of 120 km because energy is dissipated as heat at this altitude.

Mission Concept Implementation: Equipped with an instrument of modest size and mass, the baseline VAMOS spacecraft would be designed to fit within a SmallSat form factor and travel to Venus predominantly under its own power. As shown in *Figure 2*, VAMOS would enter into an orbit uniquely suited for the long-duration, full-disk staring observations required for seismic readings. VAMOS' journey would be enabled by modern solar electric propulsion technology and SmallSat avionics, which allow the spacecraft to reach the planet and autonomously filter observation data on board to detect Venus-quake events. Trade studies are conducted to determine mission architecture robustness to launch and rideshare opportunities. Key spacecraft challenges for VAMOS, just as with many SmallSat-based mission concepts, include thermal and power management, onboard processing capabilities, telecommunications throughput, and propulsion technology [5].

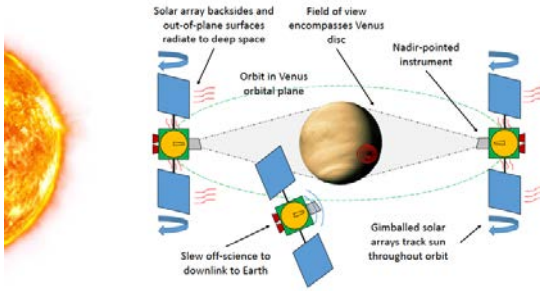

Figure 2. Illustration for pointing, cooling and operations schedule for the concept to be fully investigated during the study.

Summary: The VAMOS mission concept is studied at JPL as part of the NASA Planetary Science Deep Space SmallSat Studies (PSDS3) program, which will not only produce a viable and exciting mission concept for a Venus SmallSat, but will have the opportunity to examine many issues facing the development of SmallSats for planetary exploration. These include SmallSat solar electric propulsion, autonomy, telecommunications, and resource management that can be applied to various inner solar system mission architectures.

Our mission concept VAMOS will measure atmospheric perturbations from an orbiting platform that could provide a breakthrough in detecting seismicity on Venus and in the monitoring of seismic wave propagation.

Acknowledgements: This material is based upon work supported by the National Aeronautics and Space Administration under ROSES 2016 NNH16ZDA001N-PSDS3 issued through the Planetary Science Deep Space SmallSat Studies Program. The information about the VAMOS mission concept is pre-decisional and is provided for planning and discussion purposes only. Support to the French team has been provided by CNES. This work was conducted at the NASA Jet Propulsion Laboratory, a division of California Institute of Technology.

References:

[1] Airglow Movie for Venus (2016). http://goo.gl/j3I1bG, Movies under: ftp://sideshow.jpl.nasa.gov/pub/usrs/axk/vamos/, Accessed on Nov 5, 2016.

[2] Krasnopolsky, V. A. (2011). Excitation of the oxygen nightglow on the terrestrial planets, *Planet. Space Sci*. 59, 754–766.

[3] Lognonné, P., and Johnson, C.L. (2015). Planetary seismology. In *Treatise on Geophysics*, Edited by G. Schubert, vol 10, 2nd edn, Elsevier, Oxford, pp 65-120, DOI http://dx.doi.org/10.1016/B978-0-444-53802-4.00167-6.

[4] Makela, J. J., P. Lognonné, H. Hébert, et al. (2011). Imaging and modeling the ionospheric airglow response over Hawaii to the tsunami generated by the Tohoku earthquake of 11 March 2011, *Geophys. Res. Lett*., 38, doi:10.1029/2011GL047860.

[5] Didion, D., A. Komjathy, B. Sutin, et al., (2018). "Remote Sensing of Venusian Seismic Activity with a Small Spacecraft, the VAMOS Mission Concept." Accepted in IE*EE* Aerospace Proceedings, Big Sky, MO, March 3-10.

.

DOPPLER WIND RETRIEVALS OF PLANETARY ZONAL AND MERIDIONAL WINDS USING CONSTELLATIONS OF SMALLSATS. D.H. Atkinson[1], T.R. Spilker[2], and S.W. Asmar[1], [1]David.H.Atkinson@jpl.nasa.gov, Jet Propulsion Laboratory, California Institute of Technology, Pasadena, CA, [2]Independent Consultant

Introduction: Characterization of the dynamics of solar system atmospheres is an important element in understanding the overall structure of the atmosphere and origin, formation, and evolution of the planets. The efficacy of Doppler tracking of aerial vehicles (AV) including both probes and balloons for *in situ* retrieval of wind fields has been successfully demonstrated multiple times at Venus with Venera, VeGa, and Pioneer, and more recently at Jupiter and Titan with the Galileo and Huygens probes, respectively.

The accuracy of Doppler wind retrievals is limited by the stability of both the on-board clock used to generate the AV telemetry signal, the receiver clock that measures the received signal frequency, and by the accuracy of the AV location and reconstruction of the vertical speed. However, a primary limitation on Doppler wind retrievals of atmospheric dynamics using a single planetary AV and single receiver, whether a carrier-relay spacecraft (CRSC) or direct to Earth, is that a single Doppler profile provides only a single velocity component to represent the three-dimensional dynamics of the vehicle. In most cases, including the Galileo and Huygens probe Doppler wind retrievals, this limitation has been addressed by assuming that 1) Atmospheric Structure Instrument measurements of pressure and temperature and the assumption that the atmosphere is in hydrostatic equilibrium provides the vehicle descent speed, thereby removing one vector component of the AV motion, and 2) meridional (north-south) winds are significantly smaller than the zonal (east-west) winds. A technique for separating the aerial vehicle horizontal motions into meridional and zonal components is for the vehicle signal to be simultaneously received by the CRSC as well as from a second spacecraft or from Earth. If the aerial vehicle were to descend on the Earth-facing side of the planet and the AV-Earth telecommunications link were used in combination with the AV-carrier link to provide a second Doppler component, the measured Doppler profile provided via the Earth link would provide the important second vector of aerial vehicle motion. However, the requirement of a sub-Earth delivery and descent places significant, and sometimes prohibitive, constraints on the vehicle delivery and overall mission architecture.

It is proposed that multiple smallsats be used as secondary receive and relay systems for the aerial vehicle science telemetry. The AV would be equipped with a parachute system to provide a controlled terminal descent speed, a transmit-only telecomm system including a small ultrastable oscillator with an Allan Deviation (100 seconds) of $\sim 10^{-11}$ - 10^{-10}, and atmospheric structure sensors to measure atmospheric pressure and temperature. Including both dynamic and static pressure sensors permits the body-centered and atmosphere-relative descent speeds to be determined, thereby offering the capability of measuring vertical motions due to convection or atmospheric waves.

The smallsat receiving systems would carry a telecomm system to receive and record the descent vehicle telemetry, as well as a similar small ultrastable oscillator with a 100-second Allan Deviation of $\sim 10^{-11}$ - 10^{-10}. The Doppler profiles of the AV transmission measured by two widely separated non-collinear smallsats would provide the additional descent vehicle velocity vectors allowing the three components of descent vehicle velocity to be uniquely determined.

If the smallsats are deployed from the CRSC well in advance of the aerial vehicle entry, the ΔV requirements for sufficient separation of the smallsats from the CRSC are quite low. It is possible that the ΔV might be supplied not by a rocket propulsion system, but instead by an electromagnetic or pressurized-gas ejection system—a "gun"—on the CRSC. After ejection the smallsats could rely on standard small thrusters for attitude control, and could deploy antennas for AV signal reception and relay to the CRSC.

Radio Occultations using CubeSats on Martian Atmosphere.

Ahmed El Fadhel[1], Ozgur Karatekin[1], Olivier Witasse[2], Nicolas Bergeot[1], Bart Van Hove[1], Sami Asmar[3]

[1] Royal Observatory of Belgium, Brussels, Belgium;
[2] Scientific support office, European Space Agency, ESTEC, Noordwijk, Netherlands;
[3] Jet Propulsion Laboratory, California Institute of Technology, Pasadena, California, USA.

Abstract:

Radio waves are to transmit scientific data from Mars orbiters, rovers, and surface platforms to ground station on Earth. As the waves travel through the atmosphere, they are perturbed by the neutral atmosphere at lower altitudes and the ionosphere at higher altitudes. Radio Occultation (RO) experiments are conducted by extracting Doppler frequency changes from the received radio signal, caused by passing through different atmospheric layers on Mars. This allows to resolve the atmospheric structure in terms of density, pressure, and temperature. RO is a common measurement technique used to sound planetary atmospheres, as well as that on Earth [1].

RO experiments on Mars typically involves an orbiter that transmits directly to Earth (see figure 1). Given the known position and velocity of the orbiter relative to the ground station on Earth, the Doppler frequency contains information on the bending angle caused by the Mars atmosphere, which can be related to atmosphere density via the refractivity. Uncertainties that enter into this process include navigation errors, the influence of the Earth atmosphere, and interplanetary plasma. Advantages of RO are its altitude resolution and accuracy compared to other remote sensing methods.

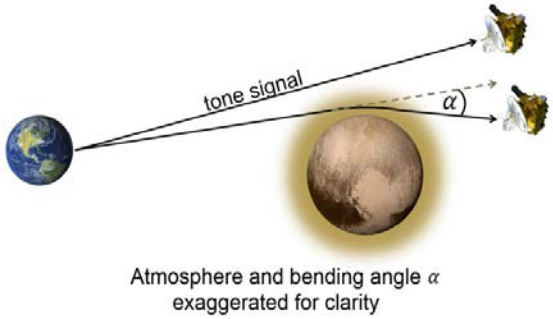

Figure 1. Illustration of the Radio Occultation method to sound the Martian atmosphere

Credit : https://blogs.nasa.gov

In this study, we investigate possible radio occultation experiments between a main spacecraft and a CubeSat, both in orbit around Mars. It has been shown that having two or more orbiters, significant improvements in spatial and temporal coverage of the atmospheric profiles can be obtained, compared to RO performed by an orbiter and a ground station located on Earth [2,3]. We assume the main spacecraft is in a high orbit, and simulate the RO performance and mission lifetime of the CubeSat in lower orbit.

References:

[1] Fjeldbo, G. and Eshleman, V. R. (1965) *J. Geophys. Res., 70(13),* 3217–3225.

[2] Asmar et al. (2016) *IEEE.*

[3] Williamson, W. ; Mannucci, A. J. and Ao, C. (2017) *LCPM-12*

GALLIUM NITRIDE MAGNETIC FIELD SENSOR PAYLOAD FOR SUBORBITAL FLIGHT.

K.M. Dowling[1], A.N. Ramirez[1], A. Garcia[2], H. S. Alpert[1], B. Plante[3], and D.G. Senesky[1],
[1]Stanford University (496 Lomita Mall, Stanford CA, 94305, kdow13@stanford.edu, aramire9@stanford.edu, halpert@stanford.edu, dsenesky@stanford.edu), [2]San Jose State University (aggarcia@gmail.com), [3]Boreal Space (bplante@borealspace.com)

Introduction: Miniaturized electronics enable the design and engineering of compact, low-cost instrumentation payloads used in space experiments. However, most silicon-based electronics are not suitable for long term space operation due to various mechanisms such as threshold voltage shifts, single event effects, and freeze out. As an alternative to silicon, wide bandgap semiconductor devices have been developed for operation under extreme environments, such as cryogenic temperatures and high levels of radiation [1, 2]. These emerging electronics often require rigourous advancement in Technology Readiness Level (TRL) for deployment on commercial satellites and other space missions. Novel device technologies, therefore, take years of reliability testing beyond academic research before they fly. CubeSats enable rapid and affordable flight testing to validate these new technologies.

Methods: Here, we present the development and implementation of a gallium nitride (GaN) based magnetic field instrumentation payload for a suborbital launch. The key payload interface choices were dictated by a rapid (< 2 months) delivery timeline. The board is affectionately named SHARK-I in honor of the team that contributed to it.

The sensor: GaN devices were manufactured with a previously reported microfabrication process [3]. To summarize, AlGaN/GaN was grown by metal organic chemical vapor deposition (MOCVD) onto a (111) silicon wafer. A stack of titanium, aluminum, platinum, and gold was evaporated and annealed to create Ohmic contacts. Finally, the devices were passivated with alumina through thermal atomic layer deposition (ALD). The sensor is shown in Figure 1. The magnetic sensors were packaged with wirebonding on a FR4 printed circuit board (PCB) and encapsualted with low-outgas resin (Masterbond® EP37-3FLFAO). The sensor was characterized in a home-built Helmholtz coil setup (Figure 2) and current spinning was leveraged to reduce the offset [4]. Figure 3 shows the measured Hall voltage with respect to various tested fields and bias currents from -5 mT to 5 mT. This sensor was then integrated into the payload SHARK-I for Boreal Space's Wayfinder II CubeSat.

Payload Sensor Amplification: The payload's biasing sheme for the device was set by the Arduino's digital pins for current spinning [4]. The sensor operates via the Hall-effect, so its differential output was amplified with an instrumentation amplifier (INA188) using a gain of 500. SHARK-I stores the hall votaltage multiplied by the amplifier gain (~500), shown on the secondary axis of Figure 3. This calibration will be important for analyzing recorded data after the flight.

Data Handling/ Payload Control: The analog signal was then digitized to 10 bits (Arduino mini pro), and was sampled at a rate of 5Hz. Two custom GaN sensors were included for redundancy. Reference silicon Hall sensors (Infineon Technologies) were also equipped on the payload. The Arduino interfaced with an Intel Edison on-board computer (OBC) via standard I^2C data communication protocol for telemetry data acquisition, and Serial Perpheral Interface (SPI) for on-board data storage in a micro SD card. The final payload's block diagram is shown in Figure 4, and Figure 5(a) shows the final payload design before integration into a 3U Cubesat (Wayfinder II from Boreal Space-Figure 5(c)). To examine the payload's signal conditioning with the sensor, a longer test duration was completed with the SHARK-I board using the magnetic test set up in Figure 2, with the data was recorded in the SD card on board. Various fields were applied, and the recorded Hall voltage (with current spinning) over time is displayed in Figure 6. This flat-sat test shows promise regarding future operation on flight – sensors are operating and data is transmitting as expected.

Future Work: Wayfinder II is scheduled to launch later this year via an Interorbital Systems launch vehicle. SHARK-I will provide important insights(e.g. launch load survival, signal integrity) into future CubeSat oribital missions with GaN-based sensing technology. Challenges discovered (e.g., signal conditioning, magnetic interference, noise reduction and radiation-hard electronics) will be addressed in future flights. Ultimately, this prototyped instrumentation payload paves the way for low TRL microdevices to be readily tested in space and launch conditions, bringing future technologies to space exploration at a rapid pace through the use of CubeSats.

References:

[1] Son, K., et al. (2010) *Nanoscience and Nanotechnology Letters 2.2*, 89-95; [2] Smorchkova, I. P., et al. (1999) *Journal of Applied Physics, 86.8*, 4520-4526; [3] Yalamarthy A.S. et al. *Advanced Materials* (2018); [4] Dowling, K.M. et al. *Hilton Head Workshop,* Accepted (2018)

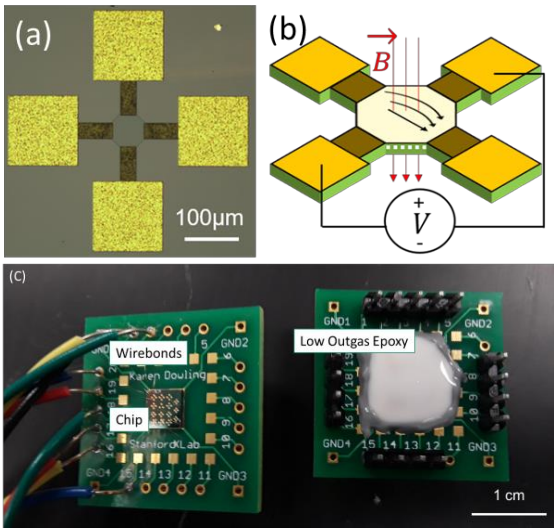

Figure 1: (a) Optical image of GaN-based Hall Sensor. (b) Sensor operation – current sourced and Hall voltage measured. (c) GaN sensor chip packaging, first wiredbonded on a PCB, then encapsulated with low-outgas epoxy.

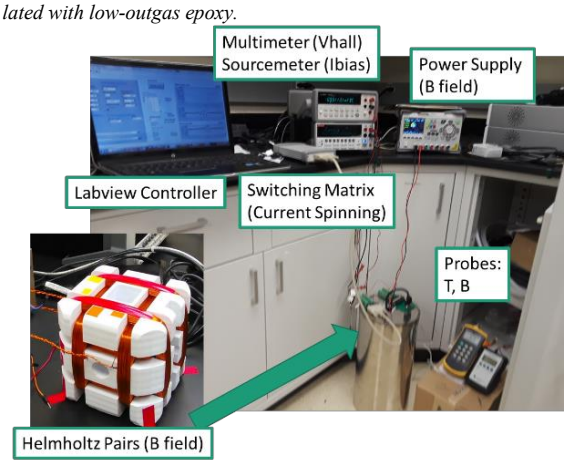

Figure 2: Experimental setup for characterizing the response of the magnetic field sensor.

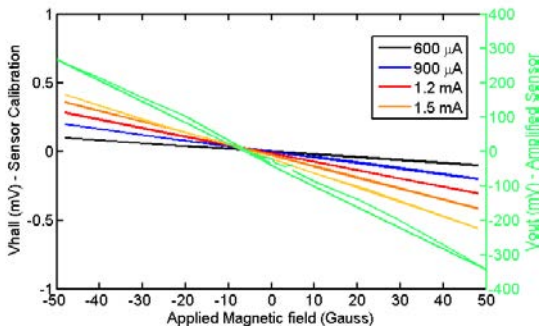

*Figure 3: Sensor voltage output from GaN-based sensor at various magnetic field value and bias currents. Secondary axis shows output voltage from amplified GaN magnetic field sensor (~Vhall *500).*

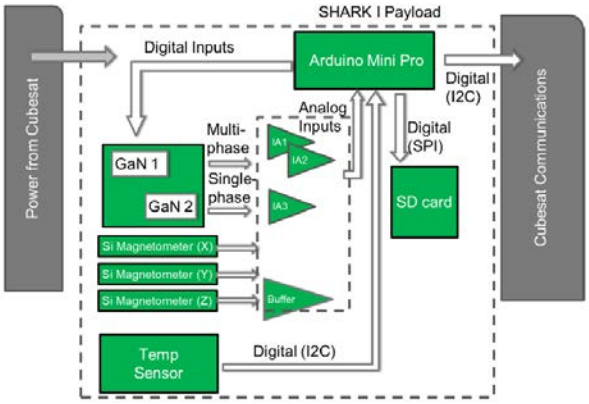

Figure 4: Schematic image detailing the block diagram of magnetic field sensolr payload.

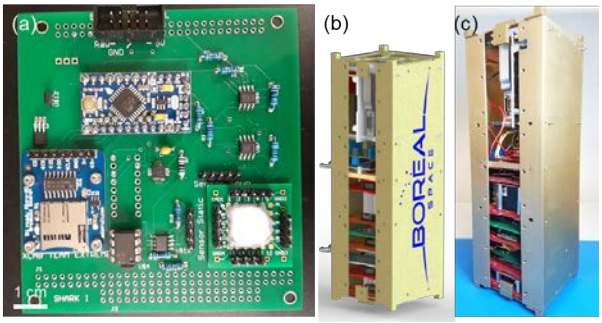

Figure 5: (a) Image of the SHARK-I payload that was implemented on Boreal Space's Wayfinder II.(b) CAD rendering of Wayfinder-II by Boreal Space (Image by Richard Casas) (c) Finaly assembly of 3U CubeSat Wayfinder-II with SHARK-I included.

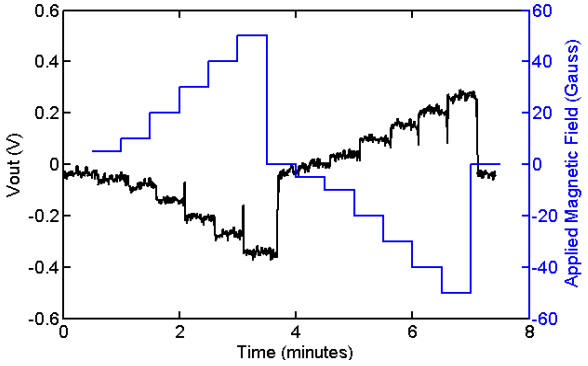

Figure 6: Data logged in SD card vs. time for GaN sensor while in magnetic field testing chamber.

RECOVERING TIME AND STATE FOR AUTONOMOUS NAVIGATION USED FOR SMALL SATELLITES. A. Dahir[1], D. Kubitschek[2] and S. Palo[3], [1]Univeristy of Colorado Boulder (1111 Engineering Dr. Boulder CO 80309, Andrew.dahir@colorado.edu) for first author, [2] LASP University of Colorado Boulder (1234 Innovation Dr. Boulder CO, [3]Univeristy of Colorado Boulder (1111 Engineering Dr. Boulder CO 80309).

Introduction: As small satellites become more abundant, the need for autonomous navigation becomes a greater necessity for deep space travel as communication resources become limited. When smallsats are in deep space, communication times between a satellite and the Earth can be prohibitive and ride-sharing opportunities as well as on-board faults can leave the smallsat without time information. The objective of this research is to investigate feasibility and develop the algorithms plus the concept of operations required to demonstrate autonomous cold-start determination of time and state for cis-Lunar and interplanetary missions utilizing an autonomous optical navigation system.

Impact: Being able to quickly and autonomously recover time and position from an environment with no Earth contact will help deliver mission success and advance technologies for smallsats from current large satellite methods which require an Earth contact. Baseline hardware for a solution approach focuses on small satellite commercial-off-the-shelf which could then be used for larger missions. The impact of this concept crosses both human (full loss of communication scenario) and robotic (autonomous recovery from on-board fault) exploration applications, where some form of spacecraft-to-ground communication is required to establish approximates for time and position. In both cases, the current state-of-the-art navigation systems require some knowledge of time and some approximate position to initialize the estimation process before the mission objectives can be obtained.

Approach: This approach uses optical observations of available planets and corresponding celestial satellites (for interplanetary operations) to initially recover the approximate time and state. These observations are then followed by precise, filter-based determination of time, position and velocity from the chosen optical beacons available in interplanetary spaceflight. The innovation of this approach is to use artificial satellites and celestial bodies periodicity to initially determine time. This capability is analogous to that of advanced star trackers that can initialize themselves by identifying any star field in the celestial sphere.

Results: The first feasibility study was to find the worst-case scenario for a star tracker to locate Jupiter given an unknown state. This was done geometrically assuming the satellite was closest to Jupiter when Jupiter was at perigee, and furthest away from Jupiter when Jupiter was at apogee. Initial feasibility studies for determining a sweep angle needed to locate Jupiter show that in ~80% of satellite location cases, Jupiter can be found with one sweep of a small satellite star tracker. This is for a worst-case scenario for instrumentation with a 5% error for sun distance measurements. The second simulation was used to discover the errors that would propagate through calculations if the sensor locating the angle of the Sun relative to the spacecraft were given a realistic error. Results were also obtained for a worst-case scenario in resolving time based on angular resolution error in the sun sensors located on the spacecraft. These results confirmed that a sensor with a resolution of 0.01° gave the best results for a range of locations based on inclination and spacecraft distance from the sun.

Conclusions: Further work will move forward on applying a full scenario in the Basilisk framework developed at the University of Colorado Boulder. By building on this framework, time and resources can be saved from having to develop a separate software environment for this research. While the solution is applicable to a wide range of missions, this presentation will focus on small satellites used for solar system exploration.

High Performance Deployable Photovoltaic Systems for Planetary Exploration – MMA HaWK Series

Eric Ruhl[1], Mark Bailey[2], ***MMA Design, LLC, 2555 55th Street, Suite 104, Boulder, CO, 80301 720-728-8491***
eruhl@mmadesignllc.com

Introduction: This paper presents an innovative deployable solar array power system architecture for spaceborne satellites. A system is presented that utilizes existing commercial technologies in space photovoltaics and structurally efficient material systems to realize a deployable power system. This innovation will address the need for high kW/m^3 and W/kg while improving life expectancy, reliability, significantly lowering mass and volume, providing higher specific power, and improving efficiency over state-of-the-art (SOA) systems. A high-performance array that stows in a 3U packing factor is supporting the Mars CubeSat One (MarCO) mission for NASA's Jet Propulsion Laboratory. MMA has developed higher power systems that similarly stow in a 3U and 6U packages, some incorporating single axis sun tracking for missions launching on NASA's SLS EM-1 launch. MMA is leveraging this technology to support even higher power densities, higher bus voltages, and other, larger small satellite platforms with power as high as 7 kW at beginning of life (BOL). The foundation of the innovation is a highly modular and customizable platform, quickly able to adapt to pivoting mission requirements. Possible applications include enhanced capability by providing high specific power for lower cost missions. Additionally, it will provide an accelerated production time frame for rapid systems development. This paper will demonstrate the feasibly of a wide range of standard and custom packaging formats to enable reduced cost and technical risk for a wide range of exploration spacecraft.

Satellite Packaging Formats: The MMA HaWK Series supports CubeSat platforms ranging from 3U-12U with powers ranging from 36Watts – 100+ Watts with optional single axis gimbal tracking.

CubeSat Packaging. Two sets of MMA HaWK arrays will launch to Mars in May of 2018 on the MarCO satellites accompanying the Mars InSight Lander.

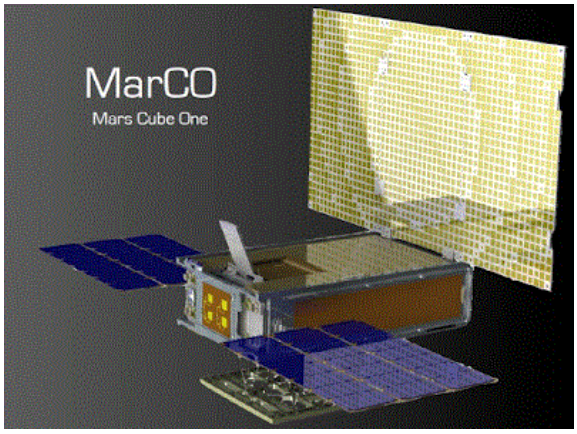

MMA HaWK solar arrays on JPL MarCO

SmallSat Packaging. MMA is leveraging the technologies developed for CubeSats to enable dramatic power increases on larger small satellite platforms. These can range from custom nanosats to standardized platforms such as ESPA and ESPA Grande. With powers ranging from 100 Watts to 7 kilowatts.

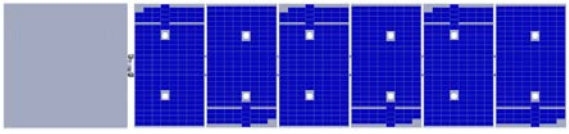

ESPA Class Satellite packaging of 1+ kW

References: :
To be supplied.

[1] Chief Engineer, 2555 55th St. #104,
[2] Director of Business Development, 2555 55th St. #104

ACTIVE CONTROL FOR MISSION EXTENSION (ACME) FOR CUBESAT PROBES. M. Costa[1], J. Ames[1], A. Enriquez[1] and P. Papadopoulos[2], [1]Student, San Jose State University, [2]Advisor, San Jose State University.

Introduction: The current work showcases the design of a 1U propulsion module (strap-on) attachment that extends the Time of Flight (TOF) of CubeSat probes and provides orbit maintenance and attitude control. The detailed design and manufacturing of the ACME system will also be presented. The ACME system fully integrates a hybrid propulsion system with reaction control to support orbital maneuvering, orbit raising, and station keeping. Typical TOF for a non-propulsive CubeSat probe system is less than one year. The presented technology extends the TOF beyond the current limitations to more than four years.

Subsystems: The primary susbsystems of the ACME system are structure, propulsion, reaction wheels and Guidance Navigation Control (GNC).The N2 represented was integrated, manufactured, and built as described below.

Structural Frame	Mass distribution, loads and moments	Mass distribution/ requirement, mounting	Mass distribution, mounting	Mass distribution, mounting	N/A	Mounting
Loads and moments from payload	Payload Mounting Mechanism	Mass properties from payload	Mass properties from payload	Mass properties from payload for calibration	Placement and codesign	N/A
Thrust forces and moments	Thrust forces and moments	Propulsion System	Control required for burns	Data on current status	N/A	Power required
Mass requirements for momentum	Payload mass properties requirements	Stabilizing action	Reaction Wheels	Data on current status	N/A	Power required
Insulation	N/A	Burn command	Control command	Controllers and Computer	Outgoing comms.	Power required
Insulation	Placement and codesign	N/A	N/A	Sensor data from payload	Payload Electrical Interface	Recharge capability
N/A	N/A	Power availability	Power availability	Power availability	Power transmission requirements	Power

Figure 1. Detail N2 ACME System Diagram

Structure: The CubeSat probe structure was manufactured using 7075 aluminum and is compliant with NASA/NanoRacks IDC requirements.

Hybrid Propulsion: the ACME system utilizes a hybrid propulsion design for Delta Velocity (ΔV) thrust maneuvers. The hybrid propulsion consists of a solid acrylic fuel grain which is oxidized using nitous oxide (N_2O) and an igniter [2]. A cutaway view of the hybrid propulsion system is show in figure 2.

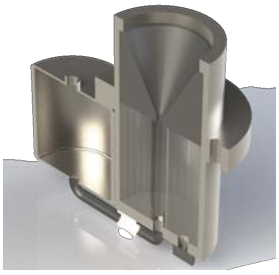

Figure 2. Hybrid Propulsion Cutaway

Reaction Wheels: Each of the three reaction wheel components feature a custom design. This subsystem utilizes low cost, COTS technologies to produce a complete six-degrees-of-freedom axis control for the complete microsatellite architecture [1, 3].

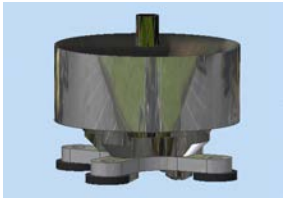

Figure 3. Reaction Wheels

GNC: The GNC subsystem is commanded by a MicroPython Trinket microcontroller. Orientation is provides by a 9-axis Inertial Measurement Unit (IMU/MPU). Orientation data is provided to the microcontroller to autonomously control the angular momentum of the reaction wheels [4].

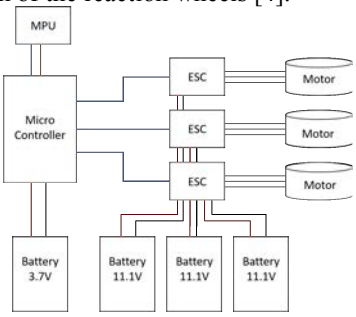

Figure 4. GNC subsystem

Conclusion: Increasing CubeSat probe TOF is critical in extending science mission in-space measurements and objectives for a significantly reduced life cycle cost. The poster will present the ACME design as well as the developed hardware to extend TOF.

References: [1] E. Oland and R. Schlanbusch, "Reaction wheel design for CubeSats," 4th Interna-

tional Conference on Recent Advances in Space Technologies, Istanbul, 2009, pp. 778-783. [2] J. Sheehan, T. Collard, F. Ebersohn and B. Longmier. “Initial Operation of the CubeSat Ambipolar Thruster.” *Joint Conference of 30th International Symposium on Space Technology and Science*. [3] S. Ge and H. Cheng, "A Comparative Design of Satellite Attitude Control System with Reaction Wheel," *First NASA/ESA Conference on Adaptive Hardware and Systems*, Istanbul, 2006, pp. 359-364. [4] C. Frost, E. Agasid. “Small Spacecraft Technology State of the Art”. *NASA Ames Research Center: Mission Design Division*.

INNOVATIVE DEPLOYABLE TELESCOPE ENABLING DRASTIC REMOTE-SENSING ENHANCEMENT CAPABILITIES OF CUBESATS WITH A MINIMAL PLATEFORM IMPACT. T. Errabih[1], E. Kostaropoulou[1], G. Bailet[2] and C. O. Laux[2], [1]CentraleSupélec, Université Paris-Saclay, 3, rue Juliot Curie, 91192 Gif-sur-Yvette Cedex, France (tarik.errabih@student.ecp.fr). [2]Laboratoire EM2C, CNRS, Université Paris-Saclay, 3, rue Juliot Curie, 91192 Gif-sur-Yvette Cedex, France (gilles.bailet@centralesupelec.fr).

Introduction: The CubeSat standard[1] created in 1999 gave the impulse for a new era for educational space programs. A CubeSat is an assembly of elementary and standardized units measuring 10x10x10 cm^3 for 1 kg called 1U. Several different configurations are possible up to 27U. This standard allows for lower budgets and shorter development periods in the space industry enabling space engineering to be much more reachable for students with hands on training. This new class of spacecraft came with the drawback of high mass/volume constraints for the avionics and the scientific payloads.

Through this publication, we are demonstrating the feasibility and interest of a compact deployable telescope fitting within the CubeSat plateform.

This multipurpose payload is currently sized for a lunar CubeSat orbiter called SIRONA (project lead by CentraleSupélec) and will contribute to the determination of the age of some of the Moon's oldest surfaces.

Conventional CubeSats' remote-sensing capabilities: Very often, CubeSats include optical systems for fulfilling their scientific goals. For instance, imaging of the Earth's surface or astrophysical bodies. In these terms, better scientific return means greater resolution. This driving parameter is currently fairly limited by the volume and mass budgets thus degrading the range of application of CubeSat plateforms.

Deployable optics to enhance Cubesats' capabilities: Deploying the optics saves the precious volume inside the Cubesat thus allowing better performing avionics or more scientific instruments. However, the idea to conceive deployable optics is not new. In fact, there are already papers from several countries treating that subject [2]. But all these papers describe either limited or large optical systems (several units inside the Cubesat). We propose an innovative instrument that will be able to fit within a volume of 10x10x3 cm^3 when packed and 10x10x25 cm^3 when deployed.

This payload will achieve resolutions as high as 1.5 meters/pixel at 200 kilometers of altitude. It is a f/10 Ritchey-Chrétien (see Fig. 1) telescope of 900 mm focal length for less than 500 grams. As its specifications show, this telescope is extremely compact, lightweight and powerful. The Ritchey-Chrétien formula already gave evidence of its power in several missions, like the Hubble Space Telescope (HWST) or Lunar Reconnaissance Orbiter (LRO).

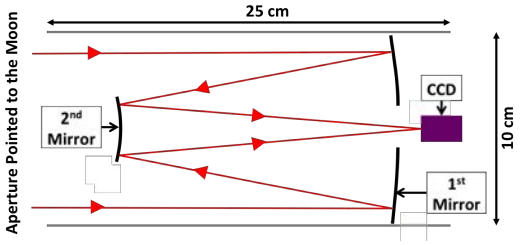

Figure 1 – Sketch of a Ritchey-Chrétien Telescope.

Application of the Payload *within SIRONA mission:* The deployable telescope is primarily designed to observe either the Moon or the Earth, onboard CubeSats. But it can be embedded and/or adapted to many space missions, to provide a budget/volume saving solution when needed.

This payload will first fly in the SIRONA mission, to image the Moon's surface in the near-UV/blue spectrum (to limit diffraction) at a high resolution (1.5 meters/pixel at 200 kilometers altitude), in order to date some of its oldest surfaces named lunar maria basins. Dating surfaces can be done wih the crater counting technique, that was pioneered by E.M. Shoemaker[3] in 1962. This technique starts from the postulate that a surface is initially untouched by craters, and is then bombarded at a constant flux. By counting craters and knowing the flux, the age of the surfaces can be well constrained.

Conclusion: For its first mission application onboard SIRONA, the deployable telescope will be able to date the lunar maria basins refining the current Solar System models which do not predict all current observations[4].

With its innovative design that mix up compacity, lightness and high performances, this instrument represents a formidable tool to expand the capabilities of CubeSats for planetary remote-sensing with a low impact on the mass/volume of such plateforms.

References:

[1] A. Mehrparvar (2014), *CubeSat Design Specification*. The CubeSat Program, CalPoly SLO.

[2] J. Champagne et al. (2014) *CubeSat Image Resolution Capabilities with Deployable Optics and Current Imaging Technology*.

[3]E.M. Shoemaker et al. (1962) *Advan. Astronaut. Sci.* 8 p70-89.

[4] National Research Council (2007) *The Scientific Context for Exploration of the Moon* Obj. 1a

VIRTUAL REALITY IN SPACE: THE NEXT FRONTIER FOR SPACE EXPLORATION

R. Bruce[1], P. Papadopoulos[1], N. Solomon[1], R. Rosila[2], J. Rosila[2], S. Chawla[2], D. Prakash Kankalale[2], M. Murbach[3], A. Guarneros Luna[3] [1]SJSU Faculty Advisors, [2]SJSU Student Researchers,[3]NASA-ARC

The virtual reality (VR) subsystem will be fully integrated with the TechEdSat 7 (Technology Educational Satellite) upcoming test flight. The flight subsystem is scheduled for system integration in summer 2018. The TechEdSat series of flights have been successfully deployed from the International Space Station while meeting complete mission success criteria. The TechEdSat series represent a space proven platform and a testbed for new technologies. The current paper will present the detailed design of the VR system currently integrated in the TechEdSat. Upon deployment from the ISS, this will be the first ever in space flight demonstration of a VR system on a on a small space craft platform.

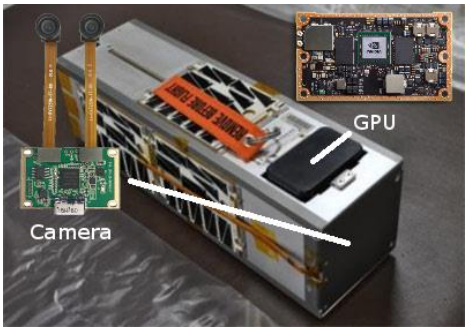

Figure 1: TechEdSat 7 VR Subsystem

Commodity-based low-power single-board computers have become wildly popular in science and engineering research. The introduction of low-power GPU computing makes high-performance computing in space possible at low cost. As shown in figure 1 TechEdSat 7 will flight-test and demonstrate the use of VR technology within CubeSat constraints such as power, thermal, size, communication bandwidth, and cost. The VR subsystem uses an Nvidia Jetson TX2 attached to a stereoscopic digital camera to capture video (to be up-linked to the Iridium satellite constellation). Nvidia's Jetson TX2 computing capability [1] is more than a teraflop (10^{12} floating point operations) per second with typical power consumption of 7.5W in a physically small form factor of 50 mm x 87 mm.

Table 1: Summary Requirements

Requirements	Performance [1]
Efficiency	Low power operation and high performance
Processing	GPU with 256 CUDA Cores
Data Acquisition	Handle 4K x 2K video at 60 fps
Fast Data Rates	802.11ac & Bluetooth wireless support, as well as 1Gbit ethernet port

As shown in table 1 the demonstrated technology enables and empowers space exploration using small form-factor space-craft for future missions. The use of GPU computing technology in small-spacecraft opens the possibility for massively parallel data analysis in-situ.

References:

[1] J. Tham, A. Hill Duin, L. Gee, N. Ernst, B. Abdelqader, M. McGrath, “Understanding Virtual Reality: Presence, Embodiment, and Professional Practice”, March 2018, DOI:10.1109/TPC.2018.2804238

Spartan Imaging Satellite

I.Quintero[1], L. Freitas[1], E. Marchan[1], C. Espinoza[1], G. Lopez-Thomas[1], P. Papadopoulos[2]
[1]Student, San Jose State University
[2]Advisor, San Jose State University

Introduction: The current paper will present the design, building, and manufacturing of a small satellite capable of multispectral imaging for advanced interplanetary exploration operations near and beyond the moon. Primary objective of this effort was to design, manufacture and ground test an imaging CubeSat with interplanetary applications that complies with NASA's International Space Station deployer/Nanoracks IDC interface design requirements. In addition, this effort demonstrates standardization, affordability, and utilization of plug-and-play technologies for interplanetary exploration architectures.

The work presented will demonstrate proper system integration techniques as shown in Figure 1. Each subsystem will be seamlessly integrated with the on board computer for command and data processing. The on board computer's function of command and data processing is also partnered with the processing of sensor data much like the design utilized in the Langmuir Probe payloads [1]. By properly integrating each subsystem, we are able to monitor status' of each subsystem as well by-pass faults when necessary. Ultimately, the design utilizes multiple folds of redundancy in both the electrical power system and communications systems to extend projected mission lifespan.

The Spartan Imaging Satellite is a 3U microsatellite that features multiple optics payloads. The work presented shows the benchmarking protocols that were implemented to comply with NASA's International Space Station Deployer. By benchmarking our system with systems containing technology readiness levels of seven and above, we are able to achieve desirable results at a fraction of the price.

The electrical power system is designed to bypass circuit faults and over-currents to ensure proper usage when the system is not running at optimal conditions. Poly switches and voltage regulators maintain proper currents and voltages for the power bus, while the implementation of multiple battery charge regulators allows for the prevention of battery failure. In the event of a battery failure, Spartan Imaging Satellite's EPS uses MOSFETs to ground the battery packs. This allows for the batteries to be bypassed when voltage is not detected allowing for the EPS to continuously supply power to the rest of the satellite.

The Communications subsystem architecture will be designed to operate with the Deep Space Network (DSN), a global array of antennas focused on communicating with interplanetary spacecraft. Aboard the cubesat, will be a high power radio operating in the X-band frequencies. This class of radio will be necessary for its directionality and higher gain, which will allow for clear transmission and reception of data across vast distances. A high-gain X-band patch antenna will be chosen as it will not require a module occupying a large portion of the cubesat volume. A UHF radio and supporting dipole antennas will be utilized when communicating with other Mars-orbiting satellites and ground stations.

This work showcases the implementation of proper system architecture redundancies for future interplanetary small satellites and probes which allow for cheaper and reliable space exploration platforms.

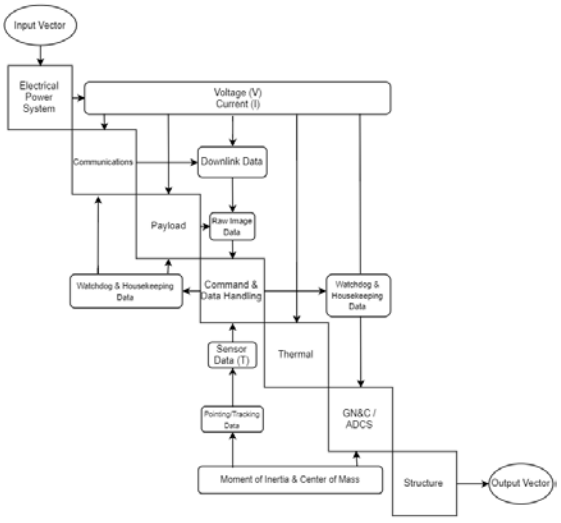

Figure 1: Spartan Imaging Satellite N2 Diagram

References:

[1] Ranvier S., Waets A., Cipriani F., Anciaux M., Gamby E., Cardoen P., Bonnewijn S., De Keyser J., Pieroux D., & Lebreton J.P. (2017, June). *SPL: A Langmuir Probe Instrument On Board A Cubesat.* Poster session presented at the International Planetary Probe Workshop, The Hague, Netherlands.

THE CU-E^3 CUBESAT: AN ENTRY IN NASA'S CUBE QUEST CHALLENGE'S DEEP SPACE DERBY

J. S. Sobtzak, Department of Aerospace Engineering Sciences, University of Colorado, 429 UCB, Boulder, CO 80309, john.sobtzak@colorado.edu.

Introduction: CubeSats have become almost ubiquitous for demonstrating and testing new technologies from low Earth orbit (LEO) but their use is expanding with CubeSats being launched into higher and higher Earth-based orbits and now even into interplanetary space. When NASA launches its new Space Launch System (SLS) on its maiden flight, Exploration Mission (EM-1), currently scheduled for December 2019, the rocket will be ferrying 13 CubeSats as secondary payloads into trans-lunar orbits and beyond. Many of these CubeSats are set to study the moon, but a few are to be sent further on into deep-space missions, including the University of Colorado's Earth Escape Explorer, or CU-E^3.

The CU-E^3 team has earned a secondary payload position on the SLS EM-1 launch through competing in NASA's Cube Quest Challenge, a NASA Centennial Challenge used to award three SLS EM-1 secondary payload positions, "… to teams that meet the challenge of designing, building, and delivering flight-qualified, small satellites capable of advanced operations near and beyond the moon."[1] Thus far, the CU-E^3 team has placed 4th, 3rd, and 2nd in the Challenge's ground tournaments GT-2, GT-3, and GT-4, respectively, earning a secondary payload slot on the EM-1 launch and $80,000 in prize money along the way and is poised to win part or all of the $1,500,000 prize money available in Deep Space Derby[2].

The CU-E^3 spacecraft will be injected into a heliocentric orbit by the SLS's upper stage and continue travelling out into deep space where its mission will be to demonstrate error-free digital radio communications from a 6U CubeSat form factor at distances greater than 4 million kilometers from Earth. The mission sounds simple, but reality is far from simple.

An overview of the design and operational concepts for the CU-E^3 CubeSat are presented in this paper. The paper starts with a short introduction to the Cube Quest Challenge and its Deep Space Derby to indicate the motivation behind the CU-E^3 design. Mission goals are stated, system architecture and subsystem details to obtain those goals are presented. Specific innovative design elements are highlighted, including a novel, student designed, reflectarray antenna and its associated feedhorn antenna element, which together provide and antenna capable of +23 dBi of gain in the 8.4-8.5 GHz deep space radio communications band. Also discussed is the High Rate CubeSat Communication System (HRCCS), an X-band transmitter previously developed thru a NASA Small Satellite Partnership Cooperative Agreement[3].

Design challenges and their solutions are emphasized and discussed at length. Of primary focus are the performance restrictions that result directly from the small form factor, i.e. the 6U size limits solar panel array size, which, in turn, limits electrical power production and, subsequently, radio transmitter power and communication range. Similarly, the small form factor also provides challenges from a thermal perspective due to the limited thermal mass available to absorb and store heat as well as the limited surface area available for radiating waste heat into space.

Finally, the expected performance of CU-E3 participation in the Cube Quest Challenge's Deep Space Derby are illustrated and quantified.

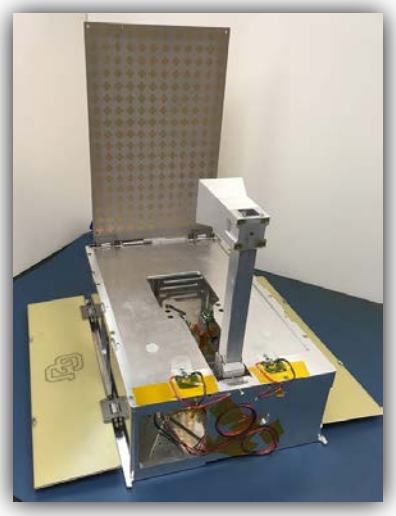

The first CU-E^3 CubeSat EDU

References:

[1] Centennial Challenges Cube Quest Challenge https://www.nasa.gov/directorates/spacetech/centennial_challenges/cubequest/index.html

2. "Cube Quest Challenge – Ground Tournaments, Deep Space Derby, and Lunar Derby – Operations and Rules", Rev. B, April 10, 2015. https://www.nasa.gov/sites/default/files/atoms/files/revision_b.pdf

3. Palo, S., O'Connor, D., DeVito, E., Kohnert, R., Crum, G., and Altunc, S., "Expanding CubeSat Capabilities with a Low Cost Transceiver", 28th Annual AIAA/USU Conference on Small Satellites, 2014.

INNOVATIVE COMPACT SOLAR AND ANTENNA ARRAY DRIVE ASSEMBLY ENABLING DEEP SPACE CUBESAT MISSIONS. M. M. Hott[1], L. Eliott[1], G. BAILET[2] and C. O. Laux[2], [1]CentraleSupélec, Université Paris-Saclay, 3, rue Juliot Curie, 91192 Gif-sur-Yvette Cedex, France (marcus.hott@student.ecp.fr). [2]Laboratoire EM2C, CNRS, 91190 Gif-sur-Yvette, France,.Université Paris-Saclay, 3, rue Juliot Curie, 91192 Gif-sur-Yvette Cedex, France (gilles.bailet@centralesupelec.fr).

Introduction: CubeSats have demonstrated their attractivity as a standardized low-cost, low mass/volume platform, with the currently biggest format (12U) not exceeding 22x22x34cm^3 and 24 kg [1]. In line with the increasing interest in long range transport and human colonies on the Moon or Mars, CubeSats find themselves on the verge of being used for scientific purpose in missions outside of their traditional terrestrial orbit, thereby coping with the challenges of deep space exploration (MarCO [2]). However, with higher mission complexity, inter alia, requirements for both the pointing accuracy of the antenna (X-band) and the electrical power budget (electric propulsion) aboard the satellite rise. To address these challenges, the design of a panel array drive assembly (PADA) for CubeSats is presented in this paper, that permits precise antenna and solar array orientation to maximize a CubeSats link and power budget.

Motivation: Development of the PADA is being conducted within the lunar SIRONA mission, which is a 12U CubeSat lead by CentraleSupélec, France [3].

In order to independently travel to the lunar orbit or beyond, some form of propulsion is required. Choosing a propulsion method heavily depends on the mass of the satellite. Large-scale satellites conventionally rely on a chemical propulsion as used by launchers. With constraints of mass and volume on a nanosatellite, electrical propulsion emerges as the primary choice to achieve long-range missions with descent payload, e.g. the SIRONA mission will use electrical propulsion to reach the lunar orbit. This mission design choice is drastically affecting the power budget, thus imposing a non-conventional power generation system compatible with the CubeSat standard.

To satisfy the mission objectives, SIRONA must be equipped with an appropriate PADA mechanism, able to orientate the solar panels towards the incoming radiation at all moments.

System design: For the PADA, the same low mass and volume constraints apply as for the whole CubeSat, hence the system design presents a particular challenge.

While the first CubeSat missions were strictly 1U CubeSats, they have grown in size. The 6U CubeSats show flight heritage since 2016, the 12U ones are in development phase. Following this trend and as a system to be tested on the SIRONA mission, the PADA is tailored to the current 12U specification of ISIS. This distinguishes it from previous PADA-equivalent concepts on 3U CubeSats, since 3Us have different cross-sections [4].

The primary design concern is to utilize free space, that would otherwise be lost. Looking at the top view of a 12U (224x224 mm^2 cross section), one finds unused areas between the 4 individual electronic assemblies (96x96 mm^2 cross section), layed out per stages (on a 12U, 3 stages of 4Us). This space dictates the dimensions of the PADA: 220x20x40 mm^3 for mechanisms and electronics, where the 40 mm depth is the only adjustable parameter.

The PADA accounts for rotation in its longitudinal axis. The accordingly designed reaction wheel on the z-axis of the ADCS (top-bottom) will complement the system and allow orientation anywhere in space.

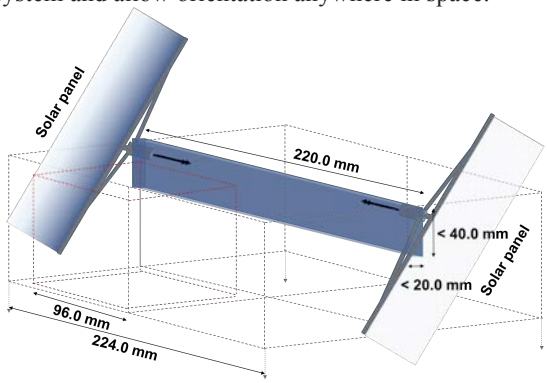

Figure 1 Sketch of the SolarArrayDriveMechanism

Conclusion: The PADA pioneers as design, that meets the increasingly complex requirements of CubeSats missions, in terms of more power demanding payloads, powerful electrical propulsion and precise antenna pointing. Simultaneously, it encourages innovation in these three sectors by providing more of the limiting resource, that the available power aboard a satellite is.

References:

[1] ISIS advised envelope (2016) *12-Unit XL CubeSat dimensions.*

[2] Klesh, A. et al. (2015) *Mars CubeSat One (MarCO)*, AIAA/USU 2015 Logan, UT.

[3] Bailet, G. et al (2018) *SIRONA-1: a selenocentric platform hosting international payloads*, 15th IPPW, Boulder, CO.

[4] Mike Passaretti and Ron Hayes. (2010) *Development of a solar array drive assembly for CubeSat*.